



HAL
open science

Études de dérivés hypervalents du silicium en conditions photoredox : de la génération de radicaux à leur utilisation en chimie organique

Etienne Levernier

► To cite this version:

Etienne Levernier. Études de dérivés hypervalents du silicium en conditions photoredox : de la génération de radicaux à leur utilisation en chimie organique. Chimie organique. Sorbonne Université, 2020. Français. NNT : 2020SORUS344 . tel-03787917

HAL Id: tel-03787917

<https://theses.hal.science/tel-03787917v1>

Submitted on 26 Sep 2022

HAL is a multi-disciplinary open access archive for the deposit and dissemination of scientific research documents, whether they are published or not. The documents may come from teaching and research institutions in France or abroad, or from public or private research centers.

L'archive ouverte pluridisciplinaire **HAL**, est destinée au dépôt et à la diffusion de documents scientifiques de niveau recherche, publiés ou non, émanant des établissements d'enseignement et de recherche français ou étrangers, des laboratoires publics ou privés.

Sorbonne Université

Ecole doctorale de Chimie Moléculaire de Paris Centre – ED 406

Institut Parisien de Chimie Moléculaire / Equipe MACO

Études de dérivés hypervalents du silicium en conditions photoredox : de la génération de radicaux à leur utilisation en chimie organique

Par **M. Etienne LEVERNIER**

Thèse de doctorat de Chimie

Dirigée par M. Louis FENSTERBANK et M. Cyril OLLIVIER

Présentée et soutenue publiquement le 25/09/2020

Devant un jury composé de :

M. Sami LAKHDAR, <i>Chargé de Recherche CNRS à l'Université Paul Sabatier</i>	Rapporteur
Mme. Clémence ALLAIN, <i>Chargée de Recherche CNRS à l'ENS Cachan</i>	Rapporteuse
M. Gérard GUILLAMOT, <i>Directeur Scientifique de SEQENS</i>	Examineur
M. Alejandro PEREZ-LUNA, <i>Directeur de Recherche CNRS à l'Université Pierre et Marie Curie</i>	Examineur
M. Cyril OLLIVIER, <i>Directeur de Recherche CNRS à l'Université Pierre et Marie Curie</i>	Directeur de thèse
M. Louis FENSTERBANK, <i>Professeur à l'Université Pierre et Marie Curie</i>	Directeur de thèse

Sorbonne Université

Ecole doctorale de Chimie Moléculaire de Paris Centre – ED 406

Institut Parisien de Chimie Moléculaire / Equipe MACO

Études de dérivés hypervalents du silicium en conditions photoredox : de la génération de radicaux à leur utilisation en chimie organique

Par **M. Etienne LEVERNIER**

Thèse de doctorat de Chimie

Dirigée par M. Louis FENSTERBANK et M. Cyril OLLIVIER

Présentée et soutenue publiquement le 25/09/2020

Devant un jury composé de :

M. Sami LAKHDAR, <i>Chargé de Recherche CNRS à l'Université Paul Sabatier</i>	Rapporteur
Mme. Clémence ALLAIN, <i>Chargée de Recherche CNRS à l'ENS Cachan</i>	Rapporteuse
M. Gérard GUILLAMOT, <i>Directeur Scientifique de SEQENS</i>	Examineur
M. Alejandro PEREZ-LUNA, <i>Directeur de Recherche CNRS à l'Université Pierre et Marie Curie</i>	Examineur
M. Cyril OLLIVIER, <i>Directeur de Recherche CNRS à l'Université Pierre et Marie Curie</i>	Directeur de thèse
M. Louis FENSTERBANK, <i>Professeur à l'Université Pierre et Marie Curie</i>	Directeur de thèse

"L'imagination est plus importante que le savoir"

Albert Einstein

Remerciements

Le travail réalisé pendant ces trois années de thèse a été effectué à l'Institut Parisien de Chimie Moléculaire dirigé par M. Louis Fensterbank.

Je tiens en premier lieu à remercier les membres de mon jury pour avoir accepté d'évaluer ce travail en tant que rapporteurs : M. Sami Lakhdar, Chargé de Recherche à l'Université Paul Sabatier et Mme. Clémence Allain, Chargée de Recherche à l'ENS Cachan, et en tant qu'examinateurs : M. Gérard Guillaumot, Directeur Scientifique de l'entreprise Seqens et M. Alejandro Perez-Luna, Directeur de Recherche à l'Université Pierre et Marie Curie.

Je souhaite ensuite dire un grand merci à mes encadrants Cyril Ollivier et Louis Fensterbank. Vous m'avez beaucoup appris durant ces trois années tant d'un point de vue humain que scientifique. Vous m'avez aussi fait confiance pour encadrer plusieurs personnes et je veux vous en remercier. Adrien, tu as été mon premier stagiaire et j'espère que travailler avec moi t'a donné envie de continuer la chimie ! Mehdi, je ne sais pas qui de nous deux a le plus appris de l'autre. Il n'y a jamais vraiment eu de relation hiérarchique entre nous car les amis, pour moi, sont au même niveau. Pour cela, je veux te dire un grand merci. J'ai aussi eu le privilège de travailler, de près ou de loin, avec plusieurs personnes que je souhaite remercier chaleureusement. Bien sûr, je suis obligé de commencer par Thibaut. Nous avons partagé le laboratoire pendant 2 ans. Toutes les émotions se sont succédées mais je pense que celle qui restera à jamais est sans nul doute l'amitié. Christophe et Vincent, pour m'avoir formé sur ce sujet et tant appris. Alex, pour m'avoir fait découvrir le Japon, on a fait une belle équipe ! Heng-Rui, tu es vraiment quelqu'un de bien et je suis convaincu qu'une carrière de chimiste t'attend. Mengxue, pour m'avoir fait découvrir et apprécier la chimie en flux continu. Alexandre M., pour ton éternelle nonchalance qui cache, j'en suis sûr, un grand cœur ! Etienne D., pour m'avoir aidé avec tes calculs et ta bonne humeur tout au long de ces années. Clément, pour m'avoir aidé lors de la rédaction de ce manuscrit. Alexandre S., Maud, Cédric, Cassandre, Julien, Anthony, Laura, Khaoula, Alexandre P., Claire, Aurélie, pour m'avoir écouté et soutenu pendant cette thèse qui fut, parfois, éprouvante. On s'est quand même bien amusés ! Ainsi que tous les autres membres passés ou présents de l'équipe MACO qui ont permis de rendre cette expérience inoubliable.

Je veux aussi remercier ma famille et mes amis car, sans eux, rien de tout cela n'aurait été possible. Noémie, Christophe, Guillaume, Johan, nous nous connaissons depuis déjà longtemps et je sais que nous serons toujours là les uns pour les autres. Guillaume, Nicolas, vous m'avez épaulé, soutenu dans les moments difficiles. Merci pour tout. Ensuite mes parents, vous m'avez rassuré et encouragé à aller toujours plus loin. Vous m'avez permis de me surpasser, et grâce à vous, j'ai pu atteindre mes objectifs. Merci.

Bien sûr je vais finir avec celle qui illumine ma vie depuis plusieurs années déjà. Adèle, bien que ces trois années aient été difficiles pour nous deux, je n'imagine plus ma vie sans toi. Tu es mon rayon de soleil et je suis convaincu que d'autres aventures, à deux ou plus, nous attendent.

Préface

Cette thèse intitulée “Études de dérivés hypervalents du silicium en conditions photoredox : de la génération de radicaux à leur utilisation en chimie organique”, est composée de quatre chapitres indépendants. Chacune de ces sections est ensuite subdivisée en plusieurs sous-parties.

Au début de chacune d'elles, une partie bibliographie peut être trouvée. Cette partie, servant à donner un aperçu de l'état de l'art, permet au lecteur de mieux appréhender la suite du travail. Ensuite, les résultats obtenus lors de cette thèse peuvent être trouvés sous la forme d'articles (publiés ou non). Il est aussi important d'ajouter que certains résultats obtenus, qui ne sont pas publiés, viennent compléter ce travail dans la partie "Additional Results". Cette partie, retranscrivant aussi des résultats négatifs, permet d'avoir un aspect global de ce qui a été effectué pendant ces trois années de recherche. Enfin, un descriptif des expériences réalisées et des analyses effectuées peut être trouvé dans la section intitulée "Supporting Information". Les références bibliographiques peuvent être trouvées à la fin de chaque sous-partie.

J'espère que ce manuscrit vous plaira et je vous souhaite une bonne lecture !

Sommaire

REMERCIEMENTS.....	7
PREFACE	9
SOMMAIRE	11
ABBREVIATIONS	17
RESUME EN FRANÇAIS.....	21
CHAPTER I. PHOTOCATALYSIS AND RADICAL PRECURSORS.....	43
I.1. GENERAL INTRODUCTION	43
I.1.1. Genesis of radical synthesis	43
I.1.2. Principle of photocatalysis	44
I.1.3. Photooxidative generation of radicals	47
I.1.3.1. Photooxidation of the carboxylates	47
I.1.3.2. Photooxidation of the trifluoroborates	49
I.1.3.3. Photooxidation of the DHPs	51
I.1.3.4. Photooxidation of silicon derivatives.....	52
a) Photooxidation of trimethylsilane derivatives	52
b) Photooxidation of the alkyl bis-catecholato silicates.....	53
b.1) Silicates synthesis	53
b.2) Crystalline form.....	55
b.3) Redox properties.....	57
b.4) Silicates reactivity: photooxidation	58
I.1.4. References	60
I.2. PHENYL BIS-CATECHOLATO SILICATES: SYNTHESIS, STRUCTURAL STUDIES AND REACTIVITY	62
I.2.1. Abstract	62
I.2.2. Introduction	62
I.2.3. Results and Discussion.....	63
I.2.4. Conclusion.....	76
I.2.5. Additional results	77
I.2.5.1. Extended catechol modifications	77

I.2.5.2.	Oxidation of the aryl silicate	78
I.2.5.3.	Oxidation of the methyl silicate	79
I.2.6.	Supporting information	81
I.2.7.	References	98
CHAPTER II.	PHOTOREDOX/TRANSITION METAL DUAL CATALYSIS AS AN	
	EFFICIENT SYNTHETIC TOOL.....	103
II.1.	DEFINITION AND GENESIS OF DUAL CATALYSIS	103
II.2.	UTILIZATION OF DIFFERENT METALS AND RADICAL PRECURSORS	106
II.2.1.	Photoreduction and organometallic catalytic cycle.....	107
II.2.1.1.	Copper catalysis	107
II.2.1.2.	Gold dual catalysis	108
II.2.2.	Photooxidation and organometallic catalytic cycle.....	109
II.2.2.1.	Chromium dual catalysis.....	109
II.2.2.2.	Cobalt dual catalysis	110
II.2.2.3.	Nickel dual catalysis	111
a)	Genesis of the nickel dual catalysis	112
b)	Trifluoroborates as efficient coupling partners.....	114
c)	Carboxylates as efficient coupling partners	118
d)	Silicates as efficient coupling partners	120
e)	Sodium sulfinates and other derivatives as efficient coupling partners.....	124
f)	DHPs as efficient coupling partners	127
g)	Mechanism of dual catalysis.....	127
h)	Extension of concept.....	130
h.1)	Multicomponent reactions	130
h.2)	Multiple	131
II.2.3.	Conclusion on dual catalysis	132
II.2.4.	References	133
II.3.	CROSS COUPLING OF ALKYL SILICATES WITH ACYLCHLORIDES VIA PHOTOREDOX/NICKEL DUAL CATALYSIS. A NEW SYNTHESIS OF KETONES	136
II.3.1.	Abstract	136
II.3.2.	Introduction	136
II.3.3.	Results and discussion.....	137
II.3.4.	Conclusion.....	144

II.3.5. Additional results	145
II.3.5.1. Formation of the side products.....	145
II.3.5.2. Additional flow chemistry: sp ³ -sp ³ cross-coupling reaction	146
II.3.5.3. Nucleophilicity of the silicates.....	147
II.3.5.4. Dual catalysis and catechol modification.....	148
II.3.6. Supporting information	150
II.3.7. References	173
CHAPTER III. VISIBLE-LIGHT PHOTOREDOX CATALYZED RADICAL CARBONYLATION.....	179
III.1. MULTICOMPONENT REACTION	179
III.1.1. Carbonylation reactions: organometallic pathway	179
III.1.2. Radical carbonylation.....	180
III.1.2.1. Genesis of radical carbonylation.....	180
III.1.2.2. Toward other systems for radical carbonylation	184
III.1.3. Photoredox radical carbonylation.....	186
III.1.3.1. Palladium chemistry and radical carbonylation	186
III.1.3.2. Radical carbonylation mediated by visible-light photoredox catalysis.....	188
a) Visible-light induced photoreductive processes	188
b) Visible-light induced photooxidative processes	190
III.1.4. References	192
III.2. ALKYL RADICAL CARBONYLATION USING ORGANOSILICATES <i>VIA</i> VISIBLE-LIGHT PHOTOREDOX CATALYSIS	193
III.2.1. Abstract	193
III.2.2. Introduction	193
III.2.3. Results and discussion.....	194
III.2.4. Conclusion.....	201
III.2.5. Additional results	202
III.2.5.1. Dual photoredox catalysis and radical carbonylation	202
III.2.5.2. Carbon monoxide releasing molecules	202
III.2.6. Supporting information	205
III.2.7. References	229
III.3. SYNTHESIS OF ALIPHATIC AMIDES THROUGH A PHOTOREDOX CATALYZED RADICAL CARBONYLATION INVOLVING ORGANOSILICATES AS ALKYL RADICAL PRECURSORS ...	232

III.3.1. Abstract	232
III.3.2. Introduction	232
III.3.3. Results and Discussion.....	233
III.3.4. Conclusion.....	238
III.3.5. Additional results	239
III.3.5.1. Amide formation under flow regimes	239
III.3.5.2. Carbonylation reactions under flow regimes	239
III.3.6. Supporting Information	241
III.3.7. References	258
CHAPTER IV. PHOTOREDUCTION OF HYPERCOORDINATED SILICON SPECIES	263
IV.1. SILICON DERIVATIVES AS EFFICIENT RADICAL PRECURSORS	263
IV.2. CHLOROSILANE AND SILICON COMPLEXES	263
IV.2.1. Synthesis of hypercoordinated chlorosilanes	263
IV.2.2. Toward other silicon complexes.....	265
IV.2.3. Chlorosilanes and silylium complexes as synthetic tools.....	267
IV.2.3.1. Chlorosilanes as reagents in organic chemistry	267
IV.2.3.2. Silyliums as reagents in organic chemistry	267
IV.2.4. References	271
IV.3. TOWARDS VISIBLE-LIGHT PHOTOCATALYTIC REDUCTION OF HYPERCOORDINATED SILICON SPECIES	272
IV.3.1. Abstract	272
IV.3.2. Introduction	272
IV.3.3. Results and Discussion.....	274
IV.3.4. Conclusion	286
IV.3.5. Supporting information	287
IV.3.6. References	295
GENERAL CONCLUSION.....	299

- Abbreviations -

Abbreviations

ATC	Atom Transfer Carbonylation
Ar	Aryl
BDE	Bond Dissociation Energy
BET	Back Electron Transfer
Bn	Benzyl
Boc	<i>tert</i> -Butoxycarbonyl
Bpin	4,4,5,5-Tetramethyl-1,3,2-dioxaborolane
CAN	Ceric ammonium nitrate ((NH ₄) ₂ Ce(NO ₃) ₆)
Cbz	Carboxybenzyl
COD	Cyclooctadiene
Cp	Cyclopentadienyl
4CzIPN	2,4,5,6-Tetra(9H-carbazol-9-yl)isophthalonitrile
DBU	1,8-Diazabicyclo(5.4.0)undec-7-ene
DFT	Density-functional theory
DHP	4-Alkyl-1,4 dihydropyridine
DIPEA	N, N-Diisopropylethylamine
DMDC	Dimethyldicarbonate
dme	ethylene glycol dimethyl ether
DMF	Dimethylformamide
dtbbpy	4,4'-di- <i>tert</i> -butyl-2,2'-dipyridyl
EBX	Ethynyl Benziiodoxolone
EPR	Electron Paramagnetic Resonance
equiv.	equivalent
<i>fac</i>	facial
h, min, s	hour, minute, second
HAT	Hydrogen Atom Transfer
HE	Hantzsch ester
HMTP	2,2,6,6-Tetramethylpiperidine
HOMO	Highest Occupied Molecular Orbital
ISC	Inter-System Crossing
IR	Infrared
[Ir]	[Ir{dFCF ₃ ppy} ₂ (bpy)]PF ₆
LA	Lewis Acid
LC	Ligand-Centered transition
LED	Light-emitting diode
LUMO	Lowest Unoccupied Molecular Orbital
LMCT	Ligand-to-Metal Charge Transfer
MC	Metal-Centered transition
Mes-Acr	9-mesityl-10-methylacridinium
MFC	Mass Flow Controller
MLCT	Metal-to-Ligand Charge Transfer

M. P.	Melting point
NMR	Nuclear magnetic resonance
<i>o, p, m</i>	ortho, meta, para
PC	Photocatalyst
1,10 phen	1,10-Phenantroline
Ph-PTZ	<i>N</i> -Phenylphenothiazine
ppy	2-Phenylpyridine
rt	room temperature
RMN	Résonance Magnétique Nucléaire
SCE	Saturated Calomel Electrode
SET	Single Electron Transfer
[Si]	Silicate
SOMO	Singly Occupied Molecular Orbital
TADF	Thermally Activated Delayed Fluorescence
TBADT	Tetrabutylammonium decatungstate
TEMPO	2,2,6,6-Tetramethylpiperidinyloxy
TFBen	Benzene-1,3,5-triyl triformate
THF	Tetrahydrofuran
THP	Tetrahydropyran
TMG	1,1,3,3 Tetramethylguanidine
TMHD	2,2,6,6-Tetramethyl-3,5-heptanedione
TMOP	1,3,5 trimethoxybenzene
TMS	Trimethylsilane
Ts	Tosyl
TTMSS	Tris(trimethylsilyl)silane
UV	Ultraviolet
XRD	X-Ray Diffraction

Résumé
- en -
français

Résumé en français

Les radicaux sont des espèces chimiques possédant un électron non apparié. Leur nature, bien souvent éphémère, a rendu compliqué l'acceptation de leur existence décrite pour la première fois par Moses Gomberg en 1900. Néanmoins, les preuves avancées au fil du temps par Paneth,¹ Hey² et Karash³ ont fini par convaincre la communauté scientifique. Pendant un temps, ces entités étaient obtenues grâce à la combinaison d'un initiateur et d'un médiateur ou bien grâce à un métal en quantité stœchiométrique. Cependant, dans un contexte où la sécurité et l'environnement ont une place chaque jour un peu plus grande, ces méthodes sont devenues obsolètes.⁴ À l'inverse, la catalyse photoredox, initiée par Kellog,⁵ Pac⁶ et Deronzier,⁷ connaît depuis une dizaine d'années un essor considérable. En effet, cette méthode douce de génération de radicaux repose sur l'utilisation d'un photocatalyseur et de lumière, ce qui permet aux chimistes d'envisager autrement la formation de liaisons carbone-carbone. Suite à une activation par un photon, un photocatalyseur est capable de promouvoir un de ses électrons dans une orbitale de plus haute énergie. Il peut alors oxyder ou réduire des molécules formant, ainsi, des radicaux. Bien que la majorité des photocatalyseurs soit basée sur un métal comme l'iridium, le ruthénium ou le cuivre,⁸ les colorants organiques tels l'éosine Y ou encore la rose de bengale se sont progressivement imposés comme alternatives efficaces (Schéma 1).

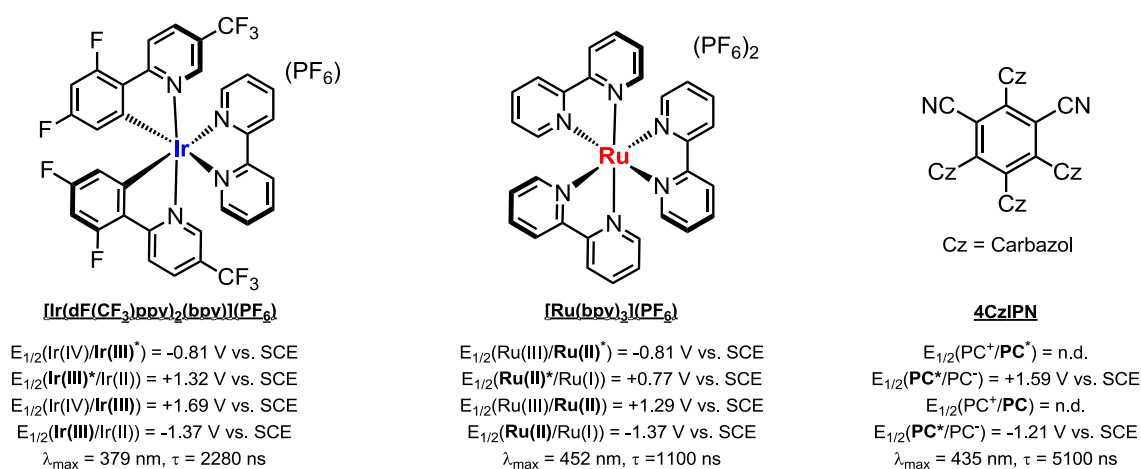


Schéma 1 : Exemples de photocatalyseurs

Sur la base de cette méthode, un grand nombre de radicaux carbonés ou centrés sur un hétéroatome (soufre, oxygène, azote) a pu être formé. Néanmoins, les radicaux alkyles non stabilisés sont restés, pendant longtemps, difficiles à obtenir. En photoréduction, des travaux très intéressants comme ceux de Stephenson sur les iodures primaires ont été réalisés. Malheureusement, le faible nombre d'exemples rapportés a considérablement limité leur utilisation (Schéma 2).⁹

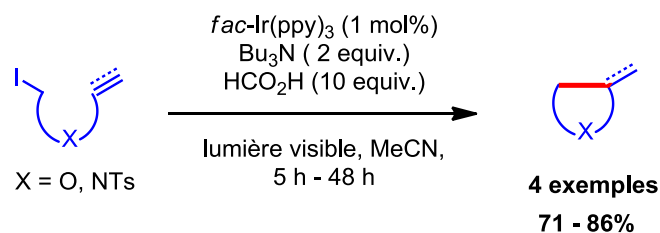


Schéma 2 : Réduction de iodures primaires puis cyclisation

Le même constat a pu être fait en photooxydation. Les travaux de MacMillan sur les α -amino/oxo carboxylates¹⁰ et ceux d'Akita sur les benzyles ou allyles trifluoroborates¹¹ ont permis de générer des radicaux alkyles. Toutefois, ceux-ci étaient stabilisés par la présence en alpha d'un hétéroélément ou d'un cycle aromatique ce qui facilitait leur génération (**Schéma 3**). Dans ces publications, le photocatalyseur $[\text{Ir}\{\text{dFCF}_3\text{ppy}\}_2(\text{bpy})]\text{PF}_6$ ($E_{1/2}(\text{Ir(III)}^*/\text{Ir(II)}) = +1.32 \text{ V vs. SCE}$ et noté [Ir]) a été utilisé.

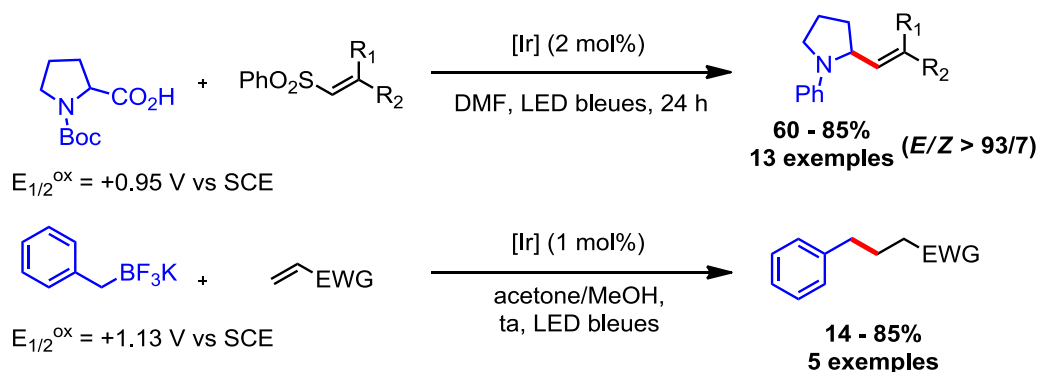


Schéma 3 : Génération de radicaux alkyles stabilisés en photooxydation

C'est dans ce contexte que notre groupe s'est intéressé aux silicates. Ces derniers peuvent être facilement synthétisés à partir d'un trialkoxysilane ou d'un trichlorosilane et de catéchols en présence d'une base (**Schéma 4**).¹²

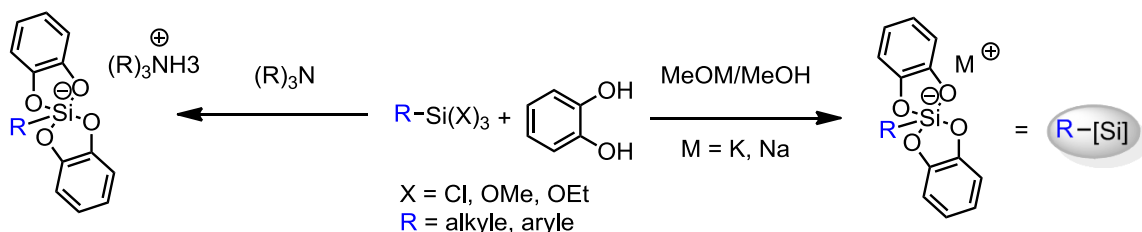


Schéma 4 : Synthèse de silicates

Ils ont aussi un potentiel d'oxydation relativement bas ($E_{1/2}^{ox} < +1$ V vs. SCE) ce qui permet la formation de radicaux alkyles stabilisés et non stabilisés. Ces derniers ont été utilisés avec succès en addition intermoléculaire et en addition/élimination sur une allylsulfone (Schéma 5).¹³

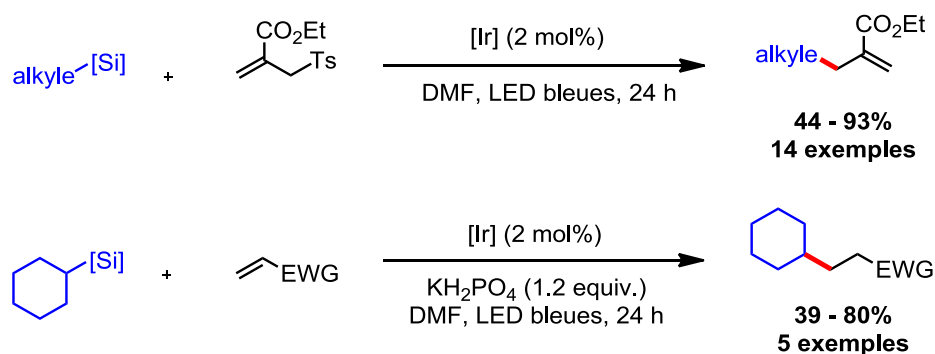


Schéma 5 : Utilisation des silicates dans des réactions de piégeage direct et d'addition/élimination

Après avoir réussi à générer des radicaux alkyles non stabilisés, nous nous sommes demandés s'ils pouvaient aussi engendrer des radicaux sp^2 . En effet, plusieurs précurseurs radicalaires peuvent être utilisés pour générer des radicaux sp^2 en réduction.¹⁴ En revanche, en oxydation, ceci semble beaucoup plus difficile. Une seule publication évoque la génération de tels radicaux dans ces conditions. Dans cet article du groupe de Yoshimi, des carboxylates d'aryles sont oxydés et piégés par différents accepteurs radicalaires (acrylonitrile, acrylamide...). Néanmoins, une grande quantité de photocatalyseur ([50 mol % - 150 mol %]) doit être utilisée sous irradiation UV et les rendements obtenus restent, pour la plupart, inférieurs à 60%.¹⁵

Intrigués par ce constat, nous avons décidé d'utiliser le phényle silicate, possédant un potentiel d'oxydation relativement bas ($E_{1/2}^{ox} = +0.89$ V vs. SCE), comme substrat modèle. Nos premiers essais se sont malheureusement soldés par des échecs. En effet, que ce soit *via* une réaction d'addition sur une allylsulfone ou bien une abstraction d'hydrogène, seules des traces de produits désirés ont été obtenues. Plus étonnant encore, cette absence de produit formé ne nous a pas semblé être due à une dégradation du silicate puisque celui-ci était toujours présent en fin de réaction. Nous nous sommes donc demandés si une variation des groupements catéchols pourrait améliorer la très faible réactivité observée. En effet, la HOMO des silicates se situe au niveau des catéchols. Ainsi, en introduisant une substitution sur ces derniers, les potentiels d'oxydation pourraient eux aussi être modifiés et nous pourrions espérer une réaction plus efficace.

Nous avons donc, tout d'abord, vérifié que de telles substitutions ne s'opposent nullement à la génération de radicaux. Pour cela, nous avons utilisé le cyclohexyle silicate, connu pour sa bonne réactivité, comme substrat modèle. Après avoir synthétisé des analogues portant des catéchols substitués, nous les avons engagés dans une réaction photochimique en présence d'une allylsulfone. Le produit désiré a pu être formé efficacement malgré une légère baisse de rendement par rapport à la réaction classique (**Schéma 6**).

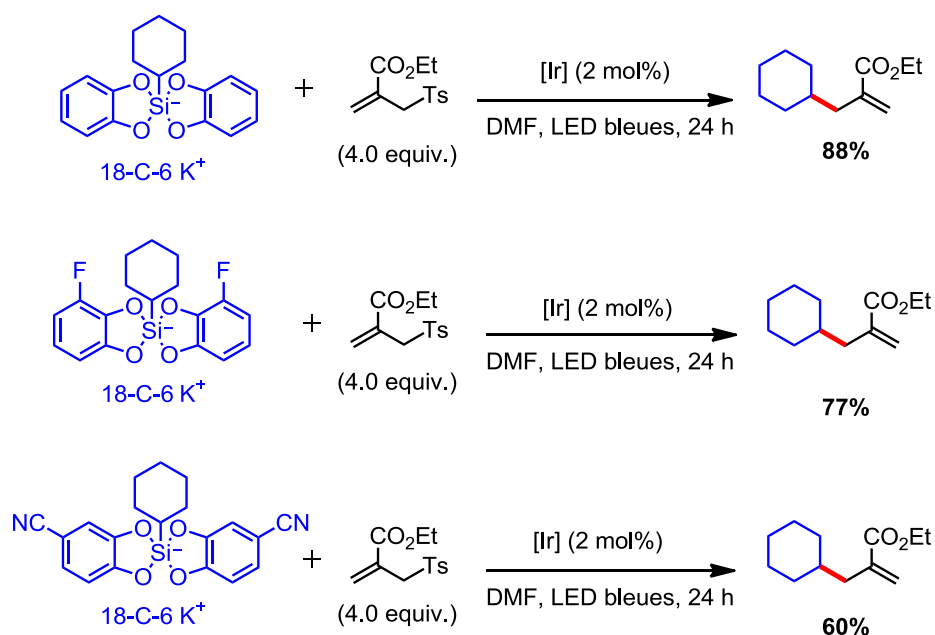


Schéma 6 : Réaction d'analogues du cyclohexyle silicate en piégeage direct

Nous avons donc pu continuer en synthétisant une large gamme de phényles silicates possédant divers groupements donneurs ou attracteurs sur les catéchols. Tel qu'attendu, leur potentiel d'oxydation s'en est trouvé modifié. Nous les avons ensuite engagés dans la même réaction photochimique qu'auparavant. Là où le silicate classique ne fournissait que des traces du produit attendu, il s'est avéré que celui possédant un nitrile en position 3 des catéchols formait le produit désiré avec un rendement de 35%. Malheureusement, même après optimisation des conditions opératoires, ce rendement n'a pu être que légèrement augmenté. Une réaction d'abstraction d'hydrogène a aussi été réalisée et le benzène deutéré résultant a pu être observé avec un rendement assez satisfaisant (**Schéma 7**).

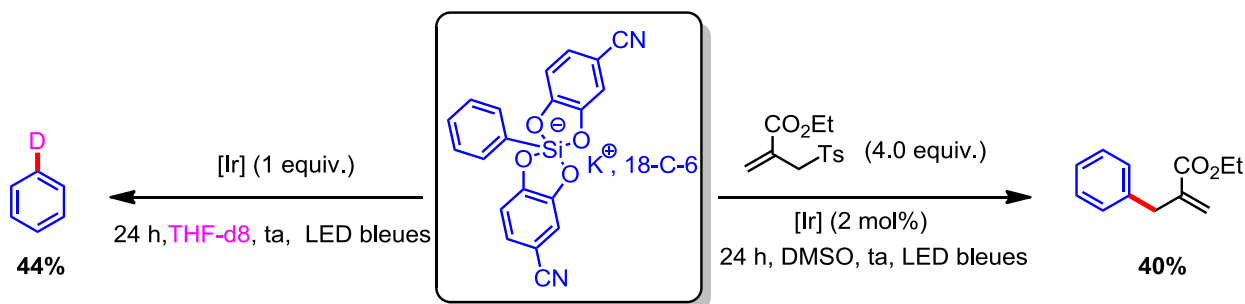


Schéma 7 : Utilisation du phényle silicate modifié en piégeage direct et abstraction d'hydrogène

L'ajout de groupements attracteurs augmentant le potentiel d'oxydation, il est surprenant que cette substitution donne les meilleurs résultats. Afin de mieux comprendre cette réactivité, nous avons réalisé des analyses structurales. Il est apparu que tous ces silicates cristallisent sous une forme pyramidale à base carrée. De plus, pour celui possédant un fluor en position 3, deux isomères ont été observés en DRX (**Schéma 8**).

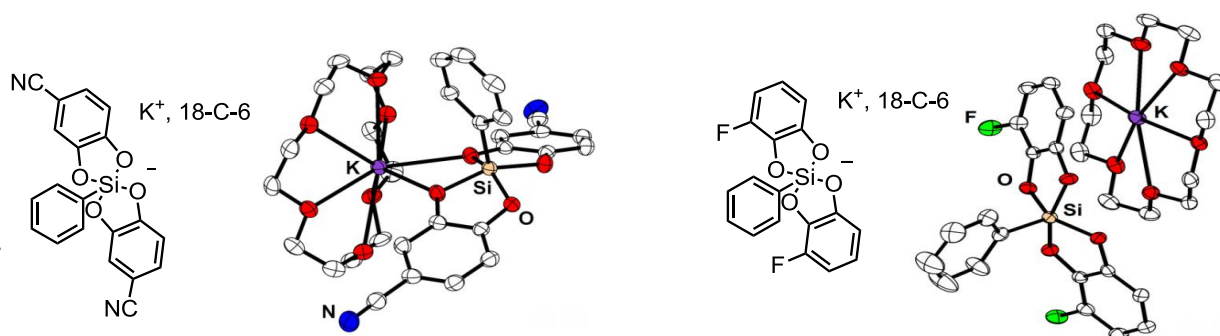


Schéma 8 : Analyse DRX de deux phényles silicates modifiés

En effet, lors de la synthèse nous pouvons obtenir soit le produit "cis", soit le "trans". Cette observation a été confirmée en RMN du ^{13}C puisque tous les pics des silicates possédant des catéchols non symétriques sont alors doublés. Nous nous sommes donc demandés si un équilibre existe entre ces deux formes. Ainsi, après avoir réalisé des RMNs à différentes températures nous avons pu mettre en lumière une coalescence des pics pour le composé possédant un nitrile en position 3 des catéchols. Nous pouvons donc en conclure qu'un équilibre existe bel et bien et il est fort probable qu'il soit le fruit de la pseudo rotation de Berry (**Schéma 9**).

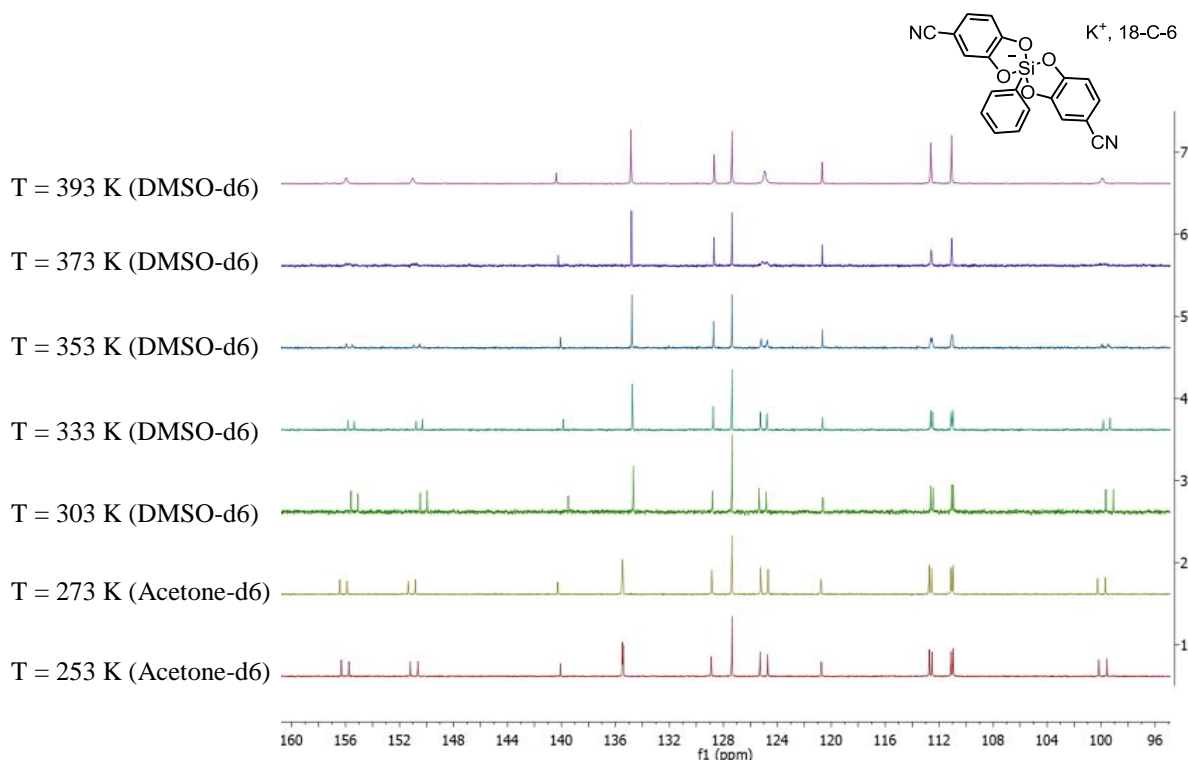


Schéma 9 : RMN du ^{13}C à différentes températures montrant l'existence d'un équilibre de produits

Nous nous sommes ensuite intéressés aux propriétés optiques de ces nouvelles structures hypervalentes du silicium. Les spectres d'absorption ont tous mis en avant une large bande d'absorption entre 270 et 320 nm (**Schéma 10**). Inspirés par les travaux de Nishigaichi,¹⁶ nous nous sommes donc demandés si nous pourrions augmenter le rendement de la réaction photocatalytique en nous plaçant dans cette gamme de longueurs d'ondes. Malheureusement, aucune amélioration n'a été observée (avec ou sans [Ir]).

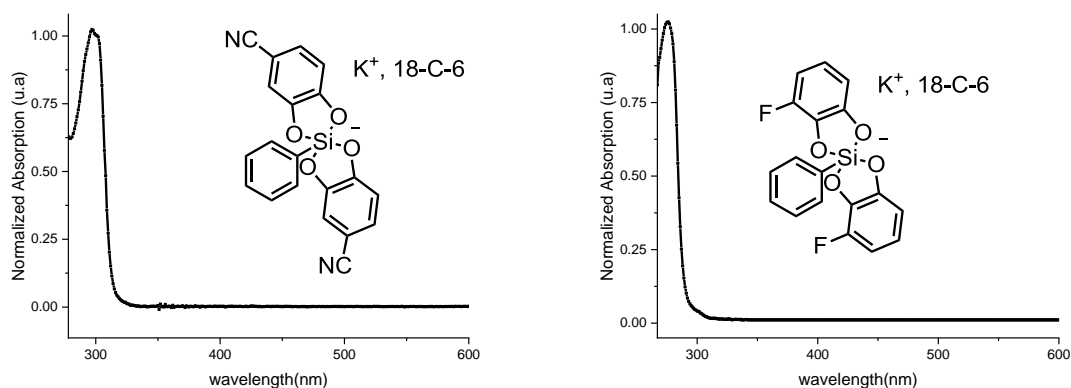


Schéma 10 : Spectres d'absorption de deux phényles silicates modifiés

Des calculs DFT ont enfin été réalisés afin d'expliquer pourquoi certaines substitutions ont un effet aussi bénéfique sur le rendement de la réaction. Il s'est avéré que, selon les catéchols utilisés, la barrière d'énergie nécessaire pour générer le radical phényle se trouve fortement modifiée. En effet, pour celui possédant un nitrile en position 3 des catéchols, une barrière de seulement 18.99 kcal/mol a été obtenue. En comparaison, pour le 3-méthoxycatéchol, qui n'a fourni que relativement peu de produit désiré, nous observons une barrière de 34.11 kcal/mol. Cette grande différence permet d'expliquer pourquoi ces silicates réagissent si différemment. Les calculs ont également mis en lumière une inversion HOMO-SOMO. Ce processus, bien que rare, montre que pour le silicate possédant des groupements cyano, la SOMO se retrouve être la HOMO - 2 alors que pour les autres, la SOMO est beaucoup plus profonde.

Ainsi, grâce à des substitutions au niveau des catéchols, un radical phényle a pu être engendré pour la première fois dans ces conditions et efficacement piégé.

Après cette étude sur la génération et le piégeage de radicaux, nous nous sommes intéressés à une autre application de ces derniers : la catalyse duale. Cette méthode est basée sur l'utilisation de deux catalyseurs. L'un d'eux sert à générer un radical alors que l'autre a pour but d'effectuer un couplage entre un partenaire électrophile et le radical formé. Initialement appliqué à des processus photoréductifs, cette méthode a été transposée en oxydation par MacMillan et Doyle¹⁷ ainsi que par Molander.¹⁸ Quelques années plus tard, notre groupe a aussi montré que les silicates peuvent être utilisés dans ces conditions (**Schéma 11**).¹³

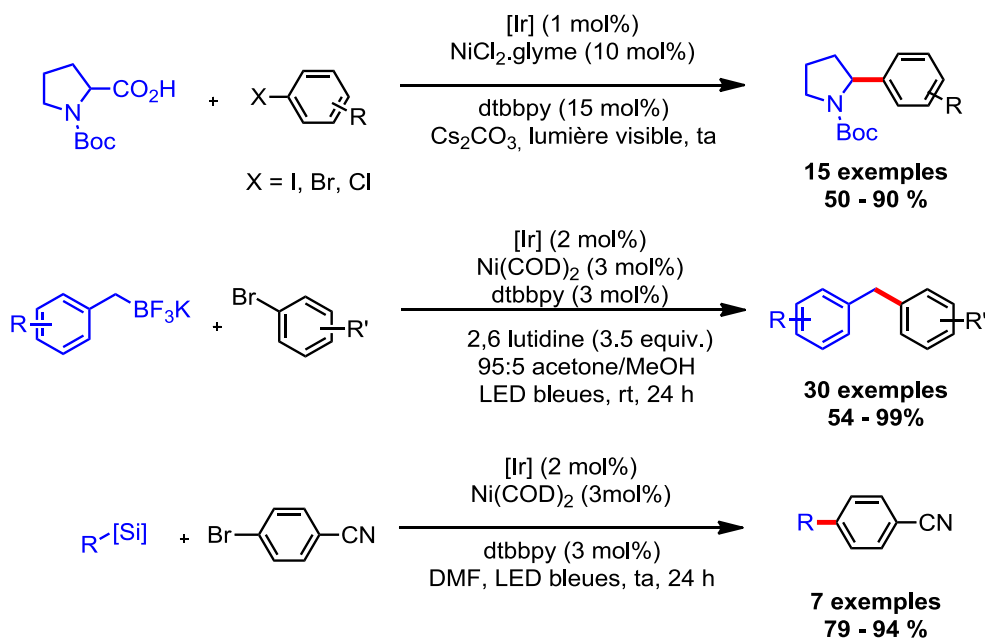


Schéma 11 : Exemples de catalyse duale en photooxydation

Ensuite, ce concept a été transposé à d'autres catalyseurs et précurseurs radicalaires.¹⁹ Même le très difficile couplage sp^3 - sp^3 a pu être réalisé de cette manière.²⁰

Encouragés par les résultats précédents, nous avons décidé d'utiliser les silicates en catalyse duale afin de synthétiser des cétones. En effet, ces dernières ont un grand intérêt en parfumerie ainsi qu'en synthèse. En nous basant sur les données de la littérature, nous avons choisi d'utiliser le chlorure de benzoyle comme partenaire électrophile et le cyclohexyle silicate afin d'optimiser le couplage. Les meilleurs résultats ont été obtenus avec le photocatalyseur $[\text{Ir}\{\text{dFCF}_3\text{ppy}\}_2(\text{bpy})]\text{PF}_6$ et le complexe de nickel $\text{NiCl}_2\cdot\text{dme}$ (**Schéma 12**).

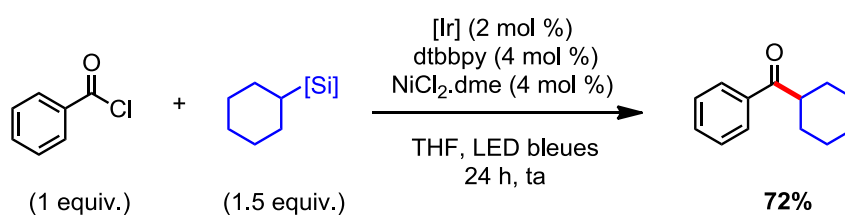


Schéma 12 : Synthèse de la cyclohexyl(phenyl)methanone après optimisation de la réaction

Plusieurs silicates ont ensuite été testés dans ces conditions. Il est apparu que seuls les silicates activés, c'est-à-dire ceux possédant un potentiel d'oxydation relativement bas, réussissent à fournir le produit désiré avec de bons rendements. Les autres mènent à des produits secondaires qui se sont avérés être les produits d'acylation des catéchols du silicate. Afin de mieux comprendre pourquoi ces produits sont formés, plusieurs réactions tests ont été réalisées. Finalement, le sous-produit de la réaction s'est avéré responsable de la formation de ces produits. Le bis-catécholsilane étant un acide de Lewis très fort, nous pensons qu'il active le site électrophile ce qui permet ensuite aux catéchols de réagir (**Schéma 13**).

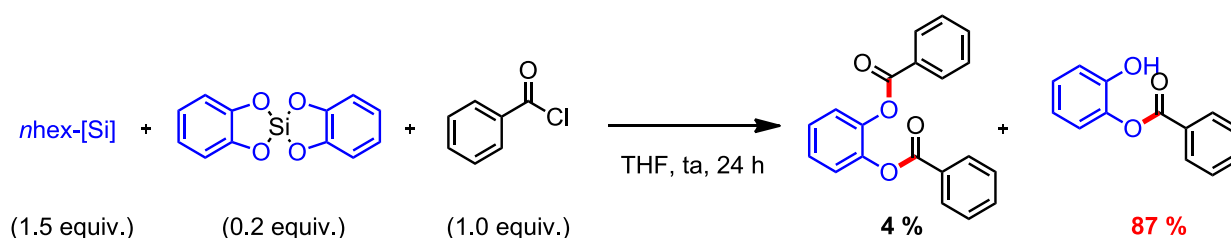


Schéma 13 : Formation des produits secondaires

Devant ces résultats, nous avons considéré la chimie en flux continu comme une solution possible à ce problème de réaction secondaire. En effet, cette approche permet d'accélérer tous les processus photochimiques puisqu'au lieu d'irradier un ballon, un tube de faible diamètre ($D \sim 0,8 \text{ mm}$) se trouve sous la lumière. Ainsi, l'ensemble de la solution peut être irradiée efficacement.²¹ Après avoir mis en œuvre plusieurs montages, nous avons obtenu, en seulement 20 minutes en flux continu, un rendement quasiment équivalent pour le benzyle silicate à celui de 24 h en batch. Cependant, pour les silicates non-activés le rendement de couplage ne s'en est pas trouvé amélioré (**Schéma 14**).

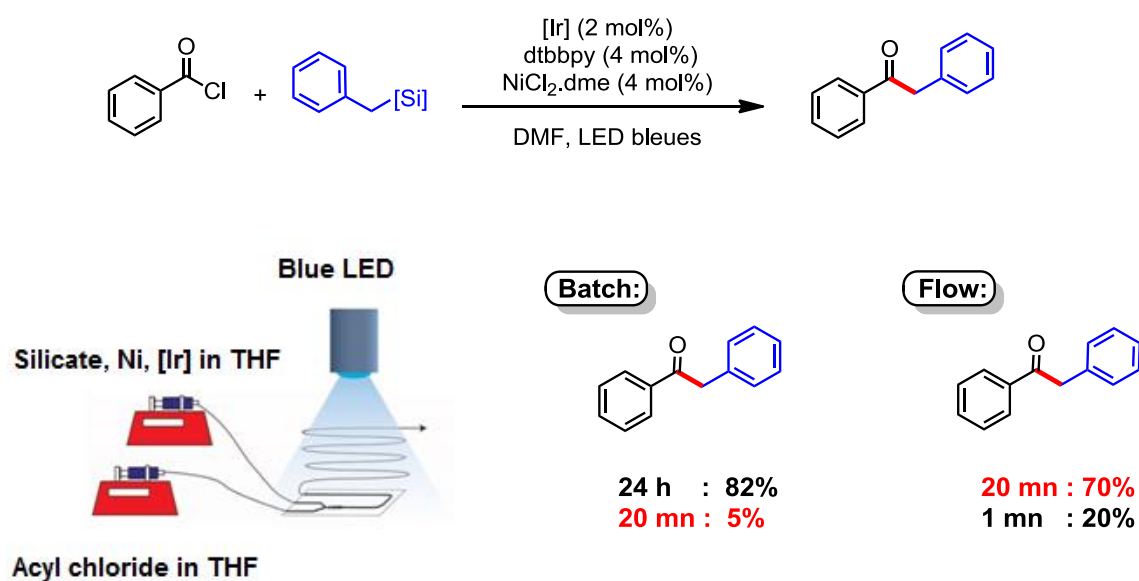


Schéma 14 : Apport de la chimie en flux continu à la catalyse duale

Nous avons ensuite fait varier le chlorure d'acyle afin de mieux appréhender ce couplage. Beaucoup ont fourni le produit attendu avec d'excellents rendements. En effet, que ce soit un chlorure d'acyle aromatique portant un groupement donneur ou bien un chlorure d'acyle alkyle, tous ont permis d'obtenir efficacement les cétones désirées (**Schéma 15**).

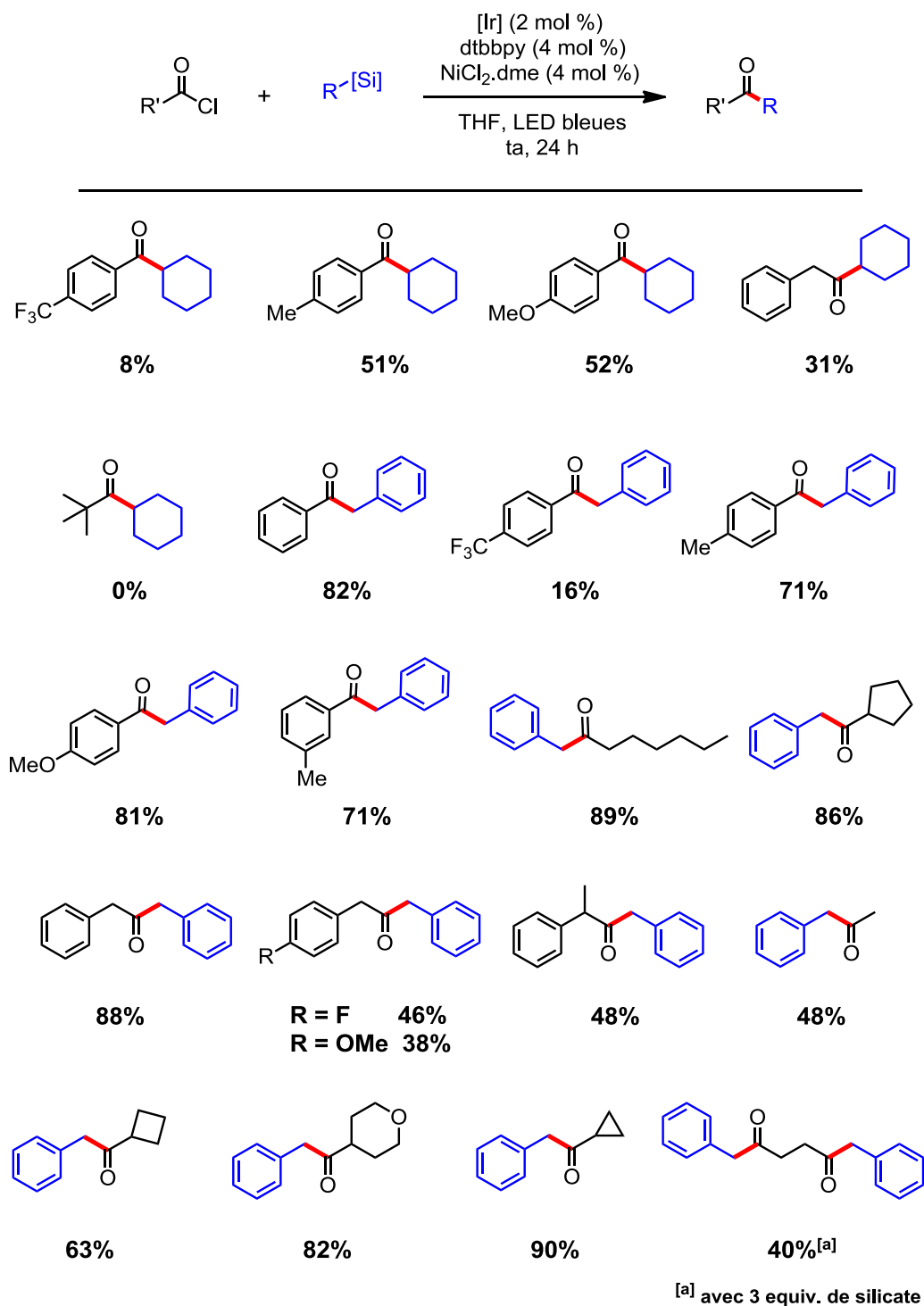


Schéma 15 : Variation du chlorure d'acyle pour la synthèse de cétones

Néanmoins, afin de réaliser cette réaction, deux catalyseurs métalliques sont nécessaires. Dans un contexte où la chimie verte est chaque jour un peu plus importante, cette approche peut poser question. Nous avons donc considéré une autre réaction afin de générer des cétones. Cette dernière s'appuie sur la carbonylation radicalaire. Bien qu'elle ait été déjà assez

étudiée en photoréduction,²² un seul papier avait pu être trouvé en photooxydation. Dans ce dernier, publié par le groupe de Xiao, une élégante méthode d'alkynylation d'acide carboxylique est reportée (**Schéma 16**).²³ Celle-ci est basée sur l'oxydation d'un carboxylate puis addition sur CO formant ainsi un radical acyle. Ce dernier réagit ensuite avec un dérivé d'ethynylbenziodoxolone (EBX). Enfin, une fragmentation permet de régénérer le photocatalyseur et de libérer le produit désiré.

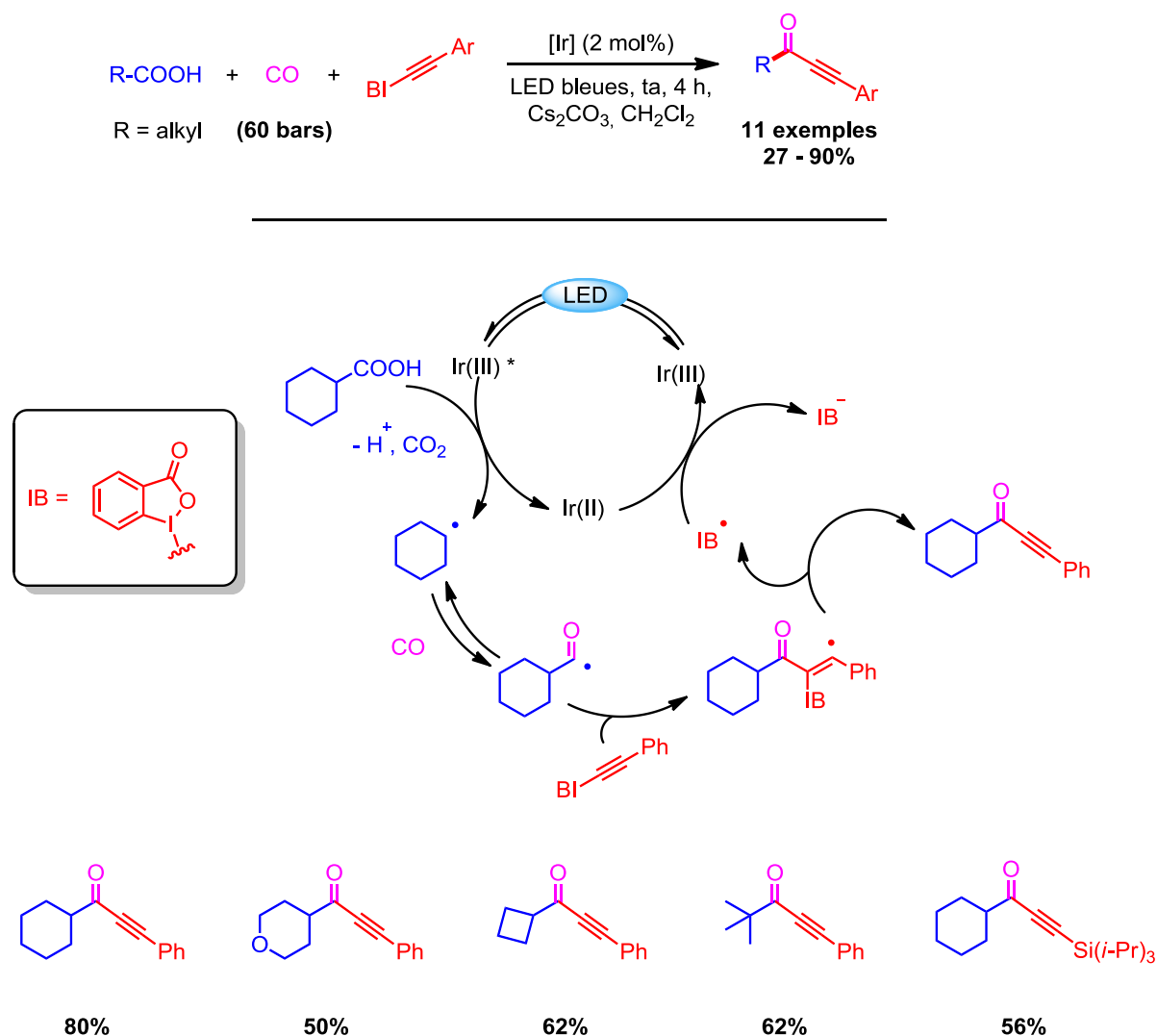
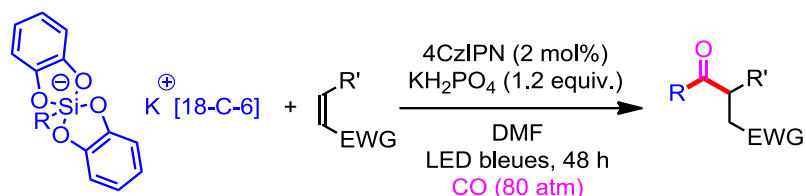


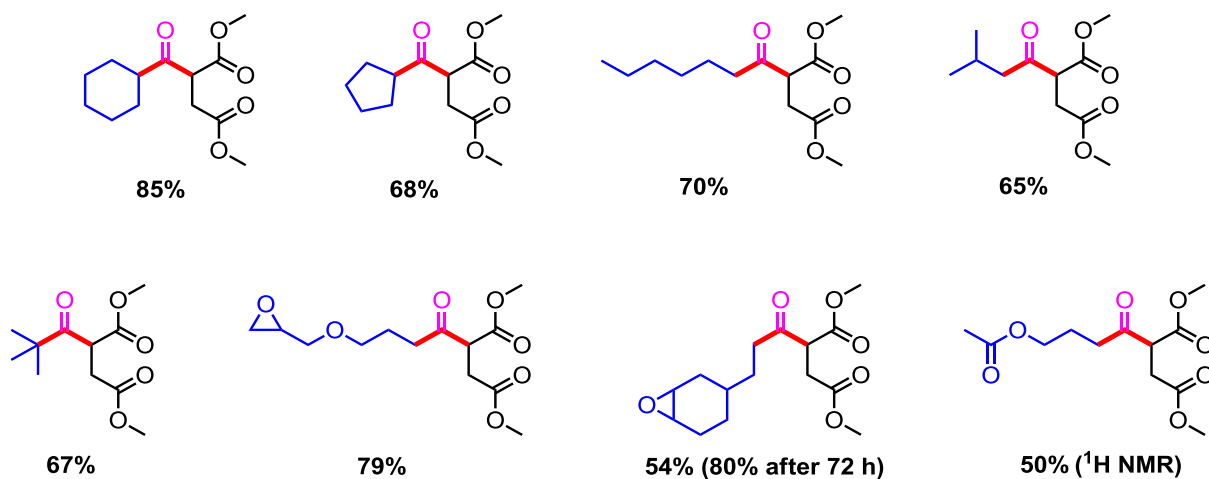
Schéma 16 : Réaction d'alkynylation de cétones

Devant ces résultats, nous nous sommes demandés si les silicates étaient eux aussi capables de réagir selon un processus de carbonylation radicalaire. Nous avons donc commencé notre étude en utilisant le cyclohexyle silicate avec le diméthyle maléate comme accepteur radicalaire. Le premier problème qui nous est apparu a été la compétition entre piégeage direct et carbonylation puis piégeage. Cependant, en modifiant les conditions réactionnelles et notamment en augmentant la pression de CO (80 bars), la formation du produit désiré a été favorisée. Il est aussi intéressant de noter que c'est le photocatalyseur organique 4CzIPN ($E_{1/2}(\text{PC}^*/\text{PC}^{\cdot-}) = +1.59 \text{ V vs. SCE}$)²⁴ qui nous a donné les meilleurs résultats. Nous avons

ensuite fait varier l'accepteur radicalaire ainsi que le silicate. La grande majorité des silicates a donné d'excellents résultats. En effet, que ce soit avec un silicate primaire, secondaire ou même tertiaire, le produit désiré était obtenu avec de très bons rendements. La même observation a été faite avec l'accepteur radicalaire. Les nitriles, cétones, esters, amides et autres groupements électro-attracteurs étaient très bien tolérés (**Schéma 17**).



Variation du silicate :



Variation de l'accepteur :

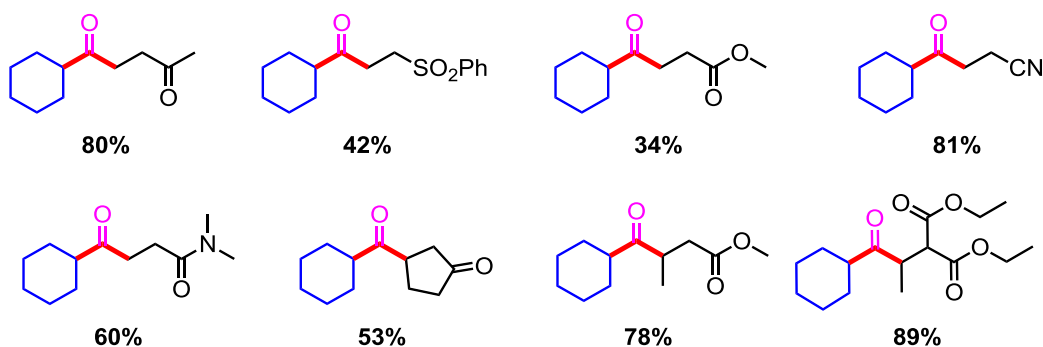


Schéma 17 : Utilisation des silicates en carbonylation radicalaire

Ensuite, nous avons étudié les réactions d'addition/élimination en utilisant, comme partenaires, les allylsulfones. De la même manière, celles-ci ont généré efficacement les produits attendus (**Schéma 18**).

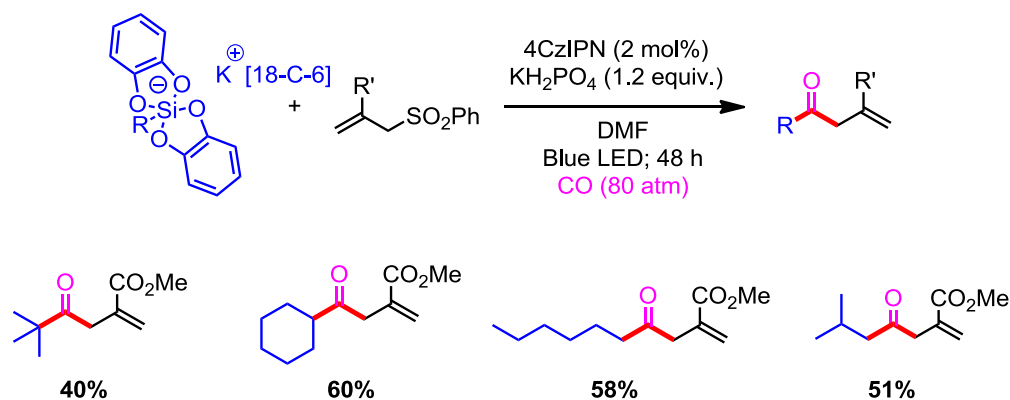


Schéma 18 : Carbonylation radicalaire et addition/élimination

Intrigués par le mécanisme de cette réaction, nous avons ensuite réalisé plusieurs expériences afin de savoir si un mécanisme en chaîne ou photocatalytique était à l'œuvre ici. Tout d'abord, une expérience "on-off" a été réalisée. Celle-ci a montré que la lumière est nécessaire à l'obtention du produit. En effet, lorsque l'on arrête l'irradiation, il semblerait que l'on stoppe aussi la réaction (**Schéma 19**).

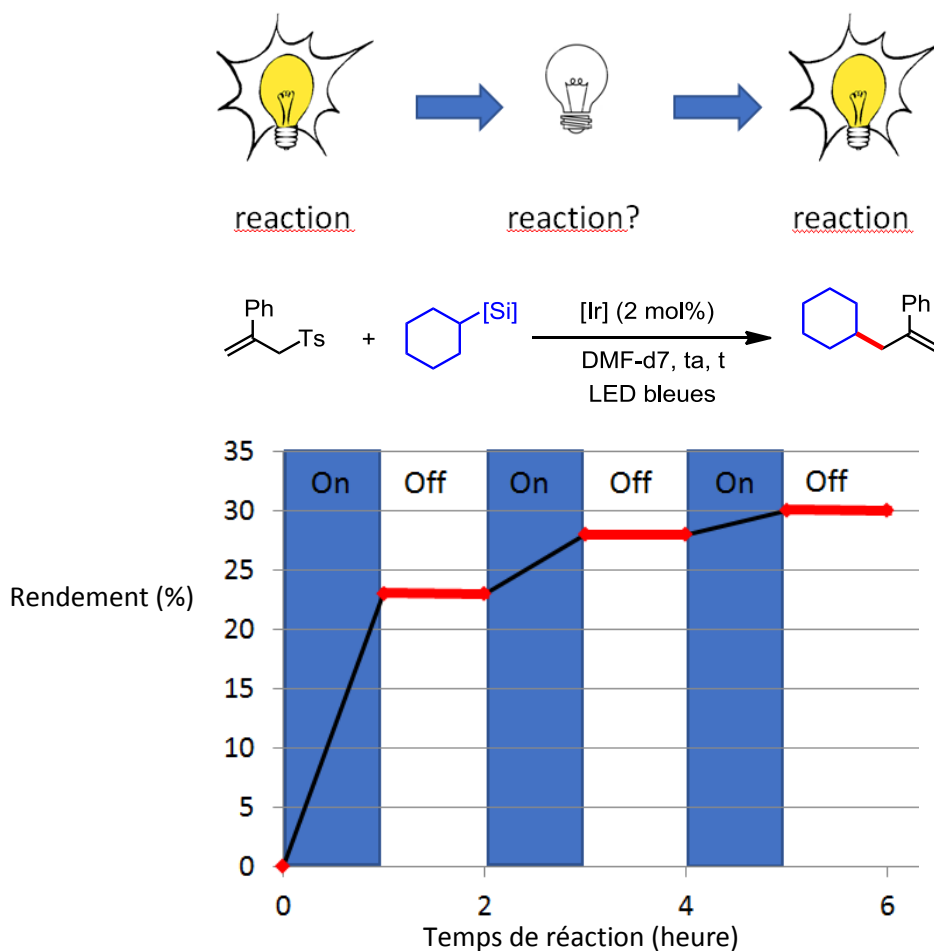


Schéma 19 : Expérience "on-off"

Ces données semblent aller dans le sens d'un processus photocatalytique. Cependant, si la chaîne étudiée est de petite taille, l'absence d'irradiation formerait aussi très rapidement un palier. Ainsi, une courbe similaire serait obtenue.²⁵ Nous avons donc complété cette expérience par la mesure des rendements quantiques de nos réactions. De très faibles valeurs ont été obtenues ce qui suggère également l'implication d'un mécanisme photocatalytique ($\phi < 1$) (**Schéma 20**).

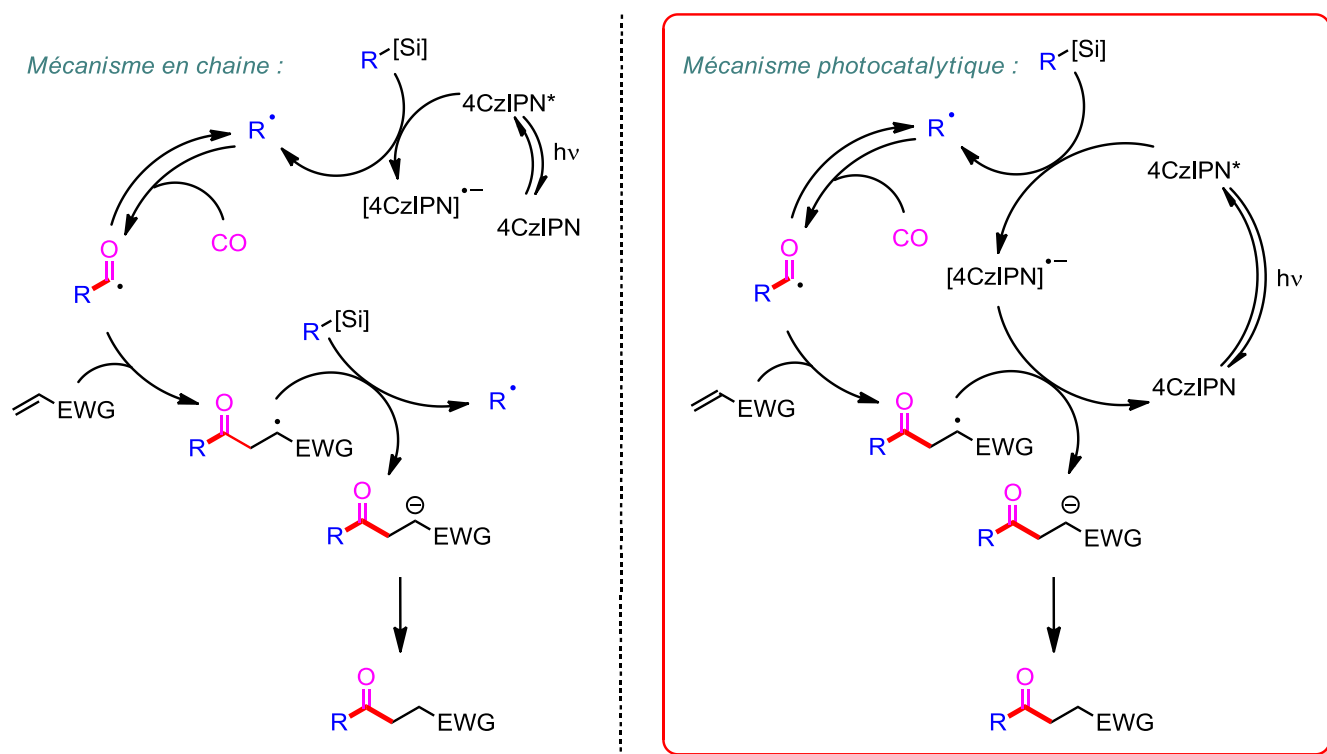
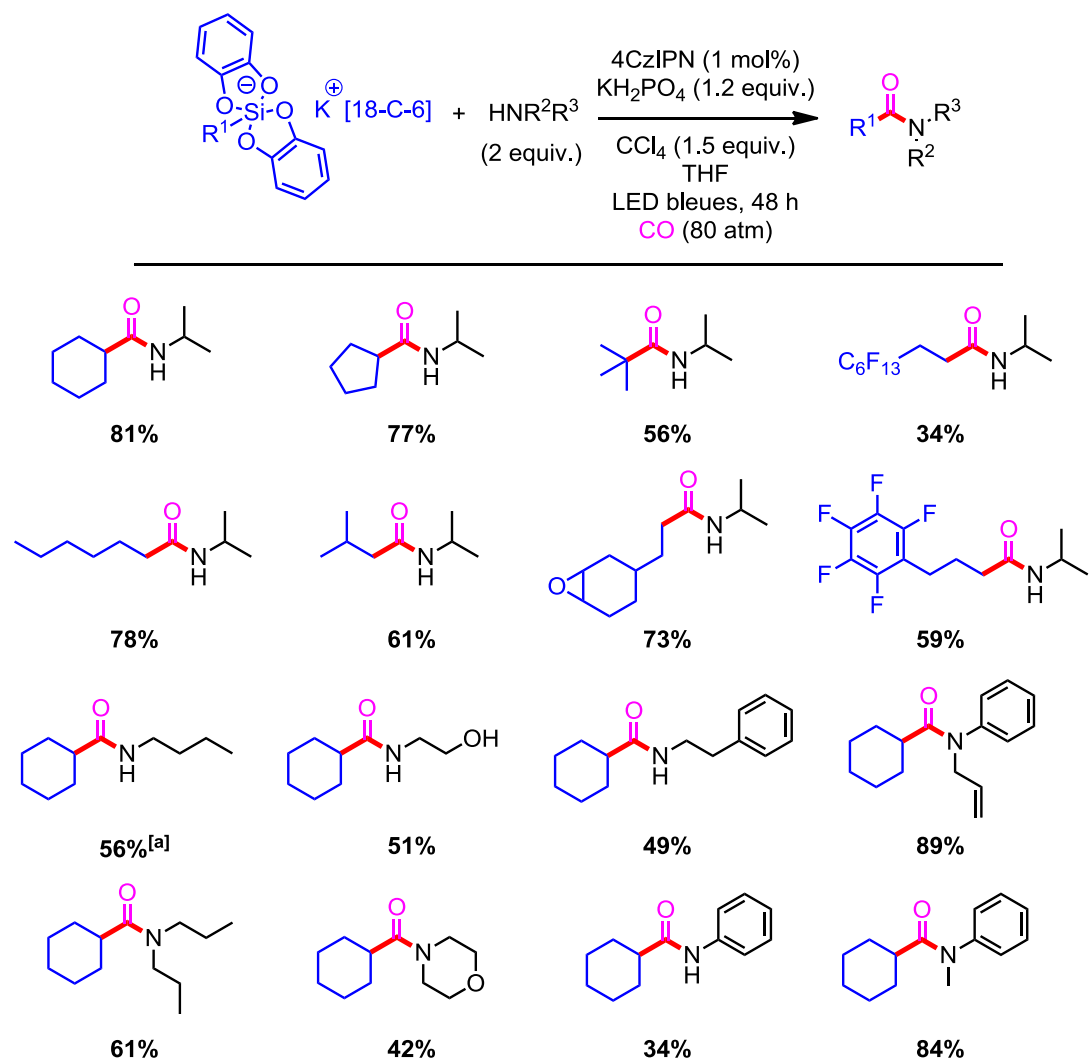


Schéma 20 : Mécanisme en chaîne (**non retenu-gauche**) et mécanisme photocatalytique (**retenu-droite**)

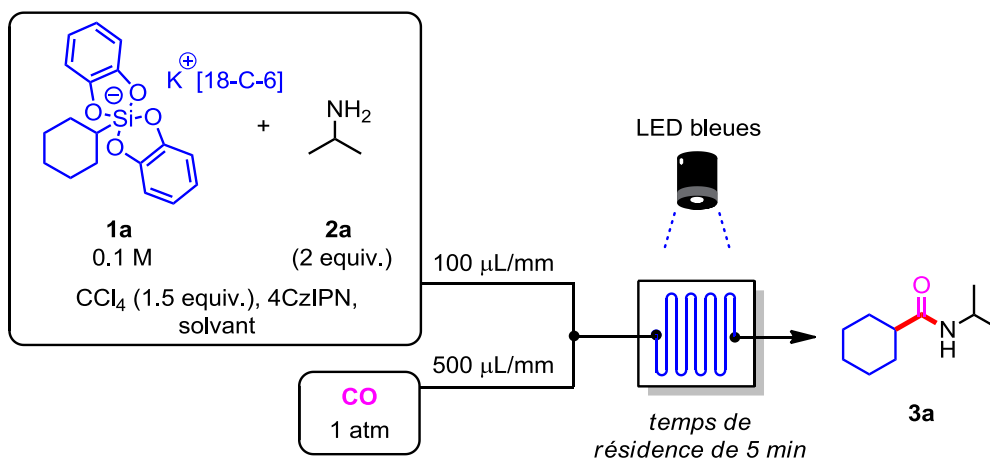
Nous avons ensuite décidé de pousser notre investigation plus loin. En effet, convaincus que le radical acyl pouvait être utilisé dans d'autres réactions, nous avons changé l'accepteur pour une amine et du tétrachlorométhane.²⁶ Grâce à cela, l'amide désiré a été obtenu très efficacement. De la même manière qu'avec l'addition directe, les silicates primaires, secondaires et tertiaires ont fourni le produit avec un bon rendement. La même observation a été faite après variation de l'amine. Toutes ces dernières nous ont permis d'isoler l'amide résultante avec des rendements allant de 34 à 89%. Plusieurs compétitions ont également été mises en œuvre. Une amine possédant un alcool potentiellement réactif a seulement mené à l'obtention de l'amide. Aucune trace de l'ester n'a été observée. Une compétition inter/intra a aussi été mise en place et, comme attendu, seul le produit de cyclisation intra a été isolé (**Schéma 21**).



[a] avec 5 equiv. de *n*-butylamine

Schéma 21 : Utilisation des silicates pour la synthèse d'amides

Même le principal problème de cette réaction, à savoir la haute pression de CO requise, a été résolu grâce à un passage en flux continu.²⁷ En effet, après optimisation des conditions opératoires, nous avons trouvé qu'un mélange 1:1 DCM:THP contenant 10 mol% de photocatalyseur ainsi que 2 équivalents d'amine et 1.5 équivalents de CCl₄ menait à la formation efficace du produit désiré en seulement 5 minutes (**Schéma 22**).



Conditions en flux continu:

THF, 4CzIPN 2 mol%, 43%
 THP:DCM 1:1, 4CzIPN 2 mol%, 50%
 THP:DCM 1:1, 4CzIPN 10 mol%, 70%

Conditions en batch: THP:DCM 1:1, 4CzIPN 10 mol%, 1 atm CO, 30 min, 0%

Schéma 22 : Apport de la chimie en flux continu à la carbonylation radicalaire

Nous avons également étudié la photoréduction de composés hypervalents du silicium. En effet, la génération de radicaux à partir de molécules organosilylées a toujours été effectuée dans des conditions photooxydantes mais rien n'avait alors été reporté en photoréduction.²⁸ Nous avons donc décidé de nous intéresser à cette pièce manquante à travers l'étude des chlorosilanes. Le phényle chlorosilane, possédant des ligands thiopyridines, s'est avéré réagir dans des conditions photoréductrices avec l'accepteur et donner le produit d'addition d'un de ses ligands sur ce dernier. Après optimisation de la réaction, un rendement de 78% a été obtenu (**Schéma 23**).

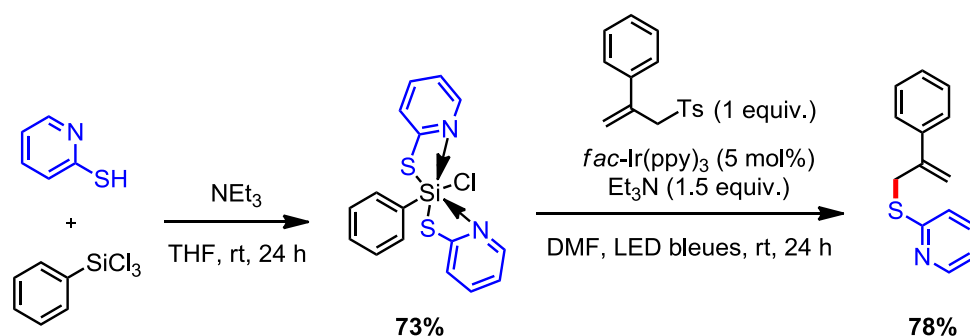


Schéma 23 : Synthèse et utilisation en photoréduction du chlorosilane d'intérêt

Nous avons ensuite confirmé que ce produit était bel et bien le résultat d'un processus radicalaire. Les analogues méthylés et benzylés ont aussi été étudiés. Néanmoins, ils n'ont fourni le produit qu'en plus faibles quantités. Il est important de noter que nous n'avons pas observé le produit résultant de l'addition d'un radical phényle, méthyle ou bien benzyle sur l'allylsulfone. Intéressés par ce phénomène, plusieurs calculs DFT ont été réalisés par E. Derat. Il s'est avéré qu'après réduction, la liaison la plus faible est la liaison Si-S (**Schéma 24, gauche**). Ceci explique pourquoi nous avons formé un radical thiopyridyle. Cependant, même si ce dernier s'additionne sur l'alcène, l'intermédiaire alors obtenu peut soit éliminer le tosylo, soit la 2-thiopyridine. Les calculs ont également pu répondre à cette question. En effet, ils ont mis en lumière l'existence d'une liaison faible résultante de l'interaction entre l'atome d'azote et l'hydrogène en position homo benzylique (**Schéma 24, droite**). Cette dernière permet d'expliquer pourquoi le tosylo est éliminé plus facilement que la 2-thiopyridine.

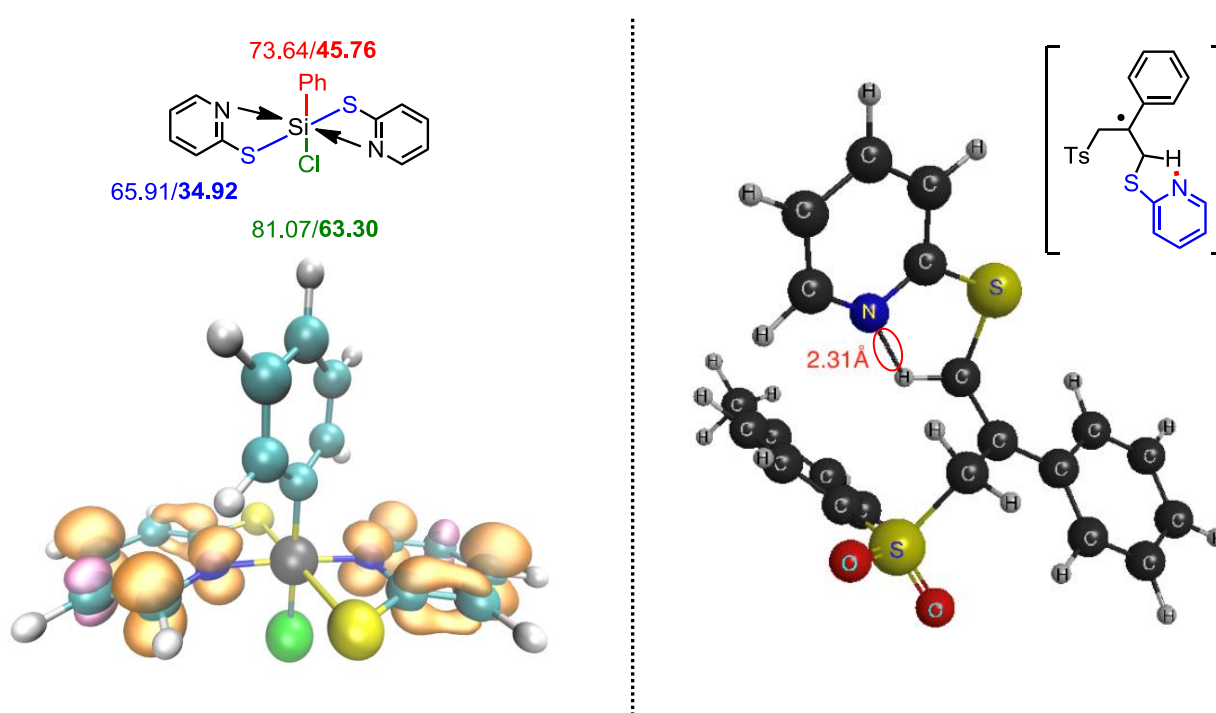


Schéma 24 : BDE avant et après réduction (**gauche**)
Intermédiaire expliquant la formation du produit désiré (**droite**)

Nous avons aussi étudié le devenir du sous-produit silylé et prédit une probable élimination du chlore menant à un silylène. Par ailleurs, la réduction du silylium a également été réalisée avec succès.

Au cours de ces trois années de doctorat, une étude sur l'utilisation de composés organosilylés en photoredox a été effectuée. Plusieurs avancées ont été réalisées en photooxydation avec les

silicates et en photoréduction avec les chlorosilanes. Après avoir généré pour la première fois des radicaux aryles avec notre système, plusieurs réactions ont été mises en oeuvre avec les silicates. Leur utilisation en catalyse duale ainsi qu'en carbonylation radicalaire a permis la formation de cétones et d'amides. Certaines de ces réactions ont aussi été transposées en flux continu ce qui peut être intéressant d'un point de vue industriel.

Des résultats préliminaires ont également montré que les silicates permettent la formation de radicaux méthyles ce qui ouvre de nouvelles perspectives en batch et en flux continu.

Références

- ¹ F. Paneth, W. Hofeditz, *Chem. Ber.* **1929**, *62*, 1335.
- ² D. H. Hey, W. A. Walters, *Chem. Rev.* **1937**, *21*, 169.
- ³ Herbert C. Brown, M. S. Kharasch, T. H. Chao, *J. Am. Chem. Soc.* **1940**, *62*, 3435.
- ⁴ P. T. Anastas, J. C. Warner in *Green Chemistry: Theory and Practice*, Oxford University Press, Oxford, **1988**.
- ⁵ D. M. Hedstrand, W. H. Kruizinga, R. M. Kellogg, *Tetrahedron Lett.* **1978**, *19*, 1255.
- ⁶ C. Pac, M. Ihama, M. Yasuda, Y. Miyauchi, H. Sakurai, *J. Am. Chem. Soc.* **1981**, *103*, 6495.
- ⁷ H. Cano-Yelo, A. Deronzier, *Tetrahedron Lett.* **1984**, *25*, 5517.
- ⁸ B. Michelet, C. Deldaele, S. Kajouj, C. Moucheron, G. Evano, *Org. Lett.* **2017**, *19*, 3576.
- ⁹ J. D. Nguyen, E. M. D'Amato, J. M. R. Narayanam, C. R. J. Stephenson, *Nature Chem.* **2012**, *4*, 854.
- ¹⁰ a) A. McNally, C. K. Prier, D. W. C. MacMillan, *Science* **2011**, *334*, 1114; b) Z. Zuo, D. W. C. MacMillan, *J. Am. Chem. Soc.* **2014**, *136*, 5257; c) A. Noble, D. W. C. MacMillan, *J. Am. Chem. Soc.* **2014**, *136*, 11602.
- ¹¹ Y. Yasu, T. Koike and M. Akita, *Adv. Synth. Catal.* **2012**, *354*, 3414.
- ¹² a) C. L. Frye, *J. Am. Chem. Soc.* **1964**, *86*, 3170; b) G. Cerveau, C. Chuit, R. J. P. Corriu, L. Gerbier, C. Reye, J. L. Aubagnac, B. El Amrani, *Int. J. Mass. Spectrom. Ion Phys.* **1988**, *82*, 259.
- ¹³ V. Corcé, L. M. Chamoreau, E. Derat, J. P. Goddard, C. Ollivier, L. Fensterbank, *Angew. Chem. Int. Ed.* **2015**, *54*, 11414.
- ¹⁴ a) H. H. Hodgson, *Chem. Rev.* **1947**, *40*, 251; b) F. Mo, G. Dong, Y. Zhang, J. Wang, *Org. Biomol. Chem.* **2013**, *11*, 1582; c) B. Olofsson, E. A. Merritt, *Angew. Chem. Int. Ed.* **2009**, *48*, 9052; d) F. Bellina, R. Rossi, *Tetrahedron* **2009**, *65*, 10269; e) E. A. Merritt, B. Olofsson, *Angew. Chem. Int. Ed.* **2009**, *48*, 9052; f) M. S. Yusubov, A. V. Maskaev, V. V. Zhdankin, *Arkivoc* **2011**, *1*, 370; g) V. V. Grushin, *Chem. Soc. Rev.* **2000**, *29*, 315.
- ¹⁵ S. Kubosaki, H. Takeuchi, Y. Iwata, Y. Tanaka, K. Osaka, M. Yamawaki, T. Morita, Y. Yoshimi, *J. Org. Chem.* **2020**, *85*, 5362.
- ¹⁶ D. Matsuoka, Y. Nishigaichi, *Chem. Lett.* **2015**, *44*, 163.
- ¹⁷ Z. Zuo, D. T. Ahneman, L. Chu, J. A. Terrett, A. G. Doyle, D. W. C. MacMillan, *Science* **2014**, *345*, 437.
- ¹⁸ J. C. Tellis, D. N. Primer, G. A. Molander, *Science* **2014**, *345*, 433.
- ¹⁹ a) Y. Yamashita, J. C. Tellis, G. A. Molander, *Prot. Natl. Acad. Sci. USA* **2015**, *112*, 12016; b) K. Matsui, G. A. Molander, *Org. Lett.* **2017**, *19*, 436.
- ²⁰ a) C. P. Johnston, R. T. Smith, S. Allmendinger, D. W. C. MacMillan, *Nature* **2016**, *536*, 322; b) C. Lévêque, V. Corcé, L. Chenneberg, C. Ollivier, L. Fensterbank, *Eur. J. Org. Chem.* **2017**, 2118.
- ²¹ D. Cambie, C. Bottecchia, N. J. W. Straathof, V. Hessel, T. Noël, *Chem. Rev.* **2016**, *116*, 10276.
- ²² a) L. Gu, C. Jin, L. Jiyan, *Green Chem.* **2015**, *17*, 3733; b) J. B. Peng, X. Qi, X. F. Wu, *ChemSusChem* **2016**, *9*, 2279; c) C. Gosset, S. Pellegrini, R. Jooris, T. Bousquet, L. Pelinski, *Adv. Synth. Catal.* **2018**, *360*, 3401.
- ²³ Q. Q. Zhou, W. Guo, W. Ding, X. Wu, X. Chen, L. Q. Lu, W. J. Xiao, *Angew. Chem. Int. Ed.* **2015**, *54*, 1196.
- ²⁴ a) H. Uoyama, K. Goushi, K. Shizu, H. Nomura and C. Adachi, *Nature* **2012**, *492*, 234; b) F. L. Vaillant, M. Garreau, S. Nicolai, G. Gryn'ova, C. Corminboeuf, J. Waser, *Chem. Sci.* **2018**, *9*, 5883.
- ²⁵ M. A. Cismesia, T. P. Yoon, *Chem. Sci.* **2015**, *6*, 5426.
- ²⁶ S. Sumino, A. Fusano, T. Fukuyama, I. Ryu, *Acc. Chem. Res.* **2014**, *47*, 1563.
- ²⁷ a) K. Mizuno, Y. Nishiyama, T. Ogaki, K. Terao, H. Ikeda, K. Kakiuchi, *J. Photochem. Photobiol. C. Photochem. Rev.* **2016**, *29*, 107; b) M. Oelgemöller, *Chem. Eng. Technol.* **2012**, *35*, 1144.
- ²⁸ a) M. Uygun, T. Danelzik, O. Garcia Mancheño, *Chem. Commun.* **2019**, *55*, 2980; N. Khatun, M. J. Sim, S. K. Woo, *Org. Lett.* **2018**, *20*, 6239; b) L. Capaldo, R. Riccardi, D. Ravelli, M. Fagnoni, *ACS Catal.* **2018**, *8*, 304.

**- Chapter I -
Photocatalysis and radical
precursors**

Chapter I. Photocatalysis and radical precursors

I.1. General introduction

I.1.1. Genesis of radical synthesis

Radicals are chemical intermediates which display one atom with an unpaired electron. The first observation of these species dates back to 1900, when Moses Gomberg managed to synthesize the triphenyl methyl radical. Even if the existence of free radicals was first quite questioned, the evidence later brought by Paneth,¹ Hey,² Karash³ as well as by the advent of EPR spectroscopy, eventually convinced the chemistry community. From that day on, a growing number of publications have been published on that topic.

Free radicals can be obtained by diverse methods that rely, for instance, on organic molecules like initiators and mediators or on metals. Nevertheless, their formation under such conditions remain quite questionable from the safety or sustainability point of view. Indeed, most of the initiators, such as azobisisobutyronitrile (AIBN), are explosives, and mediators, as exemplified by tin(IV) hydrides (e.g. $n\text{Bu}_3\text{Sn-H}$), are toxic. Moreover, the use of stoichiometric amount of metals to oxidize or reduce a species is definitely out of question nowadays (expensive, toxic wastes...). In this context, some chemists like Kellogg,⁴ Pac⁵ and Deronzier⁶ have developed new ways of generating radicals. Their idea lies on a *photocatalytic* generation of a free radical with a molecule called a “*photocatalyst*”. Nevertheless, even if this approach seemed quite interesting, chemists were reluctant to use it. Finally, it is only in the 21st century with the important work of MacMillan,⁷ Yoon⁸, Stephenson⁹ and Akita¹⁰ that photoredox catalysis experienced a rebirth (**Figure 1**).¹¹

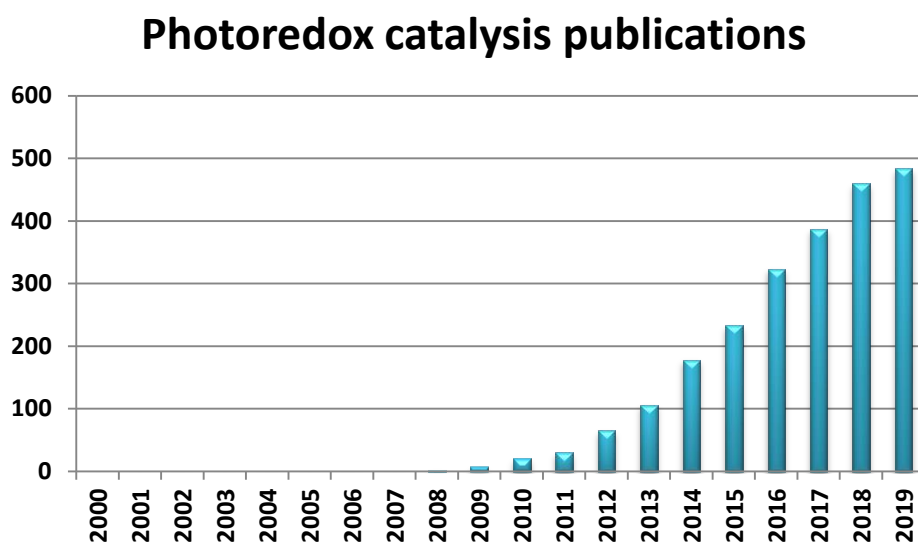


Figure 1: Photoredox catalysis publications

1.1.2. Principle of photocatalysis

In this part, the example of $\text{Ru}(\text{bpy})_3\text{Cl}_2$, the first man-made photocatalyst, synthesized by Burstall,¹² and used by Kellogg, Pac Deronzier and Lehn¹³ will help us to understand what photocatalysis is.

A *photocatalyst* is a molecule which has the capability to absorb light, bringing itself to a higher energy level. Subsequently, it can use this energy to induce a reaction. Photocatalysts can absorb light in different regions corresponding to different electronic transitions. For instance, the electronic absorption spectrum of $[\text{Ru}(\text{bpy})_3]\text{Cl}_2$ in EtOH, displayed in **Figure 2**, shows different bands. The first one is the LC (Ligand-Centered at 285nm), the second one is the MC (Metal-Centered at 322nm and 344nm) and the third one, and probably the most important one, is the MLCT (Metal-to-Ligand Charge Transfer at 240nm and 450nm). The MLCT is indeed very interesting because it usually has a band in the visible light region which is quite attractive for sustainability concerns. Importantly, some organic molecules can also have absorption properties and act as photocatalysts like Eosin Y or Fluorescein.

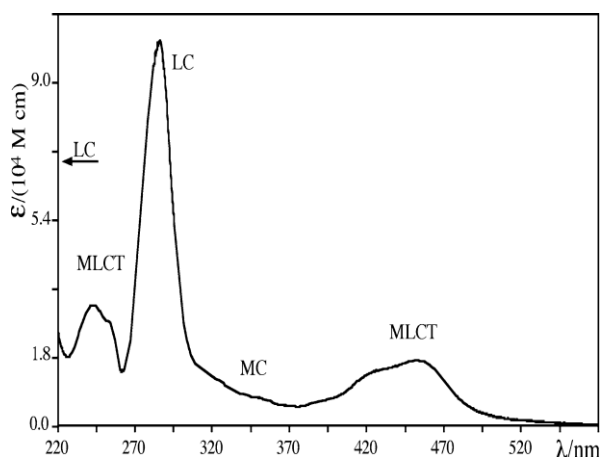


Figure 2: Electronic absorption spectrum of $[\text{Ru}(\text{bpy})_3]\text{Cl}_2$ in EtOH¹⁴

After having absorbed light, a photocatalyst has different options to go back to its ground state (S_0). They are well-explained in the following Jablonski diagram (**Figure 3**).

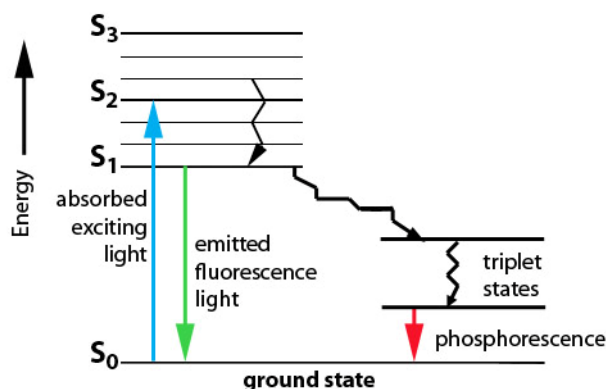


Figure 3: Jablonski diagram

Upon absorption of a photon and hence energy, the photocatalyst reaches an excited state. Then, from its singlet state, it can either emit light directly through fluorescence (radiative process), or go to a triplet state through an Inter-System-Crossing (ISC) event (non-radiative transition). Afterwards, it can release its energy *via* phosphorescence (radiative process). The photocatalyst can also go back to its ground state thanks to heat-releasing (non-radiative transition) or *via* energy or electron transfer. Indeed, when being at an excited state, its redox potentials totally change making SET possible in some cases (**Figure 4**).¹⁵ This is what is used in photoredox chemistry.

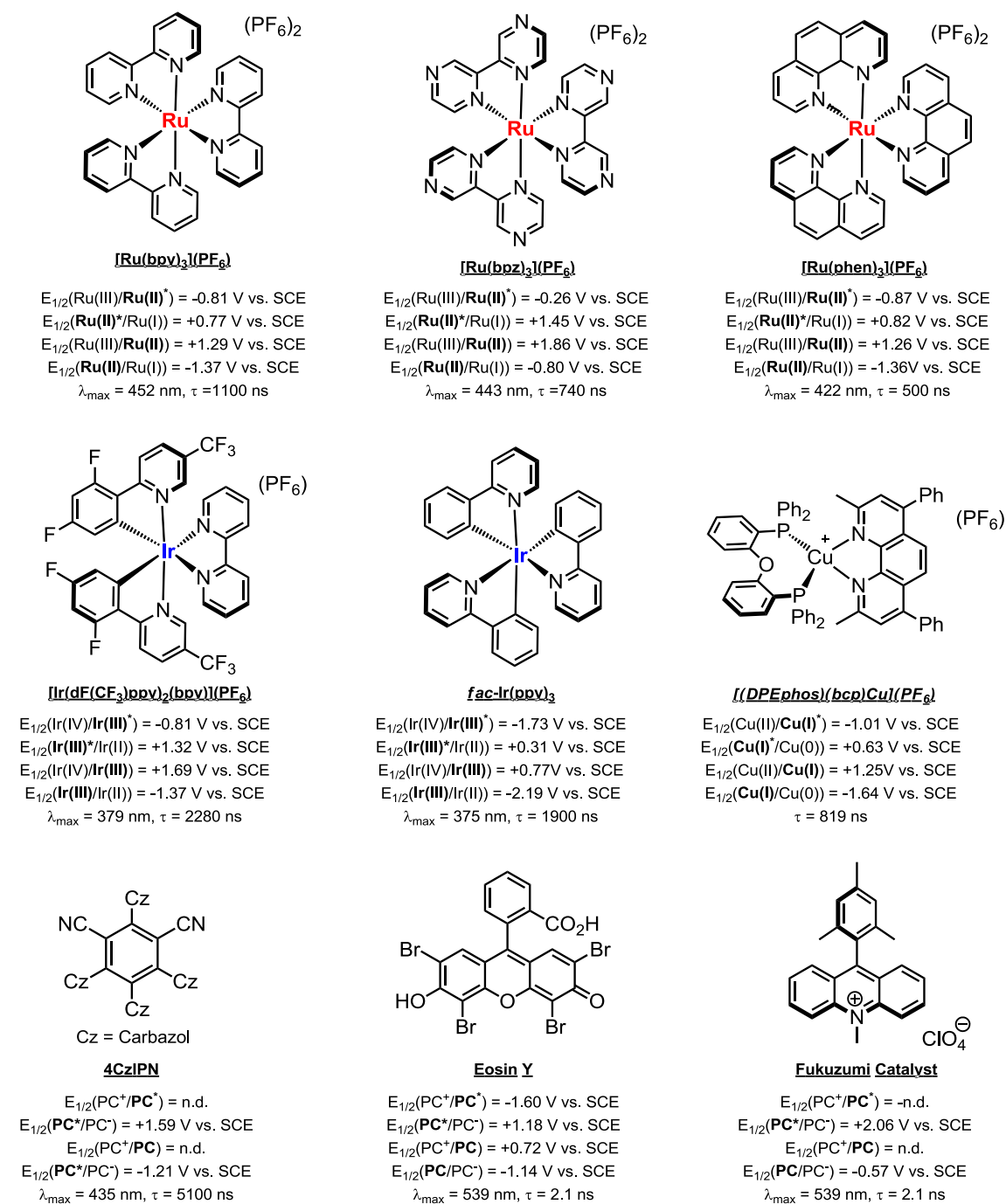
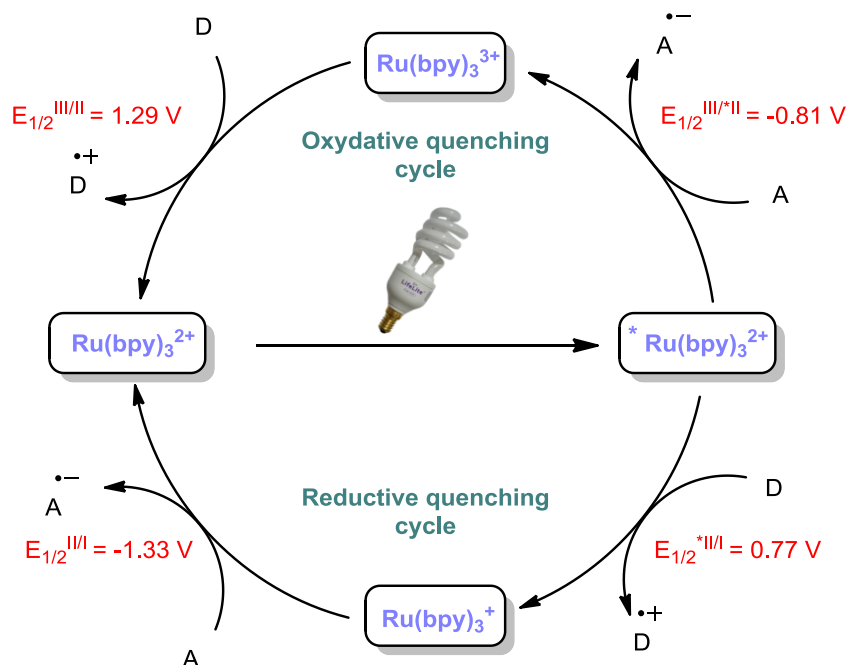


Figure 4: Example of photocatalysts

The example of $\text{Ru}(\text{bpy})_3^{2+}$ displayed by MacMillan's group can help to understand what happens (**Scheme 1**).¹⁶



Scheme 1: Reductive and oxidative quenching cycles

When the photocatalyst reaches an excited state, it can either enter an **oxidative quenching cycle** or a **reductive quenching cycle**, depending on the substrates and on the oxidation/reduction potentials:

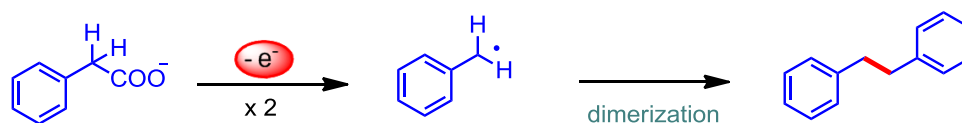
- If a molecule can be reduced in the reaction mixture, the photocatalyst will reduce it, then it will oxidize a donor to go back to its initial oxidation state.
- If a molecule can be oxidized in the reaction mixture, the photocatalyst will oxidize it, then it will reduce an acceptor to go back to its initial oxidation state.

Thus, two different families of radical precursors can be distinguished: those which can be oxidized by the excited photocatalyst to generate a radical and those which can be reduced. The photooxidative generation of radicals has been the main interest during this PhD thesis, thus, it will be developed in the following part. Nevertheless, some radical precursors, which are potent 1-electron oxidants such as diazonium salts,^{17,18} diaryl iodonium salts¹⁹ and aryl sulfonyl chlorides²⁰ for instance, are known to undergo oxidative quenching with the excited photocatalyst and can be mentioned.

1.1.3. Photooxidative generation of radicals

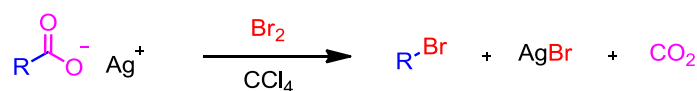
1.1.3.1 Photooxidation of the carboxylates

First, we can begin with the classical carboxylate anions. These compounds are really interesting radical precursors because of their outstanding simplicity. Moreover, most of them are usually abundant and inexpensive. The oxidation of the carboxylates ($+1.0\text{ V} < E_{1/2}^{\text{ox}} < +2.0\text{ V vs. SCE}$)²¹ has been known for quite a while now notably thanks to Kolbe electrolysis.²² In this reaction, the carboxylate is oxidized at the anode then, after decarboxylation and formation of a radical, a dimerization reaction occurs (**Scheme 2**).



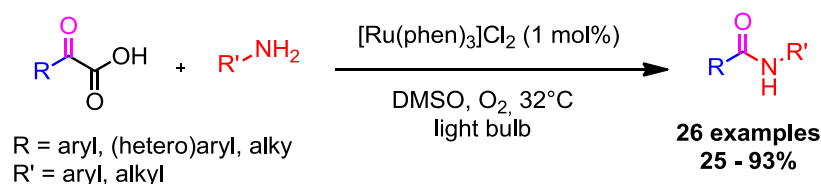
Scheme 2: Kolbe electrolysis

Following Kolbe's seminal contribution, another breakthrough was unveiled in 1939 by Hunsdiecker's group. The latter has indeed demonstrated that a carboxylic acid silver salt can efficiently undergo a radical halogenative decarboxylation to produce an organic halide (**Scheme 3**).²³



Scheme 3: Hunsdiecker reaction for organic halide synthesis

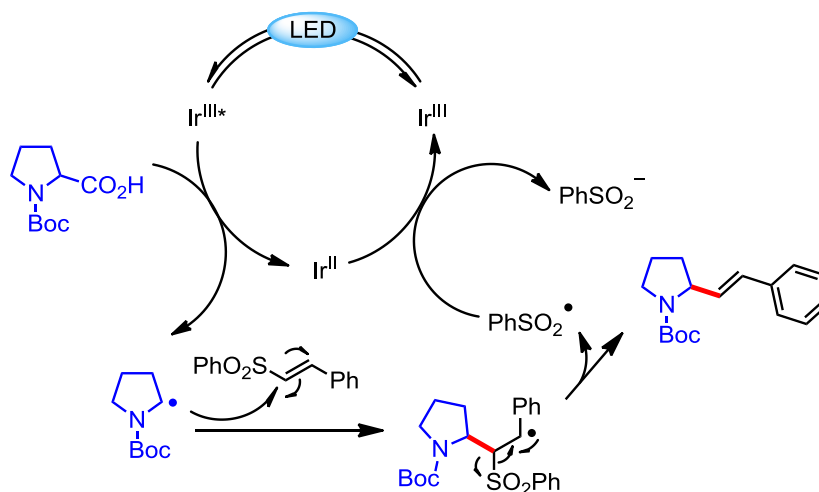
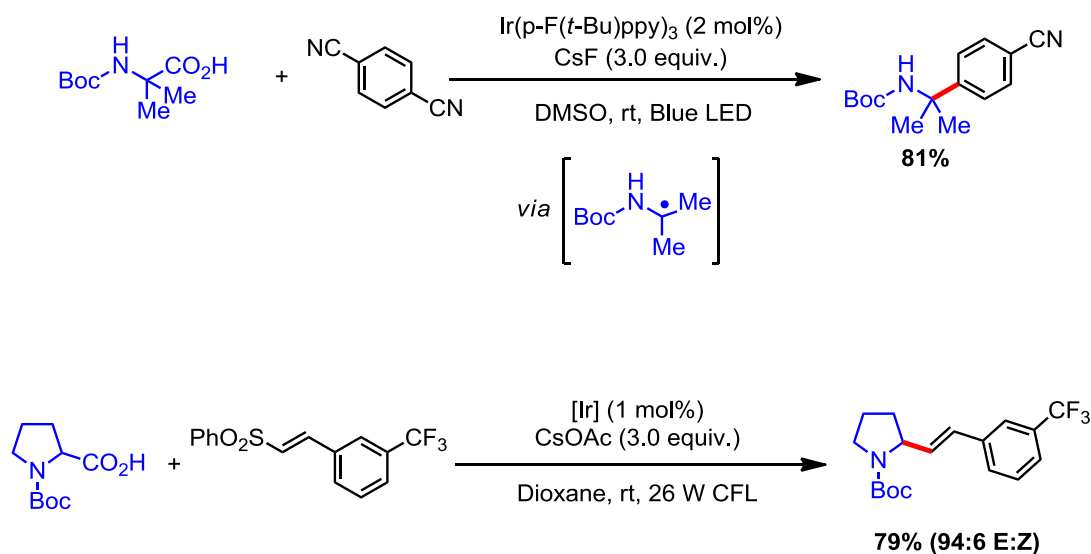
After that, different groups worked on the oxidation of carboxylate derivatives. Nevertheless, if we take for instance the example of α -keto acids ($E_{1/2}^{\text{ox}}(\text{PhCOCO}_2\text{K}) = +1.03\text{ V vs. SCE}$), most of the developed methods employ harsh conditions. Building on these previous reports, Lei's group came up in 2013 with the idea of using visible-light-induced decarboxylation.²⁴ By using such methodology, they managed to produce a large variety of amides in excellent yields and under mild conditions (**Scheme 4**).



Scheme 4: Amide synthesis thanks to visible-light-induced decarboxylative amidation of α -keto acid

Following this result, many groups have extended this concept to other substrates. Indeed, a few months after Lei's publication, α -amino carboxylates were also efficiently engaged in vinylation reactions²⁵ and in coupling reactions with dicyanobenzene²⁶ by MacMillan's group (**Scheme 5**).

For the vinylation reaction, they envisioned the following mechanism. The excited photocatalyst first oxidizes the carboxylate. Then, a decarboxylation occurs and the resulting radical is added onto the alkene. Finally, a fragmentation step extrudes the sulfonyl radical which is reduced to regenerate the photocatalyst.



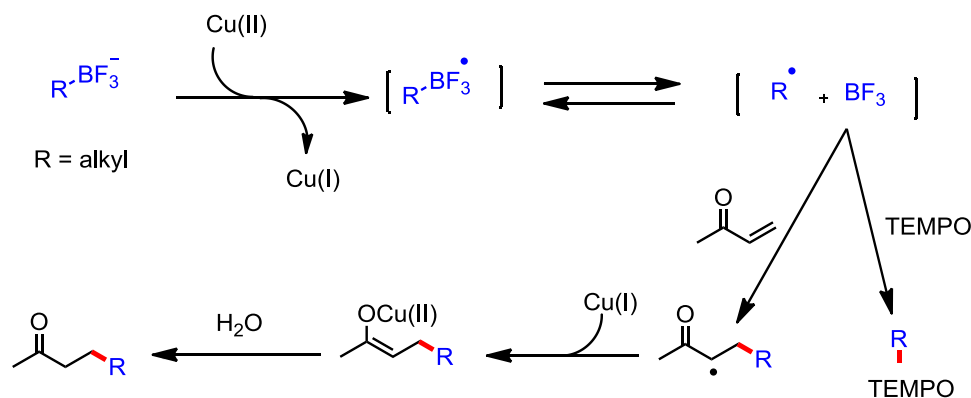
Scheme 5: Photooxidation of carboxylates

Afterwards, MacMillan's group and others have extended this conceptual framework to various interesting systems.²⁷ For instance, peptide macrocyclisation²⁸ and fluorination reactions²⁹ have been achieved.

Nevertheless, the carboxylates are not the only radical precursors that can be used under photooxidative conditions. The trifluoroborates, readily obtained by the treatment of a boronic acid with KHF_2 , are also very important ones.

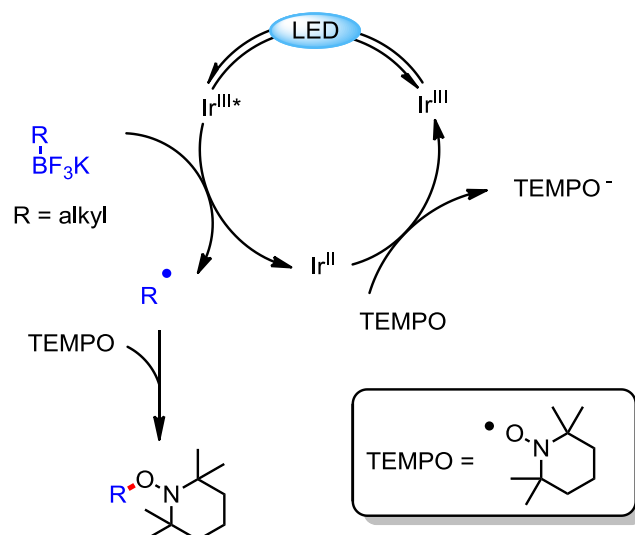
1.1.3.2. Photooxidation of the trifluoroborates

The first example of a radical generation from a trifluoroborate was reported by our group in 2010.³⁰ In this publication, a stoichiometric amount of CuCl_2 was used to oxidize the boron species and the resulting radical was trapped by TEMPO or methyl vinyl ketone (**Scheme 6**).



Scheme 6: Copper oxidation of trifluoroborates

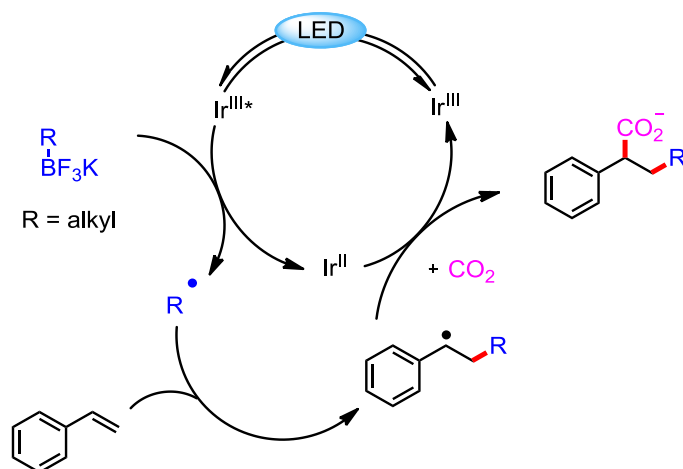
However, even if this result was of great interest, the stoichiometric amount of copper remained an issue which had to be overcome. Thus, two years later, Akita and co-workers solved this problem. They described the use of the highly oxidizing $[\text{Ir}(\text{dF}(\text{CF}_3)\text{ppy})_2(\text{bpy})](\text{PF}_6)$ photocatalyst (noted [Ir]; $E_{1/2}(\text{Ir(III)}^*/\text{Ir(II)}) = +1.32 \text{ V vs. SCE}$) to generate radicals from trifluoroborates.³¹ They also extended the concept to the cyclic organo-triol(borates) and successfully engaged them into spin trapping experiments and Giese-type additions (**Scheme 7**).



Scheme 7: Photocatalytic oxidation of trifluoroborates

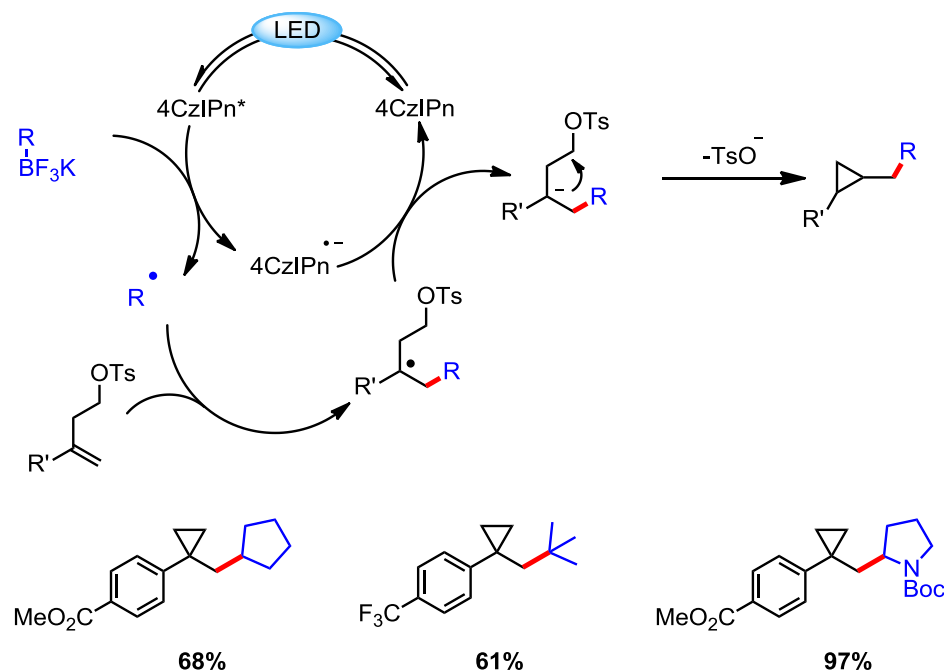
Similarly to the carboxylates, the trifluoroborates have then been engaged in various reactions which will not be developed here.³² Nevertheless, to broaden this idea, two very interesting applications of this radical precursor can be highlighted.

Firstly, radicals can also be trapped by gas (as it will be shown, as well, in chapter III).³³ For instance, in 2017, the Martin's group published a dicarbofunctionalization of styrene based on the trifluoroborates and CO₂.³⁴ They proposed that the radical, formed after oxidation, first reacts with the alkene. Then, a reduction occurs forming an anion and regenerating the photocatalyst. Finally the anion reacts with CO₂ to produce the desired product (**Scheme 8**). This mild and selective reaction also worked with other radical precursors like sulfinate salts and oxalates.



Scheme 8: Dicarbofunctionalization of styrene

Secondly, even if most of the time only radical processes are involved, sometimes, radical/polar crossover reactions, meaning a reaction featuring both radical and ionic modes of reactivity,³⁵ can be found.^{36,37} Indeed, in 2020 Molander's group disclosed successfully a cyclopropane synthesis based on this concept. They proposed the following mechanism for this reaction (**Scheme 9**).³⁸ After oxidation of the trifluoroborate by the excited photocatalyst, the produced radical is added onto the alkene. Then, this intermediate is reduced to an anion which reacts, afterwards, *via* a S_Ni to produce the desired cyclopropane.



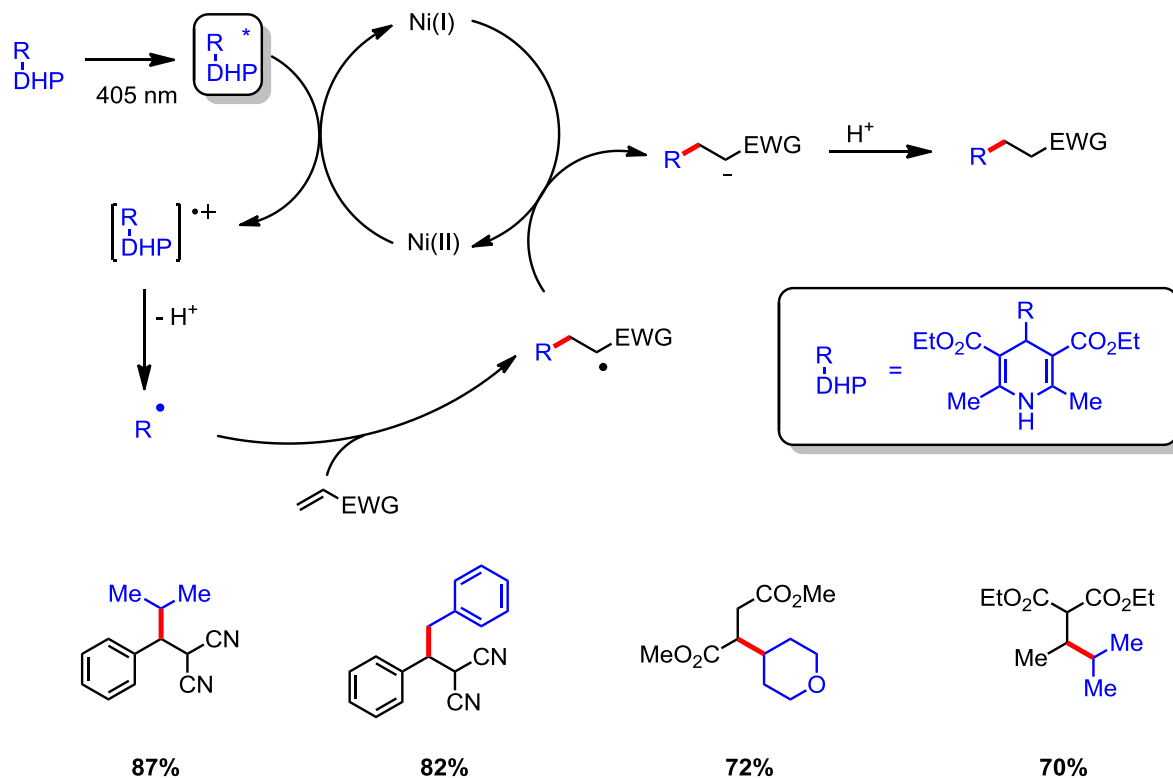
Scheme 9: Radical/polar crossover reaction for cyclopropane synthesis

Similarly to the dicarbofunctionalization reaction, this methodology is not the prerogative of trifluoroborate salts. Other radical precursors can be found in the literature to achieve this kind of reaction like the 4-alkyl-1,4 dihydropyridine also known as DHP.

1.1.3.3. Photooxidation of the DHPs

The DHPs, easily obtained *via* Hantzsch synthesis, are very interesting radical precursors. Indeed, even if they can be oxidized in a traditional way and react like carboxylates and trifluoroborates,³⁹ they can also be photoexcited as shown by Melchiorre *et al.*⁴⁰ In 2019, his group demonstrated that a nickel(II) catalyst ($Ni(bpy)_3(BF_4)_2$) could oxidize the excited DHP and trapped the resulting radical with an electro deficient alkene (**Scheme 10**). They proposed the following mechanism to explain the product formation. Under excitation at 405nm, the DHP goes to an excited state. Afterwards, it can be oxidized by the Ni(II) catalyst to form,

after fragmentation, an alkyl radical. This radical is then trapped by the alkene. Finally, the resulting intermediate is reduced to regenerate the photocatalyst. This approach tolerated a broad substrate scope and was used, later, in many different reactions.⁴¹



Scheme 10: DHPs as efficient photosensitive radical precursors

It is worth mentioning that other radical precursors such as sodium sulfonates can also be used to generate a radical after oxidation by an appropriate photocatalyst.⁴²

After this brief introduction about different radical precursors that can be used under photooxidative conditions, we can focus on the main interest of this PhD thesis: silicon derivatives.

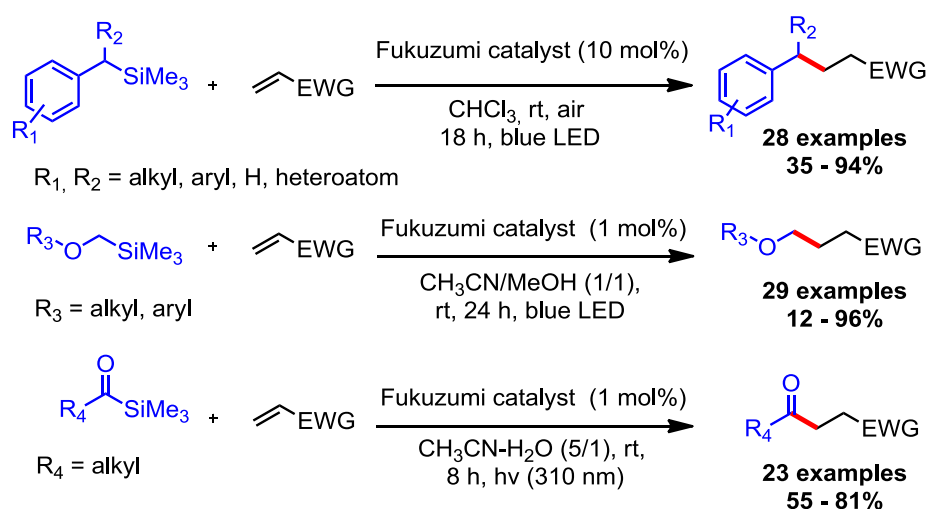
1.1.3.4. Photooxidation of silicon derivatives

Silicon is the second most abundant element in the earth's crust (27.7% approximately by weight) and different radical precursors are based on this element.

a) Photooxidation of trimethylsilane derivatives

The oxidation potentials of common silanes are usually quite high ($E^{\text{ox}} > +2 \text{ V vs. SCE}$). Nevertheless, with some activated ones, the oxidation remains possible. For instance, by using

benzyltrimethylsilane derivatives ($E^{\text{ox}} = +1.68 \text{ V vs. SCE}^{43}$) and the very strong oxidant at an excited state 9-mesityl-10-methylacridinium salt (Fukuzumi's catalyst; $E_{1/2}(\text{PC}^*/\text{PC}^{\bullet-}) = +2.06 \text{ V vs. SCE}$), Garcia Mancheño's group succeeded in generating a benzyl radical and trapping it with an electro deficient alkene.⁴⁴ In the same vein, α -alkoxymethyl radicals were efficiently generated thanks to their corresponding trimethylsilyl adduct and trapped by an acceptor.⁴⁵ Acyl silanes also afforded acyl radicals which could be quite interesting from a synthetic point of view (**Scheme 11**).⁴⁶ In this publication, they also showed that TBADT ($E_{1/2}(\text{PC}^*/\text{PC}^{\bullet-}) = +2.44 \text{ V vs. SCE}^{47}$), tetrabutylammonium decatungstate, was an efficient photocatalyst to perform this reaction.



Scheme 11: Photogeneration of radicals thanks to silane derivatives

Nevertheless, the most popular silicon-based compound for radical generation remains the bis-catecholato silicates, which, in a sense, can be seen as the silicon counterpart of the aforementioned trifluoroborate salts.

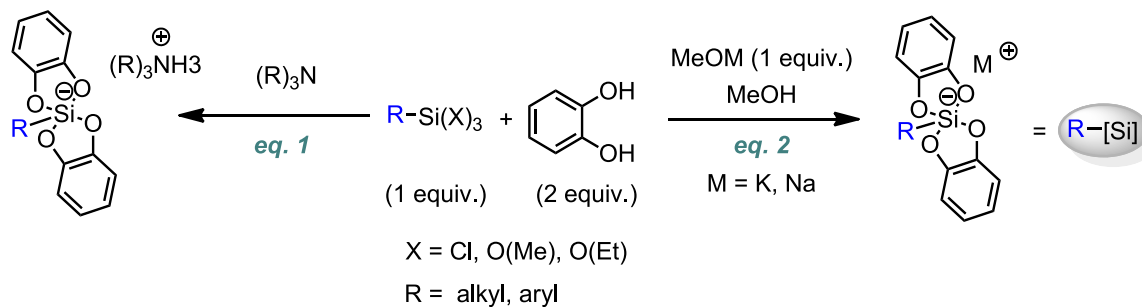
b) Photooxidation of the alkyl bis-catecholato silicates

According to the IUPAC nomenclature, a silicon atom surrounded by four oxygen atoms is called a silicate. Its general structure can be noted $(\text{RO})_a\text{Si}(\text{B})_b(\text{C})_c(\text{D})_d$ where $a+b+c+d = 4$.⁴⁸ Nevertheless, silicon derivatives can reach penta- and hexavalency. Thus, to extend this definition, we can say that if an hypervalent silicon complex bears four oxygen ligands it will also be called a silicate.

b.1) Silicates synthesis

Bis-catecholato silicates, called silicates in this PhD thesis and noted $\text{R}[\text{Si}]$ where R is an alkyl or an aryl group, were synthesized for the first time by Frye in 1964.⁴⁹ He noticed that the treatment of an alkyl trialkoxysilane solution with catechol and amine was leading to nice

crystals corresponding to the ammonium alkyl bis-catecholato silicate (*eq. 1, Scheme 12*). Pyridine and quaternary ammonium hydroxide could also be used as bases in this reaction. About 20 years later, Corriu's group completed this work by using a methanolic solution of sodium or potassium methoxide instead of an amine.⁵⁰ Thanks to this modification, he obtained the potassium or the sodium salt of the silicates (*eq. 2, Scheme 12*). It should be noted that trialkoxysilanes and trichlorosilanes can be accessed for instance, *via* Benkeser's⁵¹ or Rochow's⁵² processes or hydrosilylation reactions.⁵³

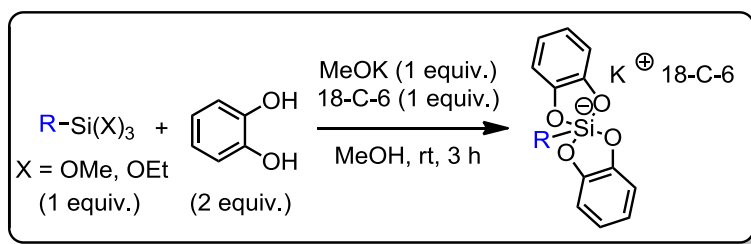


Scheme 12: General procedures for silicates synthesis

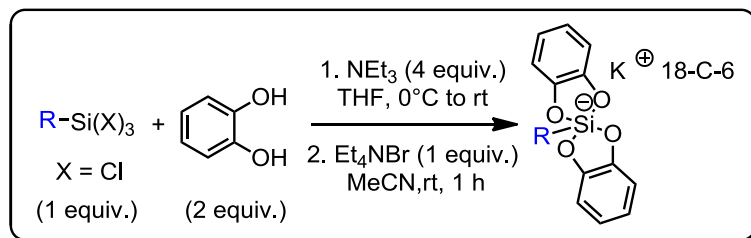
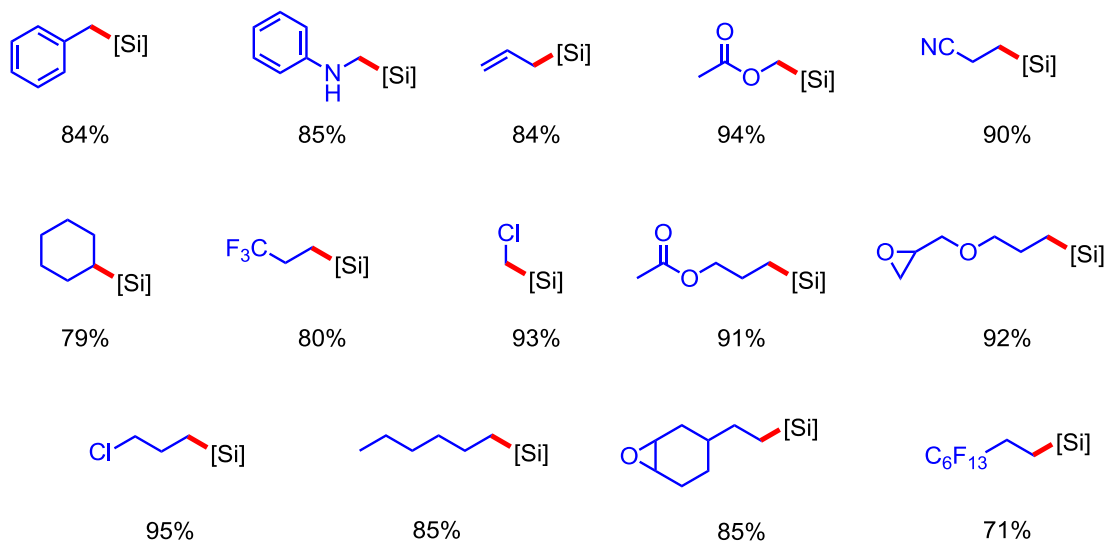
In 2015, our laboratory decided to investigate the behavior of these hypervalent silicon complexes under photooxidative conditions. The first issue encountered was the degradation of the silicates over time. However, we found that this problem could be solved by addition of [18-C-6] crown ether in the reaction mixture, which increases the charge separation and limits the introduction of water in the solid.

The standard procedure consists in dissolving catechol (2 equiv.) and 18-C-6 (1 equiv.) in dry methanol (0.1 M). Then we add the trialkoxy organosilane (1 equiv.) and the solution of potassium methoxide in methanol (1 equiv.). The reaction mixture is stirred for 3 hours. Finally, a crystallization (solvent: acetone/Et₂O) provides the pure product (yields > 70%).

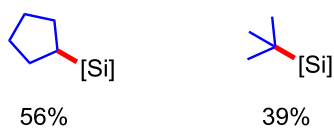
With this procedure in hand, many silicates were synthesized and stored on the bench for months (**Scheme 13**).⁵⁴



With K^+ , 18-C-6 as the counter cation



With $^+NEt_4$ as the counter cation



Scheme 13: Silicates synthesis

b.2) Crystalline form

Furthermore, because silicates are crystalline compounds, they can be analyzed by XRD. This method provides interesting information about their structure in the solid state. Surprisingly,

this analysis revealed that, depending on the base used during the synthesis, different forms could be obtained. While the silicate displays distorted square pyramidal molecular geometry when potassium methoxide is used, distorted trigonal bipyramidal structures are reached when the counter cation is an ammonium (thus when the base employed is an amine) (**Figure 5** and **Table 1**).

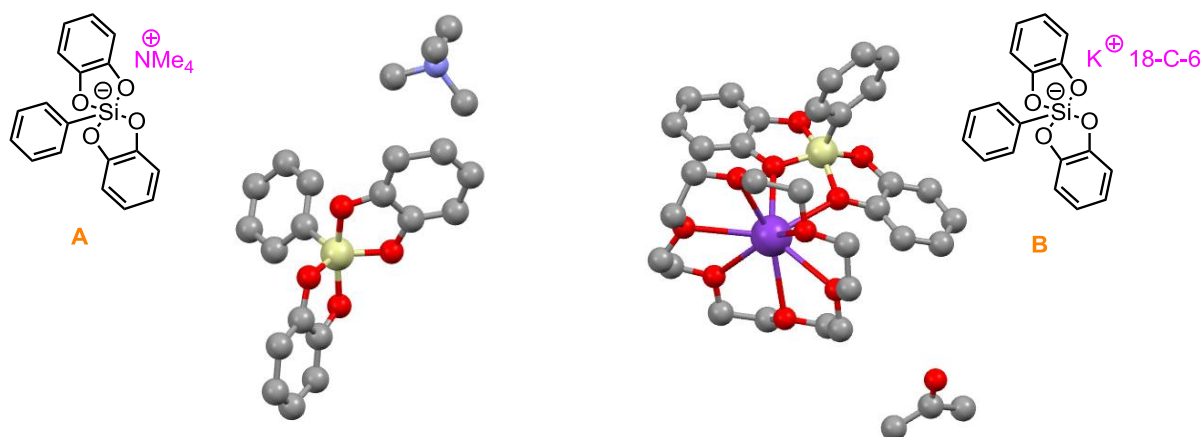


Figure 5: Crystal structure of phenyl bis-catecholato-silicate with $^+\text{NMe}_4$ (A, left)⁵⁵ and K^+ [18-Crown-6] crown ether acetone (B, right). Hydrogen atoms are omitted for clarity

The diagram illustrates the transition from structure A to structure B. A blue arrow points from left to right, with vertical lines marking the positions of structure A and structure B. A central inset shows a silicon atom (Si) coordinated to a carbon atom (C) and four oxygen atoms (O₁, O₂, O₃, O₄), with a metal cation (M⁺) coordinated to O₁ and O₄.

Silicate	$d_{\text{C-[Si]}}$ (Å)	$D_{\text{O-[Si]}}$ (Å)	$\alpha_{\text{(C-[Si]-O)}}$ (°)	$\alpha_{\text{(O-[Si]-O)}}$ (°)
With $^+\text{NMe}_4$	1.888(11)	1.700(9)	O ₁ : 116.00(5)	O ₁ -O ₃ : 127.90(4)
		1.794(5)	O ₂ : 96.10(7)	O ₂ -O ₄ : 167.70(4)
		1.701(9)	O ₃ : 116.00(5)	
		1.794(5)	O ₄ : 96.10(7)	
With K^+ [18-Crown-6]	1.869(2)	1.7631(16)	O ₁ : 102.09(9)	O ₁ -O ₃ : 154.37(9)
		1.7221(16)	O ₂ : 105.77(9)	O ₂ -O ₄ : 148.95(9)
		1.7491(16)	O ₃ : 103.52(9)	
		1.7496(16)	O ₄ : 105.27(9)	

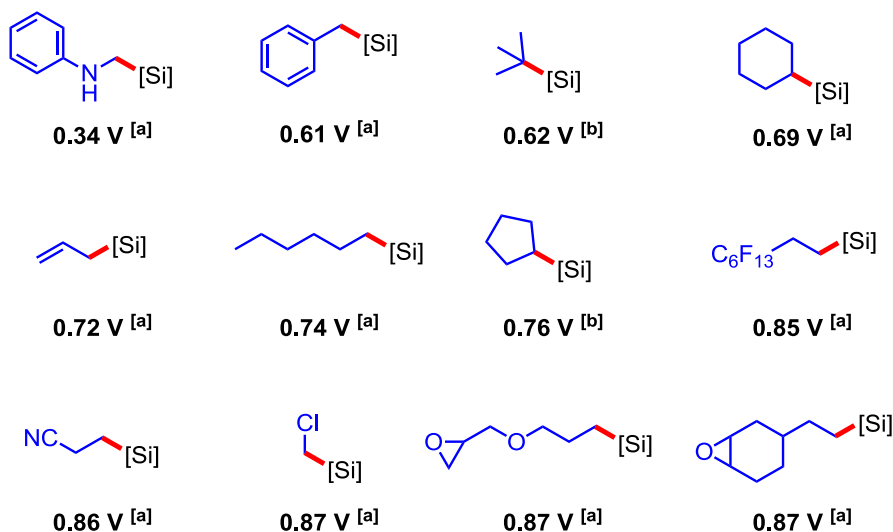
Table 1: Crystallographic data around the silicon atom for phenyl silicates

It is worth mentioning that some work is currently ongoing in our laboratory to understand if the salt modification has an impact on the yields of different photocatalytic reactions.

b.3) Redox properties

As photocatalysis generally involves SET events, the determination of the substrates redox potentials has become pivotal to design new reactions. Indeed, this information hints at whether a photocatalyst would be capable of oxidizing or reducing these molecules. Hence, the half-wave oxidation potentials of the silicates, disclosed in **Scheme 13**, were measured by cyclic voltammetry in DMF, a common solvent in photoredox chemistry (**Scheme 14**). It appeared that all of them have a half-wave oxidation potential below 1 V *vs.* SCE. For activated ones, potentials down to less than 0.5 V *vs.* SCE could even be measured. This is really interesting considering that other radical precursors, such as the carboxylates,²¹ usually have an oxidation potential above 1 V *vs.* SCE. Thus, even if these potentials are only thermodynamic parameters and not kinetic ones, it should be easy to oxidize a silicate.

Regarding the oxidation of silicates, DFT calculations suggest that it occurs on the catechols, where the highest HOMO coefficients are located. An additional information was given by Nishigaichi's group.⁵⁶ Indeed, they reported that the solvent had a great influence on the redox potential, presumably because of its possible coordination onto the silicon, generating an hexavalent silicon derivative. For instance, the allyl silicate has a peak potential of $E^{\text{ox}} = + 1.08$ V in MeCN when using DMF as a donor whereas, with *n*-butylamine, $E^{\text{ox}} = + 0.79$ V. Thus, modulation of the oxidation potential might be possible by changing the catechol moiety (different HOMO levels) and by varying the solvent.



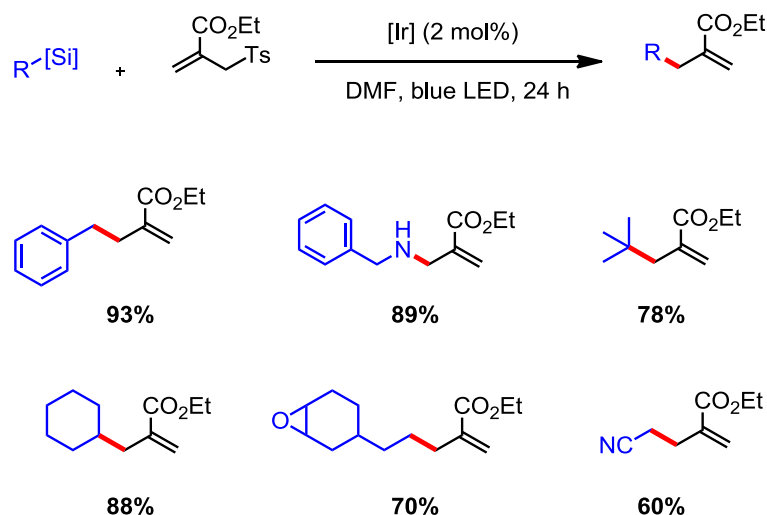
[a] K^+ , 18-C-6 as the counter cation

[b] $^+\text{NEt}_4$ as the counter cation

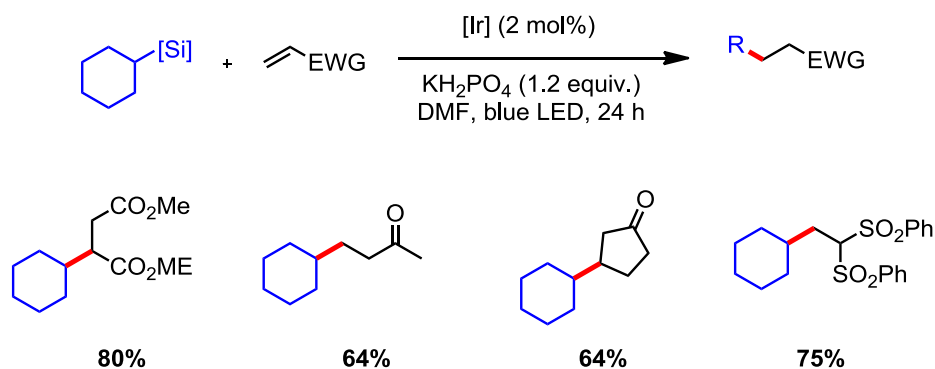
Scheme 14: Half-wave oxidation potentials of different silicates in DMF at rt (V *vs.* SCE)

b.4) Silicates reactivity: photooxidation

Inspired by the work of Kumada about the oxidation of pentafluorosilicates⁵⁷ and encouraged by the previous results, silicates photooxidation has been experienced.⁵⁴ [Ir{dFCF₃ppy}₂(bpy)]PF₆ (noted [Ir]) was found to be a very good photocatalyst for allylation (**Scheme 15**) and intermolecular reactions (**Scheme 16**). Indeed, nearly all of the tested silicates afforded the desired products in very high yields. Moreover, these reactions were found to be tolerant to many functionalities including sensitive ones such as epoxides.



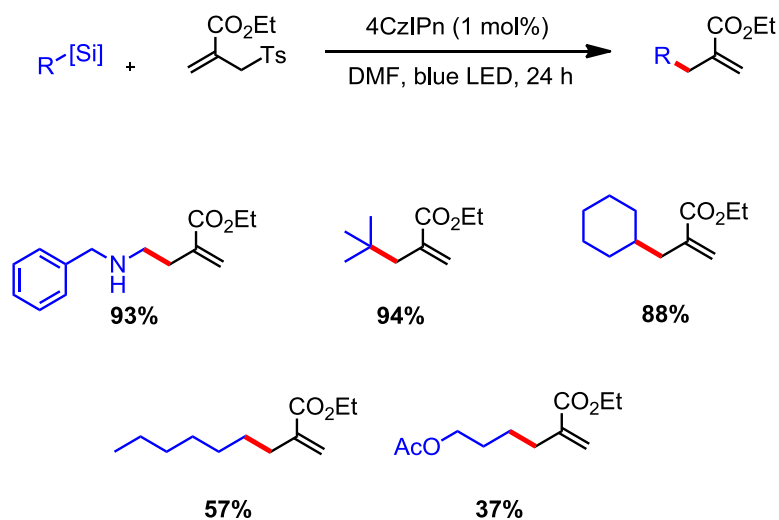
Scheme 15: Allylation reaction of various silicates



Scheme 16: Intermolecular reaction of various silicates

Nevertheless, the iridium photocatalyst used above is quite expensive. Thus, alternatives had to be searched. In 2016, the cheap and easily synthesized 4CzIPN⁵⁸ was found to be an

excellent substitute to [Ir] (see the supporting information of chapter III for synthesis details).⁵⁹ This organic dye is appealing as its reduction potential in the excited state is very high in comparison to the other ones commonly used ($E_{1/2}(\text{PC}^*/\text{PC}^{\bullet-}) = +1.59 \text{ V vs. SCE}$).⁶⁰ Furthermore, its lifetime in the excited state is relatively long (5100 ns), which probably explains why it is working so well with the silicates (**Scheme 17**). As a comparison, eosin Y has a lifetime in the excited state which is about 2500 times shorter than the one of 4CzIPN.



Scheme 17: Photooxidation of silicates using 4CzIPN as a photocatalyst

Afterwards, similarly to the carboxylates and the trifluoroborates, the silicates were utilized in many different reactions notably by our group,⁶¹ Nevado's,⁶² Molander's,⁶³ Hashmi's,⁶⁴ Boyd's,⁶⁵ Fang, Jin and Li's.⁶⁶

After this brief introduction on photocatalysis under photooxidative conditions, an interesting fact may be pointed out. In all of the previous examples, only alkyl radicals were formed. The generation of a radical centered on a sp^2 carbon has never been reported from a silicate under these photooxidative conditions. This is quite intriguing considering the quite low oxidation potential of the phenyl silicate ($E_{1/2}^{\text{ox}} = +0.89 \text{ V vs. SCE}$). Thus, before moving on, we tried to fill in this missing piece and the results can be found in the following part.

1.1.4. References

- ¹ F. Paneth, W. Hofeditz, *Chem. Ber.* **1929**, *62*, 1335.
- ² D. H. Hey, W. A. Walters, *Chem. Rev.* **1937**, *21*, 169.
- ³ Herbert C. Brown, M. S. Kharasch, T. H. Chao, *J. Am. Chem. Soc.* **1940**, *62*, 3435.
- ⁴ D. M. Hedstrand, W. H. Kruizinga, R. M. Kellogg, *Tetrahedron Lett.* **1978**, *19*, 1255.
- ⁵ C. Pac, M. Ihama, M. Yasuda, Y. Miyauchi, H. Sakurai, *J. Am. Chem. Soc.* **1981**, *103*, 6495.
- ⁶ H. Cano-Yelo, A. Deronzier, *Tetrahedron Lett.* **1984**, *25*, 5517.
- ⁷ D. A. Nicewicz, D. W. C. MacMillan, *Science* **2008**, *322*, 77.
- ⁸ M. A. Ischay, M. E. Anzovino, J. Du, T. P. Yoon, *J. Am. Chem. Soc.* **2008**, *130*, 12886.
- ⁹ J. M. R. Narayanam, J. W. Tucker, C. R. J. Stephenson, *J. Am. Chem. Soc.* **2009**, *131*, 8756.
- ¹⁰ T. Koike, M. Akita, *Chem. Lett.* **2009**, *38*, 166.
- ¹¹ Obtained by searching the concept "photoredox catalysis" in Scifinder.
- ¹² F. H. Burstall, *J. Chem. Soc.* **1936**, 173.
- ¹³ J. M. Lehn, R. Ziessel, *Prot. Natl. Acad. Sci. USA* **1982**, *79*, 701.
- ¹⁴ Figure taken from Paul Savel's PhD thesis, **2014**.
- ¹⁵ Figure taken from Christophe Lévêque PhD thesis, **2017**.
- ¹⁶ C. K. Prier, D. A. Rankic, D. W. C. MacMillan, *Chem. Rev.* **2013**, *113*, 5322.
- ¹⁷ H. H. Hodgson, *Chem. Rev.* **1947**, *40*, 251.
- ¹⁸ F. Mo, G. Dong, Y. Zhang, J. Wang, *Org. Biomol. Chem.* **2013**, *11*, 1582.
- ¹⁹ a) B. Olofsson, E. A. Merritt, *Angew. Chem. Int. Ed.* **2009**, *48*, 9052; b) F. Bellina, R. Rossi, *Tetrahedron* **2009**, *65*, 10269; c) E. A. Merritt, B. Olofsson, *Angew. Chem. Int. Ed.* **2009**, *48*, 9052; d) M. S. Yusubov, A. V. Maskaev, V. V. Zhdankin, *Arkivoc* **2011**, *1*, 370; e) V. V. Grushin, *Chem. Soc. Rev.* **2000**, *29*, 315.
- ²⁰ G. B. Deng, Z. Q. Wang, J. D. Xia, P. C. Quian, R. J. Song, M. Hu, L. B. Gong, J.H Li, *Angew. Chem. Int. Ed.* **2013**, *52*, 1535.
- ²¹ H. G. Roth, N. A. Romero, D. A. Nicewicz, *Synlett* **2016**, *27*, A.
- ²² H. Kolbe, *Justus Liebigs Annalen der Chemie* **1848**, *64*, 339.
- ²³ a) H. Hunsdiecker, C. Hunsdiecker, E. Vogt, *US 2176181*, **1939**; b) H. Hunsdiecker, C. Hunsdiecker, *Ber. Dtsch. Chem. Ges. B.* **1942**, *75*, 291; c) R. G. Johnson, R. K. Ingham, *Chem. Rev.* **1956**, *56*, 219.
- ²⁴ J. Liu, Q. Liu, H. Yi, C. Qin, R. Bai, X. Qi, Y. Lan, A. Lei, *Angew. Chem. Int. Ed.* **2014**, *53*, 502.
- ²⁵ A. Noble, D. W. C. MacMillan, *J. Am. Chem. Soc.* **2014**, *136*, 11602.
- ²⁶ Z. Zuo, D. W. C. MacMillan, *J. Am. Chem. Soc.* **2014**, *136*, 5257.
- ²⁷ J. Xuan, Z. G. Zhang, W. J. Xiao, *Angew. Chem. Int. Ed.* **2015**, *54*, 15632.
- ²⁸ S. J. McCarver, J. X. Qiao, J. Carpenter, R. M. Borzilleri, M. A. Poss, M. D. Eastgate, M. Miller, D. W. C. MacMillan, *Angew. Chem. Int. Ed.* **2016**, *55*, 1.
- ²⁹ S. Ventre, F. R. Petronijevic, D. W. C. MacMillan, *J. Am. Chem. Soc.* **2015**, *137*, 5654.
- ³⁰ G. Sorin, R. M. Mallorquin, Y. Contie, A. Baralle, M. Malacria, J. P. Goddard, L. Fensterbank, *Angew. Chem. Int. Ed.* **2010**, *49*, 8721.
- ³¹ Y. Yasu, T. Koike, M. Akita, *Adv. Synth. Catal.* **2012**, *354*, 3414.
- ³² a) J. Yi, S. O. Badir, R. Alam, G. A. Molander, *Org. Lett.* **2019**, *21*, 4853; b) J. Sim, M. W. Campbell, G. A. Molander, *ACS Catal.* **2019**, *9*, 1559; c) J. J. Dai, W. M. Zhang, Y. J. Shu, Y. Y. San, J. Xu, Y. S. Feng, H. J. Xu, *Chem. Commun.* **2016**, *52*, 6973.
- ³³ X. Su, H. Huang, W. Hong, J. Cui, M. Yi, Y. Li, *Chem Commun.* **2017**, *53*, 13324.
- ³⁴ V. R. Yatham, Y. Shen, R. Martin, *Angew. Chem. Int. Ed.* **2017**, *56*, 10915.
- ³⁵ R. J. Wiles, G. A. Molander, *Isr. J. Chem.* **2020**, *60*, 281.
- ³⁶ R. J. Wiles, G. A. Molander, *Israel Journal of Chemistry* **2020**, *60*, 281.

- ³⁷ J. A. Milligan, K. L. Burns, A. V. Le, V. C. Polites, Z. J. Wang, G. A. Molander, C. B. Kelly, *Adv. Synth. Catal.* **2020**, *362*, 242.
- ³⁸ J. A. Milligan, J. P. Phelan, V. C. Polites, C. B. Kelly, G. A. Molander, *Org. Lett.* **2018**, *20*, 6840.
- ³⁹ a) S. Fuzkumi, T. Suenobu, M. Patz, T. Hirasaka, S. Itoh, M. Fujitsuka, O. Ito, *J. Am. Chem. Soc.* **1998**, *120*, 8060; b) D. Zhang, L. Z. Wu, L. Zhou, X. Han, Q. Z. Yang, L. P. Zhang, H. H. Tung, *J. Am. Chem. Soc.* **2004**, *126*, 3440; c) J. K. Matsui, S. B. Lang, D. R. Heitz, G. A. Molander, *ACS Catal.* **2017**, *7*, 2563; d) K. Nakajima, S. Nojima, K. Sakata, Y. Nishibayashi, *Chem. Cat. Chem.* **2016**, *8*, 1028.
- ⁴⁰ T. V. Leeuwen, L. Buzzetti, L. A. Pelegro, P. Melchiorre, *Angew. Chem. Int. Ed.* **2019**, *58*, 4953.
- ⁴¹ C. Verrier, N. Alandini, C. Pezzetta, M. Moliterno, L. Buzzetti, H. B. Hepburn, A. Vega-Peñalosa, M. Silvi, P. Melchiorre, *ACS Catal.* **2018**, *8*, 1062.
- ⁴² a) R. S. Rohokale, S. D. Tambe, U. A. Kshirsagar, *Org. Biomol. Chem.* **2018**, *16*, 536; b) S. Zhu, J. Qin, F. Wang, H. Li, L. Chu, *Nat. Commun.* **2019**, *10*, 749.
- ⁴³ T. Maruyama, Y. Mizuno, I. Shimizu, S. Suga, J.-I. Yoshida, *J. Am. Chem. Soc.* **2007**, *129*, 1902.
- ⁴⁴ M. Uygur, T. Danelzik, O. Garcia Mancheño, *Chem. Commun.* **2019**, *55*, 2980.
- ⁴⁵ N. Khatun, M. J. Sim, S. K. Woo, *Org. Lett.* **2018**, *20*, 6239.
- ⁴⁶ L. Capaldo, R. Riccadi, D. Ravelli, M. Fagnoni, *ACS Catal.* **2018**, *8*, 304.
- ⁴⁷ D. Ravelli, M. Fagnoni, T. Fukuyama, T. Nishikawa, I. Ryu, *ACS Catal.* **2018**, *8*, 701.
- ⁴⁸ Definition taken from: <https://goldbook.iupac.org/html/O/OT07579.html>.
- ⁴⁹ C. L. Frye, *J. Am. Chem. Soc.* **1964**, *86*, 3170.
- ⁵⁰ G. Cerveau, C. Chuit, R. J. P. Corriu, L. Gerbier, C. Reye, J. L. Aubagnac, B. El Amrani, *Int. J. Mass. Spectrom. Ion Phys.* **1988**, *82*, 259.
- ⁵¹ a) R. A. Benkeser, W. E. Smith, *J. Am. Chem. Soc.* **1968**, *90*, 5307; b) Y. S. Cho, S. H. Kang, J. S. Han, B. R. Yoo, I. N. Jung, *J. Am. Chem. Soc.* **2001**, *123*, 5384.
- ⁵² W. J. Ward, A. Ritzer, K. M. Carroll, J. W. Flock, *J. Catal.* **1986**, *100*, 240.
- ⁵³ Y. Nakajima, S. Shimada, *RSC Adv.* **2015**, *5*, 20603.
- ⁵⁴ V. Corcé, L. M. Chamoreau, E. Derat, J. P. Goddard, C. Ollivier, L. Fensterbank, *Angew. Chem. Int. Ed.* **2015**, *54*, 11414.
- ⁵⁵ F. P. Boer, J. J. Flynn, J. W. Turley, *J. Am. Chem. Soc.* **1968**, *90*, 6973.
- ⁵⁶ Y. Nishigaichi, A. Suzuki, A. Takuwa, *Tetrahedron Lett.* **2007**, *48*, 211.
- ⁵⁷ K. Tamao, J. Yoshida, H. Yamamoto, T. Kakui, H. Matsumoto, M. Takahashi, A. Kurita, M. Murata, M. Kumada, *Organometallics* **1982**, *1*, 55.
- ⁵⁸ J. Luo, J. Zhang, *ACS Catal.* **2016**, *6*, 873.
- ⁵⁹ C. Lévêque, L. Chenneberg, V. Corcé, C. Ollivier, L. Fensterbank, *Chem. Commun.* **2016**, *52*, 9877.
- ⁶⁰ F. Le Vaillant, M. Garreau, S. Nicolai, G. Gryn'ova, C. Corminboeuf, J. Waser, *Chem. Sci.* **2018**, *9*, 5883.
- ⁶¹ a) L. Chenneberg, C. Lévêque, V. Corcé, A. Baralle, J. P. Goddard, C. Ollivier, L. Fensterbank, *Synlett* **2016**, *27*, 731; b) C. Lévêque, V. Corcé, L. Chenneberg, C. Ollivier, L. Fensterbank, *Eur. J. Org. Chem.* **2017**, 2118.
- ⁶² A. García-Domínguez, R. Mondal, C. Nevado, *Angew. Chem. Int. Ed.* **2019**, *58*, 12286.
- ⁶³ N. P. Pattel, C. B. Kelly, A. P. Siegenfeld, G. A. Molander, *ACS Catal.* **2017**, *7*, 1766.
- ⁶⁴ S. Witzel, K. Sekine, M. Rudolf, S. K. Hashmi, *Chem. Commun.* **2018**, *54*, 13802.
- ⁶⁵ K. D. Raynor, G. D. May, U. K. Bandarage, M. J. Boyd, *J. Org. Chem.* **2018**, *83*, 1551.
- ⁶⁶ a) T. Guo, L. Zhang, X. Liu, Y. Fang, X. Jin, Y. Yang, Y. Li, B. Chen, M. Ouyang, *Adv. Synth. Catal.* **2018**, *360*, 4459; b) W. Luo, Y. Fang, L. Zhang, T. Xu, Y. Liu, Y. Li, X. Jin, J. Bao, X. Wu, Z. Zhang, *Eur. J. Org. Chem.* **2020**, 1778.

I.2. Phenyl bis-Catecholato Silicates: Synthesis, Structural Studies and Reactivity

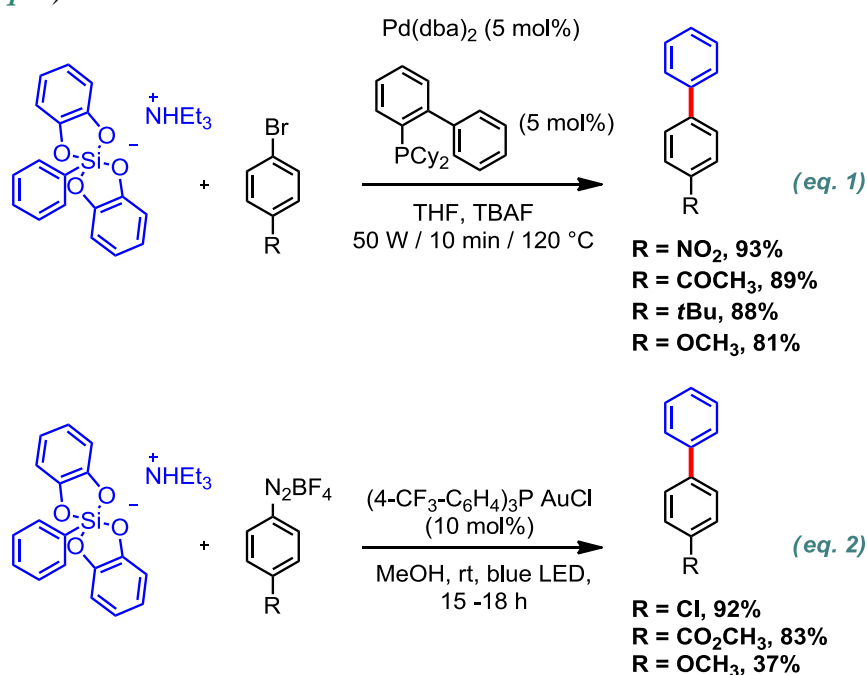
Unpublished

I.2.1. Abstract

The generation of aryl radicals by photoredox catalysis is well-documented under reductive conditions but remains challenging under oxidative pathway. Indeed, to date, only arylcarboxylates have been used under oxidative conditions despite their high oxidation potentials. Based on our previous work on the easily oxidizable silicates, a general study on phenyl silicates has been achieved and, thanks to the modification of the catechol moiety, it was found that phenyl radicals could be generated and trapped. The newly synthesized phenyl silicates have been fully characterized and their reactivity has been explored through experimental and computational studies.

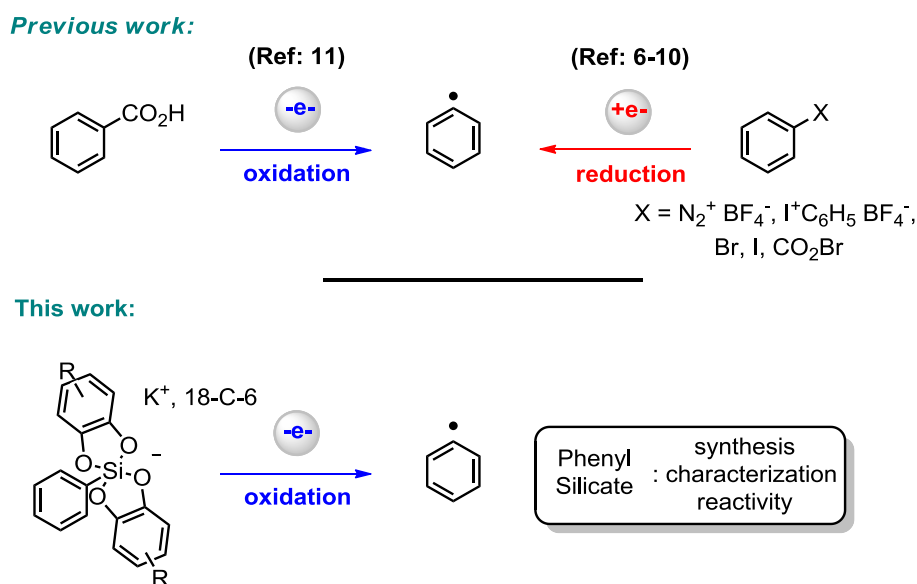
I.2.2. Introduction

Alkyl bis-catecholatosilicates have recently aroused a great interest in photooxidative catalysis as valuable alkyl radical precursors in radical addition reactions,¹ radical-polar crossover reactions² as well as dual photoredox-nickel cross-couplings.³ In contrast, aryl silicates counterparts have been much less utilized. Their main use has been disclosed by DeShong in palladium catalyzed cross-coupling reactions with arylhalides⁴ (Scheme 1, eq. 1) and by Hashmi for cross-coupling reactions with aryldiazonium salts under gold(I) catalysis⁵ (Scheme 1, eq. 2).



Scheme 1: Use of aryl silicates for $\text{sp}^2\text{-sp}^2$ cross-coupling reactions

The photooxidation of arylsilicates would be of interest for two reasons. First, the generation of aryl radicals by photoredox catalysis is well-documented under photoreductive conditions from a variety of precursors such as aryl diazoniums,⁶ iodoniums,⁷ sulfoniums,⁸ arylhalide,⁹ and also benzoyl hypohalites¹⁰ (**Scheme 2**). By contrast, only one report was published by the Yoshimi group under photooxidative conditions with aryl carboxylates.¹¹ Up to 150 mol % of photocatalyst under UV irradiation had to be used to provide moderate yields (~50%) of aryl radical adducts. This underlines that the generation of aryl radicals under photooxidative conditions is highly challenging. Second, this new class of silicate derivatives could open new perspectives in terms of reactivity either in radical addition reactions or in dual catalysis. This study aimed at determining the influence of the substitution of catechols in their ability to generate aryl radicals. We therefore undertook the synthesis of various phenyl silicates and studied their structural features and reactivity.

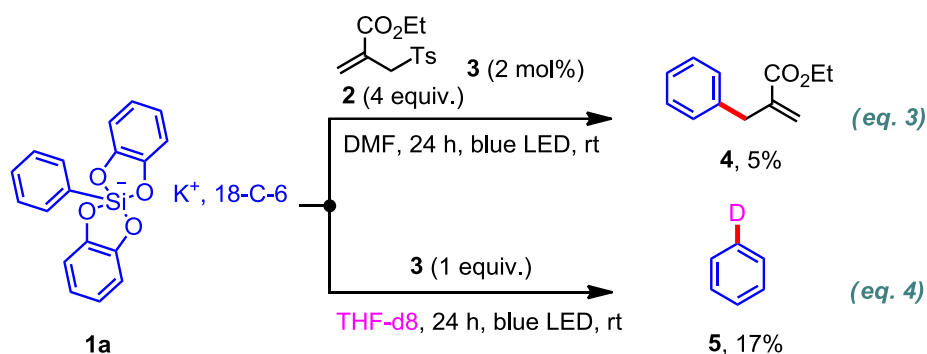


Scheme 2: Generation of aryl radical through photocatalytic conditions

1.2.3. Results and Discussion

We first focused on the reactivity of the simplest term, the phenyl bis-catecholatosilicate **1a**. It was synthesized based on a previously reported protocol,^{12,1a} using catechol (2 equiv.), 18-C-6 (1 equiv.), MeOK (1 equiv.) and phenyltrimethoxysilane (1 equiv.). Silicate **1a** was obtained in a satisfying 87% yield (reaction time : 2 h at room temperature, solvent of crystallization: acetone/Et₂O). Its half-wave oxidation potential in DMF was measured by cyclic voltammetry and the observed value ($E_{1/2}^{ox} = +0.89$ V vs. SCE 1^a) was compared with the potential of the photocatalyst [Ir(dF(CF₃)ppy)₂(bpy)]PF₆ (**3**) in its excited state ($E_{1/2}(\text{Ir(III)}^*/\text{Ir(II)}) = +1.32$ V vs. SCE¹³). These data suggest that this photocatalyst can oxidize silicate **1a**. Nevertheless, all attempts to generate a phenyl radical with photocatalyst **3** and to trap it with acceptor **2** met limited success. Product **4** was isolated in only 5 % yield albeit efficient phosphorescence quenching of **3** with **1a**. Indeed, the quenching rate constant was determined by Stern-Volmer

analysis and found to be $k_q = 5.7 \times 10^8 \text{ mol}^{-1} \text{ L s}^{-1}$. Additionally, when the reaction was performed in deuterated THF as solvent, the formation of $\text{C}_6\text{H}_5\text{D}$ could be observed (1 equiv. of **3**, 17 % NMR yield (see the supporting information for more details), **Scheme 3**).



Scheme 3: Photooxidation of phenyl silicate **1a** and aryl radical trapping

In order to check whether this low yield was due to the instability of **1a**, ^{29}Si NMR experiments were carried out before and after reaction with acceptor **2**. After 24 hours of blue LED irradiation ($\lambda_{\text{max}} = 450 \text{ nm}$), only **1a** as silicon derivative was detected in the mixture and no degradation was evidenced (**Figure 1**).

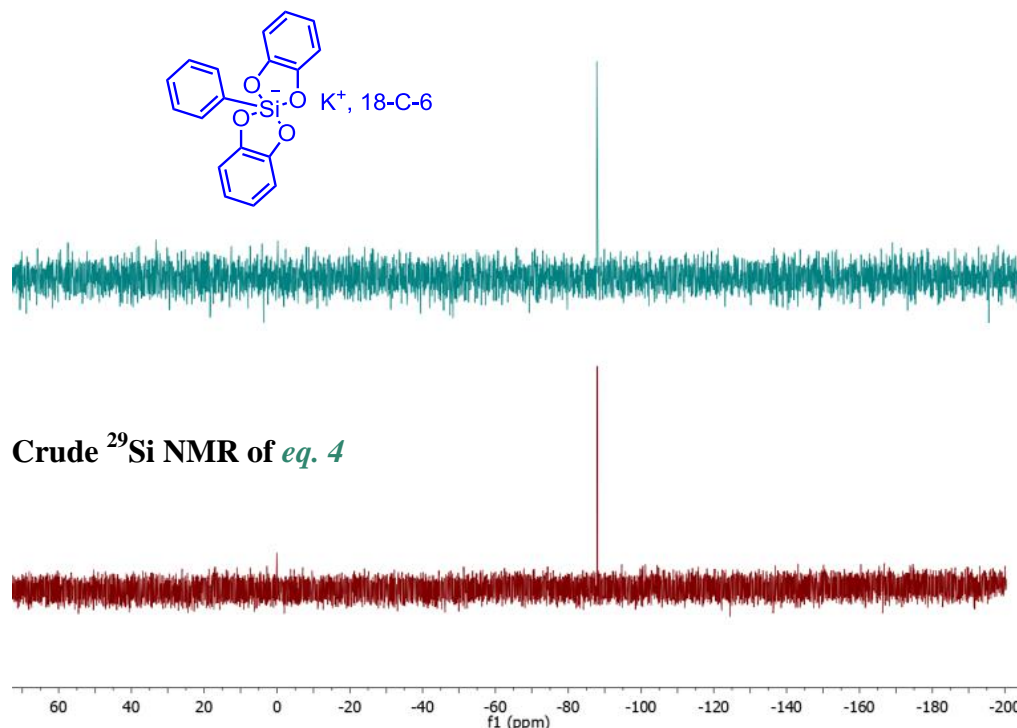
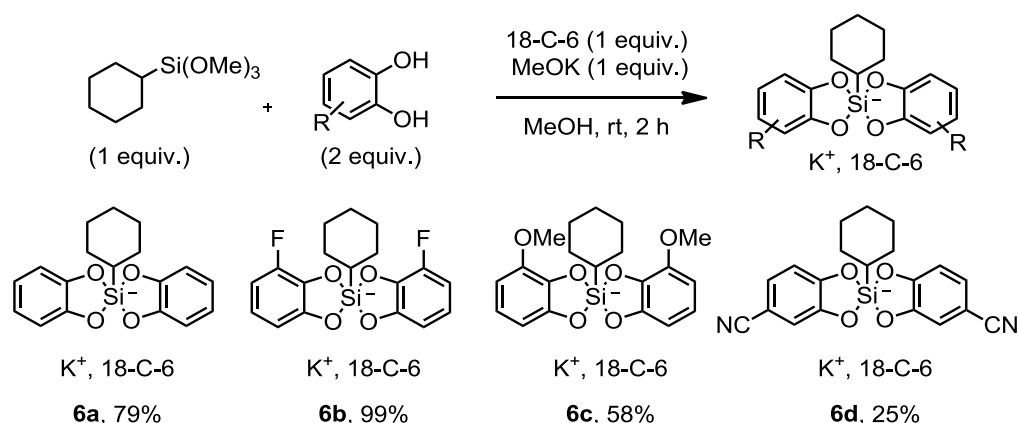


Figure 1: ^{29}Si NMR before and after the photocatalytic reaction in DMF (eq. 4)

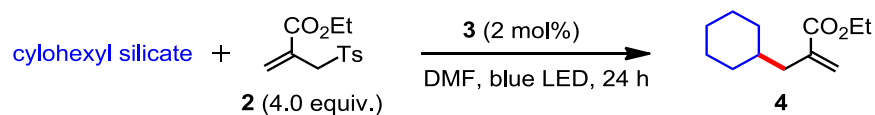
Considering the favorable redox potentials and the efficient luminescence quenching (see above), the low reactivity of **1a** was rather puzzling and led us to study the role of substituents on the catechol moiety and their effect on the reactivity of the phenyl silicates.

We first tested the substitution effect on the highly reactive cyclohexyl bis-catecholato-silicate to ensure that the formation of the cyclohexyl radical was still possible. Using the previously described procedure with appropriate catechol (18-C-6, MeOK and cyclohexyltrimethoxysilane), various cyclohexylsilicates [**6a-6d**] bearing differently substituted catechol moieties were synthesized (2 h at room temperature, solvent of crystallization: acetone/Et₂O, **Scheme 4**).^{1a,14}



Scheme 4: Synthesis of cyclohexyl silicates bearing differently substituted catechol moieties

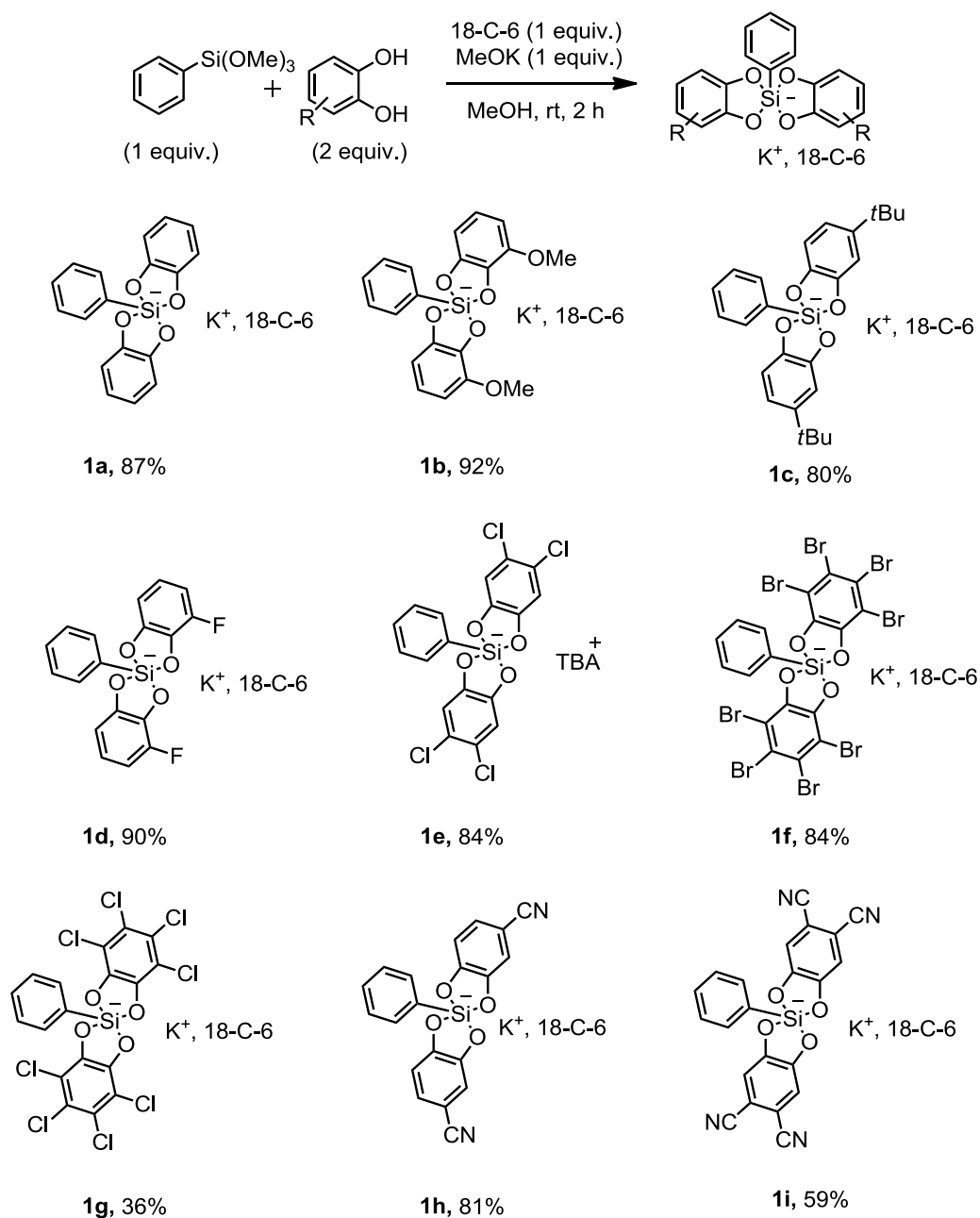
Upon treatment with photocatalyst **3** and allylsulfone **2** under blue LED irradiation, silicates **6b** ($E_{1/2}^{\text{ox}} = +0.91$ V vs. SCE) and **6d** ($E_{1/2}^{\text{ox}} = +1.01$ V vs. SCE), bearing electrowithdrawing groups, afforded the radical allylation product **4**, but in slightly lower yields (77% and 60% yields respectively) than plain silicate **6a** ($E_{1/2}^{\text{ox}} = +0.69$ V vs. SCE, 88% of **4**) (**Table 1**). Interestingly, an electrodonating group such as methoxy on the catechols (**6c**, $E_{1/2}^{\text{ox}} = +0.63$ V vs. SCE) drastically decreased the yield of this reaction and most of the starting material was recovered.



Cyclohexyl Silicate	Yield
 K^+ 18-C-6 6a	88%
 K^+ 18-C-6 6b	77%
 K^+ 18-C-6 6c	14%
 K^+ 18-C-6 6d	60%

Table 1: Generation of cyclohexyl radical from cyclohexyl silicates **6** with variously substituted catechols and allylation reaction

Encouraged by these results showing that such catechol substitutions can modulate the reactivity of the corresponding silicates but do not hamper the photooxidation process, we prepared a library of phenyl silicates with mono- and polysubstituted catechols (**Scheme 5**).



Scheme 5: Characterization of phenyl silicates bearing substituted catechols

Using the same procedure with appropriate catechol, MeOK, crown ether and phenyltrimethoxysilane, most of the silicates were efficiently prepared (yield > 80%) in crystalline form suitable for X-ray diffraction analysis. Thus, silicates **1b**, **1d** and **1h** bearing an electron-donating (MeO) and electron-withdrawing (F, CN) groups respectively were analyzed by XRD (**Figure 2**).¹⁵

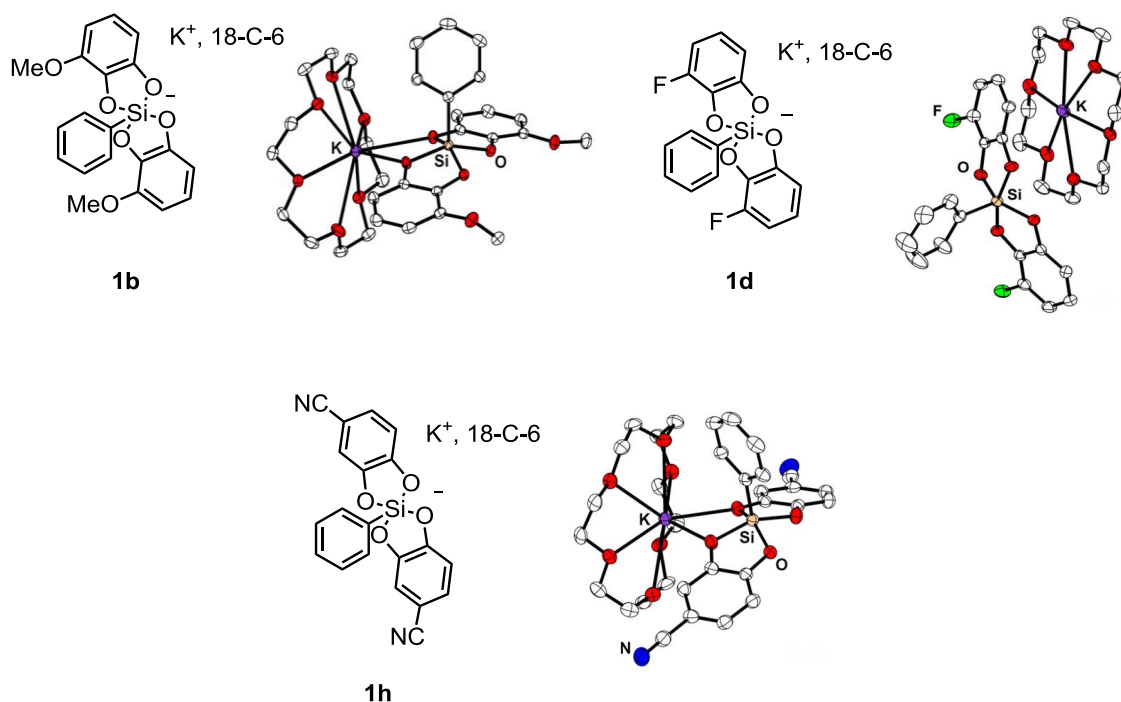


Figure 2: XRD analysis of compound **1b**, **1d** and **1h**

All of them crystallized in quite similar square pyramid structures as silicate **1a**. The electronic features of the catechols do not seem to have an impact on the crystal structure. Interestingly, while analyzing XRD data, we noticed that, for silicate **1d** bearing non symmetrical catechols, two isomers "*cis*" and "*trans*" were observed. This result was also confirmed by ^{13}C NMR. All resonances of the non-symmetrical catechol moieties in ^{13}C NMR were doubled with identical integration for both products. Thus, the synthesis furnished 1 : 1 mixtures of the two *cis* and *trans* stereoisomers. It has to be mentioned that this type of 1:1 mixture of two stereoisomers was already observed with the cyclohexyl series.

Intrigued by this finding, we wondered if an equilibrium exists between these two forms in solution. To answer this question, ^{13}C NMR of **1h** at various temperatures was conducted (in acetone- d_6 at low temperature (below 273 K) and DMSO- d_6 at higher temperature (from 303 K), **Figure 3**).¹⁶

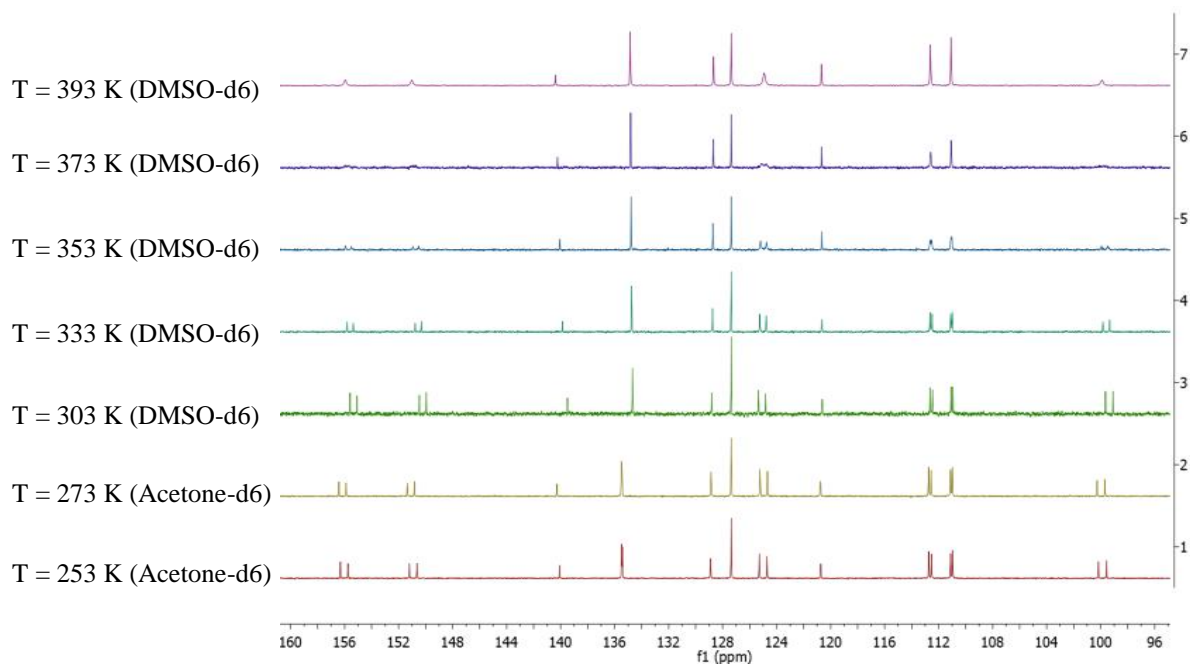
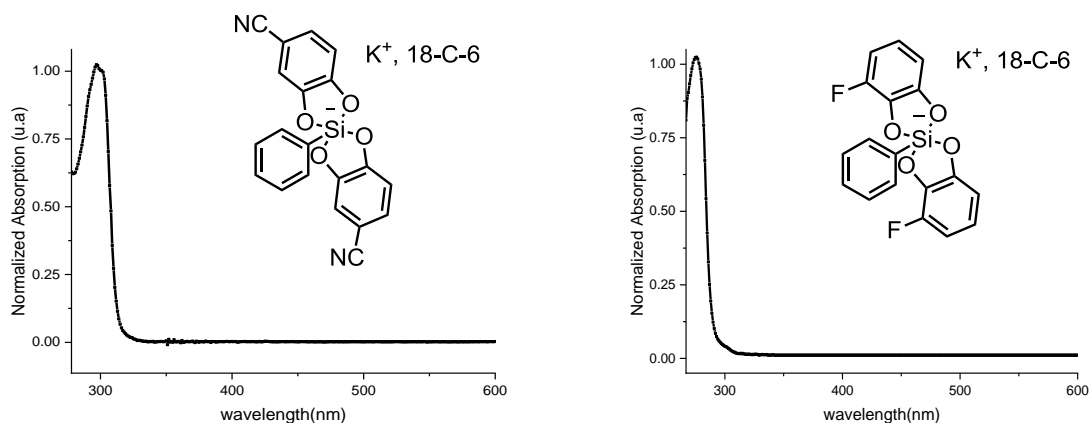


Figure 3: ^{13}C NMR of silicate **1h** at various temperatures

A coalescence of the peaks was observed, probably due to Berry pseudo-rotation,¹⁷ proving that an equilibrium exists between these two hypervalent forms.

After studying the structural features of these new silicon derivatives, we examined their behaviour upon light irradiation and oxidation. Spectroscopic analyses were conducted and UV-vis absorption spectra were recorded. All silicates exhibited a unique absorption band from 270 nm to 320 nm. No absorption was observed in the wavelength range of blue LED, previously used for the photooxidation of alkyl silicates (from 400 to 520 nm) (see **Figure 4** and the supporting information for more details and more UV spectra).



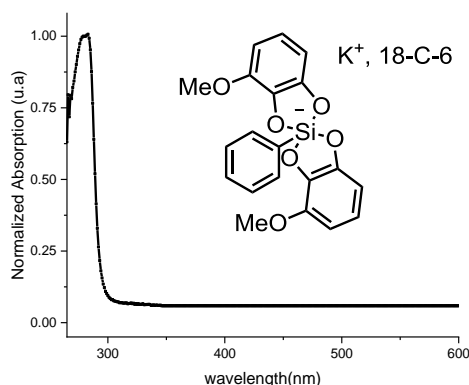


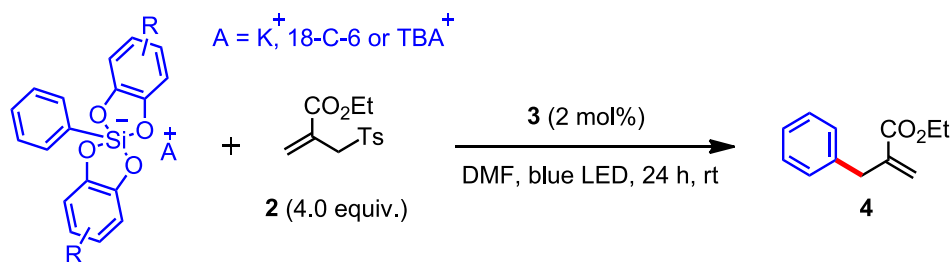
Figure 4: Absorption spectrum of silicates **1b**, **1d** and **1h**

The oxidation potentials of silicates [**1a-1i**] were measured in DMF as displayed in **Table 2**.

<i>Silicate</i>	$E_{1/2}^{ox}$ (vs. SCE in DMF)
1a	+ 0.89 V
1b	+ 0.81 V
1c	+ 1.09 V
1d	+ 1.05 V
1e	+ 1.13 V
1f	+ 1.46 V
1g	+ 1.37 V
1h	+ 1.33 V
1i	+ 1.62 V

Table 2: Half-wave oxidation potentials of silicates [**1a-1i**]

As expected, catechol modifications resulted in important variations of the oxidation potentials ($E_{1/2}^{ox}$ (**1i**) = +1.62 V vs. SCE - $E_{1/2}^{ox}$ (**1a**) = +0.73 V vs. SCE). While a donating group on the catechols was found to decrease the oxidation potential, an electron withdrawing group increased its value (**1b** $E_{1/2}^{ox}$ = +0.81 V vs. SCE / **1h** $E_{1/2}^{ox}$ = +1.33 V vs. SCE).¹⁸ Higher oxidation potentials could even be reached by using the perbromocatechol or by adding two cyano groups (**1f** $E_{1/2}^{ox}$ = +1.46 V vs. SCE / **1i** $E_{1/2}^{ox}$ = +1.62 V vs. SCE). Even if the oxidation of **1f** and **1i** by the photoactivated [Ir(dF(CF₃)ppy)₂-(bpy)]PF₆ ($E_{1/2}$ (Ir(III)* / Ir(II)) = +1.32 V vs. SCE) appears difficult, all the other silicates could potentially generate aryl radicals. Thus, we proceeded this study with the photocatalytic allylation reaction from silicates [**1a-1i**] with allylsulfone **2** and **3**. Results are summarized in **Table 3**.



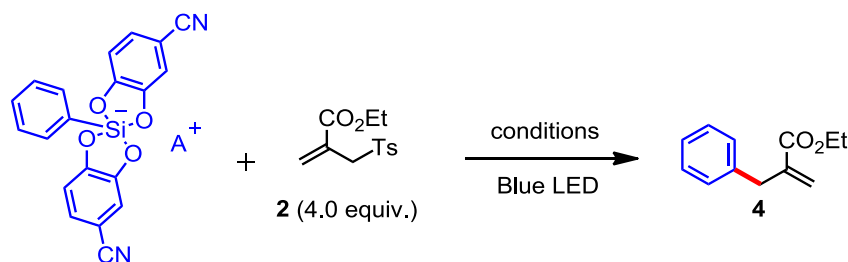
<i>Silicate</i>	<i>Yield</i>
1a	5%
1b	9%
1c	8%
1d	6%
1e	6%
1f	15%
1g	23%
1h	35%
1i	7%

Table 3: Yields of the photocatalytic allylation reaction

Although a yield < 10% was obtained with silicates [**1a-1e**, **1i**], silicate **1h** bearing a cyano group afforded **4** in 35% yield. Perbrominated and perchlorinated catechols also provided the desired product in slightly better yields than silicate **1a** (15% and 23% respectively). Nevertheless, these yields are still lower than the one obtained with silicate **1h**. The higher oxidation potentials of **1f** and **1g** in comparison to **1h** might explain this result. Also, as previously observed in **Table 1** with cyclohexyl silicates, the methoxy substitution was found to be detrimental resulting in a decreased yield.

Thus, the modification of the catechol moiety efficiently modulates the behaviour of these phenyl silicates upon this photocatalytic allylation type reaction.

Encouraged by these results, we optimized the reaction of the most promising silicate **1h** with acceptor **2** (**Table 4**). The influence of different counterions (ammoniums and potassium with and without crown ether, entry **6**, **11**, **12**) was studied but no significant improvement was observed. The temperature (room temperature or 100°C, entry **5** and **6**) did not affect the reaction efficiency. Switching to some organic photocatalysts resulted in a decreased yield (entries **1**, **2** and **3**).^{19,20} Even the very oxidizing Fukuzumi's acridinium ($E_{1/2}(\text{PC}^*/\text{PC}^{\bullet-}) = +2.06 \text{ V vs. SCE}^{21}$) did not afford **4** in a better yield. This result was consistent with what was previously observed with alkylsilicates.²² Different solvents (DMF, DMSO, MeCN, EtOH), reaction times and concentrations were also scoped but, despite all our efforts, the yield remained modest. Hence, the best conditions were found to be in DMSO with **3** at room temperature for 24 h (40%, entry **4**). Some control experiments were also carried out. The reaction in the dark or photocatalyst free conditions did not afford any product (entry **8**, **7**). Therefore, the presence of a photocatalyst under irradiation is mandatory to generate aryl radicals.



entry	Solvent	T	Photocatalyst	t	A ⁺	Yield ^[a]
1	DMF	rt	Fukuzumi's acridinium	24 h	K ⁺ / 18-C-6	6%
2	DMF	rt	Pyrylium salt ^[b]	24 h	K ⁺ / 18-C-6	7%
3	DMF	rt	4CzIPN	24 h	K ⁺ / 18-C-6	7%
4	DMSO	rt	3	24 h	K ⁺ / 18-C-6	40%
5	DMF	100°C	3	24 h	K ⁺ / 18-C-6	38%
6	DMF	rt	3	24 h	K ⁺ / 18-C-6	35%
7	DMF	rt	-	24 h	K ⁺ / 18-C-6	0%
8	DMF	rt	3	24 h	K ⁺ / 18-C-6	0% ^[c]
9	DMF	rt	3	68 h	K ⁺ / 18-C-6	35%
10	DMF	rt	3	68 h	K ⁺ / 18-C-6	41% ^[d]
11	DMF	rt	3	24 h	K ⁺	30%
12	DMF	rt	3	24 h	Et ₃ NH ⁺	35%
13	CH ₃ CN	rt	3	24 h	TBA ⁺	0%
14	EtOH	rt	3	24 h	TBA ⁺	20%
15	DMSO	rt	3	24 h	TBA ⁺	35%

^[a] [Silicate] = 0,1 mol.L⁻¹, NMR yield using 1,3,5 trimethoxybenzene as NMR standard; ^[b] 2,4,6-Tri(*p*-tolyl)pyrylium tetrafluoroborate salt; ^[c] reaction in the dark; ^[d] [Silicate] = 0,2 mol.L⁻¹.

Table 4: Optimization of the reaction

Inspired by the pioneering work of Nishigaichi showing that silicates can be photoactivated,²³ and because silicate **1h** absorbs at 300 nm (**Figure 4**), the photo allylation reaction was also tested at this wavelength with and without **3** with limited success as only 10% and 6% of product was isolated respectively. So, even if this silicate absorbs UVB light, the use of **3** under blue LED irradiation remains more efficient.

To confirm the radical character of this reaction, H abstraction from deuterated THF was also achieved and led to the formation of C₆H₅D in 44% yield (in comparison to 17% yield obtained with silicate **1a**) confirming that a radical pathway is involved.²⁴

The phosphorescence quenching of **3** with silicate **1h** was also revealed thanks to the Stern-Volmer plot and a quenching constant of $1.31 \times 10^8 \text{ mol}^{-1} \text{ L s}^{-1}$ was obtained (compared to $5.7 \times 10^8 \text{ mol}^{-1} \text{ L s}^{-1}$ for silicate **1a**). Thus, silicate **1h** does not quench the iridium photocatalyst more efficiently than silicate **1a** (Figure 5). It is worth noting that for benzyl silicate, which exhibits a good reactivity, the quenching constant of **3** is more important ($7.9 \times 10^9 \text{ mol}^{-1} \text{ L s}^{-1}$).

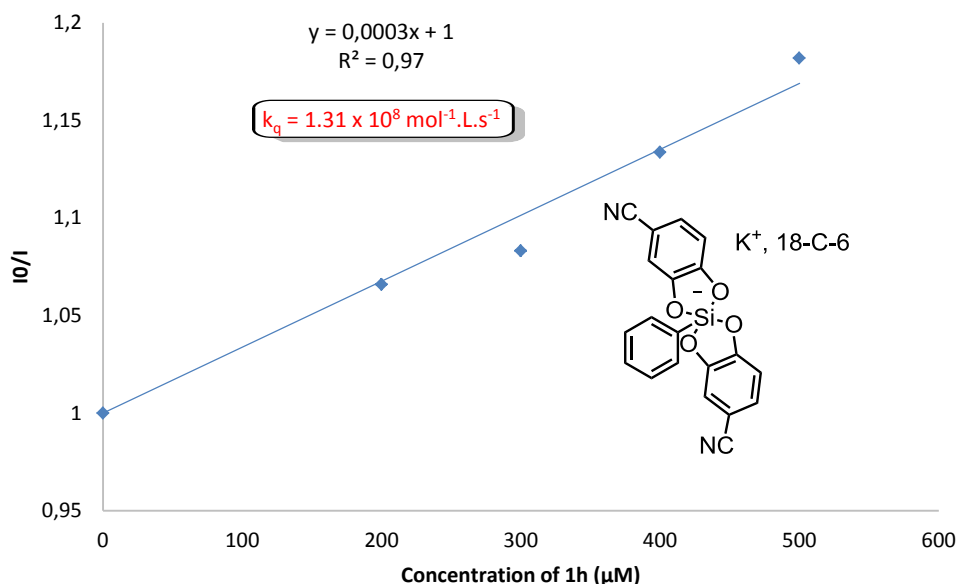
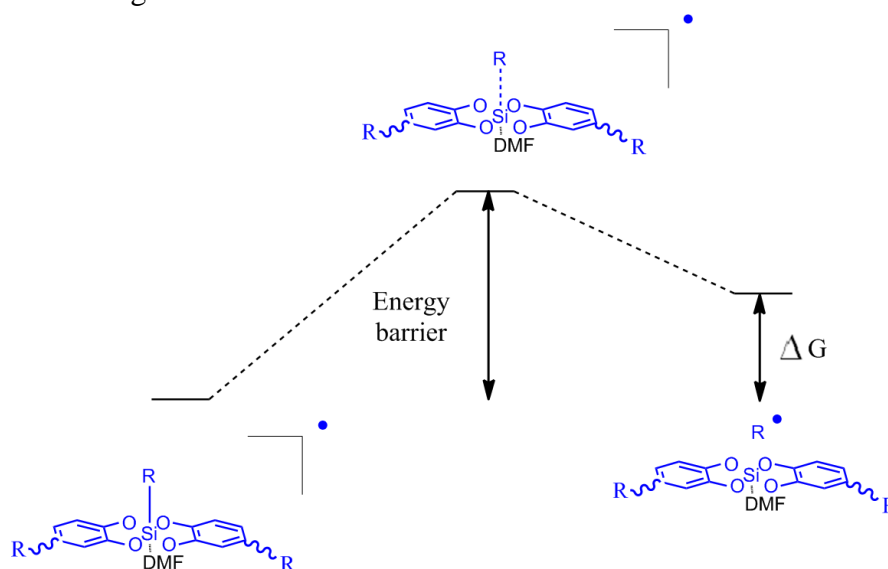


Figure 5: Stern-Volmer plot - quench of silicate **1h** and **3**

To better understand the difference of reactivity between alkylsilicates and phenyl silicates, we resorted to computational studies. The fragmentation of the intermediate hypercoordinated radical resulting from the oxidation by the photocatalyst was assessed for both types of silicates. Energy barriers for the cleavage of the silicon-carbon bond and the free energy of the reaction are summarized in **Table 5**, in the presence or absence of DMF as coordinating ligand on the silicon center. In all cases, it was found that the presence of DMF reduces the barrier of radical expulsion. With DMF, the generation of alkyl radicals is rather easy with an energy barrier of 17.45 kcal/mol, which explains why various transformations are observed with this type of substrates.^{1,3} However, aryl silicates are less prone to expel a radical upon oxidation. Without any substituent on the catechol moiety, the energy barrier was calculated to be 27.46 kcal/mol and the generated radical is rather unstable (with a Gibbs free energy of 22 kcal/mol). The situation is different with the experimentally more reactive **1h** silicate: the energy barrier to generate the radical was about 19 kcal/mol, thus more accessible but the

radical is still rather unstable with a highly endergonic process of 19 kcal/mol. These results prompted us to investigate the electronic structure of these radicals more in detail (**Figure 6**).



Silicate	Energy barrier (kcal/mol)	Free energy of reaction (kcal/mol)
	17.45 (28.88)	1.86 (13.78)
	18.99 (34.89)	19.05 (25.57)
	27.46 (36.49)	22.61 (25.98)
	34.11 (43.00)	30.20 (28.03)

Table 5: Barrier and Gibbs free energy of the reaction (in kcal/mol) corresponding to radical formation for various oxidized silicates, as calculated at the wB97M-D3BJ/def2-SV(P) level. Values in parenthesis correspond to calculations done without DMF.

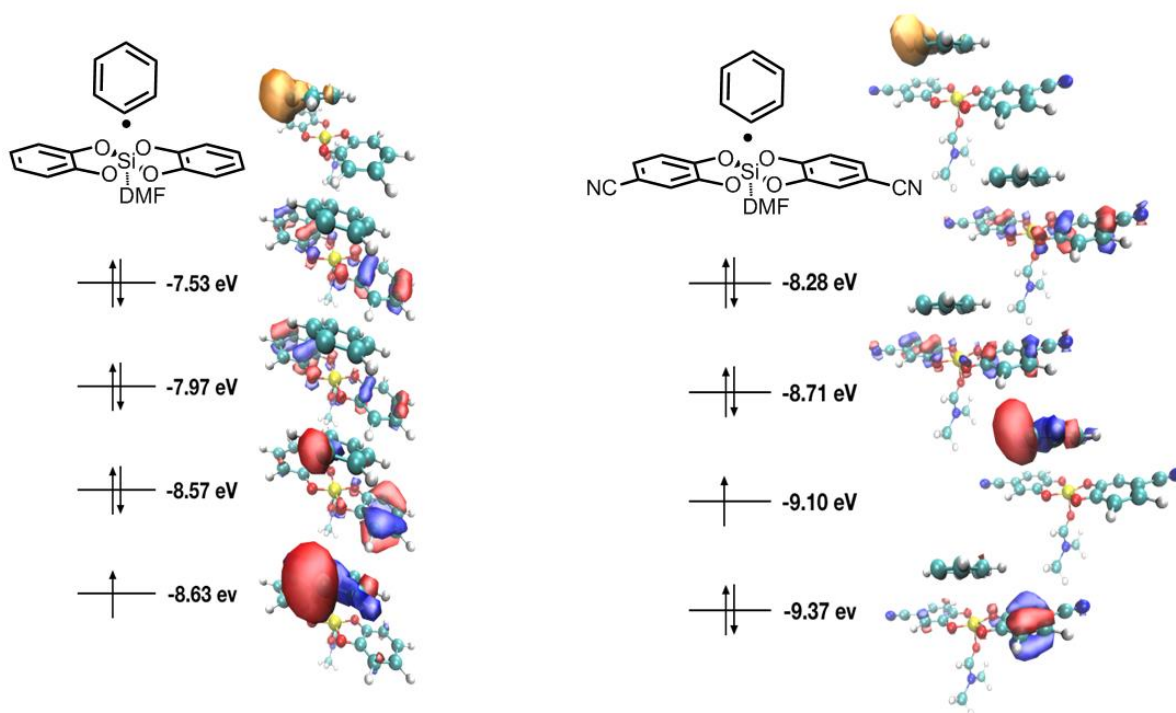


Figure 6: Spin density and frontier orbitals diagram for the oxidized aryl silicate **1a** and **1h**

To our surprise, these radicals are not classical and do not follow the Aufbau principle. For most of radicals, the orbital encompassing the unpaired electron is the highest occupied molecular orbital (HOMO). Here, the orbital better suited to describe the calculated spin density is not the HOMO but a lower lying molecular orbital. This phenomenon is known as SOMO-HOMO inversion and has been previously described for various systems, but never emerged for hypervalent species.²⁵ The frontier orbitals, as well as the spin density, are depicted in **Figures 6** and **7** for radicals arising from **1a** and **1h**. It can be observed that, in the case of the cyano substituted catechol radical species, the orbital describing the radical is lower in energy (-9.10 eV) than in the non-substituted catechol radical species (-8.63 eV). This could explain why the CN substituted silicate species is more reactive than the unsubstituted species: the radical being more stable (-9.10 eV vs. -8.63 eV), it is less prone to decompose in solution. Moreover, the barrier for radical extrusion is smaller (18.99 kcal/mol vs. 27.46 kcal/mol), allowing faster generation of the aryl radical.

Thus, the calculations explain well the strange behaviours of the phenyl silicates and are in accordance with the experimental observations.

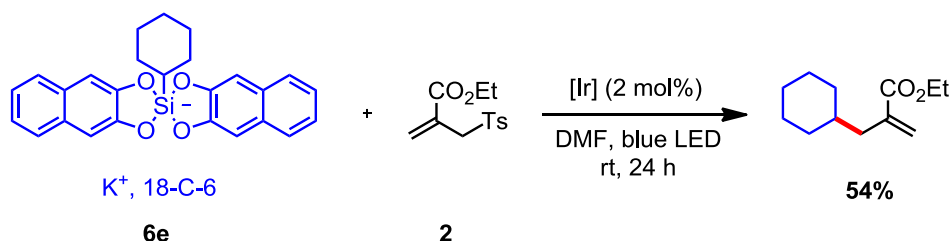
1.2.4. Conclusion

Owing to an appropriate modification of its catechol moiety, a phenyl radical was, for the first time, successfully generated from a phenyl silicate. The unusual behavior of these newly synthesized silicates has been rationalized through DFT calculations and physicochemical analyses. This result emphasizes silicates as first-rate precursors to challenging radicals.

1.2.5. Additional results

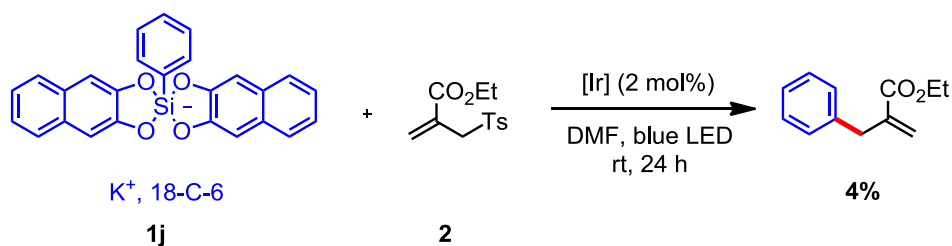
1.2.5.1. Extended catechol modifications

Inspired by Nishigaichi's reports on silicate photoexcitation,²⁶ we wondered if switching from a catechol to a naphthalene-2,3-diol could help to improve the yields of the photocatalytic reactions. In this respect, we firstly synthesized the cyclohexyl silicate **6e** and used it in the reaction with allylsulfone **2** (**Scheme 6**). The product was obtained in a satisfying yield even if a slight decrease was observed in comparison to the one obtained with silicate **6a**. Nevertheless, the oxidation potential of **6e** was found to be higher than **6a**, which might give a rationale for this lower yield (**6e**: $E_{1/2}^{ox} = +0.91$ V vs. SCE and **6a**: $E_{1/2}^{ox} = +0.69$ V vs. SCE).



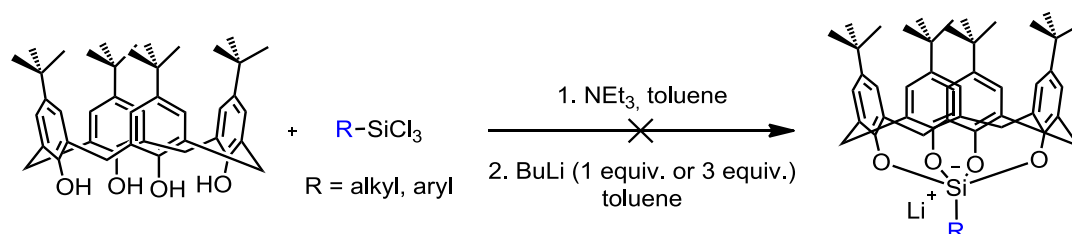
Scheme 6: Photocatalytic allylation reaction using silicate **6e**

Secondly, the phenyl analog was synthesized. Nonetheless, in that case, the reaction with allylsulfone **2** did not form any product (**Scheme 7**). Even switching the irradiation wavelength to 300 nm, which is where this compound absorbs, did not improve the yield.



Scheme 7: Photocatalytic allylation reaction using silicate **1j**

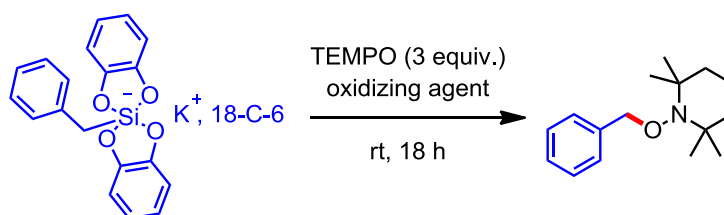
It is worth mentioning that 4-*tert*-Butylcalix[4]arene was also thought as a possible substitute to the catechol system but the synthesis turned out to be tricky and no product was obtained (**Scheme 8**).



Scheme 8: Silicate synthesis with 4-*tert*-Butylcalix[4]arene instead of catechols

1.2.5.2. Oxidation of the aryl silicate

Because photocatalysis failed in efficiently oxidizing silicate **1h**, we thought of using stoichiometric metal complexes to reach this goal. Indeed, some complexes had already been reported for the oxidation of the pentafluorosilicates²⁷ and the trifluoroborates.²⁸ Nonetheless, they had never been utilized so far with the bis-catecholato silicates. Therefore, we began our investigation by performing this reaction on the readily oxidized benzyl silicate ($E_{\text{ox}}^{1/2} = +0.61 \text{ V vs. SCE}$) to see if those oxidizing agents are compatible with our system (**Table 6**).

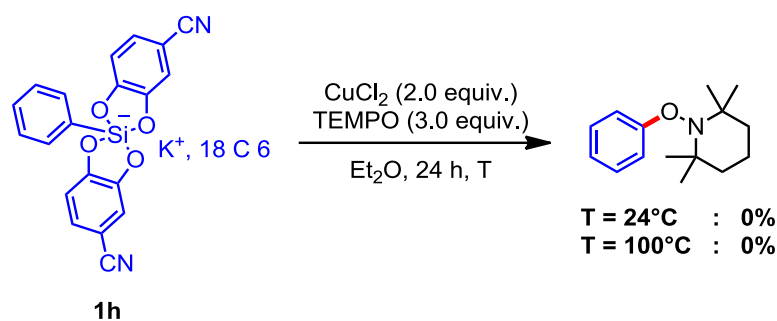


Oxidant	Solvent	Yield
Cu(OAc) ₂ (1.2 equiv.)	Et ₂ O	0%
CuCl ₂ (1.2equiv.)	Et ₂ O	75%
CuCl ₂ (2.0 equiv.)	Et ₂ O	78%
CAN (1.2 equiv.)	DMF	51%
FeCp ₂ BF ₄ (1.2 equiv.)	DMF	51%

Table 6: Oxidation of benzyl silicates thanks to metal complexes

Similarly to the trifluoroborates and the pentafluorosilicates, CuCl_2 , gave the best yield for this reaction (75%). To a lesser extent, CAN and FeCp_2BF_4 also generated the product in acceptable yields in DMF (51%) whereas $\text{Cu}(\text{OAc})_2$ did not form any benzyl-TEMPO adduct.

Encouraged by these results, we used our optimized conditions on phenyl silicate **1h** but, once again, no trace of the desired product was obtained even at a higher temperature (**Scheme 9**).

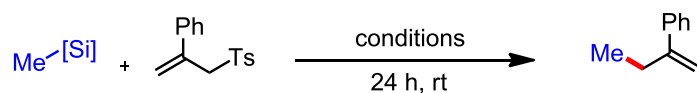


Scheme 9: Copper oxidation of phenyl silicate **1h** and trapping with TEMPO

In conclusion, the photooxidative conditions were found to be more effective even if the yields remained medium. Convinced that this difference of reactivity can be applied to other systems, we looked at other silicates reluctant to oxidation.

1.2.5.3. Oxidation of the methyl silicate

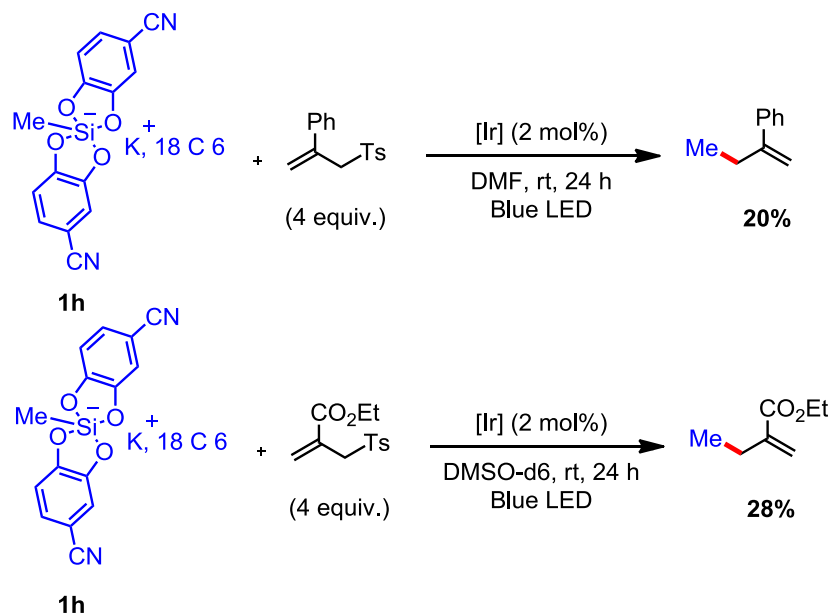
The methyl silicate is one of them. Indeed, despite all our efforts (modifications of the photocatalyst and the irradiation wavelength), we failed to generate a methyl radical and trap it with an allylsulfone (**Table 7**). Even when using TEMPO as a radical scavenger, no methyl-TEMPO adduct was formed.



Photocatalyst (2 mol%)	Wavelength (nm)	Solvent	Yield
[Ir]	470	DMF	0%
[Ir]	300	DMF	0%
4CzIPN	470	DMF	0%
Fukuzumi's acridinium	470	DMF	0%

Table 7: Oxidation of the methyl silicate

Nevertheless, based on the previous results, we synthesized the methyl silicate bearing 3,4-dihydroxybenzonnitriles instead of classical catechols. To our delight, methyl radicals were formed and the products were obtained in moderate yields (**Scheme 10**).



Scheme 10: Modified methyl silicate in photocatalytic allylation reactions

Thus, even if further work is needed, we are convinced that catechol modifications can improve the yields of some reactions and be used to reach new reactivities.

1.2.6. Supporting information

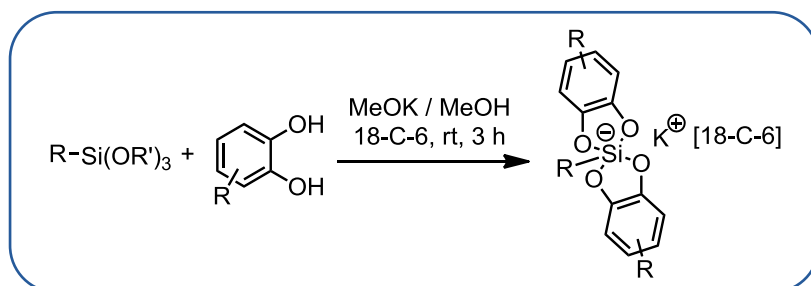
1.2.6.1. General informations

Unless otherwise noted, reactions were carried out under an argon atmosphere in oven-dried glassware. Methanol was distilled over CaH₂, THF, acetonitrile and diethyl ether were distilled over sodium/benzophenone, triethylamine over potassium hydroxide. Reagents and chemicals were purchased from commercial sources and used as received. Infrared (IR) spectra were recorded on a Bruker Tensor 27 (ATR diamond) spectrophotometer. ¹H, ¹³C, ¹⁹F NMR spectra were recorded at room temperature at 400, 100 and 377 MHz respectively, on a Bruker AVANCE III 400 spectrometer. ²⁹Si NMR spectra were recorded at 79 MHz on a Bruker AVANCE III 400 spectrometer. Chemical shifts (δ) are reported in ppm and coupling constants (J) are given in Hertz (Hz). Abbreviations used for peak multiplicity are: s (singlet); bs (broad singlet); d (doublet); t (triplet); q (quartet); quint (quintet); sept (septet); m (multiplet). Thin layer chromatographies (TLC) were performed on Merck silica gel 60 F 254 and revealed with a UV lamp ($\lambda = 254$ nm) and KMnO₄ staining. Flash Column Chromatographies were conducted on silica Geduran[®] Si 60 Å (40 – 63 μ m). High resolution mass spectrometries were performed on a microTOF (ESI).

1.2.6.2. General procedures

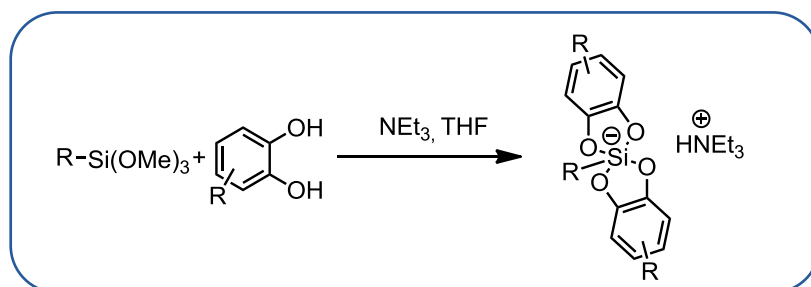
a) Synthesis of the silicates

a.1) General procedure A1 for silicates synthesis



To a stirred solution of appropriate catechol (2 equiv.) in dry methanol (0.1 or 0.13 M) was added 18-C-6 (1 equiv.). After dissolution of the crown ether, the trialkoxy organosilane (1 equiv.) was added, followed by a solution of potassium methoxide in methanol (1 equiv.). The reaction mixture was stirred for 3 hours and the solvent was removed under reduced pressure. The residue was dissolved in the minimum volume of acetone and diethyl ether was added until a cloudy solution was obtained (scrapping on the edge of the flask could be done to induce crystallization). The flask was placed at -20°C overnight. The crystals were collected by filtration, washed with diethyl ether and dried under vacuum to afford potassium [18-Crown-6] silicate.

a.2) General procedure A2 for silicates synthesis

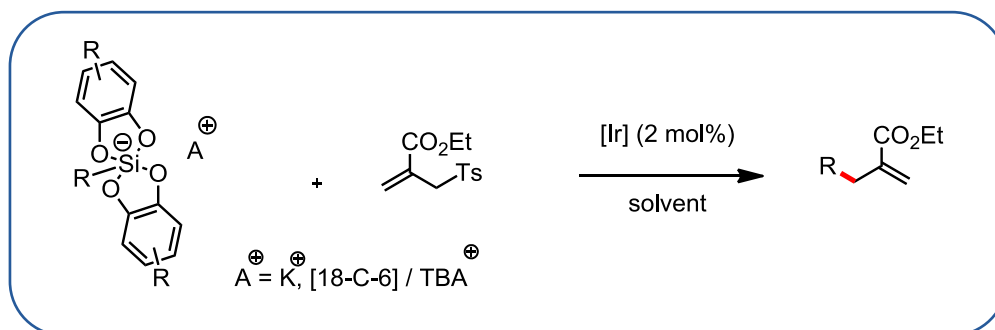


To a stirred solution of appropriate catechol (2 equiv.) in dry THF (0.1 M) was added triethylamine (4.67 equiv.). Then the corresponding trimethoxysilane (1 equiv.) was added dropwise. The reaction mixture was stirred for 20 hours under reflux and the solvent was removed under reduced pressure. The residue was dissolved in the minimum volume of acetone and diethyl ether was added until a cloudy solution was obtained (scrapping on the

edge of the flask could be done to induce crystallization). The flask was placed at -20°C overnight. The crystals were collected by filtration, washed with diethyl ether and dried under vacuum to afford triethylammonium silicate.

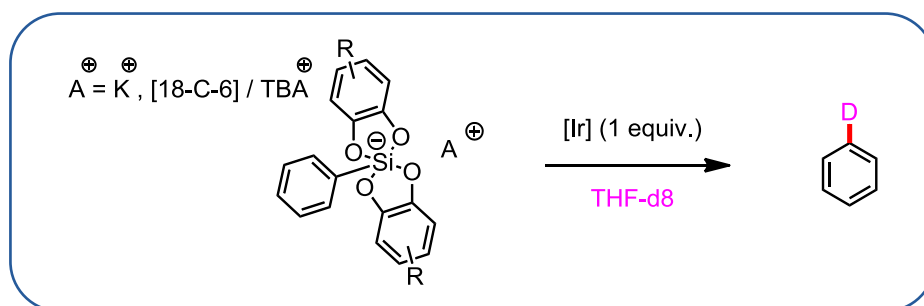
b) Photocatalytic reaction

b.1) General procedure for conjugate addition



To a dried Schlenk flask was added the appropriate silicate (1.0 equiv.), [Ir] (2 mol %), and the allylsulfone (4 equiv.). The Schlenk flask was sealed with a rubber septum and evacuated / purged with vacuum / argon three times. Then degassed solvent (0.1 M) was introduced and the reaction mixture was irradiated with blue LED (477 nm) at room temperature for 24h under an argon atmosphere. The reaction mixture was diluted with diethyl ether, washed with water (2 times), dried over MgSO_4 and evaporated under reduced pressure. The crude residue was analyzed by ^1H NMR (with 1 equiv. of 1,3,5 trimethoxybenzene as NMR standard).

b.2) General procedure for H abstraction

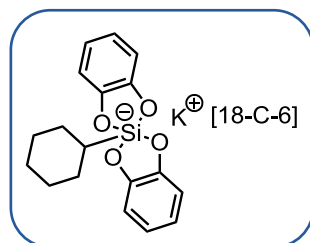


To a dried round bottom flask was added the appropriate silicate (1.0 equiv.) and [Ir] (1 equiv.). Then deuterated THF (0.017 M) was introduced and the reaction mixture was irradiated with blue LED (477 nm) at room temperature for 24h under an argon atmosphere. The mixture was analyzed by ^1H NMR (with 1 equiv. of 1,3,5 trimethoxybenzene as NMR standard). NMR references: benzene (THF-d₈),²⁹ 18-C-6 (THF-d₈),²⁹ TMOP (THF-d₈).³⁰

1.2.6.3. Compound characterizations

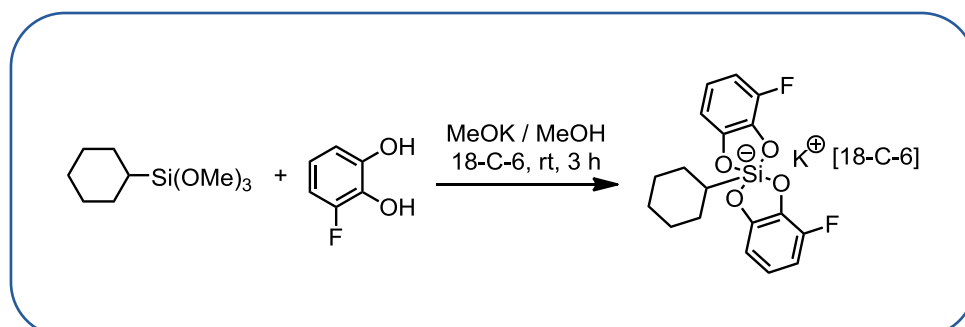
a) Cyclohexyl series

Potassium [18-Crown-6] bis(catecholato)-cyclohexylsilicate (**6a**)



Silicate **6a** was synthesized as described. The spectroscopic data are in agreement with those reported in the literature.^{1a}

Potassium [18-Crown-6] bis(3-fluorocatecholato)-cyclohexylsilicate (**6b**)



To a stirred solution of 3-fluorocatechol (5 mmol, 641 mg) in 25 mL of dry methanol (0.1 M) was added 18-C-6 (2.5 mmol, 660 mg). After dissolution of the crown ether, the cyclohexyltrimethoxysilane (2.5 mmol, 510 μ L mL) was added, followed by a solution of potassium methoxide in methanol (2.5 mmol, 700 μ L). The reaction mixture was stirred for 3 hours and the solvent was removed under reduced pressure. The residue was dissolved in the minimum volume of acetone and diethyl ether was added until a cloudy solution was obtained (scrapping on the edge of the flask could be done to induce crystallization). The flask was placed at -20°C overnight. The crystals were collected by filtration, washed with diethyl ether and dried under vacuum to afford potassium [18-Crown-6] bis(3-fluorocatecholato)-cyclohexylsilicate (**6b**) (1.65g, 99%) as a mixture of two isomers.

¹H NMR (400 MHz, Methanol-d₄): δ 6.54-6.47 (m, 4H), 6.45-6.39 (m, 2H), 3.54 (s, 24H), 1.66-1.57 (m, 5H), 1.29-1.10 (m, 5H), 0.86 (tt, $J = 12.0$ Hz and 4.0 Hz, 1H);

^{13}C NMR (75 MHz, Methanol- d_4): δ 153.9 (d, $J = 10.9$ Hz, 2C), 153.8 (d, $J = 10.9$ Hz, 2C), 149.9 (d, $J = 238.5$ Hz, 2C), 149.8 (d, $J = 238.1$ Hz, 2C), 138.4 (d, $J = 11.1$ Hz, 2C), 138.2 (d, $J = 11.1$ Hz, 2C), 118.0 (d, $J = 11.5$ Hz, 2C), 117.8 (d, $J = 11.5$ Hz, 2C), 107.4 (d, $J = 4.7$ Hz, 2C), 107.3 (d, $J = 4.6$ Hz, 2C), 107.2 (d, $J = 9$ Hz, 2C), 107.0 (d, $J = 8.9$ Hz, 2C), 69.9 (12C), 29.9, 29.8, 28.1 (4C), 27.9 (4C), 26.9 (2C);

^{29}Si NMR (79 MHz, Methanol- d_4): δ -74.9;

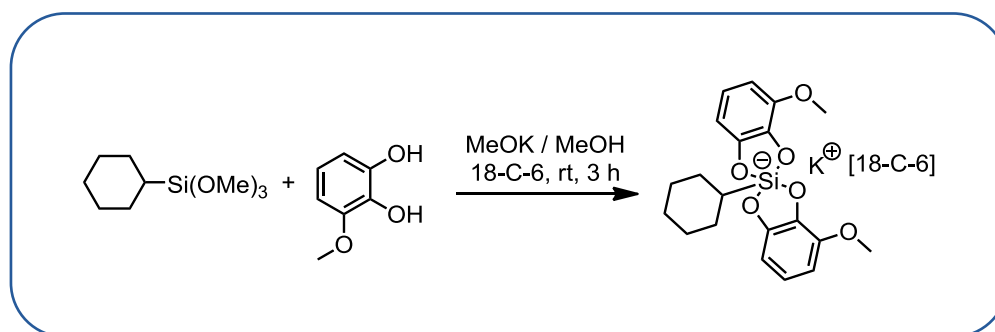
^{19}F NMR (377 MHz, Methanol- d_4): δ -141.9, -142.1;

HRMS: calc. for $[\text{C}_{18}\text{H}_{17}\text{F}_2\text{O}_4\text{Si}]^-$: 363.0870; found: 363.0869;

IR (neat): 2889, 2847, 1615, 1495, 1270, 1231, 1046, 1034, 964, 754, 723 cm^{-1} ;

M. P. 186°C.

Potassium [18-Crown-6] bis(3-methoxycatecholato)-cyclohexylsilicate (**6c**)



To a stirred solution of 3-methoxycatechol (4.0 mmol, 408 mg) in 15 mL of dry methanol was added 18-C-6 (2 mmol, 500 mg). After dissolution of the crown ether, the cyclohexyltrimethoxysilane (2.0 mmol, 410 μL) was added, followed by a solution of potassium methoxide in methanol (2.0 mmol, 560 μL). The reaction mixture was stirred for 3 hours and the solvent was removed under reduced pressure. The residue was dissolved in the minimum volume of acetone and diethyl ether was added until a cloudy solution was obtained (scrapping on the edge of the flask could be done to induce crystallization). The flask was placed at -20°C overnight. The crystals were collected by filtration, washed with diethyl ether and dried under vacuum to afford potassium [18-Crown-6] bis(3-methoxycatecholato)-cyclohexylsilicate (**6c**) (800 mg, 58%) as a mixture of two isomers.

^1H NMR (400 MHz, Methanol- d_4): δ 6.54-6.50 (m, 2H), 6.46-6.43 (m, 2H), 6.38-6.35 (m, 2H), 3.87 (m, 6H), 3.57 (s, 24H), 1.70-1.49 (m, 5H), 1.31-1.01 (m, 5H), 0.88 (tt, $J = 12.0$ Hz and 2.8 Hz, 1H);

^{13}C NMR (100 MHz, Methanol- d_4): δ 152.7 (2C), 152.6 (2C), 146.2 (4C), 140.4 (2C), 140.3 (2C), 118.0 (2C), 117.9 (2C), 106.0 (2C), 105.9 (4C), 105.83 (2C), 71.1 (12C), 57.2 (2C), 57.1 (2C), 31.5, 31.4, 29.5 (4C), 29.3 (4C), 28.2 (2C);

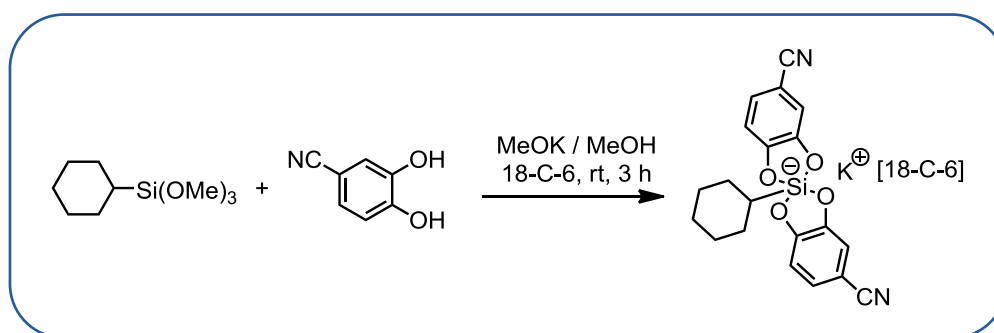
^{29}Si NMR (79 MHz, Methanol- d_4): δ -76.1, -76.2;

HRMS: calc. for $[\text{C}_{20}\text{H}_{23}\text{O}_6\text{Si}]^-$: 387.1269; found: 387.1267;

IR (neat): 2911, 1706, 1604, 1495, 1468, 1350, 1296, 1275, 1101, 964, 845, 768, 583 cm^{-1} ;

M. P. 152.6 $^\circ\text{C}$.

Potassium [18-Crown-6] bis(4-cyanocatecholato)-cyclohexylsilicate (**6d**)



To a stirred solution of 4-cyanocatechol (10 mmol, 1.35 g) in 40 mL of dry methanol was added 18-C-6 (5 mmol, 1.32 g). After dissolution of the crown ether, the cyclohexyltrimethoxysilane (5.0 mmol, 1.0 mL) was added, followed by a solution of potassium methoxide in methanol (5 mmol, 1.47 mL). The reaction mixture was stirred for 3 hours and the solvent was removed under reduced pressure. The residue was dissolved in the minimum volume of acetone and diethyl ether was added until a cloudy solution was obtained (scrapping on the edge of the flask could be done to induce crystallization). The flask was placed at -20°C overnight. The crystals were collected by filtration, washed with diethyl ether and dried under vacuum to afford potassium [18-Crown-6] bis(4-cyanocatecholato)-cyclohexylsilicate (**6d**) (850 mg, 25%) as a mixture of two isomers.

^1H NMR (400 MHz, Methanol- d_4): δ 7.06-6.92 (m, 4H), 6.79-6.71 (m, 2H), 3.61 (s, 24H), 1.66-1.56 (m, 5H), 1.35-1.10 (m, 5H), 0.88 (tt, $J = 12.0$ Hz and 4.0 Hz, 1H);

^{13}C NMR (100 MHz, Acetone- d_6): δ 157.7 (2C), 157.1 (2C), 152.5 (2C), 151.9 (2C), 125.3 (2C), 124.6 (2C), 121.4 (2C), 121.3 (2C), 112.5 (2C), 112.3 (2C), 110.9 (2C), 110.8 (2C), 100.2 (2C), 99.4 (2C), 70.7 (12C), 31.2, 31.1, 29.2, 29.1, 29.0, 28.8, 28.7, 28.6, 27.7 (4C);

^{29}Si NMR (79 MHz, Acetone- d_6): δ -75.0, -75.1;

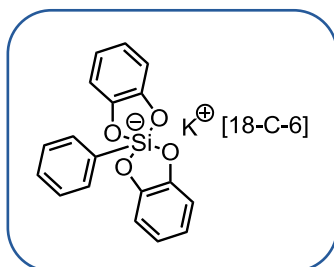
HRMS: calc. for $[C_{20}H_{17}N_2O_4Si]^-$: 377.0963; found: 377.0960;

IR (neat): 2215, 2160, 1493, 1350, 1266, 959, 831, 572 cm^{-1} ;

M.P. 147°C.

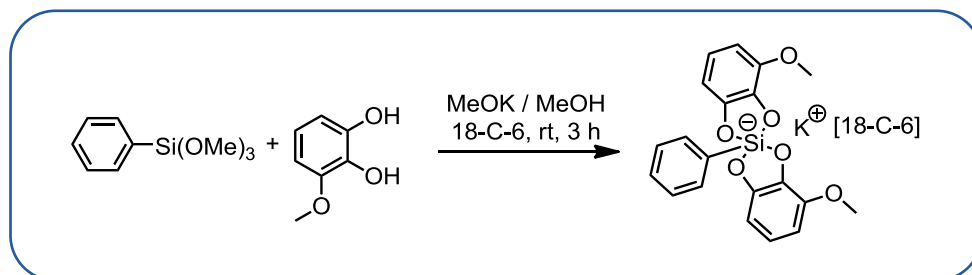
b) Phenyl series

Potassium [18-Crown-6] bis(catecholato)-phenylsilicate (**1a**)



Silicate **1a** was synthesized as described. The spectroscopic data are in agreement with those reported in the literature.^{1a}

Potassium [18-Crown-6] bis(3-methoxycatecholato)-phenylsilicate (**1b**)



To a stirred solution of 3-methoxycatechol (5.0 mmol, 701 mg) in 25 mL of dry methanol was added 18-C-6 (2.5 mmol, 660 mg). After dissolution of the crown ether, the phenyltrimethoxysilane (2.5 mmol, 466 μ L) was added, followed by a solution of potassium methoxide 3.56 M in methanol (2.5 mmol, 700 μ L). The reaction mixture was stirred for 3 hours and the solvent was removed under reduced pressure. The residue was dissolved in the minimum volume of acetone and diethyl ether was added until a cloudy solution was obtained (scrapping on the edge of the flask could be done to induce crystallization). The flask was placed at -20°C overnight. The crystals were collected by filtration, washed with diethyl ether and dried under vacuum to afford potassium [18-Crown-6] bis(3-fluorocatecholato)-phenylsilicate (**1b**) (1.43 g, 92 %) as a mixture of two isomers.

^1H NMR (400 MHz, Methanol- d_4): δ 7.69-7.66 (m, 2H), 7.19-7.17 (m, 3H), 6.58-6.52 (m, 4H), 6.44-6.41 (m, 2H), 3.85 (s, 6H), 3.53 (s, 24H);

^{13}C NMR (100 MHz, Methanol- d_4): δ 152.1 (4C), 146.6 (4C), 141.9, 141.8, 139.9, 139.8, 135.8 (4C), 129.1 (4C), 127.9 (4C), 118.5 (4C), 106.2 (4C), 106.1 (4C), 71.1 (12C), 57.1 (2C), 57.0 (2C);

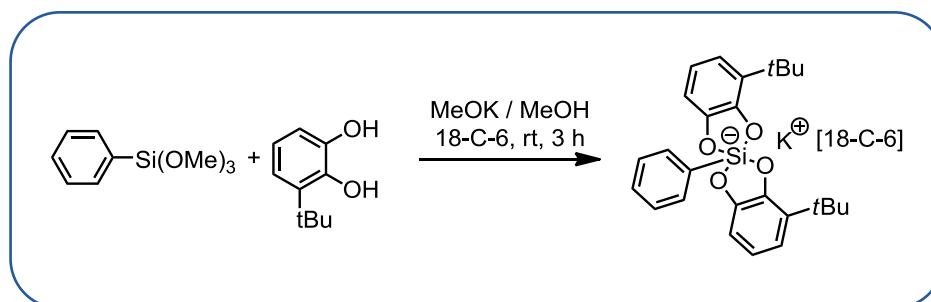
^{29}Si NMR (79 MHz, Methanol- d_4): δ -86.2, -86.3;

HRMS: calc. for $[\text{C}_{20}\text{H}_{17}\text{O}_6\text{Si}]^-$: 381.0800; found: 381.0798;

IR (neat): 2898, 1706, 1604, 1498, 1247, 1067, 964, 846, 770, 583 cm^{-1} ;

M.P. 165°C.

Potassium [18-Crown-6] bis(3-*tert*-butylcatecholato)-phenylsilicate (**1c**)



To a stirred solution of 3-*tert*-butyl catechol (5.0 mmol, 831 mg) in 25 mL of dry methanol was added 18-C-6 (2.5 mmol, 660 mg). After dissolution of the crown ether, the phenyltrimethoxysilane (2.5 mmol, 466 μL) was added, followed by a solution of potassium methoxide 3.56 M in methanol (2.5 mmol, 700 μL). The reaction mixture was stirred for 3 hours and the solvent was removed under reduced pressure. The residue was dissolved in the minimum volume of acetone and diethyl ether was added until a cloudy solution was obtained (scrapping on the edge of the flask could be done to induce crystallization). The flask was placed at -20°C overnight. The crystals were collected by filtration, washed with diethyl ether and dried under vacuum to afford potassium [18-Crown-6] bis(3-*tert*-butylcatecholato)-phenylsilicate (**1c**) (1.47 g, 80 %) as a mixture of two isomers.

^1H NMR (400 MHz, DMSO- d_6): δ 7.56-7.51 (m, 2H), 7.16-7.07 (m, 3H), 6.67-6.61 (m, 2H), 6.51-6.41 (m, 4H), 3.53(s, 24H), 1.21 (s, 18H);

^{13}C NMR (100 MHz, DMSO- d_6): δ 150.7 (2C), 150.6 (2C), 148.6 (2C), 148.5 (2C), 142.6 (2C), 142.5 (2C), 141.9 (2C), 135.5 (4C), 129.1 (2C), 127.9 (4C), 115.6 (2C), 115.5 (2C), 110.5 (4C), 109.3 (4C), 71.3 (12C), 35.1 (4C), 21.3 (12C);

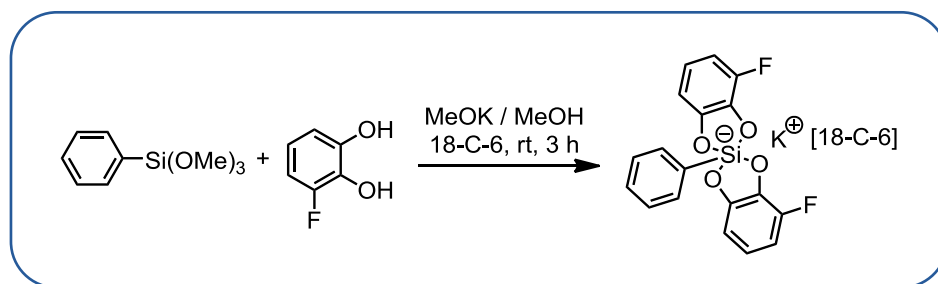
^{29}Si NMR (79 MHz, DMSO- d_6) : δ -87.1;

HRMS: calc. for $[\text{C}_{26}\text{H}_{29}\text{O}_4\text{Si}]^-$: 433.1835; found: 433.1837;

IR (neat): 2857, 1428, 1350, 1248, 1108, 820, 804, 652 cm^{-1} ;

M.P. 290°C.

Potassium [18-Crown-6] bis(3-fluorocatecholato)-phenylsilicate (**1d**)



To a stirred solution of 3-fluorocatechol (5.0 mmol, 641 mg) in 25 mL of dry methanol was added 18-C-6 (2.5 mmol, 660 mg). After dissolution of the crown ether, the phenyltrimethoxysilane (2.5 mmol, 466 μL) was added, followed by a solution of potassium methoxide 3.56 M in methanol (2.5 mmol, 700 μL). The reaction mixture was stirred for 3 hours and the solvent was removed under reduced pressure. The residue was dissolved in the minimum volume of acetone and diethyl ether was added until a cloudy solution was obtained (scrapping on the edge of the flask could be done to induce crystallization). The flask was placed at -20°C overnight. The crystals were collected by filtration, washed with diethyl ether and dried under vacuum to afford potassium [18-Crown-6] bis(3-fluorocatecholato)-phenylsilicate (**1d**) (1.48 g, 90 %) as a mixture of two isomers.

^1H NMR (400 MHz, Methanol- d_4): δ 7.70-7.67 (m, 2H), 7.24-7.22 (m, 3H), 6.67-6.65 (m, 2H), 6.63-6.57 (m, 2H), 6.55-6.49 (m, 2H), 3.52 (s, 24H);

^{13}C NMR (100 MHz, Methanol- d_4): δ 153.4 (d, $J = 11.2$ Hz, 2C), 153.3 (d, $J = 11.6$ Hz, 2C), 150.0 (d, $J = 239$ Hz, 2C), 149.9 (d, $J = 239$ Hz, 2C), 140.6 (d, $J = 1.7$ Hz, 2C), 137.8 (d, $J = 20.8$ Hz, 2C), 137.7 (d, $J = 1.6$ Hz, 2C), 135.8 (4C), 129.5 (2C), 128.1 (4C), 118.4 (d, $J = 12.6$ Hz, 2C), 118.3 (d, $J = 12.6$ Hz, 2C), 107.8 (d, $J = 5.1$ Hz, 2C), 107.7 (d, $J = 5.1$ Hz, 2C), 107.6 (d, $J = 18.2$ Hz, 2C), 107.4 (d, $J = 18.1$ Hz, 2C), 71.3 (12C);

^{29}Si NMR (79 MHz, Methanol- d_4): δ -85.1;

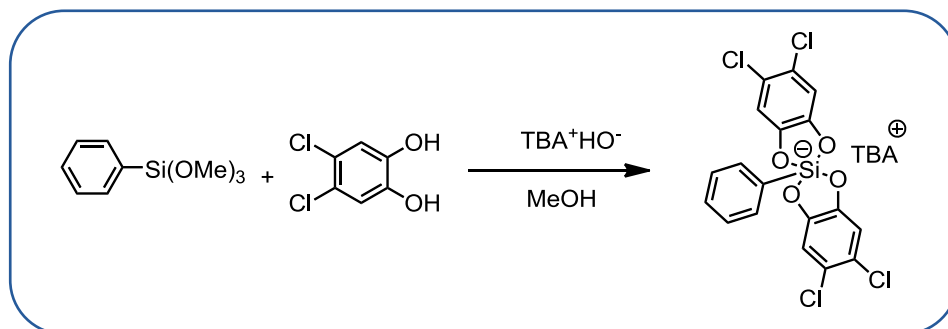
^{19}F NMR (377 MHz, Methanol- d_4): δ -141.9, -142.1;

HRMS: calc. for $[\text{C}_{18}\text{H}_{11}\text{F}_2\text{O}_4\text{Si}]^-$: 357.0395; found: 357.0391

IR (neat): 2892, 1713, 1618, 1515, 1496, 1471, 1352, 1273, 1231, 965, 868, 726, 703 cm^{-1} ;

M.P. 170°C.

Tetrabutylammonium bis(4,5-dichlorocatecholato)-phenylsilicate (1e)



To a stirred solution 4,5 dichlorocatechol (2mmol, 358 mg) in 25 mL of dry methanol was added TBA^+HO^- (1 mmol, 1 mL) (salt 1M in MeOH) and trimethoxysilane (1 mmol, 188 μL). The reaction mixture was stirred for 1 hour. After that, Et_2O was added and a white solid appeared. This solid was filtered and washed with Et_2O to afford tetrabutylammonium bis(4,5-dichlorocatecholato)-phenylsilicate (**1e**) (590mg, 84%).

^1H NMR (400 MHz, Acetone- d_6): δ 7.71-7.55 (m, 2H), 7.24-7.29 (m, 3H), 6.78 (s, 4H), 3.38 (t, $J = 11.2$ Hz, 8H), 1.84-1.65 (m, 8H), 1.47-1.31 (m, 8H), 0.94 (t, $J = 9.6$ Hz, 12H);

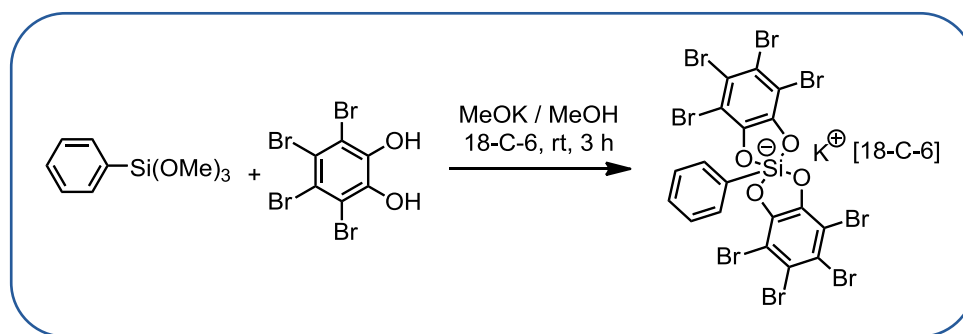
^{13}C NMR (100 MHz, Acetone- d_6): δ 152.0 (4C), 141.3, 136.0 (4C), 129.2, 127.8 (2C), 120.0 (2C), 112.0 (4C), 59.4 (4C), 24.5 (4C), 20.4 (4C), 13.9 (4C);

^{29}Si NMR (79 MHz, Acetone- d_6) : -84.4;

HRMS: calc. for $[\text{C}_{18}\text{H}_9\text{Cl}_4\text{O}_4\text{Si}]^-$: 456.9030; found: 456.9031;

IR (neat): 2961, 2873, 1482, 1427, 1377, 1239, 1093, 872, 695 cm^{-1} ;

M.P. 160.2°C.

Potassium [18-Crown-6] bis(tetrabromocatecholato)-phenylsilicate (1f**)**

To a stirred solution of tetrabromocatechol (2.0 mmol, 852 mg) in 10 mL of dry methanol was added 18-C-6 (1.0 mmol, 264 mg). After dissolution of the crown ether, the phenyltrimethoxysilane (1.0 mmol, 187 μ L) was added, followed by a solution of potassium methoxide 3.36 M in methanol (1.0 mmol, 294 μ L). The reaction mixture was stirred for 3 hours and the solvent was removed under reduced pressure. The residue was dissolved in the minimum volume of acetone and diethyl ether was added until a cloudy solution was obtained (scrapping on the edge of the flask could be done to induce crystallization). The flask was placed at -20°C overnight. The crystals were collected by filtration, washed with diethyl ether and dried under vacuum to afford potassium [18-Crown-6] bis(tetrabromocatecholato)-phenylsilicate (**1f**) (1.064 mg, 84%).

$^1\text{H NMR}$ (400 MHz, Acetone- d_6): δ 7.74-7.71 (m, 2H), 7.24-7.21 (m, 3H), 3.62 (s, 24H);

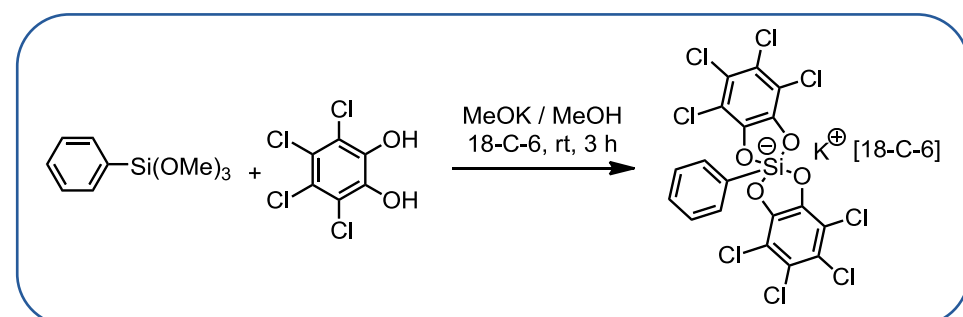
$^{13}\text{C NMR}$ (100 MHz, Acetone- d_6): δ 149.8 (4C), 138.6, 136.5 (4C), 130.0, 128.1 (4C), 115.2 (2C), 106.9 (2C), 70.8 (12C);

$^{29}\text{Si NMR}$ (79 MHz, Acetone- d_6) : δ -85.8;

HRMS: calc. for $[\text{C}_{18}\text{H}_5\text{Br}_8\text{O}_4\text{Si}]^-$: 952.3352; found:952.3358;

IR (neat): 2882, 1536, 1445, 1347, 1218, 1100, 944, 702, 678, 599 cm^{-1} ;

M.P. 266°C .

Potassium [18-Crown-6] bis(tetrachlorocatecholato)-phenylsilicate (1g**)**

To a stirred solution of tetrachlorocatechol (5.0 mmol, 1.239 g) in 25 mL of dry methanol was added 18-C-6 (2.5 mmol, 660 mg). After dissolution of the crown ether, the phenyltrimethoxysilane (2.5 mmol, 466 μ L) was added, followed by a solution of potassium methoxide 3.56 M in methanol (2.5 mmol, 700 μ L). The reaction mixture was stirred for 3 hours and the solvent was removed under reduced pressure. The residue was dissolved in the minimum volume of acetone and diethyl ether was added until a cloudy solution was obtained (scrapping on the edge of the flask could be done to induce crystallization). The flask was placed at -20°C overnight. The crystals were collected by filtration, washed with diethyl ether and dried under vacuum to afford potassium [18-Crown-6] bis(tetrachlorocatecholato)-phenylsilicate (**1g**) (810 mg, 36%).

$^1\text{H NMR}$ (400 MHz, Methanol- d_4): δ 7.51-7.49 (m, 2H), 7.29-7.24 (m, 3H), 3.51 (s, 24H);

$^{13}\text{C NMR}$ (100 MHz, DMSO- d_6): δ 146.4 (4C), 136.8, 134.5 (4C), 129.4, 127.6 (4C), 119.5 (2C), 113.3 (2C), 69.3 (12C);

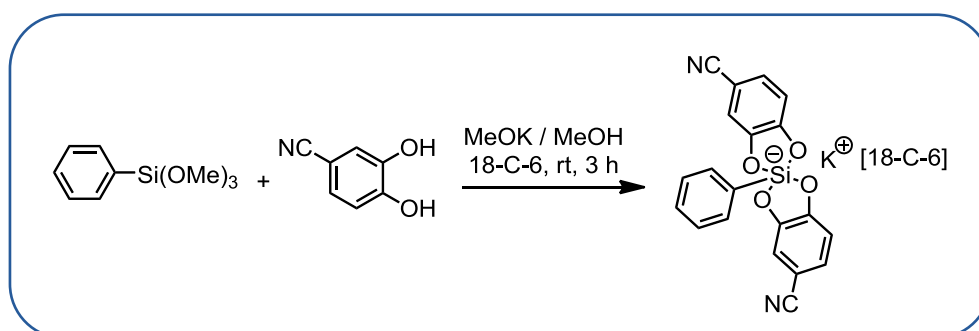
$^{29}\text{Si NMR}$ (79 MHz, DMSO- d_6): δ -84.0;

HRMS: calc. for $[\text{C}_{18}\text{H}_5\text{Cl}_8\text{O}_4\text{Si}]^-$: 594.7441; found:594.7428;

IR (neat): 2894, 1597, 1497, 1327, 1105, 1067, 963, 823, 733, 701 cm^{-1} ;

M.P. 246°C .

Potassium [18-Crown-6] bis(4-cyanocatecholato)-phenylsilicate (**1h**)



To a stirred solution of appropriate 4-cyanocatechol (5.0 mmol, 676 mg) in 25 mL of dry methanol was added 18-C-6 (2.5 mmol, 660 mg). After dissolution of the crown ether, the phenyltrimethoxysilane (2.5 mmol, 466 μ L) was added, followed by a solution of potassium methoxide in methanol (2.5 mmol, 700 μ L). The reaction mixture was stirred for 3 hours and the solvent was removed under reduced pressure. The residue was dissolved in the minimum volume of acetone and diethyl ether was added until a cloudy solution was obtained (scrapping on the edge of the flask could be done to induce crystallization). The flask was placed at -20°C overnight. The crystals were collected by filtration, washed with diethyl ether

and dried under vacuum to afford potassium [18-Crown-6] bis(4-cyanocatecholato)-phenylsilicate (**1h**) (1.37g, 81 %) as a mixture of two isomers.

¹H NMR (400 MHz, Methanol-d₄): δ 7.58-7.55 (m, 2H), 7.25-7.19 (m, 3H), 7.13-7.09 (m, 2H), 7.03 (m, 2H), 6.89-6.86 (m, 2H), 3.65 (s, 24H);

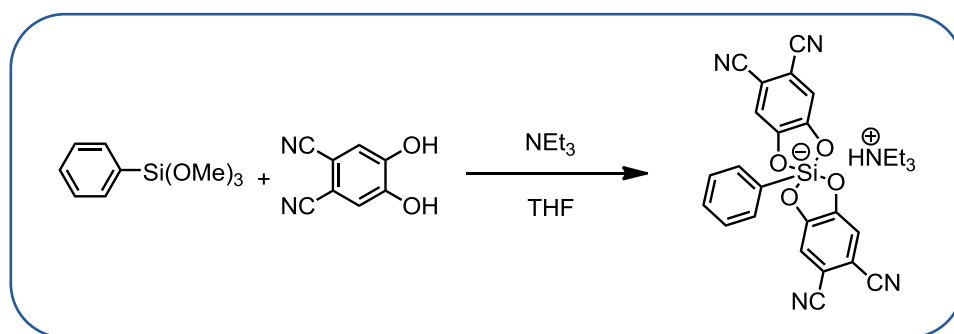
¹³C NMR (100 MHz, Methanol-d₄): δ 155.4 (2C), 154.9 (2C), 150.2 (2C), 149.7 (2C), 139.2 (2C), 134.6 (2C), 135.5 (2C), 128.6 (2C), 127.1 (4C), 125.1 (2C), 124.6 (2C), 120.4 (4C), 112.4 (2C), 112.2 (2C), 110.8 (2C), 110.7 (2C), 99.4 (2C), 98.9 (2C), 69.3(12C);

²⁹Si NMR (79 MHz, Methanol-d₄): δ -85.3;

HRMS: calc. for [C₂₀H₁₁N₂O₄Si]⁻: 371.0488; found: 371.0495;

M.P. 147°C.

Triethylammonium bis(4,5-dihydroxyphthalonitrile catecholato)-phenylsilicate (**1i**)



To a stirred solution of 4,5-dihydroxyphthalonitrile (0.9 mmol, 145mg) in 4.5 mL of dry THF added phenyltrimethoxysilane (0.45 mmol, 84 μL) and NEt₃ (2.1 mmol, 300 μL). The reaction mixture was stirred for 20 hours at reflux and the solvent was removed under reduced pressure. The residue was dissolved in the minimum volume of acetone and diethyl ether (+ pentane) was added until a cloudy solution was obtained (scrapping on the edge of the flask could be done to induce crystallization). The flask was placed at -20°C overnight. The crystals were collected by filtration, washed with diethyl ether and dried under vacuum to afford triethylammonium bis(4,5-dihydroxyphthalonitrile catecholato)-phenylsilicate (**1i**) (140 mg, 59%).

¹H NMR (400 MHz, DMSO-d₆): δ 7.46-7.43 (m, 2H), 7.38 (s, 4H), 7.28-7.21 (m, 3H), 3.09 (bs, 6H), 1.17 (bs, 9H);

¹³C NMR (100 MHz, DMSO-d₆): δ 154.1 (4C), 137.3, 134.2 (2C), 129.2, 127.5 (2C), 117.0 (4C), 114.6 (4C), 105.4 (4C), 45.8 (3C), 8.6 (3C);

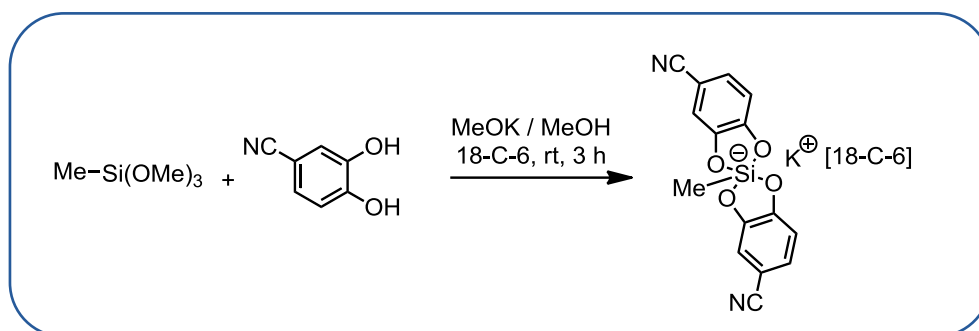
^{29}Si NMR (79 MHz, DMSO- d_6): δ -83.5;

HRMS: calc. for $[\text{C}_{22}\text{H}_9\text{N}_4\text{O}_4\text{Si}]^-$: 421.0399; found: 421.0396;

IR (neat): 3107, 2225, 1589, 1493, 1373, 1290, 1092, 876, 856, 737, 682, 596 cm^{-1} ;

M.P. 241°C.

Potassium [18-Crown-6] bis(4-cyanocatecholato)-methylsilicate



To a stirred solution of appropriate 4-cyanocatechol (5.0 mmol, 676 mg) in 10 mL of dry methanol was added 18-C-6 (2.5 mmol, 660 mg). After dissolution of the crown ether, the methyltrimethoxysilane (2.5 mmol, 356 μL) was added, followed by a solution of potassium methoxide in methanol (2.5 mmol, 700 μL). The reaction mixture was stirred for 3 hours and the solvent was removed under reduced pressure. The residue was dissolved in the minimum volume of acetone and diethyl ether was added until a cloudy solution was obtained (scrapping on the edge of the flask could be done to induce crystallization). The flask was placed at -20°C overnight. The crystals were collected by filtration, washed with diethyl ether and dried under vacuum to afford potassium [18-Crown-6] bis(4-cyanocatecholato)-methylsilicate (200 mg, 13%) as a mixture of two isomers.

^1H NMR (400 MHz, Acetone- d_6): δ 6.99-6.89 (m, 2H), 6.85-6.78 (m, 2H), 6.68-6.59 (m, 2H), 3.65 (s, 24H), 0.1 (s, 3H);

^{13}C NMR (100 MHz, Acetone- d_6): δ 157.3, 156.6, 155.8, 152.0, 151.3, 149.6, 125.5 (2C), 124.8 (2C), 124.7 (2C), 121.3, 121.2, 121.1, 117.6, 116.7, 113.01 (2C), 112.8 (2C), 111.3 (2C), 111.2 (2C), 100.4, 99.6, 99.5, 70.8 (12C), 0.5, 0.4;

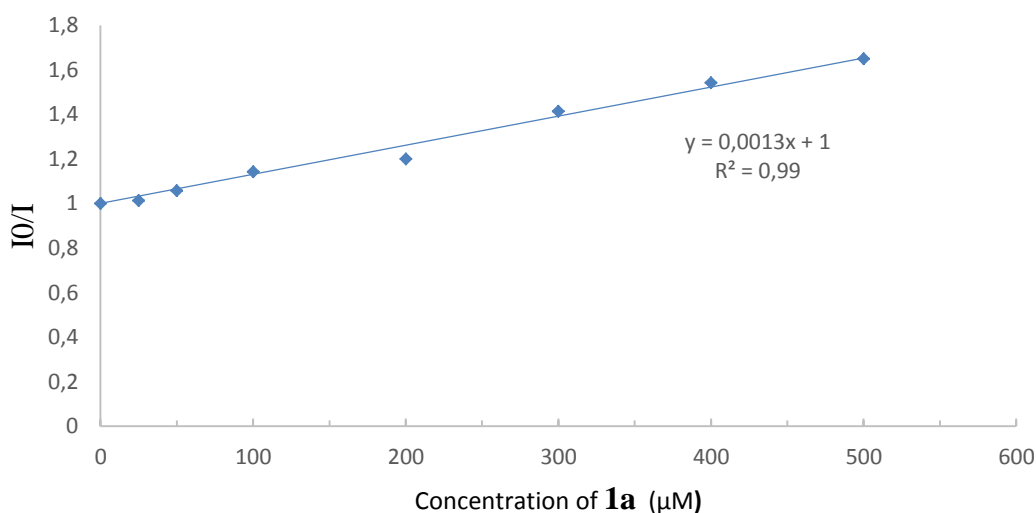
^{29}Si NMR (79 MHz, Acetone- d_6): δ -71.7;

1.2.6.4. Stern-Volmer experiments

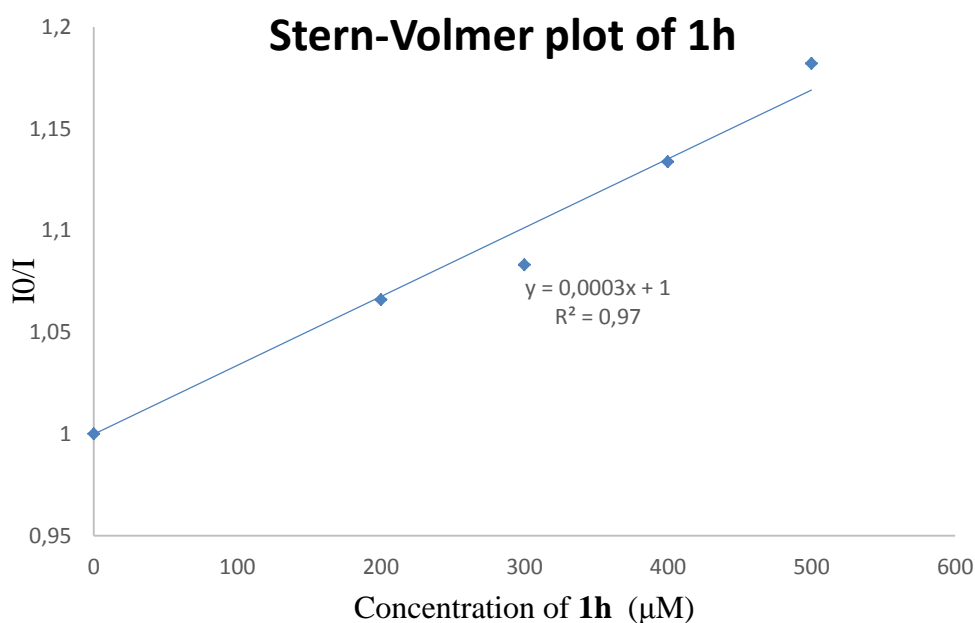
Emission intensities were recorded on a Jasco FP-6200 spectrofluorometer. Dry DMF was degassed by freeze-pump-thaw cycles before using. The photocatalyst [Ir] was excited at 436 nm and the emission spectra were recorded between 470 and 700 nm. In a typical experiment, 10 μM solutions of [Ir] in DMF were prepared with the appropriate concentration of quencher **1a** and **1h** a 1.0 cm quartz cuvette and covered. After degassing with a stream of argon for 10 minutes, the emission spectrum of the sample was recorded. The Stern-Volmer plot was done according the following equation: $\frac{I_f^0}{I_f} = 1 + k_q t_0 \cdot [Q]$.

A quenching constant of $5,7 \cdot 10^8 \text{ mol}^{-1} \cdot \text{L} \cdot \text{s}^{-1}$ for **1a** and of $1.31 \cdot 10^8 \text{ mol}^{-1} \cdot \text{L} \cdot \text{s}^{-1}$ for **1h**.

Stern-Volmer plot of 1a



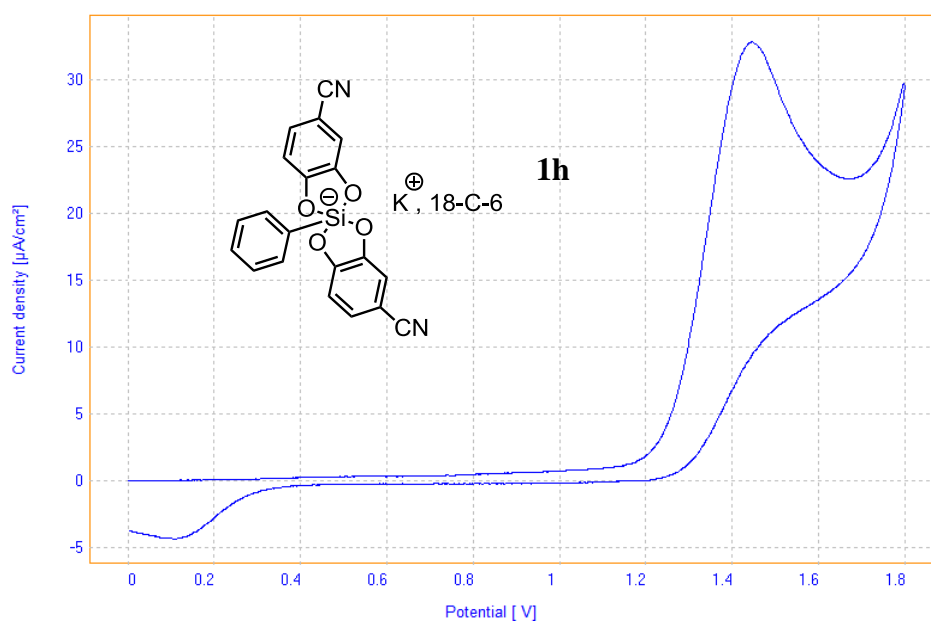
Stern-Volmer plot of 1h



1.2.6.5. Electrochemical measurements

The voltammetric measurement was recorded in a three electrodes cell in degassed DMF with Bu_4NPF_6 (0.1 M) as support electrolyte at 22°C ([Silicate] = 0.01 M). Measurements were monitored with an AutoLab PSTAT10 electrochemical workstation. Cyclic voltammetry (CV) was used to estimate the half-wave oxidation potential. The CVs were obtained with a step potential of 0.9 mV at a scan rate of 0.1 $\text{V}\cdot\text{s}^{-1}$. Glassy carbon (diameter = 2 mm), platinum plate, and saturated calomel were used as working, counter, and reference electrodes, respectively.

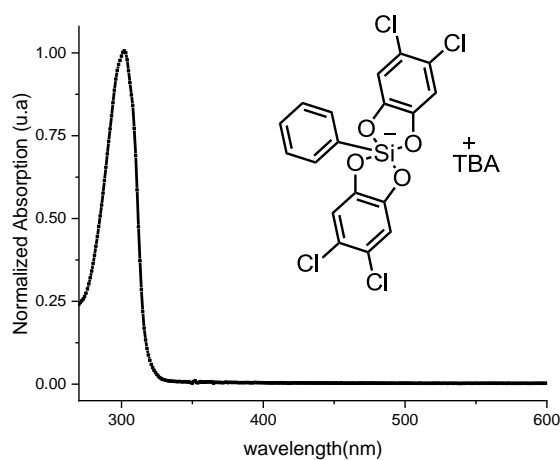
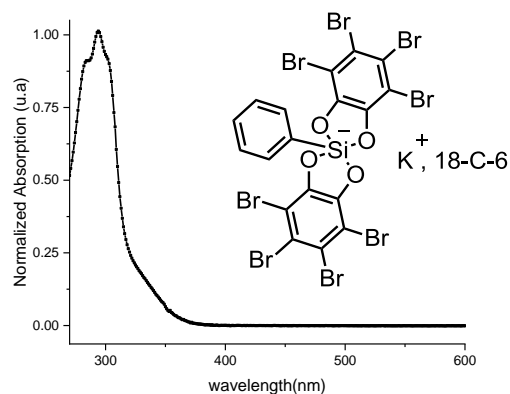
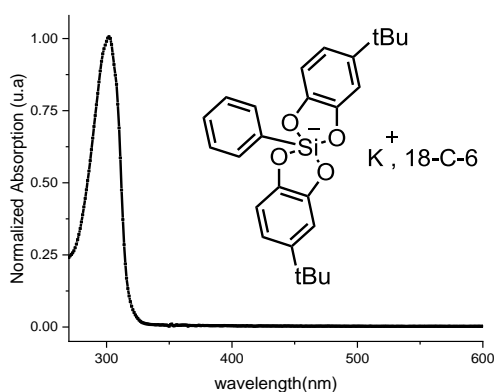
Silicate	$E_{1/2}^{ox}$ (vs. SCE in DMF)
1a	+ 0.89 V
1b	+ 0.81 V
1c	+ 1.09 V
1d	+ 1.05 V
1e	+ 1.13 V
1f	+ 1.46 V
1g	+ 1.37 V
1h	+ 1.33 V
1i	+ 1.62 V



Example of cyclic voltammetry:**1h**

1.2.6.6. Spectroscopic analyses

Absorption spectra of molecules were recorded at 25°C on a Cary 300 UV/Vis spectrophotometer (Agilent Technologies, Santa Clara, CA), equipped with a Peltier thermostated cell holder (t2x2 Sport/Cary300, Quantum Northwest, Liberty Lake, WA). The samples were placed in 2 mL quartz cuvettes (1 cm × 1 cm light path; Hellma Optics, Jena, Germany). The UV spectrums were investigated in DMF ($C = 1.6 \cdot 10^{-4} \text{ mol.L}^{-1}$).



1.2.7. References

- ¹ a) V. Corcé, L.-M. Chamoreau, E. Derat, J.-P. Goddard, C. Ollivier, L. Fensterbank, *Angew. Chem. Int. Ed.* **2015**, *54*, 11414; *Angew. Chem.* **2015**, *127*, 11576; b) A. Cartier, E. Levernier, V. Corcé, T. Fukuyama, A.-L. Dhimane, C. Ollivier, I. Ryu, L. Fensterbank, *Angew. Chem. Int. Ed.* **2019**, *58*, 1789; *Angew. Chem. Int. Ed.* **2019**, *131*, 1803; c) M. Jouffroy, D. N. Primer, G. A. Molander, *J. Am. Chem. Soc.* **2016**, *138*, 475; d) B. A. Vara, M. Jouffroy, G. A. Molander, *Chem. Sci.* **2017**, *8*, 530.
- ² a) J. P. Phelan, S. B. Lang, J. S. Compton, C. B. Kelly, R. Dykstra, O. Gutierrez, G. A. Molander, *J. Am. Chem. Soc.* **2018**, *140*, 8037; b) N. R. Patel, C. B. Kelly, A. P. Siegenfeld, G. A. Molander, *ACS Catal.* **2017**, *7*, 1766; c) T. Guo, L. Zhang, X. Liu, Y. Fang, X. Jin, Y. Yang, Y. Li, B. Chen, M. Ouyang, *Adv. Synth. Catal.* **2018**, *360*, 4459; d) R. J. Wiles, G. A. Molander, *Isr. J. Chem.* **2020**, *60*, 281.
- ³ a) C. Lévêque, L. Chennenberg, V. Corcé, J.-P. Goddard, C. Ollivier, L. Fensterbank, *Org. Chem. Front.* **2016**, *3*, 462; b) E. Levernier, V. Corcé, L.-M. Rakotoarison, A. Smith, M. Zhang, S. Ognier, M. Tatoulian, C. Ollivier, L. Fensterbank, *Org. Chem. Front.* **2019**, *6*, 1378; c) N. R. Patel, C. B. Kelly, M. Jouffroy, G. A. Molander, *Org. Lett.* **2016**, *18*, 764; d) M. Jouffroy, C. B. Kelly, G. A. Molander, *Org. Lett.* **2016**, *18*, 876; e) J. P. Phelan, S. B. Lang, J. Sim, S. Berritt, A. K. Peat, K. Billings, L. Fan, G. A. Molander, *J. Am. Chem. Soc.* **2019**, *141*, 3723; f) J. K. Matsui, S. B. Lang, D. R. Heitz, G. A. Molander, *ACS Catal.* **2017**, *7*, 2563; g) K. Lin, R. J. Wiles, C. B. Kelly, G. H. M. Davies, G. A. Molander, *ACS Catal.* **2017**, *7*, 5129; h) B. A. Vara, X. Li, S. Berritt, C. R. Walters, E. J. Petersson, G. A. Molander, *Chem. Sci.* **2018**, *9*, 336; i) S. O. Badir, J. Sim, K. Billings, A. Csakai, X. Zhang, W. Dong, G. A. Molander, *Org. Lett.* **2020**, *22*, 1046.
- ⁴ a) W. M. Seganish, P. DeShong, *J. Org. Chem.* **2004**, *69*, 1137; b) W. M. Seganish, P. DeShong, *Org. Lett.* **2004**, *5*, 4379.
- ⁵ S. Witzel, K. Sekine, M. Rudolf, S. K. Hashmi, *Chem. Commun.* **2018**, *54*, 13802.
- ⁶ For a general revue on radical precursor in reduction see: I. Ghosh, L. Marzo, A. Das, R. Shaikh, B. König, *Acc. Chem. Res.* **2016**, *49*, 1566. For a revue on diazoniums see: F. Mo, G. Dong, Y. Zhang, J. Wang, *Org. Biomol. Chem.* **2013**, *11*, 1582. a) T. Hering, D. P. Hari, B. König, *J. Org. Chem.* **2012**, *77*, 10347; b) Z. Xia, O. Khaled, V. Mouriès-Mansuy, C. Ollivier, L. Fensterbank, *J. Org. Chem.* **2016**, *81*, 7182; c) D. P. Hari, T. Hering, B. König, *Org. Lett.* **2012**, *14*, 5334; d) P. Maity, D. Kundu, B. C. Ranu, *Eur. J. Org. Chem.* **2015**, *2015*, 1727; e) J. Zhang, J. Chen, X. Zhang, X. Lei, *J. Org. Chem.* **2014**, *79*, 10682.
- ⁷ a) E. A. Merritt, B. Olofsson, *Angew. Chem. Int. Ed.* **2009**, *48*, 9052; b) A. Baralle, L. Fensterbank, J. P. Goddard, C. Ollivier, *Chem. Eur. J.* **2013**, *19*, 10809.
- ⁸ a) G. B. Deng, Z. Q. Wang, J. D. Xia, P. C. Quian, R. J. Song, M. Hu, L. B. Gong, J. H. Li, *Angew. Chem. Int. Ed.* **2013**, *52*, 1535; *Angew. Chem. Int. Ed.* **2013**, *125*, 1575; b) P. Natarajan, A. Bala, S. K. Mehta, K. K. Bhasin, *Tetrahedron* **2016**, *72*, 2521; c) J. D. Xia, G. B. Deng, M. B. Zhou, W. Liu, P. Xie, J. H. Li, *Synlett.* **2012**, *23*, 2707.
- ⁹ a) E. H. Discekici, N. J. Treat, S. O. Poelma, K. M. Mattson, Z. M. Hudson, Y. D. Luo, C. J. Hawker, J. R. de Alaniz, *Chem. Commun.* **2015**, *51*, 11705; b) I. Ghosh, B. König, *Angew. Chem. Int. Ed.* **2016**, *55*, 7676; *Angew. Chem. Int. Ed.* **2016**, *128*, 7806; c) M. Majek, U. Faltermeier, B. Dick, R. Perez-Ruiz, Jacobi vonWangelin, *Chem. Eur. J.* **2015**, *21*, 15496.
- ¹⁰ L. Candish, M. Freitag, T. Gensch, F. Glorius, *Chem. Sci.* **2017**, *8*, 3618.
- ¹¹ S. Kubosaki, H. Takeuchi, Y. Iwata, Y. Tanaka, K. Osaka, M. Yamawaki, T. Morita, Y. Yoshimi, *J. Org. Chem.* **2020**, *85*, 5362.
- ¹² a) C. L. Frye, *J. Am. Chem. Soc.* **1964**, *86*, 3170; b) G. Cerveau, C. Chuit, R. J. P. Corriu, L. Gerbier, C. Reye, J. L. Aubagnac, B. El Amrani, *Int. J. Mass. Spectrom. Ion Phys.* **1988**, *82*, 259;

- c) V. Corcé, C. Lévêque, C. Ollivier, L. Fensterbank, *Science of Synthesis: Photocatalysis in Organic Synthesis* **2019**, 427.
- ¹³ D. Hanss, J. C. Freys, G. Bernardinelli, O. S. Wenger, *Eur. J. Inorg. Chem.* **2009**, 2009, 4850.
- ¹⁴ a) C. L. Frye, *J. Am. Chem. Soc.* **1964**, 86, 3170; b) K. Lin, C. B. Kelly, M. Jouffroy, G. A. Molander, *Org. Synth.* **2017**, 94, 16.
- ¹⁵ The structures were deposited at the Cambridge Crystallographic Data Centre with numbers 2009048 (**1h**); 2009049 (**1d**); 2009050 (**1b**) and can be obtained free of charge via www.ccdc.cam.ac.uk.
- ¹⁶ R. J. Abraham, D. S. Ribeiro, *J. Chem. Soc. Perkin. Trans.* **2001**, 2, 302.
- ¹⁷ a) A. R. Bassindale, M. Sohail, P. G. Taylor, A. A. Korlyukov, D. E. Arkhipov, *Chem. Commun.* **2010**, 46, 3274; b) D. Kost, I. Kalikhman, *Acc. Chem. Res.* **2009**, 42, 303.
- ¹⁸ A. G. Larsen, A. H. Holm, M. Roberson, K. Daasbjerg, *J. Am. Chem. Soc.* **2001**, 123, 1723.
- ¹⁹ C. Lévêque, L. Chenneberg, V. Corcé, C. Ollivier, L. Fensterbank, *Chem. Commun.* **2016**, 52, 9877.
- ²⁰ J. Zhou, P.S. Mariano, *Photochem. Photobiol. Sci.* **2008**, 7, 3936404.
- ²¹ K. Ohkubo, K. Mizushima, R. Iwata, K. Souma, N. Suzuki, S. Fukuzumi, *Chem. Commun.* **2010**, 46, 601.
- ²² L. Chenneberg, C. Lévêque, V. Corcé, A. Baralle, J. P. Goddard, C. Ollivier, L. Fensterbank, *Synlett* **2016**, 27, 731.
- ²³ a) D. Matsuoka, Y. Nishigaichi, *Chem. Lett.* **2015**, 44, 163; b) Y. Nishigaichi, A. Suzuki, T. Saito, A. Takuwa, *Tetrahedron Lett.* **2005**, 46, 5149; c) Y. Nishigaichi, A. Suzuki, A. Takuwa, *Tetrahedron Lett.* **2007**, 48, 211.
- ²⁴ T. A. Halgren, J. L. Firkins, T. A. Fujimoto, H. H. Suzukawa, J. D. Roberts, *Proc. Natl. Acad. Sci. USA.* **1971**, 68, 3216.
- ²⁵ a) A. Kumar, M. D. Sevilla, *J. Phys. Chem. B* **2017**, 122, 98; b) G. Gryn'ova, M. L. Coote, *J. Am. Chem. Soc.* **2013**, 135, 15392; c) G. Gryn'ova, D. L. Marshall, S. J. Blanksby, M. L. Coote, *Nature Chem.* **2013**, 5, 474.
- ²⁶ D. Matsuoka, Y. Nishigaichi, *Chem. Lett.* **2015**, 44, 163.
- ²⁷ G. Sorin, R. M. Mallorquin, Y. Contie, A. Baralle, M. Malacria, J. P. Goddard, L. Fensterbank, *Angew. Chem. Int. Ed.* **2010**, 49, 8721; *Angew. Chem.* **2010**, 122, 8903.
- ²⁸ J. I. Yoshida, K. Tamao, T. Kakul, A. Kurita, M. Murata, K. Yamada, M. Kumada, *Organometallics* **1982**, 1, 369.
- ²⁹ G. R. Fulmer, A. J. M. Miller, N. H. Sherden, H. E. Gottlieb, A. Nudelman, B. M. Stolz, J. E. Bercaw, K. I. Goldberg, *Organometallics* **2010**, 29, 2176.
- ³⁰ E. Jürgens, B. Wucher, F. Rominger, K. W. Törnroos, D. Kunz, *Chem. Commun.* **2015**, 51, 1897.

**- Chapter II -
Photoredox/transition metal
dual catalysis as an efficient
synthetic tool**

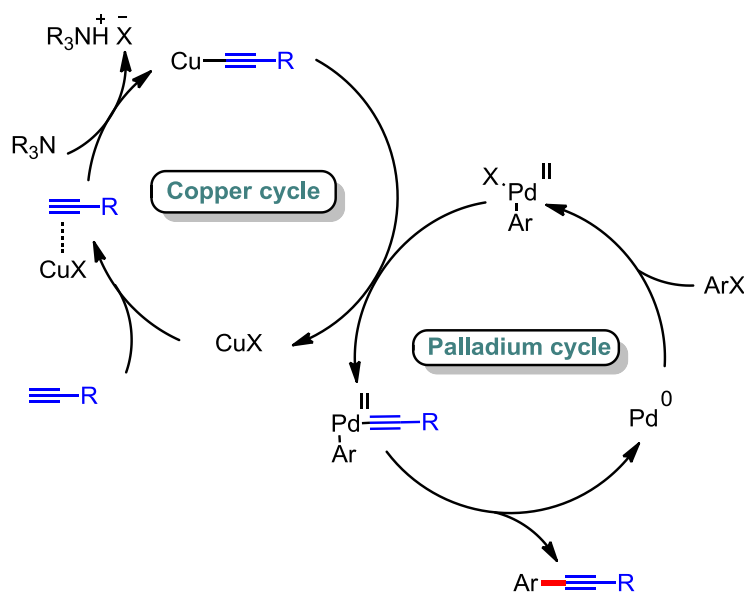
Chapter II. Photoredox/transition metal dual catalysis as an efficient synthetic tool

After this introduction about photoredox catalysis, we can focus our attention on other radical reactions. Indeed, dual catalysis can be an efficient way to functionalize radicals by merging radical chemistry and organometallic catalysis.

II.1. Definition and genesis of dual catalysis

Over the last century, a new way of forging C-C bond based on palladium/copper dual catalysis has emerged with the pioneering work of Sonogashira, Tohda and Hagihara.¹ This well-known cross-coupling reaction between a terminal alkyne and an aryl halide can illustrate the concept of “dual catalysis” or “concurrent tandem catalysis”.

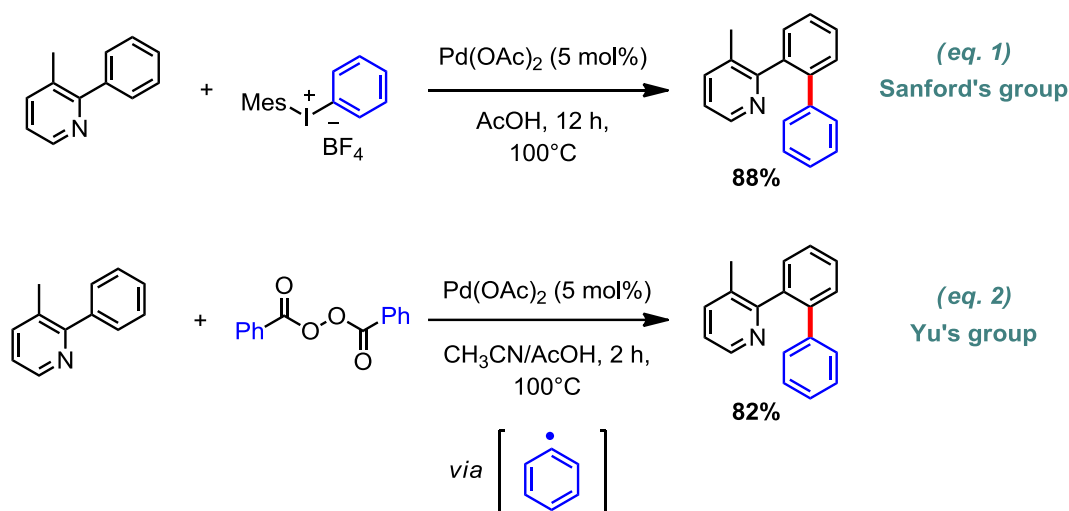
In its mechanism, two catalytic cycles work concomitantly to produce the desired product. The copper catalyst, which facilitates the deprotonation of the alkyne by the amine, produces an alkynyl copper(I). Then, this nucleophilic species reacts with the Pd(II) intermediate, resulting from the oxidative addition of the aryl halide onto the Pd(0) complex, through a transmetalation reaction. At the end, a reductive elimination releases the product and regenerates the palladium catalyst (**Scheme 1**). The copper and the palladium cycles cannot work independently and, if a problem occurs in one of them, the other one immediately stops.



Scheme 1: Mechanism of the Sonogashira reaction

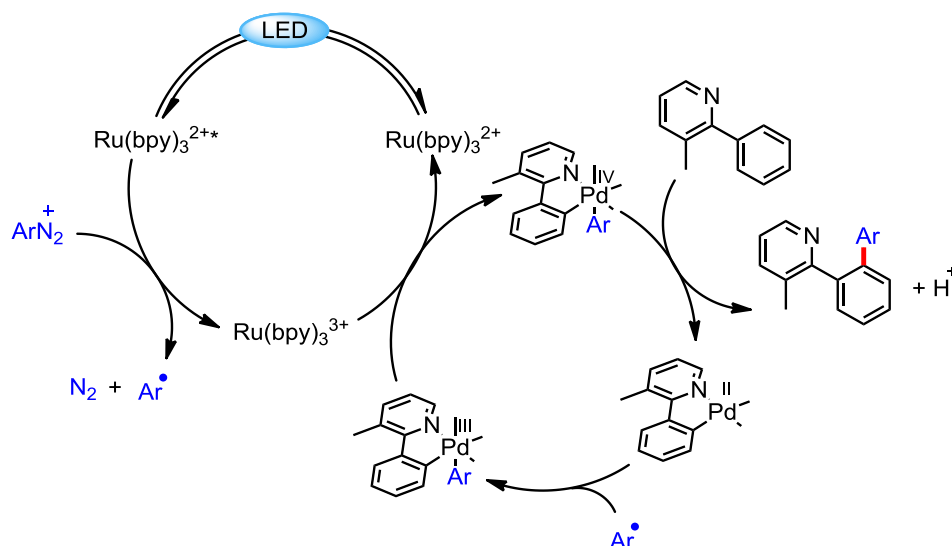
This concept, merging two organometallic cycles, has been largely used over the past years. However, what about combining a photocatalytic cycle for the generation of radicals and a transition metal cycle?

In 2009, Sanford's group demonstrated that C-H functionalization of arylpyridines was possible thermally with diaryl iodonium salts (**Scheme 2, eq. 1**).² The same year, Yu *et al.* reported the same reaction but with benzoyl peroxide which involves the generation of an aryl radical (**Scheme 2, eq. 2**).³



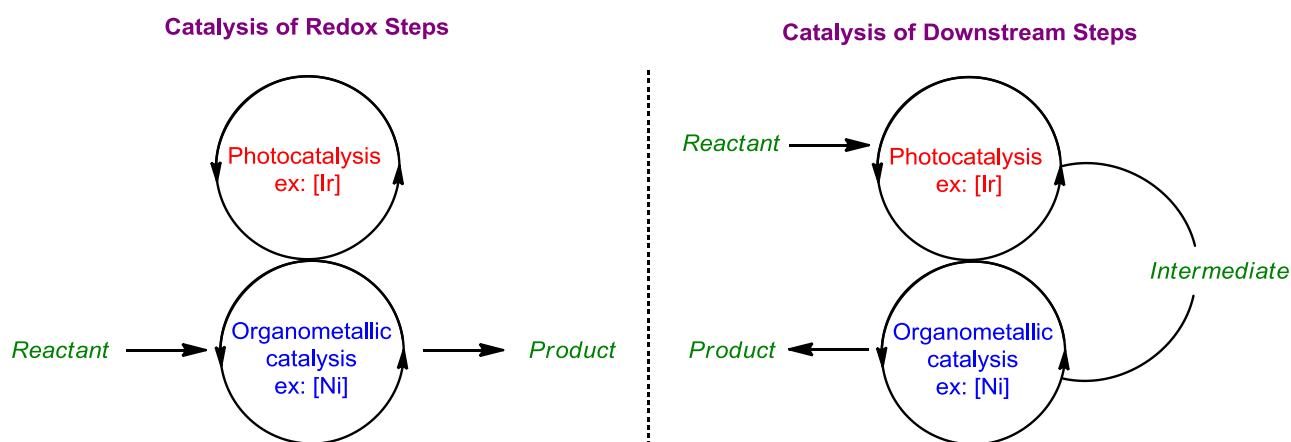
Scheme 2: Thermally activated C-H arylation of phenylpyridine with diaryl iodonium salts (*eq. 1*) and benzoyl peroxide (*eq. 2*)

Two years later, inspired by the above mentioned publications, Sanford *et al.* published the first example of photoredox/transition metal dual catalysis.⁴ In this study an aryl radical, formed by the reduction of a diazonium salt, is trapped by a palladium catalyst to achieve a cross-coupling reaction with a phenylpyridine-based substrate. Regarding the mechanism, at first, the palladium catalyst performs a CH insertion. Then, the aryl radical adds to the palladium(II) catalyst to produce a palladium(III) complex. The latter is further oxidized by the ruthenium(III) photocatalyst to palladium(IV) with the concomitant regeneration of the photocatalyst. Finally, a reductive elimination releases the desired product and regenerates the palladium catalyst (**Scheme 3**).



Scheme 3: CH arylation using a dual catalysis system

After that, many different groups all over the world applied this combination of photoredox catalysis and organometallic catalytic cycle to develop new reactions. In this context, two different ways of realizing dual catalysis can be distinguished (**Scheme 4**).



Scheme 4: Different ways of achieving dual catalysis

In the **Catalysis of Redox Steps**, the main objective of the photocatalyst is to regenerate the organometallic catalyst whereas in the **Catalysis of Downstream Steps** the radical intermediate, formed by the photocatalysis cycle, fuels the organometallic cycle.

II.2. Utilization of different metals and radical precursors

Over the last decade, many publications using both principles have been published. Gold, copper, chromium, nickel, cobalt and others, replaced the palladium catalyst and a large variety of radical precursors have been used.

Among them, we can distinguish two different families: those using a photoreductive process with an organometallic catalytic cycle, as in the previous example with palladium, and those using a photooxidative process with an organometallic catalytic cycle.

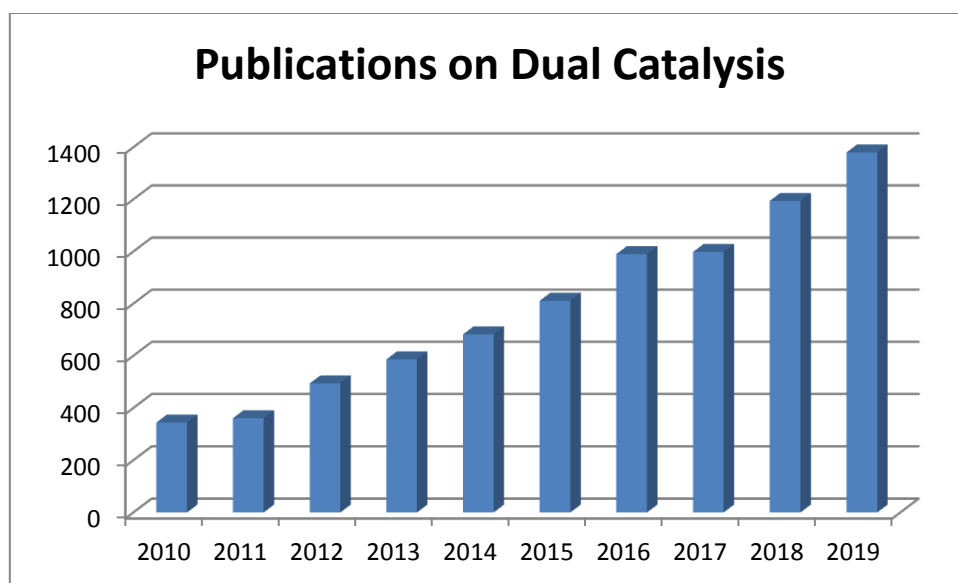


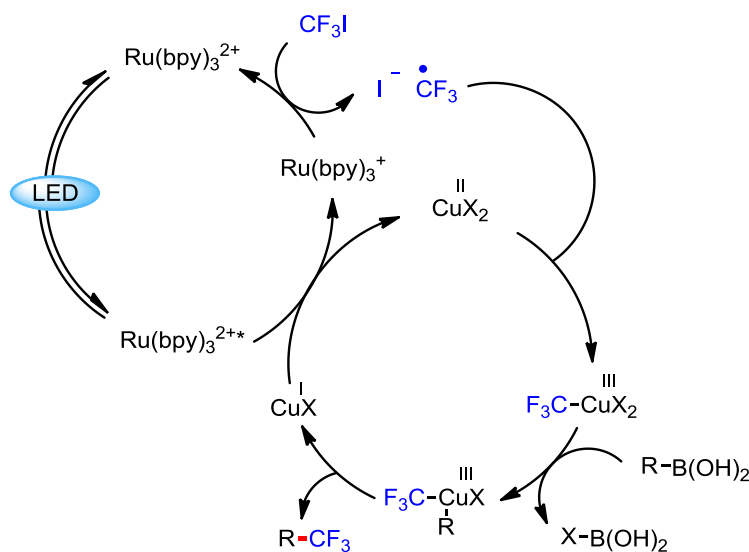
Figure 1: Number of publications about dual catalysis over the years⁵

In the following part, due to the important number of publications that appeared over the last years about dual catalysis (**Figure 1**), only a small overview will be given on different systems using photoreductive conditions. Then, photooxidative processes, which have been the main focus of this PhD thesis, will be more developed.

II.2.1. Photoreduction and organometallic catalytic cycle

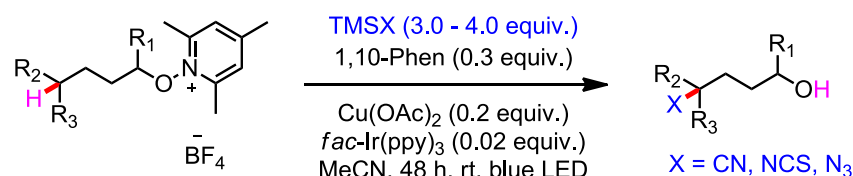
II.2.1.1. Copper catalysis

Copper(II) salts, widely used in Sonogashira reaction, for the reduction of diaryliodonium salts⁶ or the oxidation of trifluoroborates⁷ for instance, can also be used as a metal catalyst in a dual catalysis system. Indeed, one year after disclosing the palladium arylation reaction with diazonium salts, Sanford *et al.* reported a trifluoromethylation reaction of boronic acids by using the reducible CF_3I ($E^{\text{red}} = -1.22 \text{ V vs. SCE}$) and a ruthenium photocatalyst ($\text{Ru}(\text{bpy})_3\text{Cl}_2$: $E_{1/2}(\text{Ru}(\text{II})/\text{Ru}(\text{I})) = -1.37 \text{ V vs. SCE}$).⁸ Aryl boronic acids and heteroaryl boronic acids were efficiently converted to their trifluoromethylated analogs with a broad substrate scope. They proposed the following mechanism to explain the formation of the desired product. In a first step, CF_3I is reduced by the photocatalyst affording a trifluoromethyl radical that adds to the copper(II) catalyst. Subsequently, a transmetalation step occurs followed by a reductive elimination. Finally, both catalysts are regenerated by oxidation of the Cu(I) with the excited Ru(II) complex (**Scheme 5**).



Scheme 5: Trifluoromethylation of boronic acids

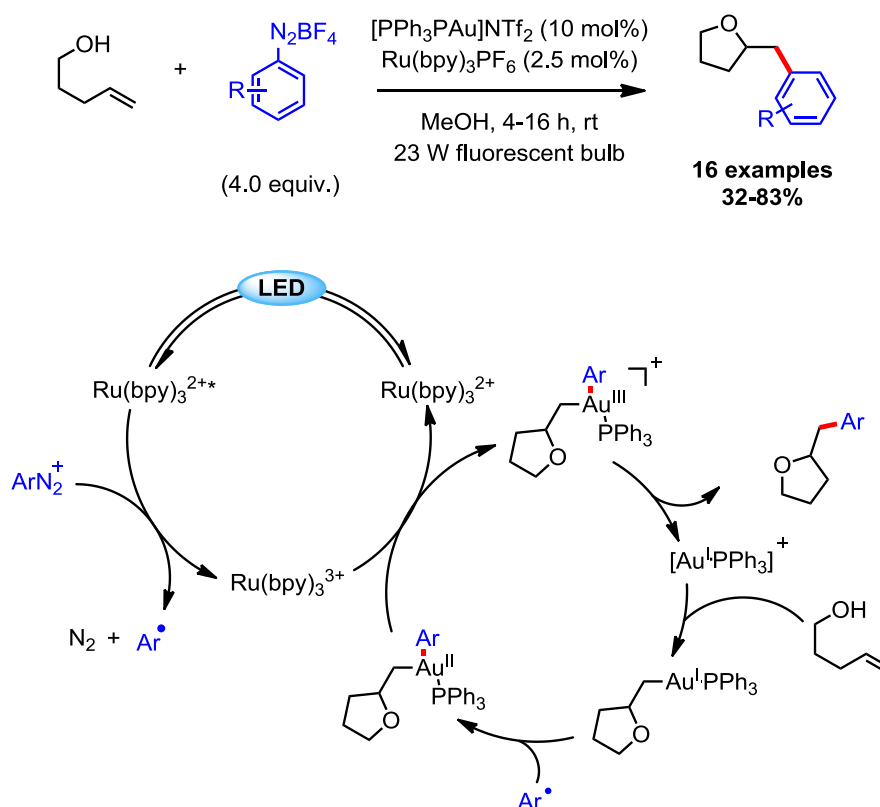
In 2019, Zhu utilized alkoxy pyridinium salts and silyl reagents to perform cyanation, thiocyanation and azidation of alcohols based on a dual copper/iridium system (**Scheme 6**).⁹ They envisioned that, thanks to the reduction of the pyridinium salt and fragmentation, an alkoxy radical was formed and, after a 1,5-HAT and copper catalysis, the desired product was obtained. These results illustrate the potential of the copper/photoredox dual catalysis and other groups, such as Yoon's or Chen's are currently studying the full implications of such processes.^{10,11}



Scheme 6: Use of alkoxy pyridinium salts and silyl reagents in a dual copper/iridium system

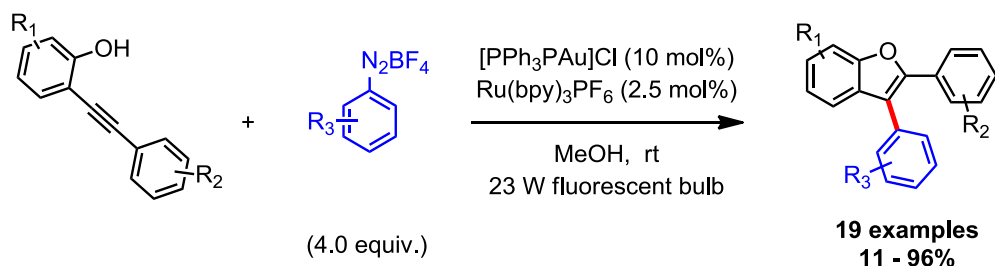
II.2.1.2. Gold dual catalysis

Copper catalysts are not the only ones which can be used concomitantly with a photoreductive cycle. In the last decades, gold catalysis has emerged as an interesting tool for synthetic chemists notably for the activation of unsaturated compounds. Moreover, this metal has also interesting reactivities toward radicals as demonstrated in 2006 by García's group. They disclosed an interesting generation of an organogold derivative by using benzyl radical and gold chloride.¹² Based on this principle, a few years later, Glorius and co-workers published the first gold/photoredox catalysis combination.¹³ They envisioned that an Au(II) complex, formed after addition of an aryl radical to a cyclic alkyl Au(I) intermediate, can be oxidized to an Au(III) complex by the Ru(III) catalyst. Finally, a reductive elimination releases the desired product. They utilized this oxy- and aminoarylation of alkenes strategy to produce a large variety of heterocycles in very good yields (**Scheme 7**).



Scheme 7: Oxyarylation of alkenes thanks to gold and ruthenium dual catalysis

Inspired by this idea, our group published a novel synthesis of benzofurans based on the arylation cyclization of *o*-alkynylphenols with aryldiazonium salts.¹⁴ This oxyarylation reaction performed well, presumably because of the high affinity of gold for the alkynes, and a large variety of benzofuran derivatives was obtained in high yields (**Scheme 8**).



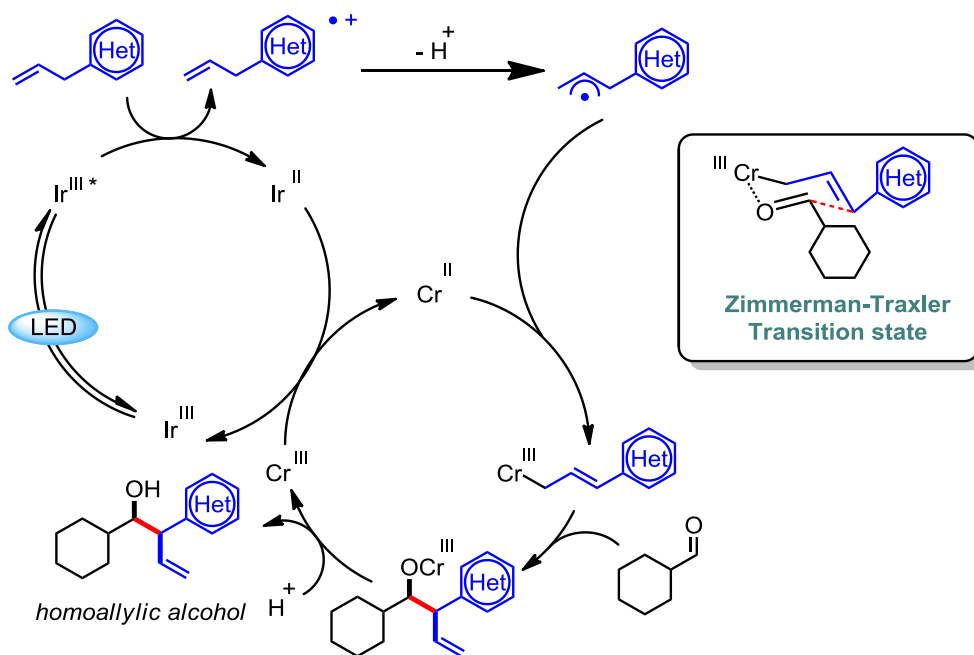
Scheme 8: Benzofuran synthesis thanks to ruthenium/gold dual catalysis

However, despite their interesting properties, gold catalysts remain relatively expensive and are mostly used with radical precursors in reduction. Because photooxidative radical generation remains an important part of photocatalysis, other metals were investigated and were found to induce cross-coupling reactions under related conditions. Selected examples in this respect are presented in the following section.

II.2.2. Photooxidation and organometallic catalytic cycle

II.2.2.1. Chromium dual catalysis

Even though chromium catalysts are quite toxic, some studies were published in the last decade to extend the aforementioned dual-catalysis systems. In 2018, Glorius's group reported a diastereoselective allylation of aldehydes by using a dual photoredox/chromium catalysis.¹⁵ Regarding the mechanism, they hypothesized that an allyl radical is formed after reductive quenching of the excited Ir(III) photocatalyst by an allyl(hetero-)arene and deprotonation. Then, this radical adds to the Cr(II) complex. Finally, this intermediate reacts with the aldehyde providing the homoallylic alcohol. The anti-selectivity obtained was best explained by invoking a Zimmerman-Traxler-type transition state (**Scheme 9**). A large variety of functional groups was tolerated and this methodology was even successfully applied to an Epiandrosterone derivative.



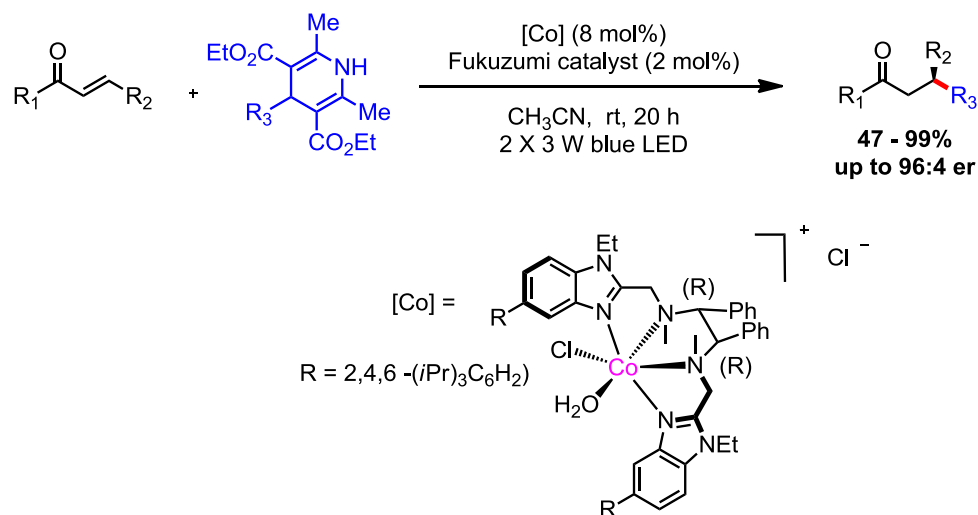
Scheme 9: Proposed catalytic cycle for the diastereoselective allylation of aldehydes

To broaden the impact of this work, the combination of radical trapping (resulting from the oxidation of a DHP derivative followed by addition onto a 1,3-diene) and allylation reaction, was also proved to work with a similar catalytic cycle to **Scheme 9**. It led to an interesting diastereoselective dialkylation of butadiene.¹⁶

However, in spite of these utilizations of some chromium catalysts, the use of this metal in dual catalysis systems remains anecdotal.

II.2.2.2. Cobalt dual catalysis

Cobalt catalysis can also be mixed with photoredox catalysis as reported by Xiao's group for enantioselective radical conjugate addition (**Scheme 10**). They used a chiral cobalt(II) complex to induce chirality thanks to its coordination to the carbonyl group of the radical acceptor and to regenerate the photocatalyst.¹⁷ The same year, cobalt dual catalysis has also been used by Kojima and Maji for alkene-alkyne coupling.¹⁸



Scheme 10: Enantioselective radical conjugate addition *via* cobalt photoredox dual catalysis

Additionally, in 2019, Breit's group developed an intermolecular reductive ene-yne coupling thanks to the Hantzsch ester (HE) and an iridium/cobalt dual catalysis system. The very mild conditions used stemmed from the ability of HE to perform both SET and HAT.¹⁹ Tunge *et al.* also showed that other radical precursors such as N-acyl amino acids could be competent substrates for this catalysis. Using this approach, they managed to efficiently synthesize some enamides.²⁰

II.2.2.3. Nickel dual catalysis

Despite other relevant publications, such as Wu's one on heterocycle synthesis²¹ or Matsunaga's one dealing with an allylic alkylation reaction,²² the most popular metal to achieve a cross-coupling reaction in a photooxidative dual catalysis system remains nickel (**Figure 2**).

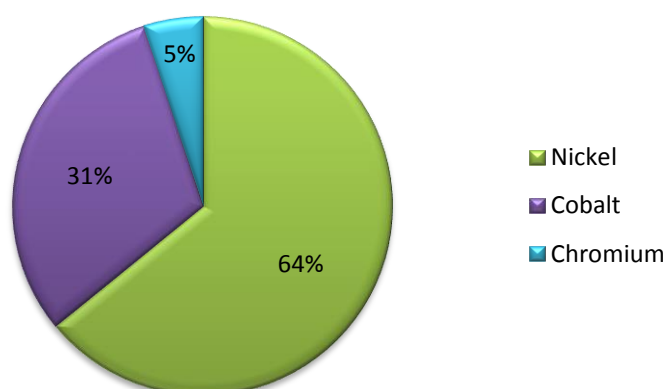
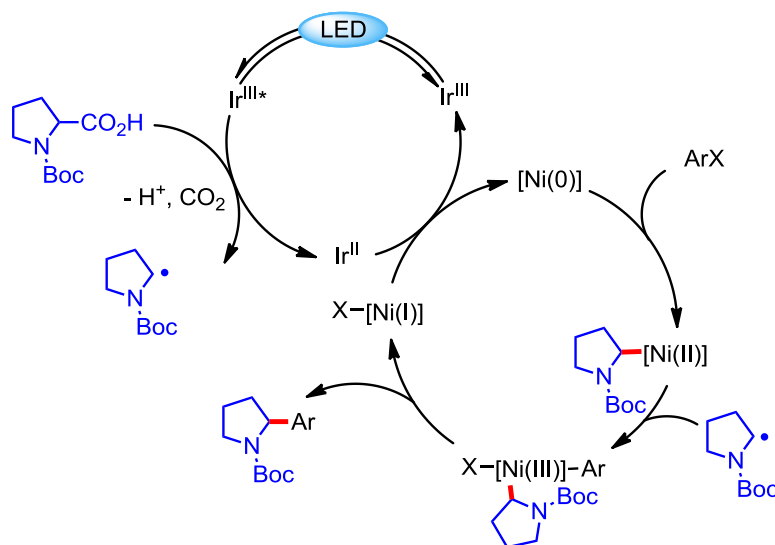


Figure 2: Proportion of each metal in photooxidative dual catalysis systems²³

Because nickel has almost exclusively been used for the design of new dual catalysis processes during this PhD thesis, the following part will describe more thoroughly the pre-existing body of literature that exists on that area.

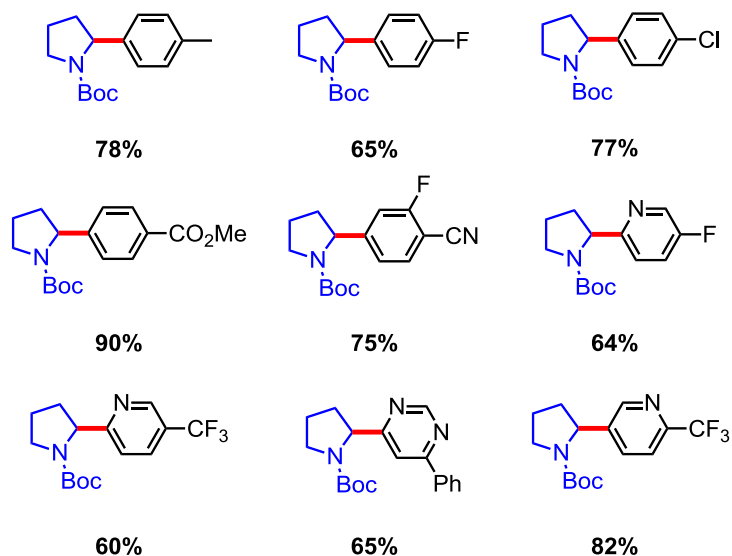
a) Genesis of the nickel dual catalysis

Seminal papers merging nickel and photoredox catalysis were published in 2014 by Doyle & MacMillan²⁴ and by Molander.²⁵ The former designed a system based on two interconnected catalytic cycles: the first one produces the radical and the second one promotes the cross-coupling reaction. For the generation of the radical, they used a decarboxylative pathway. They indeed anticipated that the activated Boc-protected proline-OH ($E_{1/2}^{ox} = +0.95$ V vs. SCE) releases CO_2 after being oxidized by a suitable excited photocatalyst. Then, the resulting radical reacts with the Ni(II) catalyst, formed after an oxidative addition of the aryl halide to the Ni(0) catalyst, producing a Ni(III) complex. Afterwards, the product is released thanks to a reductive elimination process. Finally, the two catalysts return to their ground state upon reduction of the Ni(I) to Ni(0) by the reduced photocatalyst (**Scheme 11**).



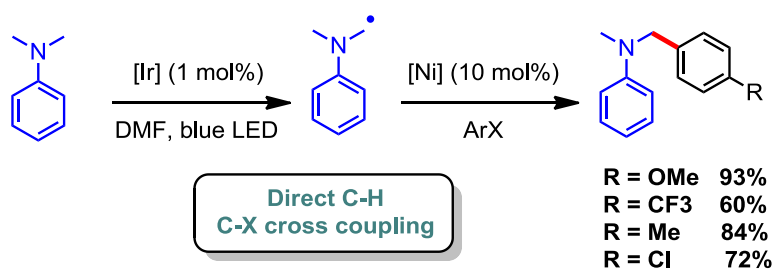
Scheme 11: Proposed mechanism for the coupling of Boc-protected prolines and heterocycles

The authors highlighted the generality of the reaction by coupling Boc-protected proline-OH to several heterocycles bearing multiple functionalities. Indeed, this reaction tolerates electron donating and withdrawing group on the aryl halide without erosion of the yield (**Scheme 12**).



Scheme 12: Scope of the proline coupling reaction

Within the same study and inspired by Reiser's work,²⁶ they also showed that aniline-based compounds were efficient substrates *via* the formation of α -nitrogen-carbon-based radicals after loss of a proton. The commercially available *N,N* dimethylaniline was used as a model substrate and very good yields were obtained for the direct C–H / C–X cross-coupling reactions (**Scheme 13**).

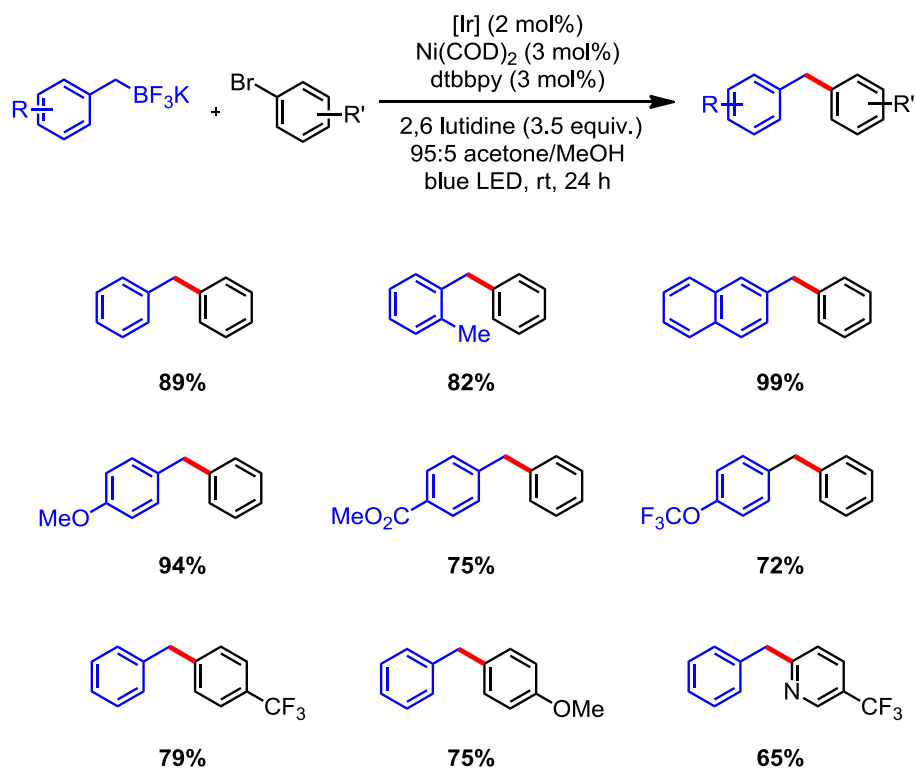


Scheme 13: Aniline-based cross-coupling reactions

Building on this novel reaction, other groups applied this nickel/photoredox dual strategy to other radical precursors.

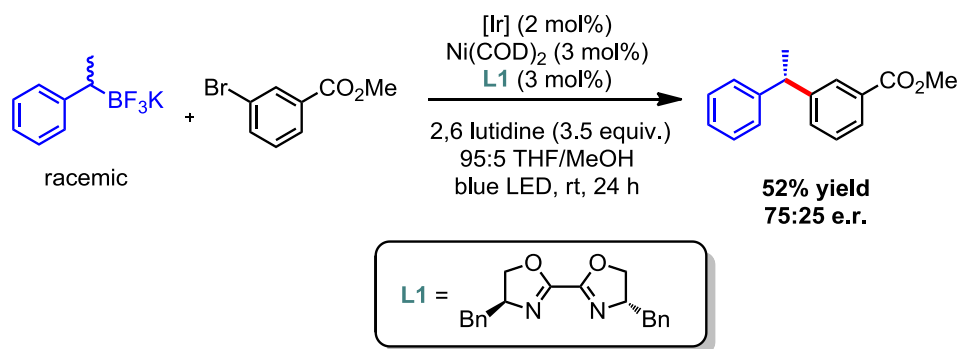
b) Trifluoroborates as efficient coupling partners

After the seminal work of our group²⁷ and the one of Akita regarding the oxidation of trifluoroborates²⁸ and inspired by MacMillan's previous publication, Molander extended, in 2014, the applications of the trifluoroborates to dual catalysis.²⁵ He showed that, in presence of Ni(COD)₂ and Ir[dFCF₃ppy]₂(bpy)PF₆, a cross-coupling reaction could occur between aryl halides and benzyl trifluoroborates (**Scheme 14**).



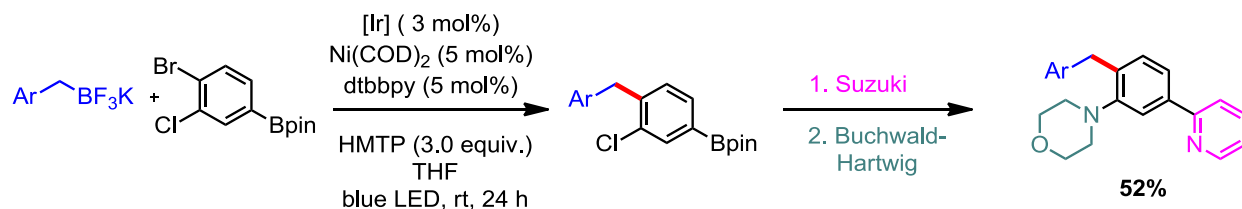
Scheme 14: Cross-coupling reactions between aryl halides and benzyl trifluoroborates

In this work, he also showed that the use of the bis(oxazoline) chiral ligand **L1** for the nickel could generate a stereoenriched cross-coupled product, while starting from the racemic methyl benzyl trifluoroborate (**Scheme 15**).



Scheme 15: Stereospecific cross-coupling reaction

A year later, Molander and co-workers completed this work by coupling activated trifluoroborates, such as benzyl trifluoroborates, to polyfunctionalized aryl halides under mild conditions.²⁹ This methodology was very selective as showed by the combination of photoredox catalysis, Suzuki coupling and Buchwald-Hartwig reaction used to form poly aromatic species (**Scheme 16**). The first coupling reaction occurred exclusively on the bromide atom without affecting the chloride. This excellent selectivity could prove valuable in total synthesis.

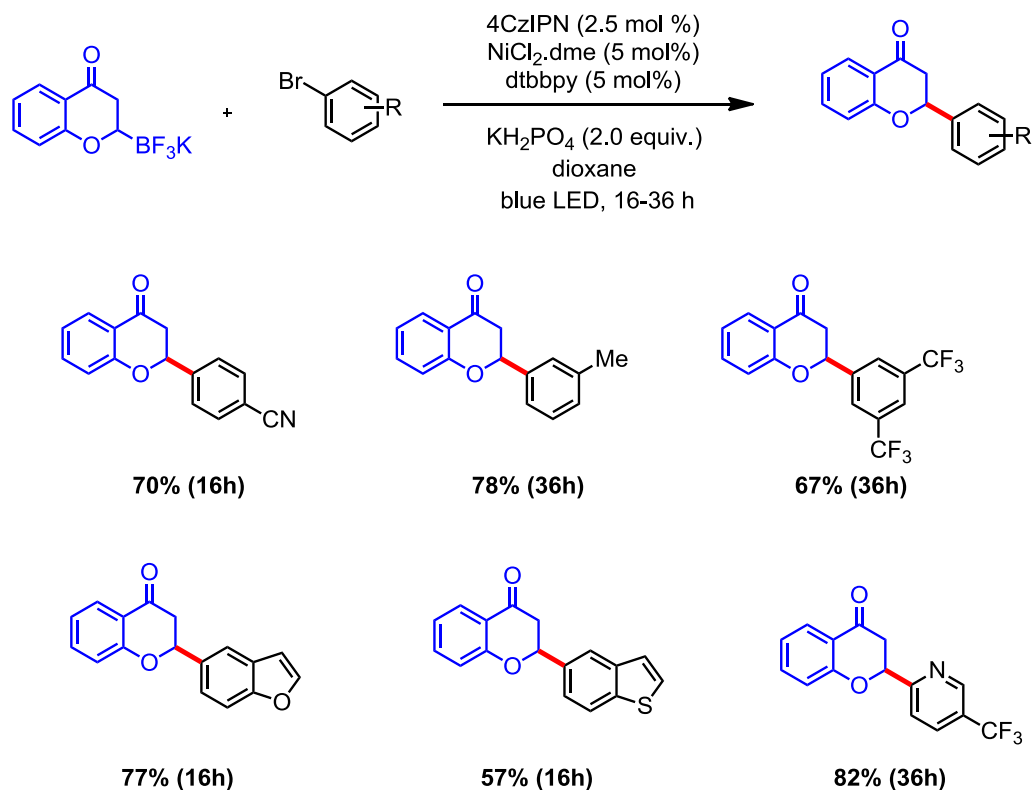


Scheme 16: Combination of photoredox/transition metal dual catalysis / Suzuki coupling / Buchwald-Hartwig reaction

Other activated trifluoroborates can also be used in such catalysis. Indeed, α -hydroxyalkyl trifluoroborates afforded, as well, the corresponding benzylic and secondary alcohols in good to excellent yields.³⁰ For this catalysis, the use of an additive such as 2,6-lutidine is mandatory to trap the boron byproduct (BF_3).

Trifluoroborates represent very interesting radical precursors because their synthesis are widely described. In this context, in 2017, Molander and co-workers showed that it was possible to synthesize new trifluoroborates by combining a β -borylation process with KHF_2 treatment. Capitalizing on this new substate class, they succeeded in producing functionalized flavanones by coupling with aryl bromides.³¹ The highly oxidant organic dye 4CzIPN, already

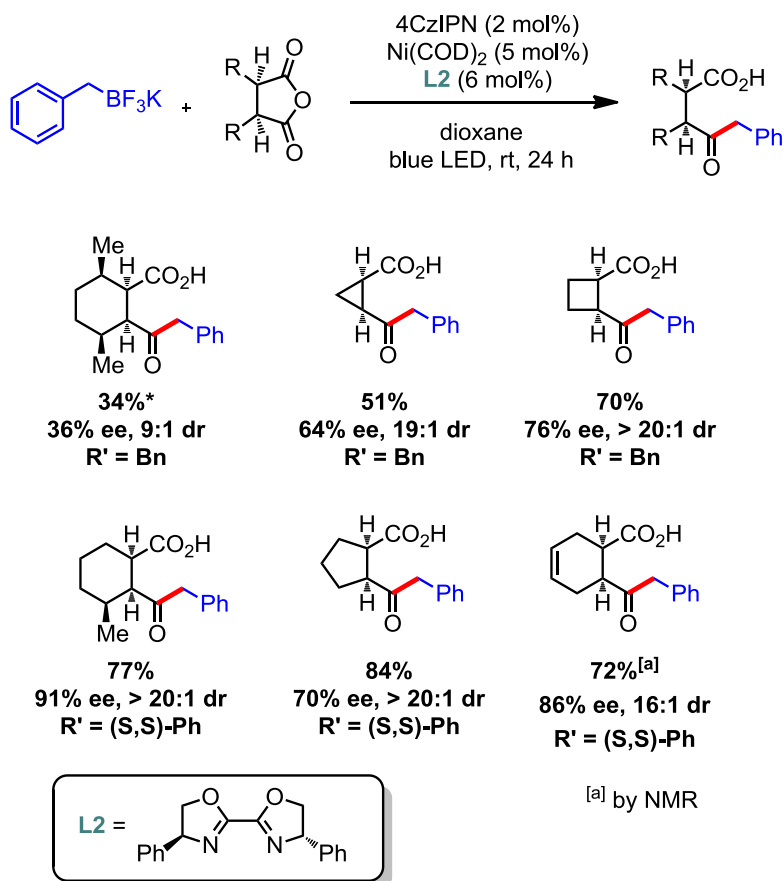
used in photoredox dual catalysis by Zhang's group one year before,³² turned out to be very efficient in this system (**Scheme 17**).^{33,34}



Scheme 17: Synthesis of new flavanones

In the same vein, Molander *et al.* showed that N-functionalized 2,1-borazaronaphthalenes were accessible through azaborinyl trifluoroborate synthesis and photoredox/nickel dual catalysis.³⁵

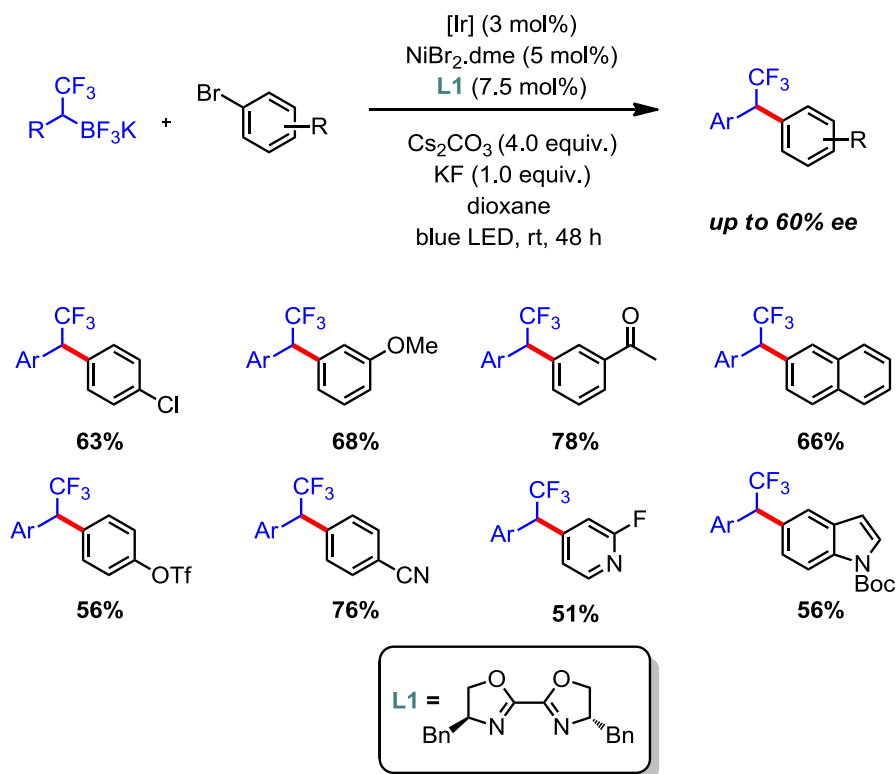
These radical precursors can also be used to produce different ketones as demonstrated by Doyle and Rovis. In 2017, they described a way to desymmetrize cyclic *meso*-anhydrides.³⁶ Compounds with an enantioselectivity up to 91% and a diastereomeric ratio up to 99:1 were obtained with BnBF₃K and the bis(oxazoline) chiral ligand **L2** (**Scheme 18**).



Scheme 18: Desymmetrization of cyclic *meso*-anhydrides

It is worth mentioning that Molander *et al.* also synthesized ketones by using acyl chlorides as electrophilic partners but this reaction will be more developed in the third part of this chapter.^{37,38}

This new way of envisioning C-C bond formation can also be very interesting for drug synthesis. Indeed, among others, the trifluoroethane synthon is of great interest in this field due to its effect on drug activity. However, its formation remains, sometimes, complicated. In that context, in 2016, a new synthesis of 1,1-diaryl-2,2,2 trifluoroethane was reported using a dual catalysis system and trifluoroborates as radical precursors.³⁹ A large variety of trifluoroethane diaryl compounds was obtained showing the interest and the versatility of the trifluoroborates (**Scheme 19**). This reaction also worked with some heterocycles which can be of interest because of the large proportion of heterocycles in common drugs.



Scheme 19: Scope of the reaction forming trifluoroethane diaryl compounds

Nevertheless, even though many interesting reactions were published using this family of radical precursor, their relatively high oxidation potential and toxicity remained a limitation.

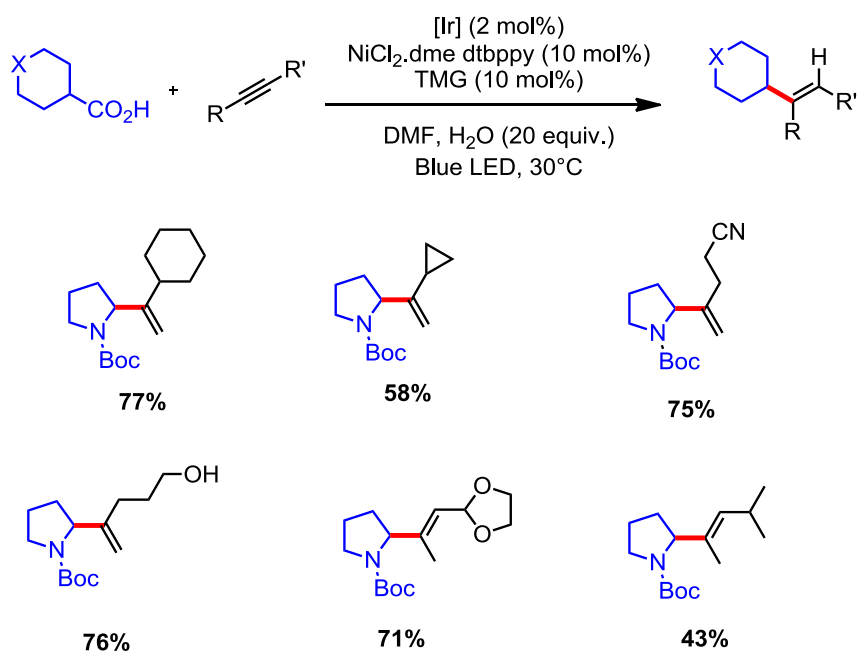
c) Carboxylates as efficient coupling partners

As previously said, carboxylates family is probably one of the simplest radical precursor class that can be found in literature. After the seminal work of Doyle & MacMillan about the coupling of α -carboxyl sp^3 -carbons with aryl halides,²⁴ MacMillan and co-workers successfully extended this reaction to less activated vinyl halides.⁴⁰

In 2017, they also published a decarboxylative process to perform an enantioselective arylation reaction of α -amino acids.⁴¹ Similarly to Doyle and Rovis,³⁶ the use of bis(oxazoline) ligands provided the desired products with very good enantioselectivity (about 90% ee). Many drugs were accessed such as a PEG₂ receptor antagonist and a glucagon receptor antagonist. Two years later, they performed a macrocyclization *via* this decarboxylative dual catalysis strategy.⁴² This reaction was applied to the synthesis of the bioactive cyclic peptide COR-005 which is a somatostatin receptor agonist.

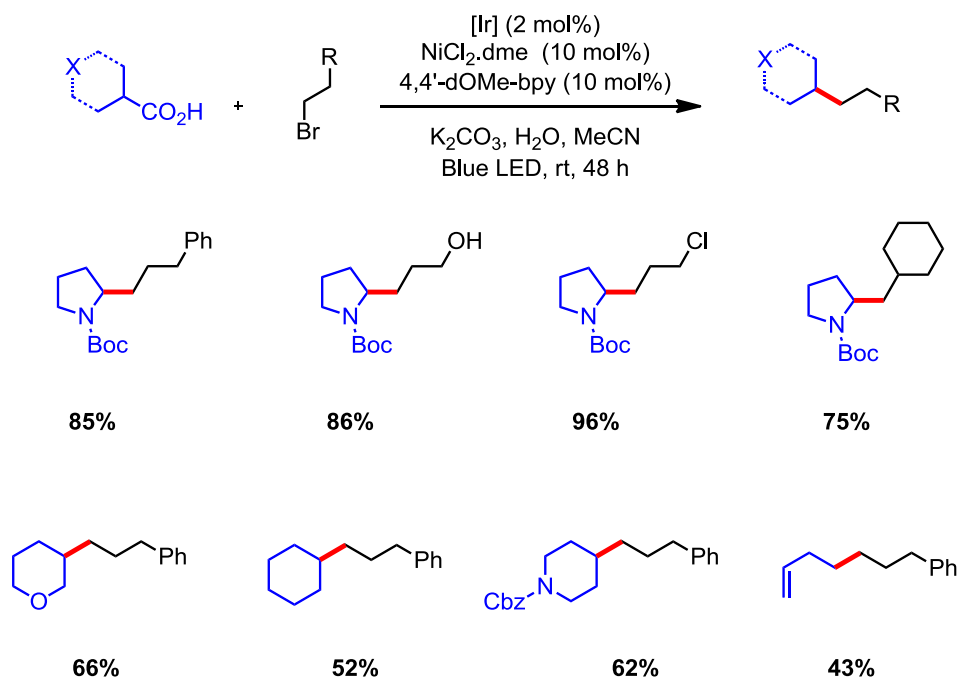
In 2018, MacMillan *et al.* extended this strategy to the hydroalkylation of alkynes (**Scheme 20**).⁴³ This reaction operates through a highly selective *cis*-carbometalation followed

by a protodemetalation by either the protonated base or the carboxylic acid and offers a broad substrate scope.



Scheme 20: Hydroalkylation of alkynes using the carboxylates as radical precursors

The carboxylates were also used to achieve the sought after sp^3 - sp^3 cross-coupling.⁴⁴ This reaction was performed with a large variety of electrophiles such as Boc-protected proline-OH which has, as already said, a low oxidation potential, but also with other carboxylates not as activated as the proline one. This reaction, which displays a high functional groups tolerance, remains a major breakthrough in radical chemistry (**Scheme 21**).

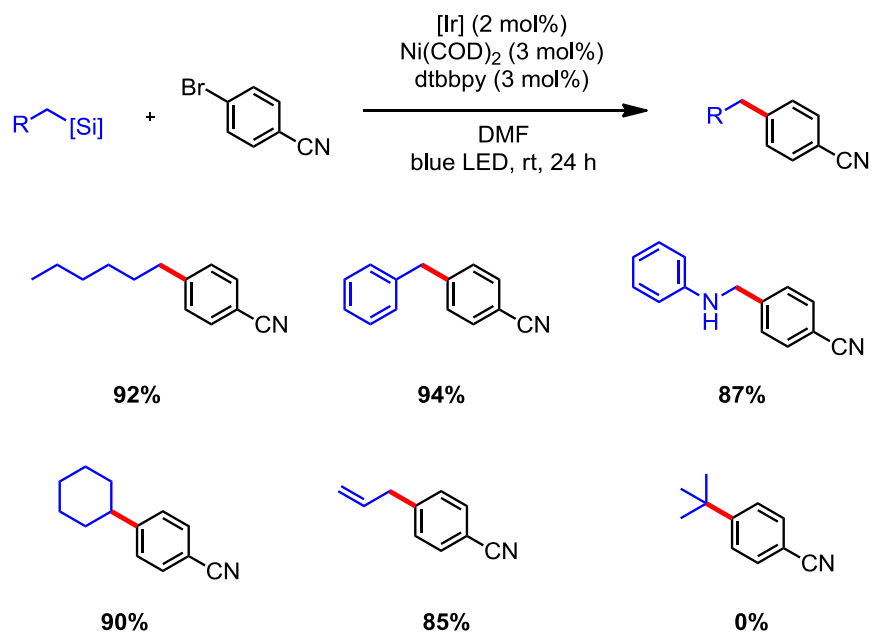


Scheme 21: $\text{sp}^3\text{-sp}^3$ cross-coupling reaction

After this proof of concept with the trifluoroborates and carboxylates, many different groups have applied this new strategy to other radical precursors.

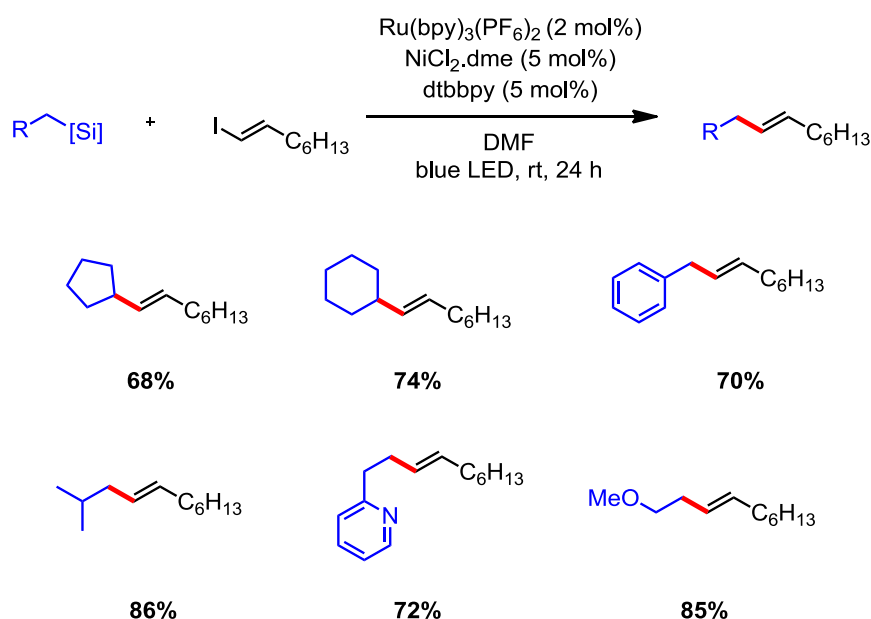
d) Silicates as efficient coupling partners

The trifluoroborates and the carboxylates, quite difficult to oxidize, are not the only radical precursors which can be used in nickel/photoredox dual catalysis. In 2015, the silicates, allowing the formation of highly unstabilized primary radicals, were also used under these conditions⁴⁵ (**Scheme 22**). The proposed mechanism remained the same as the general ones previously described.



Scheme 22: Scope of the cross-coupling using silicates and aryl bromides

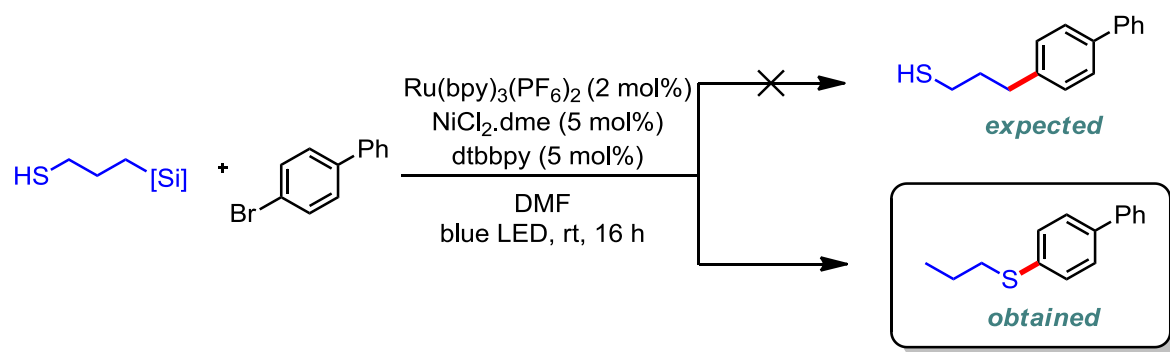
After this publication, silicates became very popular and were used in many other reactions. In 2016, Molander published a new coupling reaction using the ammonium salts of the silicates and an aryl triflate, mesylate or tosylate as electrophilic partners.⁴⁶ Similarly to the trifluoroborates, this reaction was also compatible with alkenyl halides (**Scheme 23**).⁴⁷ In 2017, they showed that the silicates react preferentially, as expected, with an iodide atom compared to bromide or a fluoride.⁴⁸ His group also demonstrated the high selectivity of this methodology by coupling DNA-tagged para-substituted aryl bromide with α -amino silicates.⁴⁹ This result might be of great interest in synthetic biology.



Scheme 23: Cross-coupling reactions between silicates and vinyl iodides

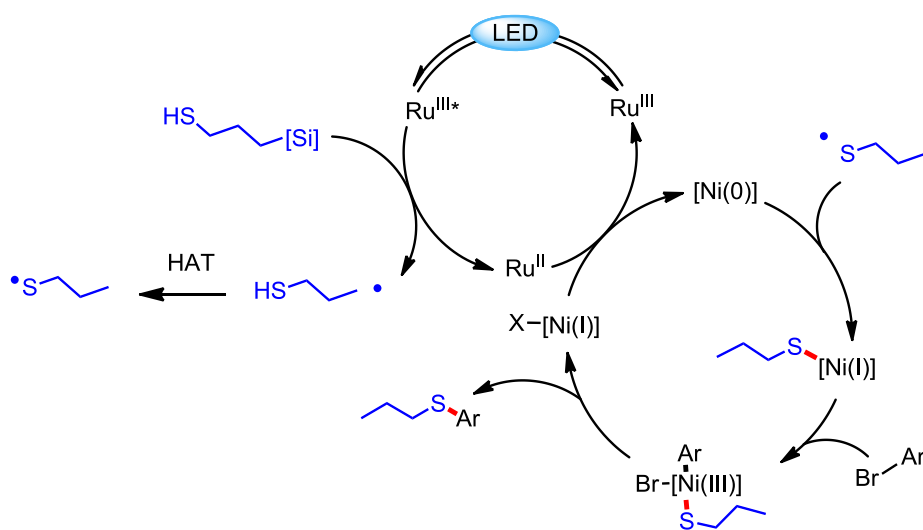
The silicates were also applied in new transformations.

In 2016, Molander's group disclosed an interesting reaction.⁵⁰ They tried to use a thiosilicate in a cross-coupling process but, instead of the expected product, they obtained the thioetherified compound (**Scheme 24**). This result can be explained by the ability of alkyl thiols (BDE (S–H) ~ 87 kcal/mol) to transfer hydrogen atoms to primary radicals very quickly ($k_{298K} = 2 \times 10^7 \text{ M}\cdot\text{s}^{-1}$).⁵¹



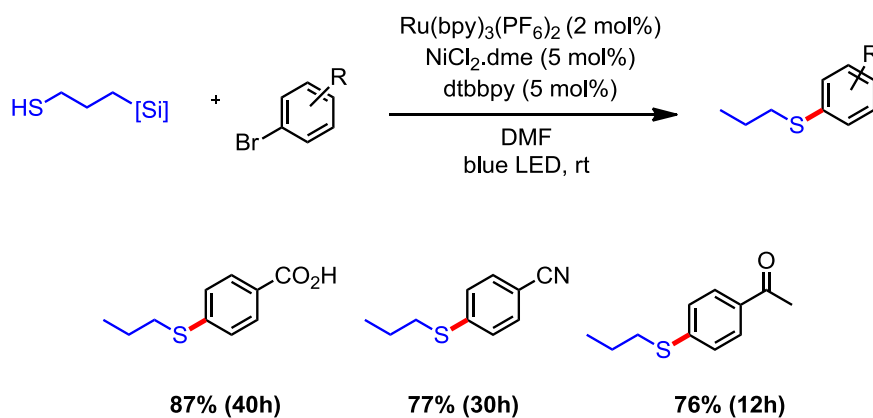
Scheme 24: Outcome of the cross-coupling reaction with a thiosilicate

They proposed the following catalytic cycle to explain the product formation (**Scheme 25**). After oxidation of the silicate by the excited photocatalyst, the alkyl radical abstracts a hydrogen atom on the sulfur to generate a thiyl radical. Afterwards, this reactive species reacts within the nickel cycle and achieves a cross-coupling reaction before releasing the product.



Scheme 25: Proposed mechanism for the thioether formation

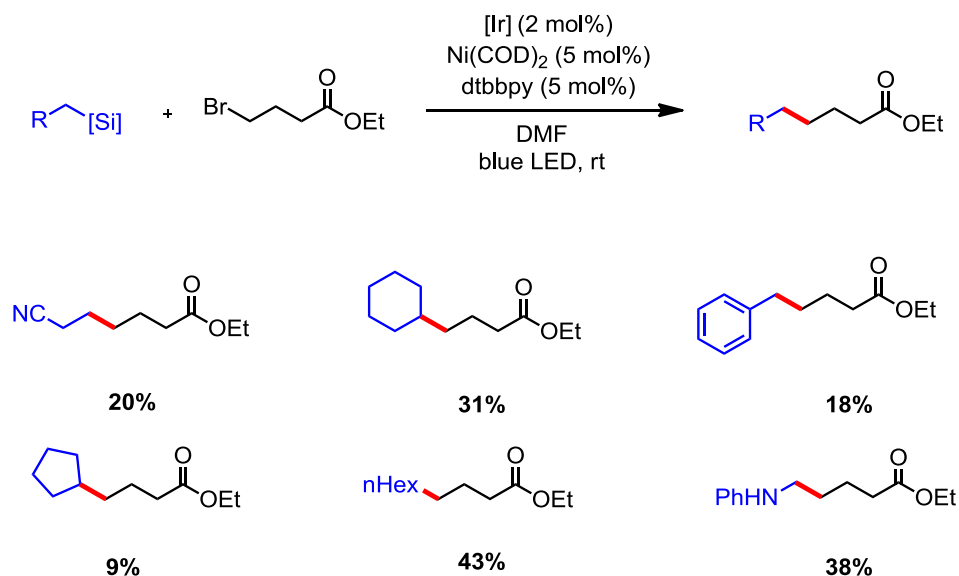
This methodology allows to prepare many different thioethers in good to excellent yields (**Scheme 26**).



Scheme 26: Synthesis of thioethers

Two years later, Molander's group went further. They exploited the ability of alkyl radicals to react rapidly through HAT to perform some thioarylation reactions of unprotected peptides.⁵² Even if this reaction can be of interest in peptide chemistry, the use of a sacrificial silicate as an HAT reagent, limits its potential.

In 2017, inspired by MacMillan's work,²⁴ our group reported another reaction concerning the silicates and dual catalysis. By using this radical precursor, we were able to perform a $\text{sp}^3\text{-sp}^3$ cross-coupling reaction.⁵³ The yield was moderate but remained definitely interesting for modern organic chemists because non-activated partners could be used. We also observed the formation of a dimer, due to the homocoupling of the bromoalkyl, but we could not explain its formation (**Scheme 27**). Some work is currently ongoing in our laboratory to understand the mechanism of this reaction.

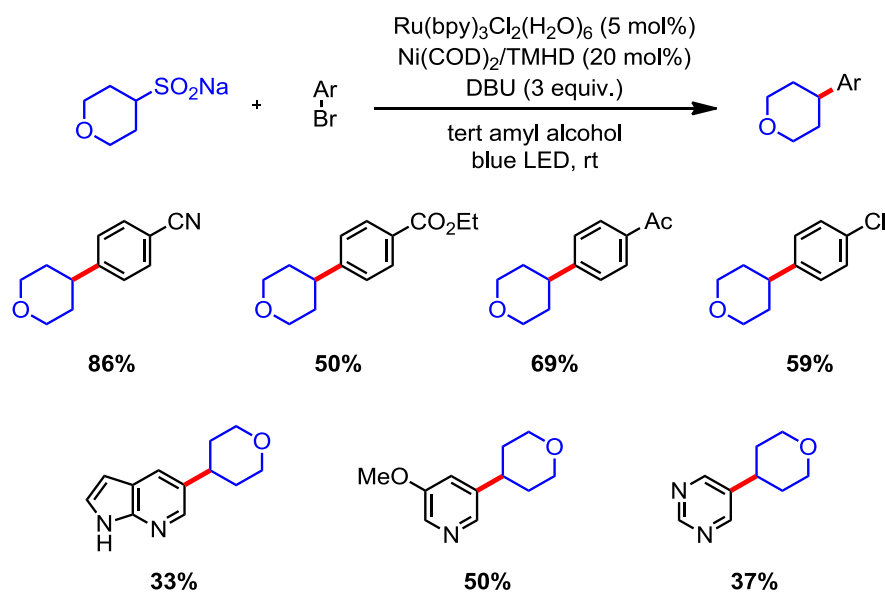


Scheme 27: Scope of the sp^3 - sp^3 cross-coupling reaction

This new reactivity clearly shows the high synthetic potential of the silicates. Moreover, photocatalysis fame has led to the discovery of new radical precursors among which many can be used in dual catalysis.

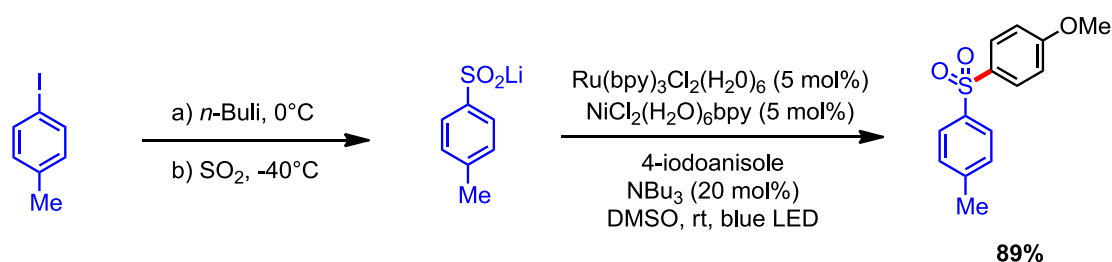
e) Sodium sulfinates and other derivatives as efficient coupling partners

In 2017, Helal and co-workers reported the cross-coupling of alkyl sulfinate salts and aryl halides *via* a dual catalysis strategy (**Scheme 28**).⁵⁴ These reactants are quite interesting because of their relatively low oxidation potential ($E_{1/2}^{ox}$ (sodium-4-tetrahydropyran sulfinate) = +0.64 V *vs.* SCE). Accordingly, an oxidant milder than the prototypical iridium photocatalyst could be used, namely the complex Ru(bpy)₃Cl₂. As an example, by using such methodology, Helal's group succeeded in synthesizing some analogs of the casein kinase 1δ inhibitor.



Scheme 28: Cross-coupling of aryl halides and alkyl sulfinate salts

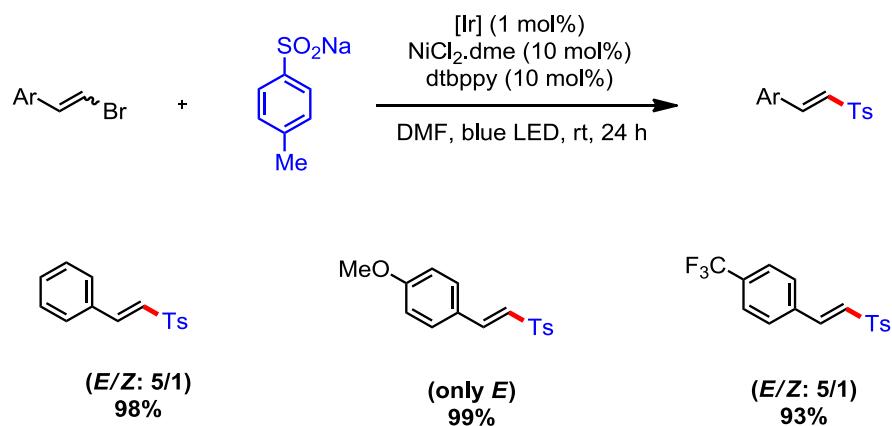
One year later, Manolikakes *et al.* reported a nickel coupling of sodium sulfinate salts with aryl halides. However, the conditions for the realization of this organometallic reaction were harsh.⁵⁵ High temperature, addition of a reducing agent and an expensive NHC ligand were mandatory, limiting the use of this discovery. Building on the already presented literature, they successfully developed a nickel/photoredox catalysis to perform this coupling under milder conditions.⁵⁶ The ruthenium photocatalyst was also found to be very efficient and the desired products were obtained in good yields. Moreover, they showed that lithium salts could be efficiently used as well (**Scheme 29**).



Scheme 29: Utilization of a lithium salt in a cross-coupling reaction

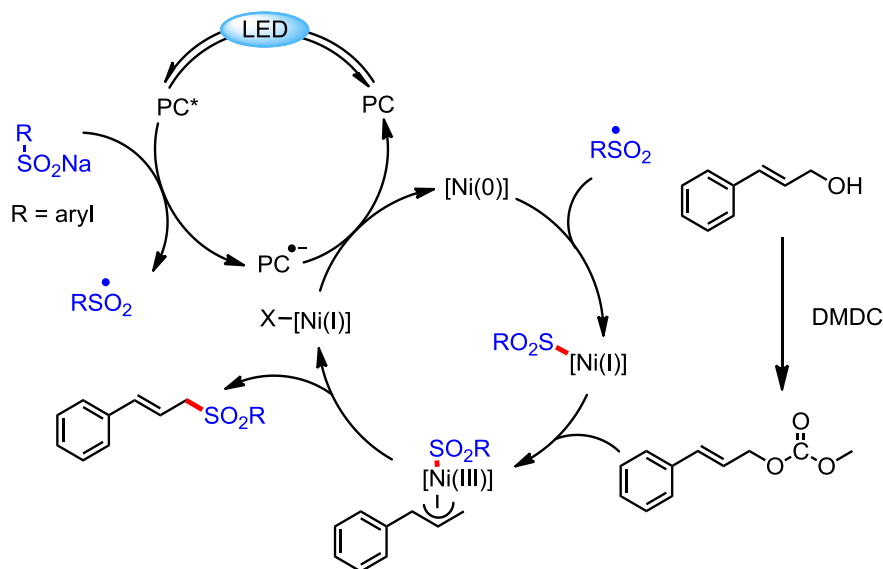
This reaction could also be achieved with benzene as a starting material resulting in the formation of the desired sulfone in 28% yield. Rueping's group extended this concept and showed that many types of coupling reactions could be achieved thanks to these sodium sulfinate salts.⁵⁷ He even showed that vinyl bromides could be used as electrophilic partners.

The products were preferentially *E* (**Scheme 30**) even if a *E/Z* mixture of reagents was used at the beginning. Electro donating or withdrawing groups were well-tolerated and no erosion of the yield occurred. They also applied this methodology to pharmaceutically relevant heteroaromatic bromides such as quinolines and thiophenes.



Scheme 30: Sulfinate salts and vinyl halides cross-coupling reactions

In 2019, another reaction with these sodium sulfinites was reported by Molander's group. With this radical precursor and allyl methyl carbonate they were able to perform a Tsuji-Trost reaction.⁵⁸ The proposed mechanism is the combination of the usual dual catalysis and Tsuji-Trost reaction (**Scheme 31**).



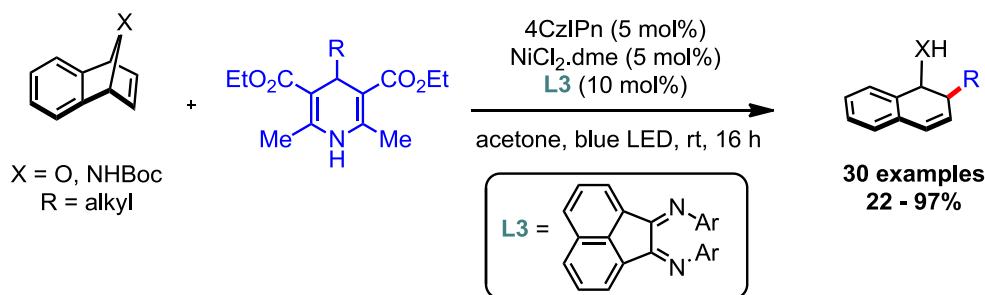
Scheme 31: Photocatalytic Tsuji-Trost reaction

In this study, they also showed that 4-alkyl-1,4 dihydropyridines (DHPs) can be used as really efficient radical precursors.

f) DHPs as efficient coupling partners

This interesting family, already presented in chapter I, was not very used in dual catalysis in comparison to others. Indeed, its quite poor atom economy limits its uses.

However, Molander and co-workers showed that some of the previous cross-coupling reactions, that were working with the silicates or the carboxylates, also worked with the DHPs.⁵⁹ Moreover, additional transformations were also developed. In 2019, Molander's group succeeded in using oxa- and azabenzonorboradienes as their electrophilic partners in a photoredox/nickel dual catalysis system. The scope of this reaction was quite broad and allowed to disclose the first regio- and diastereoselective alkylation of oxa- and azabenzonorboradienes (**Scheme 32**).⁶⁰

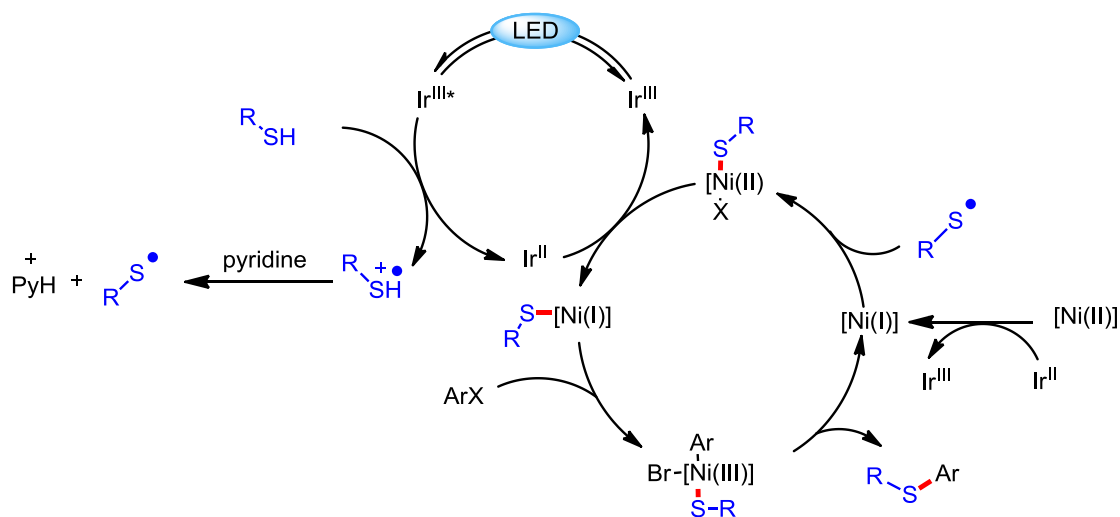


Scheme 32: Use of oxa- and azabenzonorboradienes as electrophilic partners under photoredox/nickel dual catalysis

A year later, Melchiorre *et al.* showed that amides can be formed through the carbamoylation of (hetero)aryl bromides from a DHP precursor.⁶¹ Thanks to an excited photocatalyst and the appropriate DHP, they managed to produce a carbamoyl radical that is trapped by the nickel catalyst to achieve the cross-coupling reaction with an aromatic bromide.

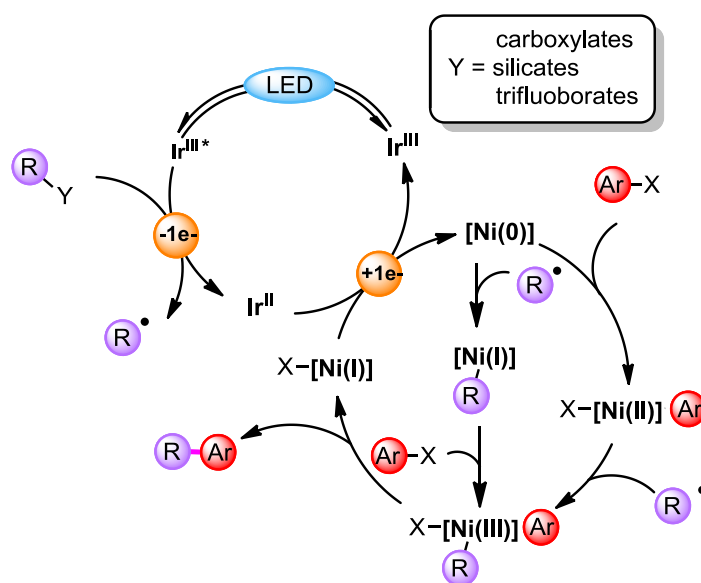
g) Mechanism of dual catalysis

All of the catalytic cycles reported in this chapter are based on a nickel(0) catalytic cycle even if a nickel(II) catalyst is added at the beginning. A proper rationale explanation for this observation is still lacking. In 2016, Johannes was the only one to propose a cycle based on a nickel(II) catalyst in his C-S cross-coupling reaction.⁶² He assumed that the nickel(II) precatalyst is first reduced by the photocatalyst. Secondly, a radical addition occurs onto that newly formed nickel(I) species. Afterwards, the resulting nickel(II) complex is, once again, reduced by the photocatalyst to Ni(I). Then, the aryl halide reacts *via* an oxidative addition. Finally, a reductive elimination releases the desired product and a Ni(I) complex (**Scheme 33**).



Scheme 33: Proposed mechanism for dual catalysis by Johannes

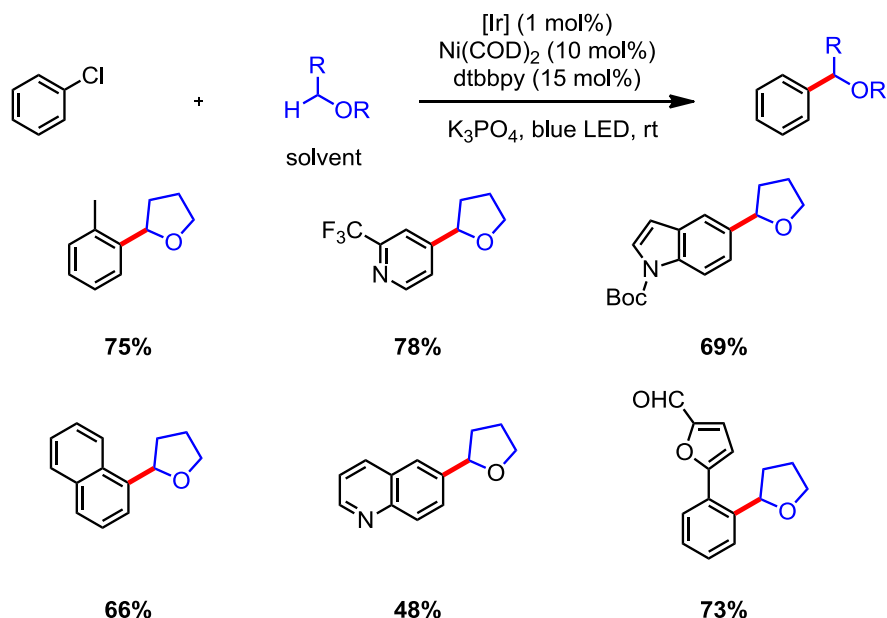
Another critical part remains the order of the different steps. Indeed, the first one may be the oxidative addition or the radical addition (**Scheme 34**). It might also depend on the system.⁶³ Thus, some works are currently ongoing in our laboratory to understand the mechanism of this reaction.



Scheme 34: Different catalytic cycles proposed

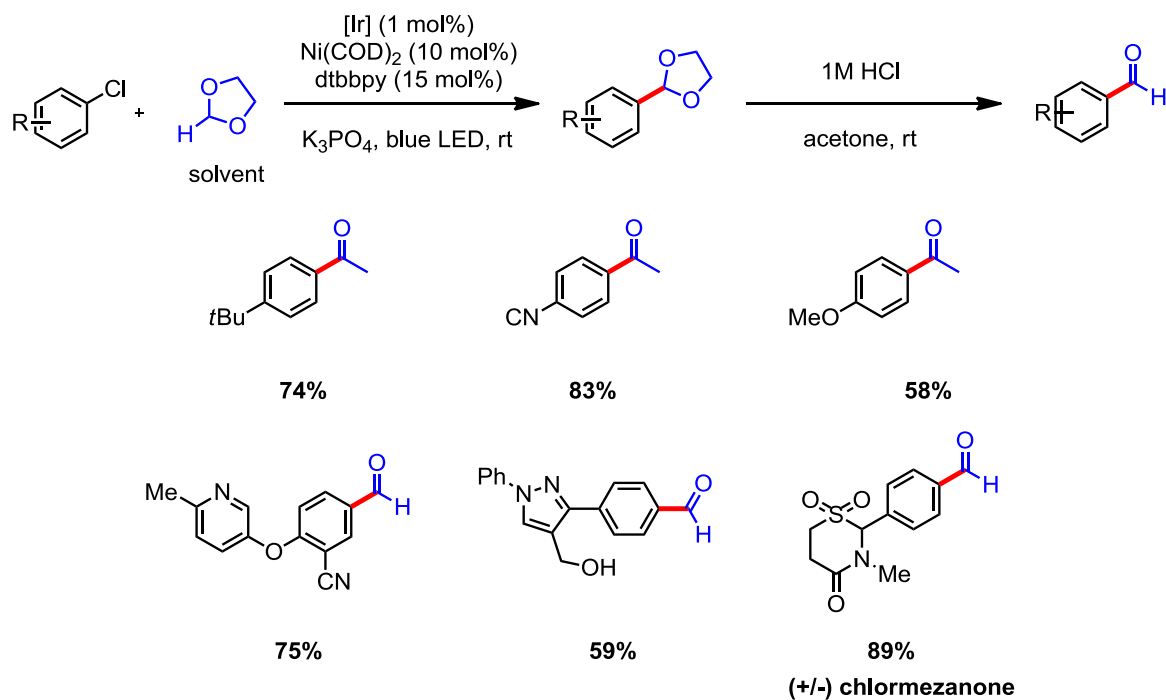
Another very interesting result about this catalytic cycle can be found in Doyle's paper.⁶⁴ She showed that the photosensitive Ni(III) intermediate, formed after the oxidative addition of an aryl halide and oxidation by the photocatalyst, could undergo a photolysis and release a

bromine or a chlorine radical. Afterwards, this radical can abstract a hydrogen atom from the solvent, which was THF in the study ($\text{H-Cl BDE} = 102 \text{ kcal.mol}^{-1}$, $\text{THF BDE} = 92 \text{ kcal.mol}^{-1}$). Then, the tetrahydrofuryl radical formed is added to the metal catalyst and the nickel(III) complex obtained undergoes a reductive elimination to produce the desired product. Thanks to that surprising reactivity, she managed to obtain many different cross-coupling products in high yields (**Scheme 35**). This methodology was also compatible with some heteroaromatic scaffolds.



Scheme 35: Cross-coupling of radical based solvent and aryl halides

One year later, she extended this concept by carrying out this reaction in the 1,3 dioxalane and using it as a coupling reagent.⁶⁵ The chlorine radical, formed after photolysis of the nickel complex, abstracts a hydrogen atom from the solvent generating a carbon centered-radical. Then, the cross-coupling reaction occurs. A large variety of compounds, which are masked aldehydes, were synthesized showing all the versatility of this reaction (**Scheme 36**).



Scheme 36: Cross-coupling of radical based 1,3 dioxalane and aryl halides

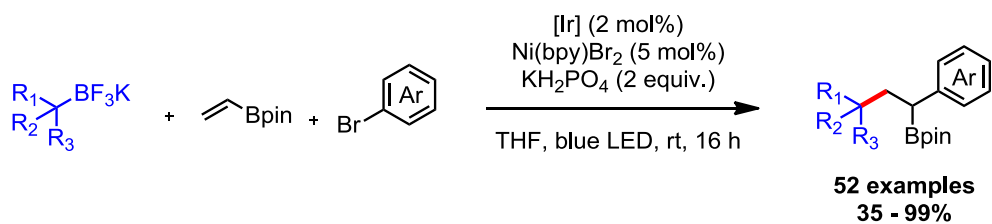
In 2018, Rueping's group complemented this work by showing that unactivated tri- and tetrasubstituted alkenes were also suitable substrates.⁶⁶ In this publication, allylic C sp³-H were efficiently coupled to vinyl or aryl bromides.

h) Extension of concept

After this discussion on the mechanism and the different radical precursors that can be used in nickel/photoredox dual catalysis, we can broaden the concept to multicomponent reactions.

h.1) Multicomponent reactions

The radical formed by photooxidation with the excited photocatalyst can react before being added onto the nickel catalyst.⁶⁷ This cascade-type reaction was already known in photoredox catalysis^{68,69} but Molander extended it to dual catalysis in 2019.⁷⁰ Indeed, his group managed to perform a three component-olefin dicarbofunctionalization by using a tertiary trifluoroborate, reluctant toward single electron metalation onto the nickel catalyst, a vinyl boronic acid pinacol ester and an aryl halide (**Scheme 37**). The scope of this reaction was quite broad and many tertiary trifluoroborates were successfully used.

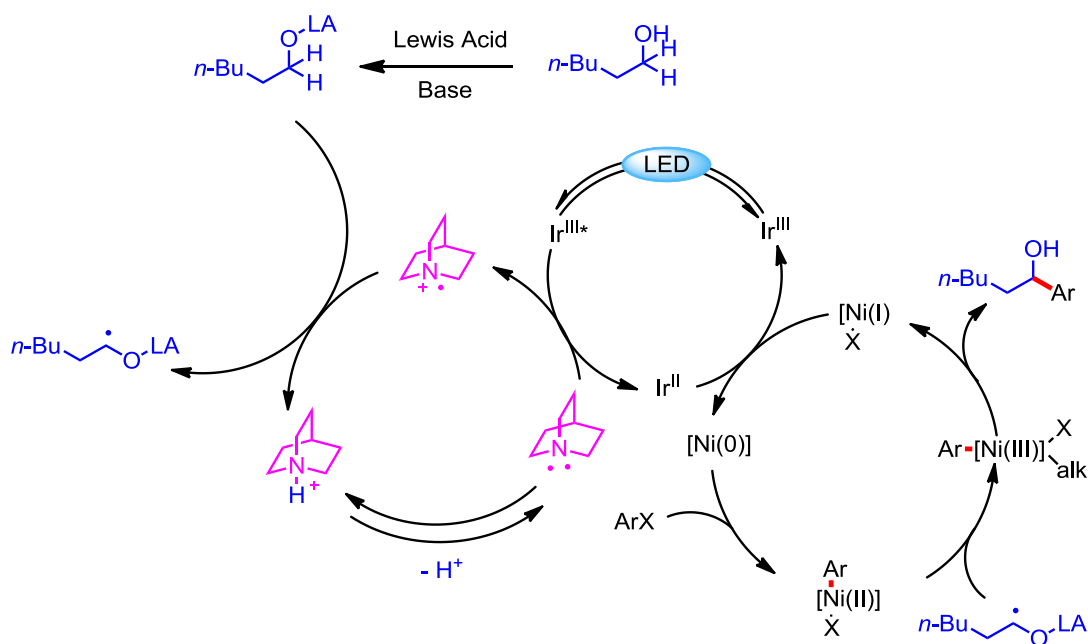


Scheme 37: Three-component olefin dicarbofunctionalization

One year later, Aggarwal and co-workers reported the same type of reaction with the Boc-protected proline OH as the radical precursor instead of a trifluoroborate.⁷¹ In 2020, Nevado extended this three-component carbofunctionalization of alkenes to secondary and tertiary silicates but also to sodium arene sulfinates.⁷² It is worth noting that this type of multicomponent reaction can also be applied under reductive conditions with a copper photocatalyst and bicyclo[1.1.1]pentane as MacMillan reported it in 2020.⁷³ These last results clearly show all the potential of this multicomponent new approach.

h.2) Multiple cycle transformations

To make this system even more complex, a third catalytic cycle can be added to the two other ones as MacMillan's group reported it in 2018.⁷⁴ Thanks to a hydrogen atom transfer enabled by the HAT catalyst quinuclidine and the Lewis acid ZnCl_2 , they were able to develop a C-C bond formation at the α -carbon of a desired alcohol (**Scheme 38**). After an oxidative quench of the quinuclidine and hydrogen atom transfer, the resulting α -alkoxy radical reacts with the nickel(II) complex and, after reductive elimination, the desired product is released.



Scheme 38: Extension to a triple catalysis

II.2.3. Conclusion on dual catalysis

In a nutshell, a large variety of metals and radical precursors can be used in a photoredox/transition metal dual catalysis system. This new way of forging C–C bonds has shown to be a highly versatile approach for the construction of a wide range of molecular scaffolds *via* C-H or C-X bond activation. After this introduction, we can focus our attention on the results obtained on this topic during this PhD thesis.

II.2.4. References

- ¹ K. Sonogashira, Y. Tohda, N. Hagihara, *Tetrahedron Lett.* **1975**, *50*, 4467.
- ² N. R. Deprez, M. S. Sanford, *J. Am. Chem. Soc.* **2009**, *131*, 11234.
- ³ W. Y. Yu, W. N. Sit, Z. Zhou, A. S.-C. Chan, *Org. Lett.* **2009**, *11*, 3174.
- ⁴ D. Kalyani, K. B. McMurtrey, S. R. Neufeldt, M. S. Sanford, *J. Am. Chem. Soc.* **2011**, *133*, 18566.
- ⁵ Results found by searching "dual catalysis" as a concept in Scifinder.
- ⁶ M. E. Lorris, R. A. Abramovitch, J. Marquet, M. Moreno-Mañas, *Tetrahedron* **1992**, *48*, 6909.
- ⁷ G. Sorin, R. M. Mallorquin, Y. Contie, A. Baralle, M. Malacria, J. P. Goddard, L. Fensterbank, L. *Angew. Chem. Int. Ed.* **2010**, *49*, 8721.
- ⁸ Y. Ye, M. S. Sanford, *J. Am. Chem. Soc.* **2012**, *134*, 9034.
- ⁹ X. Bao, Q. Wang, J. Zhu, *Angew. Chem. Int. Ed.* **2019**, *58*, 2139.
- ¹⁰ N. L. Reed, M. L. Herman, V. P. Mitchev, T. P. Yoon, *Beilstein J. Org.* **2019**, *15*, 351.
- ¹¹ J. Chen, P. Z. Wang, B. Lu, D. Liang, X. Y. Yu, W. J. Xiao, J. R. Chen, *Org. Lett.* **2019**, *21*, 9763
- ¹² C. Aprile, M. Boronat, B. Ferrer, A. Corma, H. García, *H. J. Am. Chem. Soc.* **2006**, *128*, 8388.
- ¹³ B. Sahoo, M. N. Hopkinson, F. Glorius, *J. Am. Chem. Soc.* **2013**, *135*, 5505.
- ¹⁴ Z. Xia, O. Khaled, V. Mouriès-Mansuy, C. Ollivier, L. Fensterbank, *J. Org. Chem.* **2016**, *81*, 7182.
- ¹⁵ J. L. Schwarz, F. Schäfers, A. Tlahuext-Aca, L. Lückemeier, F. Glorius, *J. Am. Chem. Soc.* **2018**, *140*, 12705.
- ¹⁶ J. L. Schwarz, H. M. Huang, T O. Paulisch, F. Glorius, *ACS Catal.* **2020**, *10*, 1621.
- ¹⁷ K. Zhang, L. Q. Lu, Y. Jia, Y. Wang, F. D. Lu, F. Pan, W. J. Xiao, *Angew. Chem. Int. Ed.* **2019**, *58*, 13375.
- ¹⁸ P. Rai, K. Maji, B. Maji, *Org. Lett.* **2019**, *21*, 3755.
- ¹⁹ M. J. González, B. Breit, *Chem. Eur. J.* **2019**, *25*, 15746.
- ²⁰ K. C. Cartwright, J. A. Tunge, *ACS Catal.* **2018**, *8*, 11801.
- ²¹ J. Hou, A. Ee, W. Feng, J. H. Xu, Y. Zhao, J. Wu, *J. Am. Chem. Soc.* **2018**, *140*, 5257.
- ²² K. Takizawa, T. Sekino, S. Sato, T. Yoshino, M. Kojima, S. Matsunaga, *Angew. Chem. Int. Ed.* **2019**, *58*, 9199.
- ²³ Results obtained by searching the concept "[metal] dual catalysis" in SciFinder.
- ²⁴ Z. Zuo, D. T. Ahneman, L. Chu, J. A. Terrett, A. G. Doyle, D. W. C. MacMillan, *Science* **2014**, *345*, 437.
- ²⁵ J. C. Tellis, D. N. Primer, G. A. Molander, *Science* **2014**, *345*, 433.
- ²⁶ P. Kohls, D. Jadhav, G. Pandey, O. Reiser, *Org. Lett.* **2012**, *14*, 672.
- ²⁷ G. Sorin, R. M. Mallorquin, Y. Contie, A. Baralle, M. Malacria, J. P. Goddard, L. Fensterbank, *Angew. Chem. Int. Ed.* **2010**, *49*, 8721.
- ²⁸ Y. Yasu, T. Koike, M. Akita, *Adv. Synth. Catal.* **2012**, *354*, 3414.
- ²⁹ Y. Yamashita, J. C. Tellis, G. A. Molander, *Prot. Natl. Acas. Sci. USA* **2015**, *112*, 12016.
- ³⁰ R. Alam, G. A. Molander, *J. Org. Chem.* **2012**, *82*, 13728.
- ³¹ J. K. Matsui, G. A. Molander, *Org. Lett.* **2017**, *19*, 436.
- ³² J. Luo, J. Zhang, *ACS Catal.* **2016**, *6*, 873.
- ³³ H. Uoyama, K. Goushi, K. Shizu, H. Nomura, C. Adachi, *Nature* **2012**, *492*, 234.
- ³⁴ For a reevaluation of the reduction and oxidation potentials of the excited state of 4CzIPN, see: F. L. Vaillant, M. Garreau, S. Nicolai, G. Gryn'ova, C. Corminboeuf, J. Waser, *Chem. Sci.* **2018**, *9*, 5883.
- ³⁵ X. Wang, G. H. M. Davies, A. Koschitzky, S. R. Wisniewsky, C. B. Kelly, G. A. Molander, *Org. Lett.* **2019**, *21*, 2880.
- ³⁶ E. E. Stache, T. Rovis, A. G. Doyle, *Angew. Chem. Int. Ed.* **2017**, *56*, 3679.
- ³⁷ J. Amani, G. A. Molander, *J. Org. Chem.* **2017**, *82*, 1856.

- ³⁸ J. Amani, E. Sodagar, G. Molander, *Org. Lett.* **2016**, *18*, 732.
- ³⁹ D. Ryu, D. N. Primer, J. C. Tellis, G. A. Molander, *Chem. Eur. J.* **2016**, *22*, 120.
- ⁴⁰ A. Noble, S. J. McCarver, D. W. C. MacMillan, *J. Am. Chem. Soc.* **2015**, *137*, 624.
- ⁴¹ Z. Zuo, H. Cong, W. Li, J. Choi, G. C. Fu, D. W. C. MacMillan, *J. Am. Chem. Soc.* **2016**, *138*, 1832.
- ⁴² S. J. McCarver, J. X. Qiao, J. Carpenter, R. M. Borzilleri, M. A. Poss, M. D. Eastgate, M. Miller, D. W. C. MacMillan, *Angew. Chem. Int. Ed.* **2016**, *55*, 1.
- ⁴³ N. A. Till, R. T. Smith, D. W. C. MacMillan, *J. Am. Chem. Soc.* **2018**, *140*, 5701.
- ⁴⁴ C. P. Johnston, R. T. Smith, S. Allmendinger, D. W. C. MacMillan, *Nature* **2016**, *536*, 322.
- ⁴⁵ V. Corcé, L. M. Chamoreau, E. Derat, J. P. Goddard, C. Ollivier, L. Fensterbank, *Angew. Chem. Int. Ed.* **2015**, *54*, 11414.
- ⁴⁶ N. R. Patel, G. A. Molander, *J. Org. Chem.* **2016**, *81*, 7271.
- ⁴⁷ N. R. Patel, C. B. Kelly, M. Jouffroy, G. A. Molander, *Org. Lett.* **2016**, *18*, 764.
- ⁴⁸ K. Lin, R. J. Wiles, C. B. Kelly, G. H. M. Davies, G. A. Molander, *ACS Catal.* **2017**, *7*, 5129.
- ⁴⁹ S. O. Badir, J. Sim, K. Billings, A. Csakai, X. Zhang, W. Dong, G. A. Molander, *Org. Lett.* **2020**, *22*, 1046.
- ⁵⁰ M. Jouffroy, C. B. Kelly, G. A. Molander, *Org. Lett.* **2016**, *18*, 876.
- ⁵¹ F. Dénès, M. Pichowicz, G. Povie, P. Renaud, *Chem. Rev.* **2014**, *114*, 2587.
- ⁵² B. A. Vara, X. Li, S. Berritt, C. R. Walters, E. J. Petersson, G. A. Molander, *Chem. Sci.* **2018**, *9*, 336.
- ⁵³ C. Lévêque, V. Corcé, L. Chenneberg, C. Ollivier, L. Fensterbank, *Eur. J. Org. Chem.* **2017**, 2118.
- ⁵⁴ T. Knauber, R. Chandrasekaran, J. W. Tucker, J. M. Chen, M. Reese, D. A. Rankic, N. Sach, C. Helal, *Org. Lett.* **2017**, *19*, 6566.
- ⁵⁵ N. W. Liu, S. Liang, N. Margraf, S. Shaaban, V. Luciano, M. Drost, G. Manolikakes, *Eur. J. Org. Chem.* **2018**, 1208.
- ⁵⁶ N. W. Liu, K. Hofman, A. Herbet, G. Manolikakes, *Org. Lett.* **2018**, *20*, 760.
- ⁵⁷ H. Yue, C. Zhu, M. Rueping, *Angew. Chem. Int. Ed.* **2018**, *57*, 1371.
- ⁵⁸ Z. J. Wang, S. Zheng, E. Romero, J. K. Matsui, G. A. Molander, *Org. Lett.* **2019**, *21*, 6543.
- ⁵⁹ J. P. Phelan, S. B. Lang, J. Sim, S. Berritt, A. J. Peat, K. Billings, L. Fan, G. A. Molander, *J. Am. Chem. Soc.* **2019**, *141*, 3723.
- ⁶⁰ Y. Luo, A. Gutiérrez-Bonet, J. K. Matsui, M. E. Rotella, R. Dykstra, O. Gutierrez, G. A. Molander, *ACS Catal.* **2019**, *9*, 8835.
- ⁶¹ N. Alandini, L. Buzzetti, G. Favi, T. Schulte, L. Candish, K. D. Collins, P. Melchiorre, *Angew. Chem. Int. Ed.* **2020**, *59*, 5248.
- ⁶² M. S. Oderinde, M. Frenette, D. W. Robbins, B. Aquila, J. W. Johannes, *J. Am. Chem. Soc.* **2016**, *138*, 1760.
- ⁶³ M. Yuan, Z. Song, S. O. Badir, G. A. Molander, O. Gutierrez, *J. Am. Chem. Soc.* **2020**, *142*, 7225.
- ⁶⁴ B. J. Shields, A. G. Doyle, *J. Am. Chem. Soc.* **2016**, *138*, 12719.
- ⁶⁵ M. K. Nielsen, B. J. Shields, J. Liu, M. J. Williams, M. J. Zacuto, A. G. Doyle, *Angew. Chem. Int. Ed.* **2017**, *129*, 7297.
- ⁶⁶ L. Huang, M. Rueping, *Angew. Chem. Int. Ed.* **2018**, *57*, 10333.
- ⁶⁷ a) T. Q. Chen, D. W. C. MacMillan, *Angew. Chem. Int. Ed.* **2019**, *58*, 14584; b) D. J. P. Kornfilt, D. W. C. MacMillan, *J. Am. Chem. Soc.* **2019**, *141*, 6853; c) M. González-Esguevillas, J. Miró, J. L. Jeffrey, D. W. C. MacMillan, *Tetrahedron* **2019**, *75*, 4222.
- ⁶⁸ X. Y. Liu, Y. Qin, *Acc. Chem. Res.* **2019**, *52*, 1877.
- ⁶⁹ V. R. Yatham, Y. Shen, R. Martin, *Angew. Chem. Int. Ed.* **2017**, *56*, 10915.
- ⁷⁰ M. W. Campbell, J. S. Compton, C. B. Kelly, G. A. Molander, *J. Am. Chem. Soc.* **2019**, *41*, 20069.
- ⁷¹ R. S. Mega, V. K. Duong, A. Noble, V. K. Aggarwal, *Angew. Chem. Int. Ed.* **2020**, *59*, 4375.
- ⁷² A. García-Domínguez, R. Mondal, C. Nevado, *Angew. Chem. Int. Ed.* **2019**, *58*, 12286.

- ⁷³ X. Zhang, R. T. Smith, C. Le, S. J. McCarver, B. T. Shireman, N. I. Carruthers, D. W. C. MacMillan, *Nature* **2020**, *580*, 220.
- ⁷⁴ J. Twilton, M. Christensen, D. A. DiRocco, R. T. Ruck, I. W. Davies, D. W. C. MacMillan, *Angew. Chem. Int. Ed.* **2018**, *57*, 1.

II.3. Cross Coupling of Alkylsilicates with Acylchlorides via Photoredox/Nickel Dual Catalysis. A New Synthesis of Ketones

Published in *Org. Chem. Front.* **2019**, *6*, 1378

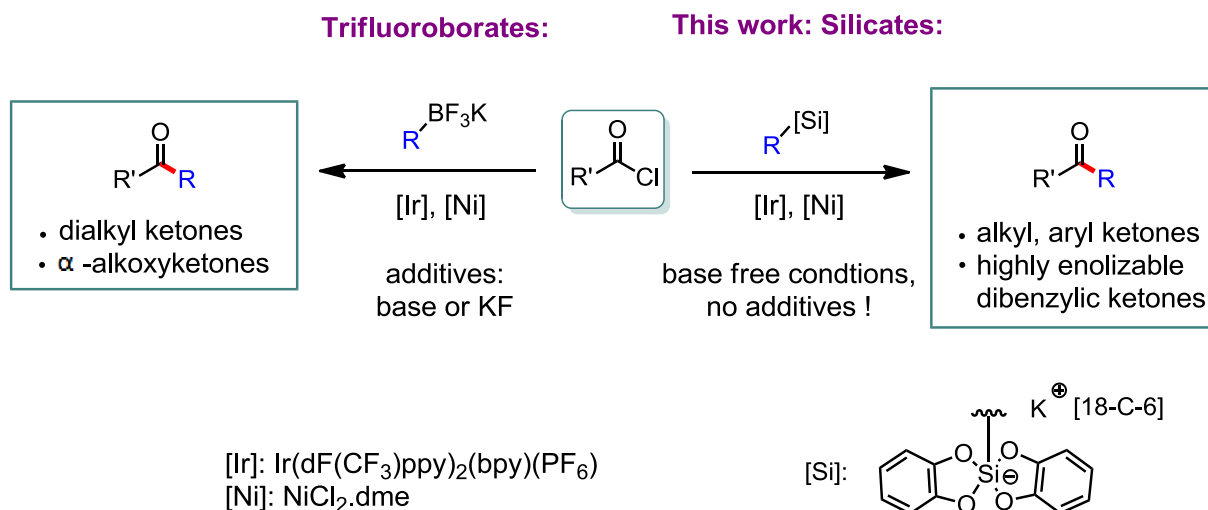
II.3.1. Abstract

Photoredox/nickel dual catalysis using easily oxidized bis-catecholato hypercoordinated silicon derivatives as radical sources and acyl chlorides as electrophiles allows a new method of formation of dialkyl and alkyl-aryl ketones as well as dibenzyl ketones which are less easily accessed. Flow chemistry can be used.

II.3.2. Introduction

Ketones are ubiquitous molecules in our daily life. They are also pivotal substrates in organic chemistry.¹ While a myriad of synthetic methods have been developed to reach them, a recurrent pitfall lies in the fact that the keto group is a highly reactive function which can overreact under a lot of experimental conditions. Recently, the emergence of dual photoredox/nickel catalysis² resulting from the pioneering studies of the groups of MacMillan, Doyle³ and Molander⁴ has profoundly changed the way of envisaging C-C bond formation by using radical precursors such as carboxylates,⁵ methylanilines or cyclic amines,^{3, 6} trifluoroborates and related derivatives,⁷ silicates,⁸ dihydropyridines⁹ and sulfinates¹⁰ as well as electrophiles such as aryl and vinyl halides and also Csp²-O-electrophiles.^{6,11}

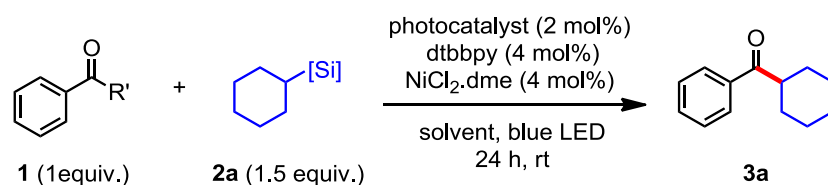
In addition to being environmentally friendly and very mild, the photoredox conditions used in these reactions are usually compatible with many functionalities.¹² They have also been found to be compatible for the delivery of ketones.^{8i,13} For instance, Doyle and co-workers showed that it is possible to obtain α -amino ketones by using N-aryl amines and electrophiles such as anhydrides or activated esters.¹⁴ In the same vein, Molander *et al.* used this approach to achieve the coupling reaction between acyl chlorides and trifluoroborates as radical precursors to obtain functionalized ketones.¹⁵ Nevertheless, this transformation relies on conditions involving the use of additives such as 2,6-lutidine or fluoride salts and does not provide highly enolizable benzylic ketones which are difficult to access. For these reasons, we turned our attention to the reactivity of the highly soluble and easily oxidized silicates toward carboxylic acid derivatives and particularly acyl chlorides in order to obtain benzylic and alkyl ketones.

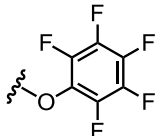
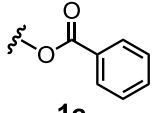
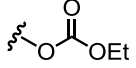


Scheme 1: Formation of ketones *via* dual photoredox/Ni catalysis using acid chloride as electrophiles

II.3.3. Results and discussion

We first tried this reaction with 1.5 equiv. of cyclohexyl silicate **2a** ($E^{\text{ox}} = +0.69$ V *vs.* SCE) as the radical source and 1 equiv. of benzoyl chloride as the electrophile in the presence of Ru(bpy)₃(PF₆) as a photocatalyst, and NiCl₂.dme and dtbbpy (4,4'-di-*tert*-butyl-2,2'-dipyridyl) as ligands in THF under blue LED irradiation at room temperature. Gratifyingly, the expected ketone **3a** was obtained in 64% yield. Following this encouraging result, we searched for the best conditions to achieve this reaction (**Table 1**). The organic photocatalyst 4CzIPN, known to have a long lived excited state and a high oxidative potential ($\tau = 5100$ ns, $E_{1/2}(\text{Ir}(\text{PC}^*)/\text{Ir}(\text{PC}^{\cdot-})) = +1.59$ V *vs.* SCE)^{16,17} and previously used to oxidize silicates,¹⁸ gave ketone **3a** in 52% yield (entry 2). To our delight, iridium photocatalyst Ir(dF(CF₃)ppy)₂(bpy)(PF₆) provided the best yield of coupling product **3a** (72%). Other solvents (dichloromethane and acetonitrile) and nickel catalysts, for instance Ni(COD)₂ as the nickel (0) source were screened but they did not show any improvement. Therefore, the Ir(dF(CF₃)ppy)₂(bpy)(PF₆)/NiCl₂.dme dual catalytic system was selected and it gave the best results.



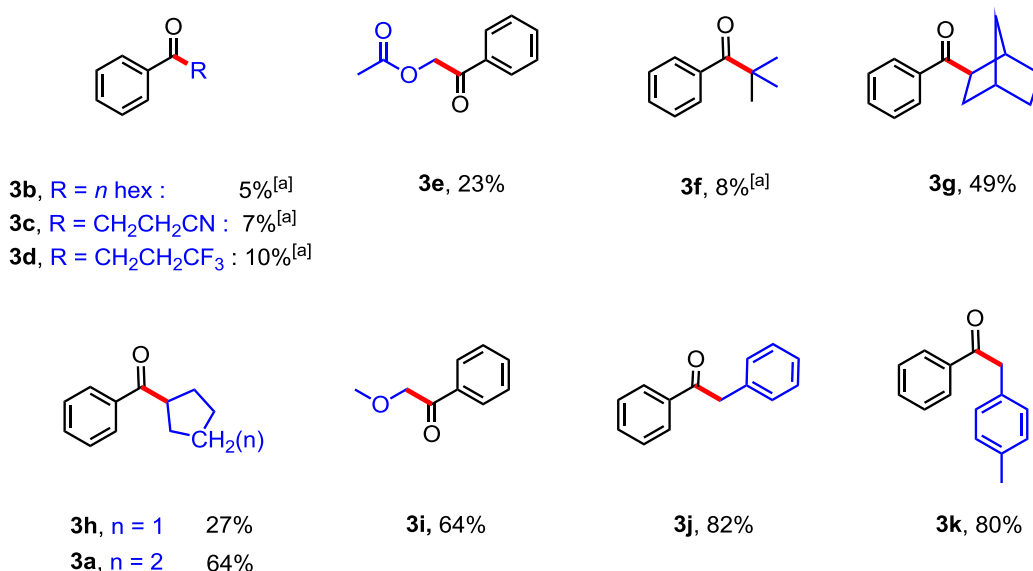
Entry	Solvent	Photocatalyst (2 mol %)	R	Yield ^[a]
1	THF	[Ru] ^[b]	Cl	64%
2	THF	4CzIPN	Cl	52%
3 ^[c]	THF	[Ir] ^[d]	Cl	54%
4	DMF	[Ir] ^[d]	Cl	6%
5	THF	[Ir] ^[d]	Cl	72%
6 ^[e]	THF	[Ir] ^[d]	Cl	42%
7	CH ₂ Cl ₂	[Ir] ^[d]	Cl	0%
8	CH ₃ CN	[Ir] ^[d]	Cl	0%
9	THF	-	Cl	0%
10 ^[f]	THF	[Ir] ^[d]	Cl	0%
11	THF	[Ir] ^[d]	F	0%
12	THF	[Ir] ^[d]		40%
13	THF	[Ir] ^[d]		31%
14	THF	[Ir] ^[c]		12%

^[a] NMR yield using 1,3,5 trimethoxybenzene as internal standard; ^[b] [Ru] = Ru(bpy)₃(PF₆)₂, ^[c] Ni(COD)₂ was used instead of NiCl₂.dme, ^[d] [Ir] = Ir(dF(CF₃)ppy)₂(bpy)(PF₆), ^[e] 16 h of blue LED irradiation (477 nm) instead of 24 h, ^[f] No NiCl₂.dme was present.

Table 1: Optimization of the reaction conditions

Under these optimized conditions other electrophiles were tested. While no product was observed with the corresponding acyl fluoride derivative, yields of 40%, 31% and 12% were obtained from activated ester **1b**, mixed anhydrides **1c** and mixed carbonate **1d**, respectively (Entries 12-14, **Table 1**). Nevertheless, these yields were lower than that previously obtained with benzoyl chloride as a partner. Therefore, we decided to continue this study with acyl chloride partners.

We first varied the silicate partner (**Scheme 2**) keeping benzoyl chloride **1a** as the electrophile. All primary radicals resulted in poor yields of products (below 10 %). The main side product in these reactions is the acylation of catechol which suggested that the rate-limiting step is the very slow oxidation of the silicate allowing the catecholate moiety to react on the acyl chloride.¹⁹ More activated α -acetoxysilicate resulted only in a slight yield increase in the yield and adding 6 equiv. of benzoyl chloride for 1 equiv. of silicate did not change it. Not surprisingly, *tert*-butyl silicate underwent little cross-coupling.^{8a} Secondary silicates proved however to be generally more rewarding since cyclopentyl, norbornane and cyclohexyl silicate precursors afforded the cross-coupling products in 27% (**3h**), 49% (**3g**) and 64% (**3a**) yields respectively. Finally, activated silicates such as the newly prepared (see ESI) methoxymethylene silicate ($E^{\text{ox}} = +0.71$ V vs. SCE **2i**) and benzyl derivatives gave the best results and provided highly enolizable ketones **3i**, **3j** and **3k** in very good yields of 64%, 82% and 80%, respectively.

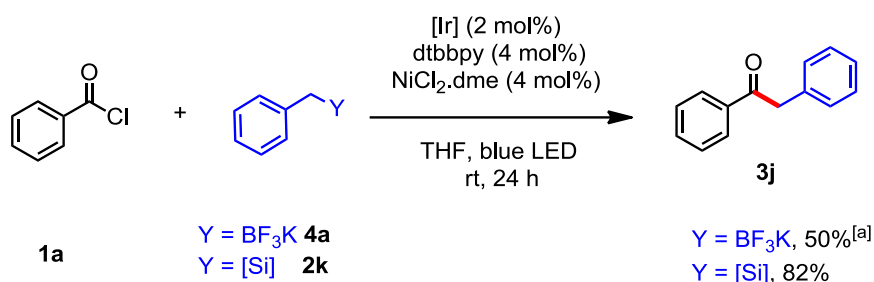


^[a] NMR yield using 1,3,5 trimethoxybenzene as internal standard

Scheme 2: Silicate scope in the coupling reaction with benzoyl chloride

It appeared also judicious to compare the reactivities of the benzyl trifluoroborate and benzyl silicate precursors under these conditions with no additive. The benzyl trifluoroborate **4a** afforded the desired product **3j** with a yield of 50% as determined by NMR (benzoic acid was also observed in the reaction mixture attesting the incomplete conversion of the reactant)

compared to the 82% isolated from benzyl silicate **1j** with full conversion of the acyl chloride (**Scheme 3**) (10% of monoacylated product was also observed in that case).

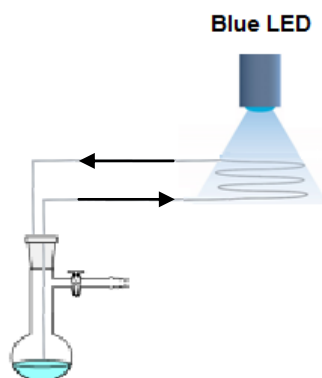


^[a] by NMR using 1,3,5 trimethoxybenzene as internal standard

Scheme 3: Comparison of the reactivity of the benzyl trifluoroborate and the benzyl silicate

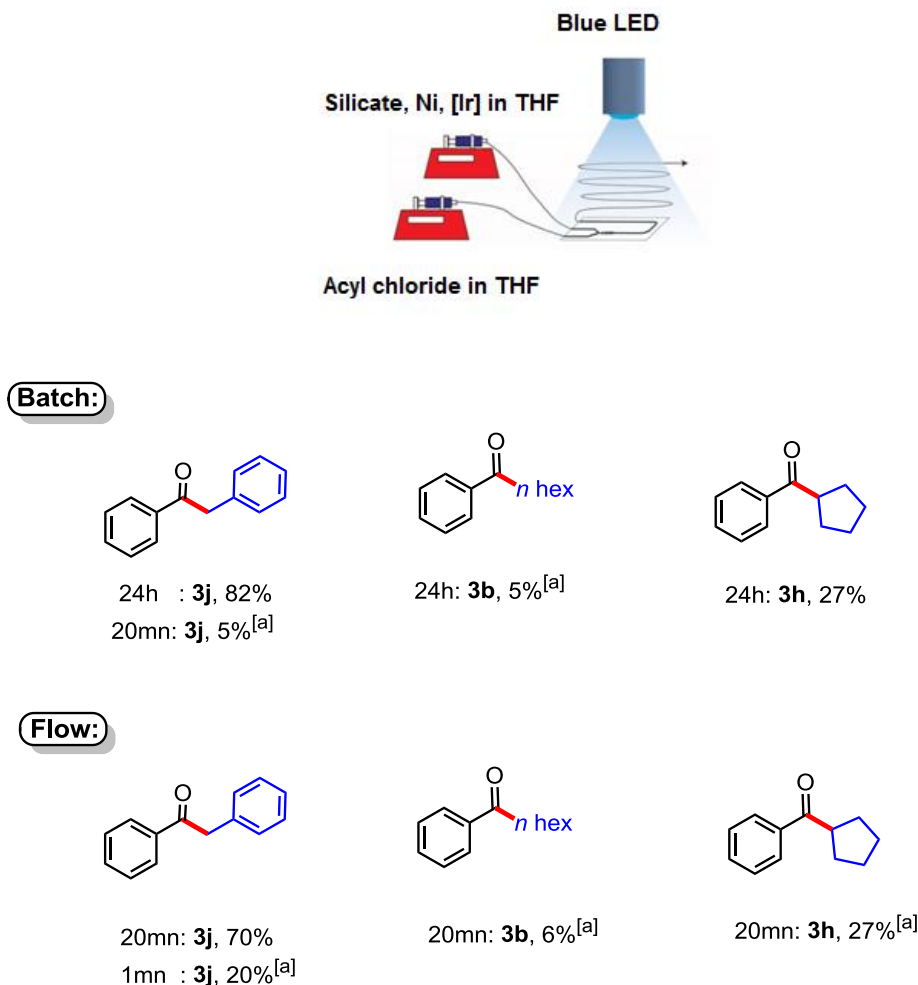
In order to avoid the previously mentioned catechol acylation side reaction, we tried to employ miniaturized flow reactors to accelerate the desired photooxidative process.²⁰

An initial flow set-up was assembled using a Schlenk flask and a recirculating pump (**Scheme 4**). The reagents were mixed by magnetic stirring inside the Schlenk flask protected from light, pumped through a PTFE tube (1/16" tubing, 134 cm, 0.67 mL at room temperature) under blue LED irradiation (477 nm) which was used as the flow reactor and re-introduced into the Schlenk flask. The coupling of benzyl silicate **2k** with benzoyl chloride was used as a model reaction and a yield of 43% for **3j** was obtained in 3.8 hours within the flow reactor. Nevertheless the formation of a larger amount of mono- and bis-acylated catechol products was observed in contrast to the trace amounts from benzyl silicate in batches. This result can be easily explained by the fact that the side reaction does not need light and that it can occur inside the Schlenk reservoir.



Scheme 4: Flow configuration with premixed reactants

Following this first attempt, a two flux process without recirculation was developed on the same scale as the previous batch reaction (**Scheme 5**).



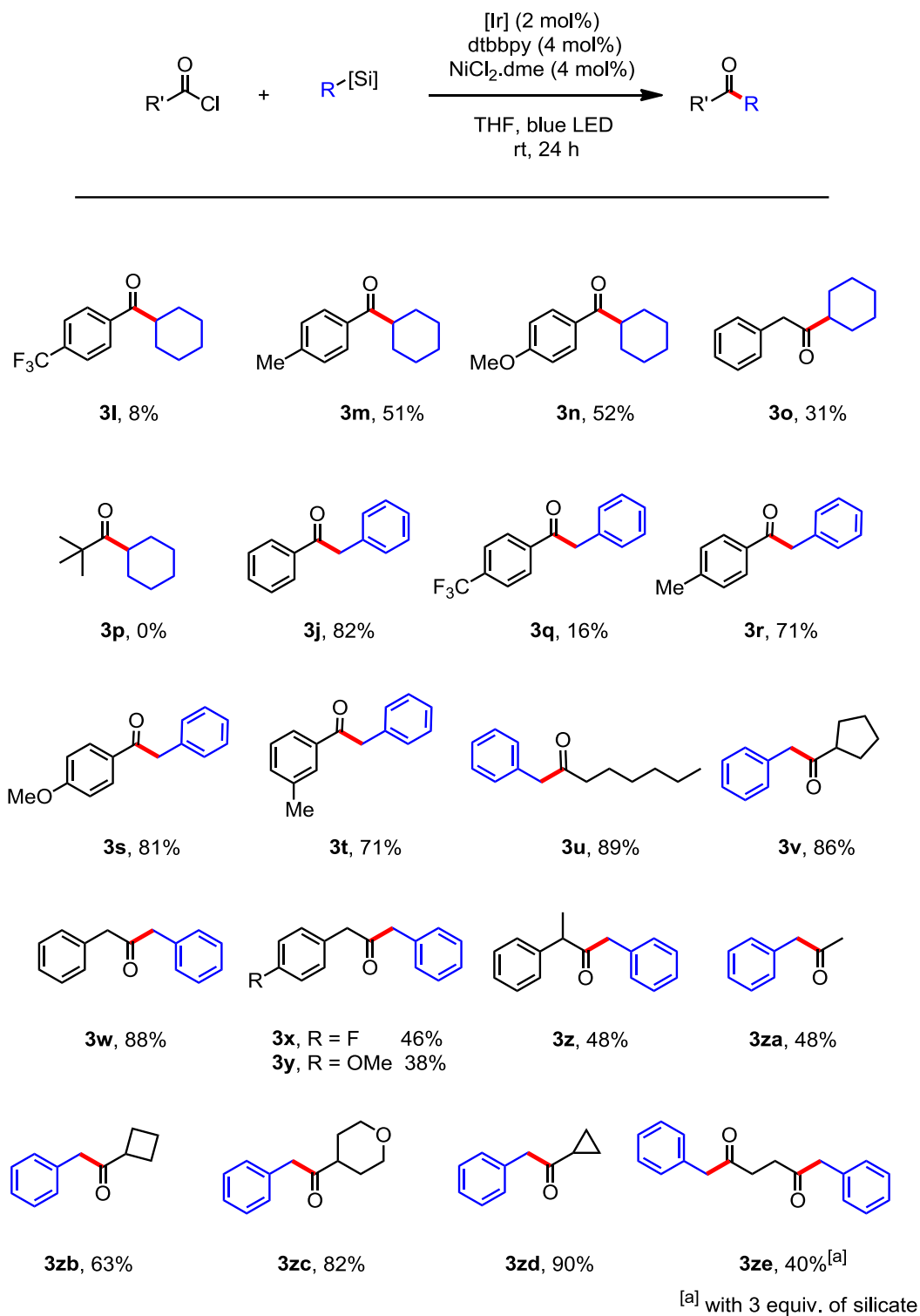
^[a] by NMR using 1,3,5 trimethoxybenzene as an internal standard

Scheme 5: Flow configuration with in-line micro reactor

One flux introduced the acyl chloride and the other one the nickel catalyst, the photocatalyst, the ligand and the silicate. The two flux components ($F = 1.305$ mL/h) were mixed within a glass milli-mixer (LTF-MX, 0.2 mL at room temperature) under blue LED irradiation (477 nm), and the mixture then flowed through a PTFE tubing (1/16" tubing, 134 cm, 0.67 mL at room temperature) under blue LED irradiation (477 nm). The resulting solution was collected in the dark and the desired product directly isolated by chromatography. A good yield (70%) of the cross-coupling product **3j** was obtained in only 20 minutes with total conversion of the acyl chloride with this flow setup (20% of the monoacetylated catechol product and traces of the bisacylated adduct were also observed), while a similar yield (81%) on the same scale can be obtained in a batch reactor after 24 hours. The flow reaction setup

enables a shorter reaction time, hence a higher energy efficiency, not to mention the ease of scaling-up with the flow chemistry.

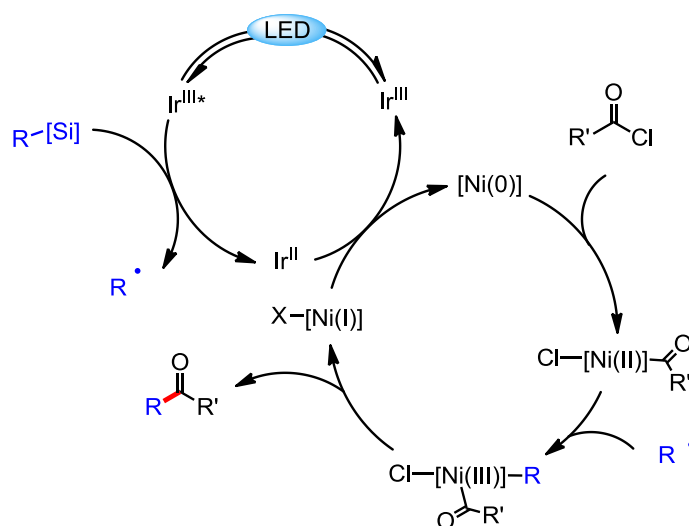
Encouraged by these series of preliminary findings and exploring the synthetic potential of this new transformation, we examined the influence of the acyl chloride partner (**Scheme 6**) using **2a** and **2j** as radical sources. The highly electrophilic *para*-CF₃ substituted benzoyl chloride mainly led to the formation of the acylated catechol (mono-acylated and bi-acylated products) with poor yields of cross-coupling ketones **3l** (8%) and **3q** (16%). In contrast, electron richer benzoyl chlorides afforded the corresponding ketones in moderate to good yields (51% and 52%, respectively, for the cyclohexyl silicate and 81% and 71%, respectively, for the benzyl silicate). To our delight, primary and secondary alkyl acyl chlorides provided the products in very high yields leading to ketones with various substitution patterns, featuring for example cyclopropyl and cyclobutyl benzylketones (**3zb** and **3zd**). It is noteworthy that double coupling from a diacyl chloride was possible (diketone **3ze**). Finally, highly enolizable dibenzyl ketones such as **3w-z** could be prepared through this method.



Scheme 6: Scope of this reaction based on the variation of the acyl chloride

Moreover, these ketones are valuable scaffolds for further elaboration. For instance, **3j** has already been used to synthesize natural products or drugs such as valdecoxib²¹, scabanca (through a Bayer-Villiger oxidation)²² and tamoxifen.²³

Based on our recent studies and those of other groups on related silicate chemistry,⁸ the following mechanism can be reasonably proposed (**Scheme 7**). The excited photocatalyst readily oxidizes the silicate to generate an iridium(II) complex and a radical intermediate. Presumably, the latter adds onto the nickel(II) intermediate resulting from the oxidative addition of the acyl chloride partner onto nickel(0). The resulting nickel(III) complex undergoes reductive elimination releasing both the desired product and a nickel (I) species and is then further reduced by iridium(II) and regenerates the iridium(III) photocatalyst.



Scheme 7: Proposed mechanism

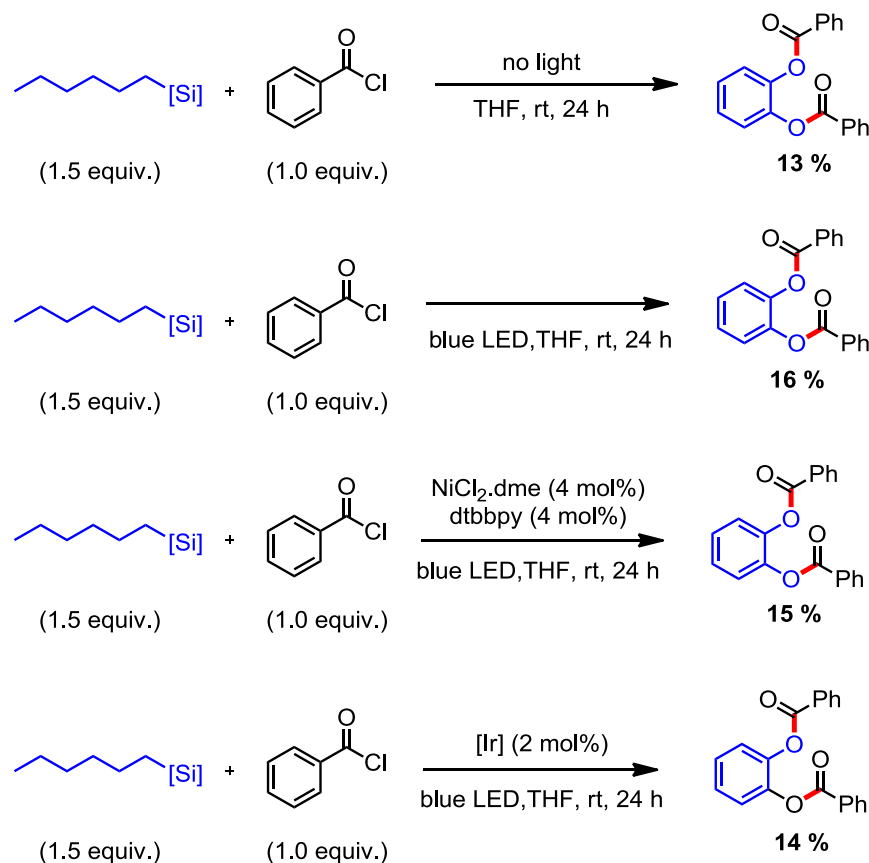
II.3.4. Conclusion

In a nutshell, a novel method has been used for obtaining ketones by dual photoredox/Ni dual catalysis using bis-catecholato silicates as radical sources and acyl chlorides as electrophiles. While the reaction proved unsatisfactory with primary silicates or highly electrophilic acid chlorides due to adventitious acylation of the catechol moieties, interesting yields of variously substituted ketones have been generally recorded. Notably the highly enolizable dibenzylic ketones could be prepared. Various applications of flow chemistry to such photoredox/nickel dual catalysis reaction have been disclosed and a shorter reaction time has been obtained.

II.3.5. Additional results

II.3.5.1. Formation of the side products

In the above-mentioned paper, we have described a new synthesis of ketones. However, non activated silicates were leading to mono and bis acylated catechols. In order to understand why we were forming these side products, different control experiments have been carried out (**Scheme 8**).



Scheme 8: Control experiments

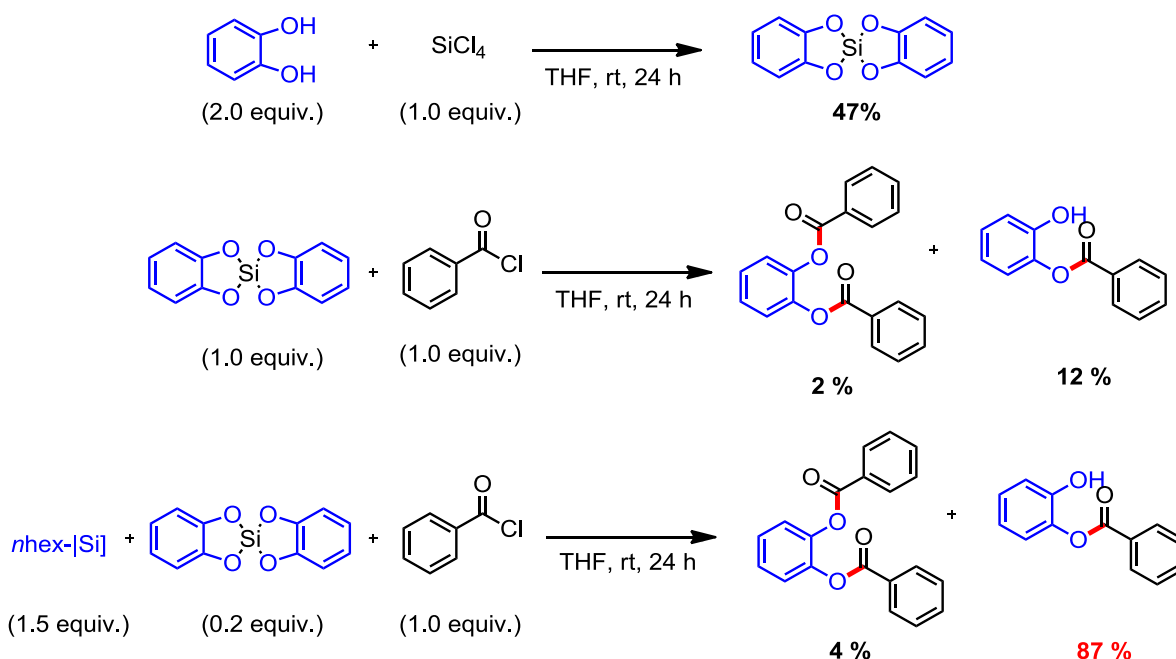
All of these control reactions led to some bis acylated products. Only about 30% of the acyl chloride was consumed, so it did not explain why only a few percents of the desired product were obtained with the non-activated silicates. None of the studied parameters (irradiation, [Ir] and NiCl₂.dme presence or absence) seemed to have an impact on the amount of side products formed.

Then, we thought that the reaction byproduct might explain these side reactions. Indeed, the biscatechol silane is a very strong Lewis acid which can activate the acyl chloride.

Thus, the biscatechol silane was synthesized and put in reaction with an acyl chloride in presence or absence of a silicate (**Scheme 9**).

When the acyl chloride was put with the Lewis acid, only a few portion reacted and led to the mono and bis acylated catechols. Nevertheless we found that, when the silicate was also present, 87% of the monoacylated adduct was obtained.

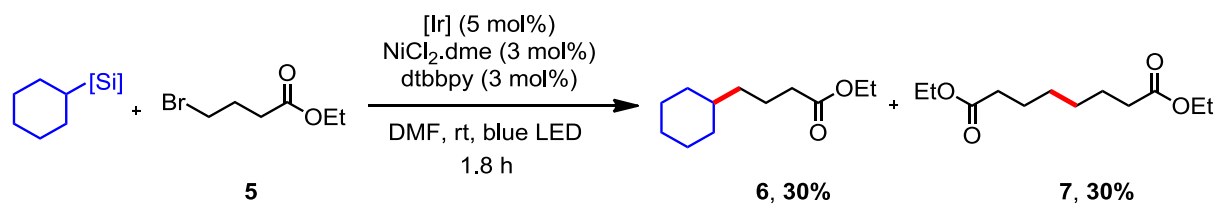
Thus, we can suppose that, once a small amount of biscatechol silane is formed, it activates the acyl chloride and the catechols of the silicate can react through a ionic or a concerted process onto this electrophile to form the acylated side products.



Scheme 9: Control experiments using the biscatechol silane

II.3.5.2. Additional flow chemistry: *sp*³-*sp*³ cross-coupling reaction

Because flow chemistry drastically accelerates the photochemical process, we had the idea of performing the previously reported *sp*³-*sp*³ cross-coupling reaction (page 124) with the silicates in flow, hoping to decrease the amount of homocoupling adduct. Indeed, the yield for this reaction in batch was only about 40% for an alkyl silicate and a ratio 50 : 50 was obtained between the coupling product and the homocoupling adduct. When we performed this reaction with the iridium photocatalyst (5 mol%) and NiCl₂.dme (3 mol%) for 1.8 hours under flow conditions, the same amount of homocoupling and desired products were obtained (**Scheme 10**). No influence on the reaction yield was observed (yield = 30%).

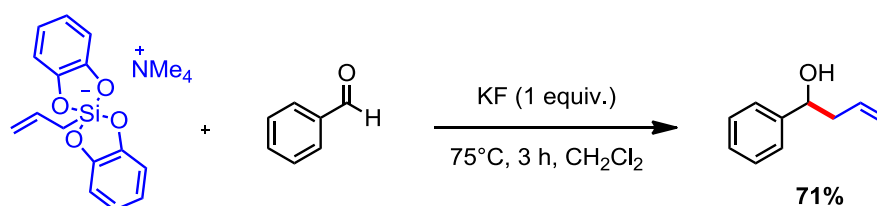


Scheme 10: $\text{sp}^3\text{-sp}^3$ cross-coupling reaction under flow conditions

In conclusion, we can say that flow chemistry usually decreases the reaction time but may not prevent side reactions.

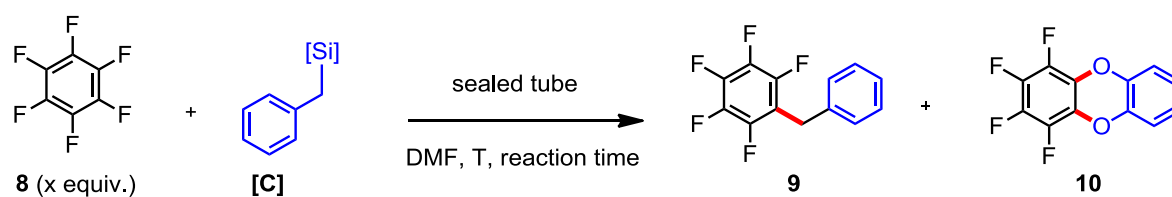
II.3.5.3. Nucleophilicity of the silicates

The side reaction between silicates and acyl chlorides shows that a certain nucleophilicity exists for these hypervalent silicon compounds. It should be noted that this nucleophilicity was already brought to light by Corriu's group. Indeed, in 1987, they showed that the tetramethylammonium salt of the allyl silicate was reacting very efficiently with benzaldehyde in presence of KF (1 equiv.) (**Scheme11**).²⁴



Scheme 11: Aldol reaction between allyl silicate and benzaldehyde

Inspired by this reaction and by the exceptional affinity between fluoride and silicon (Bond Dissociation Energy: 576 kJ/mol²⁵), we hypothesized that silicates can activate the reactivity of a fluoride atom. Our model reaction was based on hexafluorobenzene **8** toward benzyl silicate.



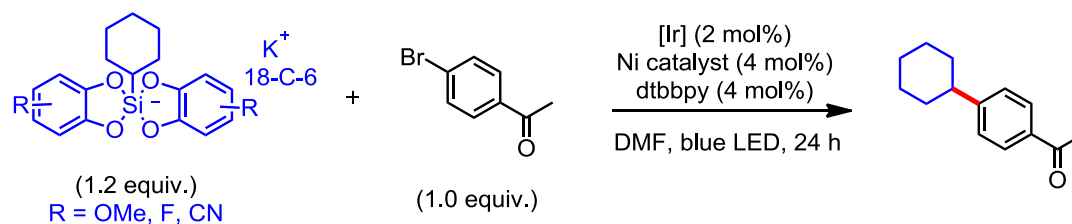
8 (x equiv.)	[C]	T	Reaction time	Yield 9/10
50	0.1 M	60°C	24h	5/29%
50	0.1 M	100°C	24h	14/26%
10	0.1 M	60°C	72h	34/38%
10	0.067 M	100°C	24h	11/20%
50	0.067 M	100°C	24h	52/50%
50	0.067 M	130°C	24h	37/17%
50	0.067 M	100°C	40h	65/21%

Table 2: Substitution reaction using hexafluorobenzene and benzyl silicate

A mixture of desired product **9** and byproduct **10**, resulting from the addition of the catechol onto the hexafluorobenzene, was obtained. After an extensive screening of the concentration, temperature and reaction time, a satisfying yield of 65% for **9** could be obtained (**Table 2**). Other electrophiles such as alkyl fluoride, aryl triflate and acyl fluoride were also tested but did not lead to any desired product. Further works are currently ongoing in our laboratory to extend the scope of this reaction.

II.3.5.4. Dual catalysis and catechol modification

Intrigued by the results obtained in the first chapter about catechol modifications, we wondered what influences such substitutions could have on a dual catalysis system. Thus we performed different reactions using cyclohexyl silicates and 4-bromoacetophenone as model substrates (**Table 3**).



Silicate	Yield (with NiCl ₂ .dme/ with Ni(COD) ₂)
	90/96%
	67/87%
	2/3%
	30/7%

Table 3: Dual catalysis reactions using cyclohexyl modified catechols silicates

Interestingly, only the 3-fluorocatechol afforded the product in good yields. The cyano and the methoxy modifications resulted in yields drops. Moreover, Ni(COD)₂ was revealed to be the best nickel catalyst for the silicate possessing 3-fluorocatechols whereas NiCl₂.dme provided the best result for the one bearing 4-cyano catechols. It is worth noting that this dual catalysis reaction was also applied to the phenyl silicate possessing 4-cyano catechols but no product was formed with NiCl₂.dme, Ni(COD)₂ or even Pd(OAc)₂ and Pd₂(dba)₃. In conclusion, catechol modifications have an impact on such systems and could be helpful in some reactions.

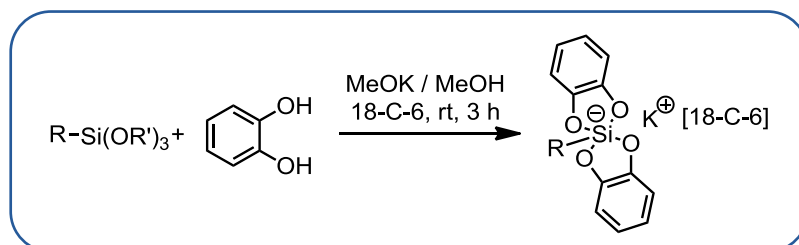
II.3.6. Supporting information

II.3.6.1. General informations

Unless otherwise noted, reactions were carried out under an argon atmosphere in oven-dried glassware. Methanol was distilled over CaH₂, THF, acetonitrile and diethyl ether were distilled over sodium/benzophenone, triethylamine over potassium hydroxide. Catechol was purchased from commercial source and purified by crystallization from toluene followed by sublimation. Reagents and chemicals were purchased from commercial sources and used as received. Infrared (IR) spectra were recorded on a Bruker Tensor 27 (ATR diamond) spectrophotometer. Melting points were determined on a melting point apparatus SMP3 (Stuart scientific) and are uncorrected. ¹H, ¹⁹F, ¹³C NMR spectra were recorded at room temperature at 400, 377 and 100 MHz respectively, on a Bruker AVANCE III 400 spectrometer. ²⁹Si NMR spectra were recorded at 79, 119 MHz on a Bruker AVANCE III 400, 600 spectrometer. Chemical shifts (δ) are reported in ppm and coupling constants (J) are given in Hertz (Hz). Abbreviations used for peak multiplicity are: s (singlet); bs (broad singlet); d (doublet); t (triplet); q (quartet); quint (quintet); sept (septet); m (multiplet). Thin layer chromatographies (TLC) were performed on Merck silica gel 60 F 254 and revealed with a UV lamp ($\lambda = 254$ nm) and KMnO₄ staining. Flash Column Chromatographies were conducted on silica Geduran[®] Si 60 Å (40 – 63 μ m). High resolution mass spectrometries were performed on a microTOF (ESI). Photocatalysts were synthesized as described.^{26,27} Silicates **2a-2h** and **2j** were synthesized as described.²⁸

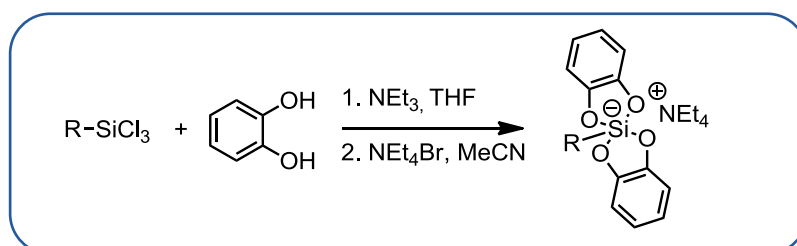
II.3.6.2. General procedures

a) General procedure A1 for silicate synthesis



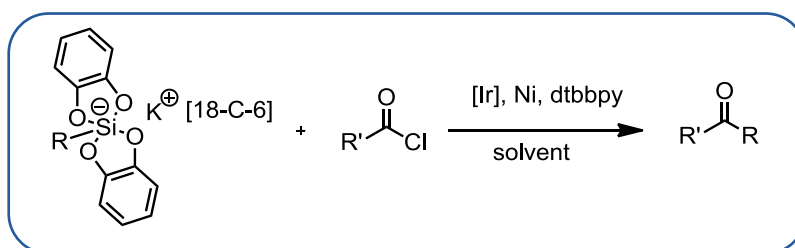
To a stirred solution of catechol (2 equiv.) in dry methanol (0.25 M) was added 18-C-6 (1 equiv.). After dissolution of the crown ether, the trialkoxy organosilane (1 equiv.) was added, followed by a solution of potassium methoxide in methanol (1 equiv.). The reaction mixture was stirred for 3 hours and the solvent was removed under reduced pressure. The residue was dissolved in the minimum volume of acetone and diethyl ether was added until a cloudy solution was obtained (scrapping on the edge of the flask could be done to induce crystallization). The flask was placed at -20°C overnight. The crystals were collected by filtration, washed with diethyl ether and dried under vacuum to afford potassium [18-Crown-6] silicate.

b) General procedure A2 for the synthesis of triethylammonium bis(catecholato) 5-(bicycloheptenyl)silicate



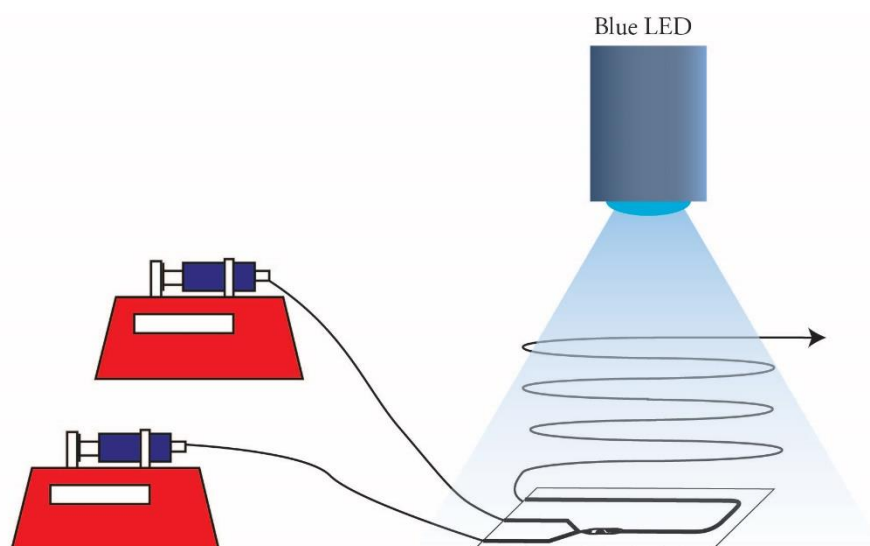
To a stirred solution of catechol (2 equiv.) in dry THF (0.1 M) was added triethylamine (4 equiv.). The reaction mixture was cooled to 0°C with an ice bath and the corresponding trichlorosilane (1 equiv.) was added dropwise. The reaction mixture was stirred for one hour at 0°C and an additional hour at room temperature. The triethylamine hydrochloride salts were filtered off and the filtrate was evaporated under reduced pressure. The residue was taken up in acetonitrile (0.3 M) and tetraethylammonium bromide (1 equiv.) was added. The reaction mixture was stirred for one hour then the mixture was evaporated under reduced mixture. The solid was taken up in water, filtered and washed again with water then dried *in vacuo* to give the corresponding tetraethylammonium silicate.

c) General procedure B for the photoredox/nickel cross-coupling dual catalysis



To a Schlenk flask was added the appropriate silicate (1.5 equiv.), [Ir] (2 mol %), 4,4'-di-*tert*-butyl-2,2'-dipyridyl (4 mol %) and NiCl₂.dme (4 mol %). The Schlenk flask was sealed with a rubber septum and evacuated / purged with vacuum / argon three times. Then degassed THF (0.1 M) was introduced followed by addition of the electrophile **2** (1 equiv.) and the reaction mixture was irradiated with blue LED (477 nm) at room temperature for 24h under an argon atmosphere. The reaction mixture was diluted with diethyl ether, washed with aqueous saturated K₂CO₃ solution (2 times), brine (2 times), dried over MgSO₄ and evaporated under reduced pressure. The crude residue was purified by flash chromatography.

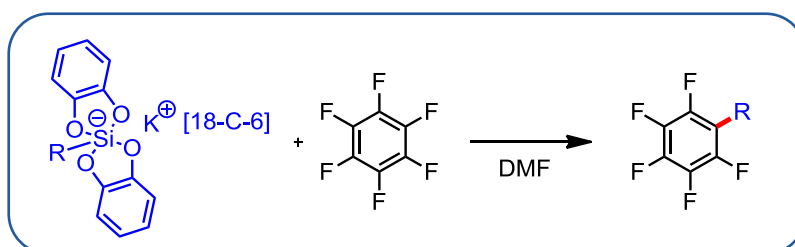
d) General procedure B2 for the continuous flow photoredox/nickel cross-coupling dual catalysis



A solution of silicate with catalysts (1.5 equiv. of the appropriate silicate, 2 mol% [Ir], 4 mol% 4,4'-di-*tert*-butyl-2,2'-dipyridyl, 4 mol% NiCl₂.dme prepared in glovebox) in degassed THF (0.2 M) and a solution of the appropriate electrophile (1 equiv.) in degassed THF(0.2 M)

were pumped by two syringe pumps (AL-300, World Precision Instruments, USA) with a flow rate of 22 $\mu\text{L}/\text{min}$ respectively. They were mixed within a glass milli-mixer (LTF-MX, 0.2 mL at room temperature, Little Things Factory, Germany) under blue LED irradiation (477 nm), and the mixture then flowed through a PTFE tubing (1/16" tubing, 134 cm, 0.67 mL at room temperature) under blue LED irradiation (477 nm). The mixer and the PTFE tubing were rinsed with degassed THF prior to use. The reaction time was calculated with the total reaction volume and the total flow rate, which gave a reaction time of 20 min. The reaction mixture was then collected, diluted with diethyl ether, washed with an aqueous saturated K_2CO_3 solution (2 times), brine (2 times), dried over MgSO_4 and evaporated under reduced pressure. The crude residue was purified by flash column chromatography on silica gel to afford the product. The reaction time is calculated as the total reaction volume (0.87 mL) divided by the total flowrate (44 $\mu\text{L}/\text{min}$), which is around 20 minutes.

e) General procedure for the reaction of a silicate with hexafluorobenzene

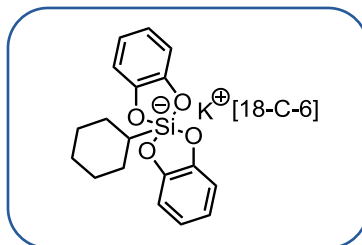


To a round bottom flask was added the appropriate silicate (1.0 equiv.) and hexafluorobenzene in DMF. The reaction mixture was heated for an appropriate time before being diluted with diethyl ether, washed with water (2 times), dried over MgSO_4 and evaporated under reduced pressure. The crude residue was analyzed by ^1H NMR using 1,3,5-trimethoxybenzene as an internal standard.

II.3.6.3. Compound characterizations

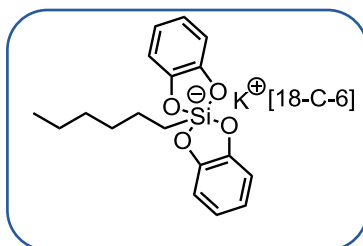
a) Synthesis and characterizations of the silicates

Potassium [18-Crown-6] bis(catecholato)-cyclohexylsilicate (**2a**)



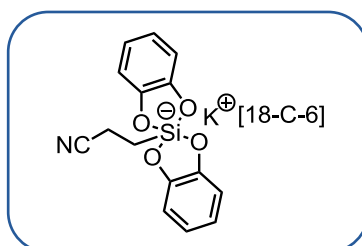
Silicate **2a** was synthesized as described. The spectroscopic data are in agreement with those reported in the literature.^{8a}

Potassium [18-Crown-6] bis(catecholato)-hexylsilicate (**2b**)

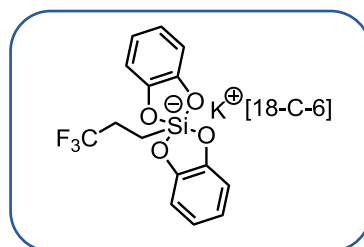


Silicate **2b** was synthesized as described. The spectroscopic data are in agreement with those reported in the literature.^{8a}

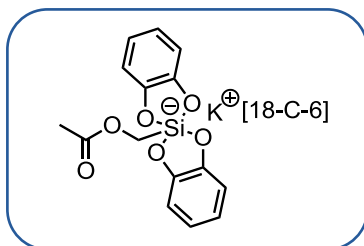
Potassium [18-Crown-6] bis(catecholato)-2-cyanoethylsilicate (**2c**)



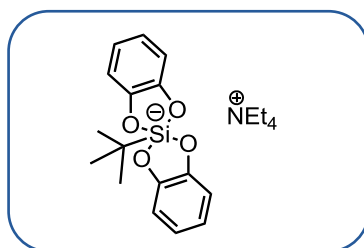
Silicate **2c** was synthesized as described. The spectroscopic data are in agreement with those reported in the literature.^{8a}

Potassium [18-Crown-6] bis(catecholato)-3,3,3-trifluoropropylsilicate (2d)

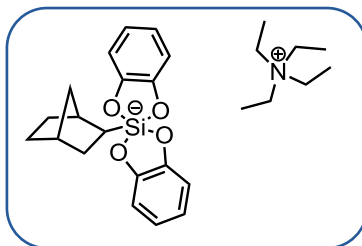
Silicate **2d** was synthesized as described. The spectroscopic data are in agreement with those reported in the literature.^{8a}

Potassium [18-Crown-6] bis(catecholato)-acetoxymethylsilicate (2e)

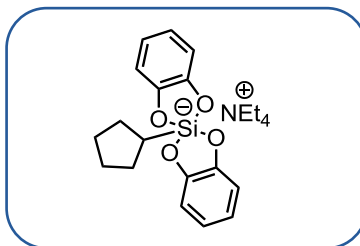
Silicate **2e** was synthesized as described. The spectroscopic data are in agreement with those reported in the literature.^{8a}

Tetraethylammonium bis(catecholato)-*tert*-butylsilicate (2f)

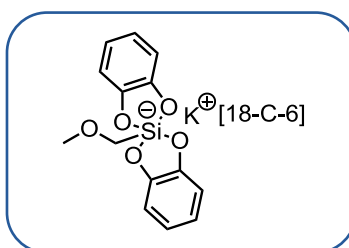
Silicate **2f** was synthesized as described. The spectroscopic data are in agreement with those reported in the literature.^{8a}

Triethylammonium exo-2-bicyclo[2.2.1]heptylbis(catecholato)silicate (2g)

Silicate **2g** was synthesized as described. The spectroscopic data are in agreement with those reported in the literature.²⁹

Cyclopentylsilicate triethylammonium (2h)

Silicate **2h** was synthesized as described. The spectroscopic data are in agreement with those reported in the literature.^{8a}

Potassium [18-Crown-6] bis(catecholato)-methoxymethylsilicate (2i)

Chloromethyltrimethoxysilane (4.0 mmol, 0.6 mL) was added to a stirred solution of potassium methoxyde 3.56 M in MeOH (4.4 mL). The resultant mixture was stirred for two days then the solvent was removed *in vacuo*. After that catechol (8.0 mmol, 880.8 mg) and 18-C-6 (4.0 mmol, 1.056 g) were added in 10 mL of MeOH. Then a solution of potassium methoxide in methanol 3.56 M (3.7 mmol, 1.04 mL) was added. The reaction mixture was stirred for 2 hours and the solvent was removed under reduced pressure. The residue was

dissolved in the minimum volume of acetone and diethyl ether was added until a cloudy solution was obtained (scrapping on the edge of the flask could be done to induce crystallization). The flask was placed at -20°C overnight. The crystals were collected to afford potassium [18-Crown-6] bis(catecholato)-methoxymethylsilicate **2i** (1.508 g, 64%).

^1H NMR (400 MHz, Methanol- d_4): δ 6.76-6.67 (m, 4H), 6.62-6.55 (m, 4H), 3.62 (s, 24H), 3.21 (s, 2H), 3.19 (s, 3H);

^{13}C NMR (100 MHz, CD_2Cl_2): δ 150.9 (4C), 118.0 (4C), 110.6 (4C), 70.1 (12C), 66.2, 61.8;

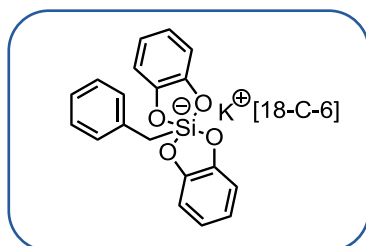
^{29}Si NMR (79 MHz, CD_2Cl_2): δ - 82.2;

HRMS: calc. for $[\text{C}_{14}\text{H}_{13}\text{O}_5\text{Si}]^-$: 289.0538, found 289.0539;

M.P. 161.9°C ;

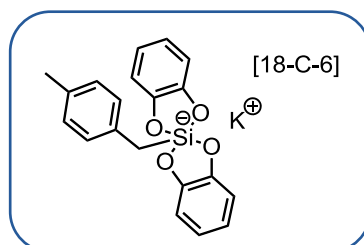
IR (neat): 2900, 1484, 1352, 1284, 1243, 1224, 1179, 1012, 956, 913, 885, 867, 583 cm^{-1} .

Potassium [18-Crown-6] bis(catecholato)-benzylsilicate (**2j**)



Silicate **2j** was synthesized as described. The spectroscopic data are in agreement with those reported in the literature.^{8a}

Potassium [18-Crown-6] bis(catecholato)-4-methylbenzylsilicate (**2k**)



To a stirred solution of dried THF were added 4-methylbenzyl bromide (5.0 mmol, 925 mg) and magnesium (6.0 mmol, 145.8 mg). The resultant mixture was heated under reflux for one hour then tetramethoxysilane (25.0 mmol, 3.70 mL) was added dropwise. The mixture was

then heated under reflux for 16 additional hours before being concentrated under reduced pressure. 20 mL of pentane were added and the mixture was filtrated. The filtrate was concentrated *in vacuo* then catechol (7.39 mmol, 814 mg) and 18-C-6 (3.7 mmol, 978 mg) were added in 10 mL of dried MeOH. Then a solution of potassium methoxide in methanol 3.56 M (3.7 mmol, 1.04 mL) was added. The reaction mixture was stirred for 3 hours and after that, the solvent was removed under reduced pressure. The residue was dissolved in the minimum volume of acetone and diethyl ether was added until a cloudy solution was obtained (scrapping on the edge of the flask could be done to induce crystallization). The flask was placed at -20°C overnight. The crystals were collected to afford potassium [18-Crown-6] bis(catecholato)-4-methylbenzylsilicate **2k** (400 mg, 12%).

¹H NMR (300 MHz, Methanol-d₄): δ 6.80-6.72 (m, 4H), 6.70-6.60 (m, 4H), 6.60-6.50 (m, 4H), 3.62 (s, 24H), 2.15 (s, 3H), 2.09 (s, 2H);

¹³C NMR (75 MHz, Methanol-d₄): δ 149.5 (4C), 128.3 (2C), 127.5 (2C), 118.9, 117.9 (4C), 114.8, 110.1 (4C), 69.9 (12C), 25.8, 19.5;

²⁹Si NMR (79 MHz, Methanol-d₄): δ - 80.6;

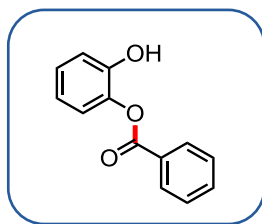
HRMS: calc. for [C₂₀H₁₇O₄Si]⁻: 349.0902, found 349.0902;

M.P. 218°C;

IR (neat): 2892, 1488, 1352, 1248, 1105, 1013, 964, 826, 767, 739, 708 cm⁻¹.

b) Characterisation of the byproducts

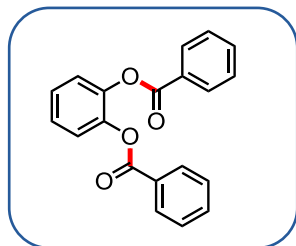
2-Hydroxyphenyl benzoate (**5a**)



The spectroscopic data are in agreement with those reported in the literature.³⁰

¹H NMR (400 MHz, CDCl₃): δ 8.30-8.15 (m, 2H), 7.72-7.64 (m, 1H), 7.58-7.51 (m, 2H), 7.23-7.16 (m, 2H), 7.11-7.04 (m, 1H), 7.01-6.95 (m, 1H);

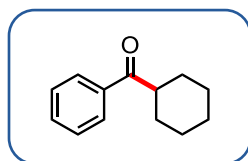
¹³C NMR (100 MHz, CDCl₃): δ 165.1, 147.4, 139.0, 134.2, 130.6 (2C), 129.0, 128.9 (2C), 127.3, 122.7, 121.4, 118.3.

1,2-Phenylene dibenzoate (5b)

The spectroscopic data are in agreement with those reported in the literature.³¹

¹H NMR (400 MHz, CDCl₃): δ 8.01-8.04 (m, 4H), 7.58-7.50 (m, 2H), 7.44-7.32 (m, 8H);

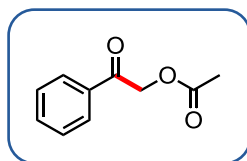
¹³C NMR (100 MHz, CDCl₃): δ 164.4 (2C), 142.8 (2C), 133.8 (2C), 130.3 (4C), 129.0 (2C), 128.6 (4C), 126.8 (2C), 123.7 (2C).

c) Synthesis and characterisation of ketones**Cyclohexyl(phenyl)methanone (3a)**

Following the general procedure **B** with benzoylchloride (0.417 mmol, 48 μL), iridium (8.34 μmol, 8.4 mg), NiCl₂.dme (16.7 μmol, 3.7 mg), 4,4'-di-*tert*-butyl-2,2'-dipyridyl (16.7 μmol, 4.5 mg) and cyclohexyl silicate (0.626 mmol, 394 mg) in 4.2 mL of dry THF. The crude product was purified according the general procedure to afford **3a** (50.0 mg, 64%) as a colorless oil. The spectroscopic data are in agreement with those reported in the literature.³²

¹H NMR (300 MHz, CDCl₃): δ 8.00-7.95 (m, 2H), 7.60-7.55 (m, 1H), 7.51-7.54 (m, 2H), 3.30-3.20 (m, 1H), 2.00-1.20 (m, 10H);

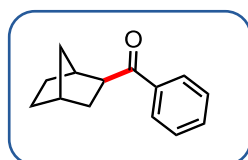
¹³C NMR (75 MHz, CDCl₃): δ 203.9, 136.5, 132.7, 128.5 (2C), 128.2 (2C), 45.7, 29.5 (2C), 26.0, 25.9 (2C).

2-Oxo-2-phenylethyl acetate (3e)

Following the general procedure **B** with benzoyl chloride (0.417 mmol, 48 μ L), iridium (8.34 μ mol, 8.4 mg), NiCl₂.dme (16.7 μ mol, 3.7 mg), 4,4'-di-*tert*-butyl-2,2'-dipyridyl (16.7 μ mol, 4.5 mg) and acetoxysilicate (0.626 mmol, 388 mg) in 4.2 mL of dry THF. The crude product was purified according the general procedure to afford **3e** (17.0 mg, 23%) as a colorless oil. The spectroscopic data are in agreement with those reported in the literature.³³

¹H NMR (300 MHz, CDCl₃): δ 7.90-7.80 (m, 2H), 7.60-7.50 (m, 1H), 7.46-7.37 (m, 2H), 5.27 (s, 2H), 2.17 (s, 3H);

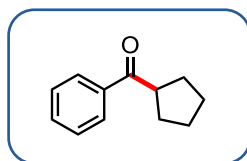
¹³C NMR (75 MHz, CDCl₃): δ 192.1, 170.5, 134.2, 133.9, 128.9 (2C), 127.8 (2C), 66.0, 20.6.

(1S,4R)-bicyclo[2.2.1]heptan-2-yl(phenyl)methanone (3g)

Following the general procedure **B** with benzoyl chloride (0.417 mmol, 48 μ L), iridium (8.34 μ mol, 8.4 mg), NiCl₂.dme (16.7 μ mol, 3.7 mg), 4,4'-di-*tert*-butyl-2,2'-dipyridyl (16.7 μ mol, 4.5 mg) and 2-(bicycloheptyl) silicate (0.626 mmol, 294 mg) in 4.2 mL of dry THF. The crude product was purified according the general procedure to afford **3g** (41.0 mg, 49%) as a colorless oil. The spectroscopic data are in agreement with those reported in the literature.³⁴

¹H NMR (300 MHz, CDCl₃): δ 8.04-7.92 (m, 2H), 7.57-7.51 (m, 1H), 7.49-7.42 (m, 2H), 3.25-3.19 (m, 1H), 2.55-2.51 (m, 1H), 2.37-2.33 (m, 1H), 2.06-1.99 (m, 1H), 1.68-1.09 (m, 7H);

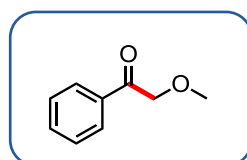
¹³C NMR (75 MHz, CDCl₃): δ 201.5, 136.8, 132.8, 128.6 (2C), 128.5 (2C), 49.7, 41.2, 36.4, 36.3, 33.8, 29.9, 29.2.

Cyclopentyl(phenyl)methanone (3h)

Following the general procedure **B** with benzoylchloride (0.417 mmol, 48 μ L), iridium (8.34 μ mol, 8.4 mg), NiCl₂.dme (16.7 μ mol, 3.7 mg), 4,4'-di-*tert*-butyl-2,2'-dipyridyl (16.7 μ mol, 4.5 mg) and cyclopentylsilicate tetraethylammonium (0.626 mmol, 277 mg) in 4.2 mL of dry THF. The crude product was purified according the general procedure to afford **3h** (21.0 mg, 27%) as a colorless oil. The spectroscopic data are in agreement with those reported in the literature.³⁵

¹H NMR (400 MHz, CDCl₃): δ 8.00-7.96 (m, 2H), 7.60-7.51 (m, 1H), 7.49-7.43 (m, 2H), 3.79-3.65 (m, 1H), 1.92 (s, 4H), 1.75-1.50 (m, 4H);

¹³C NMR (100 MHz, CDCl₃): δ 202.8, 137.0, 132.7, 128.5 (2C), 128.4 (2C), 46.3, 30.0 (2C), 26.3 (2C).

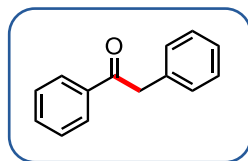
2-Methoxy-1-phenylethanone (3i)

Following the general procedure **B** with benzoyl chloride (0.417 mmol, 48 μ L), iridium (8.34 μ mol, 8.4 mg), NiCl₂.dme (16.7 μ mol, 3.7 mg), 4,4'-di-*tert*-butyl-2,2'-dipyridyl (16.7 μ mol, 4.5 mg) and methoxymethyl silicate (0.626 mmol, 370 mg) in 4.2 mL of dry THF. The crude product was purified according the general procedure to afford **3i** (40.0 mg, 64%) as a colorless oil. The spectroscopic data are in agreement with those reported in the literature.³⁶

¹H NMR (300 MHz, CDCl₃): δ 7.96-7.90 (m, 2H), 7.63-7.55 (m, 1H), 7.50-7.44 (m, 2H), 4.72 (s, 2H), 3.55 (s, 3H);

¹³C NMR (75 MHz, CDCl₃): δ 196.2, 134.9, 133.8, 128.8 (2C), 127.9 (2C), 73.4, 59.5.

1,2-Diphenylethanone (**3j**)

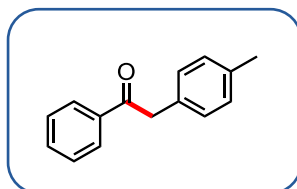


Following the general procedure **B** with benzoyl chloride (0.434 mmol, 50 μ L), iridium (8.70 μ mol, 8.7 mg), NiCl₂.dme (17.3 μ mol, 3.8 mg), 4,4'-di-*tert*-butyl-2,2'-dipyridyl (17.3 μ mol, 4.5 mg) and benzylsilicate (0.626 mmol, 416 mg) in 4.2 mL of dry THF. The crude product was purified according the general procedure to afford **3j** (70.0 mg, 82%) as a colorless oil. The spectroscopic data are in agreement with those reported in the literature.⁶

¹H NMR (300 MHz, CDCl₃): δ 8.00-7.90 (m, 2H), 7.55-7.45 (m, 1H), 7.42-7.35 (m, 2H), 7.30-7.10 (m, 5H), 4.21 (s, 2H);

¹³C NMR (75 MHz, CDCl₃): δ 197.6, 136.6, 134.6, 133.1, 129.5 (4C), 128.6 (4C), 126.9, 45.5.

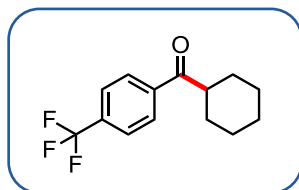
1-Phenyl-2-(*p*-tolyl)ethanone (**3k**)



Following the general procedure **B** with benzoyl chloride (0.327 mmol, 38 μ L), iridium (6.5 μ mol, 6.6 mg), NiCl₂.dme (13.1 μ mol, 2.9 mg), 4,4'-di-*tert*-butyl-2,2'-dipyridyl (13.1 μ mol, 3.5 mg) and 4-methylbenzylsilicate (0.626 mmol, 388 mg) in 4.2 mL of dry THF. The crude product was purified according the general procedure to afford **3k** (55.0 mg, 80%) as a colorless oil. The spectroscopic data are in agreement with those reported in the literature.³⁷

¹H NMR (300 MHz, CDCl₃): δ 8.00-7.89 (m, 2H), 7.51-7.45 (m, 1H), 7.42-7.33 (m, 2H), 7.12-7.00 (m, 4H), 4.17 (s, 2H), 2.25 (s, 3H);

¹³C NMR (75 MHz, CDCl₃): δ 197.8, 136.7, 136.6, 133.2, 131.3, 129.7 (2C), 129.5 (2C), 128.6 (4C), 45.1, 21.1.

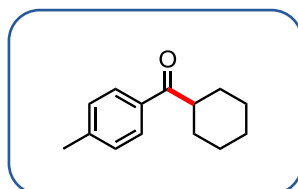
Cyclohexyl(4-(trifluoromethyl)phenyl)methanone (3l)

Following the general procedure **B** with 4-trifluoromethylbenzoyl chloride (0.834 mmol, 124 μ L), iridium (16.7 μ mol, 16.8 mg), NiCl₂.dme (33.4 μ mol, 7.3 mg), 4,4'-di-*tert*-butyl-2,2'-dipyridyl (33.4 μ mol, 7.0 mg) and cyclohexylsilicate (1.25 mmol, 788 mg) in 8.4 mL of dry THF. The crude product was purified according the general procedure to afford **3l** (20.0 mg, 8%) as a colorless oil. The spectroscopic data are in agreement with those reported in the literature.³⁸

¹H NMR (400 MHz, CDCl₃): δ 8.06 (d, J = 8.1 Hz, 2H), 7.75 (d, J = 8.1 Hz, 2H), 3.27 (tt, J = 12 Hz and 3.6 Hz, 1H), 1.95-1.70 (m, 5H), 1.45-1.20 (m, 5H);

¹³C NMR (100 MHz, CDCl₃): δ 202.8, 139.1, 134.1 (q, J = 35 Hz, 2C), 128.6, 125.6 (q, J = 5 Hz, 2C), 124.3 (q, J = 267.2 Hz), 45.9, 29.3 (2C), 25.9 (2C), 25.7;

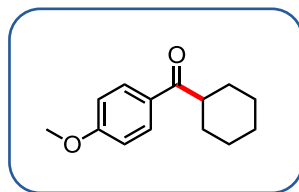
¹⁹F NMR (377 MHz, CDCl₃): δ -63.1.

Cyclohexyl(*p*-tolyl)methanone (3m)

Following the general procedure **B** with *p* toluoyl chloride (0.417 mmol, 57 μ L), iridium (8.34 μ mol, 8.4 mg), NiCl₂.dme (16.7 μ mol, 3.7 mg), 4,4'-di-*tert*-butyl-2,2'-dipyridyl (16.7 μ mol, 4.5 mg) and cyclohexyl silicate (0.626 mmol, 394 mg) in 4.2 mL of dry THF. The crude product was purified according the general procedure to afford **3m** (43.0 mg, 51%) as a colorless oil. The spectroscopic data are in agreement with those reported in the literature.³⁹

¹H NMR (300 MHz, CDCl₃): δ 7.75 (d, J = 8.2 Hz, 2H), 7.15 (d, J = 7.9 Hz, 2H), 3.15-3.21 (m, 1H), 2.40 (s, 3H), 1.85-1.10 (m, 10H);

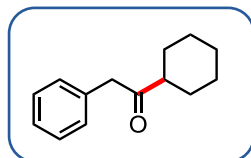
¹³C NMR (75 MHz, CDCl₃): δ 203.5, 143.5, 133.7, 129.3 (2C), 128.4 (2C), 45.5, 29.5 (2C), 26.0, 25.9 (2C), 21.5.

Cyclohexyl(4-methoxyphenyl)methanone (3n)

Following the general procedure **B** with *p* methoxy benzoylchloride (0.300 mmol, 41 μ L), iridium (6.00 μ mol, 6.0 mg), NiCl₂.dme (12.0 μ mol, 2.6 mg), 4,4'-di-*tert*-butyl-2,2'-dipyridyl (12 μ mol, 1.9 mg) and cyclohexylsilicate (0.450 mmol, 280 mg) in 4.2 mL of dry THF. The crude product was purified according the general procedure to afford **3n** (34.0 mg, 52%) as a colorless oil. The spectroscopic data are in agreement with those reported in the literature.⁴⁰

¹H NMR (400 MHz, CDCl₃): δ 8.91 (d, J = 9.2 Hz, 2H), 6.91 (d, J = 9.2 Hz, 2H), 3.87 (s, 3H), 3.28-3.19 (m, 1H), 1.92-1.85 (m, 4H), 1.60-1.20 (m, 6H);

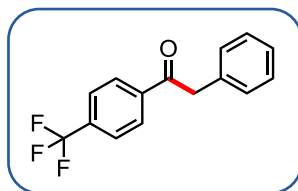
¹³C NMR (100 MHz, CDCl₃): δ 202.4, 163.2, 130.5 (2C), 129.3, 113.7 (2C), 55.5, 45.3, 29.5 (2C), 26.0 (2C), 25.9.

1-Cyclohexyl-2-phenylethanone (3o)

Following the general procedure **B** with phenylacetylchloride (0.417 mmol, 55 μ L), iridium (8.34 μ mol, 8.4 mg), NiCl₂.dme (16.7 μ mol, 3.7 mg), 4,4'-di-*tert*-butyl-2,2'-dipyridyl (16.7 μ mol, 4.5 mg) and cyclohexyl silicate (0.626 mmol, 394 mg) in 4.2mL of dry THF. The crude product was purified according the general procedure to afford **3o** (26.0 mg, 31%) as a colorless oil. The spectroscopic data are in agreement with those reported in the literature.⁴¹

¹H NMR (300 MHz, CDCl₃): δ 7.30-7.16 (m, 3H), 7.15-7.05 (m, 2H), 3.65 (s, 2H), 2.46-2.32 (m, 1H), 1.82-1.66 (m, 4H), 1.62-1.55 (m, 1H), 1.40-1.05 (m, 5H);

¹³C NMR (75 MHz, CDCl₃): δ 210.2, 133.5, 128.5 (2C), 127.5 (2C), 125.7, 49.1, 46.8, 27.5 (2C), 24.7, 24.5 (2C).

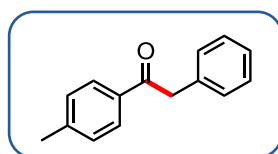
2-Phenyl-1-(4-(trifluoromethyl)phenyl)ethanone (3q)

Following the general procedure **B** with 4-trifluoromethylbenzoyl chloride (0.417 mmol, 62 μ L), iridium (8.34 μ mol, 8.4 mg), NiCl₂.dme (16.7 μ mol, 3.7 mg), 4,4'-di-*tert*-butyl-2,2'-dipyridyl (16.7 μ mol, 4.5 mg) and benzylsilicate (0.626 mmol, 400 mg) in 4.2 mL of dry THF. The crude product was purified according the general procedure to afford **3q** (18.0 mg, 16%) as a colorless oil. The spectroscopic data are in agreement with those reported in the literature.⁴²

¹H NMR (300 MHz, CDCl₃): δ 8.11 (d, J = 8.0 Hz, 2H), 7.72 (d, J = 8.0 Hz, 2H), 7.40-7.23 (m, 5H), 4.31 (s, 2H);

¹³C NMR (75 MHz, CDCl₃): δ 196.6, 139.2, 134.6 (q, J = 129.6 Hz, 2C), 133.8, 129.4 (2C), 128.9 (2C), 128.8, 127.2, 125.7 (q, J = 5 Hz, 2C), 123.8 (q, J = 295.7 Hz), 45.8;

¹⁹F NMR (376 MHz, CDCl₃): δ -63.2.

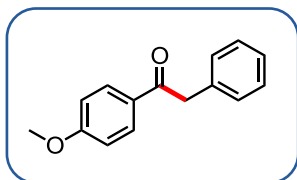
2-Phenyl-1-(p-tolyl)ethanone (3r)

Following the general procedure **B** with 4-methylbenzylchloride (0.417 mmol, 57 μ L), iridium (8.34 μ mol, 8.4 mg), NiCl₂.dme (16.7 μ mol, 3.7 mg), 4,4'-di-*tert*-butyl-2,2'-dipyridyl (16.7 μ mol, 4.5 mg) and benzyl silicate (0.626 mmol, 400 mg) in 4.2mL of dry THF. The crude product was purified according the general procedure to afford **3r** (62.0 mg, 71%) as a colorless oil. The spectroscopic data are in agreement with those reported in the literature.⁴³

¹H NMR (300 MHz, CDCl₃): δ 7.84 (d, J = 8.4 Hz, 2H), 7.28-7.11 (m, 7H), 4.18 (s, 2H), 2.34 (s, 3H);

^{13}C NMR (75 MHz, CDCl_3): δ 197.3, 144.0, 134.8, 134.1, 129.4 (2C), 129.3 (2C), 128.8 (2C), 128.6 (2C), 126.8, 45.4, 21.6.

1-(4-Methoxyphenyl)-2-phenylethanone (3s)

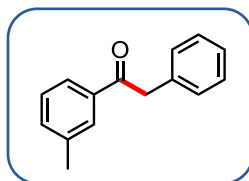


Following the general procedure **B** with 4-methoxybenzylchloride (0.417 mmol, 56 μL), iridium (8.34 μmol , 8.4 mg), $\text{NiCl}_2\cdot\text{dme}$ (16.7 μmol , 3.7 mg), 4,4'-di-*tert*-butyl-2,2'-dipyridyl (16.7 μmol , 4.5 mg) and benzyl silicate (0.626 mmol, 400 mg) in 4.2 mL of dry THF. The crude product was purified according the general procedure to afford **3s** (76.4 mg, 81%) as a colorless oil. The spectroscopic data are in agreement with those reported in the literature.⁴⁴

^1H NMR (300 MHz, CDCl_3): δ 7.95-7.87 (m, 2H), 7.29-7.11 (m, 5H), 6.88-6.80 (m, 2H), 4.14 (s, 2H), 3.75 (s, 3H);

^{13}C NMR (75 MHz, CDCl_3): δ 196.4, 163.6, 135.0, 131.0 (2C), 129.6, 129.4 (2C), 128.6 (2C), 126.8, 113.8 (2C), 55.5, 45.3.

2-Phenyl-1-(*m*-tolyl)ethanone (3t)

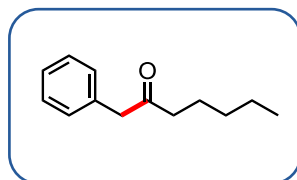


Following the general procedure **B** with *m*-toluoyl chloride (0.417 mmol, 55 μL), iridium (8.34 μmol , 8.4 mg), $\text{NiCl}_2\cdot\text{dme}$ (16.7 μmol , 3.7 mg), 4,4'-di-*tert*-butyl-2,2'-dipyridyl (16.7 μmol , 4.5 mg) and benzyl silicate (0.626 mmol, 400 mg) in 4.2 mL of dry THF. The crude product was purified according the general procedure to afford **3t** (62.0 mg, 71%) as a colorless oil. The spectroscopic data are in agreement with those reported in the literature.⁴⁵

^1H -NMR (CDCl_3 , 300 MHz): δ 7.72-7.69 (m, 2H), 7.15-7.32 (m, 7H), 4.18 (s, 2H), 2.32 (s, 3H);

^{13}C NMR (CDCl_3 , 75 MHz): δ 197.7, 138.5, 136.7, 134.7, 133.9, 129.5 (2C), 129.1, 128.6 (2C), 128.5, 126.9, 125.9, 45.5, 21.4.

1-Phenylheptan-2-one (**3u**)

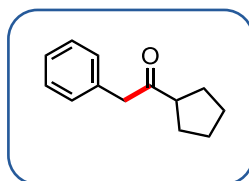


Following the general procedure **B** with hexanoylchloride (0.417 mmol, 58 μL), iridium (8.34 μmol , 8.4 mg), $\text{NiCl}_2\cdot\text{dme}$ (16.7 μmol , 3.7 mg), 4,4'-di-*tert*-butyl-2,2'-dipyridyl (16.7 μmol , 4.5 mg) and benzyl silicate (0.626 mmol, 400 mg) in 4.2 mL of dry THF. The crude product was purified according the general procedure to afford **3u** (71.0 mg, 89%) as a colorless oil. The spectroscopic data are in agreement with those reported in the literature.⁴⁶

^1H -NMR (CDCl_3 , 300 MHz): δ 7.10-7.40 (m, 5H), 3.68 (s, 2H), 2.45 (t, $J = 7.4\text{Hz}$, 2H), 1.52-1.63 (m, 2H), 1.16-1.36 (m, 4H), 0.88 (t, $J = 6.9\text{ Hz}$, 3H);

^{13}C NMR (CDCl_3 , 75 MHz): δ 208.6, 134.5, 129.5 (2C), 128.6 (2C), 127.0, 50.2, 42.0, 31.3, 23.5, 22.5, 14.0.

1-Cyclopentyl-2-phenylethanone (**3v**)

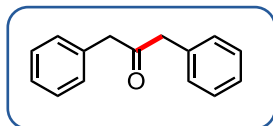


Following the general procedure **B** with cyclopentanecarbonyl chloride (0.417 mmol, 56 μL), iridium (8.34 μmol , 8.4 mg), $\text{NiCl}_2\cdot\text{dme}$ (16.7 μmol , 3.7 mg), 4,4'-di-*tert*-butyl-2,2'-dipyridyl (16.7 μmol , 4.5 mg) and benzylsilicate (0.626 mmol, 400 mg) in 4.2 mL of dry THF. The crude product was purified according the general procedure to afford **3v** (63.0 mg, 86%) as a colorless oil. The spectroscopic data are in agreement with those reported in the literature.⁴⁷

^1H NMR (300 MHz, CDCl_3): δ 7.40-7.19 (m, 5H), 3.77 (s, 2H), 3.01-2.95 (m, 1H), 1.85-1.52 (m, 8H);

^{13}C NMR (75 MHz, CDCl_3): δ 210.6, 134.5, 129.5 (2C), 128.6 (2C), 126.9, 50.6, 49.3, 29.1 (2C), 26.0 (2C).

1,3-Diphenylpropan-2-one (3w)

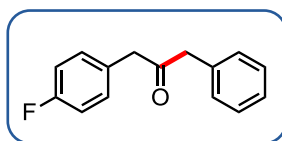


Following the general procedure **B** with phenylacetylchloride (0.417 mmol, 55 μL), iridium (8.34 μmol , 8.4 mg), $\text{NiCl}_2\cdot\text{dme}$ (16.7 μmol , 3.7 mg), 4,4'-di-*tert*-butyl-2,2'-dipyridyl (16.7 μmol , 4.5 mg) and benzyl silicate (0.626 mmol, 400 mg) in 4.2 mL of dry THF. The crude product was purified according the general procedure to afford **3w** (84.0 mg, 88%) as a colorless oil. The spectroscopic data are in agreement with those reported in the literature.⁴¹

^1H NMR (300 MHz, CDCl_3): δ 7.40-7.25 (m, 6H), 7.22-7.15 (m, 4H), 3.76 (s, 4H);

^{13}C NMR (75 MHz, CDCl_3): δ 205.6, 134.0 (2C), 129.5 (4C), 128.7 (4C), 127.0 (2C), 49.1 (2C).

1-(4-fluorophenyl)-3-phenylpropan-2-one (3x)



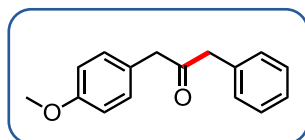
Following the general procedure **B** with 4-fluorophenylacetyl chloride (0.417 mmol, 57 μL), iridium (8.34 μmol , 8.4 mg), $\text{NiCl}_2\cdot\text{dme}$ (16.7 μmol , 3.7 mg), 4,4'-di-*tert*-butyl-2,2'-dipyridyl (16.7 μmol , 4.5 mg) and benzyl silicate (0.626 mmol, 400 mg) in 4.2 mL of dry THF. The crude product was purified according the general procedure to afford **3x** (44.0 mg, 46 %) as a colorless oil. The spectroscopic data are in agreement with those reported in the literature.⁴⁸

^1H NMR (300 MHz, CDCl_3): δ 7.37-7.26 (m, 3H), 7.19-7.14 (m, 2H), 7.12-7.05 (m, 2H), 7.04-6.95 (m, 2H), 3.73 (s, 2H), 3.69 (s, 2H);

^{13}C NMR (75 MHz, CDCl_3): δ 205.5, 162.1 (d, $J = 244$ Hz), 134.0, 131.2 (d, $J = 8$ Hz, 2C), 129.7, 129.6 (2C), 128.9 (2C), 127.3, 115.7 (d, $J = 85.2$ Hz, 2C), 49.5, 48.1;

^{19}F NMR (376 MHz, CDCl_3): δ -115.7 Hz.

1,3-Diphenylpropan-2-one (**3y**)

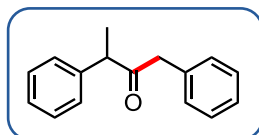


Following the general procedure **B** with 4-methoxyphenylacetyl chloride (0.417 mmol, 64 μL), iridium (8.34 μmol , 8.4 mg), $\text{NiCl}_2\cdot\text{dme}$ (16.7 μmol , 3.7 mg), 4,4'-di-*tert*-butyl-2,2'-dipyridyl (16.7 μmol , 4.5 mg) and benzyl silicate (0.626 mmol, 400 mg) in 4.2 mL of dry THF. The crude product was purified according the general procedure to afford **3y** (39.0 mg, 38 %) as a colorless oil. The spectroscopic data are in agreement with those reported in the literature.⁴⁹

^1H NMR (300 MHz, CDCl_3): δ 7.42-7.24 (m, 3H), 7.23-7.14 (m, 2H), 7.13-7.04 (m, 2H), 6.94-6.87 (m, 2H), 3.83 (s, 3H), 3.75 (s, 2H), 3.69 (s, 2H);

^{13}C NMR (75 MHz, CDCl_3): δ 206.1, 158.8, 134.2, 130.6 (2C), 129.6 (2C), 128.8 (2C), 127.1, 126.1, 114.3 (2C), 55.4, 49.0, 48.3.

1,3-Diphenylpropan-2-one (**3z**)

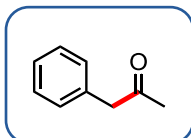


Following the general procedure **B** with 2-phenylpropionyl chloride (0.417 mmol, 62 μL), iridium (8.34 μmol , 8.4 mg), $\text{NiCl}_2\cdot\text{dme}$ (16.7 μmol , 3.7 mg), 4,4'-di-*tert*-butyl-2,2'-dipyridyl (16.7 μmol , 4.5 mg) and benzyl silicate (0.626 mmol, 400 mg) in 4.2 mL of dry THF. The crude product was purified according the general procedure to afford **3z** (45.0 mg, 48 %) as a colorless oil. The spectroscopic data are in agreement with those reported in the literature.⁵⁰

$^1\text{H NMR}$ (300 MHz, CDCl_3): δ 7.49-7.18 (m, 8H), 7.14-7.03 (m, 2H), 3.91 (q, $J = 6.9$ Hz, 1H), 3.66 (s, 2H), 1.41 (d, $J = 6.9$ Hz, 3H);

$^{13}\text{C NMR}$ (75 MHz, CDCl_3): δ 208.0, 140.5, 134.5, 129.6 (2C), 129.1 (2C), 128.6 (2C), 128.2 (2C), 127.3, 126.9, 52.2, 48.1, 17.8.

1-Phenylpropan-2-one (**3za**)

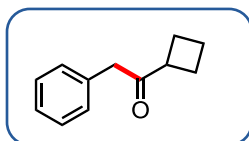


Following the general procedure **B** with acetyl chloride (0.834 mmol, 59 μL), iridium (16.68 μmol , 16.8 mg), $\text{NiCl}_2\cdot\text{dme}$ (33.4 μmol , 7.3 mg), 4,4'-di-*tert*-butyl-2,2'-dipyridyl (33.4 μmol , 8.9 mg) and benzyl silicate (1.67 mmol, 800 mg) in 4.2 mL of dry THF. The crude product was purified according the general procedure to afford **3za** (54 mg, 48%) as a colorless oil. The spectroscopic data are in agreement with those reported in the literature.⁵¹

$^1\text{H NMR}$ (300 MHz, CDCl_3): δ 7.46-7.42 (m, 3H), 7.25-7.20 (m, 2H), 3.72 (s, 2H), 2.18 (s, 3H).

$^{13}\text{C NMR}$ (75 MHz, CDCl_3): δ 206.4; 134.3, 129.5 (2C), 128.7 (2C), 127.1, 51.1, 29.3.

1-Cyclobutyl-2-phenylethanone (**3zb**)

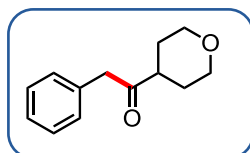


Following the general procedure **B** with cyclobutane carbonyl chloride (0.417 mmol, 47 μL), iridium (8.34 μmol , 8.4 mg), $\text{NiCl}_2\cdot\text{dme}$ (16.7 μmol , 3.7 mg), 4,4'-di-*tert*-butyl-2,2'-dipyridyl (16.7 μmol , 4.5 mg) and benzyl silicate (0.626 mmol, 400 mg) in 4.2 mL of dry THF. The crude product was purified according the general procedure to afford **3zb** (46 mg, 63%) as a colorless oil. The spectroscopic data are in agreement with those reported in the literature.⁵²

$^1\text{H NMR}$ (400 MHz, CDCl_3): δ 7.37-7.31 (m, 2H), 7.30-7.26 (m, 1H), 7.24-7.18 (m, 2H), 3.66 (s, 2H), 3.42-3.30 (m, 1H), 2.31-2.21 (m, 2H), 2.15-2.04 (m, 2H), 2.00-1.90 (m, 1H), 1.87-1.77 (m, 1H);

^{13}C NMR (100 MHz, CDCl_3): δ 209.2, 134.5, 129.6 (2C), 128.8 (2C), 127.0, 47.8, 45.0, 24.7 (2C), 17.8.

2-Phenyl-1-(tetrahydro-2H-pyran-4-yl)ethanone (**3zc**)



Following the general procedure **B** with tetrahydro-2H-pyran-4-carbonyl chloride (0.417 mmol, 52 μL), iridium (8.34 μmol , 8.4 mg), $\text{NiCl}_2\cdot\text{dme}$ (16.7 μmol , 3.7 mg), 4,4'-di-*tert*-butyl-2,2'-dipyridyl (16.7 μmol , 4.5 mg) and benzyl silicate (0.626 mmol, 400 mg) in 4.2 mL of dry THF. The crude product was purified according the general procedure to afford **3zc** (70 mg, 82%) as a colorless oil.

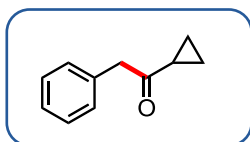
^1H NMR (300 MHz, CDCl_3): δ 7.45-7.21 (m, 5H), 4.08-3.93 (m, 2H), 3.77 (s, 2H), 3.49-3.31 (m, 2H), 2.77-2.61 (m, 1H), 1.80-1.67 (m, 4H);

^{13}C NMR (75 MHz, CDCl_3): δ 209.1, 134.0, 129.5 (2C), 128.8 (2C), 127.1, 67.2 (2C), 44.7, 46.9, 28.3 (2C);

HRMS: calc. for $[\text{C}_{13}\text{H}_{16}\text{O}_2]$: 205.1222, found 205.1223;

IR (neat): 2951, 2845, 1708, 1495, 1444, 1111, 1022, 704 cm^{-1} .

1-Cyclopropyl-2-phenylethanone (**3zd**)

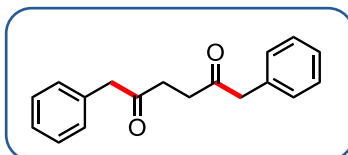


Following the general procedure **B** with cyclopropane carbonyl chloride (0.417 mmol, 37 μL), iridium (8.34 μmol , 8.4 mg), $\text{NiCl}_2\cdot\text{dme}$ (16.7 μmol , 3.7 mg), 4,4'-di-*tert*-butyl-2,2'-dipyridyl (16.7 μmol , 4.5 mg) and benzyl silicate (0.626 mmol, 400 mg) in 4.2 mL of dry THF. The crude product was purified according the general procedure to afford **3zd** (60 mg, 90%) as a colorless oil. The spectroscopic data are in agreement with those reported in the literature.⁵³

$^1\text{H NMR}$ (300 MHz, CDCl_3): δ 7.45-7.21 (m, 5H), 3.85 (s, 2H), 2.09-1.91 (m, 1H), 1.11-1.01 (m, 2H), 0.93-0.81 (m, 2H);

$^{13}\text{C NMR}$ (75 MHz, CDCl_3): δ 208.5, 134.6, 129.6 (2C), 128.8 (2C), 127.0, 58.3, 20.2, 11.4 (2C).

1-Cyclopropyl-2-phenylethanone (**3ze**)



Following the general procedure **B** with succinyl dichloride (0.417 mmol, 46 μL), iridium (8.34 μmol , 8.4 mg), $\text{NiCl}_2\cdot\text{dme}$ (16.7 μmol , 3.7 mg), 4,4'-di-*tert*-butyl-2,2'-dipyridyl (16.7 μmol , 4.5 mg) and benzyl silicate (1.252 mmol, 800 mg) in 4.2 mL of dry THF. The crude product was purified according the general procedure to afford **3ze** (45 mg, 40%) as a colorless oil. The spectroscopic data are in agreement with those reported in the literature.⁵⁴

$^1\text{H NMR}$ (300 MHz, CDCl_3): δ 7.41-7.17 (m, 10H), 3.75 (s, 4H), 2.72 (s, 4H);

$^{13}\text{C NMR}$ (75 MHz, CDCl_3): δ 207.0 (2C), 134.3 (2C), 129.6 (4C), 128.9 (4C), 127.2 (2C), 50.2 (2C), 35.8 (2C).

II.3.7. References

- ¹ The Carbonyl Group, Patai's Chemistry of Functional Groups Vol 1 & 2, **1970**, J. Wiley & Sons.
- ² For reviews, see: (a) Y.-Y. Gui, L. Sun, Z.-P. Lu, D.-G. Yu, *Org. Chem. Front.* **2016**, *3*, 522; (b) B. L. Tóth, O. Tischler, Z. Novák, *Tetrahedron Lett.* **2016**, *57*, 4505; (c) M. D. Levin, S. Kim, F. D. Toste, *ACS Cent. Sci.* **2016**, *2*, 293; (d) K. L. Skubi, T. R. Blum, T. P. Yoon, *Chem. Rev.* **2016**, *116*, 10035; (e) J. Twilton, C. Le, P. Zhang, R. W. Evans, D. W. C. MacMillan, *Nat. Rev. Chem.* **2017**, *1*, 52.
- ³ (a) Z. Zuo, D. T. Ahneman, L. Chu, J. A. Terrett, A. G. Doyle, D. W. C. MacMillan, *Science* **2014**, *345*, 437.
- ⁴ J. C. Tellis, D. N. Primer, G. A. Molander, *Science* **2014**, *345*, 433.
- ⁵ (a) A. Noble, S. J. McCarver, D. W. C. MacMillan, *J. Am. Chem. Soc.* **2015**, *137*, 624; (b) S. J. McCarver, J. X. Qiao, J. Carpenter, R. M. Borzilleri, M. A. Poss, M. D. Eastgate, M. Miller, D. W. C. MacMillan, *Angew. Chem. Int. Ed.* **2016**, *55*, 1; (c) C. P. Johnston, R. T. Smith, S. Allmendinger, D. W. C. MacMillan, *Nature* **2016**, *536*, 322; (d) N. A. Till, R. T. Smith, D. W. C. MacMillan, *J. Am. Chem. Soc.* **2018**, *140*, 5701.
- ⁶ D. T. Ahneman, A. G. Doyle, *Chem. Sci.* **2016**, *7*, 7002.
- ⁷ (a) J. K. Matsui, G. A. Molander, *Org. Lett.* **2017**, *19*, 436; (b) Y. Yamashita, J. C. Tellis, G. A. Molander, *Prot. Natl. Acad. Sci. USA* **2015**, *112*, 12016; (c) E. E. Stache, T. Rovis, A. G. Doyle, *Angew. Chem. Int. Ed.* **2017**, *56*, 3679; (d) X.-Y. Yu, Q.-Q. Zhou, P.-Z. Wang, C.-M. Liao, J.-R. Chen, W.-J. Xiao, *Org. Lett.* **2018**, *20*, 421; (e) F. Lima, M. A. Kabeshov, D. N. Tran, C. Battilocchio, J. Sedelmeier, G. Sedelmeier, B. Schenkel, S. V. Ley, *Angew. Chem. Int. Ed.* **2016**, *55*, 1; (g) F. Lima, L. Grunenberg, H. B. A. Rahman, R. Labes, J. Sedelmeier, S. V. Ley, *Chem. Commun.* **2018**, *54*, 5606.
- ⁸ (a) V. Corcé, L.-M. Chamoreau, E. Derat, J.-P. Goddard, C. Ollivier, L. Fensterbank, *Angew. Chem. Int. Ed.* **2015**, *54*, 11414; (b) M. Jouffroy, D. N. Primer, G. A. Molander, *J. Am. Chem. Soc.* **2016**, *138*, 475; (c) C. Lévêque, L. Chennenberg, V. Corcé, J.-P. Goddard, C. Ollivier, L. Fensterbank, *Org. Chem. Front.* **2016**, *3*, 462; (d) K. Lin, R. J. Wiles, C. B. Kelly, G. H. M. Davies, G. A. Molander, *ACS Catal.* **2017**, *7*, 5129; (e) N. R. Patel, C. B. Kelly, M. Jouffroy, G. A. Molander, *Org. Lett.* **2016**, *18*, 764; (f) B. A. Vara, X. Li, S. Berritt, C. R. Walters, E. J. Petersson, G. A. Molander, *Chem. Sci.* **2018**, *9*, 336; (g) K. D. Raynor, G. D. May, U. K. Bandarage, M. J. Boyd, *J. Org. Chem.* **2018**, *83*, 1551; (h) T. Guo, L. Zhang, X. Liu, Y. Fang, X. Jin, Y. Yang, Y. Li, B. Chen, M. Ouyang, *Adv. Synth. Catal.* **2018**, *360*, 4457; (i) For a very recent report, see: A. Cartier, E. Levernier, V. Corcé, T. Fukuyama, A. -L. Dhimane, C. Ollivier, I. Ryu, L. Fensterbank, *Angew. Chem. Int. Ed.* **2019**, *58*, 1789.
- ⁹ (a) Á. Gutiérrez-Bonet, J. C. Tellis, J.R.K. Matsui, B. A. Vara, G. A. Molander, *ACS Catal.* **2016**, *6*, 8004; (b) J. K. Matsui, S. B. Lang, D. R. Heitz, G.A. Molander, *ACS Catal.* **2017**, *7*, 2563; (c) K. Nakajima, S. Nojima, Y. Nishibayashi, *Angew. Chem. Int. Ed.* **2016**, *55*, 14106.
- ¹⁰ (a) H. Yue, C. Zhu, M. Rueping, *Angew. Chem. Int. Ed.* **2018**, *57*, 1371; (b) T. Knauber, R. Chandrasekaran, J. W. Tucker, J. M. Chen, M. Reese, D. A. Rankic, N. Sach, Christopher Helal, *Org. Lett.* **2017**, *19*, 6566.
- ¹¹ (a) Y.-Y. Gui, L.-L. Liao, L. Sun, Z. Zhang, J.-H. Ye, G. Shen, Z.-P. Lu, W.-J. Zhou, D.-G. Yu, *Chem. Commun.* **2017**, *53*, 1192.
- ¹² For recent books see: (a) Chemical Photocatalysis, Eds. B. König, DeGruyter Berlin, 2013; (b) Photochemically generated intermediates in Synthesis, Eds A. Albini and M. Fagnoni, Wiley, Hoboken, 2013; (c) For a recent review, see: (c) L. Marzo, S. K. Pagire, O. Reiser, B. König, *Angew. Chem. Int. Ed.* **2018**, *57*, 10034.
- ¹³ For recent reviews: (a) C. Raviola, S. Protti, D. Ravelli, M. Fagnoni, *Green Chem.* **2019**, *21*, 748 ; (b) A. Banerjee, Z. Lei, M.-Y. Ngai, *Synthesis* **2019**, *51*, 303; (c) M. Rueping, C. Vila, R. M. Koenigs, K. Poschary, D. C. Fabry, *Chem. Commun.* **2011**, *47*, 2360; (d) L. Chu, J. M. Lipshultz, D. W. C. MacMillan, *Angew. Chem. Int. Ed.* **2015**, *54*, 7929; (e) H.-T. Qin, S.-W. Wu, J.-L. Liu, F. Liu, *Chem. Commun.* **2017**, *53*, 1696; (f) G. F. P. de Souza, J. A. Bonacin, A. G. Salles, *J. Org.*

- Chem.* **2018**, *83*, 8331; (g) L. Capaldo, R. Riccardi, D. Ravelli, M. Fagnoni, *ACS Catal.* **2018**, *8*, 304; (h) M. Zhang, J. Xie, C. Zhu, *Nat. Commun.* **2018**, *9*, 3517.
- ¹⁴ (a) C. L. Joe, A. G. Doyle, *Angew. Chem. Int. Ed.* **2016**, *55*, 4040; For the use of in situ generated mixed anhydrides, see also: (b) J. Amani, G. A. Molander, *Org. Lett.* **2017**, *19*, 3612; (c) S. A. Badir, A. Dumoulin, J. K. Matsui, G. A. Molander, *Angew. Chem. Int. Ed.* **2018**, *57*, 6610.
- ¹⁵ (a) J. Amani, G. A. Molander, *J. Org. Chem.* **2017**, *82*, 1856; (b) J. Amani, E. Sodagar, G. Molander, *Org. Lett.* **2016**, *18*, 732.
- ¹⁶ H. Uoyama, K. Goushi, K. Shizu, H. Nomura and C. Adachi, *Nature* **2012**, *492*, 234.
- ¹⁷ For a reevaluation of the reduction and oxidation potentials of the excited state of 4CzIPN, see: F. L. Vaillant, M. Garreau, S. Nicolai, G. Gryn'ova, C. Corminboeuf, J. Waser, *Chem. Sci.* **2018**, *9*, 5883.
- ¹⁸ (a) C. L  v  que, L. Chenneberg, V. Corc  , C. Ollivier, L. Fensterbank, *Chem. Commun.* **2016**, *52*, 9877; (b) J. P. Phelan, S. B. Lang, J. S. Compton, C. B. Kelly, R. Dykstra, O. Gutierrez, G. A. Molander, *J. Am. Chem. Soc.* **2018**, *140*, 8037.
- ¹⁹ A series of blank experiments showed that bis-acetylated catechol was obtained in 15% and 9% from the reaction respectively of *n*-hexyl and cyclohexyl silicates (1.5 equiv.) with 1 equiv. of benzoyl chloride for 24h in THF under blue LED irradiation (the same yield was obtained without irradiation).
- ²⁰ (a) D. Cambie, C. Bottecchia, N. J. W. Straathof, V. Hessel, T. N  el, *Chem. Rev.* **2016**, *116*, 10276; (b) K. D. Raynor, G. D. May, U. K. Bandarage, M. J. Boyd, *J. Org. Chem.* **2018**, *83*, 1551; (c) J. W. Tucker, Y. Zhang, T. F. Jamison, C. R. J. Stephenson, *Angew. Chem. Int. Ed.* **2012**, *51*, 4144; (d) Z. J. Garlets, J. D. Nguyen, C. R. J. Stephenson, *Isr. J. Chem.* **2014**, *54*, 351; (e) T. J. DeLano, U. K. Bandarage, N. Palaychuk, J. Green, M. J. Boyd, *J. Org. Chem.* **2016**, *81*, 12525; (f) N. Palaychuk, T. J. DeLano, M. J. Boyd, J. Green, U. K. Bandarage, *Org. Lett.* **2016**, *18*, 6180; (g) H.-W. Hsieh, C. W. Coley, L. M. Baumgartner, K. F. Jensen, R. I. Robinson, *Org. Process Res. Dev.* **2018**, *22*, 542; (h) N. El Achi, M. Penhoat, Y. Bakkour, C. Rolando, L. Chausset-Boissarie, *Eur. J. Org. Chem.* **2016**, 4284; (i) M. Neumann and K. Zeitler, *Org. Lett.* **2012**, *14*, 2012.
- ²¹ J. J. Talley, D. L. Brown, J. S. Carter, M. J. Graneto, C. M. Koboldt, J. L. Masferrer, W. E. Perkins, R. S. Rogers, A. F. Shaffer, Y. Y. Zhang, B. S. Zweifel, K. Seibert, *J. Med. Chem.* **2000**, *43*, 775.
- ²² F. Toda, M. Yagi, K. Kiyoshige, *Chem. Commun.* **1988**, *0*, 958.
- ²³ R. J. McCague, *J. Chem. Soc. Perkin Trans.* **1987**, *1*, 1011.
- ²⁴ G. Cerveau, C. Chuit, R. J. P. Corriu, C. Reye, *Journal of Organometallic Chemistry* **1987**, 328 17.
- ²⁵ <http://staff.ustc.edu.cn/~luo971/2010-91-CRC-BDEs-Tables.pdf>.
- ²⁶ D. Hanss, J. C. Freys, G. Bernardinelli, O. S. Wenger, *Eur. J. Inorg. Chem.* **2009**, *2009*, 4850.
- ²⁷ M. S. Lowry, J. I. Goldsmith, J. D. Slinker, R. Rohl, R. A. Pascal, G. G. Malliaras, S. Bernhard, *Chem. Mater.* **2005**, *17*, 5712.
- ²⁸ V. Corc  , L.-M. Chamoreau, E. Derat, J.-P. Goddard, C. Ollivier, L. Fensterbank, *Angew. Chem. Int. Ed.* **2015**, *54*, 11414.
- ²⁹ M. Jouffroy, D.N. Primer, G. A. Molander, *J. Am. Chem. Soc.* **2016**, *138*, 475.
- ³⁰ N. Wakita, S. Hara, *Tetrahedron* **2010**, *66*, 7939.
- ³¹ W. Ren, A. Emi, M. Yamane, *Synthesis* **2011**, *14*, 2303.
- ³² T. Kondo, M. Akazome, Y. Tsuji, J. Watanabe, *J. Org. Chem.* **1990**, *55*, 1286.
- ³³ J. Sheng, X. Li, M. Tang, B. Gao, G. Huang, *Synthesis* **2007**, *8*, 1165.
- ³⁴ K.-M. Cha, E.-A. Jun, C.-H. J, *Synlett* **2009**, *18*, 2939.
- ³⁵ M. Li, C. Wang, H. Ge, *Org. Lett.* **2011**, *13*, 2062.
- ³⁶ D. L. Mo, L. X. Dai, X. L. Hou, *Tetrahedron Lett.* **2009**, *50*, 5578.
- ³⁷ B. Landers, C. Berini, C. Wang, O. Navarro, *J. Org. Chem.* **2011**, *76*, 1390.
- ³⁸ A. Takemiya, J. F. Hartwig, *J. Am. Chem. Soc.* **2006**, *128*, 14800.
- ³⁹ B. W. Fausett, L. S. Liebeskind, *J. Org. Chem.* **2005**, *70*, 4851.
- ⁴⁰ H. Li, Y. Xu, E. Shi, W. Wei, Xi. Suo, X. Wan, *Chem. Commun.* **2011**, *47*, 7880.
- ⁴¹ S. Inaba, R. D. Rieke, *J. Org. Chem.* **1985**, *50*, 1373.
- ⁴² A. Battace, M. Feuerstein, M. Lemhadri, T. Zair, H. Doucet, M. Santelli, *Eur. J. Org. Chem.* **2007**, *19*, 3122.
- ⁴³ T. Miao, G. W. Wang, *Chem. Commun.* **2011**, *47*, 9501.
- ⁴⁴ J. Ruan, O. Saidi, J. A. Iggo, J. Xiao, *J. Am. Chem. Soc.* **2008**, *130*, 10510.
- ⁴⁵ R. C. Elderfield, K. L. Burges, *J. Am. Chem. Soc.* **1960**, *82*, 1975.

- ⁴⁶ H. Okada, T. Mori, Y. Saikawa, M. Nakata, *Tetrahedron Lett.* **2009**, *50*, 1276.
- ⁴⁷ F. Cadoret, P. Retailleau, Y. Six, *Tetrahedron. Lett.* **2006**, *47*, 7749.
- ⁴⁸ N. Ishibe, S. Yutaka, J. Masui, N. Ihda, *J. Org. Chem.* **1978**, *43*, 2144.
- ⁴⁹ L. Ackermann, P. M. Vaibhav, *Chem. Eur. J.* **2012**, *18*, 10230.
- ⁵⁰ C. Gibb, A. K. Sundaresan, V. Ramamurthy, B. C. Gibb, *J. Am. Chem. Soc.* **2008**, *130*, 4069.
- ⁵¹ J. M. Zimbron, M. Seigeer-Weibel, H. Hirt, F. Gallou, *Synthesis* **2008**, *8*, 1221.
- ⁵² J. Hye-Soo and K. Seung-Hoi, *Synlett* **2015**, *26*, 666.
- ⁵³ X.-F. Fu, Y. Xiang, Z.-X. Yu, *Chem. Eur. J.* **2015**, *21*, 4242.
- ⁵⁴ S. Inaba, R. D. Rieke, *J. Org. Chem.* **1985**, *50*, 1363.

**- Chapter III -
Visible-light Photoredox
catalyzed Radical
carbonylation**

Chapter III. Visible-light Photoredox catalyzed Radical Carbonylation

The previous chapter described a novel ketone synthesis. However, some drawbacks may still be delineated:

- two metals (iridium and nickel) have to be present, which can be an issue from an environmental point of view.
- primary non-activated silicates cannot be used, which limits the reaction scope.

To overcome these limitations, we decided to investigate a new synthesis of ketones based on multicomponent radical carbonylation. This approach will be discussed in this chapter.

III.1. Multicomponent reaction

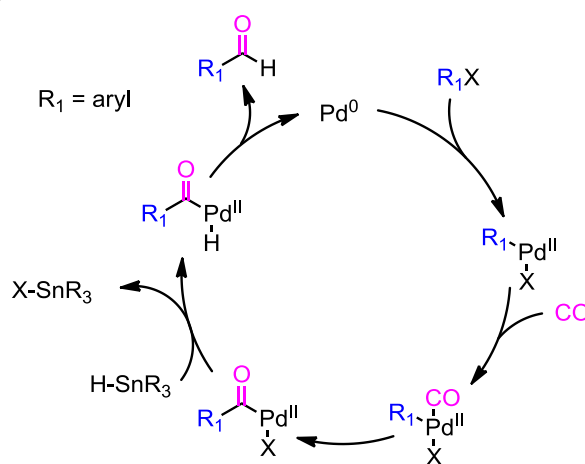
Modern chemists commonly use and develop multicomponent reactions.^{1,2} Among them, we can cite for instance the Mannich, Passerini, Ugi and Petassis reactions.

This elegant way of creating complex scaffolds is very appealing because it allows multiple transformations in only one step. Over the years, this concept has been extended to gas-based reactions including carbonylation ones

III.1.1. Carbonylation reactions: organometallic pathway

Gas-based reactions, like hydrogenations, have attracted the interest of the chemistry community for a long time. Indeed, the gas is readily incorporated in the structure, thus the atom economy is very high.

In this context, many groups used carbon monoxide as a carbonyl precursor.³ For instance, in 1986, Stille's group showed that CO is compatible with palladium chemistry to obtain, after an oxidative addition, CO insertion, transmetalation with R_3SnH and a reductive elimination, an aldehyde (**Scheme 1**).⁴



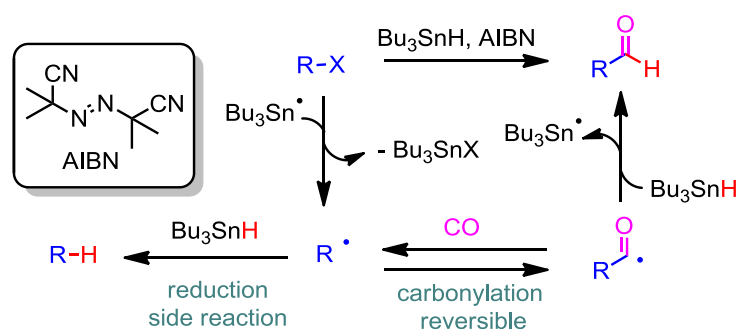
Scheme 1: Carbonylative Stille cross-coupling reaction

This method was used for the total synthesis of frenolicin in 1982⁵ and strychnine in 1993.⁶ However, this publication relies on an organometallic pathway. What about radical carbonylation?

III.1.2. Radical carbonylation

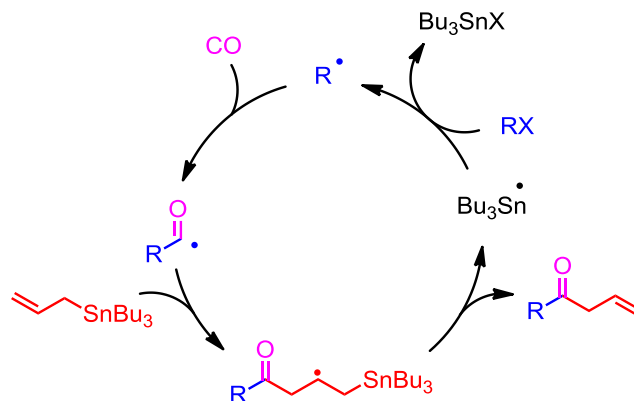
III.1.2.1. Genesis of radical carbonylation

Based on recent reports at that time,^{7,8} Sonoda *et al* developed radical carbonylation.⁹ Starting from an alkyl halide in the presence of CO and by using the well-known AIBN/Bu₃SnH conditions, they managed to produce a large variety of aldehydes in very good yields. They proposed the following mechanism. After initiation, the newly-formed alkyl radical is added to CO. The resulting acyl radical, then, abstracts a hydrogen atom to Bu₃SnH, generating the aldehyde and Bu₃Sn• which can propagate the chain reaction (**Scheme 2**). Even if this reaction is of great interest, a high CO pressure is needed for the carbonylation step to predominate over the alkyl radical reduction by tin hydride (**Scheme 2, side reaction**). But, by using such conditions, the decarbonylation of acyl radicals (back reaction) also decreases.



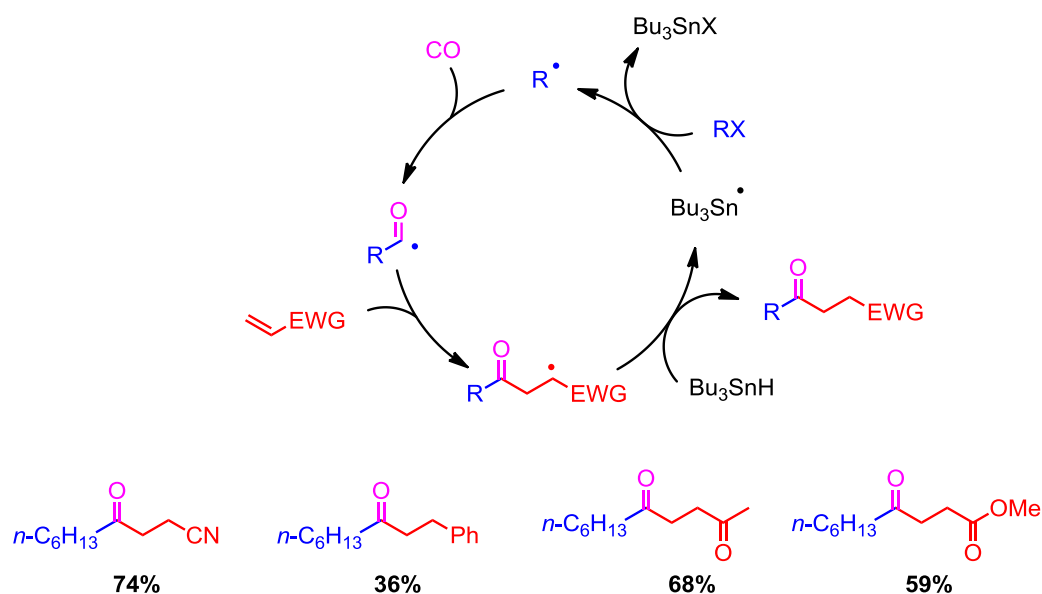
Scheme 2: Radical carbonylation using AIBN/Bu₃SnH

Because this high CO pressure could be problematic, they developed one year later new conditions based on allylstannanes instead of Bu₃SnH¹⁰ (**Scheme 3**). In that case, the side reaction, which consists on the addition of alkyl radicals onto allyltin reagents, occurs at a slower rate than hydrogen abstraction from tin hydride and radical addition to CO ($k_{\text{radical carbonylation}} = 6 \times 10^5 \text{ M}^{-1} \cdot \text{s}^{-1}$,³ $k_{\text{abstraction from tin hydride}} = 1 \times 10^6 \text{ M}^{-1} \cdot \text{s}^{-1}$,¹¹ $k_{\text{addition onto allyltin reagent}} = 3 \times 10^4 \text{ M}^{-1} \cdot \text{s}^{-1}$ at 23 °C¹²). Thus, they could successfully lower the CO pressure from 90 atm to 30 atm.



Scheme 3: Radical carbonylation using an allylstannane as a substrate and radical mediator

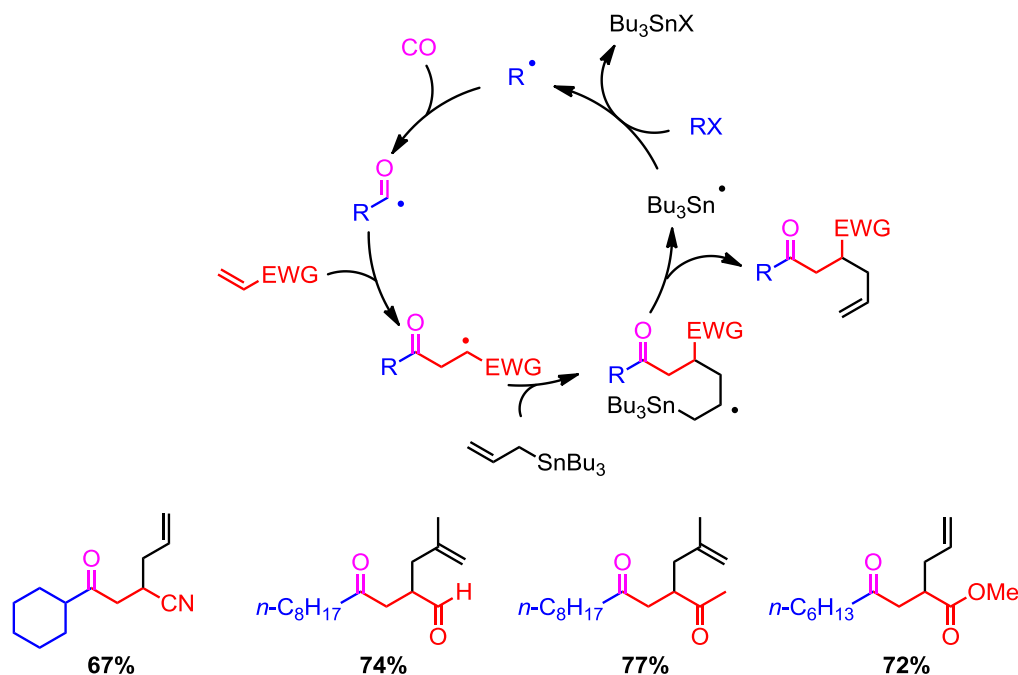
The same year, they reported the synthesis of unsymmetrical ketones by trapping the acyl radical, generated under tin hydride conditions, by an activated alkene. Fine tuning of the reaction conditions allowed the carbonylation coupling reaction to predominate over the Giese-type direct trapping (**Scheme 4**).¹³



Scheme 4: Unsymmetrical ketones synthesis *via* radical carbonylation

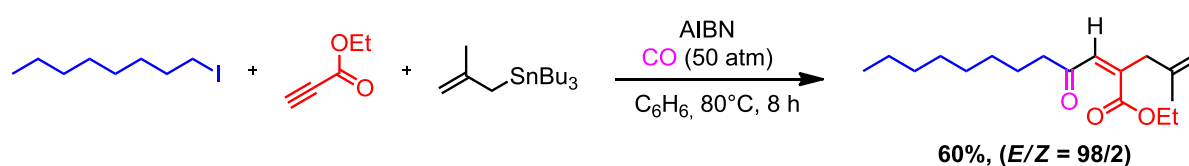
Ryu *et al.* demonstrated that a four-component reaction was also possible when replacing Bu_3SnH with methallyltin and keeping AIBN as the radical initiator. This reaction tolerated a

broad substrate scope, forming for instance 3-cyano ketones, 4-oxo aldehydes, 1,4-diketones, 4-oxo esters and 3-sulfonyl ketones (**Scheme 5**).¹⁴



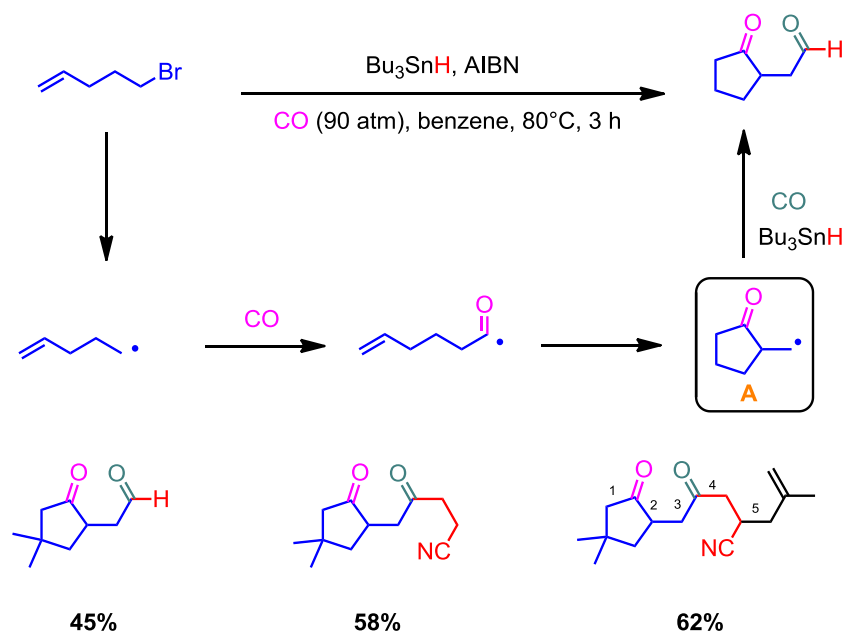
Scheme 5: Four-component radical carbonylation with activated alkenes

They also extended this process to alkynes by using ethyl propiolate as a radical acceptor. The excellent stereoselectivity obtained ($E/Z = 98/2$) might be attributed to the addition of the vinyl radical, formed after addition of the acyl radical on the triple bond, on methallyltin by its least hindered site (**Scheme 6**).



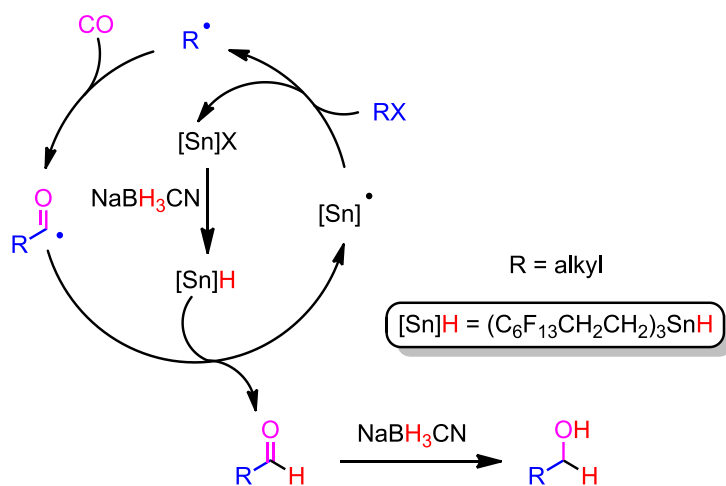
Scheme 6: Four-component radical carbonylation with ethyl propiolate as a radical acceptor

A few years later, double CO trapping reactions were also performed (**Scheme 7**).¹⁵ The intermediate **A**, formed after addition of the alkyl radical onto CO and cyclization, can indeed react once again with another molecule of CO and Bu_3SnH , forming a keto aldehyde. The scope of this reaction was found to be quite broad and, for instance, when using tributylmethallyltin and acrylonitrile, a yield of 62% was obtained. This is rather high considering that 5 C–C bonds were formed in only one step.



Scheme 7: Double CO trapping

A few years later, Ryu's group and Curran's one also showed that trialkyltin hydride reagents can be replaced by fluorinated allyltin derivatives to ease tin removal after reaction.¹⁶ By using such methodology, they were even able to perform some hydroxymethylation reactions by adding into the reaction medium NaBH_3CN , as a reductant, and a catalytic amount of $(\text{C}_6\text{F}_{13}\text{CH}_2\text{CH}_2)_3\text{SnH}$ (Scheme 8).¹⁷ In this mechanism, NaBH_3CN has a double-goal: firstly it generates $[\text{Sn}]\text{H}$ from $[\text{Sn}]\text{X}$ and secondly it reduces the aldehyde to the alcohol.

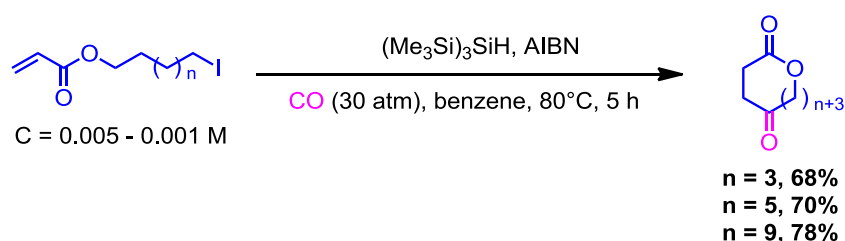


Scheme 8: Hydroxymethylation reaction

III.1.2.2. Toward other systems for radical carbonylation

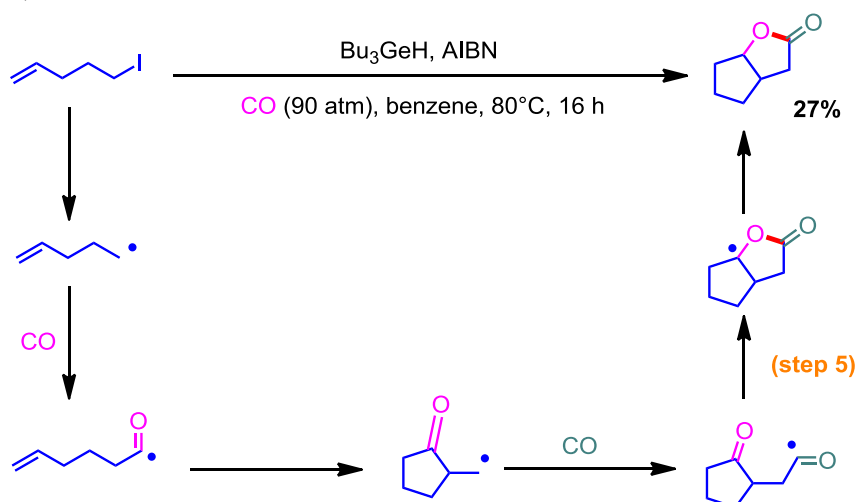
However, high CO pressure was mandatory and tin compounds are quite toxic. Thus, alternatives had to be sought to perform those reactions in a safer way.

To overcome these limitations, Sonoda and Ryu proposed in 1997 to use AIBN and $(\text{Me}_3\text{Si})_3\text{SiH}$ (TTMSS) as a radical mediator.¹⁸ Indeed, they envisioned with success that, owing to the poorer ability of $(\text{Me}_3\text{Si})_3\text{SiH}$ to transfer a hydrogen to an alkyl radical in comparison to Bu_3SnH , a "lower" CO pressure was required. Thanks to this strategy, macrocyclic ketoesters were synthesized in a quite dilute medium (**Scheme 9**).^{19,20} Of note, the rate constant for the H abstraction of a primary radical from $(\text{Me}_3\text{Si})_3\text{SiH}$ is about $3.8 \times 10^5 \text{ M}^{-1} \cdot \text{s}^{-1}$ at 25°C ²¹ (compared to $1 \times 10^6 \text{ M}^{-1} \cdot \text{s}^{-1}$ from tributyltin hydride). Under these conditions, challenging vinyl iodides were also found to undergo carbonylation reactions.



Scheme 9: Carbonylation reaction followed by a macrocyclization

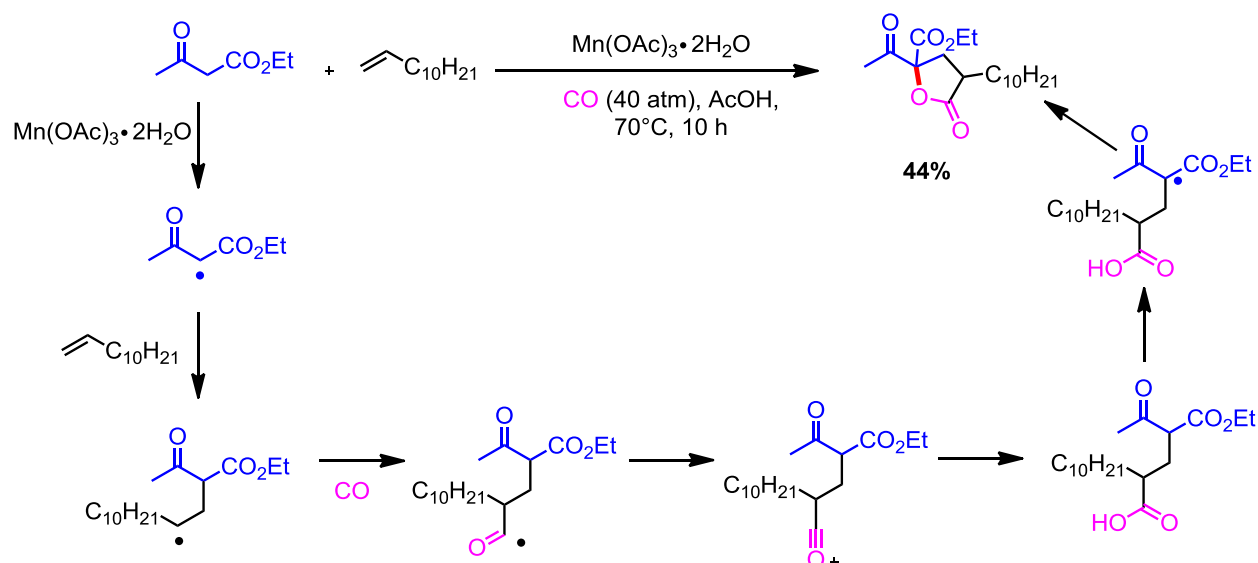
Surprisingly, when switching to tributylgermane as a radical mediator, the reaction of 4-alkenyl halides under high pressure of CO led to 2-oxa-bicyclo[3.3.0]octan-3-ones instead of 2-(formylmethyl)cyclopentanones (**Scheme 10**). This rare cyclization,²² resulting from the addition of the acyl radical to the previously formed ketone (**step 5**), can be explained by the very slow-terminating H-transfer step with the hydrogermane ($1 \times 10^5 \text{ M}^{-1} \cdot \text{s}^{-1}$ at 30°C for a primary radical).^{23, 24}



Scheme 10: Tributylgermane as a radical mediator in carbonylation reactions

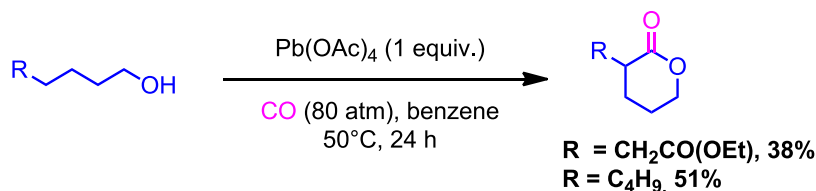
However, the use of AIBN as an initiator is still an issue due to its explosive nature.

In this context, Alper and Ryu showed that $\text{Mn}(\text{OAc})_3 \cdot 2\text{H}_2\text{O}$ could be mediated with radical carbonylation to form carboxylic acids after hydrolysis.²⁵ Indeed, the alkyl radical, formed after oxidation of the 1,3 dicarbonyl compound by $\text{Mn}(\text{OAc})_3 \cdot 2\text{H}_2\text{O}$, can react with an alkene and CO to form an acyl radical. Then, this intermediate can be oxidized by $\text{Mn}(\text{OAc})_3 \cdot 2\text{H}_2\text{O}$ to an acylium cation which is, finally, hydrolyzed. This methodology has been applied to γ -lactone synthesis (**Scheme 11**).



Scheme 11: Carbonylation reaction with $\text{Mn}(\text{OAc})_3 \cdot 2\text{H}_2\text{O}$ for γ -lactone synthesis

In 1994, Tsunoi, Ryu, and Sonoda used lead tetraacetate (LTA) for the production of δ -lactones (**Scheme 12**). The mechanism is based on the formation of the alkoxy radical thanks to LTA followed by a 1-5 HAT ($k_{1-5 \text{ HAT}} = 2.7 \times 10^7 \text{ s}^{-1}$)²⁶ and carbonylation. Finally, LTA oxidizes the acyl radical to an acyl cation which can react intramolecularly with the hydroxy moiety.²⁷



Scheme 12: Carbonylation reaction with lead tetraacetate for δ -lactone synthesis

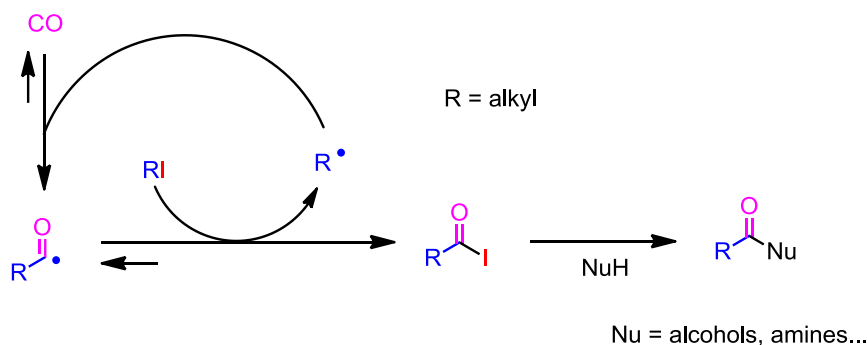
Even if all of these reactions are really interesting from a synthetic viewpoint, most of them are using toxic reagents for the radical generation. We consequently wondered whether the radical carbonylation reaction could take place under milder and safer photoredox conditions.

III.1.3. Photoredox radical carbonylation

III.1.3.1. Palladium chemistry and radical carbonylation

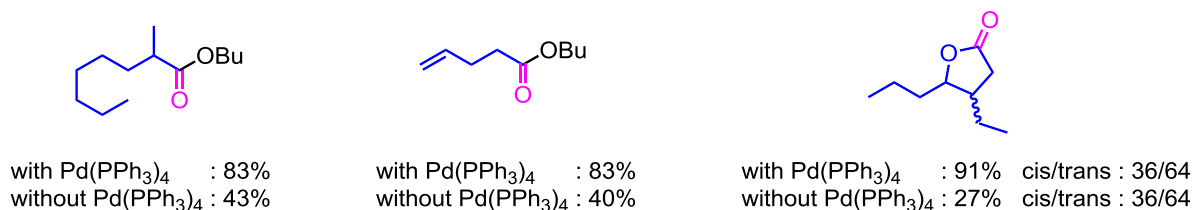
In 1980, Watanabe's group as well as Suzuki and Miyaura *et al.* reported that palladium-catalyzed carbonylation of alkyl iodide and more generally transition metal-catalyzed carbonylation of alkyl iodide, was drastically improved by photoirradiation. They hypothesized that an alkyl metal species could be formed *via* a radical process. Then, this alkyl metal intermediate underwent CO insertion to lead to the acyl metal species.^{28,29}

In 2014, inspired by this work and by the concept of Atom Transfer Carbonylation (ATC) evidencing that an alkyl iodide can react with an acyl radical to form an acyl iodide and an alkyl radical (**Scheme 13**), Ryu and co-workers published some works dealing with the interplay of carbon radicals and palladium catalysts.³



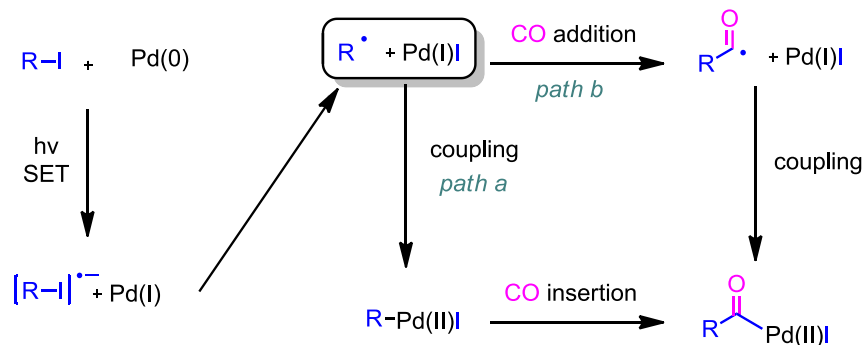
Scheme 13: Atom Transfer Carbonylation concept (ATC)

This report merged the organometallic palladium chemistry and radical carbonylation. Similarly to Watanabe, Suzuki and Miyaura, they observed a light-induced acceleration of ATC by the palladium complexes for primary, secondary, and even tertiary alkyl iodides with a Xenon pyrex lamp. Thanks to this approach, they were able to synthesize a large variety of esters in excellent yields. (**Scheme 14**).



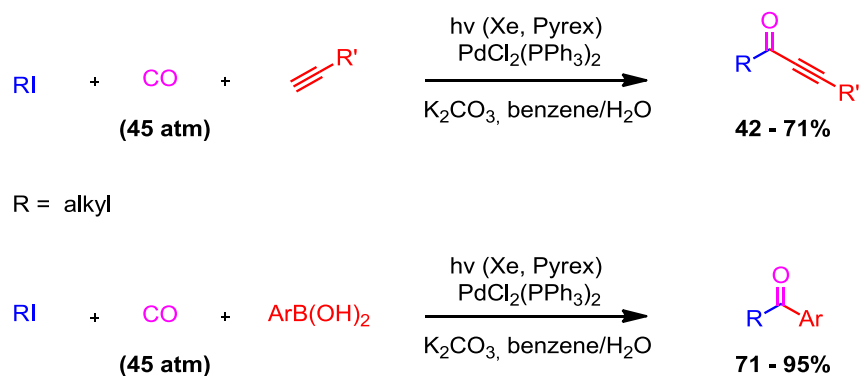
Scheme 14: Palladium/light accelerated Atom Transfer Carbonylation of Alkyl Iodides

They also showed that amides and keto amides were accessible by adding an amine instead of an alcohol into the reaction medium. Intrigued by the mechanism of this reaction, they first envisioned two possible pathways for the acyl palladium formation (**Scheme 15**).



Scheme 15: Envisioned mechanisms for acyl palladium generation

In a first step, the palladium(0) catalyst reduces the alkyl iodide forming an alkyl radical and a Pd(I). Then two possible pathways were proposed. The first one (*path a*) relies on the radical addition onto the Pd(I) followed by a CO insertion to form an acyl palladium species. The second one (*path b*), suggests first a CO addition followed by a coupling reaction. Thus, they tried to figure out which one was the correct one. When using 2-iodo-3-methylheptane, they interestingly obtained the same ratio of anti/syn diastereoisomers with and without the palladium catalyst. Consequently, this result, which cannot be a coincidence, strongly suggested that *path b* was involved in the product formation. Encouraged by this result, they went even further and synthesized some alkyl alkynyl ketones and aryl alkyl ketones (**Scheme 16**).



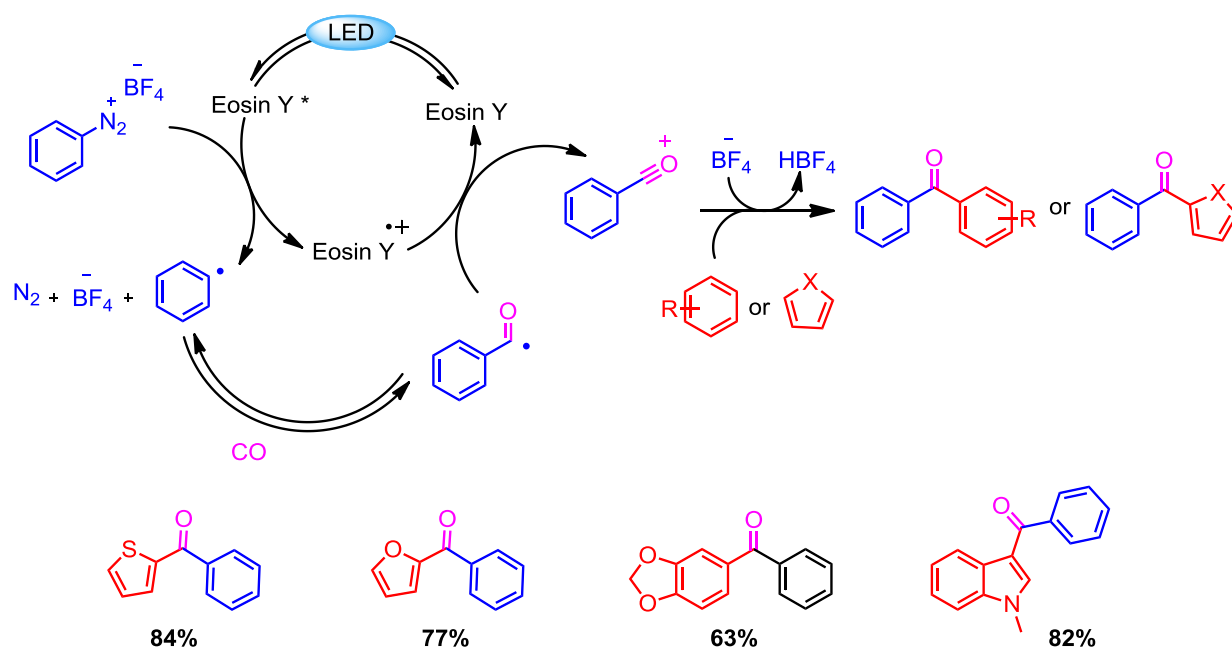
Scheme 16: Extension of the reaction

After this introduction dealing with palladium chemistry and radical carbonylation what about visible-light induced photoreductive and photooxidative carbonylation reactions?

III.1.3.2. Radical carbonylation mediated by visible-light photoredox catalysis

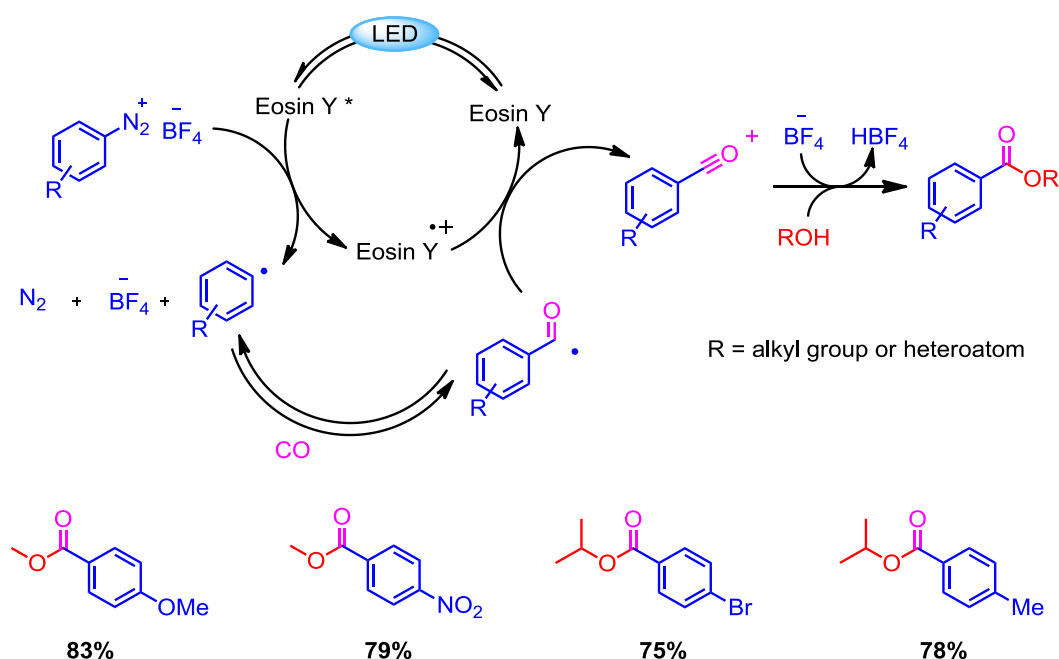
a) Visible-light induced photoreductive processes

In 2015, Gu's group get the idea of using classic photoredox catalysis and the easily reducible aryl diazonium salts to perform radical carbonylation under CO atmosphere.³⁰ The organic dye Eosin Y was found to be the best photocatalyst for this reaction. Even if high CO pressure was still needed, they managed to efficiently couple aryl radicals to (hetero)arenes. They proposed the following mechanism in which the excited photocatalyst first reduces the aryl diazonium salt (**Scheme 17**). Then, the generated aryl radical reacts with CO to form an acyl radical. Afterwards, this intermediate is oxidized to the acylium cation by the photocatalyst which is, thus, regenerated. Finally, the acylium ion reacts through a Friedel-Craft-type mechanism with the (hetero)aryl partner to provide the desired product.



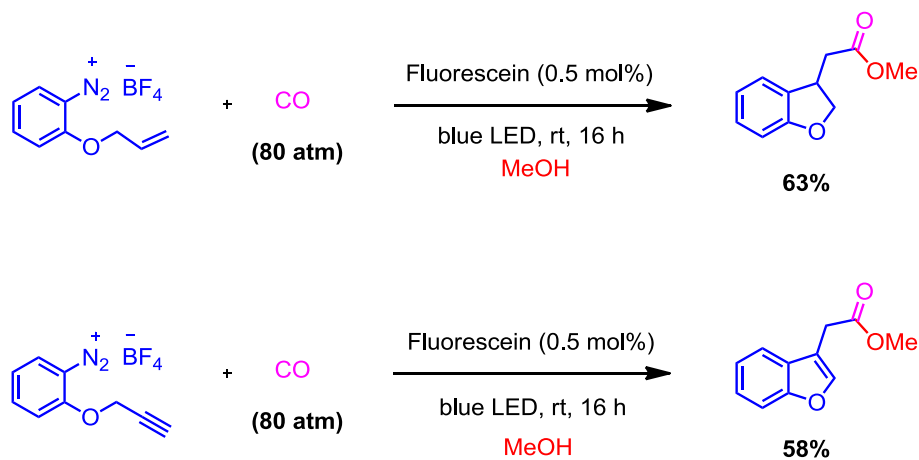
Scheme 17: Photoreductive radical carbonylation of aryl diazonium salts for the generation of diaryl ketones

At the same time, Jacobi Von Wangelin *et al.* proposed the same approach to form esters (**Scheme 18**).³¹ Their idea was based on the same principle but they used alcohols instead of (hetero)aryl reagents as nucleophiles.



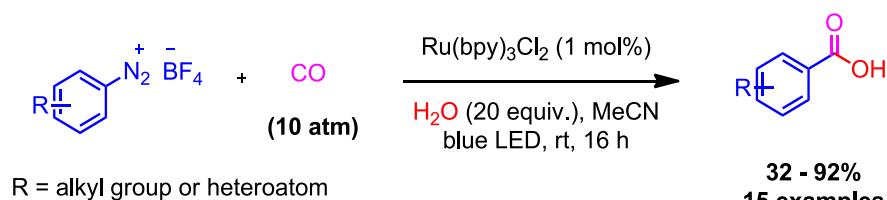
Scheme 18: Photoreductive radical carbonylation of aryl diazoniums for the generation of esters

One year later, Wu's group extended the concept to other photocatalysts.³² They also showed that the combination of fluorescein and ortho-propargyl-substituted benzenediazonium salts leads to benzofuran derivatives in very good yields (**Scheme 19**). This transformation involves a sequential radical cyclization and an alkoxy carbonylation under blue LED irradiation in the presence of CO and MeOH.



Scheme 19: Synthesis of benzofuran esters *via* a radical cyclization/alkoxy carbonylation sequence

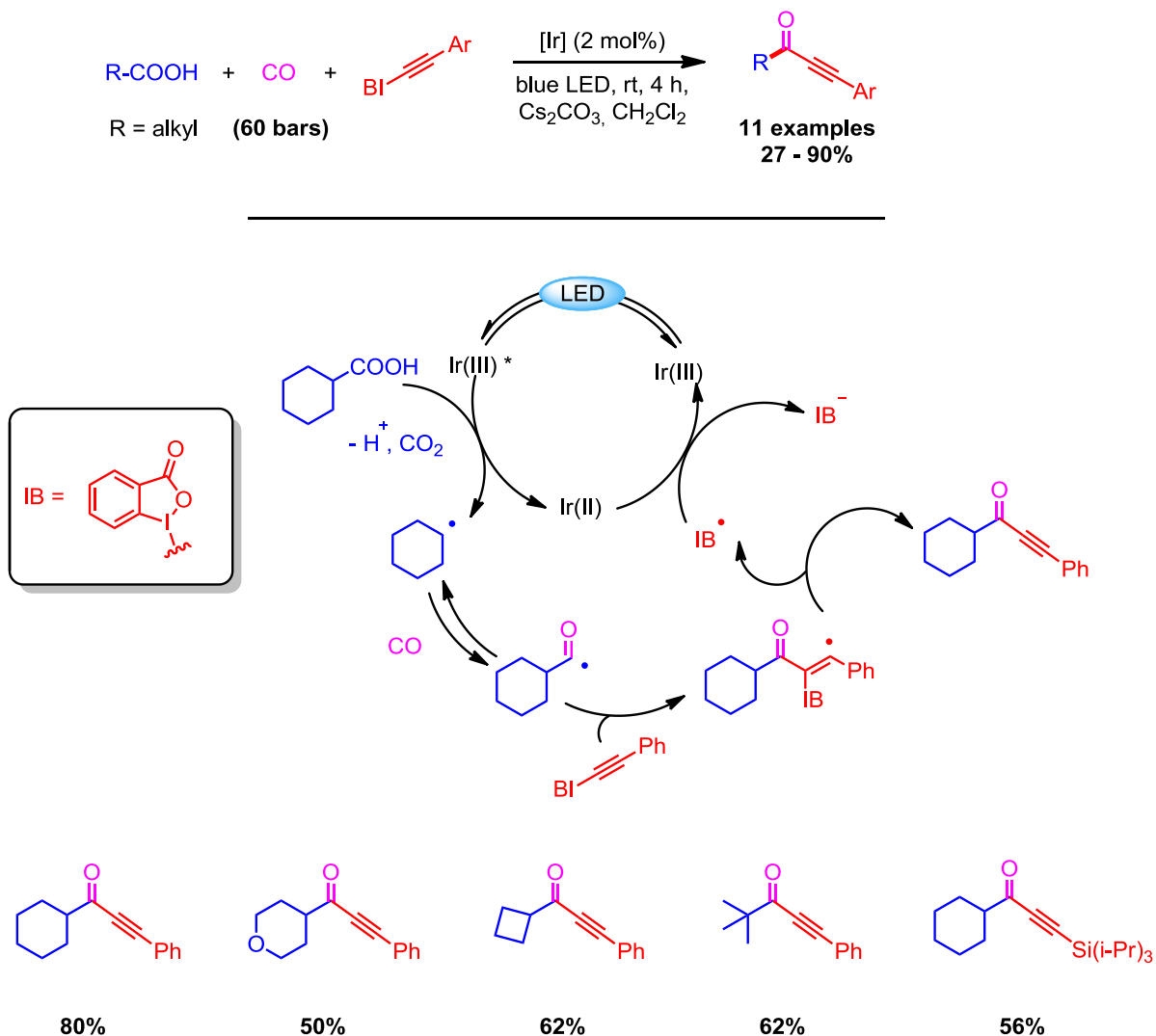
A few years later, Bousquet and co-workers extended the process to the formation of acids *via* a radical hydroxycarbonylation reaction. This way, they used water instead of an alcohol as a nucleophile (**Scheme 20**).³³ They also demonstrated that the diazonium salts could be formed *in situ* from the corresponding anilines which is a significant improvement in terms of time saving and safety.



Scheme 20: Hydroxycarbonylation reaction

b) Visible-light induced photooxidative processes

Most of the reactions were conducted under photoreductive conditions and only one study was carried out under photooxidative conditions.³⁴ In this publication, Xiao's group reported a new carbonylative alkylation of carboxylic acids in the presence of an iridium photocatalyst under blue LED irradiation. They proposed the following mechanism to explain the product formation. After oxidation of the carboxylate and decarboxylation, the alkyl radical reacts with CO to form an acyl radical. Then, this intermediate adds onto the ethynylbenziodoxolone derivative (EBX) to form, after elimination, IB[•] which regenerates the photocatalyst and liberates the desired product. This reaction tolerated a broad substrate scope and many different scaffolds were accessed (**Scheme 21**).



Scheme 21: Proposed mechanism for the carbonylative alkynylation of carboxylic acids

Based on the above state-of-the-art, we wondered if the silicates could be used within a similar system to provide another example of radical carbonylation under photooxidative conditions.

III.1.4. References

- ¹ M. Tojino, I. Ryu in *Multicomponent Reaction*, Eds. J. Zhu, H. Bienaymé, Wiley-VCH, Weinheim, **2005**, 169.
- ² V. Liautard, Y. Landais, in *Multicomponent Reactions*, Eds. J. Zhu, Q. Wang, M. X. Wang, Wiley, 2nd Edition, **2014**, 401.
- ³ S. Sumino, A. Fusano, T. Fukuyama, I. Ryu, *Acc. Chem. Res.* **2014**, 47, 1563.
- ⁴ J. K. Stille, V. P. Baillargeon, *J. Am. Chem. Soc.* **1986**, 108, 452.
- ⁵ M. F. Semmelhack, J. J. Bozell, T. Sato, W. Wulff, E. Spiess, A. Zask, *J. Am. Chem. Soc.* **1982**, 104, 5850.
- ⁶ S. D. Knight, L. E. Overman, G. Pairedeau, *J. Am. Chem. Soc.* **1993**, 115, 9293.
- ⁷ M. M. Brubaker, D. D. Coffman, H. H. Hoehn, *J. Am. Chem. Soc.* **1952**, 74, 1509.
- ⁸ a) D. D. Coffman, R. Cramer, W. E. Mochel, *J. Am. Chem. Soc.* **1958**, 80, 2882; b) C. Walling, E. S. Savas, *J. Am. Chem. Soc.* **1960**, 82, 1738.
- ⁹ I. Ryu, K. Kusano, A. Ogawa, N. Kambe, N. Sonoda, *J. Am. Chem. Soc.* **1990**, 112, 1295.
- ¹⁰ I. Ryu, H. Yamazaki, K. Kusano, A. Ogawa, N. Sonoda, *J. Am. Chem. Soc.* **1991**, 113, 8558.
- ¹¹ Y. Ryu, N. Sonoda, *Angew. Chem. Int. Ed. Engl.* **1996**, 35, 1050.
- ¹² D. P. Curran, P. A. van Elburg, B. Giese, S. Gilges, *Tetrahedron Lett.* **1990**, 31, 2861.
- ¹³ I. Ryu, K. Kusano, H. Yamazaki, N. Sonoda, *J. Org. Chem.* **1991**, 56, 5005.
- ¹⁴ I. Ryu, H. Yamazaki, A. Ogawa, N. Kambe, N. Sonoda, *J. Am. Chem. Soc.* **1993**, 115, 1187.
- ¹⁵ I. Ryu, N. Sonoda, D. Curran, *Chem. Rev.* **1996**, 96, 177.
- ¹⁶ I. Ryu, T. Niguma, S. Minakata, M. Komatsu, Z. Luo, D. P. Curran, *Tetrahedron Lett.* **1999**, 40, 2367.
- ¹⁷ I. Ryu, T. Niguma, S. Minakata, M. Komatsu, *Tetrahedron Lett.* **1997**, 38, 7883.
- ¹⁸ I. Ryu, M. Hasegawa, A. Kurihara, A. Ogawa, S. Tsunoi, N. Sonoda, *Synlett* **1993**, 2, 143.
- ¹⁹ K. Nagahara, I. Ryu, H. Yamazaki, N. Kambe, M. Komatsu, N. Sonoda, A. Baba, *Tetrahedron* **1997**, 53, 14615.
- ²⁰ I. Ryu, K. Nagahara, H. Yamazaki, S. Tsunoi, N. Sonoda, *Synlett* **1994**, 1994, 643.
- ²¹ C. Chatgililoglu, *Acc. Chem. Res.* **1992**, 25, 188.
- ²² J. Lusztyk, B. Maillard, D. A. Lindsay, K. U. Ingold, *J. Am. Chem. Soc.* **1983**, 105, 3578.
- ²³ C. Chatgililoglu, M. Ballestri, *Organometallics* **1999**, 18, 2395.
- ²⁴ For examples of 5-endocyclizations of acyl radicals, see: (a) G. D. Mendenhall, J. D. Protasiewicz, C. E. Brown, K. U. Ingold, J. Lusztyk, *J. Am. Chem. Soc.* **1994**, 116, 1718 (b) Y. Yamamoto, M. Ohno, S. Eguchi, *J. Org. Chem.* **1994**, 59, 1718; (c) A. S. Kende, J. L. Belletire, *Tetrahedron Lett.* **1972**, 13, 2145.
- ²⁵ I. Ryu, H. Alper, *J. Am. Chem. Soc.* **1993**, 115, 7543.
- ²⁶ J. H. Horner, S. Y. Choi, M. Newcomb, *Org. Lett.* **2000**, 2, 3369.
- ²⁷ a) S. Tsunoi, I. Ryu, N. Sonoda, *J. Am. Chem. Soc.* **1994**, 116, 5473; (b) S. Tsunoi, I. Ryu, Y. Tamura, S. Yamasaki, N. Sonoda, *Synlett* **1994**, 1994, 1009.
- ²⁸ a) T. Kondo, Y. Tsuji, Y. Watanabe, *Tetrahedron Lett.* **1988**, 29, 3833; (b) T. Kondo, Y. Sone, Y. Tsuji, Y. Watanabe, *J. Organomet. Chem.* **1994**, 473, 163.
- ²⁹ a) T. Ishiyama, N. Miyaura, A. Suzuki, *Tetrahedron Lett.* **1991**, 32, 6923; (b) T. Ishiyama, M. Murata, A. Suzuki, N. Miyaura, *J. Chem. Soc., Chem. Commun.* **1995**, 295.
- ³⁰ L. Gu, C. Jin, L. Jiyang, *Green Chem.* **2015**, 17, 3733.
- ³¹ M. Majek, A. Jacobi von Wangelin, *Angew. Chem. Int. Ed.* **2015**, 54, 2270.
- ³² J. B. Peng, X. Qi, X. F. Wu, *ChemSusChem.* **2016**, 9, 2279.
- ³³ C. Gosset, S. Pellegrini, R. Jooris, T. Bousquet, L. Pelinski, *Adv. Synth. Catal.* **2018**, 360, 3401.
- ³⁴ Q. Q. Zhou, W. Guo, W. Ding, X. Wu, X. Chen, L. Q. Lu, W. J. Xiao, *Angew. Chem. Int. Ed.* **2015**, 54, 1196.

III.2. Alkyl Radical Carbonylation Using Organosilicates *via* Visible-Light Photoredox Catalysis

Published in *Angew. Chem. Int. Ed.* **2019**, 58, 1803

(*Highlighted in Synfacts*, **2019**)

III.2.1. Abstract

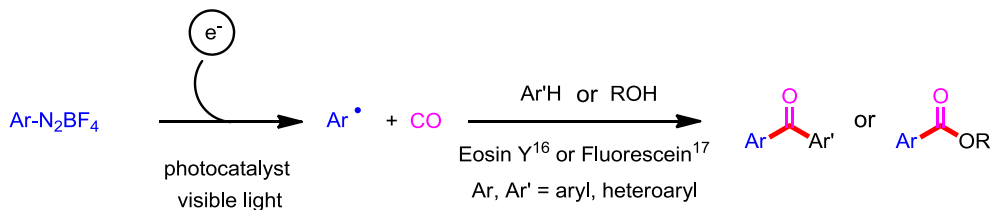
Primary, secondary and tertiary alkyl radicals, formed by photocatalyzed oxidation of organosilicates, can be involved efficiently in radical carbonylation with carbon monoxide (CO), which leads to a variety of unsymmetrical ketones. This work constitutes the first example of radical carbonylation under a photooxidative regime.

III.2.2. Introduction

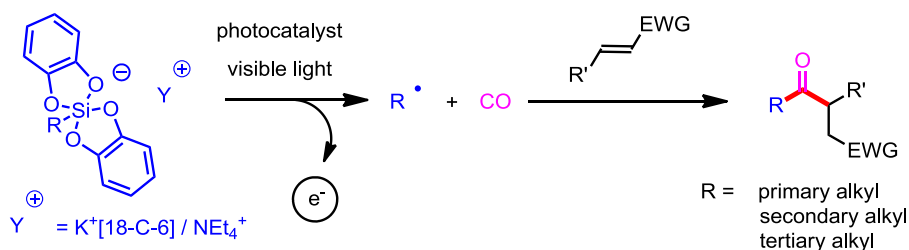
Visible-light photoredox catalysis now holds a privileged position in modern radical chemistry.^{1,2} Several families of alkyl radical precursors, such as alkylcarboxylates,³ alkyltrifluoroborates,⁴ and alkylsulfinate salts⁵ are known to use visible light irradiation to promote the efficient formation of alkyl radical species under photooxidation conditions. Recently, alkyl bis(catecholato)silicates⁶ were introduced by the Paris group⁷ and later by Molander⁸ and others⁹ to allow for the smooth generation of a variety of alkyl radicals that includes unstabilized primary radicals, and this enhancement applies to visible light photoredox-catalyzed conditions with Ru(II) or Ir(III) salts and even with organic dye 1,2,3,5-tetrakis(carbazol-9-yl)-4,6-dicyano-benzene (4CzIPN).^{7b, 10} The generated alkyl radical species can be promptly trapped by several activated alkenes, allylsulfone,^{7b, 7c} and imines.¹¹

Radical multicomponent processes are in great demand as they allow the reduction of a number of steps in order to obtain the targeted compounds.¹² In this regard, carbon monoxide (CO) is effective as a donor/acceptor type radical C1 synthon similar to isonitriles.^{13,14} Carbonylative couplings for the formation of ketones or esters by radical carbonylations have been extensively investigated by the Osaka group which include photo-induced carbonylation reactions.¹⁵ In those studies organic halides, chalcogenides, and unsaturated C-C bonds were generally used as the starting radical sources. Recently, several groups have applied aryl radical carbonylation to successful photoredox conditions, that follow a *reductive* photoredox pathway using aryl diazonium salts as aryl radical precursors. For example, Gu, Jacobi Von Wangelin, and Xiao independently reported that ketones and esters can be formed *via* the photoredox carbonylation of an aryl ring by using CO either in the presence of eosin Y¹⁶ or fluorescein as a photocatalyst (**Scheme 1**, type A).^{17,18}

Previous work (type A): Aryl radical carbonylation by *reductive* photoredox conditions



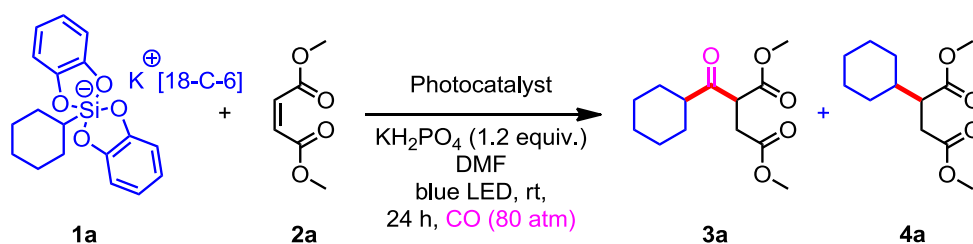
This work (type B): Alkyl radical carbonylation by *oxidative* photoredox conditions



Scheme 1: Photoredox catalysed radical carbonylation under *photoreductive* conditions (previous work) and under *photooxidative* conditions (this work).

III.2.3. Results and discussion

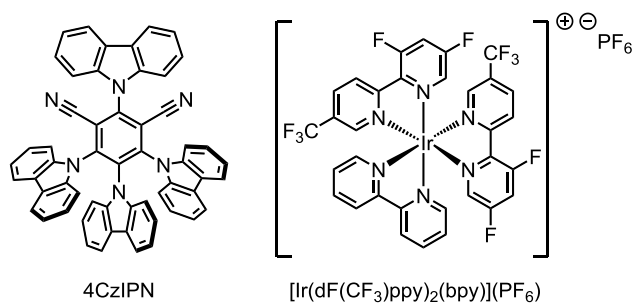
Ryu and co-workers previously reported three component types of unsymmetrical ketone synthesis for which alkyl halides, CO, and alkenes were reacted typically using tributyltin hydride¹⁹ or tris(trimethylsilyl)silane²⁰ as a radical mediator.²¹ We considered the use alkyl bis(catecholato)silicates as new substrates in this reaction. These are easily prepared from the corresponding alkoxy silanes and trichlorosilanes in a one-pot reaction (see supporting information for more details). They can be conserved weeks on the bench in contact with ambient air.⁷⁻⁹ They also exhibit relatively low oxidation potentials ($< +1$ V vs. SCE). Herein we report the first example of oxidative photocatalyzed carbonylative coupling reaction, as a novel three-component carbonylation route to unsymmetrical ketones under mild visible-light photoredox conditions that require no traditional radical mediators (**Scheme 1**, type B). As ketones are ubiquitous and important in organic chemistry due to their polyvalent reactivity, the development of new methods for their synthesis is still very useful for chemists.²²



Entry	Catalyst	[2a] [M]	Time (h)	Yield 3a ^[b]	Ratio 3a : 4a ^[d]
1	[Ir] ^[e]	0.15	24	58%	92 : 8
2	4CzIPN ^[f]	0.15	24	69%	93 : 7
3	none	0.15	24	13% ^[c]	75 : 25
4	4CzIPN ^[f]	0.02	24	49%	97 : 3
5	4CzIPN ^[f]	0.04	24	65%	97 : 3
6	4CzIPN ^[f]	0.09	24	71%	94 : 6
7	4CzIPN ^[f]	0.09	48	85%	95 : 5

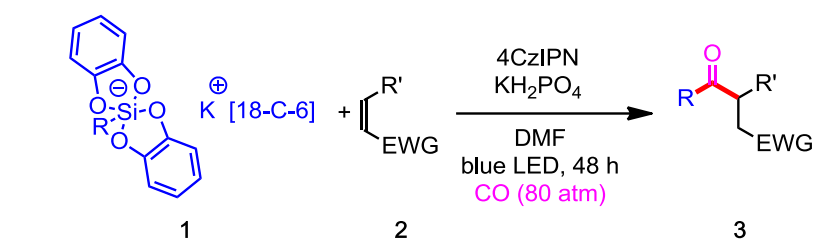
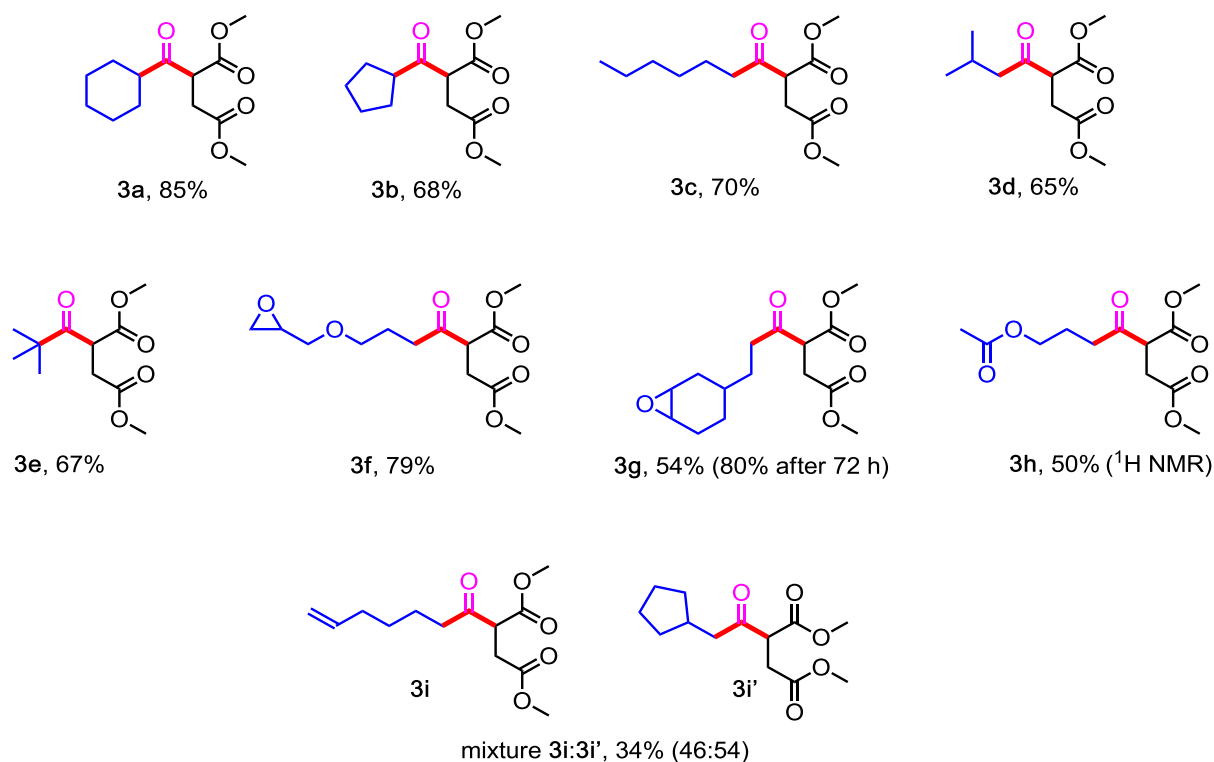
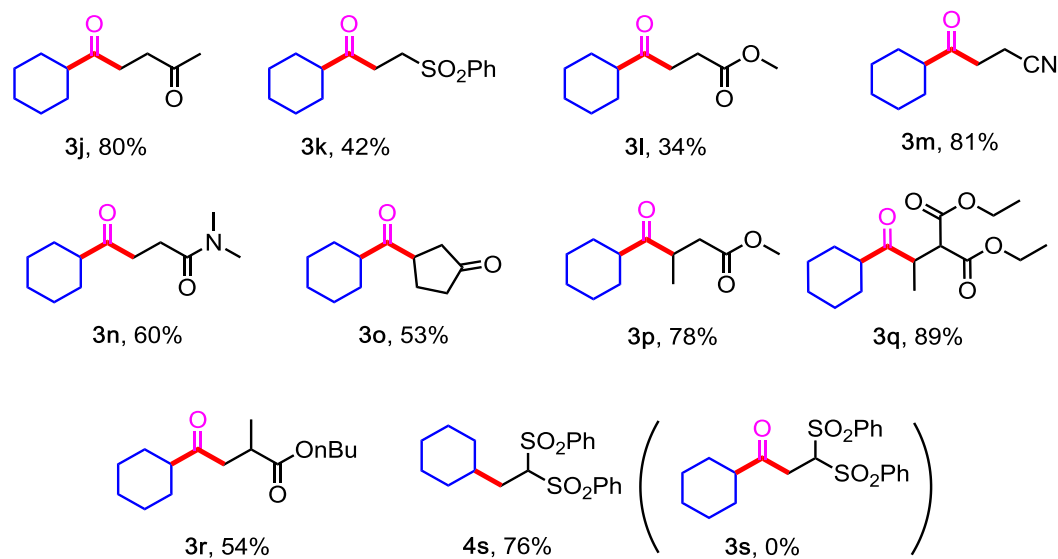
^[a] Conditions: potassium [18-Crown-6] bis(catecholato)-cyclohexylsilicate (**1a**, 0.3 mmol, 1 equiv.), dimethylmaleate (**2a**, 2 equiv.), photocatalyst (1 - 2 mol%), KH₂PO₄ (0.36 mmol), CO (80 atm), DMF (10-3 mL), irradiation by blue LED lamp (425 nm) for 24 - 48 h; ^[b] isolated yield, ^[c] determined by ¹H NMR; ^[d] determined by GC of the crude mixture, ^[e] [Ir(dF(CF₃)ppy)₂(bpy)](PF₆), 2 mol%; ^[f] 1 mol%.

Table 1: Optimization of the reaction conditions ^[a]



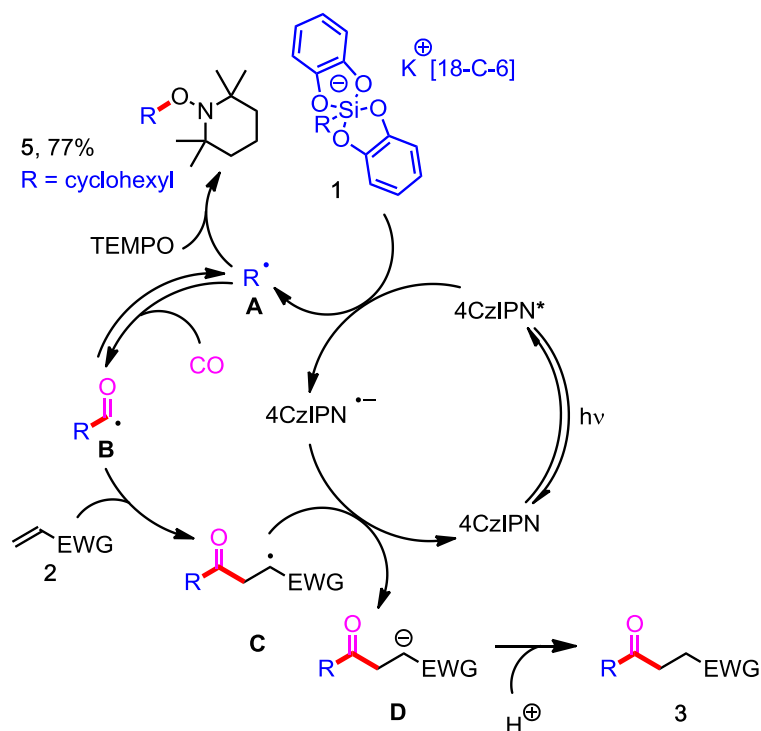
As a model, we first chose to test a three-component coupling reaction comprised of cyclohexyl bis(catecholato) silicate (**1a**), CO, and dimethylmaleate (**2a**). The experiment was

carried out in a stainless-steel autoclave equipped with two quartz glass windows that served as a pressure-durable apparatus during light irradiation (15 W blue LED, see the supporting information for details). The results are summarized in **Table 1**. When a solution of **1a**, **2a**, $[\text{Ir}(\text{dF}(\text{CF}_3)\text{ppy})_2(\text{bpy})](\text{PF}_6)$ (1 mol %), and KH_2PO_4 (1.2 equiv.) in DMF was irradiated for 24 hours under a CO pressure of 80 atm, the desired reaction proceeded to give the anticipated unsymmetrical ketone **3a** in a 58% yield after isolation by flash chromatography on silica gel (**Table 1**, entry 1). The non-carbonylated product **4a** was the only by-product of the reaction, and was present in only a small amount (**3a** : **4a** = 92 : 8). To insure effective photoredox catalysis, we used an organic dye, 1,2,3,5-tetrakis-(carbazole-yl)-4-dicyanobenzene (4CzIPN), with a long excited state lifetime (5.1 μs).^{7c, 23} It also displays interesting photoredox properties ($E_{1/2}(\text{4CzIPN}^*/[\text{4CzIPN}]^{\bullet-}) = +1.59 \text{ V vs. SCE}$ and $E_{1/2}(\text{4CzIPN}/[\text{4CzIPN}]^-) = -1.21 \text{ V vs. SCE}$);²⁴ so that this photocatalyst has proven useful for the photooxidation of alkyl bis(catecholato)silicates.^{7b,10e} To our delight, using this organic dye we obtained a better yield of 69% with similar ratios of **3a** and **4a** (93 : 7) (**Table 1**, entry 2). When the reaction was tested without the use of a photocatalyst, the yield dropped dramatically to 13% (**Table 1**, entry 3), which suggested the necessity of a photocatalyst. Next, we decreased the concentration of **2a** from 0.15 M to 0.02 and 0.04 M. At a lower concentration (0.02 M), the reaction became sluggish and the yield of **3a** was decreased to 49% (**Table 1**, entry 4). With **2a** at 0.04 M, the yield reached 65% (**Table 1**, entry 5). In these two cases, the ratio remained excellent (97 : 3). When the reaction was carried out with 0.09 M of **2a**, we observed an increased yield of product **3a** to 71% with a slightly decreased ratio of 94 : 6 (**Table 1**, entry 6). Since the reaction of entry 6 remained slow, we extended the reaction time for 48 h, which gave **3a** in an 85% isolated yield (**Table 1**, entry 7).

**Scope of the silicate:****Scope of the acceptor:****Scheme 2:** Scope of the substrates for the three-component reaction leading to unsymmetrical ketones **3**

We applied these optimized conditions to the three-component synthesis of a series of unsymmetrical ketones **3**, using a variety of alkyl bis(catecholato)silicates as substrates (**Scheme 2**). The carbonylation of the cyclopentyl derivative worked well and led to the corresponding unsymmetrical ketone **3b** in a 68% yield. Primary radicals furnished good yields, irrespective of the use of a linear alkyl (**3c**, 70%) or a branched alkyl (**3d**, 65%). The reaction of a tertiary alkylsilicate also gave ketone **3e** in a 67% yield. Interestingly, the reaction was compatible with a rather sensitive level of functionality, such as with an oxirane, and gave the desired product **3f** in a 79% yield. Product **3g** with an oxabicycloheptyl moiety was obtained in an 80% yield, albeit with an extended reaction time of 72 hours. The carbonylated adduct **3h**, bearing an acetate, appeared unstable and could not be isolated, although it was identified by ^1H NMR in the crude reaction mixture (50%). The use of the 5-hexenyl derivative **1i** was expected to provide insight into the rate of carbonylation under these conditions. Interestingly, under the employed conditions, we obtained an almost equimolar mixture of uncyclized **3i** and cyclized **3i'** in a 34% yield, with a crude NMR chart that suggested other by-products had formed *via* carbonylation.²⁵

Next, we investigated the compatibility of a variety of activated alkenes as radical acceptors (**2a-k**) by using the three-component transformation (**Scheme 2**). 1,4-Dicarbonyl derivatives still remain challenging to access.²⁶ Gratifyingly, methyl vinyl ketone **2b** was successfully used in the three-component reaction with CO and bis(catecholato-cyclo-hexyl)silicate **1a** to give the corresponding 1,4-diketone **3j** in 80% yield. By contrast, the reaction of vinylsulfone **2c**, and methyl acrylate **2d** gave the carbonylation products **3k** and **3l** in rather moderate yields (42 and 34%, respectively). When we used acrylonitrile, the expected product **3m** was obtained in an excellent yield of 81%. The compound **3n**, obtained from the *N,N*-dimethylacrylamide **2f**, was isolated in a 60% yield. Cyclopentenone **2g** led to the formation of diketone **3o** in a 53% yield. Interestingly, β -alkyl-substituted, α - β -unsaturated carbonyl compounds capably underwent the present transformation. Thus, methyl crotonate **2h** gave the corresponding 4-keto ester **3p** in a 78% yield. The reaction of diethyl 2-ethylidenemalonate **2i** gave the expected product **3q** in an 89% yield. The reaction of butyl methacrylate **2j** gave the corresponding 4-keto ester **3r** in a 54% yield. The reaction of **1a** with CO in the presence of disulfonylethene **2k**, gave non-carbonylated adduct **4s** in a 76% yield. Disulfonylethylene **2k** is such a good radical acceptor that a direct addition of a cyclohexyl radical proceeded.

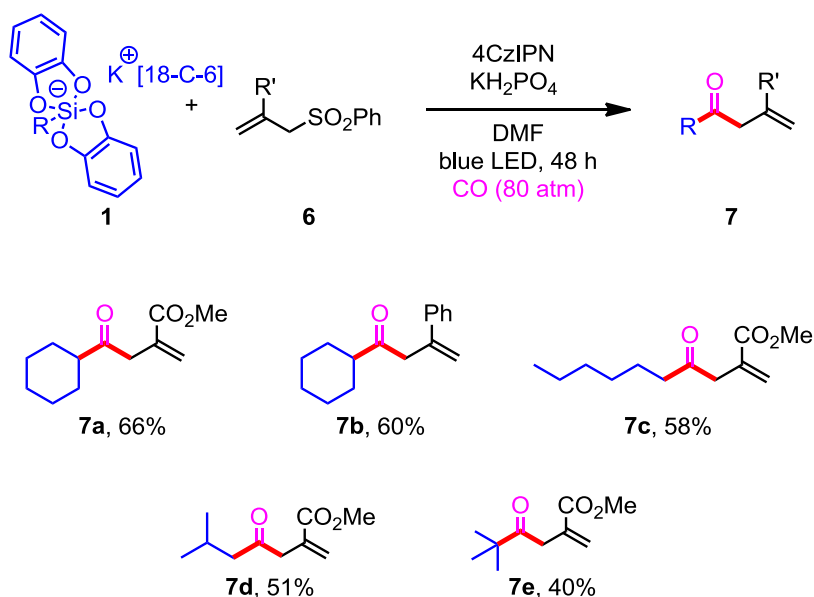


Scheme 3: Proposed mechanism

We proposed the overall mechanism illustrated in **Scheme 3**. In the first step, the photocatalyst is excited under visible-light irradiation. A SET oxidation of the alkyl bis(catecholato)silicate **1** by the excited $^*4\text{CzIPN}$,¹⁰ leads to the reduced species $[4\text{CzIPN}]^{\bullet-}$ and to the formation of the alkyl radical **A** via homolytic cleavage of the C-Si bond of the silicate radical.⁷⁻⁹ Alkyl radical **A** reacts with CO to form the acyl radical **B**,¹⁴ which adds to the acceptor alkene **2** to provide adduct radical **C**. The latter would be reduced by $[4\text{CzIPN}]^{\bullet-}$ to afford the stabilized carbanionic species **D** and regenerate the photocatalyst in its ground state, thus closing the catalytic cycle and ensuring its propagation. Finally, protonation of **D** by KH_2PO_4 yields the final product **3**.

To support this hypothetical mechanism, we conducted several experiments (see the supporting information for details). Fluorescent quenching studies of $^*4\text{CzIPN}$ by silicate **1a** in the absence of CO showed a decrease of the fluorescent intensity upon gradual addition of **1a**. The quenching rate constant k_q from the Stern-Volmer equation was determined to be $1.37 \times 10^8 \text{ mol}^{-1} \cdot \text{L} \cdot \text{s}^{-1}$ (in DMF), a value consistent with another determination in DMSO ($k_q = 2.5 \times 10^7 \text{ M}^{-1} \cdot \text{s}^{-1}$) by Molander.²⁷ Based on the redox potentials differences between $^*4\text{CzIPN}$ ($E_{1/2}(4\text{CzIPN}^*/[4\text{CzIPN}]^{\bullet-}) = +1.59 \text{ V vs. SCE}$)^{10f} and silicate **1a** ($E^{\text{ox}} = +0.69 \text{ V vs. SCE}$),^{7c} a SET consisting in the reductive quenching of the photoexcited photocatalyst $^*4\text{CzIPN}$ by silicate **1a** is presumably involved. This was confirmed by the reaction of cyclohexylsilicate **1a** with CO, in the presence of 2.2 equiv. of TEMPO which led to the exclusive formation of the non-carbonylated TEMPO adduct **5** in 77% yield, thus highlighting the formation of radical intermediates of type **A**. A “light/dark” experiment was also

conducted in the absence of CO and it appears that the product formation occurs only during periods of light irradiation. This result might support the catalytic mechanism shown in **Scheme 3**.²⁸ To ensure that no short radical chain occurs, we measured quantum yields of the reaction of silicate **1a** with different acceptors in the presence of 4CzIPN. We obtained a quantum yield of 0.066 in the conjugate addition with maleate and 0.33 for the allylation reaction with 2-phenylallyl p-tolyl sulfone with 4CzIPN. These findings show that the present mechanism does not follow a radical chain pathway but most likely a closed photoredox loop, as depicted in **Scheme 3**.



Scheme 4: Three-component reaction leading to unsaturated ketones **7**

Next, we focused on the behavior of various silicates towards carbonylative radical allylation with various allylsulfones (**6a-b**) (**Scheme 4**), for which previous work used allyltin as a radical acceptor.^{19a} The reaction of **1a** with CO and allylsulfone **6b**, which bears a methoxycarbonyl group at the 2 position, returned β,γ -unsaturated ketone **7a** in a 66% yield. When phenylallylsulfone **6b** was reacted with cyclohexylsilicate **1a** and CO, it gave the expected enone **7b** in a 60% yield. Primary radicals are good substrates for the present radical allylation regardless of whether it is a linear alkyl (**7c**, 58%), or a branched alkyl (**7d**, 51%). The reaction with a tertiary alkylsilicate gave the desired enone **7e** in a 40% yield together with a non-carbonylated addition product. These allylation reactions followed the pattern of the mechanism reported in **Scheme 3**, in which the photocatalyst was regenerated by a reduction of the phenylsulfonyl radical to a phenylsulfinate anion.^{7c} The ketones formed herein could be useful scaffolds. For instance, 1,4 ketone **3j** could be used through a Paal-Knorr reaction for the synthesis of pyrroles or thiophenes. These heteroaromatics can be found in many natural products but also in biological active compounds such as HMG-CoA reductase inhibitors and hepatitis C virus polymerase inhibitors.²⁹

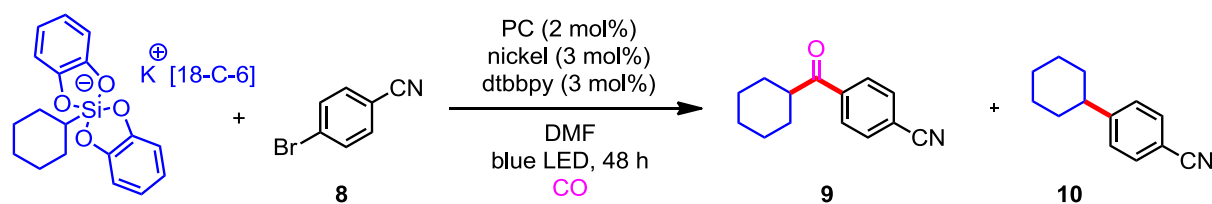
III.2.4. Conclusion

In summary, herein, we described an *oxidative* photoredox catalysis combined with radical carbonylation chemistry, for the first time. The present reaction protocol was based on the use of an inexpensive organic dye, 4CzIPN, as a photocatalyst and on a wide range of alkyl bis(catecholato)silicates that were used as alkyl radical precursors under a CO atmosphere, which afforded efficient access to a variety of functionalized unsymmetrical ketones including β,γ -unsaturated ketones. These results demonstrate the plausibility of other photocatalyzed radical carbonylation reactions under oxidative regimes that we are now exploring in our laboratory.

III.2.5. Additional results

III.2.5.1. Dual photoredox catalysis and radical carbonylation

We wondered if such methodology could be coupled to a nickel/photoredox dual catalytic system. However, whatever the nature of the nickel catalyst ($\text{Ni}(\text{COD})_2$ or $\text{NiCl}_2(\text{dme})$) or the photocatalyst ($[\text{Ir}]$ or 4CzIPN), no product was observed (carbonylated or non-carbonylated) (**Table 2**). It appeared that CO might poison the nickel based catalytic system. Only 1 atm of CO was enough to prevent the reaction to occur.



PC	Nickel catalyst	$P_{\text{CO}}(\text{atm})$	Reaction time	Yield 9/10
$[\text{Ir}]$	$\text{Ni}(\text{COD})_2$	80	24h	0/0
$[\text{Ir}]$	$\text{Ni}(\text{COD})_2$	0	24h	0/90
$[\text{Ir}]$	$\text{Ni}(\text{COD})_2$	40	24h	0/0
$[\text{Ir}]$	$\text{Ni}(\text{COD})_2$	1	24h	0/0
4CzIPN	$\text{NiCl}_2\cdot\text{dme}$	80	24h	0/0
4CzIPN	$\text{NiCl}_2\cdot\text{dme}$	1	24h	0/0

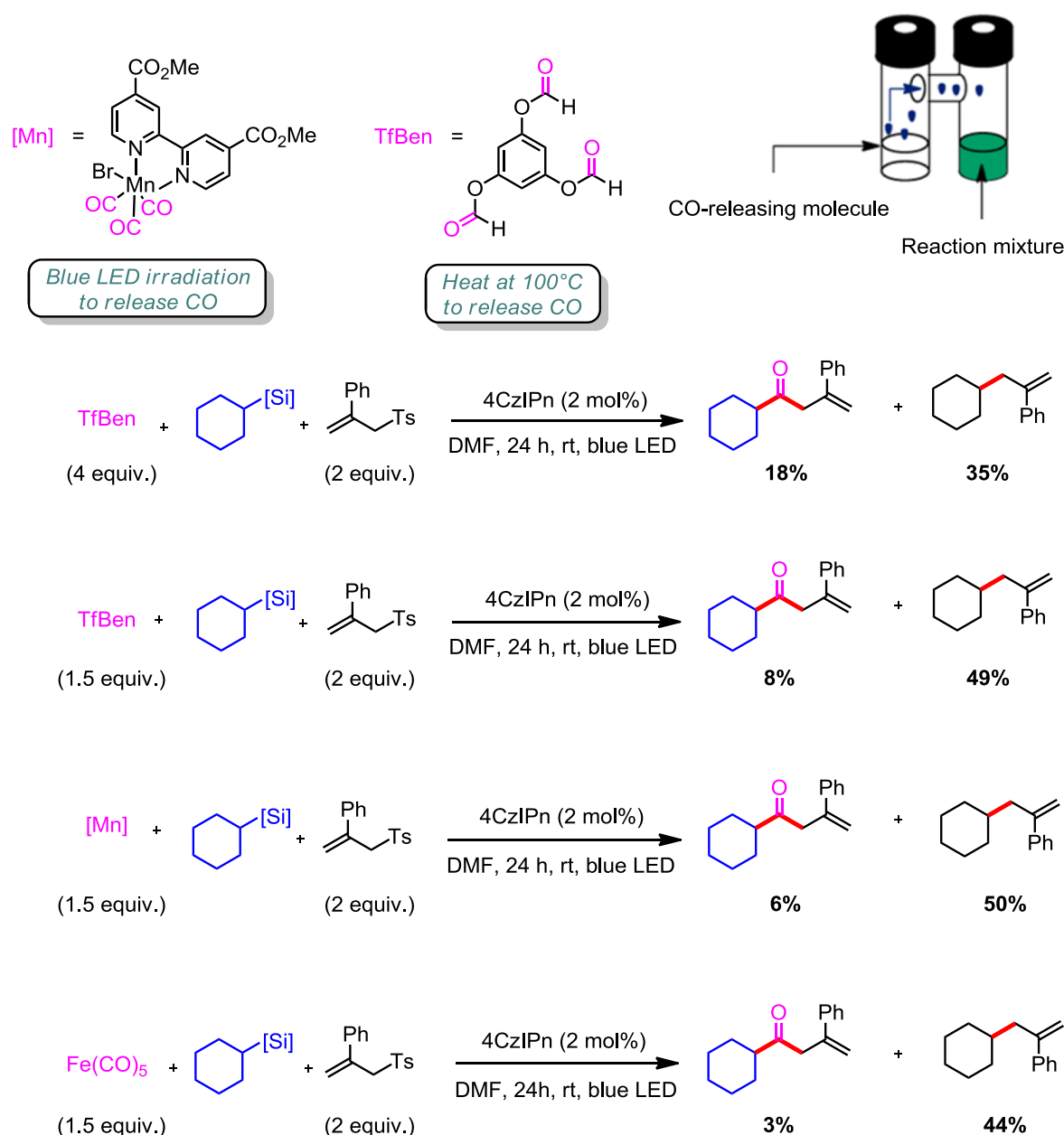
Table 2: Carbonylated dual catalysis.

Inspired by the work of Stille on palladium carbonylative cross-coupling reactions, a dual catalytic system using $\text{Pd}(\text{OAc})_2$ as the organometallic catalyst instead of nickel was also performed on the reaction of **Table 2**. However, no product was observed (carbonylated or non-carbonylated).

III.2.5.2. Carbon monoxide releasing molecules

Inspired by the work of Skrydstруп on carbonylation in H tube with CO-surrogate,³⁰ we thought of using this setup with our system. Indeed, these CO-releasing molecules are attractive from a safety point of view, because no high pressure CO bottle is needed. Furthermore, ^{14}C CO can be used and integrated in the scaffold which could be quite interesting for a pharmaceutical firm.

Thus, after choosing different CO-releasing molecules (based on their accessibility), the reaction of cyclohexyl silicate and 1-methyl-4-((2-phenylallyl)sulfonyl)benzene was performed. In one compartment, the CO-surrogate was introduced and in the other one, the silicate, the acceptor and the photocatalyst were put. Both of the compartments are connected, thus once the CO-surrogate liberates its CO (*via* irradiation or heating depending on the CO-releasing molecule), a CO atmosphere is obtained all over the H tube and the carbonylation reaction can possibly occur (**Scheme 5**).

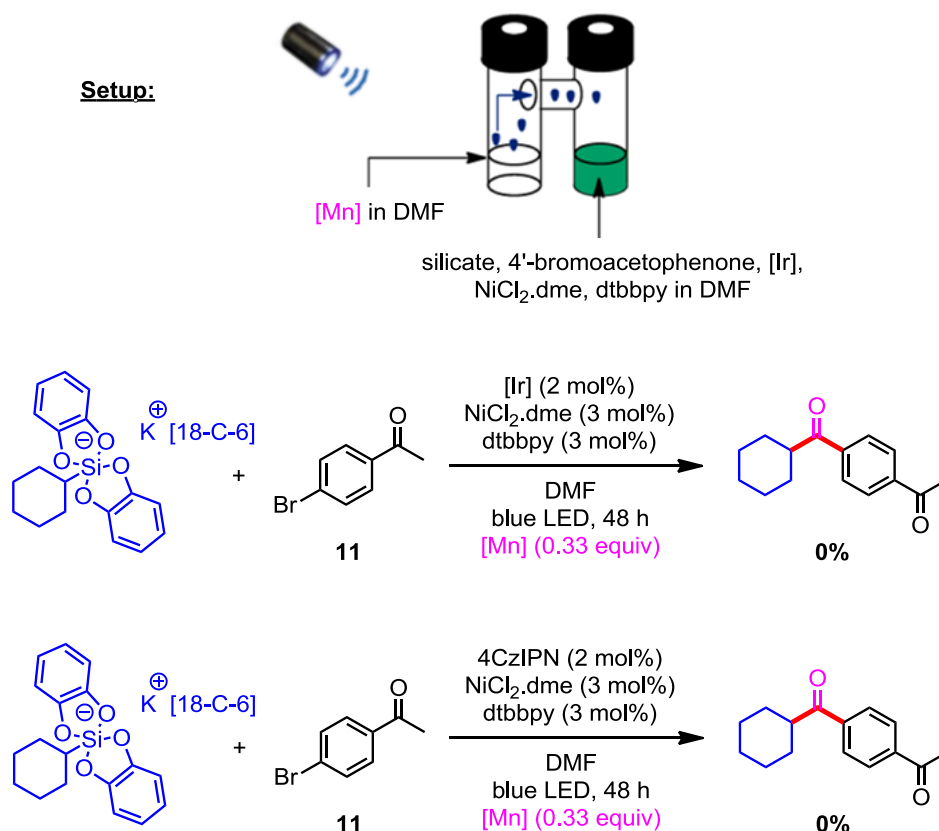


Scheme 5: Carbonylation reactions using a H tube setup

In all experiments a mixture of carbonylated and non-carbonylated products was obtained. Only traces of the carbonylated adduct were observed in most of the cases except when 4

equivalents of TfBen were used. Indeed, 18% of the desired product was formed in comparison to 35% for the non-carbonylated side product. It seems that the CO pressure inside the H tube is probably not high enough to favor the carbonylation coupling.

Dual catalysis was also performed in H tube with the manganese complex of **scheme 5** (**[Mn]**), cyclohexyl silicate, 4'-bromoacetophenone and a photocatalyst (**[Ir]** or 4CzIPN) under blue LED irradiation (**Scheme 6**). However, even with 0.33 equiv. of **[Mn]**, thus about 1 equiv. of CO, no product was formed (carbonylated and non-carbonylated) and mostly starting material was recovered.



Scheme 6: Carbonylated dual catalysis in H tube

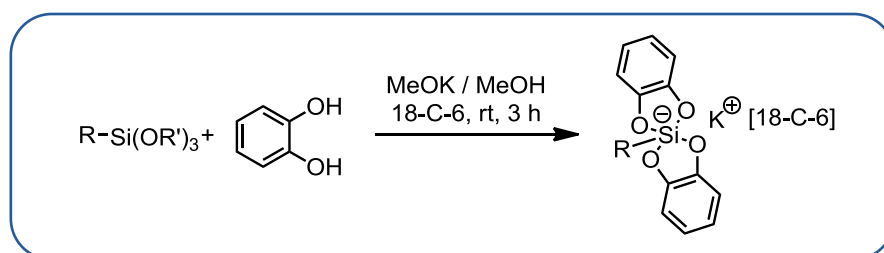
III.2.6. Supporting information

III.2.6.1. General informations

Photoinduced reactions were carried out using a 425 nm Twin LED light lamp (RelyOn Ltd.). ^1H NMR spectra were recorded with Varian MR400 (400 MHz) and JEOL ECS-400 (400 MHz) spectrometers in CDCl_3 and are referenced at 7.26 ppm for CHCl_3 . ^{13}C NMR spectra were recorded with Varian MR400 (100 MHz) and JEOL ECS-400 (100 MHz) spectrometers in CDCl_3 and are referenced at 77.00 ppm for CDCl_3 . Chemical shifts are reported in parts per million (δ). Splitting patterns are indicated as follows: b, broad; s, singlet; d, doublet; t, triplet; q, quartet; quint, quintet; sex, sextet; sept, septet; m, multiplet. Infrared spectra were obtained on a JASCO FT/IR-4100 spectrometer; absorptions were reported in reciprocal centimeters. Both conventional and high-resolution mass spectra were recorded with a JEOL MS-700 spectrometer. The products were purified by flash column chromatography on silica gel (Kanto Chem. Co. Silica Gel 60N (spherical, neutral, 40-50 μm)). Catechol was purchased from commercial source and purified by crystallization from toluene. Unless otherwise specified, all commercially available reagents were used as received. Photocatalysts were synthesized as described.^{31,32} Silicates **1a** to **1k** were synthesized as described.³³

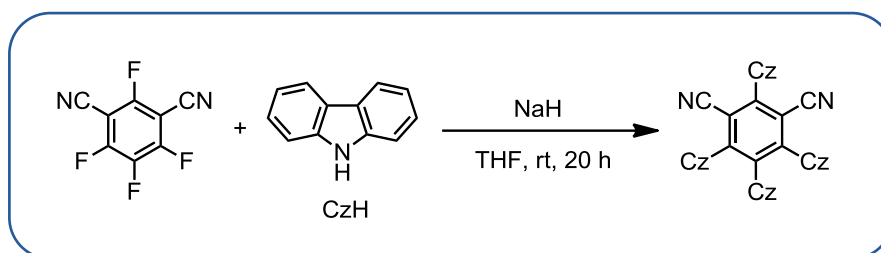
III.2.6.2. General procedures

a) Synthesis of silicates



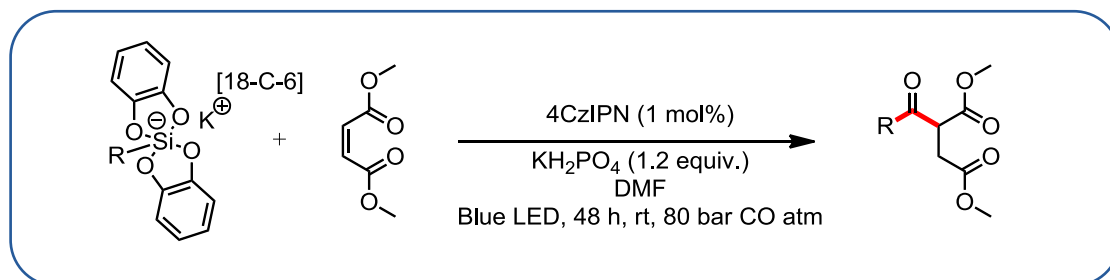
To a stirred solution of catechol (2 equiv.) in dry methanol (0.25 M) was added 18-C-6 (1 equiv.). After dissolution of the crown ether, the trialkoxy organosilane (1 equiv.) was added, followed by a solution of potassium methoxide in methanol (1 equiv.). The reaction mixture was stirred for 3 hours and the solvent was removed under reduced pressure. The residue was dissolved in the minimum volume of acetone and diethyl ether was added until a cloudy solution was obtained (scrapping on the edge of the flask could be done to induce crystallization). The flask was placed at -20°C overnight. The crystals were collected by filtration, washed with diethyl ether and dried under vacuum to afford potassium [18-Crown-6] silicate.

b) Synthesis of 4CzIPN



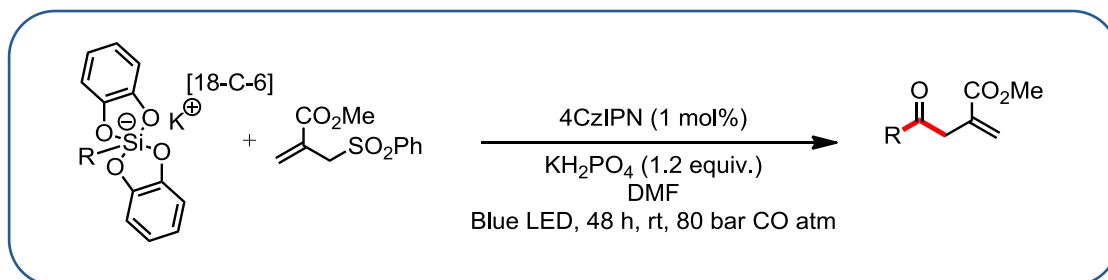
The 4CzIPN has been synthesized following a previous reported procedure.¹ To a 100 mL flask was added NaH (60% in mineral oil) (7.5 equiv., 15.0 mmol, 606 mg) in THF (40 mL). Carbazole (5 equiv., 10.0 mmol, 1.68 g) was added slowly to the mixture. After 30 min of stirring at room temperature the tetrafluoroisophthalonitrile (1 equiv., 2.00 mmol, 406 mg) was added and the mixture was stirred at room temperature for 20 hours. A brown/yellow precipitate progressively appeared. The solid was successively washed with water and ethanol. The crude product was dissolved in the minimum of DCM and crystallized by addition of hexane to give 4CzIPN as a yellow solid (1.17 g, 74% yield). The spectroscopic data are in agreement with those reported in the literature.³¹

c) Photoredox-catalyzed radical carbonylation of silicates with electron deficient alkenes



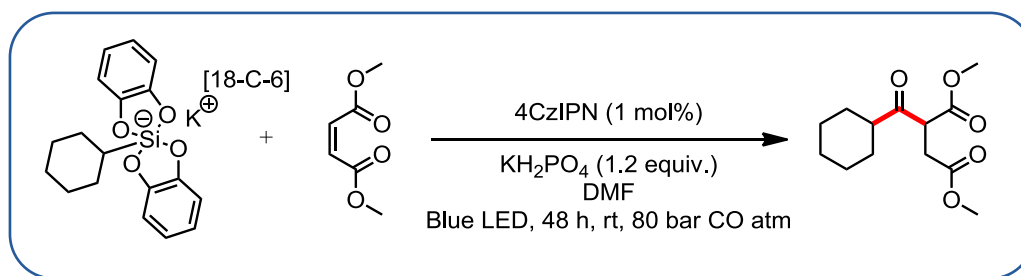
In a stainless-steel autoclave was added the appropriate silicate (1 equiv.), KH_2PO_4 (1.2 equiv.) and 4CzIPN (1 mol%). Then, DMF was added (0.043 M), followed by dimethyl maleate (2 equiv.). The autoclave was flushed 3 times under CO atmosphere and the reaction mixture was irradiated with blue LED (425 nm) under 80 bar CO pressure at rt during 48 h. The reaction was diluted with diethyl ether, washed with an aqueous saturated K_2CO_3 solution (2 times), water (2 times), dried over MgSO_4 and evaporated under reduced pressure. The crude product was purified by column chromatography.

d) Photoredox-catalyzed radical carbonylation of silicates with allylsulfones



In a pressurized autoclave was added the appropriate silicate (1 equiv.), KH_2PO_4 (1.2 equiv.) and 4CzIPN (1 mol%). Then, DMF was added (0.043 μ), followed by methyl 2-((phenylsulfonyl)methyl)acrylate (2 equiv.). The autoclave was flushed 3 times under CO atmosphere and the reaction mixture was irradiated with blue LED (425 nm) under 80 bar CO pressure at rt during 48 h. The reaction was diluted with diethyl ether), washed with an aqueous saturated K_2CO_3 solution (2 times), water (2 times), dried over MgSO_4 and evaporated under reduced pressure. The crude product was purified by column chromatography.

III.2.6.3. Control experiments



Variation from standard conditions	Yield ^[a]
none	85%
Without photocatalyst	13% ^[b]
In the dark	0%

^[a] Isolated yield; ^[b] ¹H NMR using 1 equiv. of acetanilide as internal standard.

III.2.6.4. Quantum yield measurements

All solutions were prepared and stored in the dark. Reactions were conducted in a 1 cm quartz cuvette with a rubber septum. Fluorescence quenching and quantum yield measurements were performed on a Jasco FP-6200 spectrofluorometer. UV-visible spectra were performed on a Varian Cary 50 spectrophotometer. All spectra were recorded in a thermostated cell at 25°C.

The light intensity at 436 nm of the spectrofluorometer was determined as described.³⁴

Briefly, standard ferrioxalate actinometry was used for the photon flux determination.^{35,36} Two mL of a 0.15 M solution of ferrioxalate in 0.05 M of H₂SO₄ was irradiated for 90 seconds at 436 nm (excitation slit width at 5 nm and emission slit width at 10 nm). After irradiation, 0.35 mL of a buffered solution of phenanthroline (50 mg of phenanthroline et 11.25 g of sodium acetate in 50 mL of 0.5 M H₂SO₄) was added to the cuvette. The cuvette was kept in a dark for 1 hour to ensure complete coordination of Fe²⁺ ions. The absorbance at 510 nm was measured. As a blank reaction, a similar sample was prepared without irradiation and the absorbance at 510 nm was recorded. Ferrous ions production was calculated following the *equation 1*:

$$\text{mol Fe}^{2+} = \frac{V \cdot \Delta A}{l \cdot \epsilon} \quad (\text{eq. 1})$$

Where V is the total volume (0.00235 L), ΔA is the difference of absorbance at 510 nm between irradiated and non-irradiated samples, l is path length (1 cm) and ε is the molar extinction coefficient at 510 nm (11 100 L mol⁻¹ cm⁻¹). The photon flux was calculated following the *equation 2*:

$$\text{Photon flux} = \frac{\text{mol Fe}^{2+}}{\Phi * t * f} \quad (\text{eq. 2})$$

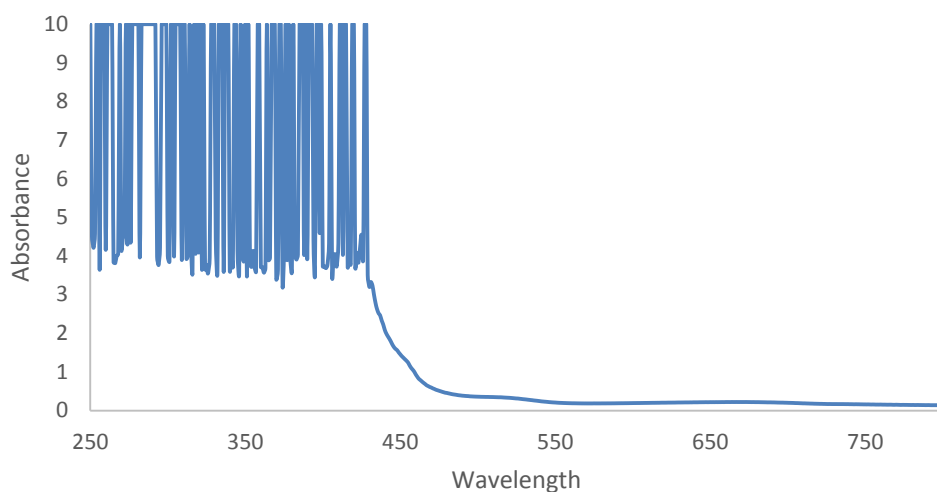
Where Φ is the quantum yield for the ferrioxalate actinometer (1.01 for a 0.15 M solution at 436 nm⁵), t is the time of irradiation (90 seconds) and f is the fraction of light absorbed at 436 nm (0.99694, *vide infra*). The photon flux was calculated (average of three experiments) to be 1.01×10^{-9} einstein.s⁻¹.

Example for one measurement:

$$\text{mol Fe}^{2+} = \frac{0.00235 * 0.37986359}{1 * 11100} = 8.04 * 10^{-8} \text{ mol}$$

$$\text{photon flux} = \frac{8.04 * 10^{-8}}{1.01 * 90 * 0.99694} = 0.88 * 10^{-9} \text{ einstein.s}^{-1}$$

a) Absorption spectrum of ferrioxalate solution

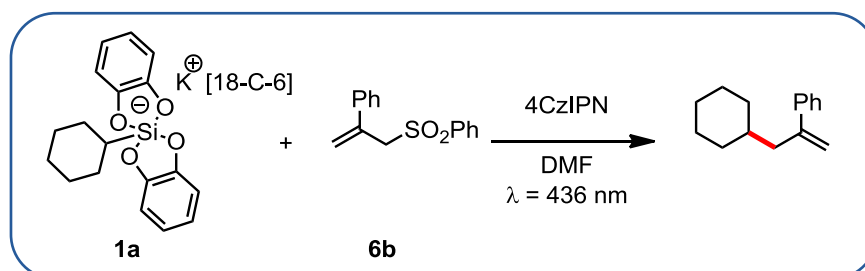


The absorption of the ferrioxalate at 436 nm was measured to be 2.5147607. The fraction of light absorbed (f) was calculating following the *equation 3*:

$$f = 1 - 10^{-A} \quad (\text{eq. 3})$$

b) Determination of the quantum yields

b.1) For allylation reaction: 4CzIpn



In a quartz cuvette was introduced **1a** (0.1 mmol, 1 equiv.), allylsulfone **6** (0.4 mmol, 4 equiv.), 4CzIPN (2 μ mol, 2 mol%) and 1 mL of DMF. The cuvette was capped with a PTFE stopper. The sample was placed in the spectrofluorometer and irradiated at 436 nm (excitation slit width at 5 nm and emission slit width at 10 nm) for 9000 seconds. The reaction mixture was transferred in a separatory funnel, partitioned between diethyl ether and water. The aqueous layer was extracted two times with diethyl ether and the combined organic layers were dried over MgSO_4 and concentrated under reduced pressure. The reaction yield was determined by ^1H NMR using 1,3,5-trimethoxybenzene as a standard. Under these conditions, the fraction of light absorbed at 436 nm (f) as a value of 0.99811 (*vide infra*).

The quantum yield was calculated according to the following the *equation 4*:

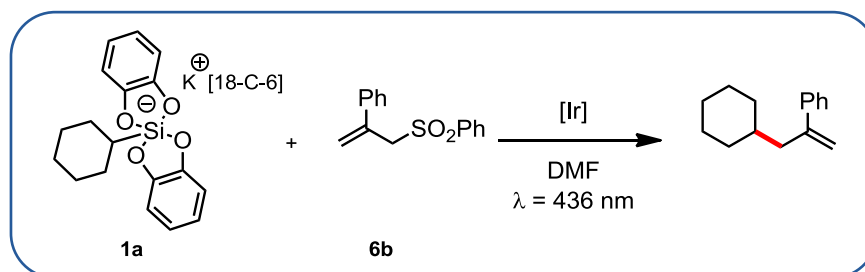
$$\Phi = \frac{\text{mol product}}{\text{flux} \cdot t \cdot f} \quad (\text{eq. 4})$$

Sample quantum yield calculation:

$$\Phi = \frac{0.000003}{1.01 \cdot 10^{-9} \cdot 9000 \cdot 0.998110737} = 0.33$$

63.1 mg of **1a** (0.1 mmol), 108.9 mg of sulfone **6** (0.4 mmol), 1.6 mg of 4CzIPN (2 μ mol) in 1 mL of DMF after 9000 seconds of irradiation yielded 3 % of product. $\Phi = 0.33$.

b.2) For allylation reaction: $[\text{Ir}(\text{dF}(\text{CF}_3)\text{ppy})_2(\text{bpy})](\text{PF}_6)$



In a quartz cuvette was introduced **1a** (0.1 mmol, 1 equiv.), allylsulfone **6** (0.4 mmol, 4 equiv.), $[\text{Ir}(\text{dF}(\text{CF}_3)\text{ppy})_2(\text{bpy})](\text{PF}_6)$ (2 μ mol, 2 mol%) and 1 mL of DMF. The cuvette was capped with a PTFE stopper. The sample was placed in the spectrofluorometer and irradiated at 436 nm (excitation slit width at 5 nm and emission slit width at 10 nm) for 9000 seconds. The reaction mixture was transferred in a separatory funnel, partitioned between diethyl ether and water. The aqueous layer was extracted two times with diethyl ether and the combined organic layers were dried over MgSO_4 and concentrated under reduced pressure. The reaction yield was determined by ^1H NMR using 1,3,5-trimethoxybenzene as a standard. Under these conditions, the fraction of light absorbed at 436 nm (f) as a value of 0.99639 (*vide infra*).

The quantum yield was calculated according to the following the *equation 4*:

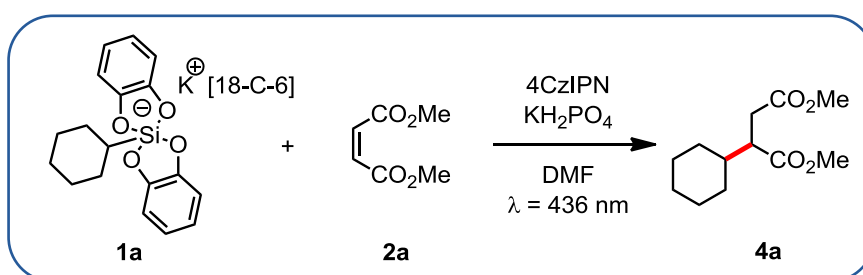
$$\Phi = \frac{\text{mol product}}{\text{flux} \cdot t \cdot f} \quad (\text{eq. 4})$$

Sample quantum yield calculation:

$$\Phi = \frac{0.000001}{1.01 \cdot 10^{-9} \cdot 9000 \cdot 0.9963899558} = 0.11$$

63.1 mg of **1a** (0.1 mmol), 108.9 mg of sulfone **6** (0.4 mmol), 2.0 mg of Ir (2 μmol) in 1 mL of DMF after 9000 seconds of irradiation yielded 1 % of product. $\Phi = 0.11$.

b.3) For Giese-type reaction



In a quartz cuvette was introduced **1a** (0.1 mmol, 1 equiv.), dimethylmaleate **2a** (0.4 mmol, 4 equiv.), KH_2PO_4 (0.12 mmol, 1.2 equiv.), 4CzIPN (2 μmol , 2 mol%) and 1 mL of DMF. The cuvette was capped with a PTFE stopper. The sample was placed in the spectrofluorometer and irradiated at 436 nm (excitation slit width at 5 nm and emission slit width at 10 nm) for 15 000 seconds. The reaction mixture was transferred in a separatory funnel, partitioned between diethyl ether and water. The aqueous layer was extracted two times with diethyl ether and the combined organic layers were dried over MgSO_4 and concentrated under reduced pressure. The reaction yield was determined by ^1H NMR using 1,3,5-trimethoxybenzene as a standard. Under these conditions, the fraction of light absorbed at 436 nm (f) as a value of 0.99811 (*vide infra*).

The quantum yield was calculated according to the following the *equation 3*:

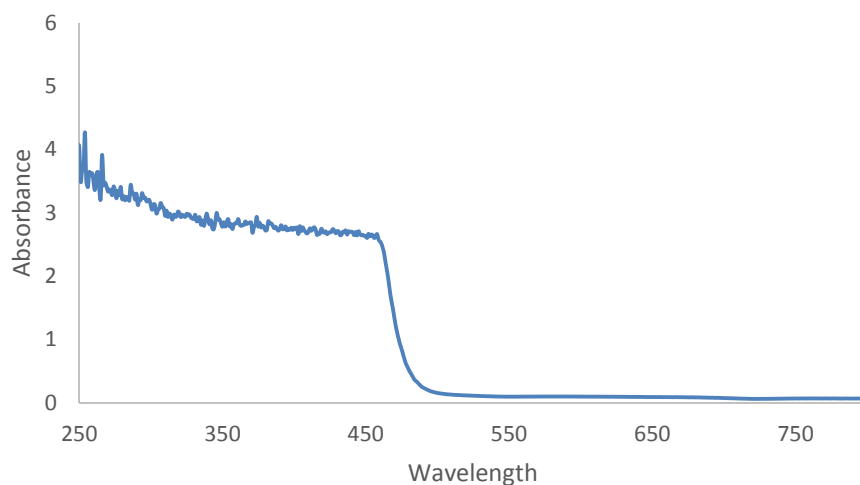
$$\Phi = \frac{\text{mol product}}{\text{flux} \cdot t \cdot f} \quad (\text{eq. 3})$$

Sample quantum yield calculation:

$$\Phi = \frac{0.000001}{1.01 \cdot 10^{-9} \cdot 15000 \cdot 0.998110737} = 0.066$$

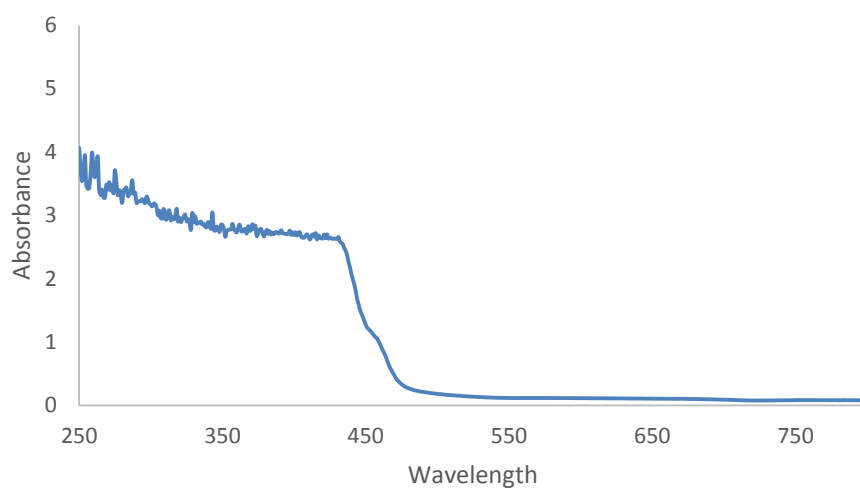
63.1 mg of **1a** (0.1 mmol), 50 μL of maleate **2a** (0.4 mmol), 16.3 mg of KH_2PO_4 (0.12 mmol), 1.6 mg of 4CzIPN (2 μmol) in 1 mL of DMF after 15 000 seconds of irradiation yielded 1 % of product. $\Phi = 0.066$.

c) Absorption spectrum of 4CzIPN solution



The absorption of 4CzIPN at 436 nm was measured to be 2,72370768. The fraction of light absorbed (f) was calculating following the *equation 3*:

$$f = 1 - 10^{-A} \quad (\text{eq. 3})$$

d) Absorption spectrum of $[\text{Ir}(\text{dF}(\text{CF}_3)\text{ppy})_2(\text{bpy})](\text{PF}_6)$ solution

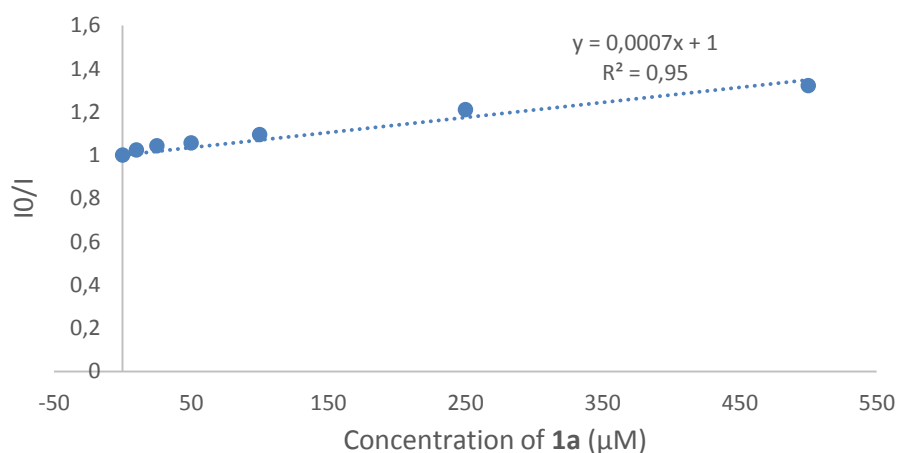
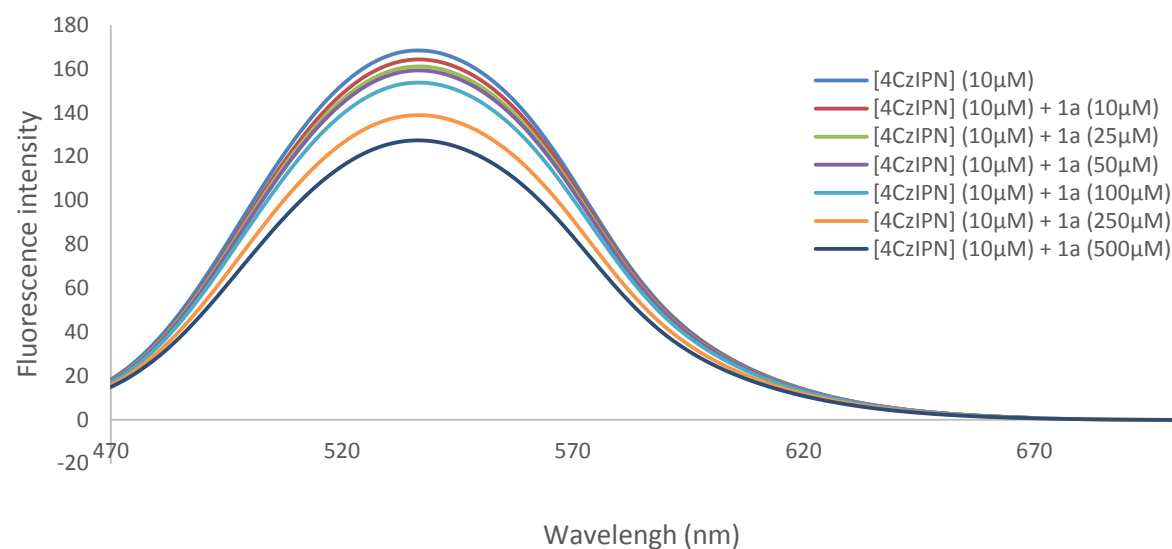
The absorption of $[\text{Ir}(\text{dF}(\text{CF}_3)\text{ppy})_2(\text{bpy})](\text{PF}_6)$ at 436 nm was measured to be 2,442487478. The fraction of light absorbed (f) was calculating following the *equation 3*:

$$f = 1 - 10^{-A} \quad (\text{eq. 3})$$

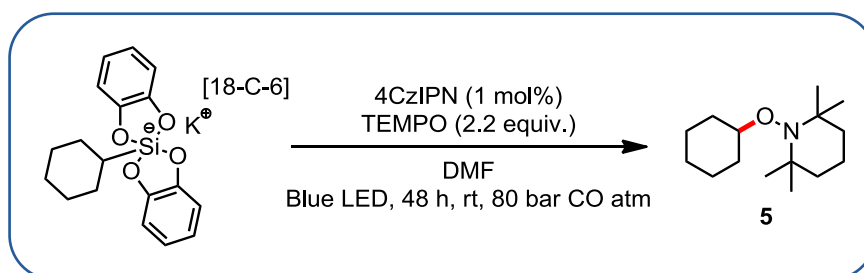
III.2.6.5. Fluorescence quenching experiments

Emission intensities were recorded on a Jasco FP-6200 spectrofluorometer. Dry DMF was degassed by freeze-pump-thaw cycles before using. The photocatalyst 4CzIPN was excited at 436 nm and the emission spectra were recorded between 470 and 700 nm. In a typical experiment, 10 μM solutions of 4CzIPN in DMF were prepared with the appropriate concentration of quencher **1a** in a 1.0 cm quartz cuvette and covered. After degassing with a stream of argon for 10 minutes, the emission spectrum of the sample was recorded.

The Stern-Volmer plot was done according the following equation: $\frac{I_f^0}{I_f} = 1 + k_q t_0 \cdot [Q]$. A quenching constant of $1.37 \times 10^8 \text{ M}^{-1} \cdot \text{s}^{-1}$ was calculated.



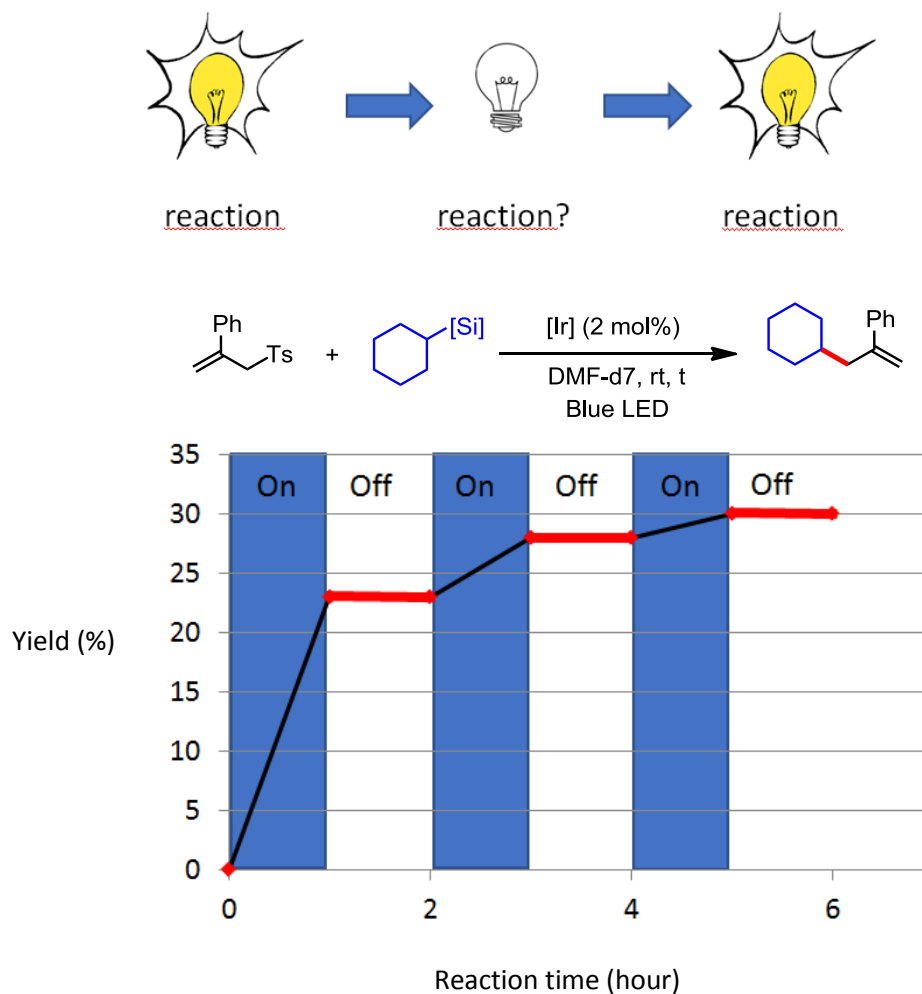
III.2.6.6. Spin-trapping experiment with TEMPO



In a stainless-steel autoclave was added potassium [18-crown-6] bis(catecholato)-cyclohexylsilicate **1a** (0.300 mmol, 187 mg), 4CzIPN (1mol%, 0.003 mmol, 2.7 mg) and TEMPO (0.693 mmol, 106 mg). DMF was added (7 mL) then the autoclave was flushed 3 times under CO atmosphere and the reaction mixture was irradiated with blue LEDs (425 nm) under 80 bar CO pressure at r.t. during 48 h. GC-MS of the crude mixture highlighted the formation of TEMPO-adduct product **5** and a yield of 77% could be obtained using acetanilide as an internal reference.

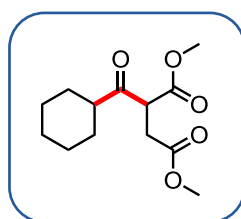
III.2.6.7. Light/dark experiment

To a schlenk flask was added potassium [18-Crown-6] bis(catecholato) cyclohexylsilicate (1 equiv., 0.1 mmol, 63.1 mg), Ir[(dF(CF₃)ppy)₂(bpy)](PF₆) (2 mol %, 2 μmol, 2 mg) and the 2-phenylallyl p-tolyl sulfone (4 equiv., 0.4 mmol, 50 μL) after that degazed and dry DMF-d₇ was added (1 mL). The reaction mixture was degassed by argon bubbling for 20 minutes and irradiated with blue LED (1 hour cycles of light and dark). t₁ = first time that the reaction is irradiated. Me₃SiPh is used as internal standard.



III.2.6.8. Spectrum data

Dimethyl 2-(cyclohexanecarbonyl)succinate (3a)

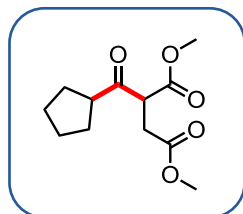


The spectroscopic data are in agreement with those reported in the literature.³⁷

¹H NMR (400 MHz, CDCl₃): δ 4.14 (dd, *J* = 8.0 Hz and 6.4 Hz, 1H), 3.74 (s, 3H), 3.66 (s, 3H), 2.94 (dd, *J* = 17.2 Hz and 8.0 Hz, 1H), 2.83 (dd, *J* = 17.2 Hz and 6.8 Hz, 1H), 2.70-2.65 (m, 1H), 2.03-1.94 (m, 1H), 1.85-1.74 (m, 3H), 1.71-1.63 (m, 1H), 1.49-1.36 (m, 1H), 1.34-1.16 (m, 4H);

^{13}C NMR (100 MHz, CDCl_3): δ 207.0, 171.9, 169.2, 52.8, 52.2, 52.1, 50.7, 32.4, 29.0, 28.0, 25.9, 25.8, 25.4.

Dimethyl 2-(cyclopentanecarbonyl)succinate (**3b**)

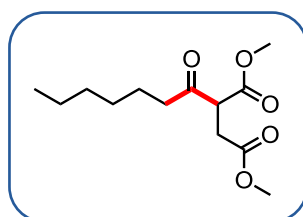


Following the general procedure with potassium [18-Crown-6] bis(catecholato)-pentylsilicate **1b** with 10% of catechol (0.294 mmol, 201 mg), KH_2PO_4 (0.376 mmol, 51.2 mg), 4CzIPN (3 μmol , 2.4 mg) and dimethyl maleate (0.600 mmol, 75.0 μL) in 7 mL of DMF. The crude product was purified to afford dimethyl 2-(cyclopentanecarbonyl)succinate **3b** (54.2 mg, 70%) as a yellow oil. The spectroscopic data are in agreement with those reported in the literature.³⁸

^1H NMR (400 MHz, CDCl_3): δ 4.10 (t, $J = 7.2$ Hz, 1H), 3.74 (s, 3H), 3.67 (s, 3H), 3.17 (dd, $J = 14.8$ Hz and 7.2 Hz, 1H), 2.95 (dd, $J = 16.8$ Hz and 7.2 Hz, 1H), 2.84 (dd, $J = 17.6$ Hz and 6.8 Hz, 1H), 2.00-1.89 (m, 1H), 1.87-1.54 (m, 7H);

^{13}C NMR (100 MHz, CDCl_3): δ 206.5, 171.9, 169.3, 53.6, 52.9, 52.2, 51.2, 32.4, 30.1, 28.8, 26.2, 26.1.

Dimethyl 2-heptanoylsuccinate (**3c**)

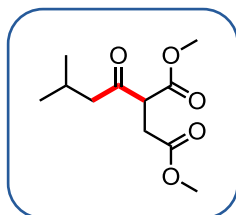


Following the general procedure with potassium [18-Crown-6] bis(catecholato)-hexylsilicate **1c** (0.304 mmol, 192 mg), KH_2PO_4 (0.361 mmol, 49.1 mg), 4CzIPN (3.00 μmol , 2.4 mg) and dimethyl maleate (0.600 mmol, 75.0 μL) in 7 mL of DMF. The crude product was purified to afford dimethyl 2-heptanoylsuccinate **3c** (54.2 mg, 70%) as a colorless oil. The spectroscopic data are in agreement with those reported in the literature.³⁹

^1H NMR (400 MHz, CDCl_3): δ 3.99 (dd, $J = 8.8$ Hz and 6.4 Hz, 1H), 3.74 (s, 3H), 2.67 (s, 3H), 2.98 (dd, $J = 17.6$ Hz and 6.8 Hz, 1H), 2.84 (dd, $J = 16.0$ Hz and 6.8 Hz, 1H), 2.76-2.54 (m, 2H), 1.60 (t, $J = 6.8$ Hz, 2H), 1.35-1.20 (m, 6H), 0.89 (t, $J = 6.4$ Hz, 3H);

^{13}C NMR (100 MHz, CDCl_3): δ 204.1, 171.9, 169.1, 53.9, 52.8, 52.1, 42.9, 32.3, 31.6, 28.7, 23.4, 22.6, 14.1.

Dimethyl 2-(3-methylbutanoyl)succinate (**3d**)

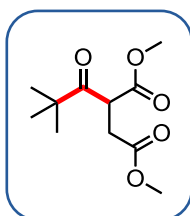


Following the general procedure with potassium [18-Crown-6] bis(catecholato)-isobutylsilicate **1d** (0.295 mmol, 178.4 mg), KH_2PO_4 (0.381 mmol, 51.8 mg), 4CzIPN (3.00 μmol , 2.50 mg) and dimethyl maleate (0.600 mmol, 75.0 μL) in 7 mL of DMF. The crude product was purified to afford dimethyl 2-(3-methylbutanoyl)succinate **3d** (44.2 mg, 65%) as a pale yellow oil. The spectroscopic data are in agreement with those reported in the literature.³⁷

^1H NMR (400 MHz, CDCl_3): δ 3.97 (dd, $J = 8.0$ Hz and 6.5 Hz, 1H), 3.74 (s, 3H), 3.68 (s, 3H), 2.97 (dd, $J = 17.5$ Hz and 8.0 Hz, 1H), 2.83 (dd, $J = 17.5$ Hz and 8.0 Hz, 1H), 2.60-2.48 (m, 2H), 2.24-2.14 (m, 1H), 0.92 (dd, $J = 12.0$ Hz and 6.4 Hz, 6H);

^{13}C NMR (100 MHz, CDCl_3): δ 203.5, 172.0, 169.0, 54.4, 52.8, 52.2, 51.7, 32.2, 24.2, 22.6, 22.4.

Dimethyl 2-pivaloylsuccinate (**3e**)



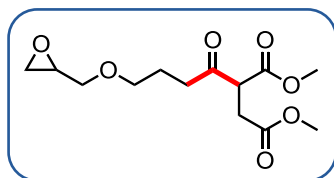
Following the general procedure with tetraethylammonium bis(catecholato)-*tert*-butylsilicate **1e** (0.300 mmol, 129.5 mg), KH_2PO_4 (0.393 mmol, 53.5 mg), 4CzIPN (3.00 μmol , 2.8 mg)

and dimethyl maleate (0.600 mmol, 75.0 μL) in 7 mL of DMF. The crude product was purified to afford dimethyl 2-pivaloylsuccinate **3e** (46.3 mg, 67%) as an incolor oil. The spectroscopic data are in agreement with those reported in the literature.⁴⁰

^1H NMR (400 MHz, CDCl_3): δ 4.40 (t, $J = 7.6$ Hz, 1H), 3.71 (s, 3H), 3.68 (s, 3H), 2.85 (d, $J = 7.6$ Hz, 2H), 1.21 (s, 9H);

^{13}C NMR (100 MHz, CDCl_3): δ 209.3, 171.6, 169.4, 52.7, 52.1, 48.1, 45.5, 33.6, 26.4 (3C).

Dimethyl 2-(3-(oxiran-2-ylmethoxy)propanoyl)succinate (**3f**)



Following the general procedure with potassium [18-Crown-6] bis(catecholato)- (2-(oxiran-2-ylmethoxy)ethyl)silicate **1f** (0.293 mmol, 194.0 mg), KH_2PO_4 (0.347 mmol, 47.2 mg), 4CzIPN (3.00 μmol , 2.5 mg) and dimethyl maleate (0.600 mmol, 75.0 μL) in 7 mL of DMF. The crude product was purified to afford dimethyl 2-(4-(oxiran-2-ylmethoxy)butanoyl)succinate **3f** (66.9 mg, 79%) as a yellow oil.

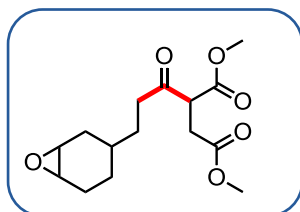
^1H NMR (400 MHz, CDCl_3): δ 4.00 (dd, $J = 8.4$ Hz and 6.8 Hz, 1H), 3.74 (s, 3H), 3.66 (s, 3H), 3.53-3.45 (m, 2H), 3.36-3.30 (m, 1H), 3.15-3.09 (m, 1H), 2.98 (dd, $J = 17.6$ Hz and 8.0 Hz, 1H), 2.88-2.70 (m, 5H), 2.60-2.57 (m, 1H), 1.89 (tt, $J = 13.2$ Hz and 6.8 Hz, 2H);

^{13}C NMR (100 MHz, CDCl_3): δ 203.7, 171.9, 169.0, 71.6, 70.3, 53.9, 52.9, 52.2, 50.9, 44.4, 39.4, 32.3, 23.7;

IR (neat): 3000, 2954, 2870, 1747, 1732, 1437, 1410, 1367, 1336, 1270, 1114, 853 cm^{-1} ;

HMRS: (ESI) m/z calc for $\text{C}_{10}\text{H}_{14}\text{O}_5$ ($[\text{M}-\text{OMe}]^+$) 257.1025; found: 257.1020.

Dimethyl 2-(3-(7-oxabicyclo[4.1.0]heptan-3-yl)propanoyl)succinate (**3g**)



Following the general procedure with potassium [18-Crown-6] bis(catecholato)-(2-(7-oxabicyclo[4.1.0]heptan-3-yl)ethyl)silicate **1g** (0.303 mmol, 204 mg), KH_2PO_4 (0.358 mmol, 48.7 mg), 4CzIPN (3.00 μmol , 2.60 mg) and dimethyl maleate (0.600 mmol, 75.0 μL) in 7 mL of DMF. The crude product was purified to afford dimethyl 2-(3-(7-oxabicyclo[4.1.0]heptan-3-yl)propanoyl)succinate **3g** (27.7 mg, 31%) as a yellow oil.

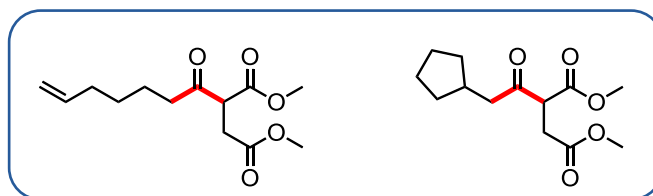
$^1\text{H NMR}$ (400 MHz, CDCl_3): δ 4.01-3.94 (m, 1H), 3.73 (s, 3H), 3.65 (s, 3H), 3.18-3.07 (m, 2H), 2.97 (dd, $J = 18.4$ Hz and 8.4 Hz, 1H), 2.83 (dd, $J = 17.2$ Hz and 6.0 Hz, 1H), 2.78-2.65 (m, 1H), 2.65-2.52 (m, 1H), 2.18-2.09 (m, 1H), 2.041.93 (m, 1H), 1.90-1.75 (m, 1H), 1.50-1.05 (m, 6H);

$^{13}\text{C NMR}$ (100 MHz, CDCl_3): δ 203.9, 171.9, 170.0, 53.8, 53.0, 52.2, 51.9, 40.5, 32.3, 31.7, 29.5, 29.2, 27.0, 25.3, 23.5;

IR (neat): 3450, 2992, 2928, 2852, 1731, 1437, 1263, 1166 cm^{-1} ;

HMRS: (ESI) m/z calc for $\text{C}_{15}\text{H}_{22}\text{O}_5$ ($[\text{M}-\text{O}]^+$) 282.1467; found: 282.1473.

Dimethyl 2-(hept-6-enoyl)succinate (**3i**) and Dimethyl 2-(3-cyclopentyl-2-oxopropyl)succinate (**3i'**)



Following the general procedure with potassium [18-Crown-6] bis(catecholato)-hexenylsilicate **1i** (0.302 mmol, 190.3 mg), KH_2PO_4 (0.394 mmol, 53.6 mg), 4CzIPN (3.00 μmol , 2.8 mg) and dimethyl maleate (0.600 mmol, 75.0 μL) in 7 mL of DMF. The crude product was purified to afford a mixture of dimethyl 2-pivaloylsuccinate **3i** and dimethyl 2-(3-cyclopentyl-2-oxopropyl)succinate **3i'** (26.0 mg, 46:54, 34%) as an incolore oil.

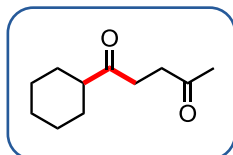
$^1\text{H NMR}$ (400 MHz, CDCl_3): δ 5.82-5.75 (m, 1H), 5.02-4.93 (m, 2H), 3.98 (t, $J = 6.0$ Hz, 2H), 3.74 (s, 6H), 3.67 (s, 6H), 3.02-2.94 (m, 2H), 2.86-2.80 (m, 2H), 2.77-2.58 (m, 4H), 2.27 (quint, $J = 7.6$ Hz, 1H), 2.06 (q, $J = 7.2$ Hz, 2H), 1.84-1.79 (m, 2H), 1.67-1.51 (m, 8H), 1.10-1.01 (m, 2H);

$^{13}\text{C NMR}$ (100 MHz, CDCl_3): δ 203.8, 203.6, 171.8 (2C), 169.0, 168.9, 138.4, 114.7, 53.9, 53.7, 52.7, 52.6, 52.0 (2C), 48.9 (2C), 35.0, 33.4, 32.5, 32.3, 32.1, 32.0, 28.1, 25.0, 24.9, 22.8;

IR (neat): 2999, 2954, 2854, 1740, 1719, 1438, 1370, 1268, 1163, 1010 cm^{-1} ;

HMRS: (ESI) m/z calc for $C_{12}H_{17}O_4^+$ ($[M-OMe]^+$) 225.1127; found: 225.1117.

1-Cyclohexylpentane-1,4-dione (**3j**)

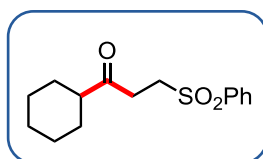


Following the general procedure with potassium [18-Crown-6] bis(catecholato)-cyclohexylsilicate **1a** (0.300 mmol, 189.0 mg), KH_2PO_4 (0.398 mmol, 54.1 mg), 4CzIPN (3.00 μ mol, 2.40 mg), and but-3-en-2-one (0.600 mmol, 30.0 μ L) in 7 mL of DMF. The crude product was purified to afford 1-cyclohexylpentane-1,4-dione **3j** (43.6 mg, 80%) as a yellow oil. The spectroscopic data are in agreement with those reported in the literature. The spectroscopic data are in agreement with those reported in the literature.³⁸

1H NMR (400 MHz, $CDCl_3$): δ 2.74-2.65 (m, 4H), 2.42-2.32 (m, 1H), 2.18 (s, 3H), 1.91-1.84 (m, 2H), 1.82-1.76 (m, 2H), 1.70-1.60 (m, 1H), 1.40-1.14 (m, 5H);

^{13}C NMR (100 MHz, $CDCl_3$): δ 212.7, 207.5, 50.8, 36.9, 34.2, 30.9, 28.6, 25.9, 25.7.

1-Cyclohexyl-3-(phenylsulfonyl)propan-1-one (**3k**)

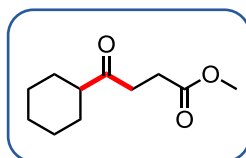


Following the general procedure C with potassium [18-Crown-6] bis(catecholato)-cyclohexylsilicate **1a** (0.299 mmol, 188.9 mg), KH_2PO_4 (0.631 mmol, 48.0 mg), 4CzIPN (3.00 μ mol, 2.50 mg), and (vinylsulfonyl)benzene (0.600 mmol, 106 mg) in 7 mL of DMF. The crude product was purified to afford 1-cyclohexylpentane-1,4-dione **3k** (35.3 mg, 42%) as a pale yellow solid (mixture of the desired product and the (vinylsulfonyl)benzene). The spectroscopic data are in agreement with those reported in the literature.³⁷

1H NMR (400 MHz, $CDCl_3$): δ 7.93-7.86 (m, 2H), 7.70-7.61 (m, 1H), 7.60-7.52 (m, 2H), 3.35 (t, $J = 7.2$ Hz, 2H), 2.95 (t, $J = 8.4$ Hz, 2H), 2.39-2.29 (m, 1H), 1.85-1.71 (m, 4H), 1.69-1.56 (m, 1H), 1.35-1.19 (m, 5H);

^{13}C NMR (100 MHz, CDCl_3): δ 209.4, 139.17, 134.0, 129.5 (2C), 128.0 (2C), 50.9, 50.8, 33.0, 28.5(2C), 25.8, 25.6(2C).

Methyl 4-cyclohexyl-4-oxobutanoate (**3l**)

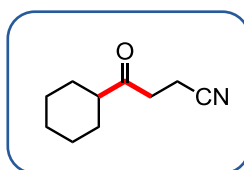


Following the general procedure with potassium [18-Crown-6] bis(catecholato)-cyclohexylsilicate **1a** (0.301 mmol, 189.8 mg), KH_2PO_4 (0.360 mmol, 49.0 mg), 4CzIPN (3.00 μmol , 2.30 mg), and methyl acrylate (0.598 mmol, 54.0 μL) in 7 mL of DMF. The crude product was purified to afford methyl 4-cyclohexyl-4-oxobutanoate **3l** (20.2 mg, 34%) as a yellow oil. The spectroscopic data are in agreement with those reported in the literature.³⁸

^1H NMR (400 MHz, CDCl_3): δ 3.67 (s, 3H), 2.75 (t, $J = 6.4$ Hz, 2H), 2.58 (t, $J = 6.4$ Hz, 2H), 2.43-2.31 (m, 1H), 1.91-1.82 (m, 2H), 1.82-1.72 (m, 2H), 1.71-1.60 (m, 1H), 1.42-1.15 (m, 5H);

^{13}C NMR (100 MHz, CDCl_3): δ 212.2, 173.5, 51.9, 50.8, 35.1, 28.6 (2C), 27.8, 26.0, 25.8 (2C).

4-Cyclohexyl-4-oxobutanenitrile (**3m**)

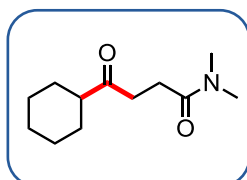


Following the general procedure with potassium [18-Crown-6] bis(catecholato)-cyclohexylsilicate **1a** (0.301 mmol, 190.1 mg), KH_2PO_4 (0.365 mmol, 49.7 mg), 4CzIPN (3.00 μmol , 2.4 mg), and acrylonitrile (0.600 mmol, 39.0 μL) in 7 mL of DMF. The crude product was purified to afford 4-cyclohexyl-4-oxobutanenitrile **3m** (40.0 mg, 80%) as a yellow oil. The spectroscopic data are in agreement with those reported in the literature.⁴¹

^1H NMR (400 MHz, CDCl_3): δ 2.83 (t, $J = 6.8$ Hz, 2H), 2.57 (t, $J = 6.4$ Hz, 2H), 2.42-2.32 (m, 1H), 1.89-1.75 (m, 4H), 1.72-1.68 (m, 1H), 1.40-1.24 (m, 5H);

^{13}C NMR (100 MHz, CDCl_3): δ 209.4, 119.3, 50.6, 35.9, 28.5 (2C), 25.8, 25.6 (2C), 11.6.

4-Cyclohexyl-N,N-dimethyl-4-oxobutanamide (**3n**)



Following the general procedure with potassium [18-Crown-6] bis(catecholato)-cyclohexylsilicate **1a** (0.300 mmol, 189.0 mg), KH_2PO_4 (0.362 mmol, 49.2 mg), 4CzIPN (3.00 μmol , 2.4 mg), and N,N-dimethylacrylamide (0.604 mmol, 62 μL) in 7 mL of DMF. The crude product was purified to afford 4-cyclohexyl-N,N-dimethyl-4-oxobutanamide **3n** (38.0 mg, 60%) as a colorless oil.

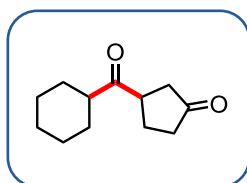
^1H NMR (400 MHz, CDCl_3): δ 3.02 (s, 3H), 2.92 (s, 3H), 2.77 (t, $J = 6.4$ Hz, 2H), 2.57 (t, $J = 6.4$ Hz, 2H), 2.45-2.38 (m, 1H), 1.92-1.68 (m, 5H), 1.38-1.18 (m, 5H);

^{13}C NMR (100 MHz, CDCl_3): δ 213.5, 171.9, 51.1, 37.2, 35.7, 35.4, 28.6 (2C), 27.1, 26.0, 25.8 (2C);

IR (neat): 2927, 2853, 1709, 1649, 1398, 1141, 1072 cm^{-1} ;

HMRS: (ESI) m/z calc for $\text{C}_{12}\text{H}_{21}\text{O}_2\text{N}$ ($[\text{M}]^+$) 211.1572; found: 211.1568.

3-(Cyclohexanecarbonyl)cyclopentan-1-one (**3o**)



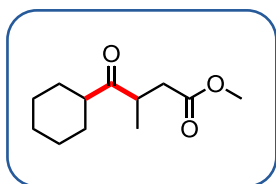
Following the general procedure with potassium [18-Crown-6] bis(catecholato)-cyclohexylsilicate **1a** (0.301 mmol, 190 mg), KH_2PO_4 (0.368 mmol, 50.1 mg), 4CzIPN (3.00 μmol , 2.30 mg), and cyclopent-2-en-1-one (0.599 mmol, 49.0 μL) in 7 mL of DMF. The crude product was purified to afford 3-(cyclohexanecarbonyl)cyclopentan-1-one **3o** (30.3 mg,

53%) as a colorless oil. The spectroscopic data are in agreement with those reported in the literature. The spectroscopic data are in agreement with those reported in the literature.³⁸

¹H NMR (400 MHz, CDCl₃): δ 3.43-3.30 (m, 1H), 2.51-2.15 (m, 5H), 2.01-1.65 (m, 6H), 1.45-1.17 (m, 6H);

¹³C NMR (100 MHz, CDCl₃): δ 217.1, 214.1, 50.2, 46.0, 40.8, 37.7, 28.8, 28.3, 26.4, 25.9, 25.8, 25.6.

Methyl 4-cyclohexyl-3-methyl-4-oxobutanoate (**3p**)

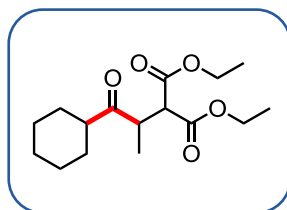


Following the general procedure with potassium [18-Crown-6] bis(catecholato)-cyclohexylsilicate **1a** (0.302 mmol, 190.5 mg), KH₂PO₄ (0.364 mmol, 49.5 mg), 4CzIPN (3.00 μmol, 2.60 mg), and pent-3-en-2-one (0.605 mmol, 59 μL) in 7 mL of DMF. The crude product was purified to afford methyl 4-cyclohexyl-3-methyl-4-oxobutanoate **3p** (45.9 mg, 78%) as a colorless oil. The spectroscopic data are in agreement with those reported in the literature.³⁸

¹H NMR (400 MHz, CDCl₃): δ 3.24-3.12 (m, 1H), 2.97 (dd, *J* = 9.2 Hz and 8.8 Hz, 1H), 2.62-2.52 (m, 1H), 2.33 (dd, *J* = 13.6 Hz and 4.4 Hz, 1H), 2.12 (s, 3H), 2.00-1.92 (m, 1H), 1.84-1.72 (m, 3H), 1.70-1.61 (m, 1H), 1.44-1.12 (m, 5H), 1.06 (d, *J* = 6.8 Hz, 3H);

¹³C NMR (100 MHz, CDCl₃): δ 216.7, 207.5, 49.6, 46.6, 39.7, 30.2, 29.1, 28.5, 26.0 (2C), 25.7, 17.0.

Diethyl 2-(1-cyclohexyl-1-oxopropan-2-yl)malonate (**3q**)

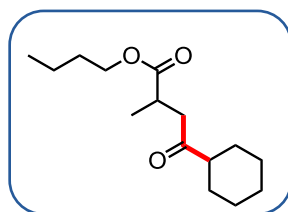


Following the general procedure with potassium [18-Crown-6] bis(catecholato)-cyclohexylsilicate **1a** (0.302 mmol, 190.5 mg), KH_2PO_4 (0.378 mmol, 51.5 mg), 4CzIPN (3.00 μmol , 2.50 mg), and diethyl 2-ethylidenemalonate (0.598 mmol, 107 μL) in 7 mL of DMF. The crude product was purified to afford diethyl 2-(1-cyclohexyl-1-oxopropan-2-yl)malonate **3q** (80.0 mg, 89%) as a colorless oil. The spectroscopic data are in agreement with those reported in the literature.³⁷

^1H NMR (400 MHz, CDCl_3): δ 4.21(q, $J = 14.4$ Hz and 7.2 Hz, 2H), 4.10 (q, $J = 7.2$ Hz and 5.2 Hz, 2H), 3.73 (d, $J = 10.4$ Hz, 1H), 3.46-3.35 (m, 1H), 2.66-2.55 (m, 1H), 2.07-1.99 (m, 1H), 1.85-1.72 (m, 3H), 1.72-1.63 (m, 1H), 1.50-1.36 (m, 1H), 1.33-1.16 (m, 10H), 1.10 (d, $J = 7.2$ Hz, 3H);

^{13}C NMR (100 MHz, CDCl_3): δ 214.7, 168.9, 168.5, 61.7, 61.6, 54.7, 49.8, 43.8, 29.2, 28.4, 26.0, 25.9, 25.7, 15.8, 14.3, 14.1.

Butyl 4-cyclohexyl-2-methyl-4-oxobutanoate (**3r**)



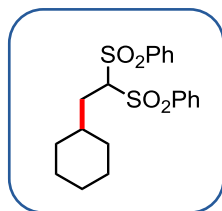
Following the general procedure with potassium [18-Crown-6] bis(catecholato)-cyclohexylsilicate **1a** (0.303 mmol, 190.7 mg), KH_2PO_4 (0.387 mmol, 52.7 mg), 4CzIPN (3.00 μmol , 2.50 mg), and butyl methacrylate (0.597 mmol, 95 μL) in 7 mL of DMF. The crude product was purified to afford butyl 4-cyclohexyl-2-methyl-4-oxobutanoate **3r** (41.6 mg, 54%) as a pale-yellow oil.

^1H NMR (400 MHz, CDCl_3): δ 4.10-4.02 (m, 2H), 2.95-2.88 (m, 1H), 2.53-2.39 (m, 1H), 2.39-1.97 (m, 2H), 1.88-1.73 (m, 3H), 1.68-1.54 (m, 4H), 1.41-1.12(m, 10H), 0.96-0.90 (m, 3H);

^{13}C NMR (100 MHz, CDCl_3): δ 212.1, 176.2, 64.6, 51.0, 43.9, 34.8, 30.8, 28.6, 28.5, 26.0, 25.8, 25.7, 19.2, 17.3, 13.9;

IR (neat): 2959, 2932, 2855, 1786, 1734, 1711, 1459, 1172, 1146 cm^{-1} ;

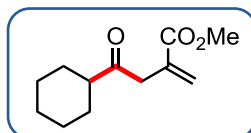
HMRS: (ESI) m/z calc for $\text{C}_{11}\text{H}_{17}\text{O}_2$ ($[\text{M-OnBu}]^+$) 181.1229; found: 181.1223.

(2-Cyclohexylethane-1,1-diyl)disulfonyl)dibenzene (4s)

Following the general procedure with potassium [18-Crown-6] bis(catecholato)-cyclohexylsilicate **1a** (0.293 mmol, 185.0 mg), KH_2PO_4 (0.378 mmol, 51.5 mg), 4CzIPN (3.00 μmol , 2.4 mg), and (ethene-1,1-diyl)disulfonyl)dibenzene (0.609 mmol, 187.9 mg) in 7 mL of DMF. The crude product was purified to afford (2-cyclohexylethane-1,1-diyl)disulfonyl)dibenzene **4s** (93.7 mg, 76%) as a pale yellow oil. The spectroscopic data are in agreement with those reported in the literature.³³

$^1\text{H NMR}$ (400 MHz, CDCl_3): δ 8.00-7.96 (m, 4H), 7.74-7.68 (m, 2H), 7.63-7.56 (m, 4H), 4.46 (t, $J = 5.6$ Hz, 1H), 2.00 (dd, $J = 6.8$ Hz and 6.4 Hz, 2H), 1.68-1.57 (m, 5H), 1.52-1.44 (m, 1H), 1.21-1.07 (m, 3H), 0.83-0.72 (m, 2H);

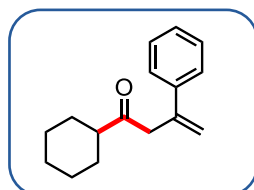
$^{13}\text{C NMR}$ (100 MHz, CDCl_3): δ 137.9 (2C), 134.6 (2C), 129.7 (4C), 129.2 (4C), 81.5, 35.7, 32.7 (2C), 32.6, 26.2, 25.9 (2C).

Methyl 4-cyclohexyl-2-methylene-4-oxobutanoate (7a)

The spectroscopic data are in agreement with those reported in the literature.⁴²

$^1\text{H NMR}$ (400 MHz, CDCl_3): δ 6.32 (d, $J = 1.2$ Hz, 1H), 5.61 (d, $J = 1.2$ Hz, 1H), 3.73 (s, 3H), 3.43 (d, $J = 0.8$ Hz, 2H), 2.47-2.38 (m, 1H), 1.91-1.85 (m, 2H), 1.81-1.76 (m, 2H), 1.69-1.64 (m, 1H), 1.40-1.22 (m, 5H);

$^{13}\text{C NMR}$ (100 MHz, CDCl_3): δ 210.5, 167.0, 134.5, 128.7, 52.2, 50.9, 43.8, 28.6 (2C), 26.0, 25.7 (2C).

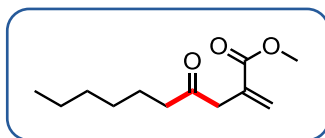
1-Cyclohexyl-3-phenylbut-3-en-1-one (7b)

Following the general procedure with potassium [18-Crown-6] bis(catecholato)-cyclohexylsilicate **1a** (0.303 mmol, 191.3 mg), KH_2PO_4 (0.360 mmol, 49.0 mg), 4CzIPN (3.00 μmol , 2.8 mg), and ((2-phenylallyl)sulfonyl)benzene (0.606 mmol, 156.4 mg) in 7 mL of DMF. The crude product was purified to afford methyl 4-cyclohexyl-2-methylene-4-oxobutanoate **7b** (41.1 mg, 60%) as a colorless oil. The spectroscopic data are in agreement with those reported in the literature.⁴²

^1H NMR (400 MHz, CDCl_3): δ 7.39-7.27 (m, 5H), 5.57 (d, $J = 0.8$ Hz, 1H), 5.16 (d, $J = 0.8$ Hz, 1H), 3.63 (s, 2H), 3.43 (d, $J = 0.8$ Hz, 1H), 1.83-1.71 (m, 5H), 1.38-1.19 (m, 5H);

^{13}C RMN (100 MHz, CDCl_3): δ 211.8, 141.7, 140.3, 128.6 (2C), 127.9, 126.0 (2C), 116.6, 50.0, 48.1, 28.8 (2C), 25.9, 25.8 (2C).

Methyl 2-methylene-4-oxodecanoate (**7c**)



Following the general procedure with potassium [18-Crown-6] bis(catecholato)-*n*-hexylsilicate **1c** (0.288 mmol, 182.3 mg), KH_2PO_4 (0.368 mmol, 50.1 mg), 4CzIPN (3.00 μmol , 2.9 mg), and methyl 2-((phenylsulfonyl)methyl)acrylate (0.608 mmol, 146.0 mg) in 7 mL of DMF. The crude product was purified to afford methyl 2-methylene-4-oxodecanoate **7c** (46 mg, 72%) as a colorless oil.

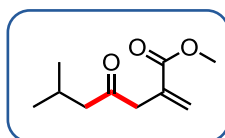
^1H NMR (400 MHz, CDCl_3): δ 6.33 (d, $J = 0.8$ Hz, 1H), 5.63 (d, $J = 0.8$ Hz, 1H), 3.74 (s, 3H), 3.40 (s, 2H), 2.47 (t, $J = 7.2$ Hz, 2H), 1.62-1.53 (m, 2H), 1.32-1.23 (m, 6H), 0.89-0.86 (m, 3H);

^{13}C NMR (100 MHz, CDCl_3): δ 207.5, 166.8, 134.3, 128.6, 52.1, 45.7, 42.7, 31.6, 28.8, 23.7, 22.5, 14.0;

IR (neat): 3422, 2955, 2932, 2856, 1729, 1715, 1636, 1439, 1338, 1307, 1204, 1149, 1069, 950, 817 cm^{-1} ;

HMRS: (ESI) m/z calc for $\text{C}_{12}\text{H}_{20}\text{O}_5$ ($[\text{M}]^+$) 212.1412; found: 212.1420.

Methyl 6-methyl-2-methylene-4-oxoheptanoate (**7d**)



Following the general procedure with potassium [18-Crown-6] bis(catecholato)-isobutylsilicate **1d** (0.301 mmol, 182.3 mg), KH_2PO_4 (0.378 mmol, 51.4 mg), 4CzIPN (3.00 μmol , 2.6 mg), and methyl 2-((phenylsulfonyl)methyl)acrylate (0.605 mmol, 145.4 mg) in 7 mL of DMF. The crude product was purified to afford methyl 6-methyl-2-methylene-4-oxoheptanoate **7d** (28 mg, 51%) as a colorless oil.

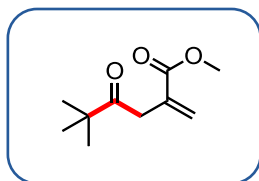
^1H NMR (400 MHz, CDCl_3): δ 6.33 (d, $J = 1.2$ Hz, 1H), 5.63 (d, $J = 1.2$ Hz, 1H), 3.74 (s, 3H), 3.38 (s, 2H), 2.37 (s, 1H), 2.35 (s, 1H), 2.16 (sept, $J = 6.8$ Hz, 1H), 0.93 (s, 3H), 0.92 (s, 3H);

^{13}C NMR (100 MHz, CDCl_3): δ 207.0, 166.8, 134.2, 128.6, 52.0, 51.7, 46.2, 24.5, 22.5 (2C);

IR (neat): 2955, 2871, 1719, 1636, 1466, 1439, 1366, 1337, 1309, 1203, 1150, 951 cm^{-1} ;

HMRS: (ESI) m/z calc for $\text{C}_9\text{H}_{13}\text{O}_2$ ($[\text{M}-\text{OMe}]^+$) 153.0916; found: 153.0925.

Methyl 5,5-dimethyl-2-methylene-4-oxohexanoate (**7e**)



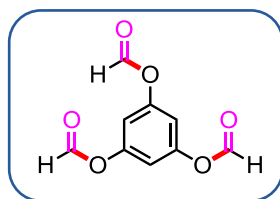
Following the general procedure with tetraethylammonium bis(catecholato)-*ter*-butylsilicate **1e** (0.296 mmol, 127.7 mg), KH_2PO_4 (0.389 mmol, 52.9 mg), 4CzIPN (3.00 μmol , 2.8 mg), and methyl 2-((phenylsulfonyl)methyl)acrylate (0.610 mmol, 146.6 mg) in 7 mL of DMF. The crude product was purified to afford a mixture of methyl 5,5-dimethyl-2-methylene-4-oxohexanoate **7e** (48 mg, 40%) as a colorless oil, and of the non-carbonylated product methyl 4,4-dimethyl-2-methylenepentanoate (59 : 41).

^1H NMR (400 MHz, CDCl_3): δ 6.33 (d, $J = 0.8$ Hz, 1H), 6.17 (d, $J = 0.8$ Hz, 0.7H), 5.59 (d, $J = 1.2$ Hz, 1H), 5.53 (bs, 0.7H), 3.76 (s, 2H), 3.73 (s, 3H), 3.52 (s, 2H), 2.50 (s, 1.5 H), 1.22-1.12 (s, 15.3 H);

^{13}C NMR (100 MHz, CDCl_3): δ 212.4, 167.5, 166.9 (0.7C), 139.4 (0.7C), 134.8, 128.4, 125.6 (0.7C), 60.4, 51.9, 51.8 (0.7C), 44.3 (0.7C), 40.2, 30.8 (0.7C), 26.4 (3C), 21.0 (2.1C).

IR (neat): 2955, 2869, 2850, 1724, 1634, 1439, 1396, 1200, 1144 cm^{-1} ;

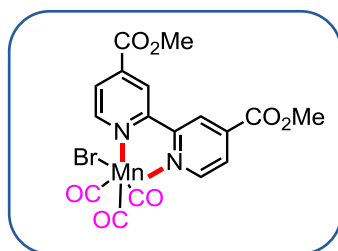
HMRS: (ESI) m/z calc for $\text{C}_9\text{H}_{13}\text{O}_2$ ($[\text{M}-\text{OMe}]^+$) 153.0916; found: 153.0921.

Synthesis of TFBen

$\text{Pd}(\text{PPh}_3)_4$ (0,16 mmol, 184 mg), benzene-1,3,5-triol (8 mmol, 1.001 g) and NaOAc (8 mmol, 656 mg) were put into an oven-dried round bottom flask filled with nitrogen and equipped with a stirring bar. Then Ac_2O (80 mmol, 7.5 mL) and HCOOH (848 mmol, 32 mL) were added. The mixture was stirred at rt for 18 h. Then, the reaction mixture was filtered and concentrated. Purification on a column chromatography (petroleum ether/ Et_2O : 8/2) gave the pure product as a white solid (750mg, 45%).

^1H NMR (400 MHz, CDCl_3) δ 8.27 (s, 3H), 6.99 (s, 3H).

^{13}C NMR (101 MHz, CDCl_3) δ 158.27 (3C), 150.22 (3C), 112.60 (3C).

Synthesis of [Mn]

Manganesepentacarbonyl bromide (500 mg, 1.8 mmol) was added to a suspension of dimethyl-2,2'-bipyridine-4,4'-dicarboxylate (544 mg, 2.0 mmol) in diethyl ether (40 mL). Then, the mixture is stirred at reflux for 3 h in the dark. The resulting precipitate was collected, washed with diethyl ether (3×10 mL) and dried to afford the manganese complex [Mn] as an orange solid (875 mg, 99%). The spectroscopic data are in agreement with those reported in the literature.⁴²

III.2.7. References

- ¹ For selected reviews, see: a) L. Marzo, S. K. Pagire, O. Reiser, B. König, *Angew. Chem. Int. Ed.* **2018**, *57*, 10034; b) J. K. Matsui, S. B. Lang, D. R. Heitz, G. A. Molander, *ACS Catal.* **2017**, *7*, 2563; c) N. A. Romero, D. A. Nicewicz, *Chem. Rev.* **2016**, *116*, 10075; d) S. Poplata, A. Tröster, Y.-Q. Zou, T. Bach, *Chem. Rev.* **2016**, *116*, 9748; e) K. Nakajima, Y. Miyake, Y. Nishibayashi, *Acc. Chem. Res.* **2016**, *49*, 1946; f) D. Ravelli, S. Proti M. Fagnoni, *Chem. Rev.* **2016**, *116*, 9850; g) T. P. Yoon, *Acc. Chem. Res.* **2016**, *49*, 2307; h) J.-R. Chen, X.-Q. Hu, L.-Q. Lu, W.-J. Xiao, *Acc. Chem. Res.* **2016**, *49*, 1911; i) J.-P. Goddard, C. Ollivier, L. Fensterbank, *Acc. Chem. Res.* **2016**, *49*, 1924; j) T. Koike, M. Akita, *Inorg. Chem. Front.* **2014**, *1*, 562; k) C. K. Prier, D. A. Rankic, D. W. C. MacMillan, *Chem. Rev.* **2013**, *113*, 5322; l) J. M. R. Narayanam, C. R. J. Stephenson, *Chem. Soc. Rev.* **2011**, *40*, 102.
- ² For recent books, see: a) *Chemical Photocatalysis*, Eds. B. König, DeGruyter Berlin, **2013**; b) *Photochemically generated intermediates in Synthesis*, Eds A. Albini, M. Fagnoni, Wiley, Hoboken, **2013**; c) *Visible Light Photocatalysis in Organic Chemistry* C. Stephenson, T. Yoon, D. W. C. MacMillan, Eds. Wiley-VCH **2018**.
- ³ a) S. J. MacCarver, J. X. Qiao, J. Carpenter, R. M. Borzirelli, M. A. Poss, M. D. Eastgate, M. M. Miller, D. W. C. MacMillan, *Angew. Chem. Int. Ed.* **2017**, *56*, 728; b) Z. Zuo, H. Cong, W. Li, J. Choi, G. C. Fu, D. W. C. MacMillan, *J. Am. Chem. Soc.* **2016**, *138*, 1832; c) C. C. Nawrat, C. R. Jamison, Y. Slutskyy, D. W. C. MacMillan, L. E. Overman, *J. Am. Chem. Soc.* **2015**, *137*, 11270; d) A. Noble, D. W. C. MacMillan, *J. Am. Chem. Soc.* **2014**, *136*, 11602.
- ⁴ a) T. Koike, M. Akita, *Org. Biomol. Chem.* **2016**, *14*, 6886; b) Y. Li, K. Miyazawa, T. Koike, M. Akita, *Org. Chem. Front.* **2015**, *2*, 319; c) Y. Yasu, T. Koike, M. Akita, *Adv. Synth. Catal.*, **2012**, *354*, 3414.
- ⁵ T. Knauber, R. Chandrasekaran, J. W. Tucker, J. M. Chen, M. Reese, D. A. Rankic, N. Sach, C. Helal, *Org. Lett.* **2017**, *19*, 6566.
- ⁶ C. L. Frye, *J. Am. Chem. Soc.* **1964**, *86*, 3170.
- ⁷ a) L. Chenneberg, C. Lévêque, V. Corcé, A. Baralle, J.-P. Goddard, C. Ollivier, L. Fensterbank, *Synlett* **2016**, *27*, 731; b) C. Lévêque, L. Chenneberg, V. Corcé, C. Ollivier, L. Fensterbank, *Chem. Commun.* **2016**, *52*, 9877; c) V. Corcé, L.-M. Chamoreau, E. Derat, J.-P. Goddard, C. Ollivier, L. Fensterbank, *Angew. Chem. Int. Ed.* **2015**, *54*, 11414.
- ⁸ M. Jouffroy, D. N. Primer, G. A. Molander, *J. Am. Chem. Soc.* **2016**, *138*, 475.
- ⁹ a) K. D. Raynor, G. D. May, U. K. Bandarage, M. J. Boyd, *J. Org. Chem.* **2018**, *83*, 1551; b) T. Guo, X. Liu, Y. Fang, X. Jin, Y. Yang, Y. Li, B. Chen, M. Ouyang, *Adv. Synth. Catal.* **2018**, *360*, 1.
- ¹⁰ For recent examples of reactions using 4CzIPN as photocatalyst, see: a) X. Wentao, J. Ma, X.-A. Yuan, J. Dai, J. Xie, C. Zhu, *Angew. Chem. Int. Ed.* **2018**, *57*, 10357; b) F. L. Vaillant, M. Garreau, S. Nicolai, G. Gryn'ova, C. Corminboeuf, J. Waser, *Chem. Sci.* **2018**, *9*, 5883; c) R. Zhou, Y. Y. Goh, H. Liu, H. Tao, L. Li, J. Wu, *Angew. Chem. Int. Ed.* **2017**, *56*, 16621; d) H. Huang, X. Li, C. Yu, Y. Zhang, P. S. Mariano, W. Wang, *Angew. Chem. Int. Ed.* **2017**, *56*, 1500; e) H. Huang, C. Yu, Y. Zhang, Y. Zhang, P. S. Mariano, W. Wang, *J. Am. Chem. Soc.* **2017**, *139*, 9799; f) B. A. Vara, M. Jouffroy, G. A. Molander, *Chem. Sci.* **2017**, *8*, 530.
- ¹¹ N. R. Patel, C. B. Kelly, A. P. Siegenfeld, G. A. Molander, *ACS Catal.* **2017**, *7*, 1766.
- ¹² For selected books and reviews, see: a) A. P. Taylor, R. P. Robinson, Y. M. Fobian, D. C. Blakemore, L. H. Jones, O. Fadeyi, *Org. Biomol. Chem.* **2016**, *14*, 6611; b) R. C. Cioc, E. Ruijter, R. V. A. Orru, *Green Chem.* **2014**, *16*, 2958; c) V. Liautard, Y. Landais, in

- Multicomponent Reactions*, Eds. Zhu, J., Wang, Q., Wang, M. X., Wiley, 2nd Edition, **2014**, 401; d) A. Dömling, W. Wang, K. Wang, *Chem. Rev.* **2012**, *116*, 3083; e) C. de Graff, E. Ruijter, V. A. Orru, *Chem. Soc. Rev.* **2012**, *41*, 3969; f) H. Pellissier, *Adv. Synth. Catal.* **2012**, *354*, 237; h) B. B. Touré, D. G. Hall, *Chem. Rev.* **2009**, *109*, 4439; i) B. Ganem, *Acc. Chem. Res.* **2009**, *42*, 463; k) M. Tojino, I. Ryu in *Multicomponent Reaction* Eds. J. Zhu, H. Bienaymé, Wiley-VCH, Weinheim, **2005**, 169.
- ¹³ For reviews on radical carbonylation, see: a) I. Ryu, Y. Uenoyama, H. Matsubara, *Bull. Chem. Soc. Jpn.* **2006**, *79*, 1476; b) I. Ryu, *Chem. Rec.* **2002**, *2*, 249; c) I. Ryu, *Chem. Soc. Rev.* **2001**, *30*, 16; d) I. Ryu, N. Sonoda, D. P. Curran, *Chem. Rev.* **1996**, *96*, 177; e) I. Ryu, N. Sonoda, *Angew. Chem. Int. Ed. Engl.* **1996**, *35*, 1050.
- ¹⁴ For a review on acyl radicals, see: C. Chatgililoglu, D. Crich, M. Komatsu, I. Ryu, *Chem. Rev.* **1999**, *99*, 1991.
- ¹⁵ (a) H. Matsubara, T. Kawamoto, T. Fukuyama, I. Ryu, *Acc. Chem. Res.* **2018**, *51*, 2023; (b) S. Sumino, A. Fusano, T. Fukuyama, I. Ryu, *Acc. Chem. Res.* **2014**, *47*, 1563. Also see some recent work of radical carbonylation: (c) T. Kawamoto, A. Sato, I. Ryu, *Chem. Eur. J.* **2015**, *21*, 14764; (d) S. Sumino, T. Ui, Y. Hamada, T. Fukuyama, I. Ryu, *Org. Lett.*, **2015**, *17*, 4952; (e) T. Kippo, K. Hamaoka, I. Ryu, *J. Am. Chem. Soc.* **2013**, *135*, 632; (f) T. Fukuyama, N. Nakashima, T. Okada, I. Ryu, *J. Am. Chem. Soc.* **2013**, *135*, 1006.
- ¹⁶ a) L. Gu, C. Jin, L. Jiyan, *GreenChem* **2015**, *17*, 3733; b) M. Majek, A. Jacobi von Wangelin, *Angew. Chem. Int. Ed.* **2015**, *54*, 2270.
- ¹⁷ W. Guo, L.-Q. Lu, Y. Wang, Y.-N. Wang, J.-R. Chen, W.-J. Xiao, *Angew. Chem. Int. Ed.* **2015**, *54*, 2265.
- ¹⁸ For flow version of an annulative carbonylation process, see: N. Micic, A. Polyzos, *Org. Lett.* **2018**, *20*, 4663.
- ¹⁹ a) I. Ryu, T. Niguma, S. Minakata, M. Komatsu, Z. Luo, D. P. Curran, *Tetrahedron Lett.* **1999**, *40*, 2367; b) I. Ryu, H. Yamazaki, K. Kusano, A. Ogawa, N. Sonoda, *J. Am. Chem. Soc.* **1991**, *113*, 8558.
- ²⁰ a) I. Ryu, K. Nagahara, A. Kurihara, M. Komatsu, N. Sonoda, *J. Organomet. Chem.* **1997**, *548*, 105; b) I. Ryu, M. Hasegawa, A. Kurihara, A. Ogawa, S. Tsunoi, N. Sonoda, *Synlett* **1993**, *2*, 143.
- For a review on TTMS, see: c) C. Chatgililoglu, C. Ferreri, Y. Landais, V. I. Timokhin, *Chem. Rev.* **2018**, *118*, 6516.
- ²¹ For decatungstate ion catalyzed C-H carbonylation, see: (a) M. Okada, T. Fukuyama, K. Yamada, I. Ryu, D. Ravelli, M. Fagnoni, *Chem. Sci.* **2014**, *5*, 2893; I. Ryu, A. Tani, T. Fukuyama, D. Ravelli, S. Montanaro, M. Fagnoni, *Org. Lett.* **2013**, *15*, 2554; (c) I. Ryu, A. Tani, T. Fukuyama, D. Ravelli, M. Fagnoni, A. Albini, *Angew. Chem. Int. Ed.* **2011**, *50*, 1869.
- ²² For selected recent examples of unsymmetrical ketones synthesis, see: a) M. Zhang, J. Xie, C. Zhu, *Nat. Commun.* **2018**, *9*, 3517; b) L. Anthore-Dalion, Q. Liu, S. Z. Zard, *J. Am. Chem. Soc.* **2016**, *138*, 8404; c) W. S. Bechara, G. Pelletier, A. B. Charette, *Nat. Chem.* **2012**, *4*, 228.
- ²³ H. Uoyama, K. Goushi, K. Shizu, H. Nomura, C. Adachi, *Nature* **2012**, *492*, 234.
- ²⁴ a) J. Luo, J. Zhang, *ACS Catal.* **2016**, *6*, 873; For a reevaluation of the reduction and oxidation potentials of the excited state of 4CzIPN, see 10f.
- ²⁵ For the rate constants of addition of primary radicals on CO (k_{CO}), see: a) K. Nagahara, I. Ryu, N. Kambe, M. Komatsu, N. Sonoda, *J. Org. Chem.* **1995**, *60*, 7384. Based on the ratio of observed products $3j:3j'$, we have $k_{cycl} = k_{CO}[CO] = 2 \times 10^5 \text{ s}^{-1}$. For the rate of the 5-exo-trig cyclization, see: b) C. Chatgililoglu, K. U. Ingold, J. C. Scaiano, *J. Am. Chem. Soc.* **1981**, *103*, 7739.

- ²⁶ a) *Organic Synthesis: The Disconnection Approach, second edition*, Eds S. Warren, P. Wyatt, John Wiley and Sons, **2011**. b) For a discussion of this, see: D. Kaldre, I. Klose, N. Maulide, *Science* **2018**, *361*, 664.
- ²⁷ J. P. Phelan, S. B. Lang, J. S. Compton, C. B. Kelly, R. Dykstra, O. Gutierrez, G. A. Molander, *J. Am. Chem. Soc.* **2018**, *140*, 8037.
- ²⁸ For practical reasons, the “light/dark” experiment was conducted without CO. We assumed that with or without CO, the reaction follows the same kind of photoredox catalyzed mechanism. However, a radical chain mechanism involving SET between intermediate **C** and silicate **1** cannot be discarded just from this single experiment, see: M. A. Cismesia, T. P. Yoon, *Chem. Sci.* **2015**, *6*, 5426.
- ²⁹ a) D. Barnes-Seeman, C. Boisselle, C. Capacci-Daniel, R. Chopra, K; Hoffmaster, C. T. Jones, M. Kato, K. Lin, S. Ma, G. Pan, L. Shu, J. Wang, L. Whiteman, M. Xu, R. Zheng, J. Fu, *Bioorg. Med. Chem. Lett.* **2014**, *24*, 3979; b) B. D. Roth, D. F. Ortwine, M. L. Hoefle, C. D. Stratton, D. R. Sliskovic, M. W. Wilson, R. S. Newton, *J. Med. Chem.* **1990**, *33*, 21.
- ³⁰ a) S. D. Friis, A. T. Lindhardt, T. Skydstrup, *Acc. Chem. Res.* **2016**, *49*, 594; K. T. Neumann, S. Klimczyk, M. N. Burhardt, B. Bang-Andersen, T. Skydstrup, A. T. Lindhardt, *ACS Catal.* **2016**, *6*, 4710.
- ³¹ D. Hanss, J. C. Freys, G. Bernardinelli, O. S. Wenger, *Eur. J. Inorg. Chem.* **2009**, 4850.
- ³² M. S. Lowry, J. I. Goldsmith, J. D. Slinker, R. Rohl, R. A. Pascal, G. G. Malliaras, S. Bernhard, *Chem. Mater.* **2005**, *17*, 5712
- ³³ V. Corcé, L.-M. Chamoreau, E. Derat, J.-P. Goddard, C. Ollivier, L. Fensterbank, *Angew. Chem. Int. Ed.* **2015**, *54*, 11414.
- ³⁴ M. A. Cismesia, T. P. Yoon, *Chem. Sci.* **2015**, *6*, 5426.
- ³⁵ C. G. Hatchard, C. A. Parker, C. A. *Proc. Roy. Soc. (London)* **1956**, A235, 518.
- ³⁶ a) H. J. Kuhn, S. E. Braslavsky, R. Schmidt, *Pure Appl. Chem.* **2004**, *76*, 2105; b) M. Monalti *et. al.* Chemical Actinometry. *Handbook of Photochemistry*, 3rd Ed. Taylor & Francis Group, LLC. Boca Raton, FL, **2006**, 601–616.
- ³⁷ V. Chudasama, R. J. Fitzmaurice, S. Caddick, *Nat. Chem.* **2010**, *2*, 592.
- ³⁸ A. Albin, D. Ravelli, T. Fukuyama, T. Akihiro, M. Fagnoni, I. Ryu, *Angew. Chem.*, **2011**, *50*, 1869.
- ³⁹ L. Capaldo, R. Riccardi, D. Ravelli, M. Fagnoni, *ACS. Catal.* **2018**, *8*, 304.
- ⁴⁰ S. Espoti, D. Dondi, M. Fagnoni, A. Albin, *Angew. Chem. Int. Ed* **2007**, *46*, 2531.
- ⁴¹ S. Sonoda, H. Yamazaki, K. Kusano, I. Ryu, *J. Org. Chem.* **1991**, *56*, 5003.
- ⁴² T. Kippo, Y. Kimura, M. Ueda, T. Fukuyama, I. Ryu, *Synlett* **2017**, *28*, 1733.

III.3. Synthesis of Aliphatic Amides through a Photoredox Catalyzed Radical Carbonylation Involving Organosilicates as Alkyl Radical Precursors

Published in *Adv. Synth. Catal.* **2020**, *362*, 2254

III.3.1. Abstract

Alkyl radicals, from primary to tertiary, formed by photocatalyzed oxidation of organosilicates, are involved efficiently in radical carbonylation with carbon monoxide (CO), in the presence of various amines and CCl₄, leading to a variety of amides in moderate to good yields.

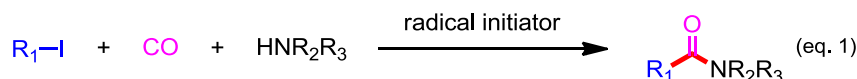
III.3.2. Introduction

Visible-light photoredox catalysis has changed the scene of radical chemistry^{1,2} by notably involving new reactants. Among them, a class of relatively low oxidation potential of alkyl (bis)catecholatosilicates³ have recently proven to be efficient radical precursors, as shown by some of us⁴ and Molander⁵ as well as other groups.⁶ They are interesting for their ease of synthesis from the corresponding alkoxy silane or trichlorosilane and for their ability to generate unstabilized primary alkyl radicals, under photoredox-catalyzed conditions, whether in the presence of classical Ru(II) or Ir(III) photocatalysts or even with an organic dye.^[4a-c] The nucleophilic radicals thus formed can be readily engaged in C-C bond formation by addition to various species such as activated alkenes,^{4d} allylsulfones,^{4d} imines⁷ or recently heteroarenes⁸ and N-acylhydrazones⁹ or by nickel catalyzed cross-coupling reactions.^[4d,5,6a,6c]

Multicomponent radical reactions have great potential in organic synthesis,¹⁰ in which carbon monoxide (CO) can be incorporated to install a carbonyl function through the formation of acyl radical intermediates.^{11,12} Recently, we reported a photoredox catalyzed carbonylation of alkyl (bis)catecholatosilicates by using 1,2,3,5-tetrakis(carbazol-9-yl)-4,6-dicyano-benzene (4CzIPN) as photocatalyst and in the presence of alkenes and allylsulfones which leads to a variety of functionalized ketones and represents one of the first radical carbonylation under a photooxidative regime.¹³ Aiming at extending this process to trivalent derivatives, we examined the possibility to develop a new synthesis of aliphatic amides. Carbonylative synthesis of aliphatic amides has been achieved by radical/ionic or radical/transition metal hybrid carbonylation of alkyl iodides (**Scheme 1**, eq 1).^{14,15} Based on the known halogenation of acyl radicals by homolytic substitution, we surmised that adding a chlorinating agent like CCl₄ could *in situ* generate acyl chlorides which would then react with an amine to lead to amides (**Scheme 1**, eq 2).¹⁶ We herein report that various aliphatic amides could indeed be synthesized from alkylsilicates under mild visible-light irradiation in metal-free conditions using 4CzIPN photocatalyst and carbon tetrachloride as a mediator.

Previous Works:

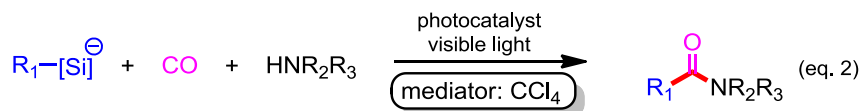
Synthesis of Aliphatic Amides *via* Atom Transfer Carbonylation of Alkyl Iodides¹³



R_1 = alkyl; R_2, R_3 = H, alkyl, aryl

This Work:

Synthesis of Aliphatic Amides *via* Photoredox Catalyzed Carbonylation of Alkyl Silicates

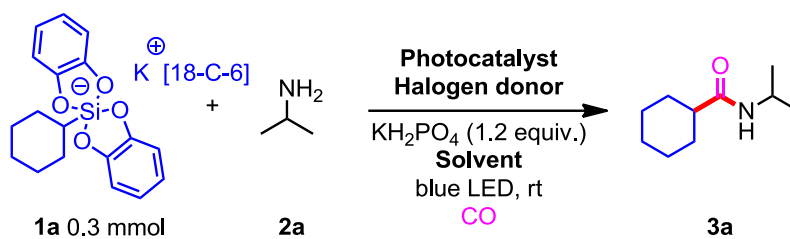


R_1 = alkyl; R_2, R_3 = H, alkyl, aryl

Scheme 1: Previous and present concepts for synthesis of aliphatic amides based on radical carbonylation

III.3.3. Results and Discussion

We chose to test the desired formation of amide using cyclohexyl bis(cathecolato)silicate **1a** in the presence of isopropylamine **2a**, CO, and 4CzIPN as photocatalyst in a series of model experiments. The latter were carried out in a stainless-steel autoclave equipped with two quartz glass windows that serve as a pressure-durable apparatus during light irradiation (15 W blue LED, see Supporting Information for details). The results are summarized in **Table 1**. Our first attempt consisted of the irradiation of **1a**, **2a**, 4CzIPN (1 mol%) and KH_2PO_4 (1.2 equiv.) in DMF under a CO pressure of 80 atm during 24 h. While expected amide **3a** was obtained in less than 5% (**Table 1**, entry 1), a significant improvement of the yield of **2a** up to 24% was observed in the presence of CCl_4 , which would work as chlorine atom donor and mediator of the reaction (**Table 1**, entry 2).¹⁷ The reaction using $[\text{Ir}(\text{dF}(\text{CF}_3)\text{ppy})_2(\text{bpy})](\text{PF}_6)$ as photocatalyst gave **3a** in 15% yield (**Table 1**, entry 3). When the reaction was carried out under a lower CO pressure (40 atm), the yield was decreased to 20% (**Table 1**, entry 4). The use of the less nucleophilic solvent THF instead of DMF improved the yield of **3a** to 51% (**Table 1**, entry 5). To our delight, with a longer reaction time of 48 h, we were able to obtain the product **3a** in 81% yield (**Table 1**, entry 6). CBrCl_3 , a bromine atom donor, was also found to work (**Table 1**, entry 7) but remained less efficient than CCl_4 . Although KH_2PO_4 is not required for the reaction to occur, it was found to increase significantly the yield of the reaction (**Table 1**, entry 8). ^1H NMR data also shown that the reaction is cleaner in the presence of KH_2PO_4 , avoiding the formation of small amounts of undesired by-products.



Entry	Catalyst	Donor	Solvent	CO (atm)	Time (h)	Yield $\text{3a}^{[b]}$
1	4CzIPN	none	DMF	80	24	< 5%
2	4CzIPN	CCl_4	DMF	80	24	24%
3	$[\text{Ir}]^{[c]}$	CCl_4	DMF	80	24	15%
4	4CzIPN	CCl_4	DMF	40	24	20%
5	4CzIPN	CCl_4	THF	80	24	51%
6	4CzIPN	CCl_4	THF	80	48	81% ^[d]
7	4CzIPN	CBrCl_3	THF	80	48	75%
8	4CzIPN	CCl_4	THF	80	48	52% ^[e]

^[a] Conditions: potassium [18-Crown-6] bis(catecholato)-cyclohexylsilicate (**1a**, 0.3 mmol, 1 equiv.), isopropylamine (**2a**, 2 equiv.), photocatalyst (1 mol%), KH_2PO_4 (1.2 equiv.), CO (40-80 atm), solvent (7 mL), irradiation by blue LED lamp (425 nm) for 24-48 h; ^[b] Determined by ^1H NMR using acetanilide as an internal standard;

^[c] $[\text{Ir}(\text{dF}(\text{CF}_3)\text{ppy})_2(\text{bpy})](\text{PF}_6)$; ^[d] Isolated yield; ^[e] Without KH_2PO_4 .

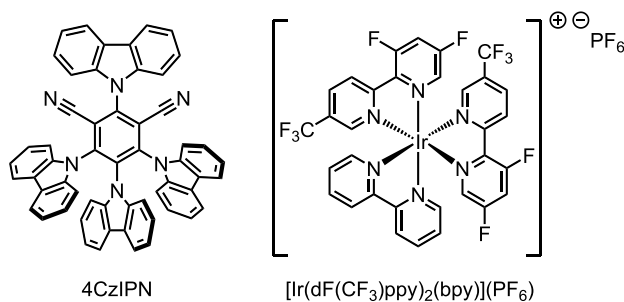
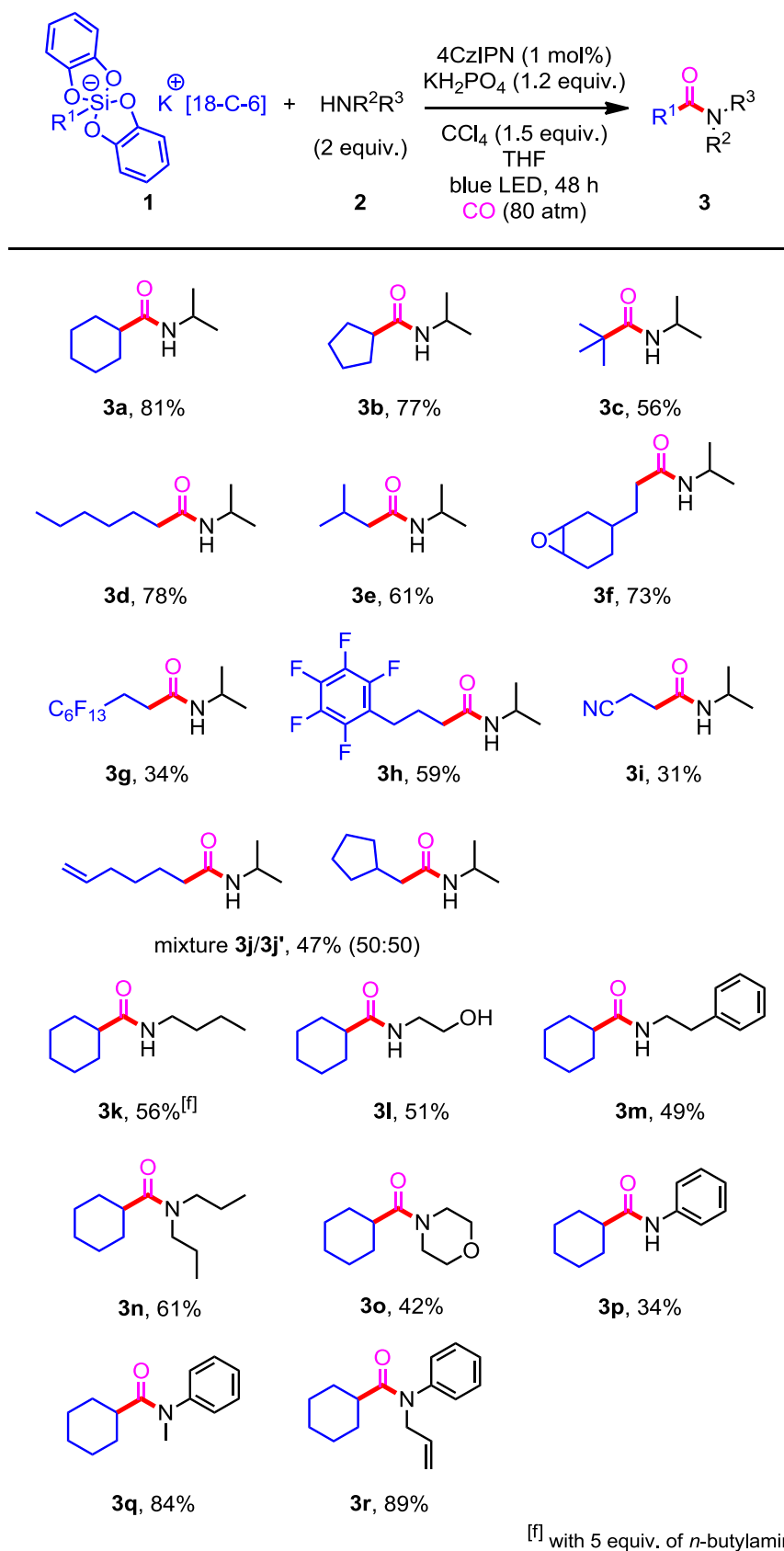


Table 1: Optimization of the reaction conditions^[a]

These promising results in hands, we applied this protocol to a series of alkyl bis(catecholato)silicates **1** and results are summarized in **Scheme 2**. Similar to cyclohexyl silicate **1a**, cyclopentyl silicate **1b**, gave the corresponding amide **3b** in 77% yield.

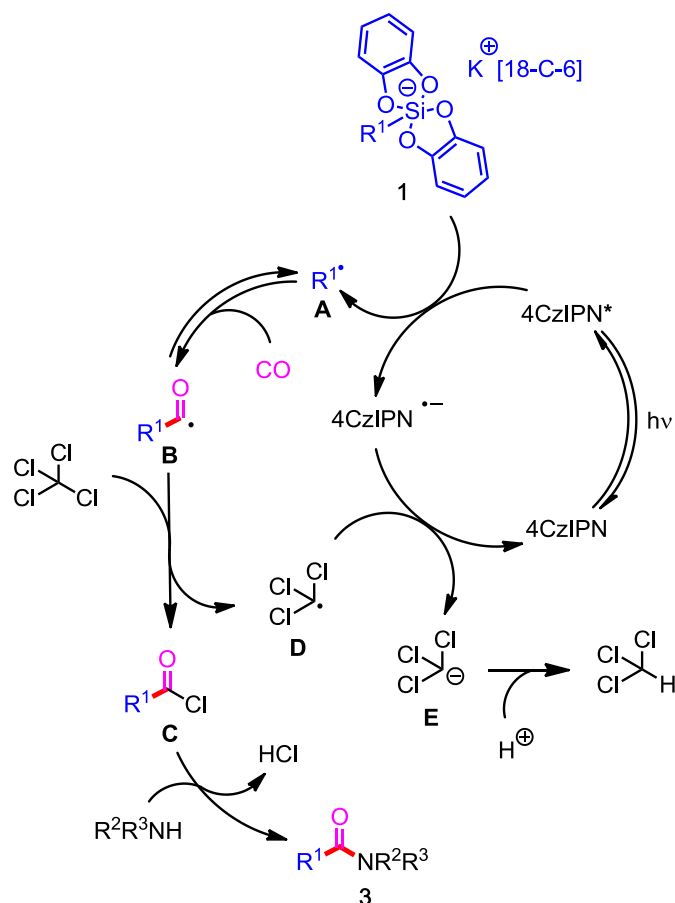
**Scheme 2:** Scope of the multicomponent reaction leading to amides **3**

Even the highly hindered *tert*-butyl silicate **1c** gave the corresponding amide **3c** in a satisfactory yield of 56%. The reaction of primary alkyl silicates **1d** and **1e** gave **3d** and **3e** in 78% and 61% yield, respectively. Knowing from these results that primary, secondary, and tertiary alkyl silicates worked well for this reaction, we next focused on the compatibility of various functional groups toward this process. The reaction of **1f**, bearing a sensitive epoxy ring was well tolerated and delivered a good yield of the corresponding amide **3f** (73%). A propyl silicate substituted by a pentafluorobenzene ring **1h** furnished the corresponding amide **3h** in 59% yield while perfluorohexyl-substituted ethyl silicate **1g** also gave the corresponding amide, albeit in low yield (34%). The amide product **3i**, bearing a nitrile functionality, was also obtained in low yield (31%). When the reaction of 5-hexenyl silicate **1j** was tested, an equimolar mixture of amides, uncyclized **3j** and cyclized **3j'**, were obtained in 47% total yield, which is consistent with our previous report on ketone synthesis.¹³

We then investigated the viability of a larger scope of nucleophile amines in this carbonylative amide synthesis. The results are also summarized in **Scheme 2**. The reaction of **1a** with the primary amine *n*-butylamine provided the desired amide **3k** in 36% yield and no double acylation was observed. This yield could be increased to 56% by using 5 equiv. of *n*-butylamine. In the case of 2-aminoethanol as nucleophile, amide **3l** was obtained in 51% yield as the sole product. Of note, no addition of the less nucleophilic alcohol to form the corresponding ester was observed. Amide **3m** was obtained in 49% yield from **1a** and 2-phenylethylamine. We also checked if the reaction could occur when using a secondary amine. The reaction of di-*n*-propylamine with cyclohexylsilicate **1a** furnished amide **3n** in good yield (61%). More modest yields were obtained from morpholine (**3o**, 42%) and aniline (**3p**, 34%). Interestingly, however, the yield was substantially increased up to 84% of desired amide **3q** when the more nucleophilic *N*-methylaniline was used instead. In the case of the *N*-allyl-substituted aniline, the reaction was even more successful, leading to amide **3r** in an excellent yield of 89%.

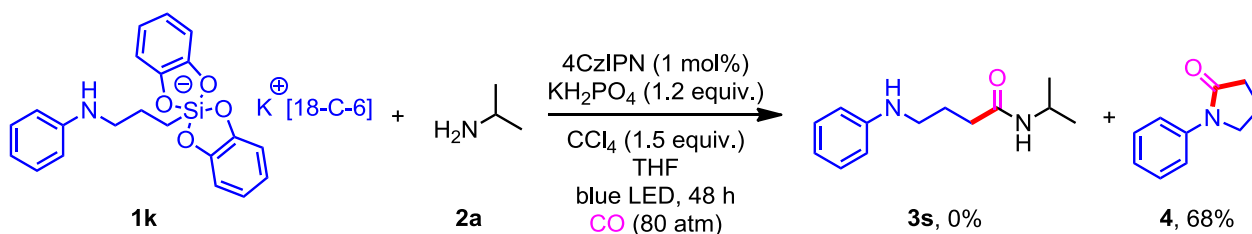
Based on our previous study¹³ and literature reports,^[12,16] a plausible mechanism is proposed on **Scheme 3**. The preliminary step is the excitation of the photocatalyst 4CzIPN by blue LED light. 4CzIPN*¹⁷ has a long lifetime at the excited state (5.1 μ s) and is also a very good oxidant ($E_{1/2}(4CzIPN^*/[4CzIPN]^{* -}) = +1.59$ V vs. SCE),¹⁸ which allows efficient single electron transfer from organosilicates ($E^{ox} < +1$ V vs. SCE)^{4b,19,20} to generate the reduced dye [4CzIPN]^{* -} and, after homolytic cleavage of the Si-C bond, the radical intermediate **A**.^[4-8] C-centered radical **A** would react with CO to form the corresponding acyl radical **B**, which after chlorine abstraction from CCl₄, generates acyl chloride **C** (detected by ¹H NMR and in accordance with the literature²⁰) *in situ* and radical intermediate **D**. An acyl chloride of type **C** was detected by ¹H NMR in the crude product of a reaction using *n*-hexyl silicate **1d** and conducted in the regular conditions except no amine was present.²¹

Acyl chloride **C** is then trapped by the amine to form the desired amide **3**. Furthermore, ¹H NMR monitoring of the crude mixture showed a chloroform peak suggesting us that [4CzIPN]^{* -} reduces radical **D** to its anionic form **E**, allowing as well the regeneration of the photocatalyst 4CzIPN in its ground state, and **E** would be protonated by KH₂PO₄ or by the protonated amide to form chloroform as by-product.



Scheme 3: Proposed mechanism

We then applied the present protocol to study the inter- vs. intramolecular competition in the amide formation. Interestingly, when we used aniline bearing silicate **1k** in the presence of 2 equiv. of isopropylamine **2a**, the intramolecular reaction occurred preferentially and only the pyrrolidinone **4** was obtained in 68% yield (**Scheme 4**).



Scheme 4: Synthesis of *N*-phenyl- γ -butyrolactam **4** from 3-(phenylamino)propane silicate **1k**

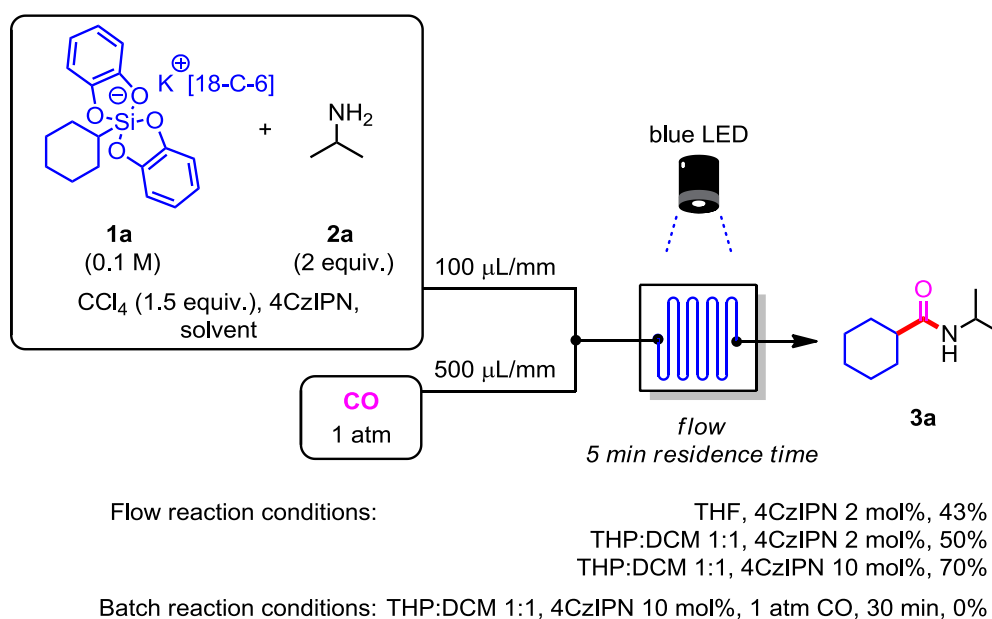
III.3.4. Conclusion

In summary, we have achieved a metal-free synthesis of aliphatic amides from a photoredox-catalyzed radical carbonylation of alkylsilicates with CO in the presence amines, in which CCl₄ works as excellent mediator. Thanks to the use of a wide range of alkyl bis(catecholato)silicates and amines, a large scope of aliphatic amides could be obtained in a multicomponent process. We are now examining the feasibility of the formation of other acyl derivatives under photooxidative regimes as well as other multicomponent reactions.

III.3.5. Additional results

III.3.5.1. Amide formation under flow regimes

Another potentially valuable extension of this reaction focuses on the development of a flow version of the amide synthesis. We notably aimed at reducing the CO pressure and shortening the reaction time.^{22,23} We tested the reaction of **1a** with **2a** and CO under flow conditions, in which we used a FEP tubing (1/16" tubing, inner diameter 0.79 mm) as the flow photoreactor. To our delight, after extensive screening, we devised a satisfactory protocol (**Scheme 5**). Thus, the reaction of **1a** with **2a** in the presence of 10 mol% 4CzIPN in THP (tetrahydropyran)/CH₂Cl₂ proceeded within 5 min residence time and gave 70% yield of **3a** (**Scheme 5**, see Supporting Information for optimization details). The use of 1 atm of CO with a shorter reaction time still gave a better yield compared to the batch conditions (after 30 min, under 1 CO atm atmosphere, no formation of the amide **3a** could be observed). This confirmed the interest of this approach for conducting this type of reactions. Presumably, an improved photon capture is at work in the flow process. It is worth noting that addition of KH₂PO₄ was not mandatory under these conditions. Further work is currently ongoing in our laboratory to extend the scope of this reaction.

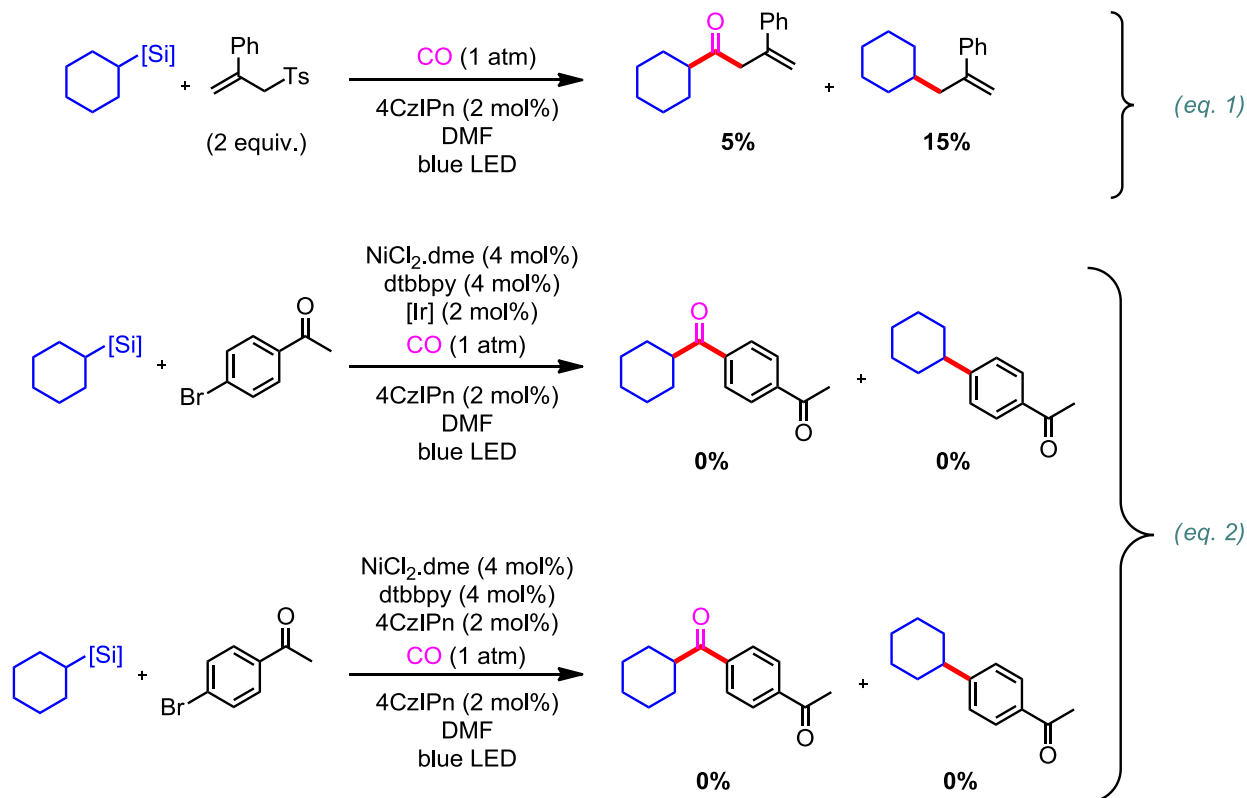


Scheme 5: Micro-flow reaction conditions

III.3.5.2. Carbonylation reactions under flow regimes

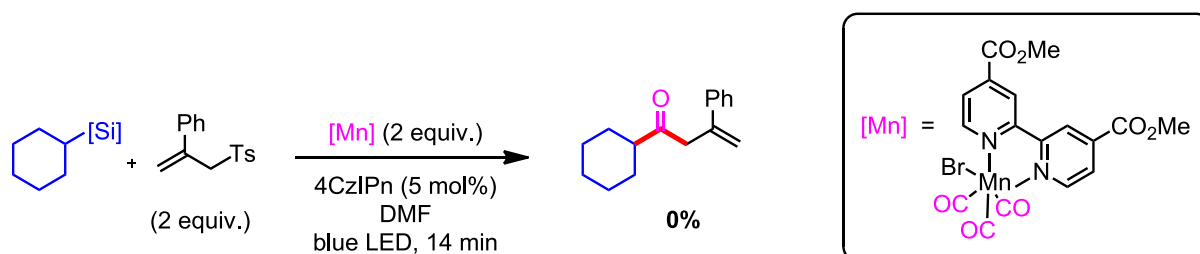
Encouraged by this result, other carbonylation reactions were performed under flow conditions (**Scheme 6**). The carbonylation reaction followed by a direct trapping by an allylsulfone led to a mixture of carbonylated and non-carbonylated products (**Scheme 6, eq. 1**). However, the yield for both of them remained very low. This could probably be due to a too

short residence time. Dual catalysis experiments using $\text{NiCl}_2\cdot\text{dme}$ and a photocatalyst ($[\text{Ir}]$ or 4CzIPN) were also performed but, similarly to the batch reaction, no product was obtained (**Scheme 6, eq. 2**). No carbonylated and non-carbonylated product was observed. The reaction seemed to be, once again, poisoned by the presence of CO .



Scheme 6: Extension of the flow reactions

In situ CO generation was also performed under flow conditions with 1-methyl-4-((2-phenylallyl)sulfonyl)benzene, cyclohexyl silicate and the blue LED sensitive manganese complex ($[\text{Mn}]$) but also without success (**Scheme 7**).



Scheme 7: *In situ* CO generation for carbonylation reaction under flow conditions

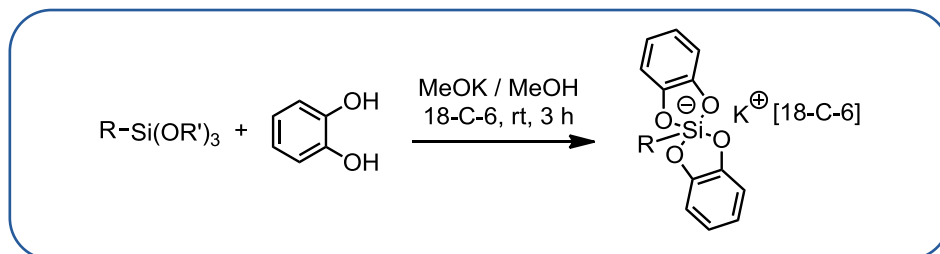
III.3.6. Supporting Information

III.3.6.1. General informations

Photoinduced reactions were carried out using a 425 nm Twin LED light lamp (RelyOn Ltd.). ^1H NMR spectra were recorded with Varian MR400 (400 MHz) and JEOL ECS-400 (400 MHz) spectrometers in CDCl_3 and are referenced at 7.26 ppm for CHCl_3 . ^{13}C NMR spectra were recorded with Varian MR400 (100 MHz) and JEOL ECS-400 (100 MHz) spectrometers in CDCl_3 and are referenced at 77.00 ppm for CDCl_3 . Chemical shifts are reported in parts per million (δ) and coupling constants (J) are given in Hertz (Hz). Splitting patterns are indicated as follows: b, broad; s, singlet; d, doublet; t, triplet; q, quartet; quint, quintet; sex, sextet; sept, septet; m, multiplet. Infrared spectra were obtained on a JASCO FT/IR-4100 spectrometer; absorptions were reported in reciprocal centimeters. Both conventional and high-resolution mass spectra were recorded with a JEOL MS-700 spectrometer. The products were purified by flash column chromatography on silica gel (Kanto Chem. Co. Silica Gel 60N (spherical, neutral, 40-50 μm)). Catechol purified by crystallization from toluene. Unless otherwise specified, all commercially available reagents were used as received. Photocatalysts were synthesized as described.^{24,25} Silicates **1a** to **1k** were synthesized as described.²⁴

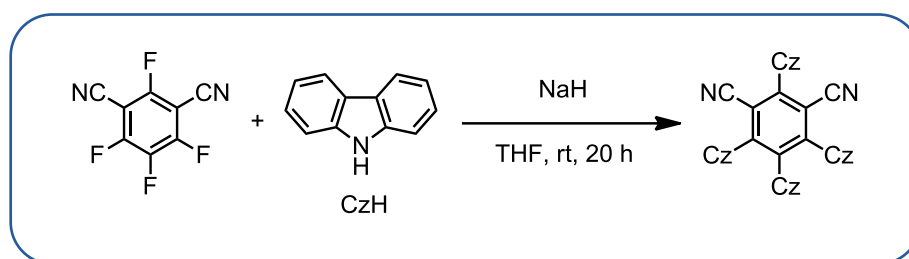
III.3.6.2. General procedures

a) Synthesis of silicates



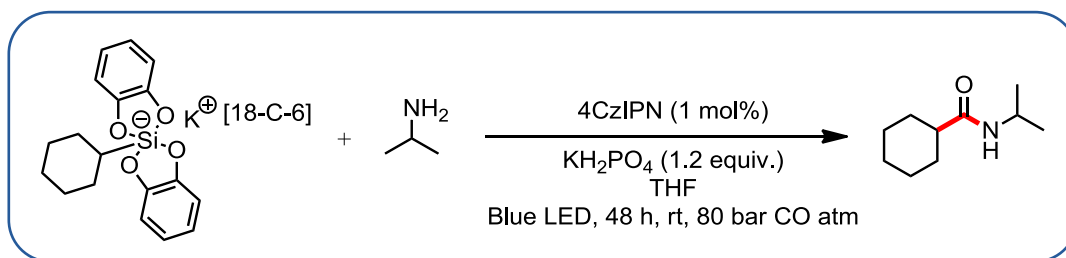
To a stirred solution of catechol (2 equiv.) in dry methanol (0.25 M) was added 18-C-6 (1 equiv.). After dissolution of the crown ether, the trialkoxy organosilane (1 equiv.) was added, followed by a solution of potassium methoxide in methanol (1 equiv.). The reaction mixture was stirred for 3 hours and the solvent was removed under reduced pressure. The residue was dissolved in the minimum volume of acetone and diethyl ether was added until a cloudy solution was obtained (scrapping on the edge of the flask could be done to induce crystallization). The flask was placed at -20°C overnight. The crystals were collected by filtration, washed with diethyl ether and dried under vacuum to afford potassium [18-Crown-6] silicate.

b) Synthesis of 4CzIPN



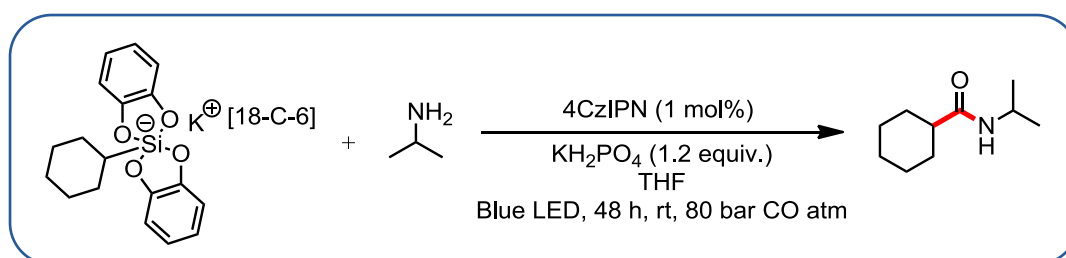
The 4CzIPN has been synthesized following a previous reported procedure.¹ To a 100 mL flask was added NaH (60% in mineral oil) (15.0 mmol, 606 mg) in THF (40 mL). Carbazole (10.0 mmol, 1.68 g) was added slowly to the mixture. After 30 min of stirring at room temperature the tetrafluoroisophthalonitrile (2.00 mmol, 406 mg) was added and the mixture was stirred at room temperature for 20 hours. A brown/yellow precipitate progressively appeared. The solid was successively washed with water and ethanol. The crude product was dissolved in the minimum of CH_2Cl_2 and crystallized by addition of hexane to give 4CzIPN as a yellow solid (1.17 g, 74% yield). The spectroscopic data are in agreement with those reported in the literature.²⁴

c) Photoredox-catalyzed radical carbonylation of silicates with amines:
example of cyclohexylsilicate with isopropylamine



In a stainless-steel autoclave was added potassium [18-crown-6] bis(catecholato)-cyclohexylsilicate **1a** (0.301 mmol, 189.7 mg), KH_2PO_4 (0.370 mmol, 50.4 mg) and 4CzIPN (1mol%, 0.003 mmol, 2.5 mg). THF was added (14 mL), followed by isopropylamine (0.595 mmol, 51 μL) and carbontetrachloride (0.455 mmol, 44 μL). The autoclave was flushed 3 times under CO atmosphere and the reaction mixture was irradiated with blue LEDs (425 nm) under 80 bar CO pressure at r.t. during 48 h. The reaction was diluted with diethyl ether (50 mL), washed with an aqueous saturated K_2CO_3 solution (20 mL x 2 times), water (20 mL x 2 times), dried over MgSO_4 and evaporated under reduced pressure. The crude product was purified to afford *N*-isopropylcyclohexanecarboxamide **3a** (41.6 mg, 82%) as a yellow solid. The spectroscopic data are in agreement with those reported in the literature.²⁶

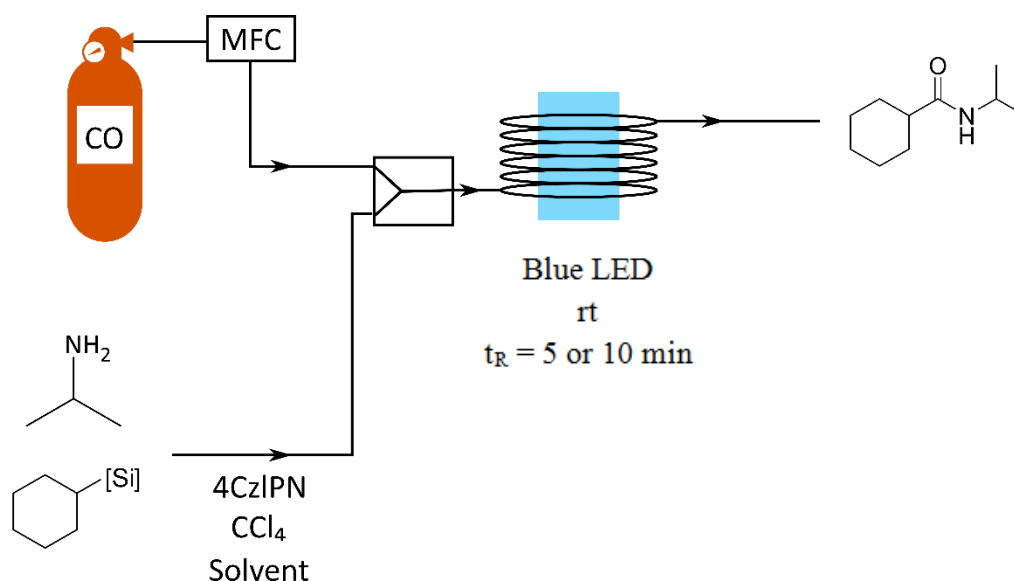
III.3.6.3. Control experiments



Variation from standard conditions	Yield ^[a]
none	81%
Without photocatalyst	< 5% ^[b]
In the dark	0%

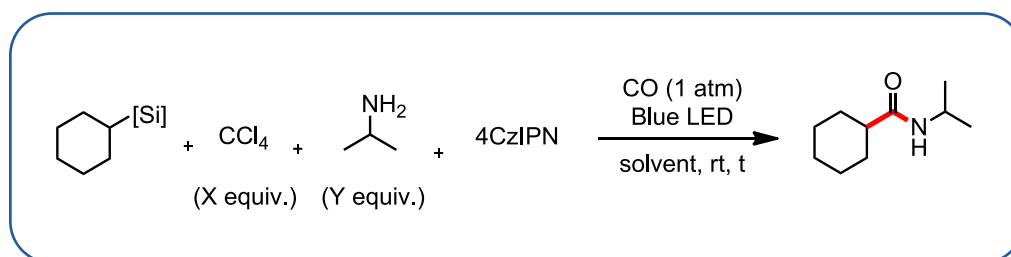
^[a] Isolated yield; ^[b] Determined by ^1H NMR analysis using acetanilide as an internal standard.

III.3.6.4. General procedure for the continuous flow carbonylation reaction



A 10 mL dried round bottom flask was charged with cyclohexyl silicate (0.2 mmol, 126.2 mg) and 4CzIPN (2 - 10 mol%). Then appropriated solvent (0.05 - 0.1 M) was added followed by addition of CCl₄ (1.5 - 4 equiv.) and amine (2 - 4 equiv.). The flask was swirled to achieve homogeneity. The liquid solution was then taken out and delivered with a 3 mL gas-tight syringe on a high precision syringe pump (KdS scientific, Legato 180). The CO was delivered from a gas cylinder and the gas flowrate was controlled by a mass flow controller (Bronkhorst EL-Flow Prestige). CO feed and liquid feed were pumped at 0.5 mL/min and 0.1 mL/min respectively. The liquid and the gas were introduced in a glass milli-mixer (LTF-MX, 0.2 mL at room temperature, Little Things Factory, Germany), which was connected to a FEP tubing (1/16" tubing, inner diameter 0.79 mm). Two tubing configurations have been used, a shorter tubing (570 cm, 2.8 mL) for a shorter residence time (t_R = 5 min) and a longer tubing (1200 cm, 5.8 mL) for a longer residence time (t_R = 10 min). Both the mixer and the tubing were under blue LED irradiation (477 nm). Regular gas slugs were formed in the mixer and were maintained in the FEP tubing. The outlet of the reactor was connected to a flask under the hood (so that excess CO can be evacuated safely). When all the mixture was passed through the reactor, the solution was extracted three times with Et₂O/H₂O or with CH₂Cl₂/H₂O (when CH₂Cl₂ is the solvent). The combined organic phases were dried over MgSO₄, evaporated under reduced pressure and analyzed by ¹H NMR using 1,3,5 trimethoxybenzene as an internal standard.

III.3.6.5. Optimization of the continuous flow carbonylation reaction



Solvent	X (equiv.)	[Silicate]	Y (equiv.)	Flow rate ^[a] (l)	Flow rate ^[a] (g)	%PC (mol%)	Time (mn)	Additive	Yield ^[e]
THF	1.5	0.1M	2	100	500	2	5	-	43%
DCM	1.5	0.1M	2	100	500	2	5	-	16%
MeCN	1.5	0.1M	2	100	500	2	5	-	0%
THF	1.5	0.1M	2	500	2500	2	1	-	20%
THP:DCM ^[c]	1.5	0.1M	2	100	500	2	5	-	48%
THP:DCM ^[d]	1.5	0.1M	2	100	500	10	5	-	70%
THP:DCM ^[d]	1.5	0.1M	2	100	500	5	5	-	55%
THP:DCM ^[d]	1.5	0.1M	2	100	500	2	5	-	50%
THP:DCM ^[d]	0	0.1M	2	100	500	2	5	-	0%
THP	1.5	0.05M	2	100	500	2	5	-	35%
THP	1.5	0.1M	2	100	500	2	5	-	35%
MeCN	4	0.1M	4	100	500	2	5	-	0%
DCM	4	0.1M	4	100	500	2	5	HFIP (1.5 equiv.)	21%
DCE	4	0.1M	4	100	500	2	5	-	7%
DCM	4	0.1M	4	100	500	2	5	-	30%
DMF	4	0.1M	4	100	500	2	5	-	8%
DCM	4	0.1M	4	100	500	2	5	-	0% ^[b]
THF	4	0.1M	4	100	500	2	5	-	41%
THF	4	0.1M	4	100	500	2	10	-	44%
DCM	4	0.1M	4	100	500	2	5	Isopropylammonium hydrochloride (1.5 equiv.)	29%
DCM	4	0.1M	4	100	500	2	5	Pyridinium hydrochloride (1.5 equiv.)	31%

^[a] Flow rate in $\mu\text{L}/\text{mn}$; ^[b] Amine put at the end, in the round bottom flask; ^[c] THP:DCM = 3:1; ^[d] THP:DCM = 1:1; ^[e] Determined by ^1H NMR analysis using 1,3,5 trimethoxybenzene as an internal standard.

Table 2: Optimization of the continuous flow carbonylation reaction

III.3.6.6. Estimation of CO concentration in various solvents

The concentrations $[\text{CO}]_{\text{liquid}}$ in different solvents have been calculated using thermodynamics data from the NIST database (**Table 3**).

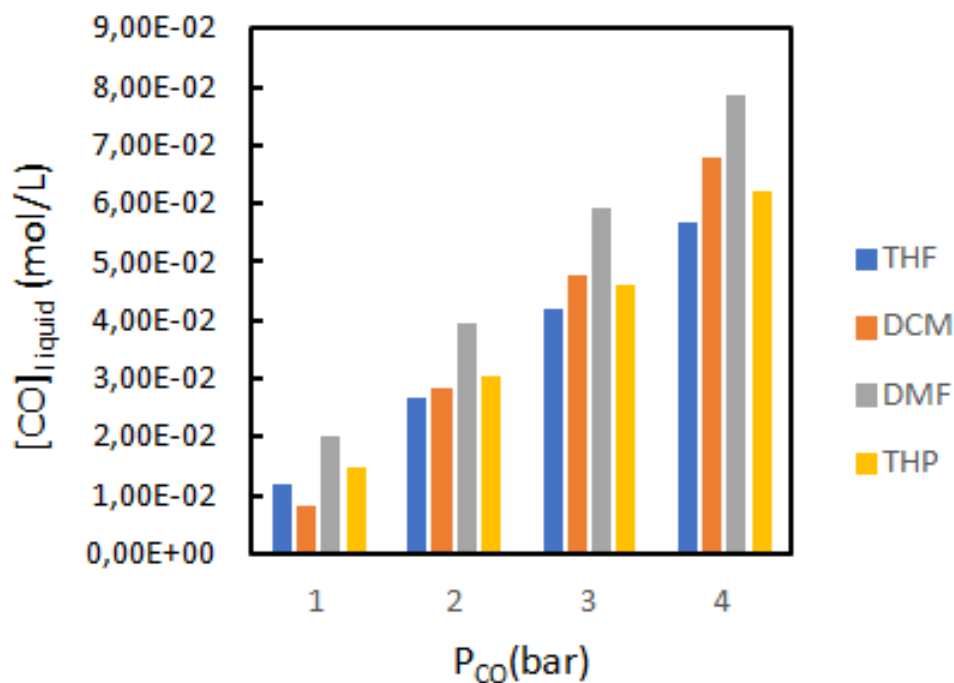
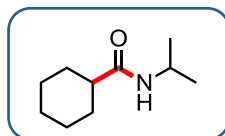


Table 3: Carbon monoxide concentration in the liquid phase at different pressures

III.3.6.7. Spectrum data for 3a-r

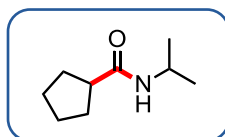
N-isopropylcyclohexanecarboxamide (**3a**)



$^1\text{H NMR}$ (400 MHz, CDCl_3): δ 5.23 (bs, 1H), 4.06 (sept, $J = 7.0$ Hz, 1H), 2.00 (tt, $J = 11.6$ Hz and 3.6 Hz, 1H), 1.85-1.65 (m, 5H), 1.45-1.36 (m, 2H), 1.30-1.21 (m, 3H), 1.12 (d, $J = 7.0$ Hz, 6H);

$^{13}\text{C NMR}$ (100 MHz, CDCl_3): δ 171.6, 50.9, 37.1, 35.5, 35.3, 28.5 (2C), 27.0, 25.7 (2C).

N-isopropylcyclopentanecarboxamide (**3b**)



Following the general procedure with potassium [18-Crown-6] bis(catecholato)-pentylsilicate **1b** with 10% of catechol (0.197 mmol, 135.2 mg), KH_2PO_4 (0.257 mmol, 35.1 mg), 4CzIPN (3 μmol , 2.2 mg) followed by isopropylamine (0.595 mmol, 51 μL) and carbontetrachloride (0.300 mmol, 29 μL) in 14 mL of THF. The crude product was purified to afford *N*-isopropylcyclopentanecarboxamide **3b** (23.9 mg, 77%) as a white solid.

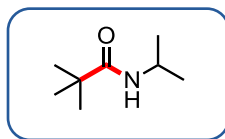
$^1\text{H NMR}$ (400 MHz, CDCl_3): δ 5.24 (bs, 1H), 4.07 (sept, $J = 6.0$ Hz, 1H), 2.43 (quint, $J = 8$ Hz, 1H), 1.87-1.67 (m, 6H), 1.60-1.55 (m, 2H), 1.13 (d, $J = 6.0$ Hz, 6H);

$^{13}\text{C NMR}$ (100 MHz, CDCl_3): δ 175.3, 46.0, 41.1, 30.4 (2C), 25.9 (2C), 22.9 (2C);

IR (neat): 3294, 2963, 1643, 1552, 1455, 1238 cm^{-1} ;

HMRS: (ESI) m/z calc for $\text{C}_9\text{H}_{17}\text{NNaO}$ ($[\text{M}+\text{Na}]^+$) 172.1208; found: 172.1205;

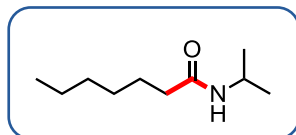
M. P. 101.9 $^\circ\text{C}$.

***N*-isopropylpivalamide (3c)**

Following the general procedure with tetraethylammonium bis(catecholato)-*ter*-butylsilicate **1c** (0.292 mmol, 126 mg), KH_2PO_4 (0.364 mmol, 49.5 mg), 4CzIPN (3.00 μmol , 2.6 mg) followed by isopropylamine (0.595 mmol, 51 μL) and carbontetrachloride (0.455 mmol, 44 μL) in 14 mL of THF. The crude product was purified to afford *N*-isopropylpivalamide **3c** (23.2 mg, 54%) as a white solid. The spectroscopic data are in agreement with those reported in the literature.²⁷

^1H NMR (400 MHz, CDCl_3): δ 5.40 (bs, 1H), 4.06 (sept, $J = 6.4$ Hz, 1H), 1.18 (s, 9H), 1.14 (d, $J = 6.4$ Hz, 6H);

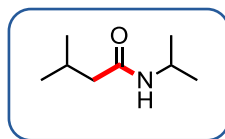
^{13}C NMR (100 MHz, CDCl_3): δ 177.6, 41.1, 29.7, 27.5 (3C), 22.8 (2C).

***N*-isopropylheptanamide (3d)**

Following the general procedure with potassium [18-Crown-6] bis(catecholato)-hexylsilicate **1d** (0.299 mmol, 178.4 mg), KH_2PO_4 (0.364 mmol, 49.6 mg), 4CzIPN (3.00 μmol , 2.8 mg) followed by isopropylamine (0.595 mmol, 51 μL) and carbontetrachloride (0.455 mmol, 44 μL) in 14 mL of THF. The crude product was purified to afford *N*-isopropylheptanamide **3d** (42.1 mg, 82%) as a pale-yellow oil. The spectroscopic data are in agreement with those reported in the literature.²⁸

^1H NMR (400 MHz, CDCl_3): δ 5.24 (bs, 1H), 4.08 (sept, $J = 6.4$ Hz, 1H), 2.12 (t, $J = 7.2$ Hz, 2H), 1.62-1.57 (m, 2H), 1.34-1.25 (m, 6H), 1.14 (d, $J = 6.4$ Hz, 6H), 0.89-0.86 (m, 3H);

^{13}C NMR (100 MHz, CDCl_3): δ 172.2, 41.1, 37.0, 31.5, 28.9, 25.8, 22.8 (2C), 22.5, 14.0.

***N*-isopropyl-3-methylbutanamide (3e)**

Following the general procedure with potassium [18-Crown-6] bis(catecholato)-isobutylsilicate **1e** (0.300 mmol, 181.3 mg), KH_2PO_4 (0.408 mmol, 55.5 mg), 4CzIPN (3.00 μmol , 3.0 mg) and dimethyl maleate (0.600 mmol, 75.0 μL) followed by isopropylamine (0.595 mmol, 51 μL) and carbontetrachloride (0.455 mmol, 44 μL) in 14 mL of THF. The crude product was purified to afford *N*-isopropyl-3-methylbutanamide **3e** (26.2 mg, 61%) as a light brown solid.

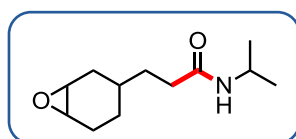
$^1\text{H NMR}$ (400 MHz, CDCl_3): δ 5.22 (bs, 1H), 4.10 (sept, $J = 7.2$ Hz, 1H), 2.11 (sept, $J = 6.8$ Hz, 1H), 1.98 (d, $J = 6.8$ Hz, 2H), 1.14 (d, $J = 6.8$ Hz, 6H), 0.94 (d, $J = 6.8$ Hz, 6H);

$^{13}\text{C NMR}$ (100 MHz, CDCl_3): δ 171.6, 46.4, 41.1, 26.2, 22.8 (2C), 22.4 (2C);

IR (neat): 3302, 3072, 2958, 1638, 1548, 1465 cm^{-1} ;

HMRS: (ESI) m/z calc for $\text{C}_8\text{H}_{17}\text{NNaO}$ ($[\text{M}+\text{Na}]^+$) 166.1208; found: 166.1194;

M. P. 62.2 $^\circ\text{C}$.

3-(7-oxabicyclo[4.1.0]heptan-3-yl)-*N*-isopropylpropanamide (3f)

Following the general procedure with potassium [18-Crown-6] bis(catecholato)-(2-(7-oxabicyclo[4.1.0]heptan-3-yl)ethyl)silicate **1f** (0.306 mmol, 206.0 mg), KH_2PO_4 (0.364 mmol, 49.6 mg), 4CzIPN (3.00 μmol , 2.8 mg) followed by isopropylamine (0.595 mmol, 51 μL) and carbontetrachloride (0.455 mmol, 44 μL) in 14 mL of THF. The crude product was purified to afford 3-(7-oxabicyclo[4.1.0]heptan-3-yl)-*N*-isopropylpropanamide **3f** (46.3 mg, 73%, 52 : 48 ratio) as a yellow oil.

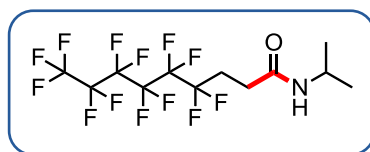
^1H NMR (400 MHz, CDCl_3): δ 5.28 (bs, 1H), 4.07 (sept, $J = 6.4$ Hz, 1H), 3.90-3.71 (m, 2H), 2.16-2.11 (m, 3H), 2.01-1.80 (m, 4H), 1.67-1.50 (m, 4H), 1.14 (d, $J = 6.4$ Hz, 6H);

^{13}C NMR (100 MHz, CDCl_3) (diastereomers were observed): 172.1, 171.9, 70.6, 62.1, 42.1, 41.3, 36.5, 34.7, 34.6, 34.5, 31.4, 30.1, 29.4, 29.0, 27.4, 26.5, 23.4, 22.7 (2C);

IR (neat): 3300, 3084, 2978, 1650, 1556, 1240, cm^{-1} ;

HMRS: (ESI) m/z calc for $\text{C}_{12}\text{H}_{21}\text{NNaO}_2$ ($[\text{M}+\text{Na}]^+$) 234.1470; found: 234.1462.

4,4,5,5,6,6,7,7,8,8,9,9,9-tridecafluoro-*N*-isopropylnonanamide (**3g**)



Following the general procedure with potassium [18-Crown-6] bis(catecholato)-(4,4,5,5,6,6,7,7,8,8,9,9,9-tridecafluorooctyl)silicate **1g** (0.302 mmol, 232 mg), KH_2PO_4 (0.420 mmol, 57.2 mg), 4CzIPN (3.00 μmol , 2.80 mg) followed by isopropylamine (0.595 mmol, 51 μL) and carbontetrachloride (0.455 mmol, 44 μL) in 14 mL of THF. The crude product was purified to afford 4,4,5,5,6,6,7,7,8,8,9,9,9-tridecafluoro-*N*-isopropylnonanamide **3g** (31.2 mg, 24%) as a light brown solid.

^1H NMR (400 MHz, CDCl_3): δ 5.31 (bs, 1H), 4.10 (sept, $J = 7.0$ Hz, 1H), 2.55-2.40 (m, 4H), 1.16 (d, $J = 7.0$ Hz, 6H);

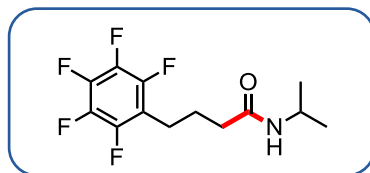
^{13}C NMR (100 MHz, CDCl_3): 168.8, 120-100 (m, 5 CF_2 , 1 CF_3), 41.7, 27.3, 26.7 (t, $J = 21$ Hz), 22.7 (2C);

^{19}F NMR (376 MHz, CDCl_3): -80.84 (t, $J = 10$ Hz, 3F), -114.60(-114.68) (m, 2F), -121.95 (bs, 2F), -122.93 (bs, 2F), -123.58 (bs, 2F), -126.16(-126.24) (m, 2F);

IR (neat): 3304, 2978, 1650, 1556, 1240, cm^{-1} ;

HMRS: (ESI) m/z calc for $\text{C}_{12}\text{H}_{12}\text{F}_{13}\text{NNaO}$ ($[\text{M}+\text{Na}]^+$) 456.0609; found: 456.0604;

M. P. 48.0 $^\circ\text{C}$.

***N*-isopropyl-4-(perfluorophenyl)butanamide (3h)**

Following the general procedure with potassium [18-Crown-6] bis(catecholato)-4-(perfluorophenyl)proylsilicate **1h** (0.296 mmol, 224.0 mg), KH_2PO_4 (0.418 mmol, 56.9 mg), 4CzIPN (3.00 μmol , 2.8 mg) followed by isopropylamine (0.595 mmol, 51 μL) and carbontetrachloride (0.455 mmol, 44 μL) in 14 mL of THF. The crude product was purified to afford *N*-isopropyl-4-(perfluorophenyl)butanamide **3h** (52.3 mg, 59%) as a white solid.

^1H NMR (400 MHz, CDCl_3): δ 5.22 (bs, 1H), 4.08 (sept, $J = 6.4$ Hz, 1H), 2.75 (t, $J = 7.6$ Hz, 2H), 2.16 (t, $J = 7.6$ Hz, 2H), 1.94 (quint, $J = 7.6$ Hz, 2H), 1.14 (d, $J = 6.4$ Hz, 6H);

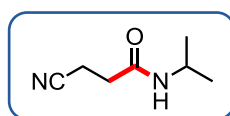
^{13}C NMR (100 MHz, CDCl_3): δ 170.7, 145.0 (d, $J = 242$ Hz), 139.8 (d, $J = 223$ Hz, 2C), 137.3 (d, $J = 235$ Hz, 2C), 114.5 (t, $J = 18$ Hz), 41.4, 35.6, 24.9, 22.7 (2C), 21.7;

^{19}F NMR (376 MHz, CDCl_3): -143.96 – (-144.01) (m, 2F), -157.45 – (-157.55) (m, 1F), -162.61- (-162.72) (m, 2F);

IR (neat): 3310, 2975, 2936, 1636, 1502 cm^{-1} ;

HMRS: (ESI) m/z calc for $\text{C}_{13}\text{H}_{14}\text{F}_5\text{NNaO}$ ($[\text{M}+\text{Na}]^+$) 318.0893; found: 318.0888;

M. P. 109.3°C.

3-cyano-*N*-isopropylpropanamide (3i)

Following the general procedure with potassium [18-Crown-6] bis(catecholato)-3-cyanoethylsilicate **1i** (0.299 mmol, 180.0 mg), KH_2PO_4 (0.377 mmol, 51.3 mg), 4CzIPN (3.00 μmol , 2.7 mg) followed by isopropylamine (0.595 mmol, 51 μL) and carbontetrachloride (0.455 mmol, 44 μL) in 14 mL of THF. The crude product was purified to afford 3-cyano-*N*-isopropylpropanamide **3i** (13.0 mg, 31%) as a white solid.

¹H NMR (400 MHz, CDCl₃): δ 5.33 (bs, 1H), 4.11 (sept, *J* = 6.8 Hz, 1H), 2.68 (t, *J* = 7.2 Hz, 2H), 2.48 (t, *J* = 7.2 Hz, 2H), 1.17 (d, *J* = 6.8 Hz, 6H);

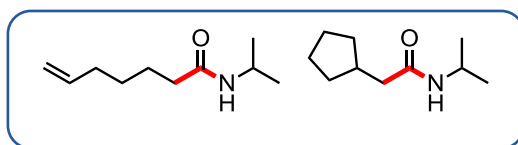
¹³C NMR (100 MHz, CDCl₃): δ 167.7, 119.0, 41.9, 31.8, 22.7 (2C), 13.2;

IR (neat): 3308, 3200, 2960, 2251, 1672, 1600, 1544 cm⁻¹;

HMRS: (ESI) *m/z* calc for C₇H₁₂N₂NaO ([M]⁺) 140.0950; found: 140.0905;

M. P. 74.4 °C.

N-isopropylhept-6-enamide (**3j**) and 2-cyclopentyl-*N*-isopropylacetamide (**3j'**)



Following the general procedure with potassium [18-Crown-6] bis(catecholato)-hexenylsilicate **1j** (0.305 mmol, 192.1 mg), KH₂PO₄ (0.367 mmol, 50.0 mg), 4CzIPN (3.00 μmol, 2.5 mg) followed by isopropylamine (0.595 mmol, 51 μL) and carbontetrachloride (0.455 mmol, 44 μL) in 14 mL of THF. The crude product was purified to afford an inseparable mixture of *N*-isopropylhept-6-enamide **3j** and 2-cyclopentyl-*N*-isopropylacetamide **3j'** (23.9 mg, 50:50, 47%) as a yellow oil.

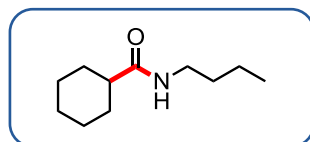
¹H NMR (400 MHz, CDCl₃): δ 5.79-5.75 (m, 1H), 5.28 (bs, 2H), 5.01-4.92 (m, 2H), 4.11-4.05 (m, 2H), 2.14-2.05 (m, 8H), 1.80-1.78 (m, 2H), 1.67-1.51 (m, 7H), 1.40 (quint, *J* = 7.6 Hz, 2H), 1.13 (d, *J* = 6.8 Hz, 12H);

¹³C NMR (100 MHz, CDCl₃): δ 172.0, 171.9, 138.5, 114.6, 43.2 (2C), 41.2, 41.1, 37.3, 36.8, 33.4, 32.5, 28.5, 25.2, 24.9 (2C), 22.8 (4C);

IR (neat): 3296, 3078, 2970, 1640, 1547, 1457 cm⁻¹;

HMRS: (ESI) *m/z* calc for C₁₂H₁₇O₄⁺ ([M-OMe]⁺) 225.1127; found: 225.1117.

N-butylcyclohexanecarboxamide (**3k**)

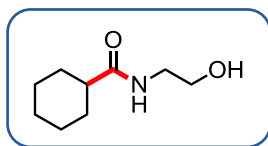


Following the general procedure with potassium [18-Crown-6] bis(catecholato)-cyclohexylsilicate **1a** (0.301 mmol, 188.9 mg), KH_2PO_4 (0.427 mmol, 58.1 mg), 4CzIPN (3.00 μmol , 2.5 mg) followed by butan-1-amine (0.607 mmol, 60 μL) and carbontetrachloride (0.455 mmol, 44 μL) in 14 mL of THF. The crude product was purified to afford *N*-butylcyclohexanecarboxamide **3k** (19.8 mg, 36%) as a yellow oil containing a small amount of catechol impurities. The spectroscopic data are in agreement with those reported in the literature.²⁹

^1H NMR (400 MHz, CDCl_3): δ 5.43 (bs, 1H), 3.24 (q, $J = 6.8$ Hz, 2H), 2.05 (tt, $J = 11.6$ Hz and 3.6 Hz, 1H), 1.87-1.65 (m, 6H), 1.49-1.22 (m, 8H), 0.92 (t, $J = 6.8$ Hz, 3H);

^{13}C NMR (100 MHz, CDCl_3): δ 176.2, 45.7, 39.1, 31.7, 29.7 (2C), 25.7 (3C), 20.0, 13.7.

N-(2-hydroxyethyl)cyclohexanecarboxamide (**3l**)

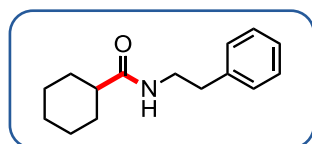


Following the general procedure with potassium [18-Crown-6] bis(catecholato)-cyclohexylsilicate **1a** (0.297 mmol, 187.2 mg), KH_2PO_4 (0.406 mmol, 55.3 mg), 4CzIPN (3.00 μmol , 3.0 mg) followed by 2-aminoethan-1-ol (0.661 mmol, 40 μL) and carbontetrachloride (0.455 mmol, 44 μL) in 14 mL of THF. The crude product was purified to afford *N*-(2-hydroxyethyl)cyclohexanecarboxamide **3l** (26.0 mg, 51%) as a brown solid containing a small amount of catechol impurities. The spectroscopic data are in agreement with those reported in the literature.³⁰

^1H NMR (400 MHz, CDCl_3): δ 6.00 (bs, 1H), 3.87 (bs, 1H), 3.72 (t, $J = 5.0$ Hz, 2H), 3.42 (q, $J = 5.0$ Hz, 2H), 2.11 (tt, $J = 11.6$ Hz and 3.6 Hz, 1H), 1.88-1.77 (m, 3H), 1.69-1.66 (m, 1H), 1.44-1.41 (m, 2H), 1.29-1.21 (m, 4H);

^{13}C NMR (100 MHz, CDCl_3): δ 177.7, 62.7, 45.4, 42.4, 29.6 (2C), 25.7 (3C).

N-phenethylcyclohexanecarboxamide (**3m**)

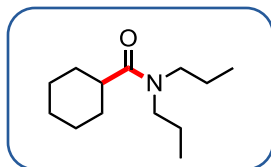


Following the general procedure with potassium [18-Crown-6] bis(catecholato)-cyclohexylsilicate **1a** (0.301 mmol, 190.2 mg), KH_2PO_4 (0.399 mmol, 54.3 mg), 4CzIPN (3.00 μmol , 2.9 mg), followed by 2-phenylethan-1-amine (0.597 mmol, 75 μL) and carbontetrachloride (0.455 mmol, 44 μL) in 14 mL of THF. The crude product was purified to afford *N*-phenethylcyclohexanecarboxamide **3m** (34.0 mg, 49%) as a white solid. The spectroscopic data are in agreement with those reported in the literature.³¹

^1H NMR (400 MHz, CDCl_3): δ 7.33-7.29 (m, 2H), 7.25-7.16 (m, 3H), 5.43 (bs, 1H), 3.51 (q, $J = 6.4$ Hz, 2H), 2.81 (t, $J = 6.4$ Hz, 2H), 2.00 (tt, $J = 11.6$ Hz and 3.6 Hz, 1H), 1.81-1.66 (m, 5H), 1.42-1.17 (m, 5H);

^{13}C NMR (100 MHz, CDCl_3): δ 176.0, 139.0, 128.8 (2C), 128.6 (2C), 126.5, 45.5, 40.3, 35.7, 29.6 (2C), 25.7 (3C).

N,N-dipropylcyclohexanecarboxamide (**3n**)



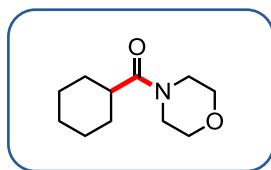
Following the general procedure with potassium [18-Crown-6] bis(catecholato)-cyclohexylsilicate **1a** (0.299 mmol, 188.7 mg), KH_2PO_4 (0.390 mmol, 53.1 mg), 4CzIPN (3.00 μmol , 2.4 mg), followed by dipropylamine (0.600 mmol, 82 μL) and carbontetrachloride (0.455 mmol, 44 μL) in 14 mL of THF. The crude product was purified to afford *N,N*-dipropylcyclohexanecarboxamide **3n** (38.7 mg, 61%) as a yellow oil.

^1H NMR (400 MHz, CDCl_3): δ 3.28-3.06 (m, 4H), 2.41 (tt, $J = 11.6$ Hz and 3.6 Hz, 1H), 1.80-1.67 (m, 4H), 1.61-1.49 (m, 6H), 1.29-1.22 (m, 4H), 0.92 (t, $J = 7.6$ Hz, 3H), 0.86 (t, $J = 7.6$ Hz, 3H);

^{13}C NMR (100 MHz, CDCl_3): δ 176.0, 49.3, 47.4, 40.9, 29.6 (2C), 25.9 (2C), 25.8, 22.8, 21.0, 11.3, 11.2;

IR (neat): 3328, 2930, 1616, 1599, 1468, 1274 cm^{-1} ;

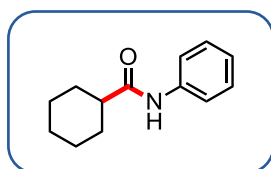
HMRS: (ESI) m/z calc for $\text{C}_{12}\text{H}_{17}\text{O}_4$ ($[\text{M}-\text{OMe}]^+$) 225.1127; found: 225.1117.

Cyclohexyl(morpholino)methanone (3o)

Following the general procedure with potassium [18-Crown-6] bis(catecholato)-cyclohexylsilicate **1a** (0.302 mmol, 190.8 mg), KH_2PO_4 (0.397 mmol, 54.0 mg), 4CzIPN (3.00 μmol , 2.6 mg), followed by morpholine (0.603 mmol, 52 μL) and carbontetrachloride (0.455 mmol, 44 μL) in 14 mL of THF. The crude product was purified to afford cyclohexyl(morpholino)methanone **3o** (24.9 mg, 42%) as a pale-yellow solid containing catechol impurities. The spectroscopic data are in agreement with those reported in the literature.²⁶

$^1\text{H NMR}$ (400 MHz, CDCl_3): δ 3.68-3.51 (m, 8H), 2.43 (tt, $J = 11.6$ Hz and 3.6 Hz, 1H), 1.83-1.79 (m, 2H), 1.73-1.70 (m, 2H), 1.58-1.49 (m, 3H), 1.29-1.26 (m, 3H);

$^{13}\text{C NMR}$ (100 MHz, CDCl_3): δ 174.9, 67.0, 66.9, 45.9, 42.0, 40.3, 29.3, 25.8 (2C), 25.7 (2C).

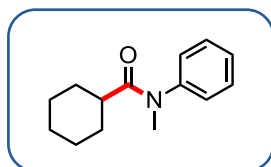
***N*-phenylcyclohexanecarboxamide (3p)**

Following the general procedure with potassium [18-Crown-6] bis(catecholato)-cyclohexylsilicate **1a** (0.499 mmol, 315.0 mg), KH_2PO_4 (0.614 mmol, 83.5 mg), 4CzIPN (5.00 μmol , 4.1 mg), followed by aniline (0.997 mmol, 91 μL) and carbontetrachloride (0.755 mmol, 73 μL) in 14 mL of THF. The crude product was purified to afford *N*-phenylcyclohexanecarboxamide **3p** (34.6 mg, 34%) as a light brown solid. The spectroscopic data are in agreement with those reported in the literature.³²

$^1\text{H NMR}$ (400 MHz, CDCl_3): δ 7.52 (d, $J = 7.6$ Hz, 2H), 7.31 (t, $J = 7.6$ Hz, 2H), 7.19 (bs, 1H), 7.09 (t, $J = 7.6$ Hz, 1H), 2.23 (tt, $J = 12.0$ Hz and 3.2 Hz, 1H), 1.96 (d, $J = 12$ Hz, 2H), 1.85-1.82 (m, 2H), 1.72-1.69 (m, 1H), 1.59-1.50 (m, 2H), 1.36-1.23 (m, 3H);

^{13}C NMR (100 MHz, CDCl_3): δ 174.4, 138.0, 129.0 (2C), 124.1, 119.7 (2C), 46.6, 29.6 (2C), 25.6 (3C);

N-methyl-*N*-phenylcyclohexanecarboxamide (**3q**)

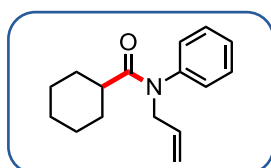


Following the general procedure with potassium [18-Crown-6] bis(catecholato)-cyclohexylsilicate **1a** (0.301 mmol, 190.0 mg), KH_2PO_4 (0.391 mmol, 53.2 mg), 4CzIPN (3.00 μmol , 2.5 mg), followed by *N*-methylaniline (0.603 mmol, 61 μL) and carbontetrachloride (0.455 mmol, 44 μL) in 14 mL of THF. The crude product was purified to afford *N*-methyl-*N*-phenylcyclohexanecarboxamide **3q** (54.7 mg, 84%) as a light brown solid. The spectroscopic data are in agreement with those reported in the literature.³³

^1H NMR (400 MHz, CDCl_3): δ 7.43-7.40 (m, 2H), 7.36-7.32 (m, 1H), 7.18-7.16 (m, 2H), 3.24 (s, 3H), 2.20-2.15 (m, 1H), 1.63-1.47 (m, 7H), 1.25-1.13 (m, 1H), 1.00-0.94 (m, 2H);

^{13}C NMR (100 MHz, CDCl_3): δ 176.4, 144.3, 129.7 (2C), 127.6, 127.2 (2C), 41.3, 37.4, 29.4 (2C), 25.6, 25.5 (2C).

N-allyl-*N*-phenylcyclohexanecarboxamide (**3r**)



Following the general procedure with potassium [18-Crown-6] bis(catecholato)-cyclohexylsilicate **1a** (0.307 mmol, 193.4 mg), KH_2PO_4 (0.404 mmol, 55.0 mg), 4CzIPN (3.00 μmol , 2.5 mg), followed by *N*-allylaniline (0.605 mmol, 82 μL) and carbontetrachloride (0.455 mmol, 44 μL) in 14 mL of THF. The crude product was purified to afford *N*-allyl-*N*-phenylcyclohexanecarboxamide **3r** (65.0 mg, 89%) as a brown oil.

^1H NMR (400 MHz, CDCl_3) (*E* and *Z* isomers were observed) : δ 7.42-7.39 (m, 2H), 7.15-7.13 (m, 1H), 7.00-6.91 (m, 1H), 6.72-6.70 (m, 1H), 5.98-5.81 (m, 1H), 5.10-5.02 (m, 2H),

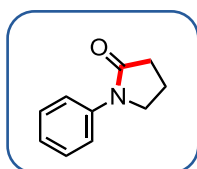
4.26 (d, $J = 6.0$ Hz, 2H), 2.14 (t, $J = 11.6$ Hz, 1H), 1.66-1.51 (m, 7H), 1.25-1.13 (m, 1H), 0.99-0.90 (m, 2H);

^{13}C NMR (100 MHz, CDCl_3) (E and Z isomers were observed): δ 175.9, 144.0, 142.7, 134.4, 133.4, 129.5 (2C), 128.2, 127.8 (2C), 127.0, 125.0, 117.6, 54.5, 52.1, 41.6, 29.4 (2C), 25.6, 25.5 (2C);

IR (neat): 3062, 2927, 1656, 1595, 1485, 1396, 1261 cm^{-1} ;

HMRS: (ESI) m/z calc for $\text{C}_{16}\text{H}_{21}\text{NNaO}_4$ ($[\text{M}+\text{Na}]^+$) 266.1521; found: 266.1513.

1-phenylpyrrolidin-2-one (4)



Following the general procedure with potassium [18-Crown-6] bis(catecholato)-3-(phenylamino)propanylsilicate **1a** (0.295 mmol, 201.2 mg), KH_2PO_4 (0.404 mmol, 56.1 mg), 4CzIPN (3.00 μmol , 2.5 mg), followed by isopropylamine (0.595 mmol, 51 μL) and carbontetrachloride (0.455 mmol, 44 μL) in 14 mL of THF. The crude product was purified to afford 1-phenylpyrrolidin-2-one **4** (31.0 mg, 64%) as a white solid. The spectroscopic data are in agreement with those reported in the literature.³⁴

^1H NMR (400 MHz, CDCl_3): δ 7.62-7.60 (d, $J = 8.0$ Hz, 2H), 7.39-7.35 (t, $J = 8.0$ Hz, 2H), 7.17-7.13 (t, $J = 8.0$ Hz, 1H), 3.89-3.86 (t, $J = 7.6$ Hz, 2H), 2.64-2.60 (t, $J = 7.6$ Hz, 2H), 2.21-2.13 (quint, $J = 7.6$ Hz, 2H);

^{13}C NMR (100 MHz, CDCl_3): δ 174.2, 139.4, 128.8 (2C), 124.5, 120.0 (2C), 48.8, 32.8, 18.0.

III.3.7. References

- ¹ For recent books, see: a) *Visible Light Photocatalysis in Organic Chemistry*, (Eds. C. Stephenson, T. Yoon, D. W. C. MacMillan) Wiley-VCH, Weinheim, **2018**. For selected reviews, see: b) L. Marzo, S. K. Pagire, O. Reiser, B. König, *Angew. Chem. Int. Ed.* **2018**, *57*, 10034; c) J. K. Matsui, S. B. Lang, D. R. Heitz, G. A. Molander, *ACS Catal.* **2017**, *7*, 2563; d) D. Ravelli, S. Proti, M. Fagnoni, *Chem. Rev.* **2016**, *116*, 9850; e) T. P. Yoon, *Acc. Chem. Res.*, **2016**, *49*, 2307; f) J.-R. Chen, X.-Q. Hu, L.-Q. Lu, W.-J. Xiao, *Acc. Chem. Res.* **2016**, *49*, 1911; g) J.-P. Goddard, C. Ollivier, L. Fensterbank, *Acc. Chem. Res.* **2016**, *49*, 1924; h) J. Xuan, Z.-G. Zang, W.-J. Xiao, *Angew. Chem. Int. Ed.* **2015**, *54*, 15632; *Angew. Chem.* **2015**, *127*, 15847.
- ² For selected examples, see: a) F.-D. Lu, D. Liu, L. Zhu, L.-Q. Lu, Q. Yang, Q.-Q. Zhou, Y. Lan, W.-J. Xiao, *J. Am. Chem. Soc.* **2019**, *141*, 6167; b) T. Wang, D.-H. Wang, *Org. Lett.* **2019**, *21*, 3981; c) Q.-Q. Zhou, S. J. S. Düsel, L.-Q. Lu, B. König, W.-J. Xiao, *Chem. Commun.* **2019**, *55*, 107; d) I. Ghosh, J. Khamrai, A. Savateev, N. Shlapakov, M. Antonietti, B. König, *Science* **2019**, *365*, 360; e) W. Wei, P. Bao, Y. Shao, H. Yue, D. Yang, X. Yang, X. Zhao, H. Wang, *Org. Lett.* **2018**, *20*, 7125; f) S. J. MacCarver, J. X. Qiao, J. Carpenter, R. M. Borzirelli, M. A. Poss, M. D. Eastgate, M. M. Miller, D. W. C. MacMillan, *Angew. Chem. Int. Ed.* **2017**, *56*, 728; *Angew. Chem.* **2017**, *129*, 746; g) M. O. Akram, P. S. Mali, N. T. Patil, *Org. Lett.* **2017**, *19*, 3075; h) M. Daniel, G. Dagousset, P. Diter, P.-A. Klein, B. Tuccio, A.-M. Goncalves, G. Masson, E. Magnier, *Angew. Chem.* **2017**, *56*, 3997; i) L. Candish, M. Freitag, T. Gensch, F. Glorius, *Chem. Sci.* **2017**, *8*, 3618; j) Z. Zuo, H. Cong, W. Li, J. Choi, G. C. Fu, D. W. C. MacMillan, *J. Am. Chem. Soc.* **2016**, *138*, 1832; k) C. C. Nawrat, C. R. Jamison, Y. Slutskyy, D. W. C. MacMillan, L. E. Overman, *J. Am. Chem. Soc.* **2015**, *137*, 11270; l) W. Guo, L.-Q. Lu, Y. Wang, Y.-N. Wang, J.-R. Chen, W.-J. Xiao, *Angew. Chem. Int. Ed.* **2015**, *54*, 2265; m) A. Gutierrez-Bonet, J. C. Tellis, J. K. Matsui, B. A. Vara, G. A. Molander, *ACS Catal.* **2016**, *6*, 8004.
- ³ C. L. Frye, *J. Am. Chem. Soc.* **1964**, *86*, 3170.
- ⁴ a) E. Levernier, V. Corcé, L.-M. Rakotoarison, A. Smith, M. Zhang, S. Ognier, M. Tatouliau, C. Ollivier, L. Fensterbank, *Org. Chem. Front.* **2019**, *6*, 1378; b) C. Lévêque, L. Chenneberg, V. Corcé, C. Ollivier, L. Fensterbank, *Chem. Commun.* **2016**, *52*, 9877; c) L. Chenneberg, C. Lévêque, V. Corcé, A. Baralle, J.-P. Goddard, C. Ollivier, L. Fensterbank, *Synlett* **2016**, *27*, 731; d) V. Corcé, L.-M. Chamoreau, E. Derat, J.-P. Goddard, C. Ollivier, L. Fensterbank, *Angew. Chem. Int. Ed.* **2015**, *54*, 11414.
- ⁵ M. Jouffroy, D. N. Primer, G. A. Molander, *J. Am. Chem. Soc.* **2016**, *138*, 475.
- ⁶ a) K. D. Raynor, G. D. May, U. K. Bandarage, M. J. Boyd, *J. Org. Chem.* **2018**, *83*, 1551; b) T. Guo, X. Liu, Y. Fang, X. Jin, Y. Yang, Y. Li, B. Chen, M. Ouyang, *Adv. Synth. Catal.* **2018**, *360*, 4457; c) A. García-Domínguez, R. Mondal, C. Nevado, *Angew. Chem. Int. Ed.* **2019**, *58*, 2.
- ⁷ N. R. Patel, C. B. Kelly, A. P. Siegenfeld, G. A. Molander, *ACS Catal.* **2017**, *7*, 1766.
- ⁸ Z.-J. Wang, S. Zheng, J. K. Matsui, Z. Lu, G. A. Molander, *Chem. Sci.* **2019**, *10*, 4389.
- ⁹ S. T. J. Cullen, G. K. Friestad, *Org. Lett.* **2019**, *21*, 8290.
- ¹⁰ For selected reviews by radical methods, see: a) V. Liautard, Y. Landais, in *Multicomponent Reactions*, (Eds. J. Zhu, Q. Wang, M. X. Wang), Wiley, 2nd Edition, **2014**, 401; b) M. Tojino, I. Ryu in *Multicomponent Reaction* Eds. J. Zhu, H. Bienaymé, Wiley-VCH, Weinheim, **2005**, 169; c) A. Fusano, I. Ryu in *Science of Synthesis, Multicomponent Reactions*, (Eds. J. J. Thomas, T. J. J. Müller), Georg Thieme Verlag KG; Stuttgart, **2014**, vol. 2, 409.

- ¹¹ For reviews on radical carbonylations, see: a) I. Ryu, N. Sonoda, *Angew. Chem. Int. Ed.* **1996**, *35*, 1050; b) I. Ryu, N. Sonoda, D. P. Curran, *Chem. Rev.* **1996**, *96*, 177; c) I. Ryu, T. Fukuyama in *Topics in Heterocyclic Chemistry*, (Eds. X.-F. Wu, M. Beller), Springer, Cham, **2016**, 101; d) H. Matsubara, T. Kawamoto, T. Fukuyama, I. Ryu, *Acc. Chem. Res.* **2018**, *51*, 2023; d) Q.-Q. Zhou, W. Guo, W. Ding, X. Wu, X. Chen, L.-Q. Lu, W.-J. Xiao, *Angew. Chem. Int. Ed.* **2015**, *54*, 1196.
- ¹² For a review on acyl radicals, see a) C. Chatgililoglu, D. Crich, M. Komatsu, I. Ryu, *Chem. Rev.* **1999**, *99*, 1991. Also see: b) A. Banerjee, Z. Lei, M.-Y. Ngai, *Synthesis* **2019**, *51*, 303.
- ¹³ A. Cartier, E. Levernier, V. Corcé, T. Fukuyama, A.-L. Dhimane, C. Ollivier, I. Ryu, L. Fensterbank, *Angew. Chem. Int. Ed.* **2019**, *58*, 1789.
- ¹⁴ For a review on atom transfer carbonylation, see: a) I. Ryu, *Chem. Soc. Rev.* **2001**, *30*, 16; b) I. Ryu, K. Nagahara, N. Kambe, N. Sonoda, S. Kreimerman, M. Komatsu, *Chem. Commun.* **1998**, 1953.
- ¹⁵ For a review on Pd/light system: a) S. Sumino, A. Fusano, T. Fukuyama, I. Ryu, *Acc. Chem. Res.* **2014**, *47*, 1563. Also see selected papers: a) I. Ryu, S. Kreimerman, F. Araki, S. Nishitani, Y. Oderaotoshi, S. Minakata, M. Komatsu, *J. Am. Chem. Soc.* **2002**, *124*, 3812; b) T. Fukuyama, T. Inouye, I. Ryu, *J. Organomet. Chem.* **2007**, *692*, 685; c) A. Fusano, S. Sumino, S. Nishitani, T. Inoue, K. Morimoto, T. Fukuyama, I. Ryu, *Chem. Eur. J.* **2012**, *18*, 9415; d) M. Sardana, J. Bergman, C. Ericsson, L. P. Kingston, M. Schou, C. Dugave, D. Audisio, C. S. Elmore, *J. Org. Chem.* **2019**, *84*, 16076.
- ¹⁶ a) R. E. Fostser, A. W. Larchar, R. D. Lipscomb, B. C. McKusick, *J. Am. Chem. Soc.* **1956**, *78*, 5606; b) D. Ginsburg, *J. Am. Chem. Soc.* **1951**, *73*, 702; c) T. Suzuki, J. Tsuji, *J. Org. Chem.* **1970**, *35*, 2982.
- ¹⁷ To suppress any risk of premature quenching of alkyl radicals by CCl₄, we maintained a high pressure of CO in all trials. We are now trying to decrease the CO pressures and the results will be reported in due course.
- ¹⁸ a) M. Yokoyama, K. Inada, Y. Tsuchiya, H. Nakanotani, C. Adachi, *Chem. Commun.* **2018**, *54*, 8261; b) H. Uoyama, K. Goushi, K. Shizu, H. Nomura, C. Adachi, *Nature* **2012**, *492*, 234.
- ¹⁹ Photoredox potentials of 4CzIPN $E_{1/2}(4CzIPN^*/[4CzIPN]^-) = +1.59$ V vs. SCE and $E_{1/2}(4CzIPN/[4CzIPN]^-) = -1.21$ V vs. SCE, see: a) J. Luo, J. Zhang, *ACS Catal.* **2016**, *6*, 873; For a reevaluation of the reduction and oxidation potentials of the excited state of 4CzIPN, see F. Le Vaillant, M. Garreau, S. Nicolai, G. Gryn'ova, C. Corminboeuf, J. Waser, *Chem. Sci.* **2018**, *9*, 5883.
- ²⁰ For recent examples of reactions using 4CzIPN as photocatalyst, see: a) T.Y. Shang, L.-H. Lu, Z. Cao, Y. Liu, W.-M. He, B. Yu, *Chem. Commun.* **2019**, *55*, 5408; b) Q.-Y. Meng, T. E. Schirmer, A. L. Berger, K. Donabauer, B. König, *J. Am. Chem. Soc.* **2019**, *141*, 11393; c) Q.-Y. Meng, T. E. Schirmer, K. Katou, B. König, *Angew. Chem. Int. Ed.* **2019**, *58*, 5723; d) C. Shu, R. S. Mega, B. J. Andraessen, A. Noble, V. X. Aggarwal, *Angew. Chem. Int. Ed.* **2018**, *57*, 15430; e) T. Ju, J.-H. Ye, Z. Zhang, L.-L. Liao, S.-S. Yan, X.-Y. Tian, S.-P. Luo, J. Li, D.-G. Yu, *Angew. Chem. Int. Ed.* **2018**, *57*, 13897; f) F. L. Vaillant, M. Garreau, S. Nicolai, G. Gryn'ova, C. Corminboeuf, J. Waser, *Chem. Sci.* **2018**, *9*, 5883; g) R. Zhou, Y. Y. Goh, H. Liu, H. Tao, L. Li, J. Wu, *Angew. Chem. Int. Ed.* **2017**, *56*, 16621; h) B. A. Vara, M. Jouffroy, G. A. Molander, *Chem. Sci.* **2017**, *8*, 530.
- ²¹ Characteristic signals of n-heptanoyl chloride by ¹H NMR were observed and consistent with literature data, see: Spectral Database for Organic Compounds (SDBS) of the National Institute of Advanced Industrial Science and Technology (AIST), Japan: https://sdb.sdb.aist.go.jp/sdb/cgi-bin/direct_frame_top.cgi.

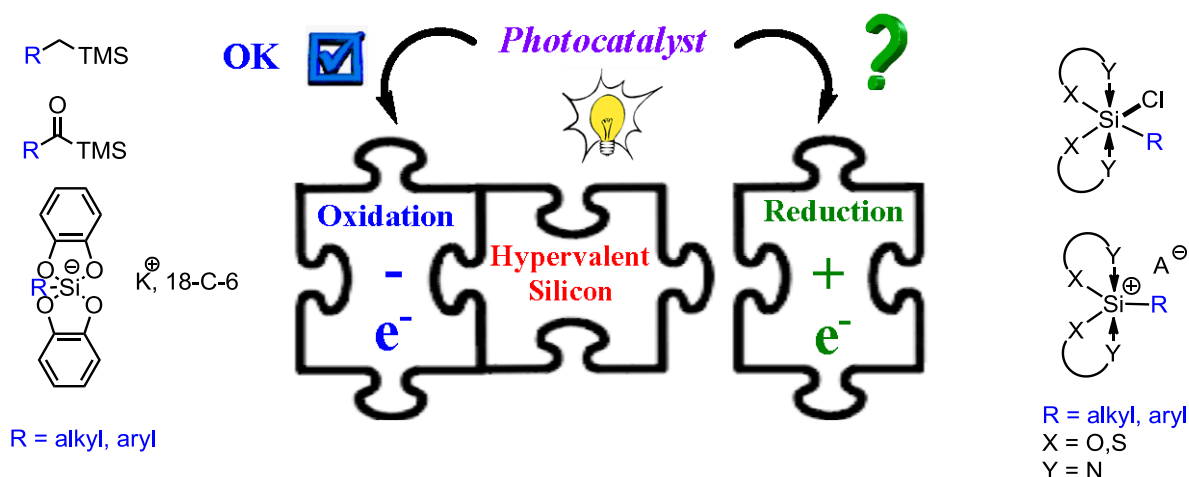
- ²² For reviews on flow photoreactions, see: a) D. Cambié, C. Bottecchia, N. J. W. Straathof, V. Hessel, T. Noël, *Chem. Rev.* **2016**, *116*, 10276; (b) K. Mizuno, Y. Nishiyama, T. Ogaki, K. Terao, H. Ikeda, K. Kakiuchi, *J. Photochem. Photobiol. C. Photochem. Rev.* **2016**, *29*, 107; (c) M. Oelgemöller, *Chem. Eng. Technol.* **2012**, *35*, 1144.
- ²³ For a review on flow carbonylation, see: a) T. Fukuyama, T. Totoki, I. Ryu, *Green Chem.* **2014**, *16*, 2042. Also see selected recent work: b) C. Brancour, T. Fukuyama, Y. Mukai, T. Skrydstrup, I. Ryu, *Org. Lett.* **2013**, *15*, 2794; c) T. Fukuyama, T. Totoki, I. Ryu, *Org. Lett.* **2014**, *16*, 56325; d) H. Akinaga, N. Masaoka, K. Takagi, I. Ryu, T. Fukuyama, *Chem. Lett.* **2014**, *43*, 1456; e) C. J. Mallia, G. C. Walter, I. R. Baxendale, Beilstein J. Org. Chem. **2016**, *12*, 1503; f) N. Micic, A. Polyzos, *Org. Lett.* **2018**, *20*, 4663.
- ²⁴ a) E. Levernier, V. Corcé, L.-M. Rakooarison, A. Smith, M. Zhang, S. Ognier, M. Tatoulian, C. Ollivier, L. Fensterbank, *Org. Chem. Front.* **2019**, *6*, 1378; b) A. Cartier, E. Levernier, V. Corcé, T. Fukuyama, A.-L. Dhimane, C. Ollivier, I. Ryu, L. Fensterbank, *Angew. Chem. Int. Ed.* **2019**, *58*, 1789; c) C. Lévêque, L. Chenneberg, V. Corcé, C. Ollivier, L. Fensterbank, *Chem. Commun.* **2016**, *52*, 9877; d) L. Chenneberg, C. Lévêque, V. Corcé, A. Baralle, J.-P. Goddard, C. Ollivier, L. Fensterbank, *Synlett* **2016**, *27*, 731; e) V. Corcé, L.-M. Chamoreau, E. Derat, J.-P. Goddard, C. Ollivier, L. Fensterbank, *Angew. Chem. Int. Ed.* **2015**, *54*, 11414.
- ²⁵ a) D. Hanss, J. C. Freys, G. Bernardinelli, O. S. Wenger, *Eur. J. Inorg. Chem.* **2009**, 4850; b) M. S. Lowry, J. I. Goldsmith, J. D. Slinker, R. Rohl, R. A. Pascal, G. G. Malliaras, S. Bernhard, *Chem. Mater.* **2005**, *17*, 5712.
- ²⁶ J. E. Dander, E. L. Baker, N. K. Garg, *Chem. Sci.* **2017**, *8*, 6433.
- ²⁷ M. Salamone, F. Basili, R. Mele, M. Cianfanelli, M. Bietti, *Org. Lett.* **2014**, *16*, 6444.
- ²⁸ G. N. Papadopoulos, G. G. Kokotos, *J. Org. Chem.* **2016**, *81*, 7023.
- ²⁹ T. McCallum, L. Barriault, *J. Org. Chem.* **2015**, *80*, 2874.
- ³⁰ a) Y. Nishii, S. Akiyama, Y. Kita, K. Mashima, *Synlett* **2015**, *26*, 1831; b) Y. Kita, Y. Nishii, T. Higuchi, K. Mashima, *Angew. Chem. Int. Ed.* **2012**, *51*, 5723.
- ³¹ K. Mishiro, T. Kimura, T. Furuyama, M. Kunishima, *Org. Lett.* **2019**, *21*, 4101.
- ³² L. Liang, C. Chen, M. Luo, X. Zeng, *Org. Lett.* **2019**, *21*, 1912.
- ³³ S. Y. Chow, M. Y. Stevens, L. Åkerbladh, S. Bergman, L. R. Odell, *Chem. Eur. J.* **2016**, *22*, 9155.
- ³⁴ Y. Zheng, X. Nie, Y. Long, L. Ji, H. Fu, X. Zheng, H. Chen, R. Li, *Chem. Commun.* **2019**, *55*, 12384.

**- Chapter IV -
Photoreduction of
Hypercoordinated Silicon
Species**

Chapter IV. Photoreduction of Hypercoordinated Silicon Species

IV.1. Silicon derivatives as efficient radical precursors

In the previous chapters, we saw that silicon-based reagents such as silanes or silicates were quite efficient radical precursors. Nevertheless, all of them were used under photooxidative conditions and, to date, nothing can be found in the literature about photoreduction of silicon derivatives. Intrigued by this finding, we decided to investigate the behavior of some hypercoordinated silicon structures under photoreductive conditions. Our first idea was to study a variety of chlorosilane and silylium complexes (**Scheme 1**). Indeed, preliminary calculations by E. Derat on the phenyl chlorosilane bearing two 2-mercaptopyridine ligands, suggested the feasibility of the Si-R homolytic cleavage after electron capture. Thus, we first searched what is known about these compounds and how to synthesize them.

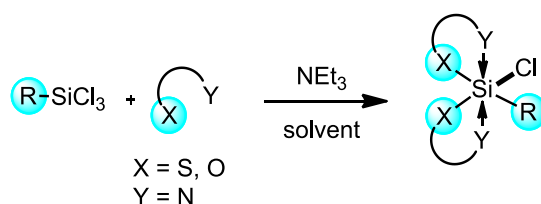


Scheme 1: Radical generation from hypercoordinated silicon derivatives under photoredox conditions

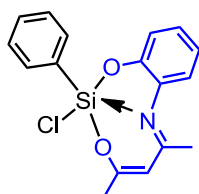
IV.2. Chlorosilane and silicon complexes

IV.2.1. Synthesis of hypercoordinated chlorosilanes

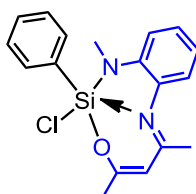
The synthesis of chlorosilane derivatives is mostly based on the utilization of a nucleophile (oxygen-, sulfur- or nitrogen-based), a trichlorosilane and a base (**Scheme 2**). Their synthesis is relatively straightforward but has to be done in a water-free environment because of their high reactivity toward nucleophiles which can lead to sol-gel side reactions.

**Scheme 2:** General synthesis of chlorosilanes

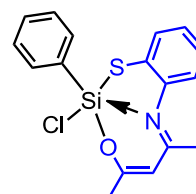
In the past few years, thanks to the work of Tacke's,¹ Wagler's,² Roewer's³ and Kraft's groups,⁴ various nucleophiles were utilized to produce different pentavalent and hexavalent silicon structures (**Scheme 3**). Even if most of the time phenyl trichlorosilane was used, other trichlorosilanes such as benzyl trichlorosilane and methyltrichlorosilane were found to react efficiently.

Pentavalent silicon complexes:

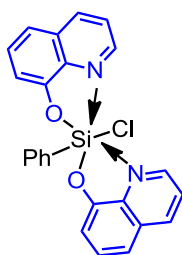
Tacke (2014)
 $\delta^{29}\text{Si}$ NMR (CD_2Cl_2): -97
 distorted trigonal bipyramid



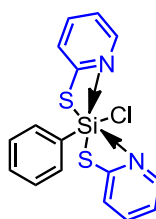
Tacke (2014)
 $\delta^{29}\text{Si}$ NMR (CD_2Cl_2): -96
 distorted trigonal bipyramid



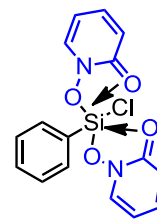
Tacke (2014)
 $\delta^{29}\text{Si}$ NMR (CD_2Cl_2): -83
 distorted trigonal bipyramid

Hexavalent silicon complexes:

Wagler (2014)
 $\delta^{29}\text{Si}$ NMR (solid state): -152
 distorted-octahedral



Tacke (2013)
 $\delta^{29}\text{Si}$ NMR (CD_2Cl_2): -154.1
 distorted-octahedral



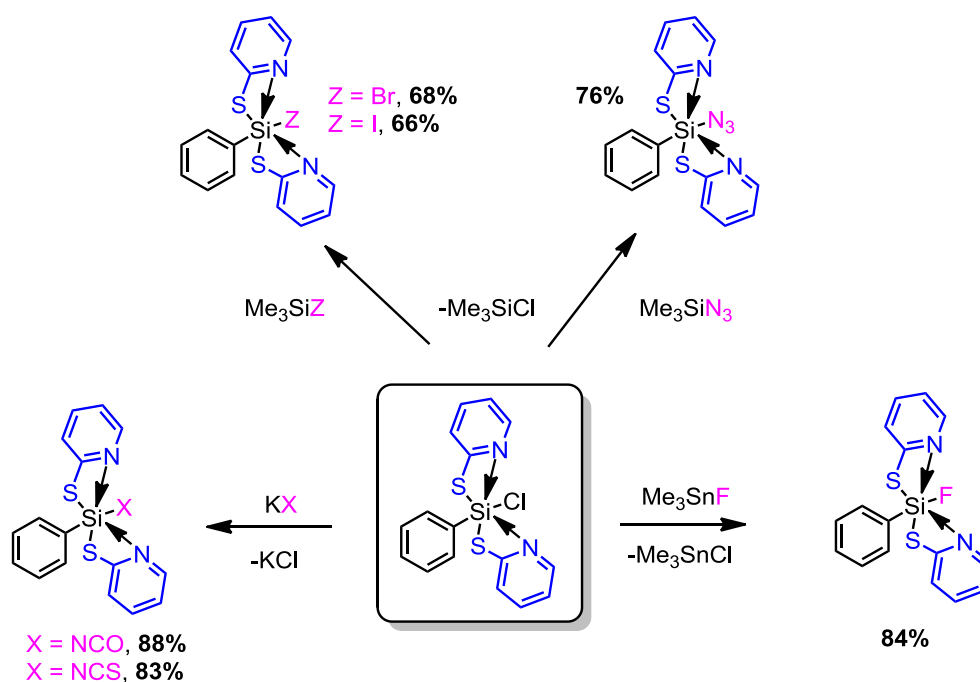
Kraft (2017)
 $\delta^{29}\text{Si}$ NMR (DMSO-d_6): -145.6
 distorted-octahedral

Scheme 3: Variety of chlorosilane complexes

In addition to highlight the ability of silicon to reach hypervalency, these compounds can also be used as building blocks to access other silicon complexes.

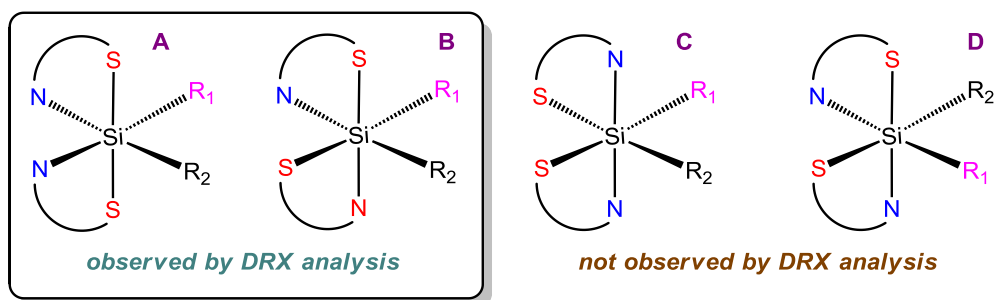
IV.2.2. Toward other silicon complexes

In 2013, Tacke *et al.* showed that various silicon complexes could be obtained by treating a chlorosilane derivative with different appropriate reagents (**Scheme 4**).^{1b} Me_3SiBr , Me_3SiI , Me_3SiN_3 , KNCO , KNCS and Me_3SnF were found to be very efficient and provided the corresponding products in good to excellent yields.



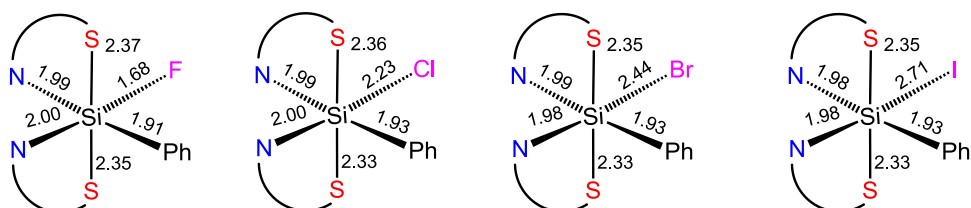
Scheme 4: Chlorosilanes as building blocks to access a variety of silicon complexes

Furthermore, during this investigation, Tacke's group made different observations. Firstly, only two of the four possible diastereoisomers were observed by XRD (**Scheme 5**). Thus, either only two diastereoisomers are formed during the synthesis or the two other ones are not crystalline. Then, depending on the studied complex, both **A** and **B** or either one or the other were observed. Moreover, all of these products crystallized in a distorted octahedral form except for the iodide one which crystallized in a strongly distorted trigonal bipyramid.



Scheme 5: Possible diastereomers

Secondly, changing the complex resulted in variations of the silicon-X bond lengths ($X = \text{F}, \text{Cl}, \text{Br}, \text{I}$). This trend was observed by XRD but, as the same diastereoisomer was not always obtained, the values could not be directly compared. Thus, they also computed the different bond lengths for each diastereoisomer. The result for diastereoisomer **A** can be found in **Scheme 6**. Even though, the length did not seem to be highly modified for the other bonds, a variation of more than 1 Å could be observed for the Si-X bond ($d_{\text{Si-F}} = 1.68 \text{ \AA}$, $d_{\text{Si-I}} = 2.71 \text{ \AA}$). As expected, the weakest Si-X bond, namely the Si-I bond, was the longest. For this complex, a dissociation even occurred leading to a silylium complex. This finding was also confirmed by XRD analysis. It is worth noting that all of the computed values were in agreement with the experimental data.



Scheme 6: Bond lengths (Å) of the different silicon complexes

After this publication, the same strategy has been applied to some of the structures represented in **Scheme 3** leading to even more silicon derivatives.⁴

Now that we know how to synthesize these compounds, we can focus on their utilization in organic synthesis.

IV.2.3. Chlorosilanes and silylium complexes as synthetic tools

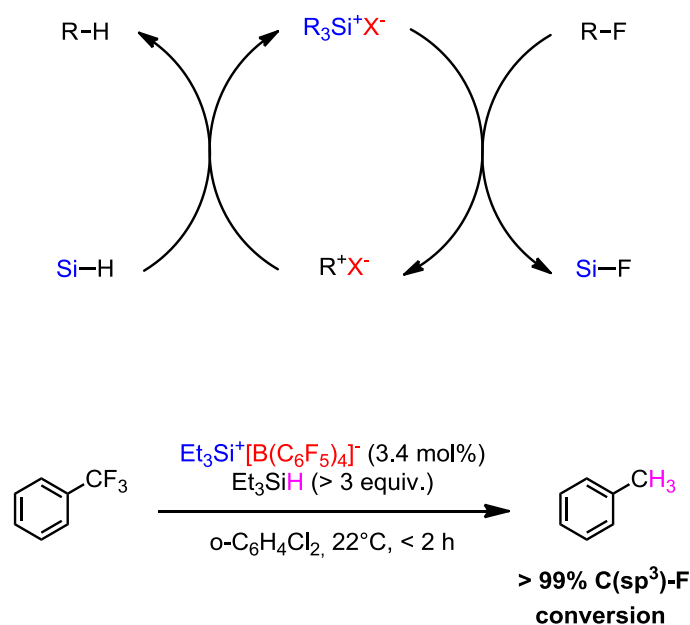
IV.2.3.1. Chlorosilanes as reagents in organic chemistry

The organic chemistry applications of such structures turned out to be quite limited in terms of “general reactions”. Indeed, chlorosilanes can be used as precursors to silyl anions⁵ or polysilanes⁶ but, due to their high sensitivity toward nucleophiles, they were mostly used as electrophiles (alcohol protection, Grignard addition...⁷).

On the contrary, silylium complexes were found to be efficient catalysts in various reactions.

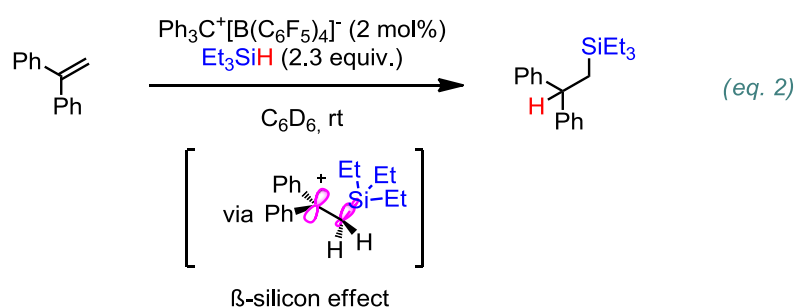
IV.2.3.2. Silyliums as reagents in organic chemistry

The first application which can be mentioned is the C-F bond activation. This general idea, represented in **Scheme 7**, was introduced by Ozerov *et al.* in 2005.⁸ In a first step, the silicon cation R_3Si^+ abstracts a fluoride ion. Then, the produced carbenium ion reacts with a triorganosilane R_3SiH to produce the hydrodefluorinated product and regenerate the silicon cation. This process is thermodynamically downhill because Si-F bonds (~159 kcal/mol) are stronger than C-F bonds (~108 kcal/mol).⁹ Of note, C-H bonds (~100 kcal/mol) are also stronger than Si-H bonds (~90 kcal/mol). By using such methodology, his group managed to produce different hydrocarbons from their fluorinated analogues. Later, this catalytic activity has been extended to other silylium complexes and to alkyl fluorides.¹⁰



Scheme 7: Si-H / C-F metathesis

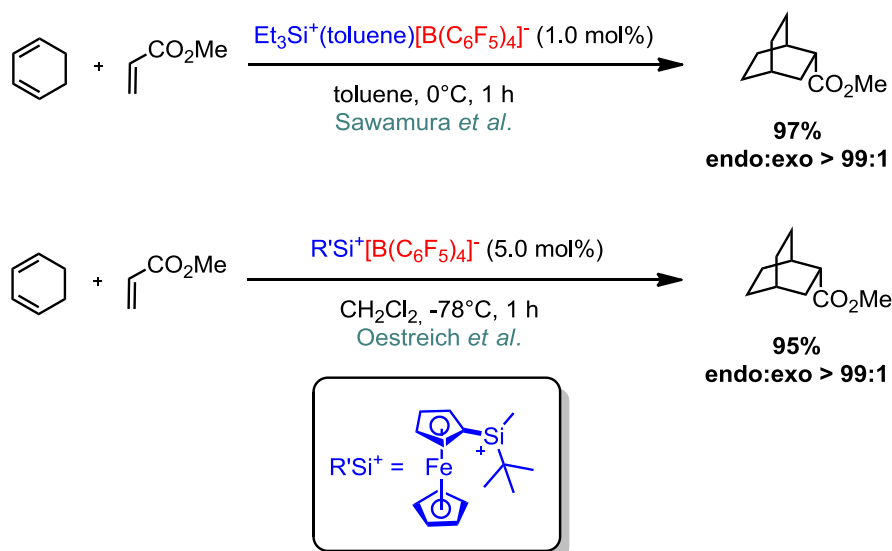
Silicon cations can also perform hydrosilylation reactions. In 1999, Lambert's group demonstrated that the silylium ion, formed after the silicon-to-carbon hydride transfer between $\text{Ph}_3\text{C}^+[\text{B}(\text{C}_6\text{F}_5)_4]^-$ and Et_3SiH (**Scheme 8**, *eq. 1*),¹¹ could react with alkenes through a hydrosilylation process (**Scheme 8**, *eq. 2*). This reaction was possible thanks to the β -silicon effect, meaning the stabilization of a carbocation in the β -position due to the overlaps of the σ orbital of the C–Si bond with the p orbital of the carbocation. Olefins with internal double bonds were also found to work. Nevertheless, because they are less reactive than terminal olefins, higher reaction temperatures and increased catalyst loadings are usually needed.¹²



Scheme 8: Hydrosilylation reaction

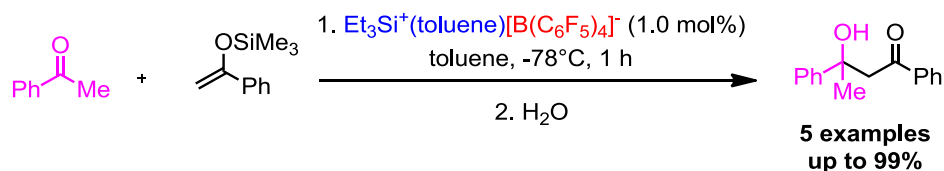
Later, this reactivity has been extended to other systems such as unactivated cyclopropanes and intramolecular hydrosilylation reactions by Oestreich's¹³ and Auner's¹⁴ groups.

Moreover, a trivalent silicon cation is also an outstanding Lewis Acid. This property was used in 2005 by Sawamura's group¹⁵ and by Oestreich's one¹⁶ in 2009 to perform some Diels Alder reactions at very low temperatures (**Scheme 9**). Only a catalytic amount of silylium, was needed to obtain excellent yields (> 95%) and endo:exo ratio up to 99:1 at very low temperature (0°C or -78°C) in only one hour. It is worth mentioning that, by using such methodology, other systems including challenging ones have also been found to work nicely.¹⁷



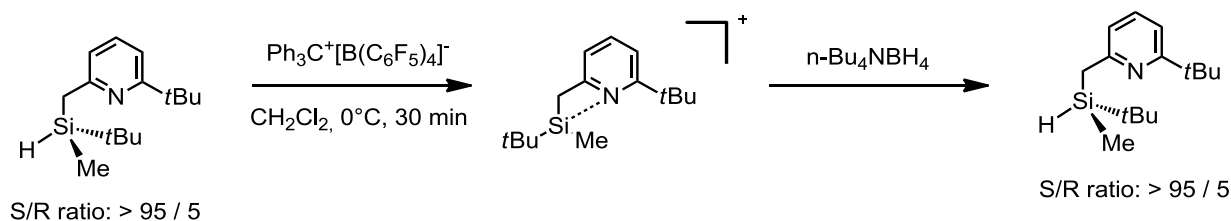
Scheme 9: Silylium as catalysts for Diels-Alder reactions

In 2005, Sawamura *et al.* extended silyliums utilization as Lewis acidic catalysts to Mukaiyama aldol reactions.¹⁴ By using only 1 mol% of a silicon cation, his group managed to produce the desired products in excellent yields in only one hour at -78°C (**Scheme 10**).



Scheme 10: Mukaiyama aldol reaction catalyzed by silylium

Landais's group also exhibited a memory of chirality at the silicon atom in various heterocycles-stabilized silyl cations (**Scheme 11**).¹⁸ This finding will probably be used in future development of catalysis.



Scheme 11: Chiral memory at the silicon atom

Nevertheless, even if a growing number of publications are using silyl cations, their high sensitivities and ability to form Lewis pairs remain an issue in numerous catalysis and reactions.¹⁹

After this introduction on chlorosilane and silylium complexes, we can present our study of their potential use under photoreductive conditions. The results can be found in the following publication.

IV.2.4. References

- ¹ a) J. Weiß, B. Theis, S. Metz, C. Burschka, C. F. Guerra, F. M. Bickelhaupt, R. Tacke, *Eur. J. Inorg. Chem.* **2012**, 2012, 3216; b) J. A. Baus, C. Burschka, R. Bertemann, C. F. Guerra, F. M. Bickelhaupt, R. Tacke, *Inorg. Chem.* **2013**, 52, 10664; c) B. Theis, S. Metz, F. Back, C. Burschka, R. Tacke, *Z. Anorg. Allg. Chem.* **2009**, 635, 1306.
- ² E. Wächtler, A. Kämpfe, K. Krupinski, D. Gerlach, E. Krokea, E. Brendlerb, J. Wagler, *Z. Naturforsch.* **2014**, 69b, 1402.
- ³ J. Wagler, U. Böhme, E. Brendler, B. Thomas, S. Goutal, H. Mayr, B. Kempf, G. Y. Remennikov, G. Roewer, *Inorganica Chimica Acta* **2005**, 38, 4270.
- ⁴ J. G. Koch, W. W. Brennessel, B. M. Kraft, *Organometallics* **2017**, 36, 594.
- ⁵ a) M. D. Visco, J. M. Wieting, A. E. Wattson, *Org. Lett.* **2016**, 18, 2883; b) V. Murugesan, V. Balakrishnan, R. Rasappan, *Journal of Catalysis* **2019**, 377, 293.
- ⁶ P. D. Lickiss, R. Lucas, *Journal of Organometallic Chemistry* **1993**, 44, 25.
- ⁷ a) M. N. Missaghi, C. M. Downing, M. C. Kung, H. H. Kung, *Organometallics* **2008**, 27, 6364; b) N. Kano, F. Komatsu, M. Yamamura, T. Kawashima, *J. Am. Chem. Soc.* **2006**, 128, 7097; c) A. Kawachi, H. Morisaki, M. Zaima, T. Teranishi, Y. Yamamoto, *Journal of Organometallic Chemistry* **2010**, 695, 2167.
- ⁸ V. J. Scott, R. Çelenligil-Çetin, O. V. Ozerov, *J. Am. Chem. Soc.* **2005**, 127, 2852.
- ⁹ M. A. Brook, *Silicon in Organic, Organometallic, and Polymer Chemistry*, Wiley, New York, **2000**, 30.
- ¹⁰ R. Panisch, M. Bolte, T. Müller, *J. Am. Chem. Soc.* **2006**, 128, 9676.
- ¹¹ J. Y. Corey, *J. Am. Chem. Soc.* **1975**, 97, 3237.
- ¹² E. Fritz-Langhals, *Org. Process. Res. Dev.* **2019**, 23, 2369.
- ¹³ a) M. Oestreich, *Angew. Chem. Int. Ed.* **2016**, 55, 494; b) A. Roy, V. Bonetti, G. Wang, Q. Wu, H. F. T. Klare, M. Oestreich, *Org. Lett.* **2020**, 22, 1213.
- ¹⁴ H. U. Steinberger, C. Bauch, T. Müller, N. Auner, *Can. J. Chem.* **2003**, 81, 1223.
- ¹⁵ K. Hara, R. Akiyama, M. Sawamura, *Org. Lett.* **2005**, 7, 5621.
- ¹⁶ a) H. F. T. Klare, K. Bergander, M. Oestreich, *Angew. Chem. Int. Ed.* **2009**, 48, 9077.
- ¹⁷ a) R. K. Schmidt, H. F. T. Klare, R. Frölich, M. Oestreich, *Chem. Eur. J.* **2016**, 22, 5376; b) P. Shaykhutdinova, M. Oestreich, *Org. Lett.* **2018**, 20, 7029; c) T. Gatzemeier, M. V. Gemmeren, Y. Xie, D. Höfler, M. Leutzsch, B. List, *Science* **2016**, 351, 949.
- ¹⁸ a) A. Fernandes, C. Laye, S. Pramanik, D. Palmeira, Ö. Ö. Pekel, S. Massip, M. Schmidtman, T. Müller, F. Roberts, Y. Landais, *J. Am. Chem. Soc.* **2020**, 142, 564; b) P. Ducos, V. Liautard, F. Roberts, Y. Landais, *Chem. Eur. J.* **2015**, 21, 11573.
- ¹⁹ H. F. T. Klare, M. Oestreich, *Dalton. Trans.* **2010**, 39, 9176.

IV.3. Towards Visible-Light Photocatalytic Reduction of Hypercoordinated Silicon Species

Published in *Helv. Chim. Acta.* **2019**, *103*, e1900238

IV.3.1. Abstract

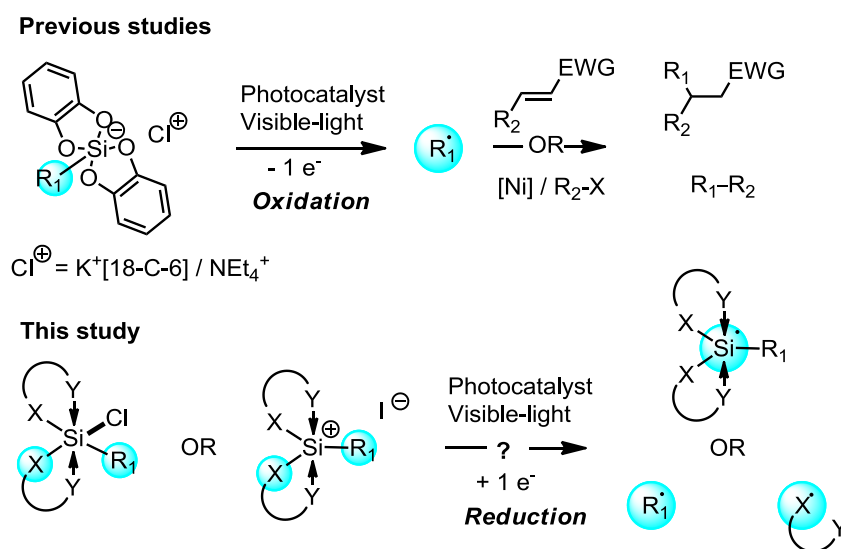
Nowadays, the quest of new radical precursors based on heteroatom complexes occupies an increasingly prominent position in contemporary research. Herein, we investigated the behavior and the limitations of hexa- or pentacoordinated organochlorosilanes and related pentacoordinated silyliums as new families of complexes for the generation of radicals under photocatalytic reductive conditions. Particularly, treatment of chlorophenylbis[N,S-pyridine-2-thiolato(-)]silicon(IV) or the related silylium derivative with the *fac*-Ir(ppy)₃ (5 mol%)/NEt₃ (1.5 equiv.) system under blue LED irradiation generates a thiopyridyl radical which can participate in the formation of a carbon-sulfur bond by reaction with an allylsulfone. Computational studies supported this experimental finding, and particularly by showing that homolytic fragmentation of C-Ts bond is favored over the fragmentation of thiopyridyl radical.

IV.3.2. Introduction

Over the last few decades, organosilicon compounds have received a great deal of attention in organic synthesis,^{1,2} and particularly radical synthetic chemistry, with the generation of transient silicon-centered radicals from silyl hydrides,^[3-8] behaving both as an effective mediator of radical reactions starting from a range of radical precursors (halides, chalcogens, xanthates, *etc.*) and as substrates for radical functionalization such as the hydrosilylation of unsaturated systems.^[3-8] The homolytic Si-H cleavage can be obtained for instance with the (TMS)₃SiH *Chatgialiloglu's* reagent^{[3-6],9,10} or the Et₃SiH/RSH system for polarity reversal catalysis introduced by *Roberts*.¹¹ More anecdotal, silyl radicals can be generated by photolysis of a Si-B bond for the silylboration of olefins¹² or by photocatalytic oxidation of the supersilanol (TMS)₃SiOH to perform halogen abstraction for Nickel/photoredox sp³-sp³ cross-coupling reactions.¹³ As another interesting property, organosilicons with an activated C-Si bond as well as hypercoordinated - penta- or hexacoordinated - silicon derivatives^[14-17] have revealed as a potential source of carbon-centered radicals under oxidative conditions, which can participate in further synthetic transformations.

A SET oxidation-desilylation of benzyltrimethylsilanes involving visible-light excited chiral iminium ions,¹⁸ 9-mesityl-10-methylacridinium perchlorate salt¹⁹ or graphitic carbon nitride²⁰ as a catalytic and strong photooxidant, allowed the formation of benzylic radicals which can be trapped by ground-state iminium ions or *Michael*-type acceptors respectively. In the same vein, α -alkoxymethyl radicals were successfully generated from the corresponding α -silyl ethers^[21-23] by photocatalyzed oxidation, as well as acyl radicals from acyl silanes.²⁴ But interestingly, what about the reactivity of hypercoordinated silicon derivatives under oxidative

conditions? This question was first answered by *Kumada* who reported the oxidation of organopentafluorosilicates to provide organic radicals which can react with a second equivalent of copper chloride and liberate the chlorinated product. However, this transformation required stoichiometric amount of copper salts and the low solubility of these substrates limits their use for synthesis.^{25,26} In that context, *Nishigaishi* reported the photoallylation^{27,28} of benzyl-type derivatives and dicyanobenzene with the more soluble allyl bis-catecholato silicate²⁹ but these studies were limited to the generation of allylic radical. Following our initial work on the oxidation of alkyltrifluoroborates in 2010,³⁰ we prepared a series of bench stable alkyl biscatecholato silicates with a low oxidation potential ($< +1$ V vs. SCE) and tested them under visible-light photooxidative condition³¹ in order to generate functionalized alkyl radicals and particularly primary ones.^{32,33,[34-49]} The scope of substrates for simple radical trapping and also for photoredox/nickel dual catalysis proved to be quite large from primary to tertiary radicals^{31,32, [50-54]}

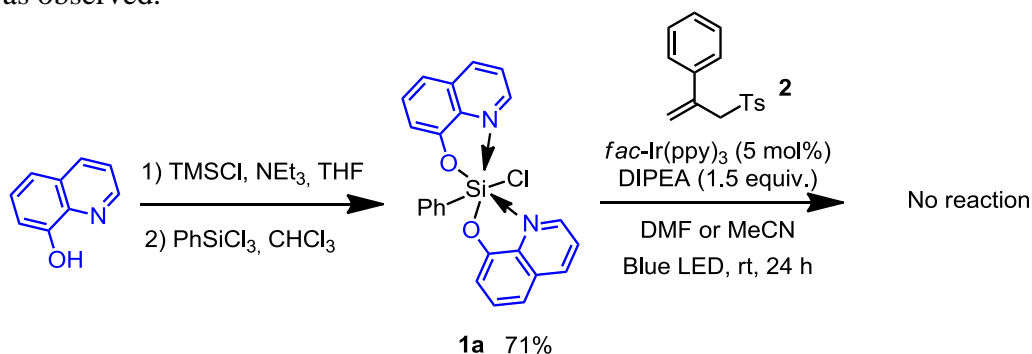


Scheme 1: Hypercoordinated silicon compounds as a source of radicals under photooxidative or photoreductive conditions

To date, the use of hypercoordinated silicon derivatives in radical synthesis has been limited to the generation of radicals under oxidative regimes and no attempt has been made in a reductive manner. Herein, we reported the first results about the behavior of hypercoordinated chlorosilanes and the related cationic silicon derivatives under visible-light photoreductive conditions to generate radical species. We presumed that the presence of hypercoordinated ligands or the formation of silylium salts would favor the labilization of the Si-Cl bond during the reduction step to provide the formation of hypercoordinated silyl radicals. The latter may subsequently expel a carbon- or heteroatom-centered radical (R_1 or X, respectively) (**Scheme 1**).

IV.3.3. Results and Discussion

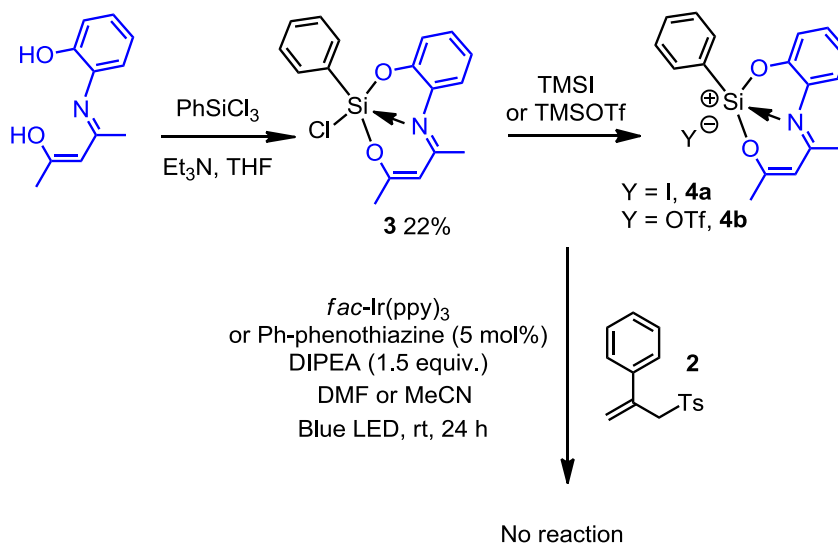
We thus tested the photoreduction of a set of hypercoordinated chlorosilanes whose synthesis has already been described in the literature. We started to investigate the reactivity of hexacoordinated silicon compounds with bidentate N,O ligands such as 8-oxyquinolinato ligands. We first prepared compound **1a** from phenyltrichlorosilane and 8-hydroxyquinoline using the procedure developed by Wägler in 2014 (Scheme 2).⁵⁵ We tried to evaluate the reduction potential of **1a** by cyclic voltammetry (CV) but, due to the insolubility of this organosilicon in acetonitrile and THF, it could not be determined. Nevertheless, we explored the photoreduction of **1a** using the highly reductant photocatalyst *fac*-Ir(ppy)₃ (5 mol%, E Ir (IV)/ Ir (III)* = -1.7 V vs. SCE) under blue LED irradiation in the presence 1.5 equiv. of allylsulfone **2** as a radical acceptor and 1.5 equiv. of N,N-diisopropylethylamine (DIPEA) as sacrificial electron donor for the regeneration of the photocatalyst (Scheme 2). Whatever the nature of the solvent (0.1 mol/L), acetonitrile (CH₃CN) or dimethylformamide (DMF), no reaction occurred leaving the allylsulfone **1a** unchanged. Butyl and benzyl chlorosilanes were also efficiently synthesized (86% and 84% yield, respectively) and investigated but no reaction was observed.



Scheme 2: Synthesis of hexacoordinated silicon compound **1a** with 8-oxyquinolinato ligands and reactivity in the presence of allylsulfone **2** under visible-light photoreductive conditions

In a second phase, we looked at more soluble silicon derivatives. In 2012, Tacke's group reported the formation of pentacoordinate chlorosilicon(IV) complexes with tridentate dianionic O, N, O ligands such as the tridentate 2-((E)-(Z)-4-hydroxypent-3-en-2-ylidene)amino)phenol ligand.⁵⁶ We then synthesized the corresponding complex **3** as reported in Scheme 3 and measured its reduction potential by CV. To our delight, we were pleased to see that the reduction potential of the hypercoordinated species **3** is higher than the tetravalent phenyl trichlorosilane (PhSiCl₃), that is, -1.60 V vs. SCE compared to -1.95 V vs. SCE (see cyclic voltammogram of **3** (Figure 1) and Supporting Information). This suggests that this tridentate ligand significantly increases the ability of the chlorosilane to be reduced. Compound **3** was then subjected to the same reaction conditions used for **1a**, but again no reaction was observed by TLC and confirmed by ¹H NMR (Scheme 3). Only starting materials were recovered. Even after addition of additives such as TMSI or TMSOTf to generate *in situ* the corresponding electron deficient silylium derivatives **4a** and **4b** (not characterized),⁵⁷ no product was obtained and only degradation was seen. Switching from *fac*-

$\text{Ir}(\text{ppy})_3$ to a highly reducing organic photocatalyst such as N-phenylphenothiazine (Ph-PTZ) ($E \text{ Ph-PTZ}^{*+} / \text{P Ph-PTZ}^* = -2.5 \text{ V vs. SCE}$),⁵⁸ did not afford any product either.



Scheme 3: Synthesis of pentacoordinated silicon compound **3**, using 2-{(E)-(Z)-4-hydroxypent-3-en-2-ylidene}amino}phenol ligand, and the corresponding silylium derivatives **4a** and **4b** as well as their reactivity in the presence of allylsulfone **2** under visible-light photoreductive conditions

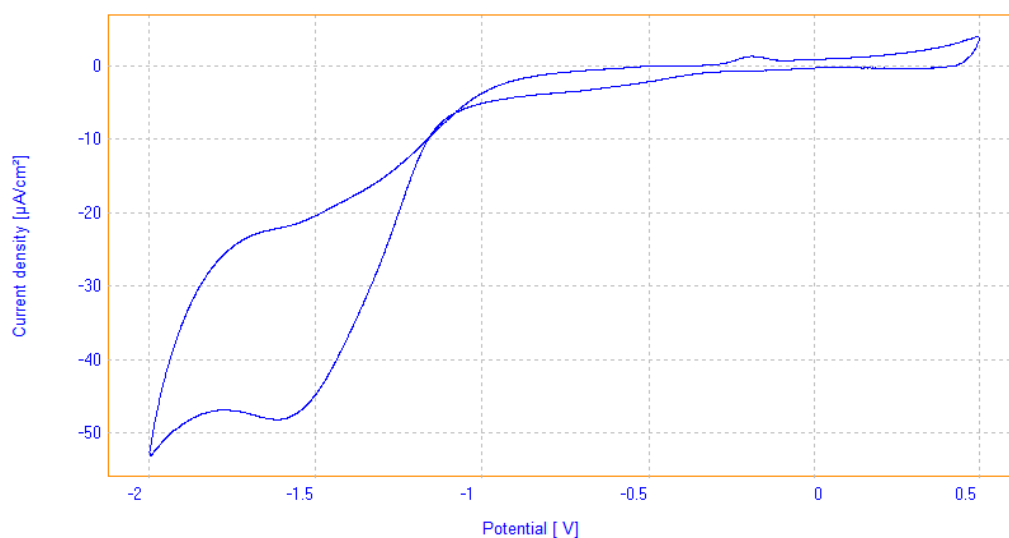
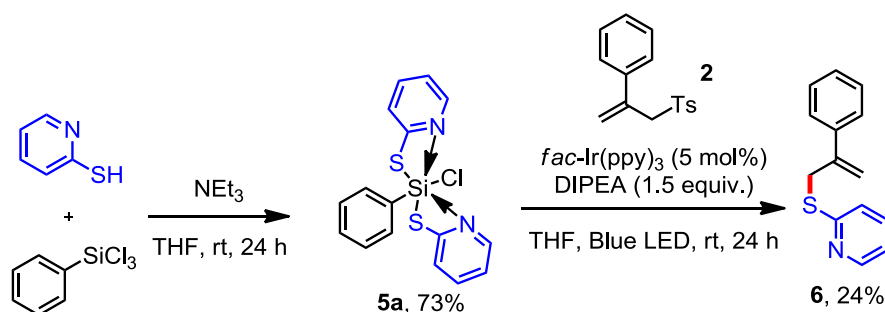


Figure 1: Electrochemical studies: Cyclic voltammogram of **3** (10 mM) performed at 22°C in dried and degassed THF containing Bu_4NPF_6 (100 mM) as the supporting electrolyte at a scan rate of 0.1 V.s^{-1} . Glassy carbon, platinum plate and saturated calomel were used as working, counter and reference electrodes respectively

Thereafter, we were particularly interested in the photoreduction of hexacoordinated silicon complexes with two bidentate N,S-pyridine-2-thiolato ligands.⁵⁷ In this case, we may benefit from the possible stabilization of the generated silyl radical by the sulfur atom as already observed in the disulfide bond.⁵⁹ Chlorophenylbis[N,S-pyridine-2-thiolato(-)]silicon(IV) (**5a**) was then synthesized following the protocol reported by *Tacke* in 2013 as outlined in **Scheme 4**. Its reduction potential can be estimated by CV and showed a value of about -1.49 V vs. SCE (**Figure 2**), higher than the reduction potentials previously determined for the hypercoordinated silicon species **3** (*vide supra*). This increase of potential should facilitate the reduction of compound **5a** by the excited state of the photocatalyst *fac*-Ir(ppy)₃ (**Scheme 4**). This substrate was then treated under the same conditions as **1a** and **3**. Allylsulfide **6**, resulting from the addition of the ligand 2-thiopyridine to the allylsulfone **2**, was obtained in a 24% yield. We wondered if the yield in **6** can be improved and if this transformation involves a radical or an ionic pathway.



Scheme 4: Synthesis of hexacoordinated silicon compound **5a**, using N,S-pyridine-2-thiolato ligand followed by their reactivity in the presence of allylsulfone **2** under visible-light photoreductive conditions. Formation of allylsulfide **6**

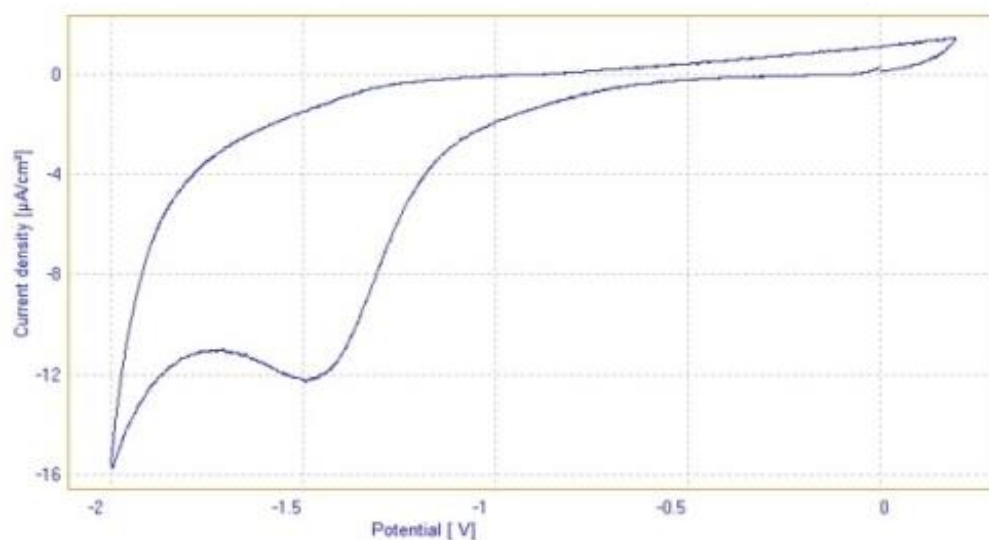


Figure 2: Electrochemical studies: Cyclic voltammogram of **5a** (10 mM) performed at 22°C in dried and degassed THF having Bu₄NPF₆ (100 mM) as the supporting electrolyte at a scan

rate of $0.1 \text{ V}\cdot\text{s}^{-1}$. Glassy carbon, platinum plate and saturated calomel were used as working, counter and reference electrodes respectively

Encouraged by these preliminary results, we first optimized the reaction conditions by screening the nature of the photocatalyst or the electron donor, by using different solvents and by modulating the reaction time or the ratio radical trap/hypercoordinated silicon (**2/5a**). Both DMF and CH_3CN have proved to be beneficial solvents for the reaction, while the reaction was less effective in THF (**Table 1**, entries 1- 3 and 9). With respect to the sacrificial electron donor, changing DIPEA to triethylamine gave a comparable yield while no reaction was observed with Hantzsch ester (**Table 1**, entries 2, 3 and 4). An extended irradiation time from 24 h to 48 h did not improve the photoreductive process (**Table 1**, entries 3 and 5). No more than 45% yield was reached with an excess of allylsulfone **2** (4 equiv., **Table 1**, entry 6). By contrast, if we consider allylsulfone **2** as the limiting substrate, addition of 2 or 3 equiv. of organochlorosilane **5a** led to 66 or 78% of **6**, respectively (**Table 1**, entries 7 and 8). An organic dye such as fluorescein (F) ($E(\text{F}^+/\text{F}^*) = -1.61 \text{ V vs. SCE}$) was investigated as an alternative to *fac*- $\text{Ir}(\text{ppy})_3$ but only 4% of **6** was obtained after 24h of irradiation (**Table 1**, entry 10).

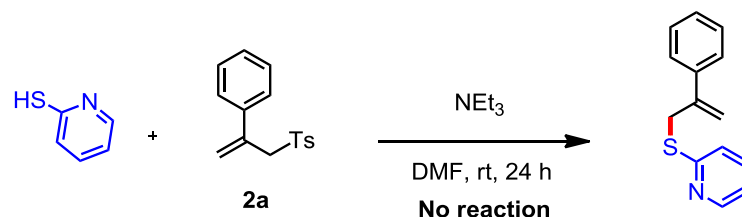
Entry	Solvent	PCat	Equiv. (2/5a)	Time (h)	Donor	yield ^[a]
1	THF	<i>fac</i> -Ir(ppy) ₃	1.5/1	24	DIPEA	24%
2	DMF	<i>fac</i> -Ir(ppy) ₃	1.5/1	24	DIPEA	35%
3	DMF	<i>fac</i> -Ir(ppy) ₃	1.5/1	24	Et ₃ N	36%
4	DMF	<i>fac</i> -Ir(ppy) ₃	1.5/1	24	Hantzsch ester	0%
5	DMF	<i>fac</i> -Ir(ppy) ₃	1.5/1	48	Et ₃ N	37%
6	DMF	<i>fac</i> -Ir(ppy) ₃	4/1	24	DIPEA	45%
7	DMF	<i>fac</i> -Ir(ppy) ₃	1/2	24	Et ₃ N	66%
8	DMF	<i>fac</i>-Ir(ppy)₃	1/3	24	Et₃N	78%
9	MeCN	<i>fac</i> -Ir(ppy) ₃	1.5/1	24	Et ₃ N	32%
10	MeCN	Fluorescein	1.5/1	24	DIPEA	4%
11	DMF	-	1/3	24	Et ₃ N	33%
12	DMF	<i>fac</i> -Ir(ppy) ₃	1/3	24	-	26%
13	DMF	<i>fac</i> -Ir(ppy) ₃	1/3	24	Et ₃ N	0% ^[b]
14	DMF	-	1/3	24	-	26%

^[a] NMR yield using TMOP as internal standard; ^[b] in the dark

Table 1: Optimization of the reaction conditions and control reactions

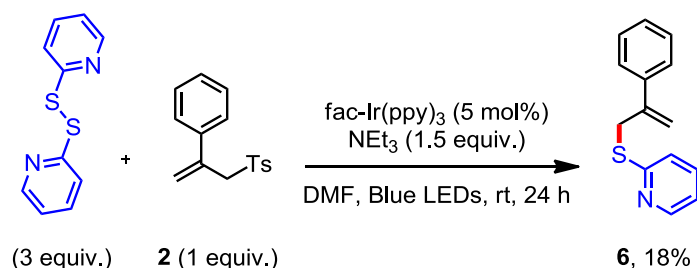
Control experiments have been performed to secure the role of the photocatalyst and a radical process (**Table 1**, entries 11- 13). Without any photocatalyst and amine, 26% of product was obtained due to the degradation of the silicon complex (**Table 1**, entry 14). In the absence of photocatalyst, we ran the reaction under blue LED irradiation and allylsulfide **6** was obtained in 33% yield (**Table 1**, entry 11). This slight increase of yield in comparison to entry **16** may arise from a photoinduced electron-transfer (PET) between NEt₃ and the organosilane **5a**. No reaction occurred without blue LED activation. Only 26% for **6** was obtained when NEt₃ was omitted (due to the degradation of the complex). Even if we showed that the presence of the photocatalyst *fac*-Ir(ppy)₃ is required to reach a good yield, we tested the reactivity between pyridine-2-thiol and acceptor allylsulfone **2** under basic conditions. As expected, no trace of **6** was formed showing that the formation of the allylation adduct does not involve an ionic pathway and a radical process is likely to occur (**Scheme 5**). Of note, addition of *fac*-Ir(ppy)₃ (5 mol%) to this mixture led to only 9% yield of **6**. From these last studies, we can deduce that most of thiopyridyl radicals were generated by reduction of silane **5a** leading to adduct **6**,

and not from the decomposition of **5a**. We also can mention that energy transfer instead of electron transfer from the iridium complex *fac*-Ir(ppy)₃ is probably negligible.ⁱ



Scheme 5: Control experiment: reactivity between pyridine-2-thiol and acceptor allylsulfone **2** under basic conditions

In parallel, we examined the behavior of the commercially available *Aldrithiol*TM under the same photocatalytic conditions, as a potential source of thiopyridyl radical. Starting from three equivalents of this compound, only a 18% yield of **6** was obtained compared to 78% from **5a**. This study showed all the interest of **5a** as an efficient precursor of thiopyridyl radical for synthetic transformations (**Scheme 6**).



Scheme 6: Photocatalytic reaction using *Aldrithiol*TM as a radical precursor

Computational studies have been realized, namely at the B3LYP-D3/def2-SV(P) level with the TURBOMOLE suite of programs. Upon reduction, it was showed that the SET process is occurring on the π system of the pyridine moiety of **5a** (**Figure 3**, lower part), in a similar manner to what have been observed with our biscatecholato silicates except that in this case this is an electron capture by the photocatalyst.³¹ If we compare the various BDEs of the substrates before and after oxidation, this reduction strongly weakens all Si-X (X = C, S, Cl) bonds. Particularly, the energy of the Si-S bond (35 kcal/mol) is lower than the one of the Si-C bond (46 kcal/mol) and the Si-Cl bond (63 kcal/mol) and should favor the formation of the thiopyridyl radical (**Figure 3**). We also investigated the non-hypercoordinated tetravalent

ⁱ In response to a referee that we thank for her/his suggestions, we first measured the UV/Visible spectrum which showed a characteristic band centered at 290 nm and a large one between 320 nm and 440 nm. This might explain the formation of thiopyridyl radical both under UV (350 nm) or blue LED irradiation. Thus, we performed a reaction with benzophenone as photosensitizer (with a triplet energy (69.1 kcal/mol) higher than that of *fac*-Ir(ppy)₃ (58.1 kcal/mol) under UV irradiation (350 nm). The yield did not increase significantly which suggests that the energy transfer from the iridium complex *fac*-Ir(ppy)₃ would be negligible compared to the electron transfer process. This was also supported by the photoinduced electron-transfer (PET) reaction observed between NEt₃ and the organosilane **5a** in **Table 1**, Entry 11.

species with two phenylthio ligands, to directly compare the various BDE values with **5a**. This species is plotted on the right side of **Figure 3**. The reduction process is taking place on the phenylthio moiety but the energy of the Si-S bond before reduction (76 kcal/mol) is higher than for the hypervalent silane **5a** (66 kcal/mol). This comparison shows also that while **5a** has a positive electron affinity (10.35 kcal/mol), this is not the case for (PhS)₂Si(Cl)Ph (-1.96 kcal/mol), highlighting the ease of reduction of **5a**. As for **5a**, we also observed a small BDE of 27 kcal/mol after reduction. The other bonds are similarly affected by the reduction with the Si-Cl bond having a BDE of 64.5 kcal/mol and the Si-Ph being at 40 kcal/mol.

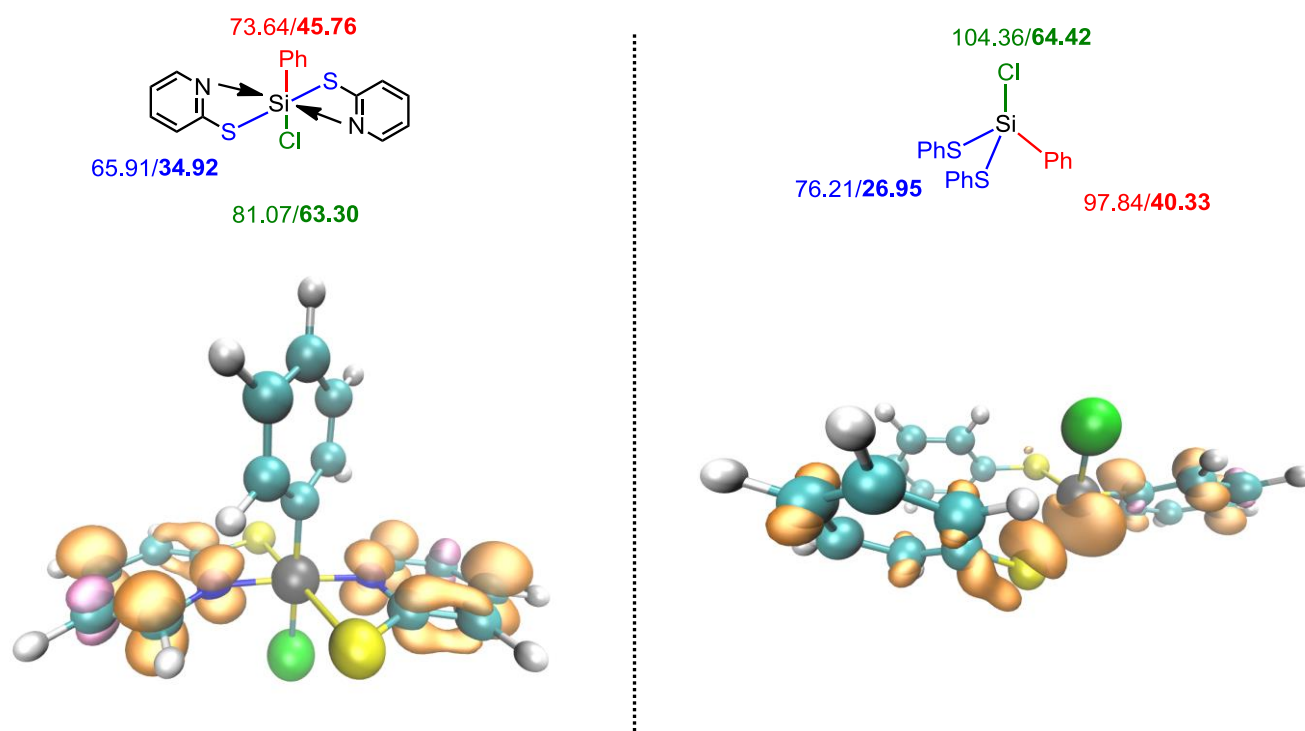


Figure 3: Computational studies on **5a** and on phenylbis(phenylthiol)chlorosilane. Upper part: bond dissociation energies before and after reduction. Lower part: spin density isosurfaces

Based on these experimental studies, DFT calculations and in accordance with the literature,^[33-48] we can propose the following mechanism where the photoactivated catalyst under blue LED irradiation reduces hypercoordinated phenylchlorosilane **5a** at the pyridine moiety and promotes preferentially the homolytic cleavage of the Si-S bond between the thiopyridine ligand and silicon atom. The expelled thiopyridyl radical can be trapped by allylsulfone **2**. The photocatalyst is regenerated by action of NEt₃ (**Scheme 7**). It should be mentioned that formation of **6** involved sequential addition of the thiopyridine radical, generation of the transient radical intermediate **A** and homolytic fragmentation of the C-Ts bond. We were surprised by the fact that intermediate **A** is more prone to give the homolytic

fragmentation of the C-Ts bond rather than the reversible extrusion of the thiopyridine radical moiety. It is indeed known in the literature that a thiophenyl radical is a good leaving group, presumably better than the phenylsulfonyl one.^{60,61} To rationalize the observed selectivity, DFT calculations of β -fragmentation processes on intermediate **A** and on an analogous intermediate (**A'**) where the pyridine moiety is replaced by a phenyl were thus conducted, at the same level of theory (namely B3LYP-D3/def2-SV(P)). On **A'**, calculations indicate that departure of the tosyl radical is slightly favored over the thiophenyl radical fragmentation (barriers of 8.4 kcal/mol vs. 9.3 kcal/mol). But the situation is different in the case of intermediate **A**: while the tosyl radical departure is still in the same energetic range with a barrier of 9 kcal/mol, the thiopyridyl radical extrusion proves to be unfeasible with an always increasing potential energy surface (see **Figure 4**), reaching value over 18 kcal/mol. It turns out that the thiopyridyl radical is particularly unstable, and observation of the geometry highlights that this radical is trying to establish non-covalent interactions between the nitrogen of the pyridine moiety and the homobenzylic C-H to stabilize itself (see **Figure 5**). Therefore, the mechanism proposed in **Scheme 7** is supported by this computational analysis

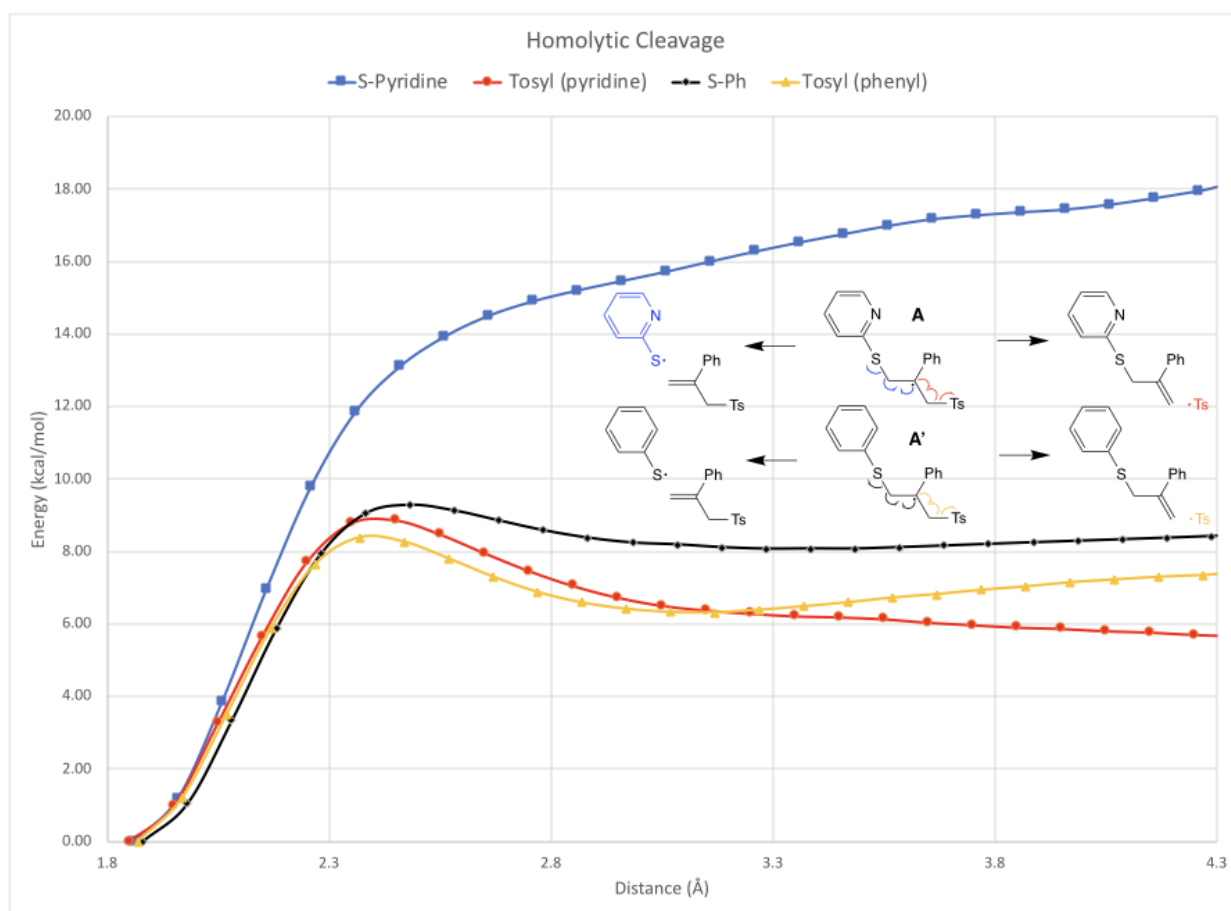


Figure 4: Calculated β -fragmentation processes for intermediate **A** and **A'**, at the B3LYP-D3/def2-SV(P) level

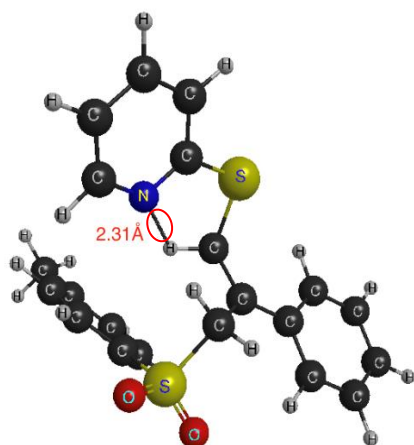
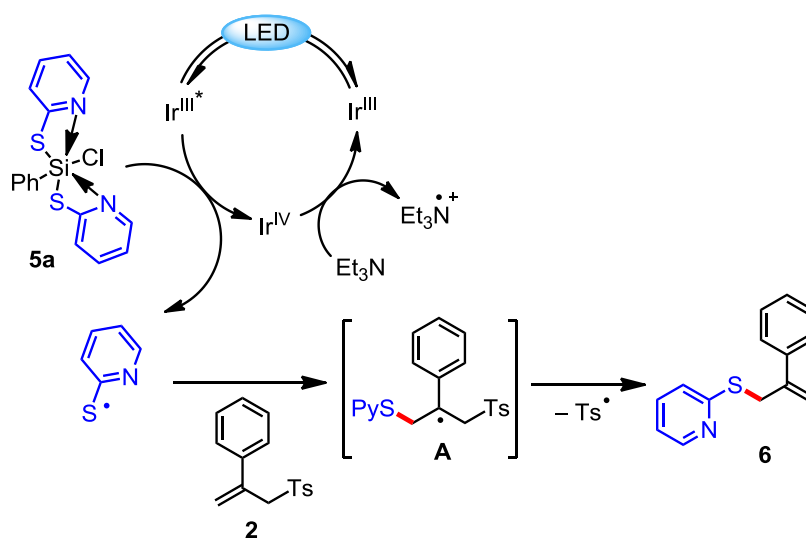
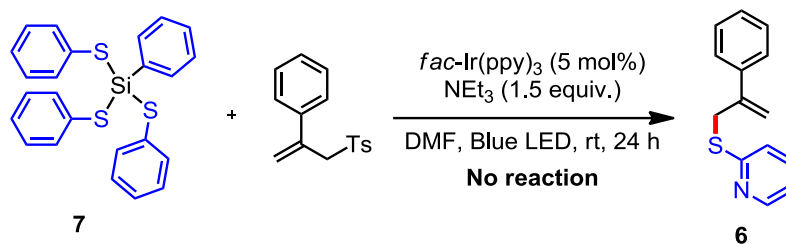


Figure 5: Structure of the intermediate A

Scheme 7: Proposed mechanism for the formation of **6**

Due to the weakness of the Si-S bond and its ability to generate thiyl radicals under reductive conditions, we compared the reactivity of our previous system (**5a**) with the non-hypercoordinated tetravalent phenylsilane bearing three phenylthio ligands **7** (Scheme 8). This one was synthesized from phenylsilane and thiophenol according to the literature procedure.⁶² Its reduction potential was then measured. A value of -2.00 V vs. SCE was obtained which appears to be lower than the reduction potential of **5a** (Figure 6). This difference of potential may explain why no allylation adduct **6** was formed from **7** under the same reductive conditions (Scheme 8).



Scheme 8: Photocatalytic reaction using phenyltris(phenylthio)silane as a radical precursor

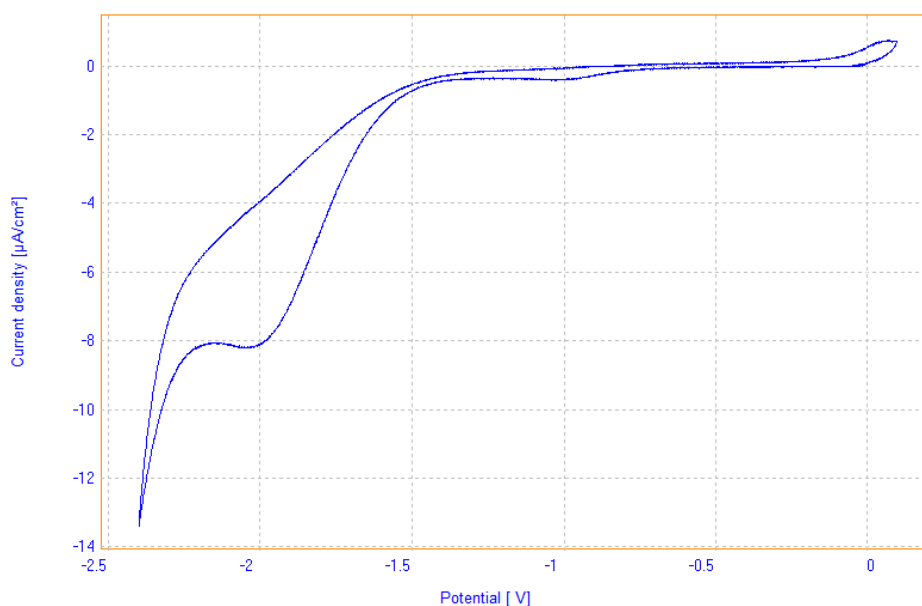
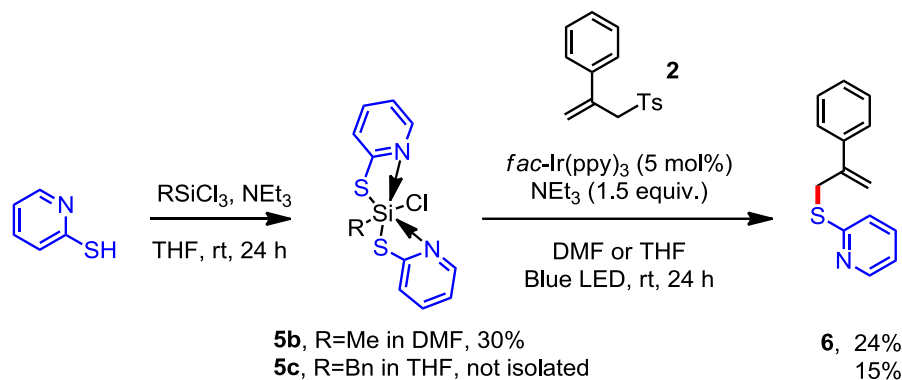


Figure 6: Electrochemical studies: cyclic voltammetry of **7** (10 mM) performed at 22°C in dried and degassed THF containing Bu_4NPF_6 (100 mM) as the supporting electrolyte at a scan rate of $0.05 \text{ V}\cdot\text{s}^{-1}$. Glassy carbon, platinum plate and saturated calomel were used as working, counter and reference electrodes, respectively

We next evaluated the reactivity of the hypercoordinated methylchlorosilane **5b** under photocatalytic reductive conditions. We first prepared it by using the same procedure as for **5a** starting from methyltrichlorosilane and then we measured its reduction potential, which was estimated by CV at about -1.68 V (*vs.* SCE) (**Figure 7**). This value still suggests that the photo-excited photocatalyst fac-Ir(ppy)_3 ($E \text{ Ir(IV)/Ir(III)}^* = -1.7 \text{ V vs. SCE}$) can reduce this substrate. Treatment of **5b** (3 equiv.) with **2** (1 equiv.) in the presence of fac-Ir(ppy)_3 (5 mol%) and Et_3N (1.5 equiv.) in DMF under blue LED irradiation gave **6** in 31% yield (**Scheme 9**). It should be noted that no addition of the methyl group was observed. For comparison, its benzyl analog **5c** has also been investigated. This compound was prepared *in-situ* from benzyltrichlorosilane but could not be isolated. Nevertheless, the photocatalytic reaction was carried on the crude mixture and the allylsulfide **6** was obtained in 15% yield as the only product.

From those experiments, only the thiopyridyl radical was formed as evidenced by trapping experiments with allylsulfone **2**. The phenyl derivative was revealed to be the most reactive and provided the best yield in allylsulfide **6**. Interestingly, formation of phenyl, methyl or benzyl radical was never observed in these studies.



Scheme 9: Synthesis of hexacoordinated silicon compounds **5b** and **5c**, using N,S-pyridine-2-thiolato ligand followed by their reactivity in the presence of allylsulfone **2** under visible-light photoreductive conditions. Formation of allylsulfide **6**.

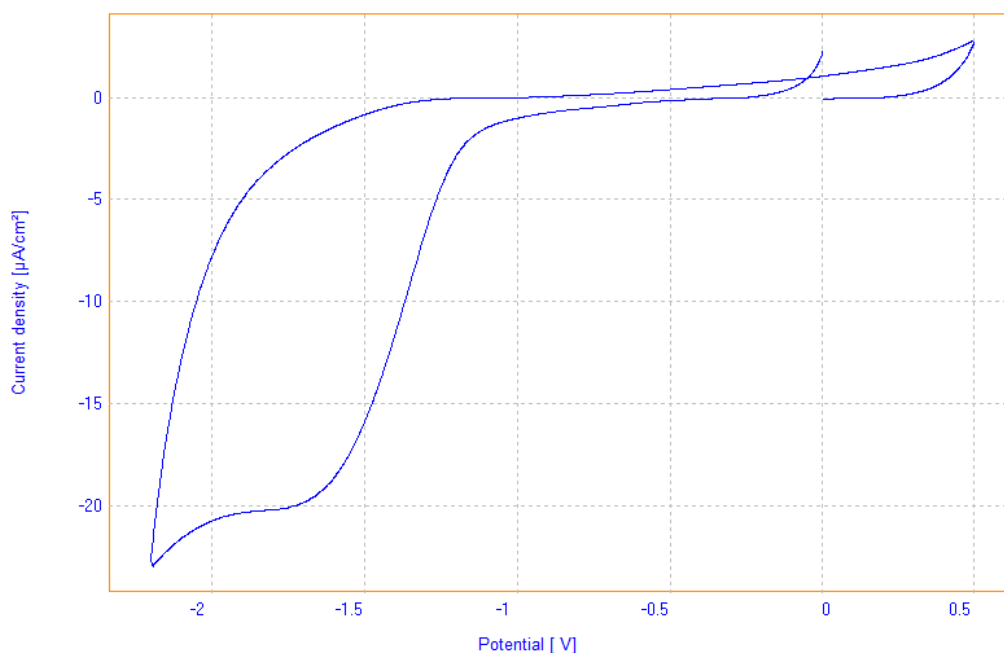
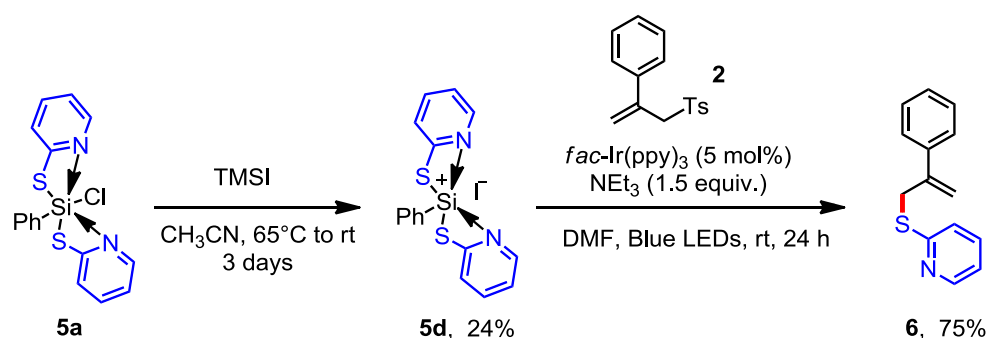


Figure 7: Electrochemical studies: Cyclic voltammogram of **5b** (10 mM) performed at 22°C in dried and degassed THF containing Bu_4NPF_6 (100 mM) as the supporting electrolyte at a scan rate of $0.1 \text{ V}\cdot\text{s}^{-1}$. Glassy carbon, platinum plate and saturated calomel were used as working, counter and reference electrodes, respectively

We investigated by DFT calculations the fate of the silyl anion originating from the reduction of hypercoordinated alkylchlorosilanes **5** and subsequent fragmentation of the thiopyridyl radical. We found that chloride anion dissociation occurs with an energy barrier of 8.6 kcal/mol providing the formation of a transient highly reactive silylene.ⁱⁱ

Finally, we looked at the photoreduction of the highly electron deficient silylium derivative **5d** readily obtained by action of TMSI on the corresponding phenylchlorosilane **5a**.⁵⁷ Under the optimized photocatalytic conditions determined for **5a**, **5d** provided **6** as the sole product with the same yield as **5a**. This result showed that silylium **5d** can be reduced as efficiently as phenylchlorosilane **5a** and participate in radical reactions (**Scheme 10**).



Scheme 10: Synthesis of silylium derivative **5d**, using N,S-pyridine-2-thiolato ligand followed by their reactivity in the presence of allylsulfone **2** under visible-light photoreductive conditions. Formation of allylsulfide **6**.

Interestingly, as the thiopyridine moiety is encountered in various bioactive molecules (**Figure 8**),^{63,64} efficient reactions allowing the synthesis of these compounds in mild conditions remains interesting.⁶⁵

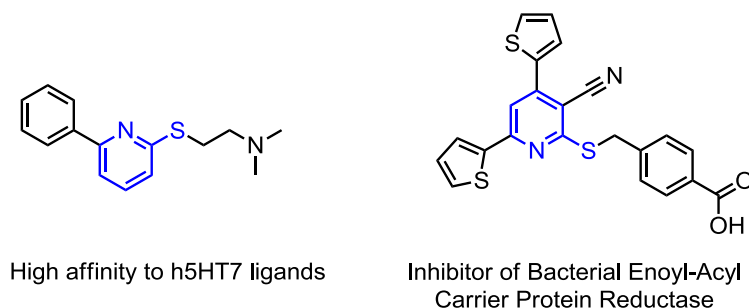


Figure 8: Bioactive molecules containing a thiopyridine scaffold

ⁱⁱ We are grateful to the referees for their questions on the nature of the generated Si-species generated after the reaction, and particularly the fate of the silyl anion.

IV.3.4. Conclusion

In conclusion, we have demonstrated that the modification of the ligands of hexacoordinated chlorosilane derivatives can efficiently modulate their reactivity towards photoreductive conditions. By using a thiopyridine ligand, the corresponding thiyl radical has been liberated and efficiently trapped by an allylsulfone as an acceptor. Even if these radicals could be formed through the oxidation of pyridine thiolate like phenyl thiolate,⁶⁶ no methodology has already been reported by using a reductive pathway. Experiments are currently ongoing in our laboratory for the formation of carbon-centered radicals by photoreduction of other types of hypercoordinated silicon species.

IV.3.5. Supporting information

IV.3.5.1. General informations

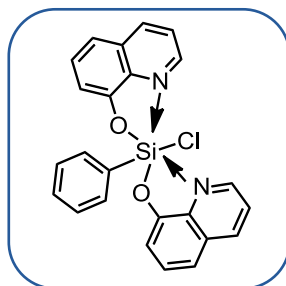
Unless otherwise noted, reactions were carried out under an argon atmosphere in oven-dried glassware. THF, acetonitrile and diethyl ether were distilled over sodium/benzophenone, triethylamine over potassium hydroxide. Reagents and chemicals were purchased from commercial sources and used as received. Infrared (IR) spectra were recorded on a Bruker Tensor 27 (ATR diamond) spectrophotometer. ^1H , ^{13}C NMR spectra were recorded at room temperature at 400 and 100 MHz respectively, on a Bruker AVANCE III 400 spectrometer. Chemical shifts (δ) are reported in ppm and coupling constants (J) are given in Hertz (Hz). Abbreviations used for peak multiplicity are: s (singlet); bs (broad singlet); d (doublet); t (triplet); q (quartet); quint (quintet); sept (septet); m (multiplet). Thin layer chromatographies (TLC) were performed on Merck silica gel 60 F 254 and revealed with a UV lamp ($\lambda = 254$ nm) and KMnO_4 staining. Flash Column Chromatographies were conducted on silica Geduran® Si 60 Å (40 – 63 μm). High resolution mass spectrometries were performed on a microTOF (ESI).

IV.3.5.2. General Procedures

a) Synthesis of the silicon complexes

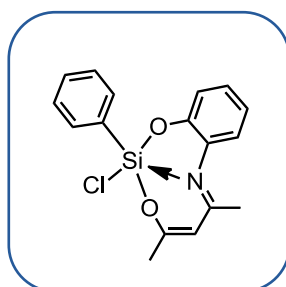
All these complexes were previously described by Tacke's,^{67, 68} Yamamoto's⁶⁹ or Wagler's groups.⁷⁰

8,8'-((chloro(phenyl)silanediy)bis(oxy))diquinoline (**1a**)



To a dried Schlenk flask with 8-Oxyquinoline (2.00 g, 13.7 mmol) and triethylamine (2.89 mL, 20.7 mmol) in THF (50 mL) was added dropwise chlorotrimethylsilane (2.07 mL, 16.3 mmol) at 0°C. The triethylammonium salt was filtered off and washed with THF (2 x 10 mL). The residue was dissolved in chloroform (30 mL) and cooled to 0°C. At this temperature, phenyltrichlorosilane (1.1 mL, 6.86 mmol) was added and the solution was stored at room temperature. The yellow crystalline product was filtered off, washed with chloroform (2 x 5 mL) and dried in vacuo to afford 8,8'-((chloro(phenyl)silanediy)bis(oxy))diquinoline (**1a**) (2.1 g, 71%). No analysis could be done due to the very poor solubility of this compound.

2-chloro-4,6-dimethyl-2-phenylbenzo[d][1,3,6,2]dioxazasilonine (**3**)



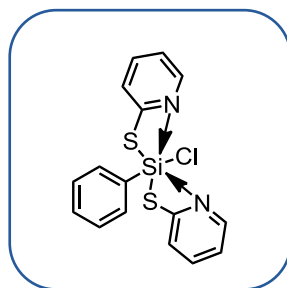
Triethylamine (40 mmol, 5.6 mL) and trichlorophenylsilane (20 mmol, 3.2 mL) were added at 0°C to a stirred suspension of 2-((E)-((Z)-4-hydroxypent-3-en-2-ylidene)amino)phenol (20.0 mmol, 3.82 g) in tetrahydrofuran (60 mL). After that, the resulting mixture was warmed to 20°C and was stirred at this temperature for 24h. The triethylammonium salt was filtered off and washed with tetrahydrofuran (2 x 10 mL). The solvent was removed under reduced pressure before addition of DCM (15 mL) and *n*-pentane (15 mL) on the residue. The

resulting solution was kept undisturbed at room temperature for 24 h. The yellow crystalline product was isolated by filtration, washed with diethyl ether (15 mL), and dried *in vacuo* to afford 2-chloro-4,6-dimethyl-2-phenylbenzo[d][1,3,6,2]dioxazasilonine (**3**) (1.49 g, 22 %). The spectroscopic data are in agreement with those reported in the literature.⁶⁷

¹H NMR (400 MHz, CD₂Cl₂): δ 7.41 (dd, J = 8.0 Hz and 1.2 Hz, 1H), 7.37-7.32 (m, 2H), 7.31-7.24 (m, 2H), 7.24-7.15 (m, 3H), 7.01-6.93 (m, 1H), 5.72 (d, J = 0.4 Hz, 1H), 2.44 (s, 3H), 2.26 (s, 3H);

¹³CNMR (100 MHz, CD₂Cl₂): δ 172.1, 169.3, 151.6, 138.3, 132.6, 132.5 (2 C), 129.8, 129.2, 127.9 (2 C), 121.1, 120.7, 115.8, 107.0, 24.8, 24.3.

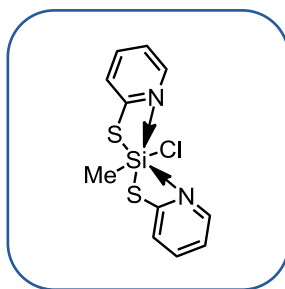
Chlorophenylbis[N,S-pyridine-2-thiolato(-)]silicon(IV) (5a)



To a Schlenk flask with a stirred solution of 2-pyridinethiol (14.2 mmol, 1.59 g) in tetrahydrofuran (30 mL) was added triethylamine (14.2 mmol, 1.44 g) and trichlorophenylsilane (7.09 mmol, 1.50 g). The reaction mixture was then stirred at room temperature for 16 h. The resulting triethylammonium salt was filtered off, washed with tetrahydrofuran (2×5 mL) and discarded. The solvent was concentrated *in vacuo*, then acetonitrile (20 mL) was added. The resulting suspension was heated until a clear solution was obtained, which was then cooled slowly to 20°C then put in a freezer and kept undisturbed for 6 days. The resulting yellow crystalline solid was isolated by filtration and washed with diethyl ether (2×10 mL) before being dried *in vacuo* to afford chlorophenylbis[N,S-pyridine-2 thiolato(-)]silicon(IV) (**5a**) (1.87 g, 73%). The spectroscopic data are in agreement with those reported in the literature.⁶⁸

¹H NMR (400 MHz, CD₂Cl₂): δ 8.17 (bs, 2H), 7.77-7.70 (m, 2H), 7.66-7.60 (m, 2H), 7.48-7.43 (m, 2H), 7.24-7.18 (m, 3H), 7.12-7.05 (m, 2H);

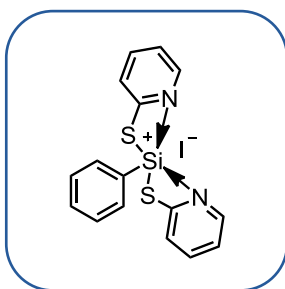
¹³CNMR (100 MHz, CD₂Cl₂): δ 166.6 (2C), 152.7, 141.3 (2C), 140.9 (2C), 132.7 (2C), 127.9, 127.4 (2C), 125.6 (2C), 118.2 (2C).

Chloromethylbis[N,S-pyridine-2-thiolato(-)]silicon(IV) (5b)

To a Schlenk flask with a solution of 2-pyridinethiol (13.7 mmol, 1.547 g) in tetrahydrofuran (27.8 mL) was added triethylamine (13.7 mmol, 1.81 mL) and methyltrichlorosilane (6.96 mmol, 0.817 mL). The reaction mixture was then stirred at room temperature for 16 h. The resulting precipitate was filtered off, washed with tetrahydrofuran (2×5 mL) and discarded. The solvent was concentrated *in vacuo*, followed by the addition of acetonitrile (15 mL) and Et₂O (15 mL). The resulting suspension was heated until a clear solution was obtained, which was then cooled slowly to 20°C then put in a freezer and kept undisturbed for 3 days. The resulting colorless crystalline solid was isolated by filtration and washed with diethyl ether (2×10 mL) before being dried *in vacuo* to afford chloromethylbis[N,S-pyridine-2 thiolato(-)]silicon(IV) (**5b**) (320 mg, 30%). The spectroscopic data are in agreement with those reported in the literature.⁶⁸

¹H NMR (400 MHz, CD₂Cl₂): δ 8.10-7.99 (m, 2H), 7.77-7.67 (m, 2H), 7.50-7.42 (m, 2H), 7.11-6.98 (m, 2H), 1.16 (s, 3H);

¹³CNMR (100 MHz, CD₂Cl₂): δ 168.2 (2C), 141.0 (2C), 140.4 (2C), 125.4 (2C), 117.9 (2C), 26.0.

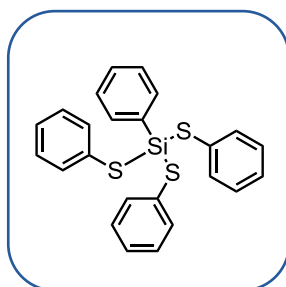
Phenylbis[N,S-pyridine-2-thiolato(-)]silicon(IV) Iodide (5d)

Iodotrimethylsilane (6.95 mmol, 1.39 g) was added in a single portion to a stirred solution of chlorophenylbis[N,S-pyridine-2 thiolato(-)]silicon(IV) (**6a**) (2.77 mmol, 1.00 g) in acetonitrile (30 mL). The resulting reaction mixture was then stirred at 65°C for 3 hours and at room temperature for 3 days. After that, the reaction mixture was concentrated *in vacuo*,

then dissolved in acetonitrile (30 mL). The resulting suspension was heated until a clear solution was obtained, which was then cooled slowly to 20°C then put in a freezer and kept undisturbed at this temperature for 3 days. The resulting colorless crystalline solid was isolated by filtration, washed with diethyl ether (2×5 mL), and dried in to afford phenylbis[N,S-pyridine-2-thiolato(-)]silicon(IV) Iodide (**5d**) (300 mg, 24%). The spectroscopic data are in agreement with those reported in the literature.⁶⁸

¹H NMR (400 MHz, CD₂Cl₂): δ 8.46-8.22 (m, 2H), 8.06-7.82 (m, 2H), 7.73-7.57 (m, 4H), 7.43-7.24 (m, 5H).

Phenyltris(phenylthio)silane (**7**)

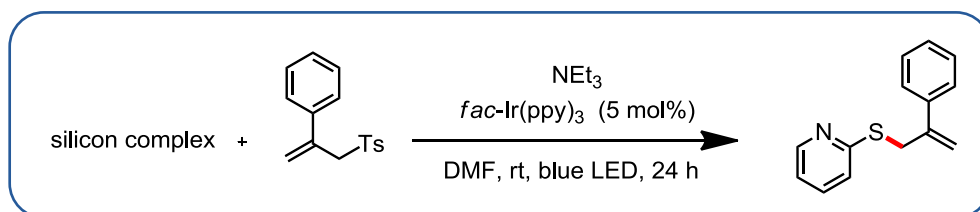


To a Schlenk flask was added the phenyl silane (4 mmol, 0.49 mL), the thiopyridine (12 mmol, 1.32 g) and RhCl(PPh₃)₃ (0.128 mmol, 120 mg) in 10 mL of hexane. The reaction mixture was stirred for 15 hours then filtrated, concentrated under vacuo and pentane was added. An oil appeared and this was taken out to give pure product phenyltris(phenylthio)silane (**7**) (600 mg, 35%). The spectroscopic data are in agreement with those reported in the literature.⁶⁹

¹H NMR (400 MHz, CDCl₃): δ 7.65-7.09 (m, 20H);

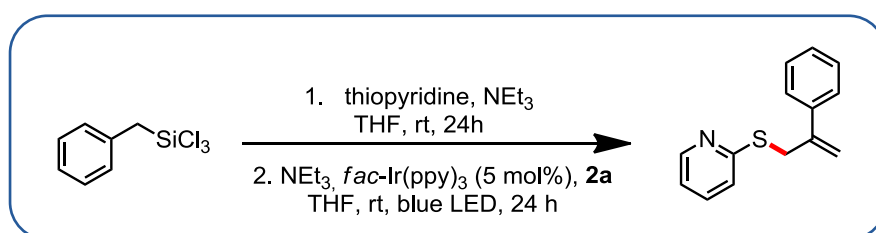
¹³C NMR (100 MHz, CDCl₃): δ 135.1 (6C), 134.9 (3C), 132.0, 131.1, 128.9 (6C), 128.8 (2C), 128.0 (2C), 127.6 (3C).

b) Photocatalytic reactions



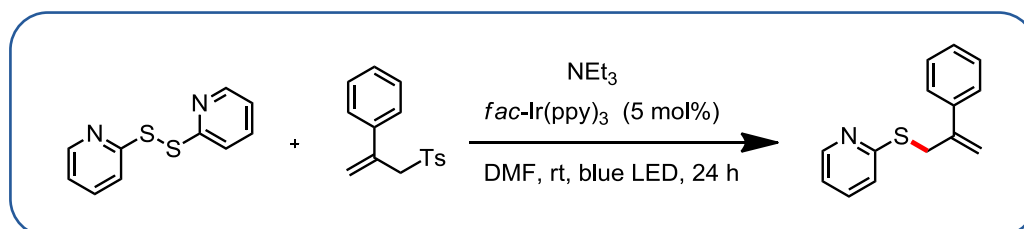
To a Schlenk flask was added the silicon complex **5a-d**, *fac*-Ir(ppy)₃ (5 mol %), and allylsulfone **2**. The degassed solvent (0.1 mol.L⁻¹ or 0.067 mol.L⁻¹) was then introduced followed by the amine (1.5 equiv.) and the reaction mixture was irradiated with blue LED (470 nm) at room temperature for 24h under an argon atmosphere. The reaction mixture was diluted with diethyl ether, washed with water (2 times), dried over MgSO₄ and evaporated under reduced pressure. The crude residue was purified by flash chromatography.

Photocatalytic reaction using Chlorobenzylbis[N,S-pyridine-2-thiolato(-)]silicon(IV) complex



To a dry Schlenk flask was added the benzyl trichlorosilane (2.0 mmol, 0.35 mL), triethylamine (4.0 mmol, 0.56 mL) and thiopyridine (4.0 mmol, 445 mg). The Schlenk flask was sealed with a rubber septum and evacuated / purged with vacuum / argon three times. Then 14 mL of dry and degazed THF were added and the solution was stirred for one day. The triethylammonium salt was filtrated off by canula then 7 mL of this solution were added to a dry schlenk flask containing *fac*-Ir(ppy)₃ (0.0255 mmol, 14.73 mg) triethylamine (1 mmol, 0.14 mL) and allylsulfone **2** (0.45 mmol, 122 mg). The reaction mixture was irradiated with blue LED (470 nm) at room temperature for 24h under an argon atmosphere. The reaction mixture was diluted with diethyl ether, washed with water (2 times), dried over MgSO₄ and evaporated under reduced pressure and analyzed by NMR using TMOP (1 equiv.) as an internal standard.

Photocatalytic reaction using aldrithiolTM

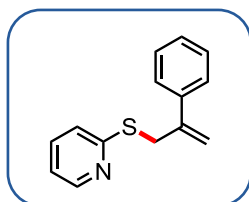


To a dry Schlenk flask was added *Aldrithiol*TM (0.3 mmol, 66 mg), the *fac*-Ir(ppy)₃ (0.005 mol, 3.2 mg) and the allylsulfone **2** (0.1 mmol, 27.2 mg). The Schlenk flask was sealed with a

rubber septum and evacuated / purged with vacuum / argon three times. Then 1.5 mL of dry and degazed DMF was introduced followed by addition of the triethylamine (0.15 mmol, 0.021 mL) and the reaction mixture was irradiated with blue LED (470 nm) at room temperature for 24h under an argon atmosphere. The reaction mixture was diluted with diethyl ether, washed with water (2 times), dried over MgSO_4 and evaporated under reduced pressure. The crude residue was analyzed by NMR using TMOP (1 equiv.) as an internal standard.

IV.3.5.3. Characterization of the product

2-((2-phenylallyl)thio)pyridine (3b)



To a dried Schlenk flask was added the silicon complex (3 equiv.), the acceptor (1 equiv.), the *fac*-Ir(ppy)₃ (5 mol%), and the NEt_3 (1.5 equiv.) in dried and degassed DMF (0.66M). The reaction mixture was irradiated with blue LEDs (477 nm) for 24h then diluted with diethyl ether washed with water (2 times) dried over MgSO_4 , filtered, evaporated under reduced pressure and analyzed by ^1H NMR CDCl_3 .

^1H NMR (400 MHz, CDCl_3): δ 8.47 (d, $J = 4.8$ Hz, 1H), 7.54-7.42 (m, 3H), 7.38-7.27 (m, 3H), 7.16-7.01 (m, 1H), 7.02-6.95 (m, 1H), 5.48 (s, 1H), 5.43 (s, 1H), 4.35 (s, 2H);

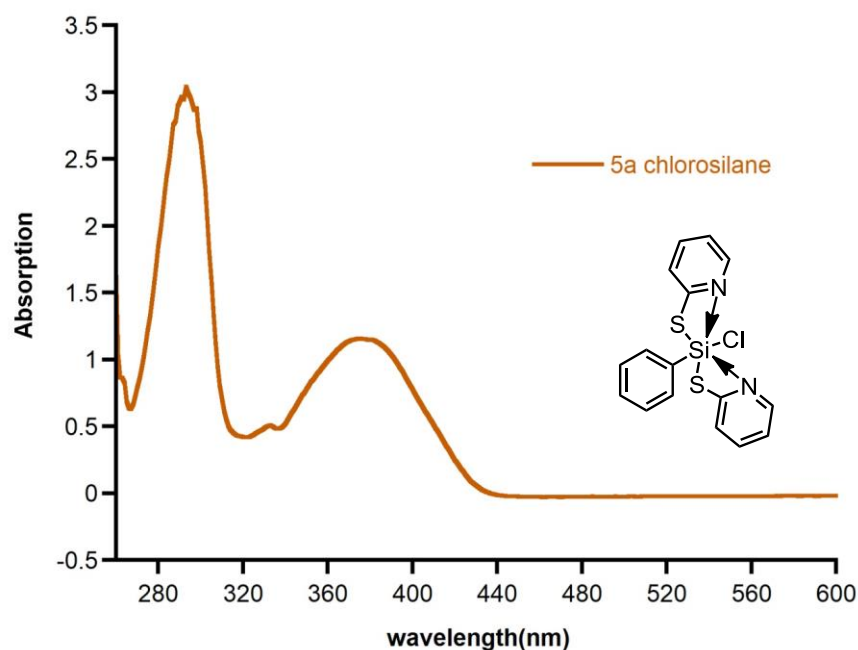
^{13}C NMR (100 MHz, CDCl_3): δ 158.9, 149.6, 143.7, 139.7, 136.0, 128.5 (2C), 128.0, 126.4 (2C), 122.6, 119.7, 115.7, 34.7;

HRMS: calc. for $[\text{C}_{14}\text{H}_{14}\text{NS}]$: 228.0841 found 228.0841;

IR (neat): 3051, 928, 1577, 1557, 1495, 1454, 1413, 1281, 1122 cm^{-1} .

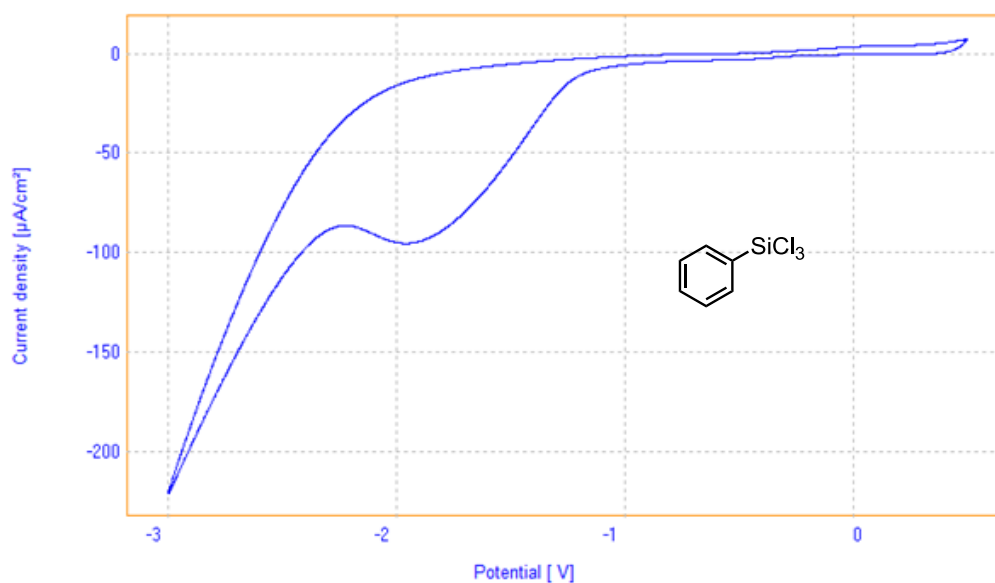
IV.3.5.4. Absorption spectra of 5a

Absorption spectra of 5a in DMF ($C = 3.33 \times 10^{-6} \text{ mol.L}^{-1}$)



IV.3.5.5. Electrochemical measurements

The voltammetric measurement was recorded with a three electrodes apparatus in degassed THF with Bu_4NPF_6 (100 mM) as support electrolyte at 22°C. Measurements were monitored on an AutoLab PSTAT10 electrochemical workstation. Cyclic voltammetry (CV) was used to estimate the redox potential (peak potential). The CVs were obtained with a step potential of 0.009 V at a scan rate of 0.1 V.s^{-1} (0.05 V.s^{-1} for **7**). Glassy carbon, platinum plate, and saturated calomel were used as working, counter, and reference electrodes, respectively



IV.3.6. References

- ¹ S. E. Thomas, 'Organic Synthesis: The Roles of Boron and Silicon', Oxford Chemistry Primers series, **1991**.
- ² G. R. Jones, Y. Landais, *Tetrahedron* **1996**, *52*, 7599.
- ³ C. Chatgililoglu, *Acc. Chem. Res.* **1992**, *25*, 188.
- ⁴ C. Chatgililoglu, *Chem. Rev.* **1995**, *95*, 1229.
- ⁵ C. Chatgililoglu, C. H. Schiesser, 'Silyl radicals in The Chemistry of Organic Silicon Compounds', Vol. 3, Z. Rappoport, Y. Apeloig Eds., Wiley, Chichester, **2001**, 341.
- ⁶ Y. Landais, 'Silyl Radicals in *Science of Synthesis*', D. Bellus, S. Ley, R. Noyori, B. Trost, Eds. G. Thieme, **2013**, Vol. 26, chap. 4.
- ⁷ H. Qrareya, D. Dondi, D. Ravelli, M. Fagnoni, *ChemCatChem*. **2015**, *7*, 3350.
- ⁸ R. Zhou, Y. Goh, H. Liu, H. Tao, L. Li, J. Wu, *Angew. Chem. Int. Ed.* **2017**, *56*, 16621.
- ⁹ C. Chatgililoglu, J. Lalevée, *Molecules* **2012**, *17*, 527.
- ¹⁰ C. Chatgililoglu, C. Ferreri, Y. Landais, V. I. Timokhin, *Chem. Rev.* **2018**, *118*, 6516.
- ¹¹ B. P. Roberts, *Chem. Soc. Rev.* **1999**, *28*, 25.
- ¹² A. Matsumoto, Y. Ito, *J. Org. Chem.* **2000**, *65*, 5707.
- ¹³ R. T. Smith, X. Zhang, J. A. Rincón, J. Aregas, C. Mateos, M. Barberis, S. García-Cerrada, O. de Frutos, D. W. C. MacMillan, *J. Am. Chem. Soc.* **2018**, *140*, 17433.
- ¹⁴ R. J. P. Corriu, R. Perz, C. Réye, *Tetrahedron* **1983**, *39*, 999.
- ¹⁵ C. Chult, R. J. P. Corriu, C. Reye, J. C. Young, *Chem. Rev.* **1993**, *93*, 1371.
- ¹⁶ R. R. Holmes, *Chem. Rev.* **1996**, *96*, 927.
- ¹⁷ S. Rendler, M. Oestreich, *Synthesis* **2005**, *11*, 1727.
- ¹⁸ M. Silvi, C. Verrier, Y. P. Rey, L. Buzzetti, P. Melchiorre, *Nat. Chem.* **2017**, *9*, 868.
- ¹⁹ M. Uygur, T. Danelzik, O. Garcia-Mancheño, *Chem. Commun.* **2019**, *55*, 2980.
- ²⁰ Y. Cai, Y. Tang, L. Fan, Q. Lefebvre, H. Hou, M. Rueping, *ACS Catal.* **2018**, *8*, 9471.
- ²¹ G. Gutenberger, E. Steckhan, S. Blechert, *Angew. Chem. Int. Ed.* **1998**, *37*, 660.
- ²² M. K. Jackl, L. Legnani, B. Morandi, J. W. Bode, *Org. Lett.* **2017**, *19*, 4696.
- ²³ N. Khatun, M. J. Kim, S. K. Woo, *Org. Lett.* **2018**, *20*, 6239.
- ²⁴ L. Capaldo, R. Riccardi, D. Ravelli, M. Fagnoni, *ACS Catal.* **2018**, *8*, 304.
- ²⁵ J. I. Yoshida, K. Tamao, T. Kakui, A. Kurita, M. Murata, K. Yamada, M. Kumada, *Organometallics* **1982**, *1*, 369.
- ²⁶ T. Wang, D.-H. Wang, *Org. Lett.* **2019**, *21*, 3981.
- ²⁷ Y. Nishigaichi, A. Suzuki, A. Takuwa, *Tetrahedron Lett.* **2007**, *48*, 211.
- ²⁸ D. Matsuoka, Y. Nishigaishi, *Chem. Lett.* **2014**, *43*, 559.
- ²⁹ C. L. Frye, *J. Am. Chem. Soc.* **1964**, *86*, 3170.
- ³⁰ G. Sorin, R. Martinez Mallorquin, Y. Contie, A. Baralle, M. Malacria, J.-P. Goddard, L. Fensterbank, *Angew. Chem. Int. Ed.* **2010**, *49*, 8721.
- ³¹ V. Corcé, L.-M. Chamoreau, E. Derat, J.-P. Goddard, C. Ollivier, L. Fensterbank, *Angew. Chem. Int. Ed.* **2015**, *54*, 11414.
- ³² M. Jouffroy, D. N. Primer, G. A. Molander, *J. Am. Chem. Soc.* **2016**, *138*, 475.
- ³³ J. M. R. Narayanam, C. R. J. Stephenson, *Chem. Soc. Rev.* **2011**, *40*, 102.
- ³⁴ C. K. Prier, D. A. Rankic, D. W. C. MacMillan, *Chem. Rev.* **2013**, *113*, 5322.
- ³⁵ J. Xuan, L.-Q. Lu, J.-R. Chen, W.-J. Xiao, *Eur. J. Org. Chem.* **2013**, *30*, 6755.
- ³⁶ T. Koike, M. Akita, *Inorg. Chem. Front.* **2014**, *1*, 562.
- ³⁷ M. H. Shaw, J. Twilton, D. W. C. MacMillan, *J. Org. Chem.* **2016**, *81*, 6898.
- ³⁸ J. Xuan, Z.-G. Zang, W.-J. Xiao, *Angew. Chem. Int. Ed.* **2015**, *54*, 15632.

- ³⁹ I. Ghosh, L. Marzo, A. Das, S. Rizwan, B. König, *Acc. Chem. Res.* **2016**, *49*, 1566.
- ⁴⁰ J.-R. Chen, X.-Q. Hu, L.-Q. Lu, W.-J. Xiao, *Acc. Chem. Res.* **2016**, *49*, 1911.
- ⁴¹ J.-P. Goddard, C. Ollivier, L. Fensterbank, *Acc. Chem. Res.* **2016**, *49*, 1924.
- ⁴² K. Nakajima, Y. Miyake, Y. Nishibayashi, *Acc. Chem. Res.* **2016**, *49*, 1946.
- ⁴³ T. P. Yoon, *Acc. Chem. Res.* **2016**, *49*, 2307.
- ⁴⁴ J.-R. Chen, X.-Q. Hu, L.-Q. Lu, W.-J. Xiao, *Chem. Soc. Rev.* **2016**, *45*, 2044.
- ⁴⁵ N. A. Romero, D. A. Nicewicz, *Chem. Rev.* **2016**, *116*, 10075.
- ⁴⁶ S. Poplata, A. Tröster, Y.-Q. Zou, T. Bach, *Chem. Rev.* **2016**, *116*, 9748.
- ⁴⁷ D. Ravelli, S. Proti M. Fagnoni, *Chem. Rev.* **2016**, *116*, 9850.
- ⁴⁸ J. K. Matsui, S. B. Lang, D. R. Heitz, G. A. Molander, *ACS Catal.* **2017**, *7*, 2563.
- ⁴⁹ L. Marzo, S. K. Pagire, O. Reiser, B. König, *Angew. Chem. Int. Ed.* **2018**, *57*, 10034.
- ⁵⁰ C. Lévêque, L. Chennenberg, V. Corcé, J.-P. Goddard, C. Ollivier, L. Fensterbank, *Org. Chem. Front.* **2016**, *3*, 462.
- ⁵¹ C. Lévêque, L. Chennenberg, V. Corcé, C. Ollivier, L. Fensterbank, *Chem. Commun.* **2016**, *52*, 9877.
- ⁵² C. Lévêque, V. Corcé, L. Chennenberg, C. Ollivier, L. Fensterbank, *Eur. J. Org. Chem.* **2017**, 2118.
- ⁵³ A. Cartier, E. Levernier, V. Corcé, T. Fukuyama, A.-L. Dhimane, C. Ollivier, I. Ryu, L. Fensterbank, *Angew. Chem. Int. Ed.* **2019**, *58*, 1789.
- ⁵⁴ E. Levernier, V. Corcé, L.-M. Rakotoarison, A. Smith, M. Zhang, S. Ognier, M. Tatoulian, C. Ollivier, L. Fensterbank, *Org. Chem. Front.* **2019**, *6*, 1378.
- ⁵⁵ E. Wächtler, A. Kämpfe, K. Krupinski, D. Gerlach, E. Kroke, E. Brendler, J. Wägler, *Z. Naturforsch.* **2014**, *69b*, 1402.
- ⁵⁶ J. Weiß, B. Theis, S. Metz, C. Burschka, C. F. Guerra, F. M. Bickelhaupt, R. Tacke, *Eur. J. Inorg. Chem.* **2012**, 3216.
- ⁵⁷ J. A. Baus, C. Burschka, R. Bertemann, C. F. Guerra, F. M. Bickelhaupt, R. Tacke, *Inorg. Chem.* **2013**, *52*, 10664.
- ⁵⁸ F. Speck, D. Rombach, H. A. Wagenknecht, *Beilstein J. Org. Chem.* **2019**, *15*, 52.
- ⁵⁹ B. Braïda, S. Hazebroucq, P. C. Hiberty, *J. Am. Chem. Soc.* **2002**, *124*, 2371.
- ⁶⁰ P. J. Wagner, J. H. Sedon, M. J. Lindstrom, *J. Am. Chem. Soc.* **1978**, *100*, 2579.
- ⁶¹ V. I. Timokhin, S. Gastaldi, M. P. Bertrand, C. Chatgililoglu, *J. Org. Chem.* **2003**, *68*, 3532.
- ⁶² J. B. Baruah, K. Osakada, T. Yamamoto, *Organometallics* **1996**, *15*, 456.
- ⁶³ C. G. Thomson, M. S. Beer, N. R. Curtis, H. J. Diggle, E. Handford, J. J. Kulagowski, *Bioorg. Med. Chem. Lett.* **2004**, *14*, 677.
- ⁶⁴ L. L. Ling, J. Xian, S. Ali, B. Geng, J. Fuan, D. M. Mills, A. C. Arvanites, H. Orgueira, M. A. Aswhell, G. Carmel, Y. Xiang, D. T. Moir, *Antimicrob. Agents Chemother.* **2004**, *48*, 1541.
- ⁶⁵ D. H. R. Barton, D. Crich, G. Kretzschmar, *J. Chem. Soc. Perkin Trans. 1* **1986**, 39.
- ⁶⁶ For a recent review: A. V. Bordoni, M. V. Lombardo, A. Wolosiuk, *RSC Adv.* **2016**, *6*, 77410.
- ⁶⁷ B. Theis, S. Metz, F. Back, C. Burschka, R. Tacke, *Z. Anorg. Allg. Chem.* **2009**, 635, 1306.
- ⁶⁸ J. A. Baus, C. Burschka, R. Bertemann, C. F. Guerra, F. M. Bickelhaupt, R. Tacke, *Inorg. Chem.* **2013**, *52*, 10664.
- ⁶⁹ J. B. Baruah, K. Osakada, T. Yamamoto, *Organometallics* **1996**, *15*, 456.
- ⁷⁰ E. Wächtler, A. Kämpfe, K. Krupinski, D. Gerlach, E. Kroke, E. Brendler, J. Wägler, *Z. Naturforsch.* **2014**, *69b*, 1402.

- General - Conclusion -

General Conclusion

As shown in this manuscript, visible-light photoredox catalysis has proven to be an efficient tool for radical generation. In a context where sustainability and safety stand at the forefront, the use of a photocatalyst to replace tin-mediated and stoichiometric redox methodologies seems highly attractive. Over the last decades, a large number of radical precursors have been disclosed, allowing the modern chemists to change the way they envision C–C bond formation. Furthermore, among all the available radical precursors, silicon-based ones, and more specifically the silicates, have revealed all their potential.

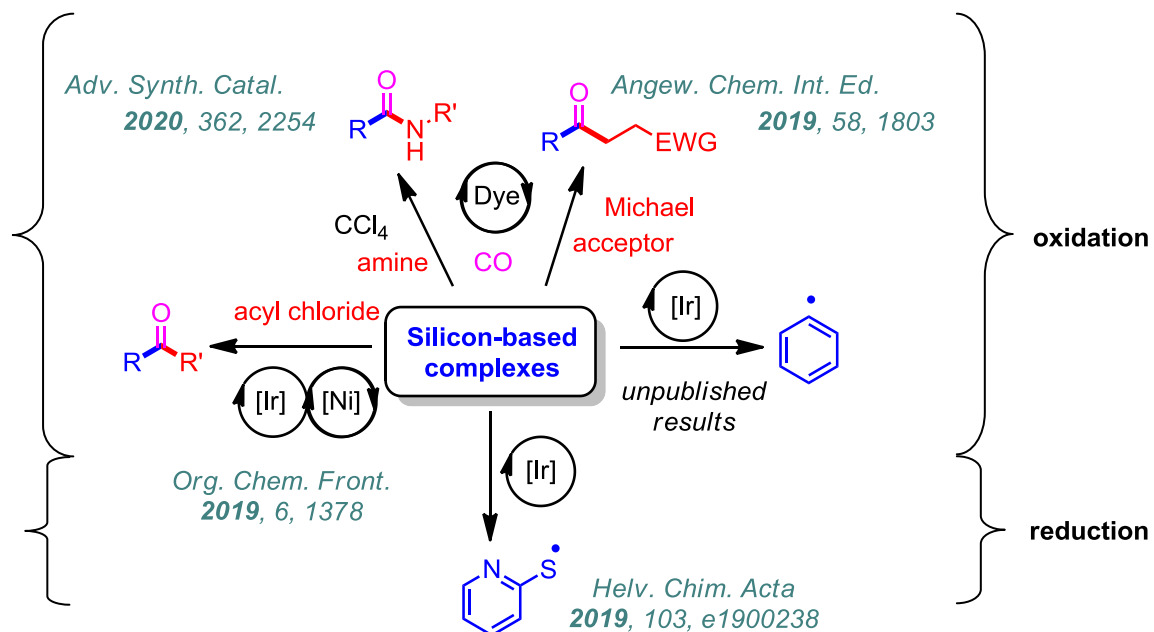
In the first part of this PhD thesis, the generation of a phenyl radical has been disclosed thanks to an efficient catechol modification. Even if the yield remains modest, it is, to the best of our knowledge, the first photooxidative generation of such radical from a silicate. Moreover, we are convinced that this finding, allowing us to gain more insight on these structures, can be extended to other challenging systems. Indeed, preliminary results suggest that methyl silicate also reacts more efficiently with similar modifications. Thus, even if further work is still needed, new interesting reactivities can probably be reached.

In a second part, a nickel/photoredox dual catalysis system for ketone synthesis has been reported. Even though the scope is limited to the activated silicates, the electrophilic partner has been found to be quite diverse. Indeed, aromatic and alkyl acyl chlorides have been shown to react efficiently. Moreover, flow chemistry can be used to reduce the reaction time which can be of great interest from an industrial point of view. Additionally, the observed side product allowed us to design a new metal-free cross-coupling reaction between an aryl fluoride and a silicate. This synthetic transformation is currently under investigation.

Then, radical carbonylation has been studied to overcome the limitations encountered with the nickel/photoredox dual catalysis system. This type of reactions was already well-known under photoreductive conditions but remained quite unexplored under photooxidative ones. Thus, after showing that silicates also perform very efficiently radical carbonylation, the system has been successfully extended to amide formation. Even the main drawback of this new strategy, namely the need of a high CO pressure, has been overcome with the aid of flow chemistry. Arguably, this finding is of great interest and we are now examining the feasibility of the formation of other acyl derivatives under photooxidative batch and flow regimes. Moreover, carbon monoxide is probably not the only gas that can be used. Other challenging ones, like CO₂ or SO₂, can be quite interesting from a synthetic point of view and might be studied later on.

In a last part, the photoreduction of hypercoordinated silicon complexes has been investigated. Indeed, no radical generation under photoreductive conditions from silicon-based structures had ever been reported. Thus, chlorosilane derivatives have been studied to fill in this missing gap. Even if no carbon-centered radical has been formed within these conditions, the thiopyridyl radical has been efficiently trapped. This interesting result

discloses the first photoreduction of a silicon complex. Experiments are currently ongoing in our laboratory for the formation of carbon-centered radicals by photoreduction of other types of hypercoordinated silicon species.



Études de dérivés hypervalents du silicium en conditions photoredox : de la génération de radicaux à leur utilisation en chimie organique.

Au cours des quinze dernières années, la catalyse photoredox s'est imposée comme une méthode douce et efficace de génération de radicaux permettant ainsi d'envisager autrement la formation de liaisons carbone-carbone. En effet, grâce au grand nombre de précurseurs radicalaires disponibles, un large panel de réactions devient accessible. Parmi eux, une grande famille se détache de par sa capacité à engendrer facilement des radicaux primaires : les bis-catécholatosilicates. Bien que cette dernière classe de précurseurs s'est déjà avérée d'un grand intérêt en chimie organométallique, ce n'est vraiment qu'avec la catalyse photoredox qu'elle a révélé tout son potentiel. Que ce soit en addition directe ou en catalyse duale, les silicates se sont révélés très efficaces. Ainsi, au cours de ces travaux de thèse, nous avons montré que de nouvelles structures pouvaient être accessibles grâce à ces derniers. En effet, pour la première fois à partir de silicates et grâce à l'utilisation de catéchols substitués, des radicaux aryles ont été formés et piégés. La catalyse duale iridium/nickel nous a aussi permis de synthétiser des cétones possédant des positions fortement énolisables. La carbonylation radicalaire a de même très bien fonctionné avec ces substrats menant à des cétones ou des amides selon le système mis en œuvre. De plus, une utilisation de la carbonylation en flux continu nous a permis de surmonter le plus grand désavantage de cette technique, à savoir la haute pression de CO requise. Enfin, la réduction de dérivés hypervalents du silicium a été étudiée et a permis la génération de radicaux thiopyridyles.

Mots clés : silicate, oxydation, catalyse duale, carbonylation, radicaux, flux continu.

Hypervalent silicon compounds under photoredox conditions: from the generation of radicals to their applications in organic chemistry.

Over the last fifteen years, the photoredox catalysis has profoundly changed the way that modern chemists envisioned C-C bond formation. Among all of the available radical precursors, the bis-catecholatosilicates have been shown to be very effective in a large variety of reactions. Indeed, thanks to their low oxidation potentials, they allow the formation of highly unstabilized primary radicals which can be used, later on, in synthetic transformations. During this PhD thesis, we developed new reactions based on this type of radical precursors. We showed that a phenyl radical could be formed and trapped thanks to the oxidation of a phenyl silicate bearing substituted catechols. Moreover, a dual catalysis system for highly enolizable ketones synthesis was found and extended to flow chemistry. Radical carbonylation was also revealed to work very nicely with the silicates and, thanks to this approach, ketones and amides were synthesized in high yields. Furthermore, this reaction was studied under flow conditions and exhibited a reduced reaction time and carbon monoxide pressure required. Finally, we studied the reduction of silicon complexes. Even if no carbon-centered radical was formed, a thiopyridyl radical was efficiently trapped showing that the reduction of such derivatives is possible.

Keywords: silicate, oxidation, dual catalysis, carbonylation, radical, flow chemistry.